DISSERTATION

REDUCTIVE COUPLING REACTIONS OF ORGANOSILANES FOR THE MONOSELECTIVE C–F FUNCTIONALIZATION OF TRIFLUOROMETHYLARENES

Submitted by

Shawn E. Wright

Department of Chemistry

In partial fulfillment of the requirements

For the Degree of Doctor of Philosophy

Colorado State University

Fort Collins, Colorado

Summer 2022

Doctoral Committee:

Advisor: Jeffrey Bandar

Robert Paton
Thomas Borch
Margarita Herrera-Alonso

ABSTRACT

REDUCTIVE COUPLING REACTIONS OF ORGANOSILANES FOR THE MONOSELECTIVE C–F FUNCTIONALIZATION OF TRIFLUOROMETHYLARENES

The mono-selective defluorofunctionalization of trifluoromethylarenes is an emerging strategy to access α,α-difluorobenzylic derivatives, which are difficult to access in a divergent manner. Fluorine incorporation is a common strategy employed during the optimization of potential pharmaceuticals in the drug discovery process. Much effort has been spent over the past few decades in developing fluorination methodologies, and the result has been tremendous growth in aryl and alkyl fluorination and trifluoromethylation reactions. On the other hand, methods to install other fluoroalkyl motifs are less developed. Due to the abundant availability of trifluoromethylarenes, mono-selective defluorofunctionalization reactions would be an ideal route to access α,α-difluorobenzylic derivatives, which are becoming increasing examined in drug discovery settings.

Chapter one will provide the necessary background to understand the context of the work described throughout the following chapters. First, there will be an overview of the importance of fluorine for the development of pharmaceutical compounds. Then there will be a brief summary of the different strategies that have been developed to achieve the trifluoromethylation of arenes as well as the common routes to access α,α-difluorobenzylic compounds. Finally, a thorough discussion of the challenges and reported solutions to achieve mono-selective defluorofunctionalization of trifluoromethylarenes will be provided.

Chapter two will describe the initial discovery, development, and mechanistic investigation of the defluoroallylation reaction reported by the Bandar group. This discovery led to the identification of a new strategy to achieve reductive coupling through the use of Lewis base activated organosilanes, which provides the basis for the reactions discovered and developed in chapters three and four.

Chapter three will describe the discovery, development, and mechanistic investigation of a reductive coupling reaction of trifluoromethylarenes with formamides. This reaction generates a silylated hemiaminal product which is a valuable synthetic intermediate to access a broad scope of α,α-difluorobenzylic derivatives. Mechanistic investigations support the generation of a α,α-difluorobenzylsilane intermediate in the reaction. Isolated of the α,α-difluorobenzylsilane and subsequent derivatizations further broaden the scope of transformations accessible via this reductive coupling process.

Chapter four will describe the discovery and preliminary development of the mono-selective hydrodefluorination of trifluoromethylarenes using hydrosilanes activated by a Lewis basic catalyst. Two different catalytic systems are demonstrated that operate via different mechanisms, which provides access to different reaction scopes. A short discussion on the future work of this project will also be provided, where a junior graduate student is developing conditions to enable the mono-selective hydrodefluorination of electron-neutral trifluoromethylarenes.

ACKNOWLEDGEMENTS

As I near the end of this long and incredible journey I am filled with gratitude. I have received so much support throughout every part of this journey, and I know that I could not have reached this point if not for everyone along the way. I will take this opportunity to thank some of those people.

First, I would like to thank my committee: Professors Robert Paton, Thomas Borch, and Margarita Herrera-Alonso. Your time and consideration have been crucial in progressing towards my degree, thank you all very much.

Thu-Thai Le Douglass and Roselle Schmidt, thank you for being great managers and great people. You gave me the hours I needed to afford school and attend classes. You built great teams that made work fun and led to friends and memories that I will forever cherish.

Professor Linda Woods, thank you for making the community college more than just a place to take cheap classes. You instituted programs that gave us opportunity and encouraged us on. I know that I would not have finished college without those opportunities.

Professor Timothy Clark, thank you for being a great mentor. I wouldn't have been accepted to the university if it wasn't for your lab, and it is because of that opportunity to do research that I was able to go to graduate school. Most of all, your high expectations from everyone in the group, and the care you take in teaching us, is what shaped me into the chemist that exists today.

Professor Jeffrey Bandar, thank you for being a great advisor, a great mentor, a great boss, and a great person. Thank you especially for giving me the flexibility I needed to always put my family first. You push all your students in the ways that they need to be pushed while giving us

the freedom that we need to succeed in our own way. Your mentorship has taught me what it takes to be successful and how to achieve that success. I will use these lessons for the rest of my life.

Mom and dad, thank you for teaching me how to work hard and how to value the most important things in life, and thank you for loving me and supporting me throughout my life. Stanley, thank you for being the best brother I have ever had and for always being there for me.

Patrick, thank you for being a part of my life and for being you. You left everything you know to come with me. I hope that the opportunities provided to us will make it so that you won't have to struggle in the way that your mom and I had to, and I hope that I can help you in achieving your goals and dreams—whatever they may be.

Stephanie, thank you for accepting me, thank you for believing in me, thank you for always supporting me, and thank you for always being there for me. This has been a long journey, but I hope that this is still just the beginning our life together. I look forward to a lifetime of moments together. I hope to support you in achieving everything that you want, and I will spend the rest of my life returning, in kind, the love and support that you have given me.

TABLE OF CONTENTS

CHAPTER ONE

DEFLUOROFUNCTIONALIZATION AS AN EMERGING STRATEGY TO ACCESS DIFLUOROBENZYLIC COMPOUNDS

1.1 Chapter Overview

This chapter is intended to provide the necessary background to appreciate the utility of selective defluorofunctionalization reactions for accessing difluorobenzylic compounds from trifluoromethylarenes. A brief introduction to the unique and desirable effects of fluorine incorporation on the pharmacokinetic properties of potential drugs will be provided. Then, an overview of common methods of benzylic fluorination will be described, with a focus on the well-developed trifluoromethylation methodologies that have been reported. Finally, recent developments towards the mono-selective defluorofunctionalization of trifluoromethylarenes will be summarized to provide the necessary context for the state of the field in which the work presented herein will advance.

1.2 Unique Properties of Fluorine for Drug Discovery

The incorporation of fluorine into bioactive molecules can have subtle or substantial effects on stability, solubility, conformation, and biological activity.[1-9] Currently, about 20% of commercial pharmaceuticals contain at least one fluorine atom and there has been an upward trend in the proportion of FDA-approved drugs that contain fluorine in recent years.[8] Fluorinated motifs are therefore in high demand for drug discovery efforts and methods to incorporate them have been the focus of intensive research efforts over the past several decades.[10-12] Although much effort has been spent developing new methods of fluorination and fluoroalkylation, increased

incorporation of fluorine in drug design and development is still limited primarily by synthetic accessibility.[3]

The combination of fluorine's small size (1.47 Å van der Waals radius, about 20% larger than hydrogen) and high electronegativity (3.98 Pauling scale, the most electronegative atom) impart unique properties that are often used for modulating the physiochemical and pharmacokinetic properties of a potential pharmaceutical, particularly when multiple fluorine atoms are attached to the same carbon.[9] Trifluoro- and *gem*-difluoro substituents are strongly electron-withdrawing and this inductive effect can alter the acidity or basicity of nearby functional groups which can affect binding interactions to biological targets.[5] The high strength of the C–F bond (115 kcal/mol for $PhCF_2$–F and 99 kcal/mol for $PhCH_2$–F)[13-14] has increased oxidative and thermal stability and consequently C–F substitution is a commonly used strategy to prevent *in vivo* oxidation of labile C–H bonds (90 kcal/mol for $PhCH_2$–H)[15], particularly at benzylic positions. Additionally, these inductive effects can also increase the metabolic stability of electron rich (hetero)arenes that are susceptible to oxidation. Increases in metabolic stability often lead to increased half-life and a reduction in the formation of toxic metabolites. [16]

Unlike the other halogens (chlorine, bromine, iodine), fluorine possesses low polarizability, which effectively increases the lipophilicity of a difluoro- or trifluoromethylarene. From a pharmacokinetic perspective, the lipophilicity of a compound is often correlated with adsorption, distribution, and route of elimination within the body.[17] Of particular importance is the bioavailability of a potential drug after oral dosage. Absorption via passive diffusion across membranes within the stomach, intestinal lining, and the blood brain barrier to reach the central nervous system are affected by the lipophilicity of a potential drug. To provide an example of the enhanced pharmacokinetic properties due to the fluorine incorporation, the substitution of a

chlorine atom in the benzothiazole core of the antipsychotic chlorpromazine with a trifluoromethyl group resulted in a five-fold increase in potency.[3]

The focus of the work described in Chapters 2,3, and 4 is on the α,α-difluorobenzylic substructure specifically (generic figure shown in Figure 1-1). A unique feature of the α,α-difluorobenzylic group ($ArCF_2$–R) is the presence of an R substituent that be used as a point of modularity. Structure optimization of lead and late-stage compounds is a critical part of the drug discovery process, therefore examination of a variety of fluoroalkyl motifs can be crucial in obtaining the optimal pharmacological profile. For example, Novartis screened four subtly different fluoroalkyl motifs, among other substituents of varying size and polarity, as a bioisostere of an *iso*-propyl substituent during the development of LSZ102, a selective estrogen receptor degrader currently in clinical trials for the treatment of breast cancer (Figure 1-2).[18] Examination of trifluoromethyl, difluoromethyl, α-fluoroethyl, and α,α-difluoroethyl moieties revealed the α,α-difluoroethyl structure as the optimal structure to achieve a desirable balance of potency and bioavailability. An x-ray crystal structure of LSZ102 bound to the estrogen receptor alpha (ERα) protein shows that the α,α-difluoroethyl substituent is an optimal size to adequately occupy space within the hydrophobic binding pocket, with additional interactions to several phenylalanine, leucine, and methionine residues observed.

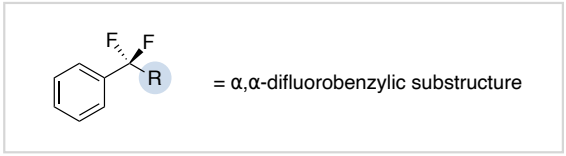

Figure 1-1. The α,α-difluorobenzylic substructure.

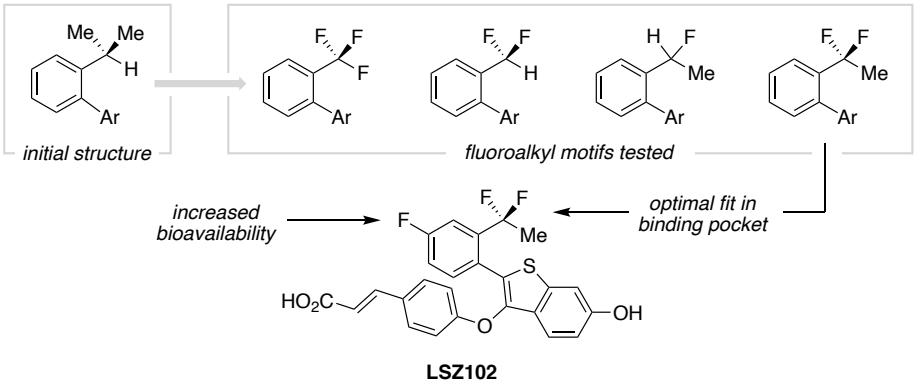

Figure 1-2. Novartis structure optimization of LSZ102, currently in clinical trials for the treatment of breast cancer.

In another example of potential bioisosterism enabled by the difluorobenzylic motif, Merck was developing a thrombin inhibitor that failed phase 3 clinical trials due to poor bioavailability (Figure 1-3).[3,5] Extensive structure-activity relationship studies led to the identification of difluorobenzylic compounds with similar potency and higher bioavailability. The α,α-difluoroethyl substructure serves two functions: (1) as a lipophilic bioisostere by mimicking the shape and dipole of the sulfonamide moiety, and (2) blocks metabolic oxidation of the benzyl moiety. The beneficial effect of the difluorobenzylic substructure is verified by the observation that replacing the *gem*-difluoride with either a *gem*-dimethyl or a methylene both resulted in roughly six-fold decrease in activity. The previous two examples are from drug discovery campaigns and they highlight how the difluorobenzylic motif can act as a lipophilic bioisostere to optimize potential drug candidates.

Figure 1-3. Merck structural optimization of a thrombin inhibitor, RWJ-445167, that failed clinical trials due to poor bioavailability.

A particularly useful bioisostere is the difluoromethylarene ($ArCF_2H$) functional group as a lipophilic bioisostere of alcohols, thiols, and amines with weak hydrogen bond donating capabilities.[19-21] Hydrogen bonding is an important non-covalent interaction that can increase the binding affinity of drugs to their target proteins and result in a more potent pharmaceutical. A lipophilic hydrogen bond donator is a useful tool to possess as hydrogen bond donating functional groups are typically polar and hydrophilic, such as alcohols, thiols, and amines; therefore, having access to a lipophilic bioisostere can be useful in complementary situations to traditional hydrogen bond donators. As an example, a pyrazole carboxamide fungicide was examined with both a trifluoro- and difluoromethyl group on the pyrazole ring.[19] The difluoromethyl version was nearly twice as effective and it was suggested that the greater activity was due to increased enzyme-inhibitor interactions.

Due to the myriad effects that trifluoro- and difluoromethyl substituents can impart on a compound, much effort has been devoted to the development of methods to install these substituents on arenes. The next section will provide a brief background on the methods to access difluoro- and trifluoromethylarenes.

1.3 Methods to Access Trifluoromethylarenes

The trifluoromethylation of arenes has been the focus of intensive research efforts and consequently has the most developed methodologies of any fluoroalkyl group. This section will briefly provide an overview of methods to achieve trifluoromethylation of an arene by providing examples of representative reported strategies.

Many simple building-block trifluoromethylarenes are produced industrially from the methylarene through the two-step Swarts reaction, utilizing chlorine gas and antimony trifluoride

or hydrogen fluoride (Figure 1-4, a).[22-23] While this is a reliable route to simple trifluoromethylarenes, the harsh reaction conditions and dangerous reagents used limit functional group compatibility and prevent use for most purposes beyond the use of highly specialized equipment. Alternatively, robust condensation/annulation reactions employing trifluoroacetate derivatives have been used to generate trifluoromethyl(hetero)arenes. For example, trifluoroacetic anhydride was used for acylation followed by annulation in a process route to the top-selling DPP-4 inhibitor diabetic drug sitagliptin.[24] Careful consideration must be employed as this strategy can result in regioisomers and the scope of accessible (hetero)arenes is limited to the specific structural arrangements amenable to condensation/annulation type reactions (Figure 1-4, b).

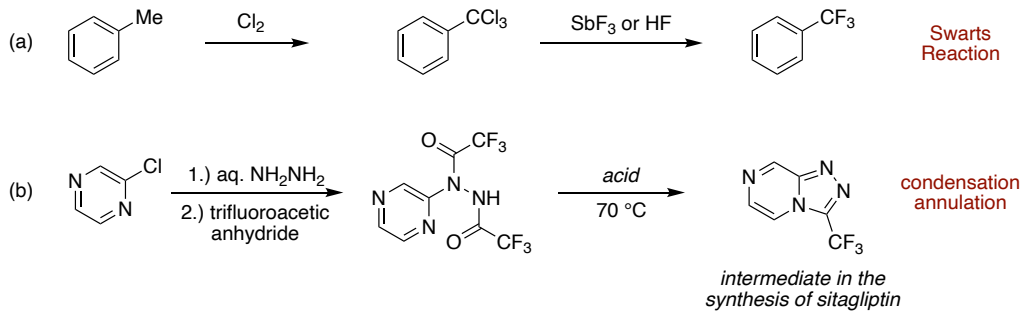

Figure 1-4. Common industrial routes towards trifluoromethylarene building block compounds.

There has been much effort devoted towards the mild trifluoromethylation of arenes and only a few examples will be provided here, though several reviews have been published on the subject.[10,11,22,23] *Ipso*-substitution of aryl iodides, bromides, and chlorides by stoichiometric $CuCF_3$ generated *in situ* or preformed is well-developed.[22] A Sandmeyer-type trifluoromethylation of primary anilines was developed by Fu in 2013 utilizing an electrophilic trifluoromethyl source and copper metal.[25] Copper mediated oxidative coupling of aryl boronates with trifluorotrimethylsilane has also been developed.[26] The cost and waste associated with stoichiometric metal use are undesirable and significant effort has been spent on developing catalytic methods for aromatic trifluoromethylation. Over the last decade photoredox and

transition metal-catalyzed methods have greatly expanded access to trifluoromethyl(hetero)arenes. In 2009, Amii reported the copper-catalyzed trifluoromethylation of aryl iodides, discovering that the use of the diamine ligand 1,10-phenanthroline accelerated the rate of oxidative insertion enough to prevent decomposition of the trifluoromethyl source.[27] In 2010, Buchwald disclosed the palladium-catalyzed trifluoromethylation of aryl chlorides, where the identity of trifluoromethyl source, to limit degradation, and bulky monophosphine ligand, to promote the challenging reductive elimination, were crucial for the success of the reaction.[28] In 2011, MacMillan utilized photocatalysis for with the C–H trifluoromethylation of (hetero)arenes employing a ruthenium photocatalyst to reduce trifluoromethylsulfonyl chloride and generate a trifluoromethyl radical that adds to (hetero)arenes.[29] In 2018, MacMillan impressively combined photo- and copper catalysis for the trifluoromethylation of aryl bromides—key aspects were the identification of a silyl radical, generated by oxidation of the excited photocatalyst, that could abstract the bromide providing the aryl radical, and a trifluoromethyl source that could reduce the photocatalyst and generate the trifluoromethyl radical.[30] In summary, the tremendous development of mild and catalytic methods to install trifluoromethyl groups on arenes from a variety of precursors has enabled its ubiquitous presence in drug-discovery efforts.

1.4 Methods to Access Difluorobenzylic Compounds

There are far fewer methods available for the preparation of α,α-difluorobenzylic compounds when compared to the trifluoromethylation of arenes. Difluoromethylarenes are typically synthesized from deoxyfluorination of the corresponding carbonyl using highly reactive and potentially explosive sulfur(IV) fluoride reagents, such as dimethylaminosulfur trifluoride, which greatly limits functional group compatibility.[31] Therefore, accessing a diverse array of

difluorobenzylic structures, such as for understanding structure-activity relationships, requires multi-step syntheses for access to the carbonyl prior to deoxyfluorination. Additionally, installation of the difluorobenzylic moiety must typically be performed early in the synthetic sequence, or incorporated later in a convergent synthesis, because of functional group incompatibilities (including alcohols, other carbonyls, and basic amines) with the harsh deoxyfluorination reagents. While there has been progress in the difluoromethylation of aryl (pseudo)halides and boronates utilizing transition metals, these reactions frequently require expensive stoichiometric reagents.[32] Additionally, available $–CF_2R$ coupling partners are generally limited to α,α-difluorocarbonyls.[33-36] Several radical-based methods to achieve benzylic C–H fluorination[37] or aryl difluoromethylation[38-39] have been reported, though it can be challenging to control regioselectivity for many classes of aromatic substrates. As another alternative approach, Qing recently reported in 2018 the regioselective oxidative difluoromethylation of acidic heteroaryl C–H bonds.[40]

The lack of methods to rapidly access diverse α,α-difluorobenzylic substructures and the prevalence of trifluoromethylarenes in drug discovery positions the trifluoromethyl group as the most logical choice as a synthetic handle to streamline access to these highly desired derivatives; unfortunately, numerous challenges have hindered progress in this regard and these will be discussed in the next section.

1.5 Selective C–F Functionalization of Trifluoromethylarenes

A major challenge to the mono-selective C–F functionalization of trifluoromethylarenes is the high trifluoromethyl C–F bond strength that decreases upon each C–F substitution (115 kcal/mol for $PhCF_2–F$ and 99 kcal/mol for $PhCH_2–F$). Thus, traditional activation strategies are

unable to provide selectivity since any products formed will have weaker C–F bonds than the reactants and will thus result in unselective or exhaustive defluorination. Therefore, any strategy to selectively functionalize a single C–F bond in trifluoromethylarenes must also be prevented from activating the weaker remaining C–F bonds in the product. This section provides an overview of the reported strategies to overcome these limitations to provide a mono-selective defluorofunctionalized product. Currently, there exist five strategies for the selective substitution of a single C–F bond of a trifluoromethylarene: (1) electrochemical or low valent metal reductions, (2) Lewis acid activation, (3) transition metal catalysis, and (4) photoredox catalysis will be discussed in this section. The fifth strategy encompasses the developments of the Bandar Group, the Lewis base activation of organosilanes, and will be the focus of Chapters 2 and 3, as well as part of Chapter 4.

1.5.1 Electrochemical and Low-Valent Metal Reductive Defluorofunctionalization of Trifluoromethylarenes

The earliest reports of the selective trifluoromethylarene defluorofunctionalization date back to 1989 using electrochemistry. Saboureau and coworkers demonstrated that careful control of the electrical current allows a two electron reduction, generating a radical anion that undergoes mesolytic cleavage. The resulting benzylic radical is then reduced to a benzylic anion which acts as a nucleophile to add into the electrophilic (co)solvent (Figure 1-5).[41] Following this work in 1998, Clavel and coworkers reported a selective defluorosilylation reaction using chlorotrimethylsilane as an electrophile compatible with the highly reducing conditions necessary for reduction of the trifluoromethylarene ($PhCF_3$ E_{red} = –2.61 V vs. SCE in DMF).[42] These reports demonstrate impressive selectivity through careful control of the current, but the highly reducing

conditions are a major limiting factor for the substrates amenable to this reactivity and consequently the scopes of trifluoromethylarenes and electrophiles are rather limited.

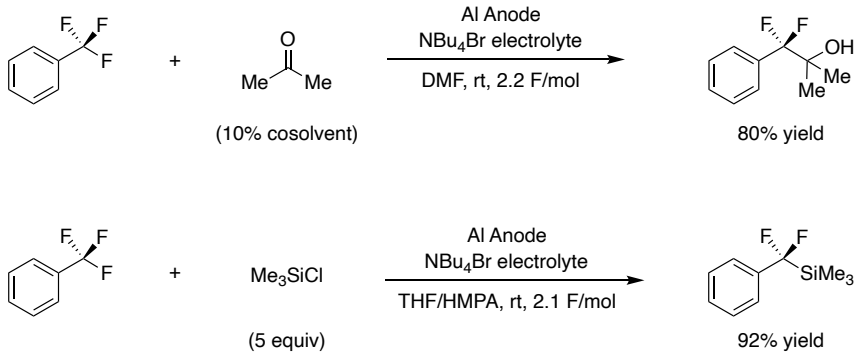

Figure 1-5. Early reports by Saboureau in 1989 (top) and Clavel in 1998 (bottom) of selective electrochemical defluorofunctionalization of trifluoromethylarenes.

Another early strategy uses low valent metals, such as elemental magnesium, to reduce trifluoromethylarenes. An important consideration in these methods is potential overreduction due to the inherent reducing power of low valent metals. A 2014 report from Syngenta describes their use of magnesium metal, combined with iron(II) chloride and magnesium(II) chloride Lewis acid cocatalysts, to reduce a bis(trifluoromethyl)-1,2,3-triazle to generate the defluorosilylation product as a route to a new class of potential herbicides (Figure 1-6).[43]

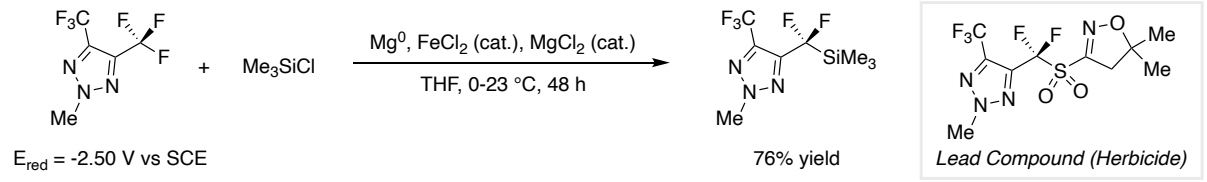

Figure 1-6. Syngenta 2014 disclosure of a defluorosilylation reaction using magnesium metal.

Prakash reported the reduction of bis(trifluoromethyl)arenes in 2017 using magnesium metal under acidic conditions, with varying amounts of selectivity illustrating the added difficulty to selectively reduce electron-deficient trifluoromethylarenes due to their increased electron affinity (Figure 1-7).[44] The 1,3-bis(trifluoromethyl)benzene model substrate has a reduction potential of –2.68 V vs Fc^{+}/Fc while the hydrodefluorination product 3-

(difluoromethyl)benzotrifluoride has a reduction potential of –2.85 V vs Fc^{+}/Fc. The reported scope was limited to substitution at the 5 position of 1,3-bis(trifluoromethyl)benzenes, and a few substituents severely eroded the mono-selectivity.

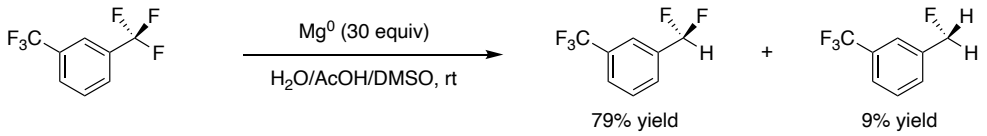

Figure 1-7. Prakash 2017 report for the mono-selective reduction of bis(trifluoromethyl)arenes using magnesium metal.

These reports demonstrate the ability of electrochemistry and low valent metals to reduce trifluoromethylarenes. Electrochemistry has been shown to work well for electron-neutral trifluoromethylarenes, but the highly reducing conditions necessary limit the functional group tolerance of both the arene and electrophile coupling partner. Meanwhile, low valent metals have been shown to be selective with careful consideration of reaction conditions but overreduction is still present to some degree, particularly for electron-deficient trifluoromethylarenes.

1.5.2 Lewis Acid Assisted Defluorofunctionalization of Trifluoromethylarenes

While there has been much progress using Lewis acids to promote defluorinative functionalizations, there have been relatively few reports of mono-selective defluorinative functionalization reactions of trifluoromethylarenes. Typically, a Lewis acid present in solution will indiscriminately activate any C–F bond present, ultimately leading to exhaustive defluorofunctionalization.[45-51] This section will provide an overview of strategies to selectively achieve mono-selective defluorofunctionalization using Lewis acids.

In 2016 Yoshida disclosed the use of an *ortho*-silylium cation to control the mono-selective defluoroallylation of trifluoromethylarenes (Figure 1-8).[52] First, hydride abstraction occurs using a tritylium cation, then the resulting silylium cation abstracts a fluorine from an *ortho*-

trifluoromethyl group, and the difluorobenzylic cation couples with an allylic silane to furnish the product. Further reports by Yoshida in 2020 and 2022 expand the scope of defluorinative functionalizations from a variety of heteroatomic nucleophiles as well as derivatizations of the *ortho*-silane moiety.[53-55] The requirement for a directing group is the major limitation of this strategy, while the generation of a benzylic cation in the mechanism also places a lower limit of reactivity in regards to the electronic nature of the trifluoromethylarene.

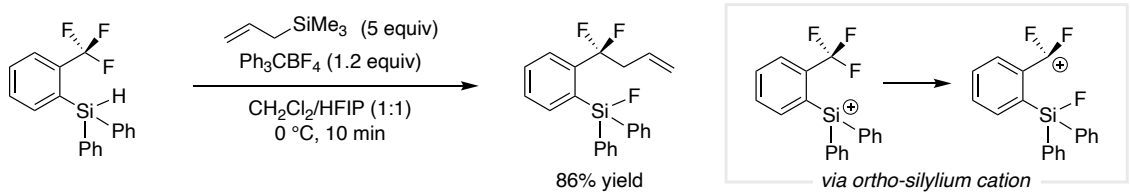

Figure 1-8. Yoshida 2016 report of *ortho*-silylium cation for mono-selective defluoroallylation of trifluoromethylarenes.

In 2020 Young reported the use of a frustrated Lewis pair to achieve mono-selective defluorinative functionalization (Figure 1-9).[56] A strong Lewis acid catalyst, tris(pentafluorophenyl)borane, abstracts a fluorine from a trifluoromethylarene and a bulky, neutral Lewis base, 2,4,6-triphenylpyridine or tris(*ortho*-tolyl)phosphine, adds into the difluorobenzylic cation to generate an isolable cationic product. The Lewis acid catalyst is regenerated through the formation of trimethylsilylfluoride gas through the inclusion of trimethylsilyl additives. The generation of an electrophilic cationic product is key to preventing over-functionalization as the cationic nature prevents further fluoride abstraction, and the cationic product is additionally valuable as an electrophilic synthon amenable to nucleophilic substitution with a wide variety of heteroatom salts. Similar to Yoshida's strategy, the generation of a benzylic cation prevents electron-deficient trifluoromethylarenes from performing well in this reaction.

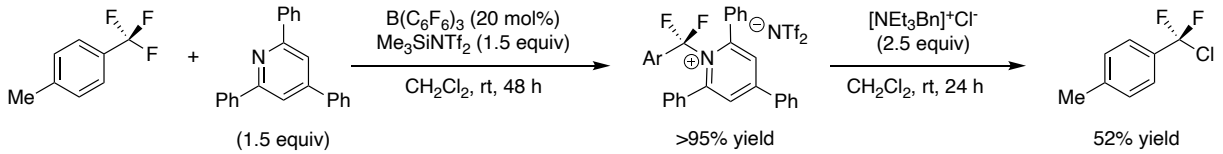

Figure 1-9 Young 2020 report using frustrated Lewis pairs for the mono-selective defluorofunctinalization of trifluoromethylarenes.

Compared to the numerous reports of unselective or exhaustive defluorinative functionalization of trifluoromethylarenes, these reports by Yoshida and Young represent the state of the art for mono-selective C–F functionalization using Lewis acids and provide routes to valuable electrophilic difluorobenzyl synthons for further structural elaboration of trifluoromethylarene building blocks.

1.5.3 Transition Metal Catalyzed Defluorofunctionalization of Trifluoromethylarenes

There have been limited reports of transition metals promoting the selective defluorofunctionalization of trifluoromethylarenes, likely due to the difficulty in oxidative addition of a transition metal into the strong trifluoromethyl C–F bond. A 2016 report by Lalic demonstrates the mono-selective hydrodefluorination of six *para*-substituted trifluoromethylarenes using catalytic palladium, copper, and 2-pyridone (Figure 1-10).[57] The mechanism of this reaction is unclear but possibly operates through a hemiaminal intermediate with evidence that the reaction solvent, DMF, is incorporated into the intermediate (*vide infra*, the work detailed in Chapter 3 generates an isolable hemiaminal product through incorporation of the formamide solvent). After activation of the C–F bond, addition of a proton source with heating results in protonation, supported with deuterium studies, to furnish the hydrodefluorination product selectively. The authors hypothesize the reaction operates through a single electron

reduction mechanism from the observation that difluoromethylarenes, with weaker C–F bonds but higher reduction potentials, are less reactive.

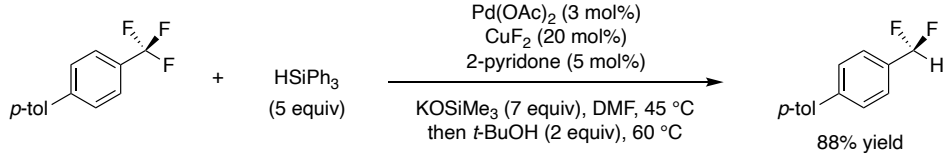

Figure 1-10. 2016 report by Lalic for the catalytic activation of trifluoromethylarenes for mono-selective hydrodefluorination.

In 2021, Zhang reported the ability of a photo-excited palladium complex to reduce electron deficient trifluoromethylarenes through a SET process and ultimately effect defluoroarylation using aryl boronic acids (Figure 1-11).[58] After reduction and mesolytic cleavage of the trifluoromethylarene, generation of a F–Pd^{II}–CF_2Ar complex is reminiscent of a formal oxidative addition process which then undergoes transmetallation with an aryl boronic acid followed by reductive elimination to generate the net defluoroarylation product. A low amount of benzyl radical homocoupling occurs due to the similar reduction potentials of the substrates and products in this SET process (E_{red} = –2.68 V vs Fc^+/Fc for both substrate and product in Figure 1-11). The authors found that both the trifluoromethylarene's redox potential and substituent identity were critical to the efficiency of the reaction.

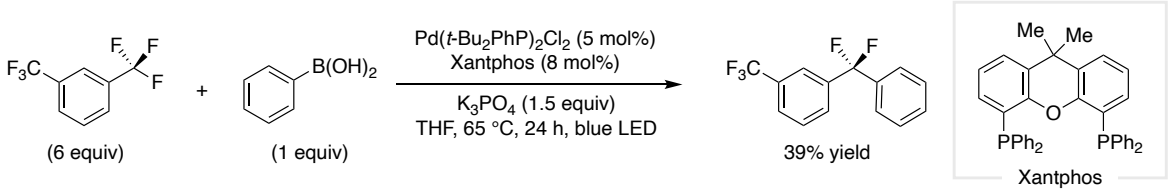

Figure 1-11. Zhang 2021 report of trifluoromethylarene defluoroarylation via excited-state Pd-catalyzed SET reduction

Zhang's discovery of a visible light induced pathway for palladium complexes to engage in the SET reduction of trifluoromethylarenes is an exciting development with much promise for future applications.

1.5.4 Photoredox-Catalyzed Defluorofunctionalization of Trifluoromethylarenes

The emergence of modern photoredox catalysis a little over a decade ago has opened new synthetic pathways to enable highly desirable transformations. Use of a photoredox catalyst with an appropriate reduction potential has allowed for the selective reduction of trifluoromethylarenes. König was the first to exploit this mode of activation in 2017 to enable a mono-selective defluorinative alkylation through a Giese-type addition into *N*-phenylacrylamides (Figure 1-12).[59] Reduction of the photoexcited iridium(III) complex generates a highly reducing iridium(II) species (E_{red} = –2.19 V vs SCE) that can directly reduce a trifluoromethylarene via single electron transfer (E_{red} = –1.91 V vs SCE for 4-trifluromethylbenzonitrile). Importantly, tetramethylpiperidine (TMP) and pinacolborane (HBpin) form an electrophilic cationic complex that assists C–F cleavage.

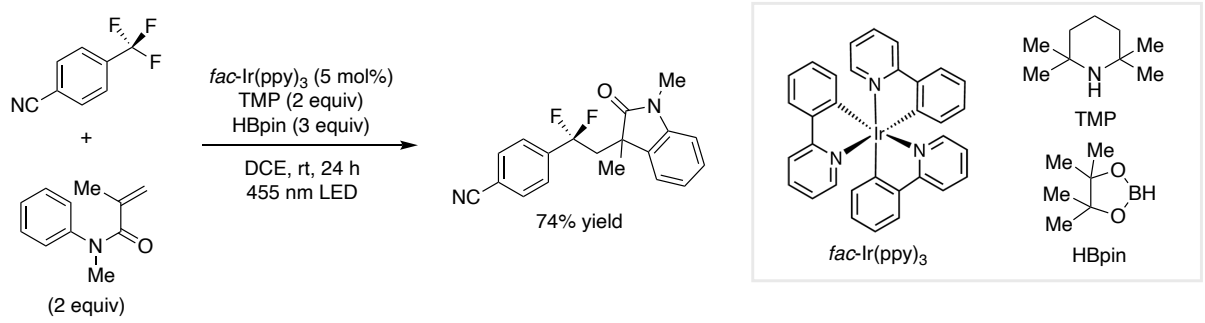

Figure 1-12. König 2017 report of the photoredox-catalyzed, Lewis acid assisted mono-selective defluoroalkylation of trifluoromethylarenes.

In a significant step forward, the photoredox-catalyzed defluoroalkylation was extended to unactivated alkene coupling partners with a report by Jui in 2018 (Figure 1-13).[60] Critical to this transformation were the inclusion of cyclohexanethiol as a hydrogen atom transfer (HAT) catalyst and sodium formate to regenerate both the photocatalyst and thiol catalyst through SET and HAT, respectively. Additionally, this protocol uses the organic photoredox catalyst, *N*-

phenylphenothiazine (PTH, E_{red} = –2.10 V vs SCE), which has advantages in regards to sustainability and toxicity concerns as it is an organic compound.

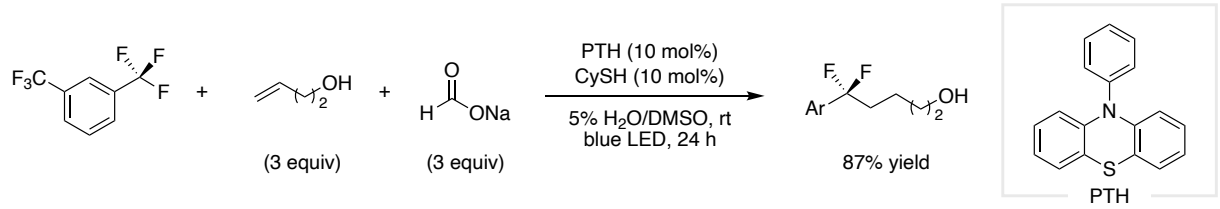

Figure 1-13. Jui 2018 report of the photoredox-catalyzed mono-selective defluoroalkylation of trifluoromethylarenes with unactivated alkenes.

The Jui Group further expanded their defluoroalkylation method in 2019 with a report extending the scope to electron-neutral trifluoromethylarene substrates (Figure 1-14).[61] Their photocatalyst investigations led to the key insight that conversion to product was closely related to excited state lifetimes rather than reduction potentials. Thus, they identified Miyake's phenoxazine photocatalyst[62] (Miyake PC, E_{red} = –1.70 V vs SCE) as the optimal photocatalyst with an excited state lifetime of 480 μs (compared to the excited state lifetime of 3 ns for PTH). Selective hydrodefluorination of unactivated trifluoromethylarenes was also shown by omission of both the alkene coupling partner and the thiophenol, along with slight modifications to the reaction conditions, with selectivity for the desired hydrodefluorination product to the overreduction product ($ArCF_2H$:$ArCFH_2$) ranging from >99:1 to 3:1.

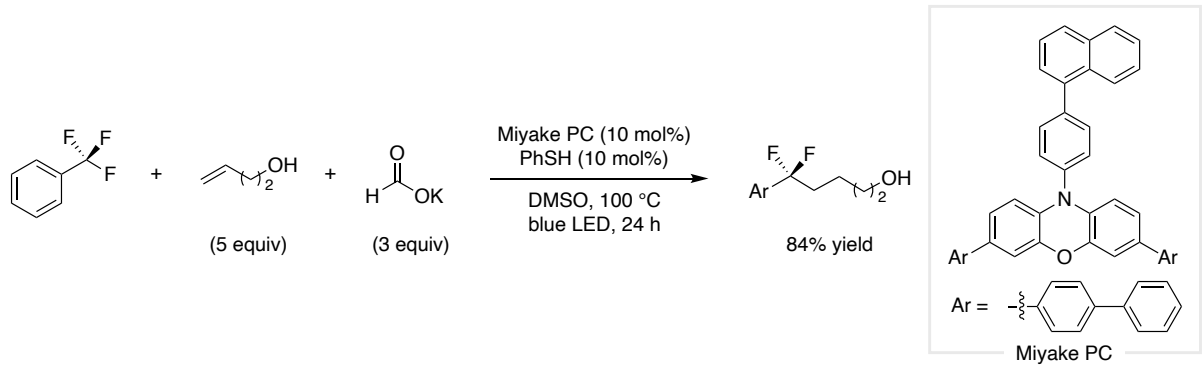

Figure 1-14. Jui 2019 report of defluoroalkylation and hydrodefluorination on unactivated trifluoromethylarenes.

In 2020, Gouverneur reported the use of organic photocatalyst 4-DPA-IPN (E_{red} = –1.52 V vs SCE) to catalyze the hydrodefluorination of electron-deficient trifluoromethylarenes with selectivity for the desired hydrodefluorination product to the overreduction product ($ArCF_2H$:$ArCFH_2$) ranging from >20:1 to 3:1 (Figure 1-15).[63] Importantly, the 4-hydroxythiophenol reduces the excited photocatalyst and provides the hydrogen atom to generate the final product.

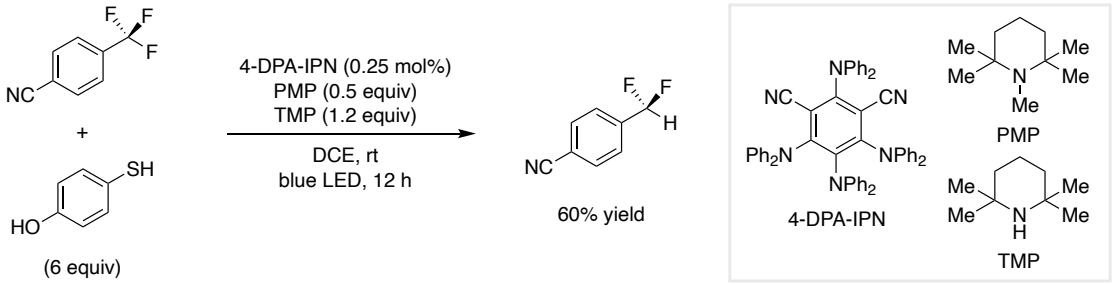

Figure 1-15. Gouverneur 2020 report of the mono-selective hydrodefluorination of electron-deficient trifluoromethylarenes.

Since König's first report in 2017, photoredox catalysis has emerged as the premier strategy to selectively reduce trifluoromethylarenes for C–F functionalization. Important insight and development of photocatalyst structure has revealed both reducing power and excited state lifetime are key factors enabling successful and selective C–F transformations of a broad scope of trifluoromethylarenes. The major limitation of this strategy is the limited scope of coupling partners amenable to the reaction mechanism using photoredox catalysis, with only hydroalkyation (via radical addition into alkenes) and hydrodefluorination (via direct hydrogen atom transfer) reported.

1.6 Conclusion

This chapter provided an overview of the importance of benzylic fluorination for drug discovery and a background on methods to access the difluoro- and trifluoromethyl aryl motif.

Particularly, Section 1.5 provided a thorough overview of methods to selectively substitute a single C–F bond of an aryl trifluoromethyl group, a relatively challenging transformation with limited reports to date. The following chapter, Chapter 2, will discuss the discovery and development of Lewis base activation of organosilanes to promote C–C coupling, beginning with the defluoroallylation reaction reported by the Bandar Group.[64]

REFERENCES

[1] Hagmann, W. K. The Many Roles for Fluorine in Medicinal Chemistry. *J. Med. Chem.* **2008**, *51*, 4359−4369.

[2] Wang, J.; Sánchez-Roselló, M.; Aceña, J. L.; Pozo, C. d.; Sorochinsky, A. E.; Fustero, S.; Soloshonok, V. A.; Liu, H. Fluorine in the Pharmaceutical Industry: Fluorine-Containing Drugs Introduced to the Market in the Last Decade (2001–2011). *Chem. Rev.* **2013**, *114*, 2432–2506.

[3] Gillis, E. P.; Eastman, K. J.; Hill, M. D.; Donnelly, D. J.; Meanwell, N. A. Applications of Fluorine in Medicinal Chemistry. *J. Med. Chem.* **2015**, *58*, 8315−8359.

[4] Zhou, Y.; Wang, J.; Gu, Z.; Wang, S.; Zhu, W.; Aceña, J. L.; Soloshonok, V. A.; Izawa, K.; Liu, H. Next Generation of Fluorine-Containing Pharmaceuticals, Compounds Currently in Phase II−III Clinical Trials of Major Pharmaceutical Companies: New Structural Trends and Therapeutic Areas. *Chem. Rev.* **2016**, *116*, 422−518.

[5] Meanwell, N, A. Fluorine and Fluorinated Motifs in the Design and Application of Bioisosteres for Drug Design. *J. Med. Chem.* **2018**, *61*, 5822–5880.

[6] Wiberg, K. B.; Bailey, W. F.; Lambert, K. M. Unrecognized Intramolecular and Intermolecular Attractive Interactions between Fluorine-Containing Motifs and Ether, Carbonyl, and Amino Moieties. *J. Org. Chem.* **2019**, *84*, 5783–5789.

[7] Johnson, B. M.; Shu, Y.-Z.; Zhuo, X.; Meanwell. N. A. Metabolic and Pharmaceutical Aspects of Fluorinated Compounds. *J. Med. Chem.* **2020**, *63*, 6315–6386.

[8] Inoue, M.; Sumii, Y.; Shibata, N. Contribution of Organofluorine Compounds to Pharmaceuticals. *ACS Omega*, **2020**, *5*, 10633–10640.

[9] Bégué, J.-P.; Bonnet-Delpon, D. *Bioorganic and Medicinal Chemistry of Fluorine*; John Wiley & Sons: Hoboken, N.J., 2008.

[10] Liang, T.; Neumann, C. N.; Ritter, T. Introduction of fluorine and fluorine-containing functional groups. *Angew. Chem., Int. Ed.* **2013**, *52*, 8214−8264.

[11] Ahrens, T.; Kohlmann, J.; Ahrens, M.; Braun, T. Functionalization of fluorinated molecules by transition-metal-mediated C−F bond activation to access fluorinated building blocks. *Chem. Rev.* **2015**, *115*, 931−972.

[12] Caron, S. Where Does the Fluorine Come From? A Review on the Challenges Associated with the Synthesis of Organofluorine Compounds. *Org. Process Res. Dev.* **2020**, *24*, 470–480.

[13] Luo, Y. R. Comprehensive Handbook of Chemical Bond Energies; CRC Press: Boca Raton, FL, 2007.

[14] O'Hagan, D. Understanding organofluorine chemistry. An introduction to the C–F bond. *Chem. Soc. Rev.* **2008**, *37*, 308–319.

[15] Nam, P.-C.; Nguyen, M. T.; Chandra, A. K. The C–H and α(C–X) Bond Dissociation Enthalpies of Toluene, C6H5–CH2X (X = F, Cl), and Their Substituted Derivatives: A DFT Study. *J. Phys. Chem. A* **2005**, *109*, 10342–10347.

[16] Park, B. K.; Kitteringham, N. R.; O'Neill, P. M. Metabolism of Fluorine-Containing Drugs. *Annu. Rev. Pharmacol. Toxicol.* **2001**, *41*, 443–470.

[17] McGinnity, D.F.; Grime, K. ADME Optimization in Drug Discovery. In *Comprehensive Medicinal Chemistry III*; Elsevier Ltd., 2017; pp 34–44.

[18] Tria, G. S.; Abrams, T.; Baird, J.; Burks, H. E.; Firestone, B.; Gaither, L. A.; Hamann, L. G.; He, G.; Kirby, C. A.; Kim, S.; Lombardo, F.; Maccho, K. J.; McDonnell, D. P.; Mishina, Y.; Norris, J. D.; Nunez, J.; Springer, C.; Sun, Y.; Thomsen, N. M.; Wang, C.; Wang, J.; Yu, B.; Tiong-Yip, C.-L.; Peukert, S. Discovery of LSZ102, a Potent, Orally Bioavailable Selective Estrogen Receptor Degrader (SERD) for the Treatment of Estrogen Receptor Positive Breast Cancer. *J. Med. Chem.* **2018**, *61*, 2837–2864.

[19] Erickson, J. A.; McLoughlin, J. I. Hydrogen Bond Donor Properties of the Difluoromethyl Group. *J. Org. Chem.* **1995**, *60*, 1626–1631.

[20] Sessler, C. D.; Rahm, M.; Becker, S.; Goldberg, J. M.; Wang, F.; Lippard, S. J. CF_2H, a Hydrogen Bond Donor. *J. Am. Chem. Soc.* **2017**, *139*, 9325–9332.

[21] Zafrani, Y.; Sod-Moriah, G.; Yeffet, D.; Berliner, A.; Amir, D.; Marciano, D.; Elias, S.; Katalan, S.; Ashkenazi, N.; Madmon, M.; Gershonov, E.; Saphier, S. CF_2H, a Functional Group-Dependant Hydrogen-Bond Donor: Is It a More or Less Lipophilic Bioisostere of OH, SH, and CH_3? *J. Med. Chem.* **2019**, *62*, 5628–5637.

[22] Tomashenko, O. A.; Grushin, V. V. Aromatic Trifluoromethylation with Metal Complexes. *Chem. Rev.* **2011**, *111*, 4475–4521.

[23] Schlosser, M. CF_3-Bearing Aromatic and Heteroaromatic Building Blocks. *Angew. Chem. Int. Ed.* **2006**, *45*, 5432–5446.

[24] Hansen, K. B.; Balsells, J.; Dreher, S.; Hsiao, Y.; Kubryk, M.; Palucki, M.; Rivera, N.; Steinhuebel, D.; Armstrong, J. D.; Askin, D.; Grabowski, E. J. J. First Generation Process for the Preparation of the DPP-IV Inhibitor Sitagliptin. *Org. Process. Res. Dev.* **2005**, *9*, 634–639.

[25] Dai, J.-J.; Fang, C.; Xiao, B.; Yi, J.; Xu, J.; Liu, Z.-J.; Lu, X.; Liu, L.; Fu, Y. Copper-promoted Sandmeyer Trifluoromethylation Reaction. *J. Am. Chem. Soc.* **2013**, *135*, 8436–8439.

[26] Senecal, T. D.; Parsons, A. T.; Buchwald, S. L. Room Temperature Aryl Trifluoromethylation via Copper-Mediated Oxidative Cross-Coupling. *J. Org. Chem.* **2011**, *76*, 1174–1176.

[27] Oishi, H.; Kondo, H.; Amii, H. Aromatic trifluoromethylation catalytic in copper. *Chem. Commun.* **2009**, 1909–1911.

[28] Cho, E. J.; Senecal, T. D.; Kinzel, T.; Zhang, Y.; Watson, D.A.; Buchwald, S. L. The Palladium-Catalyzed Trifluoromethylation of Aryl Chlorides. *Science*, **2010**, *328*, 1679–1681.

[29] Nagib, D. A.; MacMillian, D. W. C Trifluoromethylation of arenes and heteroarenes by means of photoredox catalysis. *Nature*, **2011**, *480*, 224–228.

[30] Le, C.; Chen, T. Q.; Liang, T.; Zhang, P.; MacMillian, D. W. C. A radical approach to the copper oxidative addition problem: Trifluoromethylation of bromoarenes. *Science*, **2018**, *360*, 1010–1014.

[31] Shreeve, J. M.; Singh, R. P. Recent Advances in Nucleophilic Fluorination Reactions of Organic Compounds Using Deoxofluor and DAST. *Synthesis* **2002**, *17*, 2561–2578.

[32] Rong, J.; Ni, C.; Hu, J. Metal-Catalyzed Direct Difluoromethylation Reactions. *Asian J. Org. Chem.* **2017**, *6*, 139–152.

[33] Fujikawa, K.; Fujioka, Y.; Kobayashi, A.; Amii, H. A New Method for Aromatic Difluoromethylation: Copper-Catalyzed Cross-Coupling and Decarboxylation Sequence from Aryl Iodides. *Org. Lett.* **2011**, *13*, 5560–5563.

[34] Feng, Z.; Min, Q.-Q.; Xiao, Y.-L.; Zhang, B.; Zhang, X. Palladium-Catalyzed Difluoroalkylation of Aryl Boronic Acids: A New Method for the Synthesis of Aryldifluoromethylated Phosphonates and Carboxylic Acid Derivatives. *Angew. Chem. Int. Ed.* **2014**, *53,* 1669–1673.

[35] Guo, C.; Wang, R.-W.; Qing, F.-L. Palladium catalyzed direct α-arylation of α,α-difluoroketones with aryl bromides. *J. Fluorine Chem.* **2012**, *143*, 135–142.

[36] Ge, S.; Chaładaj, W.; Hartwig, J. F. Pd-Catalyzed α-Arylation of α,α-Difluoroketones with Aryl Bromides and Chlorides. A Route to Difluoromethylarenes. *J. Am. Chem. Soc.* **2014**, *136*, 4149–4152.

[37] Xia, J.-B.; Zhu, C.; Chen. C Visible Light-Promoted Metal-Free C–H Activation: Diarylketone-Catalyzed Selective Benzylic Mono- and Difluorination. *J. Am. Chem. Soc.* **2013**, *135*, 17494–17500.

[38] Fijuwara, Y.; Dixon, J. A.; Rodriguez, R. A.; Baxter, R. D.; Dixon, D. D.; Collins, M. R.; Blackmond, D. G.; Baran, P. S. "A New Reagent for Direct Difluoromethylation" *J. Am. Chem. Soc.* **2012***, 134*, 1494–1497.

[39] Sakamoto, R.; Kashiwagi, H.; Maruoka, K. "The Direct C–H Difluoromethylation of Heteroarenes Based on the Photolysis of Hypervalent Iodine(III) Reagents That Contain Difluoroacetoxy Ligands" *Org. Lett.* **2017**, *19*, 5126–5129.

[40] Zhu, S.-Q.; Liu, Y.-I.; Li, H.; Xu, X.-H.; Qing, F.-L. "Direct and Regioselective C–H Oxidative Difluoromethylation of Heteroarenes" *J. Am. Chem. Soc.* **2018**, *140*, 11613–11617.

[41] Saboureau, C.; Troupel, M.; Sibille, S.; Périchon, J. Electroreductive Coupling of Trifluoromethylarenes with Electrophiles: Synthetic Applications. *J. Chem. Soc., Chem. Commun.* **1989**, 1138−1139.

[42] Clavel, P.; Léger-Lambert, M.-P.; Biran, C.; Serein-Spirau, F.; Bordeau, M.; Roques, N.; Marzouk, H. Selective Electrosynthesis of (Trimethylsilyldifluoro)methylbenzene, a $PhCF_2^-$ Precursor; Conditions for a Molar Scale Preparation without HMPA. *Synthesis* **1999**, *5*, 829−834.

[43] Belie, C.; Boehmer, J.; Clarke, E.; Dalençon, A.; Dallimore, J.; Diggelmann, M.; Qacemi, M. E.; Ingram, K.; Knee, A.; Kozakiewicz, T.; Longstaff, A.; McCormack, D.; McLachlan, M.; Mulholland, N.; Plant, A.; Williams, J. An Improved Process for the Preparation of an α,α-Difluorosulfonylisoxazoline Herbicide. *Chimia*, **2014**, *68*, 442–445.

[44] Munoz, S. B.; Ni, C.; Zhang, Z.; Wang, F.; Shao, N.; Mathew, T.; Olah, G. A.; Prakash, G. K. S. Selective Late-Stage Hydrodefluorination of Trifluoromethylarenes: A Facile Access to Difluoromethylarenes. *Eur. J. Org. Chem.* **2017**, 2322–2326.

[45] Saito, K.; Umi, T.; Yamada, T.; Suga, T.; Akiyama, T. Niobium(V)-catalyzed defluorinative triallylation of α,α,α-trifluorotoluene derivatives by triple C−F bond activation. *Org. Biomol. Chem.* **2017**, *15*, 1767−1770.

[46] Scott, V. J.; Çelenligil-Çetin, R.; Ozerov, O. V. Room-Temperature Catalytic Hydrodefluorination of C(sp^3)−F Bonds. *J. Am. Chem. Soc.* **2005**, *127*, 2852−2853.

[47] Gu, W.; Haneline, M. R.; Douvris, C.; Ozerov, O. V. Carbon−Carbon Coupling of C(sp^3)−F Bonds Using Alumenium Catalysis. *J. Am. Chem. Soc.* **2009**, *131*, 11203−11212.

[48] Henne, A. L.; Newman, M. S. The Action of Aluminum Chloride on Fluorinated Compounds. *J. Am. Chem. Soc.* **1938**, *60*, 1697−1698.

[49] Zhu, J.; Pérez, M.; Caputo, C. B.; Stephan, D. W. Use of Trifluoromethyl Groups for Catalytic Benzylation and Alkylation with Subsequent Hydrodefluorination. *Angew. Chem. Int. Ed.* **2016**, *55*, 1417−1421.

[50] Stahl, T.; Klare, H. F. T.; Oestreich, M. Main-Group Lewis Acids for C–F Bond Activation. *ACS Catal.* **2013**, *3*, 1578–1587.

[51] Shen, Q.; Huang, Y.-G.; Liu, C.; Xiao, J.-C.; Chen, Q.-Y.; Guo, Y. Review of recent advances in C−F bond activation of aliphatic fluorides. *J. Fluorine Chem.* **2015**, *179*, 14−22

[52] Yoshida, S.; Shinomori, K.; Kim, Y.; Hosoya, T. Single C–F Bond Cleavage of Trifluoromethylarenes with an *ortho*-Silyl Group. *Angew. Chem. Int. Ed.* **2016**, *55*, 10406–10409.

[53] Idogawa, R.; Kim, Y.; Shinomori, K.; Hosoya, T.; Yoshida, S. Single C–F Transformations of *o*-Hydrosilyl Benzotrifluorides with Trityl Compounds as All-in-One Reagents. *Org. Lett.* **2020**, *22*, 9292–9297.

[54] Kim, Y.; Kanemoto, K.; Shinomori, K.; Hosoya, T.; Yoshida, S. Functionalization of a Single C–F Bond of Trifluoromethylarenes Assisted by an *ortho*-Silyl Group Using a Trityl-Based All-in-One Reagent with Ytterbium Triflate Catalyst. *Chem. Eur. J.* **2020**, *26*, 6136–6140.

[55] Idogawa, R.; Kobayashi, A.; Kim, Y.; Shimomori, K.; Hosoya, T.; Yoshida, S. Hydride reduction of *o*-(fluorosilyl)benzodifluorides for subsequent C–F transformations. *Chem. Commun.*, **2022**, *58*, 3521–3524.

[56] Mandal, D.; Gupta, R.; Jaiswal, A. K.; Young, R. D. Frustrated Lewis-Pair-Mediated Selective Single Fluoride Substitution in Trifluoromethyl Groups. *J. Am. Chem. Soc.* **2020**, *142*, 2572–2578.

[57] Dang, H.; Whittaker, A. M.; Lalic, G. Catalytic activation of a single C–F bond in trifluoromethylarenes. *Chem. Sci.* **2016**, *7*, 505–509.

[58] Luo, Y.-C.; Tong, F.-F.; Zhang. Y.; He, C.-Y.; Zhang, X. Visible-Light-Induced Palladium-Catalyzed Selective Defluoroarylation of Trifluoromethylarenes with Arylboronic Acids. *J. Am. Chem. Soc.* **2021**, *143*, 139741–13979.

[59] Chen, K.; Berg, N.; Gschwind, R.; König, B. Selective Single C(sp^3)–F Bond Cleavage in Trifluoromethylarenes: Merging Visible-Light Catalysis with Lewis Acid Activation. *J. Am. Chem. Soc.* **2017***, 139*, 18444–18447.

[60] Wang, H.; Jui, N. T. Catalytic Defluoroalkylation of Trifluoromethylaromatics with Unactivated Alkenes. *J. Am. Chem. Soc.* **2018**, *140*, 163–166.

[61] Vogt, D. B.; Seath, C. P.; Wang, H.; Jui, N. T. Selective C–F Functionalization of Unactivated Trifluoromethylarenes. *J. Am. Chem. Soc.* **2019**, *141*, 13203–13211.

[62] Pearson, R. M.; Lim, C.-H.; McCarthy, B. G.; Musgrave, C. B.; Miyake, G. M. Organocatalyzed Atom Transfer Radical Polymerization Using N-Aryl Phenoxazines as Photoredox Catalysts. *J. Am. Chem. Soc.* **2016**, *138*, 11399−11407.

[63] Sap, J. B. I.; Straathof, N. J. W.; Knauber, T.; Meyer, C. F.; Médebielle, M.; Buglioni, L.; Genicot, C.; Trabanco, A. A.; Noël, T.; Ende, C. W. a.; Gouverneur, V. Organophotoredox Hydrodefluorination of Trifluoromethylarenes with Translational Applicability to Drug Discovery. *J. Am. Chem. Soc.* **2020**, *142*, 9181–9187.

[64] Luo, C.; Bandar, J. S. Selective Defluoroallylation of Trifluoromethylarenes. *J. Am. Chem. Soc.* **2019**, *141*, 14120–14125.

CHAPTER TWO

LEWIS BASE ACTIVATION OF ORGANOSILANES TO PROMOTE TRIFLUOROMETHYLARENE C–F CROSS COUPLING

2.1 Chapter Overview

The previous chapter set the stage for the motivation and the current state of the field for the mono-selective defluorofunctionalization of trifluoromethylarenes. This chapter will provide an overview of the Bandar Group's initial contribution to the field of selective trifluoromethylarene C–F functionalization with a 2019 report, pioneered by the group post-doc Dr. Chaosheng Luo, utilizing a new mechanistic approach and will provide the immediate precedent for my work described in Chapters 3 and 4.

2.2 Discovery of a Trifluoromethylarene Defluoroallylation Reaction

Building upon the use of organic superbase catalysts[1] to promote unique reactivity, the Bandar Group began exploring new deprotonative functionalization reactions in 2018. The deprotonation of difluoromethylarenes is a challenging process due to the facile α-fluoride elimination that can occur upon deprotonation, especially when using basic metal salts (lithium, sodium, potassium alkoxides and amides) with metal cations that generate stable alkali fluoride salts (e.g. LiF, NaF, KF), although there have been a few reports of this strategy being successfully applied at cryogenic temperatures[2] or with designer Lewis acids[3] in recent years. Organic superbases possess unique properties when compared to basic metal salts, including a large size and a neutral structure combined with extremely high basicity, that allow for new reactivity.[1] The Bandar Group hypothesized that the unique properties of organic superbases could allow for the

deprotonation of difluoromethylarenes and subsequent stabilization of the reactive difluorobenzylic anion to allow for nucleophilic addition to electrophiles.

First attempts by Dr. Chaosheng Luo, a Bandar Group post-doc, to functionalize difluoromethylarenes *via* deprotonation with an organic superbase resulted in an unexpected C–F substitution reaction. Subjecting 1-(difluoromethyl)-3-nitrobenzene (**2-1**) to catalytic P_4-t-Bu in the presence of allyltrimethylsilane resulted in a defluoroallylation product (**2-2**) in modest yield without any observed product corresponding to deprotonation of the benzylic C–H bond (**2-3**) (Figure 2-1). Hypothesizing that a deprotonation pathway was not occurring, a trifluoromethylarene, 1,3-bis(trifluoromethyl)benzene (**2-4**) was subjected to similar reaction conditions and a similar defluoroallylation product (**2-5**) was observed, and after a brief optimization, cesium fluoride was found to promote this reaction efficiently (Figure 2-2). This transformation is the first report of a Lewis base activated organosilane engaging trifluoromethylarenes in a defluorinative C–C bond-forming process and was disclosed in 2019.[4]

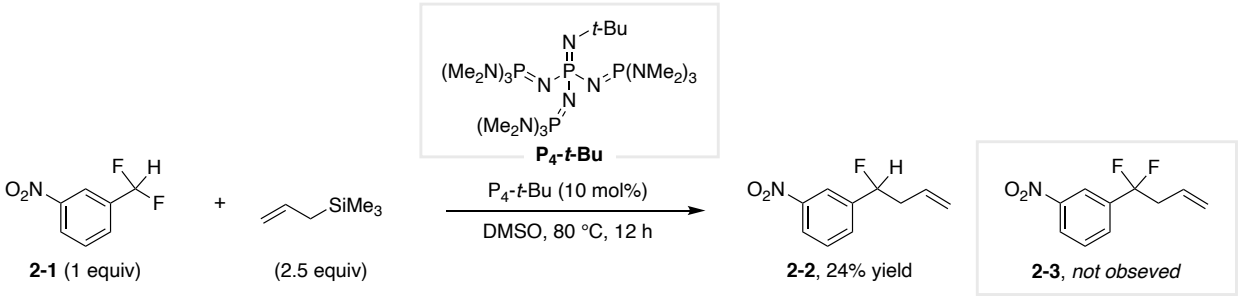

Figure 2-1. Unexpected difluoromethylarene C–F allylation reaction by the Bandar Group.

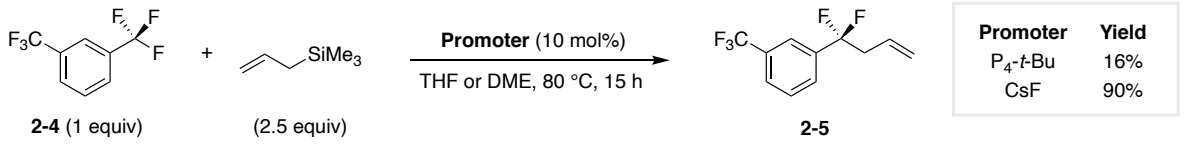

Figure 2-2. Discovery of a mono-selective defluoroallylation reaction by the Bandar Group.

2.3 Defluoroallylation Reaction Mechanism

Several experiments were then conducted to probe the reaction mechanism. Addition of the radical trap 2,2,6,6-Tetramethylpiperidine-1-oxyl free radical (TEMPO) to the reaction resulted in the formation of allylated TEMPO (**2-6**) in 23% yield, providing support for the intermediacy of an allyl radical under the reaction conditions (Figure 2-3). Conducting the reaction in strict absence of light resulted in no decrease of yield for the model reaction. A key insight gained from examining the scope of amenable arenes in that reactivity seems to correlate with reduction potential, where electron deficient difluoro- and trifluoromethylarenes react under the standard reaction conditions, but electron neutral substrates, such as benzotrifluoride, result in no reactivity. The proposed mechanism is shown at the bottom of Figure 2-3: (1) cesium fluoride activates the allyltrimethysilane, generating a silicate intermediate that (2) reduces the trifluoromethylarene via single electron transfer, generating a pair of radical ions that (3) fragment, generating trimethylsilylfluoride by-product and an equivalent of cesium fluoride to propagate the cycle, then (4) the resulting radicals couple to generate the defluoroallylation product. It is important to note that a radical chain process may be operative that combines the individual steps of this cycle. Furthermore, the reaction generates fluoride as a byproduct, which allows the fluoride to be pseudocatalytic and thus explains why only catalytic amounts of fluoride are needed to initiate this reaction. Importantly, the mono-selectivity of the defluoroallylation reaction arises from the change in reduction potential from the starting trifluoromethylarene (**2-4**: E_{red} = –2.67 V vs Fc^+/Fc^0) versus the allylated product (**2-5**: E_{red} = –3.21 V vs Fc^+/Fc^0) once the $ArCF_2$–C bond is formed.[5]

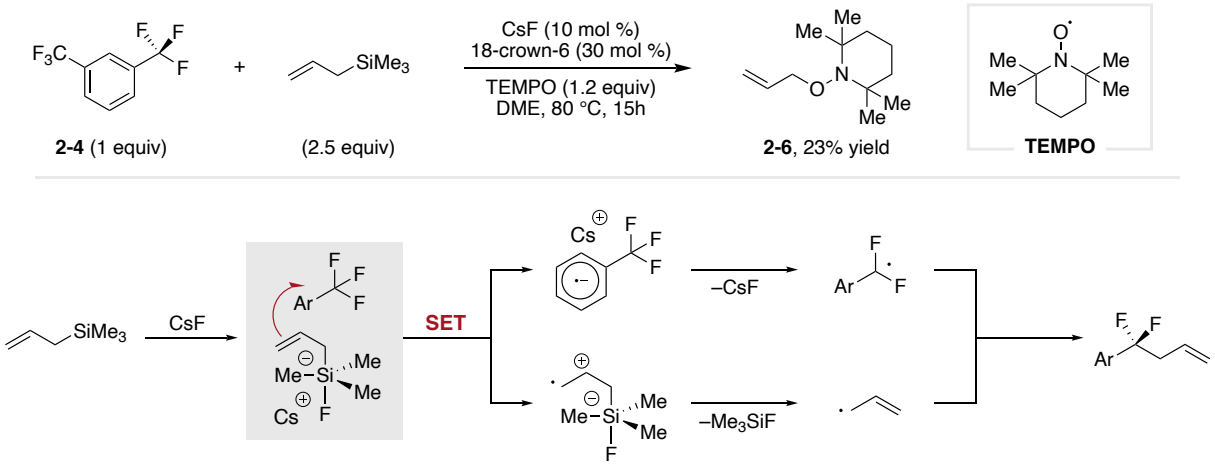

Figure 2-3. (top) Radical trap experiment to probe mechanism of defluoroallylation reaction and (bottom) proposed mechanism for the defluoroallylation reaction.

2.4 Defluoroallylation Reaction Scope and Derivatizations

A representative defluoroallylation scope is shown below in Figure 2-4. A variety of electron-withdrawing substituents sufficiently activate the trifluoromethylarene, including: trifluoromethyl (**2-7**, **2-8**, **2-9**, **2-10**), nitrile (**2-11**, **2-14**), sulfonamide (**2-12**), and phosphonate ester (**2-13**) functional groups in the meta position. Heterocyclic substrates were also amenable to this reactivity including benzo[*c*]-1,2,5-thiadiazole (**2-15**) and 3-trifluoromethylpyridines (**2-16**, **2-17**, **2-18**). Chemoselectivity for the electron-deficient trifluoromethylarene is observed when multiple trifluoromethyl groups of differing electronic properties are present (**2-18**). Some of the allylated products were functionalized, either by alkene reduction with Schwartz's reagent (Cp_2ZrHCl) or debromination with bromine (Br_2), before isolation due to sensitivity to silica gel chromatography, otherwise significant decomposition was observed.

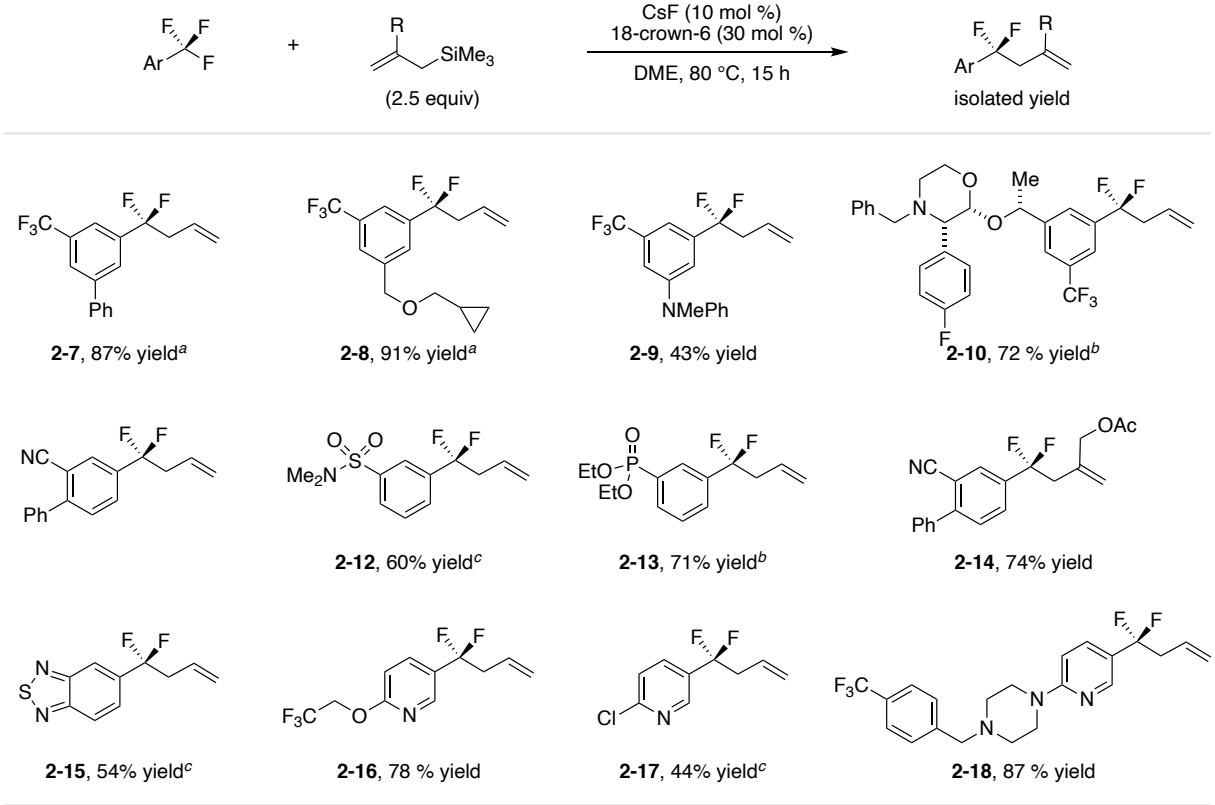

[a] Product isolated as saturated product following alkene reduction using Schwartz's reagent. [b] 48 h reaction time. [c] Product isolated as dibrominated adduct.

Figure 2-4. Representative reaction scope of the defluoroallylation of trifluoromethylarenes.

The allyl group is a valuable synthetic handle and several subsequent functionalizations were demonstrated in a one-pot defluoroallylation/derivatization process (Figure 2-5). Hydroboration/oxidation (**2-19**), hydroiodination (**2-20**), hydroalkylation (**2-21**, **2-24**), ozonolysis and reduction (**2-22**), and Heck coupling (**2-23**) are demonstrated on several substrates highlighting the synthetic utility of the allyl group. Of note is that these difluorobenzylic derivatives possess at least a 2 carbon framework that is a specific consequence of C–C bond formation with the allyl group.

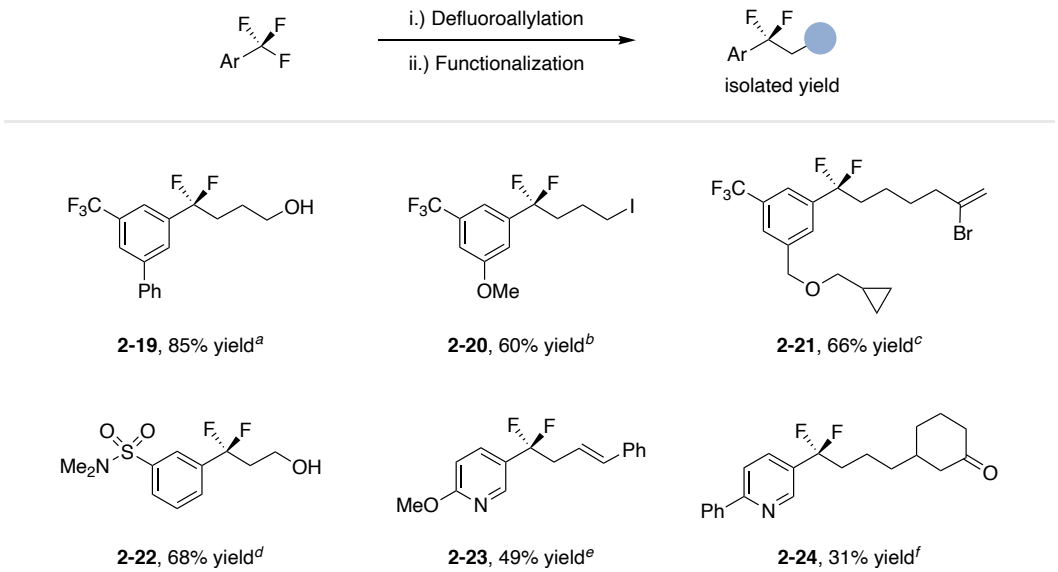

Defluoroallylation reaction conditions: Trifluoromethylarene (1 equiv), allyltrimethylsilane (2.5 equiv), cesium fluoride (10 mol%), 18-crown-6 (30 mol%), DME, 80 °C, 15 h. Functionalization conditions as follows: [a] 9-BBN, THF, rt; H_2O_2, NaOH; [b] (C_5H_5)ZnHCl, DCM, rt; I_2; [c] C_5H_5)ZnHCl, THF, rt; CuCN, 2,3-dibromopropene; [d] O_3, MeOH, -78 °C; NaBH4; [e] PhI, $Pd(OAc)_2$, PPh_3, K_2CO_3, DMF, 100 °C; [f] (C_5H_5)ZnHCl, THF, rt; CuCN, 2-cyclohexen-1-one.

Figure 2-5. One-pot defluoroallylation/functionalization of trifluoromethylarenes.

2.5 Conclusion

The discovery that Lewis base activation of allyltrimethylsilane can promote single electron transfer to trifluoromethylarenes to enable a defluoroallylation reaction has provided a new mechanistic avenue to achieve selective C–F functionalization of trifluoromethylarenes. While this reaction is practical and a novel strategy to achieve trifluoromethylarene C–F functionalization, the major limitation is that it only provides allyl products. My goal was to overcome this limitation and develop a defluorinative transformation to access a broad scope of difluorobenzylic derivatives from a single precursor, and the discovery and development of such a transformation will be the focus of Chapter 3.

REFERENCES

[1] Puleo, T. R.; Sujansky, S. J.; Wright, S. E.; Bandar, J. S. Organic Superbases in Recent Synthetic Methodology Research. *Chem. Eur. J.* **2021**, *27*, 4216–4229.

[2] Santos, L.; Panossian, A.; Donnard, M.; Vors, J.-P.; Pazenok, S.; Bernier, D.; Leroux, F. R. Deprotonative Functionalization of the Difluoromethyl Group. *Org. Lett.* **2020**, *22*, 8741–8745.

[3] Geri, J. B.; Wade Wolfe, M. M.; Szymczak, N. K. The Difluoromethyl Group as a Masked Nucleophile: A Lewis Acid/Base Approach. *J. Am. Chem. Soc.* **2018**, *140*, 9404–9408.

[4] Luo, C.; Bandar, J. S. Selective Defluoroallylation of Trifluoromethylarenes. *J. Am. Chem. Soc.* **2019**, *141*, 14120–14125.

[5] Experimentally calculated reduction potentials courtesy of the Shores group at CSU.

CHAPTER THREE

BASE-PROMOTED REDUCTIVE COUPLING REACTIONS FOR THE DIVERGENT DEFLUOROFUNCTIONALIZATION OF TRIFLUOROMETHYLARENES

3.1 Chapter Overview

This chapter details the discovery, development, and mechanistic investigations of a reductive coupling reaction of trifluoromethylarenes that dramatically expands the scope of difluorobenzylic substructures accessible via C–F functionalization. This transformation is achieved using a catalytic quantity of a Lewis basic salt to activate a commercially available disilane reagent to reduce and couple to a trifluoromethylarene to generate two isolable difluorobenzylic synthons capable of a divergent array of transformations. The work presented in this chapter represents the bulk of my doctoral research.

3.2 Introduction

The α,α-difluorobenzylic substructure ($ArCF_2R$) is becoming increasingly examined in the development of pharmaceuticals and agrochemicals because it imparts the beneficial effects of benzylic fluorination, such as enhanced bioavailability and metabolic stability, while also possessing a diversifiable R substituent.[1-8] The challenge of exploring this chemical space lies in the lack of general methods to access this substructure in a diversifiable fashion from a single precursor.[9-10] The direct and selective C–F functionalization of trifluoromethylarenes is an ideal route towards this motif due to the wide accessibility of trifluoromethylarenes as either building blocks or in late-stage pharmaceutical settings. Currently, the methods to achieve mono-selective C–F functionalization are generally limited to three specific structural motifs (all methods previously summarized in Chapter 1 and 2): hydrodefluorination, hydroalkylation (via radical

addition to alkenes or allylation), and nucleophilic heteroatom addition. Therefore, there is still a need for a reactivity platform to divergently access a broad scope of α,α-difluorobenzylic substructures.

Three examples of pharmaceutical compounds containing a difluorobenzylic motif that are currently in clinical trials or approved are shown below in Figure 3-1. Abediterol is a dual β_2 adrenergic agonist and muscarinic antagonist in phase II clinical trials for the treatment of asthma and chronic obstructive pulmonary disease (COPD).[5] Glecaprevir is a hepatitis C virus nonstructural protein 3/4A protease inhibitor that was FDA approved in 2017 for the treatment of chronic hepatitis C infection.[7,12] LSZ102 is a selective estrogen receptor degrader currently in phase Ib clinical trial for the treatment of breast cancer.[8] These examples illustrate the structural diversity present in the difluorobenzylic motif.

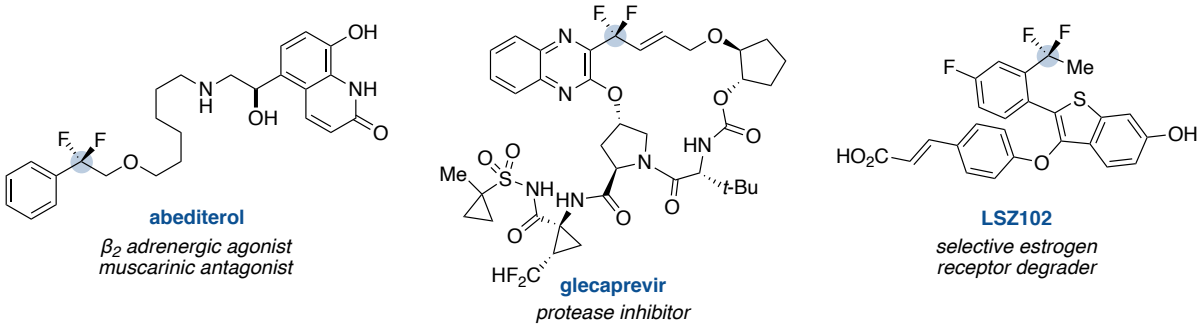

Figure 3-1. Examples of pharmaceutical compounds in clinical trials or FDA approved containing the difluorobenzylic substructure.

The structural diversity of bioactive difluorobenzylic compounds necessitates a singular, divergent method that can access these frameworks in a diversifiable fashion. Accessing difluorobenzylic analogues typically requires the synthesis of a unique precursor for each derivative of interest, either via deoxyfluorination or cross-coupling reactions, which can limit the functional tolerance or diversity through the incompatibility to harsh reaction conditions or the limited availability of coupling partners.[12-19] An overview of the strategies to incorporate a

difluorobenzylic motif was presented in Chapter 1. Despite the impressive synthetic advancements over the past decade, there is still the need for a unified, divergent method to access diverse substructures from a common precursor using a single coupling reagent. Following the discovery of Lewis base activated organosilanes promoting the single electron transfer reduction of trifluoromethylarenes (discussed previously in Chapter 2), we wondered whether other organosilanes could promote new C–F functionalization reactions and began examining other classes of organosilanes.

3.3 Discovery of a Trifluoromethylarene Reductive Coupling Reaction with Formamides

We hypothesized that Lewis base activation of a disilane, a compound containing a Si–Si bond, could generate a highly reactive silyl anion to reduce a trifluoromethylarene and subsequently engage in radical-radical coupling to generate a α,α-difluorobenzylsilane. Silyl anions have multiple modes of reactivity and have been calculated to have extremely high basicity, have been reported to engage in halophilic substitution, and are known to be highly reducing ($E_{red} \lesssim -3.0$ V vs Fc^+/Fc).[23-25]

To test this hypothesis, commercially available tris(trimethylsilyl)silane (TTMSS) was activated with catalytic cesium fluoride in DMF at room temperature (rt) in the presence of the model substrate 1-(benzyloxy)-3,5-bis(trifluoromethyl)benzene (**3-1**). Surprisingly, a C–F reductive coupling product from addition into the carbonyl of the *N*,*N*-dimethylformamide (DMF) solvent, compound **3-2,** was formed in 5% ^{1}H NMR yield referenced to an internal standard (Eq. 1). Notably, there are reports from the early 2000's, primarily by Langlois, that describe isolable silylated trifluoromethyl-formamide adducts and their use as anionic CF_3 synthons and CF_3–C

synthons.[26-33] We therefore anticipated that this unexpected and unusual structure formed from this reductive coupling reaction would be valuable as a difluorobenzylic synthon.

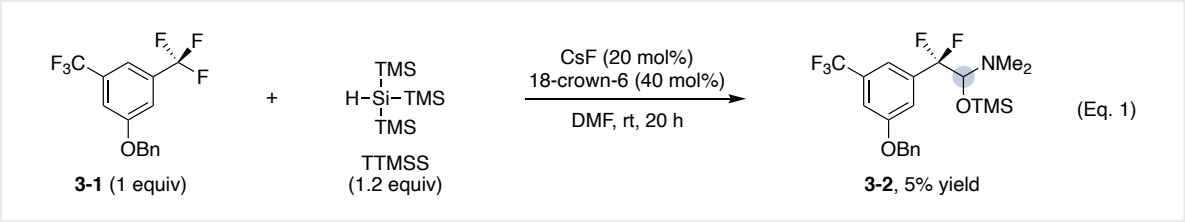

My initial efforts to optimize the model reaction focused on the examination of other Lewis basic catalysts (Figure 3-2). Use of potassium methoxide provides an increased yield of 30% (Entry 2). The organic superbase P_4-*t*-Bu provides a higher yield of 46% (Entry 3). Formate salts were found to be particularly effective at promoting this reaction, with potassium formate providing 42% yield and cesium formate providing 76% yield, the highest of any Lewis base examined (Entries 4 and 5). Cesium acetate and pivalate were less effective, providing 57% and 19% yield, respectively (Entries 6 and 7). The cesium cation is not necessary to achieve high reactivity, as tetrabutylammonium acetate provides a 69% yield (Entry 8). Omitting 18-crown-6 reduces the yield slightly to 63% (Entry 9), although adding more cesium formate can alleviate the reduction in yield (Entries 10 and 11). Generation of a carboxylate anion *in situ*, using either P_4-*t*-Bu and a carboxylic acid or cesium formate and a silylated carboxylate, is also effective in promoting this reaction (Entries 12-16). Use of other commercially available disilanes, hexamethyldisilane or tetrakis(trimethylsilyl)silane, were ineffective at promoting this reaction, providing 0% and 7% yield, respectively (Entries 17 and 18).

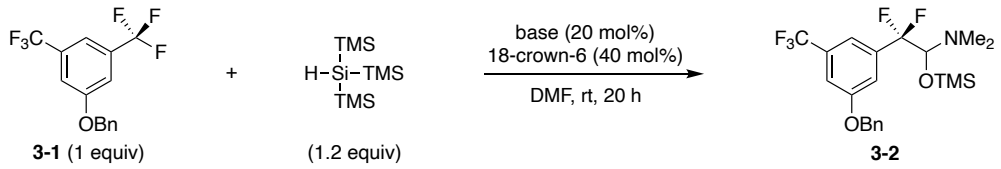

Entry	Base	Variation from standard conditions	Yield
1	CsF	-	5%
2	KOMe	-	30%
3	P_4-*t*-Bu	no 18-crown-6	46%
4	HCO_2K	-	42%
5	HCO_2Cs	-	76%
6	CsOAc	-	57%
7	CsOPiv	-	19%
8	Bu_4NOAc	no 18-crown-6	69%
9	HCO_2Cs	no 18-crown-6	63%
10	HCO_2Cs	50% base, no 18-crown-6	70%
11	HCO_2Cs	100% base, no 18-crown-6	68%
12	P_4-*t*-Bu	no 18-crown-6, 20 mol% HCO_2H	52%
13	P_4-*t*-Bu	no 18-crown-6, 20 mol% $PhCO_2H$	69%
14	P_4-*t*-Bu	no 18-crown-6, 20 mol% *c*-Pr-CO_2H	61%
15	CsF	20 mol% AcOTMS	69%
16	CsF	20 mol% $PhCO_2TMS$	73%
17	HCO_2Cs	Si_2Me_6 instead of TTMSS	0%
18	HCO_2Cs	$Si(TMS)_4$ instead of TTMSS	7%

Figure 3-2. Optimization of Lewis basic catalyst for a trifluoromethylarene reductive coupling reaction.

Unfortunately, my attempts at chromatographic purification of the silylated DMF adduct **3-2**, with either silica or alumina, resulted in complete decomposition. The instability towards purification of the structurally related trifluoromethyl-DMF silylated hemiaminal adduct has been reported by Langois.[26] In an attempt at finding a silica stable formamide adduct, several formamides were examined as a 1:1 solvent mixture with NMP (Figure 3-3). Use of any formamides with a free N–H bond resulted in no reactivity (NR), with full trifluoromethylarene starting material remaining at the end of the reaction (Entries 1 and 3). *N*-aryl substitution provides much decreased reactivity (Entry 2). *N*-formylpiperidine provides a moderate yield of product (59% yield, Entry 4). Use of 4-formylmorpholine provides the highest yield of all coupling partners tested under these conditions, with a 69% ^{1}H NMR yield and a 66% isolated yield *via* silica gel column chromatography at a 1 mmol scale. For reference, use of NMP/DMF (1:1 ratio) provided 68% yield (Entry 8). Use of a cosolvent is necessary when using 4FM, evidenced by a

diminished yield (38% yield, Entry 9) when the reaction is run in only 4FM. We speculate this is due to competing direction reduction of 4FM by the silyl anion intermediate. Alternatively, use of benzotrifluoride ($PhCF_3$) as a cosolvent with 4FM (1:1 ratio) also provides high yields (68%), and for some substrates gives improved yields (*vide infra*). Use of ethylformate as a cosolvent with NMP provides no reactivity (Entry 6).

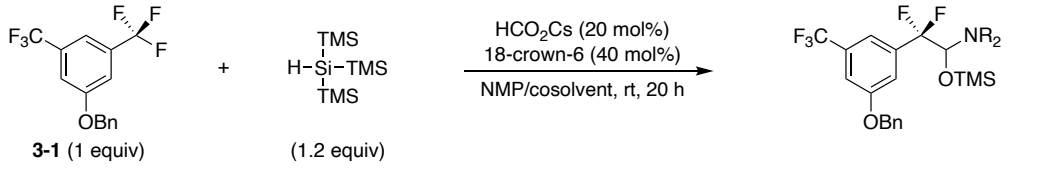

cosolvent:

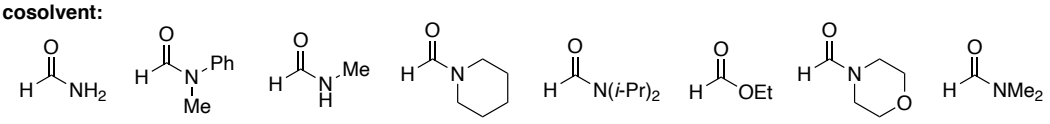

Entry	NMP : Cosolvent (1:1)	Yield[a]
1	Cosolvent = A	NR
2	Cosolvent = B	8%
3	Cosolvent = C	NR
4	Cosolvent = D	59%
5	Cosolvent = E	0%
6	Cosolvent = F	NR
7	Cosolvent = 4FM	69% (66%)
8	Cosolvent = DMF	68%
9	Solvent = 4FM only (no NMP)	38%
10	Solvent = 4FM / $PhCF_3$ (1:1, no NMP)	68%

[a] Yield is ^1H NMR yield referenced to an internal standard. Yield in parenthesis is an isolated yield after silica gel column chromatography. NR = no reaction, 100% substrate remaining.

Figure 3-3. Identification of a high yielding, silica stable formamide coupling partner.

3.4 Trifluoromethylarene Reductive Coupling Scope

After identifying reaction conditions to generate a silica stable silylated hemiaminal, I next examined the scope of trifluoromethylarenes amenable to this reaction. Figure 3-4 shows a series of trifluoromethylarenes that undergo the mono-selective reductive coupling. 1,3-bis(trifluoromethyl)arenes provide good yields, even scaled up to 10 mmol (**3-3**), with a free

phenolic O–H (**3-4**), and with a terminal alkene (**3-5**). Other *meta* electron-withdrawing groups are effective to activate the benzotrifluoride, including sulfonamides (**3-6**) and phosphonate esters (**3-7**). Heterocyclic substrates are also effective, with 2-, 3- and 4-trifluoromethylpyridines providing moderate to good yields (**3-8, 3-9, 3-10, 3-11**). Drug-like substrates also undergo selective C–F substitution, shown with the benzylated aprepitant precursor (**3-12**) and a fluoxetine-pyrimidine derivative (**3-13**). An x-ray crystal structure was obtained for Compound **3-6** to conclusively support the structure of the indicated silylated hemiaminal product (Figure 3-5).

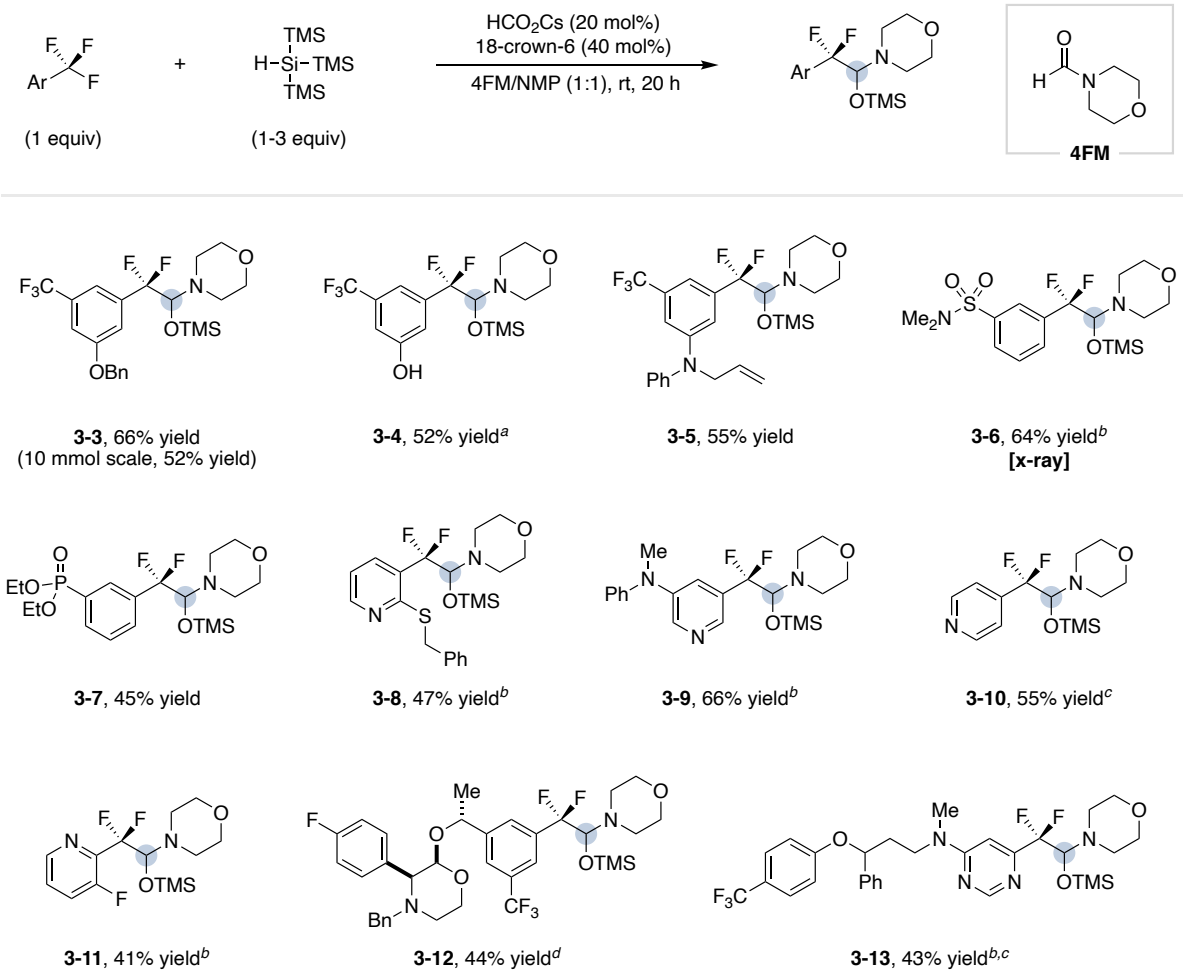

Yields are Isolated yields via silica gel column chromatography. [a] Isolated as a roughtly 2:1 adduct with NEt_3. [b] $PhCF_3$ as colsolvent instead of NMP. [c] Reaction heated to 80 °C. [d] Extra portion of base (20 mol%) and TTMSS (1 equiv) added after 16 h.

Figure 3-4. Trifluoromethylarene reductive coupling substrate scope.

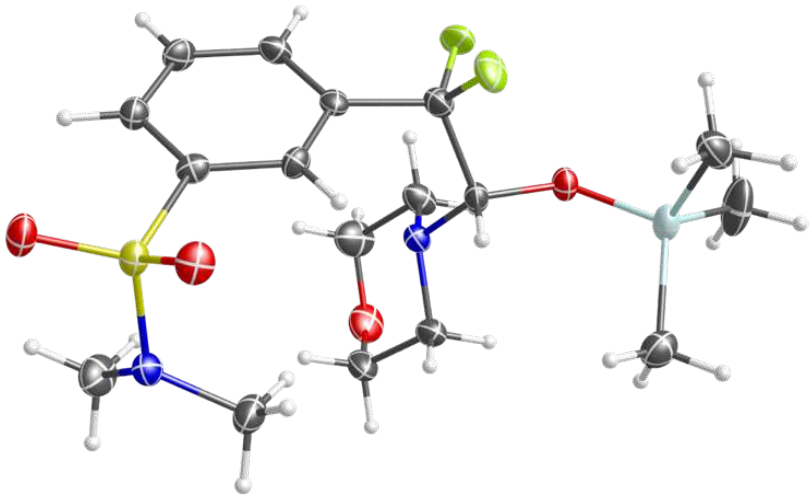

Figure 3-5. X-ray crystal structure of Compound **3-6**. Thermal ellipsoids are at 50% probability. Colors of atoms are as follows: carbon (black), oxygen (red), nitrogen (blue), fluorine (green), sulfur (yellow), silicon (light blue), hydrogen (white).

The value of this transformation lies in the ability to transform these silylated hemiaminal products into desirable and diverse structural motifs. Consideration of the silylated hemiaminal structure predicts that there are two major reactivity modes in equilibrium: the iminium form and the aldehyde form. Previous work by Langlois and others have demonstrated the synthetic utility of these different forms using the structurally similar trifluoromethyl silylated hemiaminal analogue.[26-33] I found that careful choice of reaction conditions can allow for selective access to just one mode of reactivity (Figure 3-6). Reactions that are selective for iminium ions provide efficient access to a diverse array of difluorobenzylic products, including condensation to form the oxime (**3-14**), condensation followed by dehydration to form the nitrile (**3-15**), reduction to access the tertiary amine (**3-16**), oxidation to access the *N*-morpholino amide (**3-17**), Petasis-type reactivity to access allylic amines (**3-18**), and Mannich-type reactivity to access beta-aminoketones (**3-19**). To selectively access the reactivity of an aldehyde, simply subjecting the silylated hemiaminal to catalytic acid in an alcoholic solvent results in quantitative conversion to the hemiacetal, a functional group useful as a masked aldehyde, which can be used without further

purification. From the hemiacetal intermediate many classical aldehyde transformations can be performed, including borohydride reduction to the hydroxymethyl (**3-20**), reductive amination (**3-21**), condensation-oxidation to form a heterocycle (**3-22**), silylation for an isolable hemiacetal (**3-23**), Wittig olefinations (**3-24** and **3-25**), nucleophilic cyanation to form an α-hydroxy nitrile (**3-26**), oxidation to form the carboxylic acid (**3-27**), and nitro-aldol to access 1,2-aminoalcohol derivatives (**3-28**). Additionally, base-induced cleavage of the silylated hemiaminal occurs readily through a Haller-Bauer-type mechanism to generate the valuable difluoromethylarene (**3-29**), and high deuterium incorporation can be achieved using D_2O (**3-30**)—a notable transformation that currently is difficult to achieve with high deuterium incorporation.[34]

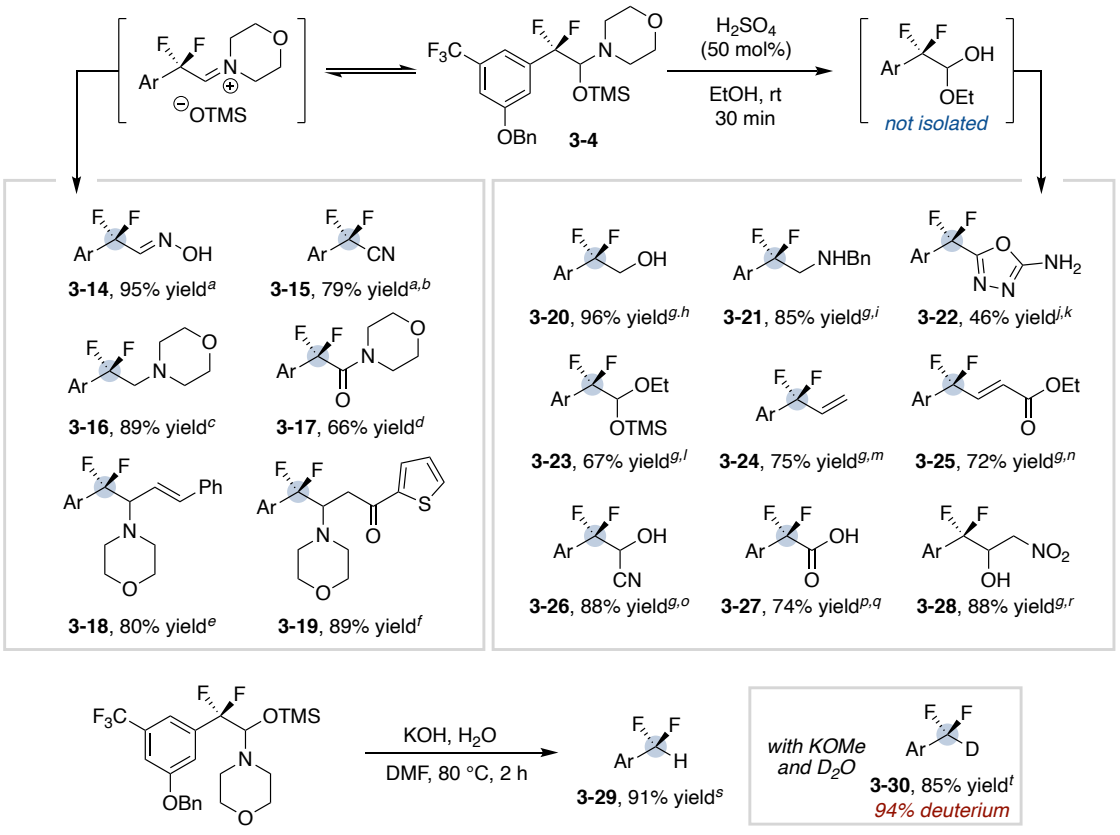

Yields reported are isolated yields starting from the silylated hemiaminal. [a] $NH_2OH{\cdot}HCl$, DMSO, 80 °C; [b] Ac_2O, NEt_3, rt; [c] $NaBH(OAc)_3$, AcOH, DCE, rt; [d] Dess-Martin Periodinane, CH_2Cl_2, rt; [e] $BF_3{\cdot}OEt_2$, styrenylBF_3K, CH_2Cl_2, rt; [f] CsF, 2-acetylthiophene, DME, 50 °C; [g] H_2SO_4, EtOH, rt; [h] then NaBH4, rt; [i] H_2NBn, AcOH, DCE, then $NaBH(OAc)_3$; [j] semicarbazide·HCl, $MeOH/H_2O$; [k] I_2, K_2CO_3, dioxane, 120 °C; [l] TMSCl, NEt_3, CH_2Cl_2, rt; [m] Ph_3PCH_3Br, KO-*t*-Bu, THF, 0 °C; [n] $Ph_3PCCHCO_2Et$, NEt_3, LiBr, THF, rt; [o] ZnI_2, TMSCN, dioxane, 120 °C; [p] H_2SO_4, $DMSO/H_2O$, rt; [q] Dess-Martin Periodinane, CH_2Cl_2, rt; [r] $MeNO_2$, K_2CO_3, THF, 50 °C; [s] KOH, H_2O, DMF, 80 °C; [t] KOMe, D_2O, DMF, 80 °C.

Figure 3-6. The silylated hemiaminal as a platform for trifluoromethylarene C–F diversification.

Further demonstration of the utility of this method is shown by the C–F reductive coupling and subsequent derivatization of complex, drug-like trifluoromethylarenes with only a single purification step (Figure 3-7). We sought to show that this chemistry can work in late-stage settings, hoping to inspire medicinal chemists to utilize this chemistry to for structure activity relationship studies of difluorobenzylic substructures. A bis(trifluoromethyl) analog of aripiprazole could provide the hydrodefluorination (**3-31**) and the hydroxymethylation (**3-32**) products in 59% and 56% yield, respectively. The benzylated aprepitant precursor could provide the hydrodefluorination (**3-33**) and vinylation (**3-34**) products in 43% and 59% yield, respectively. These two examples highlight divergent reactivity as diverse substructures can be readily accessed from a single late-stage precursor. Trifluoromethylated heteroarenes were also effective in this two-step process. A fluoxetine-pyrimidine derivative, bearing two electronically distinct trifluoromethylarenes, was hydroxymethylated (**3-35**) in 95% yield with complete selectivity for the trifluoromethyl group on the electron deficient aromatic ring. A bepotastine-pyridazine derivative was hydrodefluorinated (**3-36**) in 28% yield. A trifluoromethyl quinoline substrate was aminomethylated (**3-37**) in 62% yield. These examples particularly demonstrate the synthetic use of the trifluoromethyl group as an orthogonal synthetic disconnection that can be carried on into the late-stage diversification of complex molecules. Of note, some substrates react better when the reaction solvent is DMF and an aqueous work-up allows for use of the DMF adduct without decomposition from chromatography, which leads to increased yields in this sequenced two-step operation compared to independent preparation and isolation of the hemiaminal intermediate.

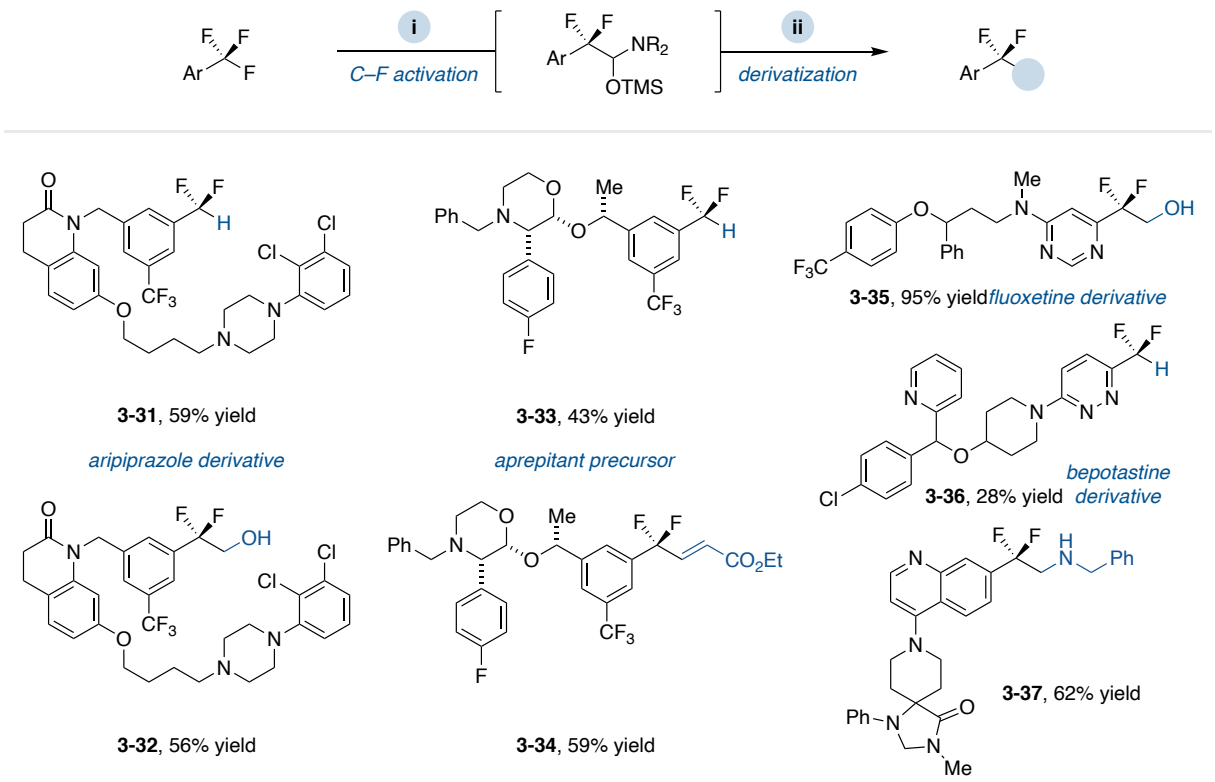

Yields are isolated yields starting from the trifluoromethylarene.

Figure 3-7. One-pot reductive coupling and subsequent derivatization of medicinally relevant trifluoromethylarenes.

3.5 Experiments to Investigate the Reaction Mechanism

Several experiments were carried out to probe the mechanism of this transformation. A key observation was that changing the solvent of the model reaction results in different products: in NMP the major product is the difluorobenzylsilane (**3-38**) and in acetonitrile (MeCN) the major product is the difluoromethylarene (**3-29**) (Figure 3-8, a). Based on these observations, our initial mechanistic hypothesis involves the generation of a benzylsilane intermediate. If a benzylsilane intermediate is formed, then *in situ* desilylation under the basic conditions could generate the difluoromethylarene *via* protonation or the hemiaminal *via* addition to the formamide solvent.[35-37] Subjecting the isolated benzylsilane **3-38** to cesium formate in MeCN and DMF provided the

protodesilylation product **3-29** and the formamide addition adduct **3-2**, respectively, in high yield (Figure 3-8, b). A reaction profile of the reductive coupling was conducted in DMF to provide support for the formation of postulated reaction intermediates. The reaction profile shows the consumption of trifluoromethylarene **1** and concurrent formation of benzylsilane **3-38** and hemiaminal **3-2,** with the rate of benzylsilane formation initially occurring faster. Once the starting material is completely consumed, the conversion of benzylsilane **3-38** into hemiaminal **3-2** can be observed until only the hemiaminal remains, which is not subject to further reduction under the reaction conditions (Figure 3-8, c). The stability of the hemiaminal product to the reductive conditions arises from the difference in reduction potentials from the starting material and the product—once the C–F bond is transformed into a C–C bond the reduction potential lowers substantially ($\Delta \approx -0.6$ V vs Fc^{+}/Fc^{0}), preventing any further C–F functionalization.

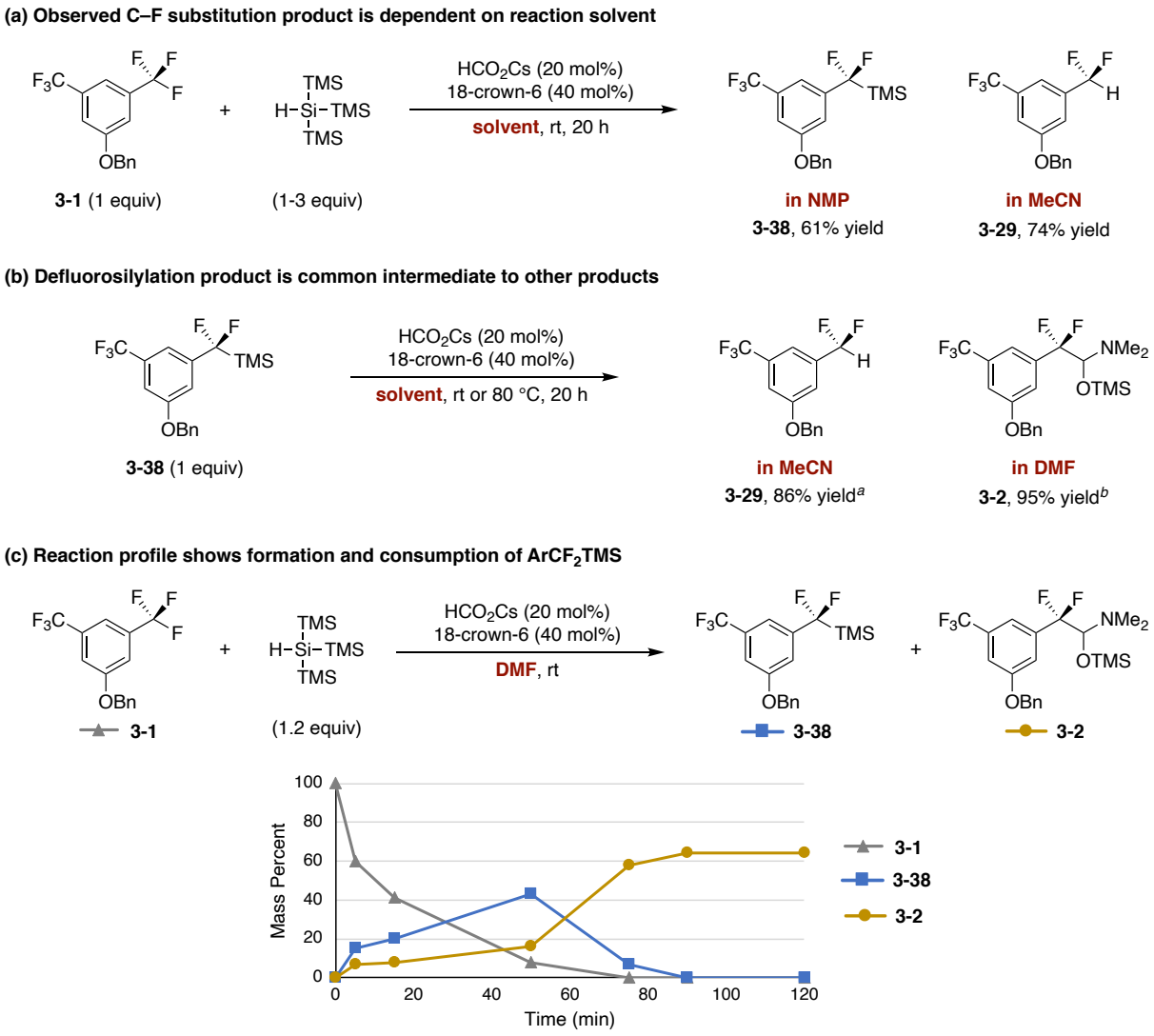

Yields are ^{1}H NMR yields referenced to an internal standard. [a] Reaction run at 80 °C. [b] Reaction run at rt.

Figure 3-8. Mechanistic experiments to probe intermediacy of benzyl silane.

Several mechanistic experiments were then conducted to gauge the presence of any silyl anions under the reductive coupling reaction conditions. Silyl anions are highly reactive intermediates and possess multiple modes of reactivity. Calculations estimate that silyl anions are extremely basic, where trimethylsilyl anion pK_a, = 44.9 in DMSO.[23] Dervan has shown that trimethylsilyl anions are halophilic, attacking the σ-holes of bromo- and iodoarenes to generate aryl anions.[24] Trimethylsilyl anions have also been reported by Sakurai to reduce naphthalene

(naphthalide anion E_{red} = –3.0 V vs Fc/Fc^+).[25] With these reports of the varying modes of reactivity that silyl anions possess, it is feasible that they may play a role in the reductive coupling reaction mechanism.

We hypothesized that replacement of the trifluoromethylarene with other electrophiles would allow for the formation of a product associated with silyl anion reactivity. The loading of cesium formate and 18-crown-6 were increased relative to the standard conditions due to the potential lack of any catalyst regeneration pathways without the presence of a trifluoromethylarene (which produces fluoride as a byproduct). Treatment of 1,2,3,4-tetrafluorobenzene with half an equivalent of TTMSS, cesium formate, and 18-crown-6 in DMF provided the defluorosilylation product **3-39** in 59% yield (Figure 3-9, a). This substitution product likely is generated by nucleophilic aromatic substitution (S_NAr) of the electron-deficient arene by a trimethylsilyl anion generated *in situ*. Trimethylsilyl anions have been reported to engage haloarenes in S_NAr reactions.[24] Subjecting styrene oxide to equimolar amounts of TTMSS, cesium formate, and 18-crown-6 in DMF generates styrene in 34% yield (Figure 3-9, b). This product likely arises from nucleophilic addition of a trimethylsilyl anion to open the epoxide. Once the epoxide is opened, the oxyanion attacks the geminal trimethylsilyl group and eliminates out via a Peterson-olefination pathway.[38] The presence of hexamethyldisiloxane (TMS_2O) in 35% yield supports this mechanism, as the trimethylsilyloxy anion is formed from the Peterson olefination in a 1:1 ratio with the styrene and, presumably, silylated by additional polysilane in solution (either TTMSS or silane by-product produced from the generation of the trimethylsilyl anion). Treatment of 3-phenylpropyl chloride to equimolar amounts of TTMSS, cesium formate, and 18-crown-6 in DMF generates a 1,1,1,3,3,3-hexamethyltrisilyl ($SiH(TMS)_2$) anion substitution product **3-40** in 50% yield (Figure 3-9, c). The $SiH(TMS)_2$ anion that substitutes into the product must arise from

desilylation of a trimethylsilyl group of TTMSS by cesium formate to generate trimethylsilyl formate and the $SiH(TMS)_2$ anion. The generation of $SiH(TMS)_2$ anion from TTMSS is unprecedented in the literature, but isolation and characterization of **3-40** provide unambiguous support for the proposed structure. Taken together, these experiments support our initial hypothesis of Lewis base-promoted generation of a silyl anion that allows for reduction and subsequent functionalization of the trifluoromethylarene. Currently, the exact role of each silyl anion in this process is not clear, and the exact process of benzyl silane formation is unclear as well (it could potentially proceed through radical-radical coupling with a trimethylsilyl radical and the difluorobenzylic radical or radical nucleophilic unimolecular substitution ($S_{RN}1$)[39] by a trimethylsilyl anion with the difluorobenzylic radical) and in-depth mechanistic investigations are currently underway in the Bandar lab.

Conducting the model reaction with addition of one equivalent of an additive in a Glorius-type screen[40] shows that addition of bromo- and iodobenzene completely shut reactivity down (Figure 3-9, d). These substrates are known to be attacked by trimethylsilyl anions and could potentially sequester formation of silyl anion species necessary to promote the reductive coupling reaction. Inclusion of phenyl triflone also completely inhibits reactivity, possibly by preferential SET reduction over the trifluoromethylarene. Addition of common radical traps (TEMPO and BHT) had a negligible effect on the reaction yield, suggesting that any possible radical coupling processes occur faster than the rate of diffusion. Notably, use of hexamethyldisilane, a disilane that can only generate the trimethylsilyl anion, does not promote the reductive coupling reaction under the standard conditions, suggesting that TTMSS is critical to promote the reductive coupling process (Figure 3-9, e).

Substitution of the H substituent of the silane reagent (H–Si(TMS)$_3$ to R–Si(TMS)$_3$) reveals that TTMSS is the optimal disilane for promoting this reaction (Figure 3-10). Substitution of the R = H to trimethylsilyl, methyl, phenyl, pyrrolidine, or allyl drastically reduces the yield (<12% yield for all other R substituents). This suggests that TTMSS possesses the ideal balance of Lewis acidity and steric accessibility and rules out the necessity of the H-atom to successfully promote this reaction.

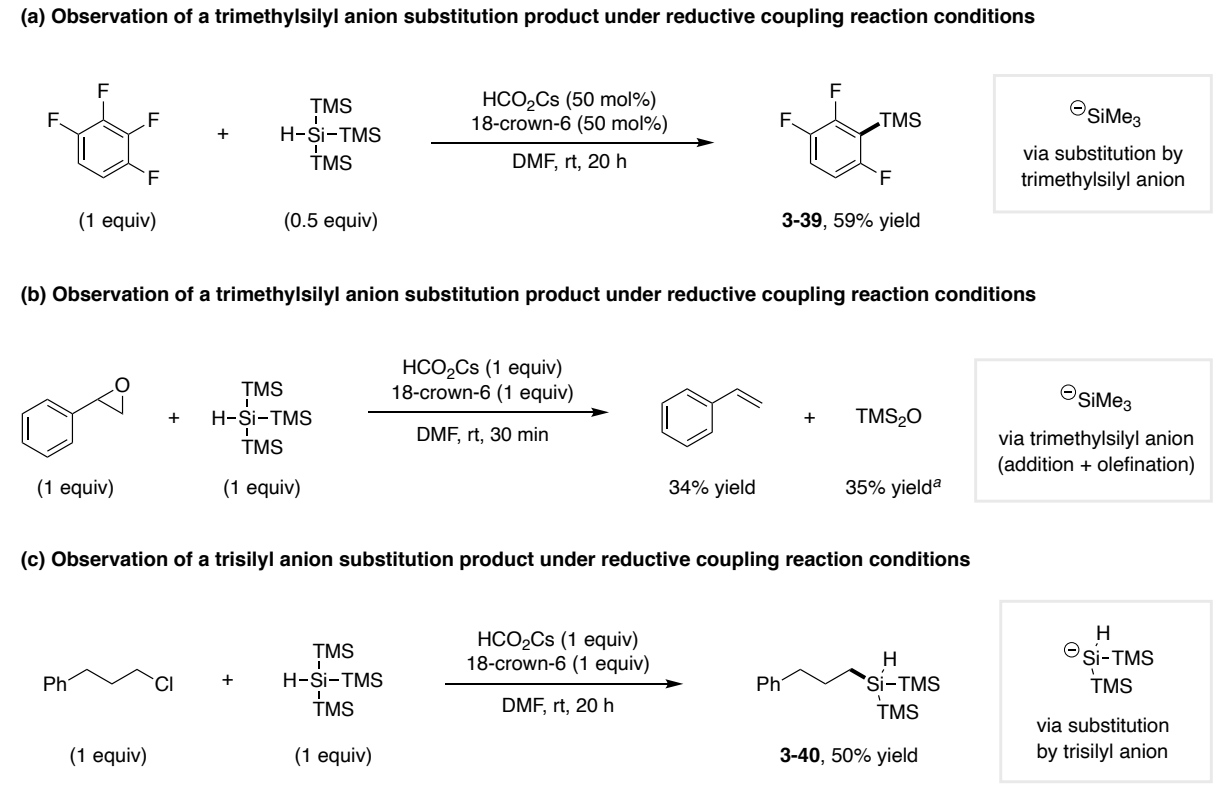

Yields are ^{1}H NMR yields referenced to an internal standard. [a] Yield is a GC yield derived from a calibration curve and referenced to an internal standard.

Figure 3-9. Mechanistic experiments to probe presence of silyl anions under the reductive coupling reaction conditions

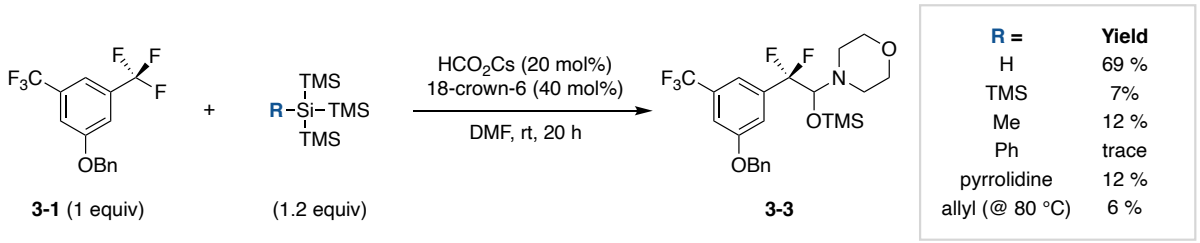

Yields are ^{1}H NMR yields referenced to an internal standard.

Figure 3-10. Effect of variation of tris(trimethylsilyl)silane structure on reductive coupling yield.

3.6 Defluorosilylation and Use as a Nucleophilic Difluorobenzylic Synthon

Once the difluorobenzylic silane intermediate was identified, I realized that it could be intercepted if the reaction was conducted without the formamide coupling partner. Use of the difluorobenzylsilane product as an anionic $ArCF_2^-$ synthon allows for additional transformations that are challenging to access directly from the hemiaminal.[35-37] The model substrate underwent defluorosilylation to provide **3-38** in 40% isolated yield at a 5 mmol scale (Eq. 2). An x-ray crystal structure of **3-38** was also determined (Figure 3-11). From difluorobenzylsilane **3-38**, arylation and alkylation reactions were performed with activation by cesium fluoride (Figure 3-12). Fluoride-promoted C–CN coupling provided the net C–F arylation to access a cyanoarene product (**3-41**) in 78% yield and a quinazoline product (**3-42**) in 38% yield.[41] Nucleophilic substitution reactions of primary alkyl iodides were also readily demonstrated, providing the net defluoromethylation product (**3-43**) as well as the isotopic analogues (**3-44** and **3-45**) in high yields. Defluoroethylation (**3-46**) provided a lower yield (76% NMR yield vs. 42% isolated) due to challenges in separating the elimination side product (16% hydrodefluorination NMR yield) *via* column chromatography. Use of the electrophilic trifluoromethylating reagent, 1-trifluoromethyl-1,2-benziodoxol-3-(1*H*)-one (Togni II), provides the pentafluoroethyl product **3-47** in a modest 31% yield, representing a novel, formal perfluoro homologation of a trifluoromethylarene—in

other words, the C–F bond has been extended into a CF_3 group. These nucleophilic substitution reactions highlight the ability to rapidly access difluorobenzylic analogues with minor structural changes that could be useful in a drug discovery campaign to optimize, for example, the compound's ability to fit into a binding pocket.[8]

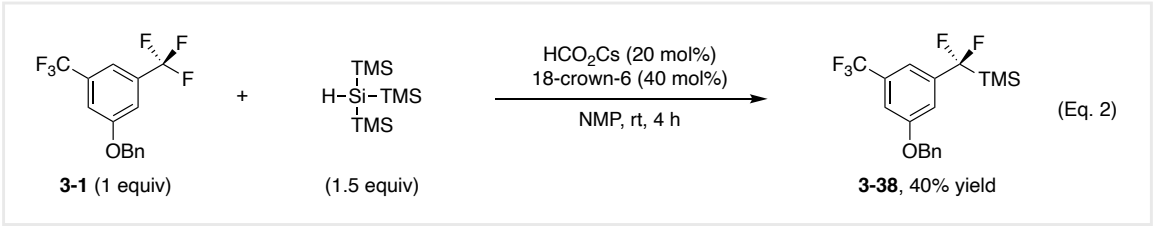

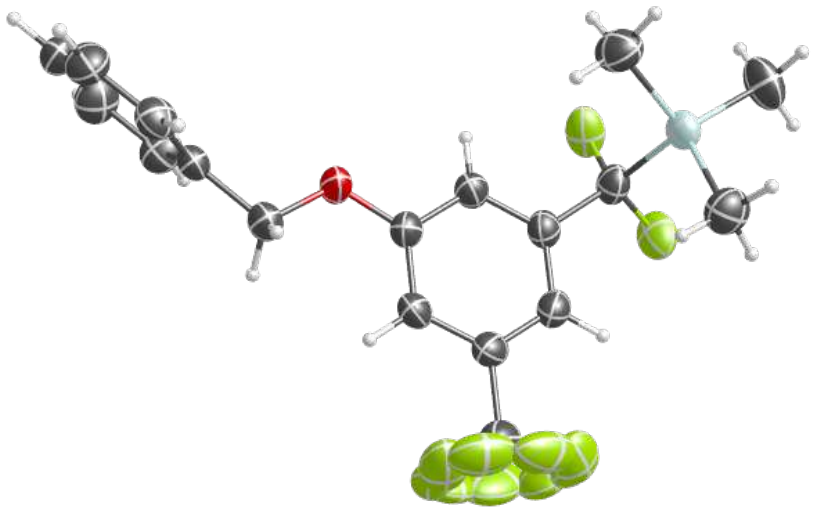

Figure 3-11. X-ray crystal structure of Compound **3-38**. Thermal ellipsoids are at 50% probability. Colors of atoms are as follows: carbon (black), oxygen (red), fluorine (green), silicon (light blue), hydrogen (white).

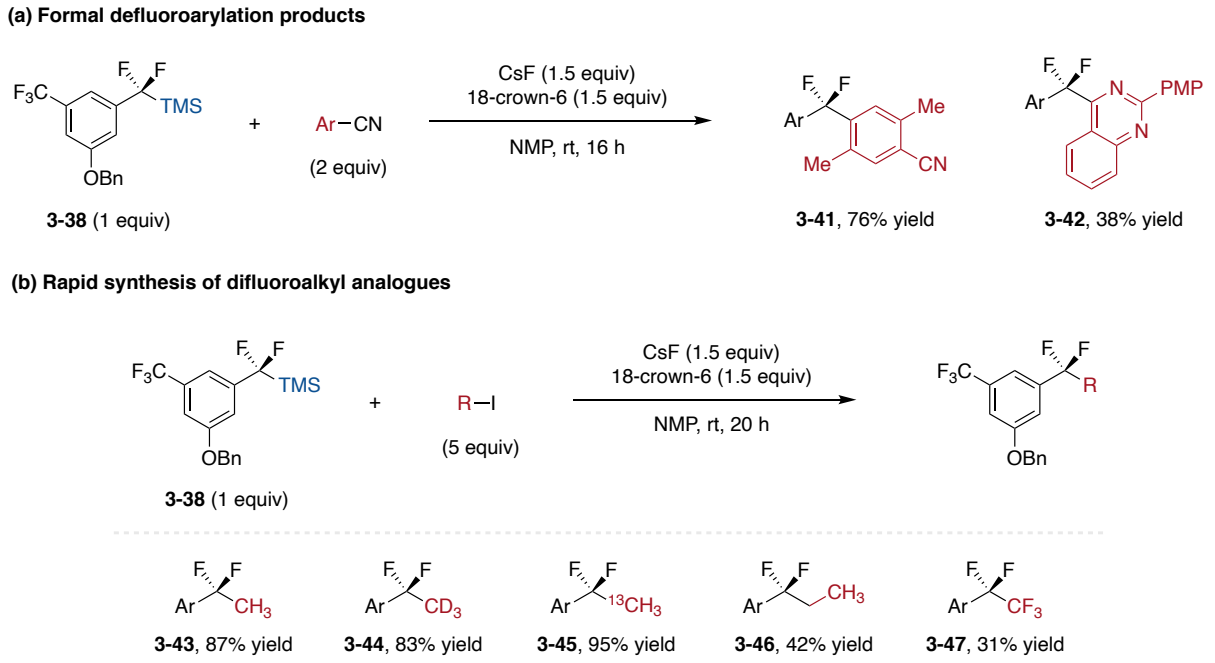

Figure 3-12. Fluoride-promoted arylations and alkylations of the difluorobenzylsilane **3-38**.

3.7 C–H Functionalization of a Difluoromethylarene

Since the reductive coupling reaction operates through a single electron reduction pathway, I wondered if difluoromethylarenes would undergo similar C–F substitution as their reduction potentials are similar to their trifluoromethyl counterparts. Subjecting 1-(difluoromethyl)-3-(trifluoromethyl)benzene (**3-48**) to the reductive coupling reaction does not provide a C–F substitution product, but instead C–H functionalization occurs with a 41% isolated yield of the silylated hemiaminal (**3-49**) obtained after silica gel column chromatography (Eq. 3). This reaction is believed to occur *via* direct deprotonation of the difluoromethyl C–H bond (estimated pK_a = 19.3 in DMSO)[42] by a silyl anion generated *in situ* (trimethylsilyl anion p$K_{a'}$ = 44.9 and SiH(TMS)$_2$ anion p$K_{a'}$ = 30.2 in DMSO[23], acetic acid pK_a = 12.6 in DMSO for reference). From the resulting difluorobenzylic anion either direct addition into the formamide solvent or

silylation/desilylation are possible and further investigation into this reactivity is currently under investigation. This reactivity would be useful to rapidly derivatize difluoromethylarenes with diverse C–C fragments.

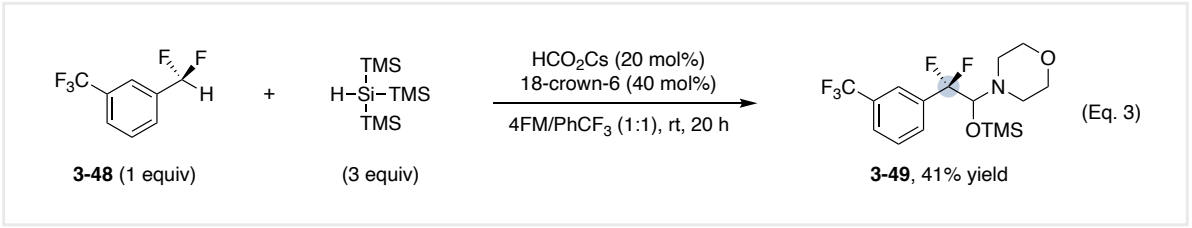

3.8 Conclusion

In conclusion, my initial investigations into the Lewis base activation of organosilanes to promote the defluorofunctionalization of trifluoromethylarenes resulted in the discovery of a reductive coupling reaction that generates a synthetically versatile silylated hemiaminal product. The products generated from this reaction greatly expand the scope of trifluoromethylarene C–F transformations now possible. This reaction uses a cheap Lewis basic salt as the catalyst and the commercially available tris(trimethylsilyl)silane as the key enabling reagent to promote this unique reactivity. Mechanistic studies have provided key insights into the reductive coupling process and allowed for the isolation of a key benzylsilane intermediate that allows for an additional scope of C–F transformations. Silyl anion trapping experiments support the generation of two different silyl anion species under the standard reaction conditions that potentially promote this reductive coupling process, with tris(trimethylsilyl)silane uniquely capable of effectively promoting this reaction. Since this reaction operates *via* a reductive process, the scope encompasses electron-deficient trifluoromethylarenes, but current work in the Bandar Group is expanding the scope to electron-neutral trifluoromethylarenes and will be discussed in Chapter 4.

REFERENCES

[1] Coteron, J. M.; Marco, M.; Esquivias, J.; Deng, X.; White, K. L.; White, J.; Koltun, M.; El Mazouni, F.; Kokkonda, S.; Katneni, K.; Bhamidipati, R.; Shackleford, D. M.; Angulo-Barturen, I.; Ferrer,S.B.;Jimeńez-Díaz,M.B.;Gamo,F.-J.;Goldsmith,E.J.; Charman, W. N.; Bathurst, I.; Floyd, D.; Matthews, D.; Burrows, J. N.; Rathod, P. K.; Charman, S. A.; Phillips, M. A. Structure-Guided Lead Optimization of Triazolopyrimidine-Ring Substituents Identifies Potent Plasmodium falciparum Dihydroorotate Dehydrogenase Inhibitors with Clinical Candidate Potential. *J. Med. Chem.* **2011**, *54*, 5540−5561.

[2] Anderson, M. O.; Zhang, J.; Liu, Y.; Yao, C.; Phuan, P.-W.; Verkman, A. S. Nanomolar Potency and Metabolically Stable Inhibitors of Kidney Urea Transporter UT-B. *J. Med. Chem.* **2012**, *55*, 5942−5950.

[3] Jeppsson, F.; Eketjäll, S.; Janson, J.; Karlström, S.; Gustavsson, S.; Olsson, L.-L.; Radesäter, A.-C.; Ploeger, B.; Cebers, G.; Kolmodin, K.; Swahn, B.-M.; Berg, S. v.; Bueters, T.; Fälting, J. Discovery of AZD3839, a Potent and Selective BACE1 Inhibitor Clinical Candidate for the Treatment of Alzheimer Disease. *J. Biol. Chem.* **2012**, *287*, 41245–41257.

[4] Cui, J. J. Targeting Receptor Tyrosine Kinase MET in Cancer: Small Molecule Inhibitors and Clinical Progress. *J. Med. Chem.* **2014**, *57*, 4427−4453.

[5] Timmer, W.; Massana, E.; Jimenez, E.; Seoane, B.; de Miquel, G.; Ruiz, S. First-in-human study of the safety, tolerability, pharmacokinetics and pharmacodynamics of abediterol (LAS100977), a novel long-acting B2-agonist. *J. Clin. Pharmacol.* **2014**, *54*, 1347−1353.

[6] Stroebel, D.; Buhl, D. L.; Knafels, J. D.; Chanda, P. K.; Green, M.; Sciabola, S.; Mony, L.; Paoletti, P.; Pandit, J. A Novel Binding Mode Reveals Two Distinct Classes of NMDA Receptor GluN2B-selective Antagonists. *Mol. Pharmacol.* **2016**, *89*, 541−551.
Jeschke, P. Latest generation of halogen-containing pesticides. *Pest Manage. Sci.* **2017**, *73*, 1053−1066.

[7] Besandre, R.; Liu, H. Biochemical Basis of Vosevi, a New Treatment for Hepatitis C. *Biochemistry* **2018**, *57*, 479−480.

[8] Tria, G. S.; Abrams, T.; Baird, J.; Burks, H. E.; Firestone, B.; Gaither, L. A.; Hamann, L. G.; He, G.; Kirby, C. A.; Kim, S.; Lombardo, F.; Maccho, K. J.; McDonnell, D. P.; Mishina, Y.; Norris, J. D.; Nunez, J.; Springer, C.; Sun, Y.; Thomsen, N. M.; Wang, C.; Wang, J.; Yu, B.; Tiong-Yip, C.-L.; Peukert, S. Discovery of LSZ102, a Potent, Orally Bioavailable Selective Estrogen Receptor Degrader (SERD) for the Treatment of Estrogen Receptor Positive Breast Cancer. *J. Med. Chem.* **2018**, *61*, 2837–2864.

[9] a) Belhomme, D.-C.; Besset, T.; Poisson, T.; Pannecoucke, X. Recent Progress toward the Introduction of Functionalized Difluoromethylated Building Blocks onto C(sp2) and C(sp) Center. *Chem. Eur. J.* **2015**, *21*, 12836–12865.

[10] (b) Koperniku, A.; Liu, H.; Hurley, P. B. Mono- and Difluorination of Benzylic Carbon Atoms. *Eur. J. Org. Chem.* **2016**, 871–886.

[11] Lawitz, E. J.; O'Riordan, W. D.; Asatryan, A.; Freilich, B. L.; Box, T. D.; Overcash, J. S.; Lovell, S.; Ng, T. I.; Liu, W.; Campbell, A.; Lin, C.-W.; Yao, B.; Kort, J. Potent Antiviral Activities of the Direct-Acting Antivirals ABT-493 and ABT-530 with Three-Day Monotherapy for Hepatitis C Virus Gentotype 1 Infection. *Antimicrob. Agents Chemother.* **2016**, *60*, 1546–1555.

[12] Singh, R. P.; Shreeve, J. M. Recent Advances in Nucleophilic Fluorination Reactions of Organic Compounds Using Deoxofluor and DAST. *Synthesis* **2002**, *17*, 2561–2578.

[13] Ni, C.; Hu, M.; Hu, J. Good Partnership between Sulfur and Fluorine: Sulfur-Based Fluorination and Fluoroalkylation Reagents for Organic Synthesis. *Chem. Rev.* **2015**, *115*, 765– 825.

[14] Feng, Z.; Xiao, Y.-L.; Zhang, X. Transition-Metal (Cu, Pd, Ni)-Catalyzed Difluoroalkylation via Cross-Coupling with Difluoroalkyl Halides. *Acc. Chem. Res.* **2018**, *51*, 2264–2278.

[15] Xiao, Y.-L.; Min, Q.-Q.; Xu, C.; Wang, R.-W.; Zhang, X. Nickel-Catalyzed Difluoroalkylation of (Hetero)Arylborons with Unactivated 1-Bromo-1,1-difluoroalkanes. *Angew. Chem., Int. Ed.* **2016**, *55*, 5837–5841.

[16] Min, Q.-Q.; Yin, Z.; Feng, Z.; Guo, W.-H.; Zhang, X. Highly Selective gem-Difluoroallylation of Organoborons with Bromodifluoromethylated Alkenes Catalyzed by Palladium. *J. Am. Chem. Soc.* **2014**, *136*, 1230–1233.

[17] Ge, S.; Chaladaj, W.; Hartwig, J. F. Pd-Catalyzed α-Arylation of α,α-Difluoroketones with Aryl Bromides and Chlorides. A Route to Difluoromethylarenes. *J. Am. Chem. Soc.* **2014**, *136*, 4149–4152.

[18] Ge, S.; Arlow, S. I.; Mormino, M. G.; Hartwig, J. F. Pd-Catalyzed α-Arylation of Trimethylsilyl Enolates of α,α-Difluoroacetamides. *J. Am. Chem. Soc.* **2014**, *136*, 14401–14404.

[19] An, L.; Xiao, Y.-L.; Zhang, S.; Zhang, X. Bulky Diamine Ligand Promotes Cross-Coupling of Difluoroalkyl Bromides by Iron Catalysis. *Angew. Chem., Int. Ed.* **2018**, *57*, 6921– 6925.

[20] Luo, Y. R. Comprehensive Handbook of Chemical Bond Energies; CRC Press: Boca Raton, FL, 2007.

[21] O'Hagan, D. Understanding organofluorine chemistry. An introduction to the C–F bond. *Chem. Soc. Rev.* **2008**, *37*, 308–319.

[22] Luo, C.; Bandar, J. S. Selective Defluoroallylation of Trifluoromethylarenes. *J. Am. Chem. Soc.* **2019**, *141*, 14120–14125.

[23] Fu, Y.; Liu, L.; Li, R.-Q.; Liu, L.; Guo, Q.-X. First-Principal Predictions of Absolute pK_a's of Organic Acids in Dimethyl Sulfoxide Solution. *J. Am. Chem. Soc.* **2003**, *126*, 814–822.

[24] Shippey, M. A.; Dervan, P. B. Trimethylsilyl Anions. Direct Synthesis of Trimethylsilylbenzenes. *J. Org. Chem.* **1977**, *42*, 2654–2655.

[25] Sakurai, H.; Akane, O.; Umino, H.; Kira, M. Silyl anions. IV. New convenient method of producing radical anions involving one-electron transfer from trimethylsilylsodium. *J. Am. Chem. Soc.* **1973**, *95*, 955–956.

[26] Billard, T.; Bruns, S.; Langlois, B. R. New Stable Reagents for the Nucleophilic Trifluoromethylation. 1. Trifluoromethylation of Carbonyl Compounds with *N*-Formylmorpholine Derivatives. *Org. Lett.* **2000**, *2*, 2101–2103.

[27] Billard, T.; Langlois, B. R.; Blond, G. New stable reagents for the nucleophilic trifluoromethylation. Part 2: Trifluoromethylation with silylated heminals of trifluoroacetaldehyde. *Tetrahedron Lett.* **2000**, *41*, 8777–8780.

[28] Large, S.; Roques, N.; Langois, B. R. Nucleophilic Trifluoromethylation of Carbonyl Compounds and Disulfides with Trifluoromethane and Silicon-Containing Bases. *J. Org. Chem.* **2000**, *65*, 8848–8856.

[29] Billard, T.; Langlois, B. R.; Blond, G. Trifluoromethylation of Nonenolizable Carbonyl Compounds with a Stable Piperazino Hemiaminal of Trifluoroacetaldehyde. *Eur. J. Org. Chem.* **2001**, 1467–1471.

[30] Blond, G.; Billard, T.; Langlois, B. R. New stable reagents for the nucleophilic trifluoromethylation. Part 4: Trifluoromethylation of disulfides and diselenides with hemiaminals of trifluoroacetaldehyde. *Tetrahedron Lett.* **2001**, *42*, 2473–2475.

[31] Blond, G.; Billard, T.; Langlois, B. R. Reactivity of Stable Trifluoroacetaldehyde Hemiaminals. 1. An Unexpected Reaction with Enolizable Carbonyl Compounds. *J. Org. Chem.* **2001**, *66*, 4826–4830.

[32] Billard, T.; Langlois, B. R. Reactivity of Stable Trifluoroacetaldehyde Hemiaminals. 2. Generation and Synthetic Potentialities of Fluorinated Iminiums. *J. Org. Chem.* **2002**, *67*, 997–1000.

[33] Leuger, J.; Blond, G.; Fröhlich, R.; Billard, T.; Haufe, G.; Langlois, B. R. Synthetic Applications of α-Fluoroalkylated Enones. 1. Use as Dienophiles in Diels–Alder Cycloadditions. *J. Org. Chem.* **2006**, *71*, 2735–2739.

[34] Huang, L.; Liu, W.; Zhao, L.-L.; Zhang, Z.; Yan, X. Base-Catalyzed H/D Exchange Reaction of Difluoromethylarenes. *J. Org. Chem.* **2021**, *86*, 3981–3988.

[35] Zhang, W.-X.; Ding, C.-H.; Luo, Z.-B.; Hou, X.-L.; Dai, L.-X. Addition of benzyltrimethylsilane to imines triggered by tetrabutylammonium fluoride. *Tetrahedron Lett.* **2006**, *47*, 8391–8393.

[36] Aikawa, K.; Maruyama, K.; Nitta, J.; Hashimoto, R.; Mikami, K. Siladifluoromethylation and Difluoromethylation onto C(sp^3), C(sp^2), and C(sp) Centers Using Ruppert–Prakash Reagent and Fluoroform. *Org. Lett.* **2016**, *18*, 3354–335.

[37] (a) Santos, L.; Panossian, A.; Donnard, M.; Vors, J.-P.; Pazenok, S.; Bernier, D.; Leroux, F. R. Deprotonative Functionalization of the Difluoromethyl Group. *Org. Lett.* **2020**, *22*, 8741–8745. (b) Geri, J. B.; Wade Wolfe, M. M.; Szymczak, N. K. The Difluoromethyl Group as a Masked Nucleophile: A Lewis Acid/Base Approach. *J. Am. Chem. Soc.* **2018**, *140*, 9404–9408.

[38] Chan, T.-H. Alkene Synthesis via β-Functionalized Organosilicon Compounds. *Acc. Chem. Res.* **1977**, *10*, 442–448.

[39] Rossi, R. A.; Pierini, A. B.; Santiago, A. N. Aromatic Substitution by the $S_{RN}1$ Reaction. *Org. React.* **1999**, *54*, 1–178.

[40] (a) Collins, K. D.; Glorius, F. A robustness screen for the rapid assessment of chemical reactions. *Nature Chemistry*, **2013**, *5*, 597–603. (b) Collins, K. D.; Glorius, F. Intermolecular Reaction Screening as a Tool for Reaction Evaluation. *Acc. Chem. Res.* **2015**, *48*, 619–627. (c) Gensch, T.; Teders, M.; Glorius, F. Approach to Comparing the Functional Group Tolerance of Reactions. *J. Org. Chem.* **2017**, *82*, 9154–9159.

[41] Reidl, T. W.; Bandar, J. S. Lewis Basic Salt-Promoted Organosilane Coupling Reactions with Aromatic Electrophiles. *J. Am. Chem. Soc.* **2021**, *143*, 11939–11945.

[42] Yang, Q.; Li, Y.; Yang, J.-D.; Liu, Y.; Zhang, L.; Luo, S.; Cheng, J.-P. Holistic Prediction of pK_a in Diverse Solvents Based on Machine Learning Approach. *Angew. Chem. Int. Ed.* **2020**, *59*, 19282-19291.

CHAPTER FOUR

DIRECT HYDRODEFLUORINATION OF TRIFLUOROMETHYLARENES

4.1 Chapter Overview

This chapter will provide an introduction to the difluoromethylarene functional group and will describe the discovery and initial investigations into a two mechanistically different hydrodefluorination reactions of trifluoromethylarenes using Lewis base activated organosilane reagents. Within the Bandar Group, there is ongoing development of new reactions using the mechanistic insight provided by the work in the Chapter 3. To highlight those efforts, the expansion of the hydrodefluorination reaction scope to electron-neutral trifluoromethylarenes by a junior graduate student will also be briefly described.

4.2 Introduction

The difluoromethyl group is the second most common benzylic fluoroalkyl group after the trifluoromethyl group.[1] The difluoromethyl substituent can engage in weak hydrogen bonding interactions and has been investigated as a lipophilic bioisostere of alcohols, thiols, and amines.[2-4] Additionally, the weakly acidic difluoromethylarene C–H bond has been the subject of C–H deprotonation methodologies to access difluorobenzylic derivatives.[5-6] It is for these reasons that the difluoromethyl group is a unique fluoroalkyl functional group and has been the target of much methodological development to access this fluorinated motif. It would be powerful if one could directly transform a trifluoromethyl group into a difluoromethyl group to test for these potential benefits.

4.3 Increased pharmacological activity of difluoromethyl- versus trifluoromethyl substitution

There are a few instances reported of the substitution of a trifluoromethyl group with a difluoromethyl group on an arene during the optimization of a potential drug resulting in a significant increase in biological activity. In one example, a pyrazole carboxamide fungicide was examined with both a trifluoro- and difluoromethyl substituent on the pyrazole ring.[7] The difluoromethyl version was nearly twice as potent and it was suggested that the greater potency was due to increased enzyme-inhibitor interactions arising from the intramolecular hydrogen bonding of the difluoromethyl C–H bond with the amide oxygen, thereby locking the molecule in the preferred confirmation for substrate-protein interaction. In another example, the mTOR inhibitor PQR309 was further optimized to increase potency and selectivity, culminating in the development of PQR620 (Figure 4-1).[8] Substitution of the trifluoromethyl group with a difluoromethyl group resulted in more than thirteen times the potency, which is ascribed to increased interaction with the negatively charged glutamate (Glu) residue and a nearby isoleucine (< 7 Å) that reinforces the CF_2H-Glu interaction.

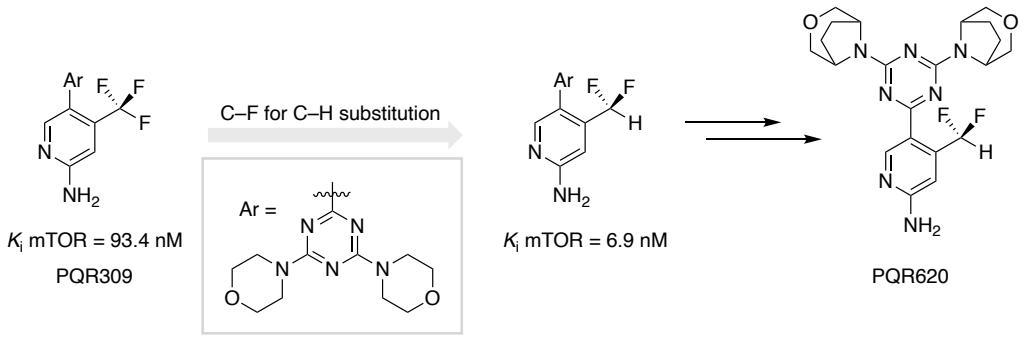

Figure 4-1. Examples of increased potency upon aryl trifluoromethyl substitution with a difluoromethyl group.

4.4 Methods to incorporate the difluoromethyl group into arenes

The synthetic methods to incorporate the difluoromethyl group into arenes are not as well developed as the trifluoromethyl group. The mechanistic strategies towards incorporation of the difluoromethyl group are generally similar to those of the trifluoromethyl group. This section will briefly provide an overview of methods to achieve difluoromethylation of an arene by providing examples of different strategies that have been reported than those discussed in Chapter 1.

Deoxyfluorination of aryl aldehydes using sulfur(IV) fluoride reagents (such as sulfur tetrafluoride (SF_4) or diethylaminosulfur trifluoride (DAST)) is one of the most common strategies to access difluoromethylarenes, though care must be taken as these reactions can be highly exothermic and potentially explosive.[9-10] The aldehydes required for this transformation typically come from the aryl halide precursor through carbonylation or metalation/trapping reactions such that this approach requires multiple steps to access the difluoromethylarene.

In 2012 Baran reported the Minisci-type addition of difluoromethyl radicals to heteroarenes. The radicals are generated from zinc difluoromethylsulfinate salts using *tert*-butyl hydroperoxide and possess nucleophilic character, in contrast to trifluoromethyl radicals which possess electrophilic character. Other reagents to generate difluoromethyl radicals have also been developed.[11-12] This strategy provides direct C–H difluoromethylation but possesses substrate-dependent selectivity.

There has been much effort in utilizing transition metals to promote and catalyze the difluoromethylation of aryl halides. In 2016 Vivec reported the nickel-catalyzed difluoromethylation of aryl (pseudo)halides using an isolable difluoromethyl zinc reagent at room temperature.[13] Since then, other transition metals have been shown competent to catalyze this transformation under a variety of conditions.

4.5 Hydrodefluorination of trifluoromethylarenes

While there has been much effort in developing methodologies to install the difluoromethyl group on arenes, there is still a greater ability to incorporate trifluoromethyl groups onto arenes. Therefore, methods to mono-selectively reduce trifluoromethylarenes to access difluoromethylarenes would be useful. Since 2016 there have been four reports for the mono-selective hydrodefluorination of trifluoromethylarenes. These reports were discussed in Chapter 1 and are restated here. Lalic reported in 2016 the use of catalytic palladium, copper, and 2-pyridone in combination with a hydrosilane and alkoxide base to promote the mono-selective hydrodefluorination of a limited scope of trifluoromethylarenes.[14] Prakash in 2017 reported the use of magnesium metal in acidic conditions to mono-selectively reduce bis(trifluoromethyl)arenes.[15] Jui in 2019 leveraged the use of photoredox catalysis to mono-selectively reduce electron-neutral trifluoromethylarenes.[16] In 2020 Gouverneur reported the photoredox catalyzed mono-selective reduction of electron-deficient trifluoromethylarenes.[17]

4.6 Lewis base activation of hydrosilanes for the hydrodefluorination of trifluoromethylarenes

Following the defluoroallylation work reported by the Bandar group in 2019 (described in Chapter 2), we speculated that Lewis base activation of hydrosilanes could effect a single electron transfer to a trifluoromethylarene and, after mesolytic cleavage of the radical anion, could be a hydrogen atom donor to the resulting benzylic radical to mono-selectively provide the difluoromethylarene.

To begin, I conducted initial investigations using the optimized conditions from the defluoroallylation reactions. The model substrate, 1,3-bis(trifluoromethyl)benzene was subjected

to catalytic cesium fluoride ligated by 18-crown-6 and triethylsilane in dimethoxyethane (DME) at 50 °C, but no reaction took place and only starting material was remaining (Figure 4-2, top). Changing the Lewis basic catalyst to the polyphosphazene organic superbase P_4-*t*-Bu provided the hydrodefluorination product (**4-1**) in 66% ^{1}H NMR yield referenced to an internal standard, with 8% of the over-reduced benzyl fluoride product (**4-2**), equaling an 8:1 mono-selective hydrodefluorination reaction. Examination of other commercially available hydrosilanes demonstrates that triethylsilane provides the highest yields of all hydrosilanes tested, and the hydrogen atom is crucial for reactivity as tetraethylsilane was unreactive under the standard reaction conditions (Figure 4-2, bottom). It is unclear at this time why cesium fluoride was ineffective at promoting this transformation while P_4-*t*-Bu can catalyze it effectively. P_4-*t*-Bu typically acts as a strong Brønsted base (pK_a' = 30.2 in DMSO)[18] but has also been shown to coordinate and activate organosilanes catalytically, for example the generation of aryl anions from aryltrimethylsilanes and the activation of triethylsilane to deprotonate alcohols for S_NAr were reported by Kondo.[19-20] The calculated pK_a of trimethylsilane is 44.9 in DMSO, so it is unlikely that P_4-*t*-Bu is operating as a Brønsted base in this reaction.[21] Other alkoxide, amide, and fluoride bases, and also a weaker polyphosphazene base, P_2-Et (p*K*a' = 21.1 in DMSO), were examined and found to be ineffective promoters for this reaction.

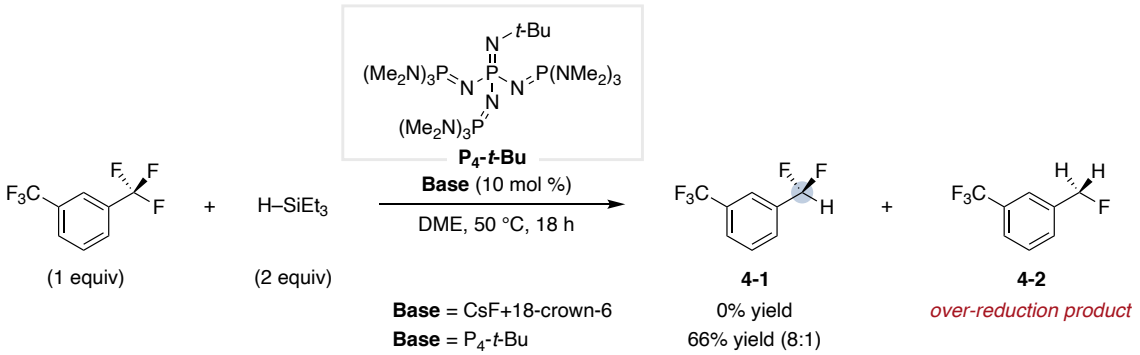

Silane screen with P_4-t-Bu as base

Silane:	H–Si(*i*-Pr)$_3$	H–SiMe$_2$Ph	H–SiPh$_3$	H–SiPh$_2$H	H–Si(OMe)$_2$Me	H–Si(OEt)$_3$	H–Si(TMS)$_3$	SiEt$_4$
Yield of 4-1: (4-1:4-2 ratio)	55% yield (9:1)	27% yield (2:1)	<5% yield (n/a)	0% yield (n/a)	10% yield (1:1)	11% yield (1:1)	0% yield (n/a)	0% yield (n/a)

Figure 4-2. (top) Discovery of Lewis base catalyzed hydrodefluorination of trifluoromethylarenes with hydrosilanes and (bottom) effect of hydrosilane structure on reaction yield.

An optimization of the reaction variables was conducted, and it was found the 3 equivalents of triethylsilane and 0.2 equivalents of P_4-*t*-Bu at 50 C in DME at 0.25 M was the optimal set of reaction conditions for the model reaction. A brief substrate scope is demonstrated below in Figure 4-3, but although work is still ongoing to develop this reaction with other members of the Bandar Group. Electron-deficient substrates that are amenable to this reaction include 1,2- and 1,3-bis(trifluoromethyl)arenes, 3-trifluoromethylbenzonitriles, 3-trifluoromethylpyridines, 3-trifluoromethylsulfonamides, and 3-trifluoromethylphosphonate esters. The similarities of the scope to that of the defluoroallylation reaction suggest a similar mechanism might be in effect. Conducting the reaction in deuterated tetrahydrofuran (THF-d_8) does not incorporate any deuterium into the product, suggesting that the hydrogen atom source is the hydrosilane.

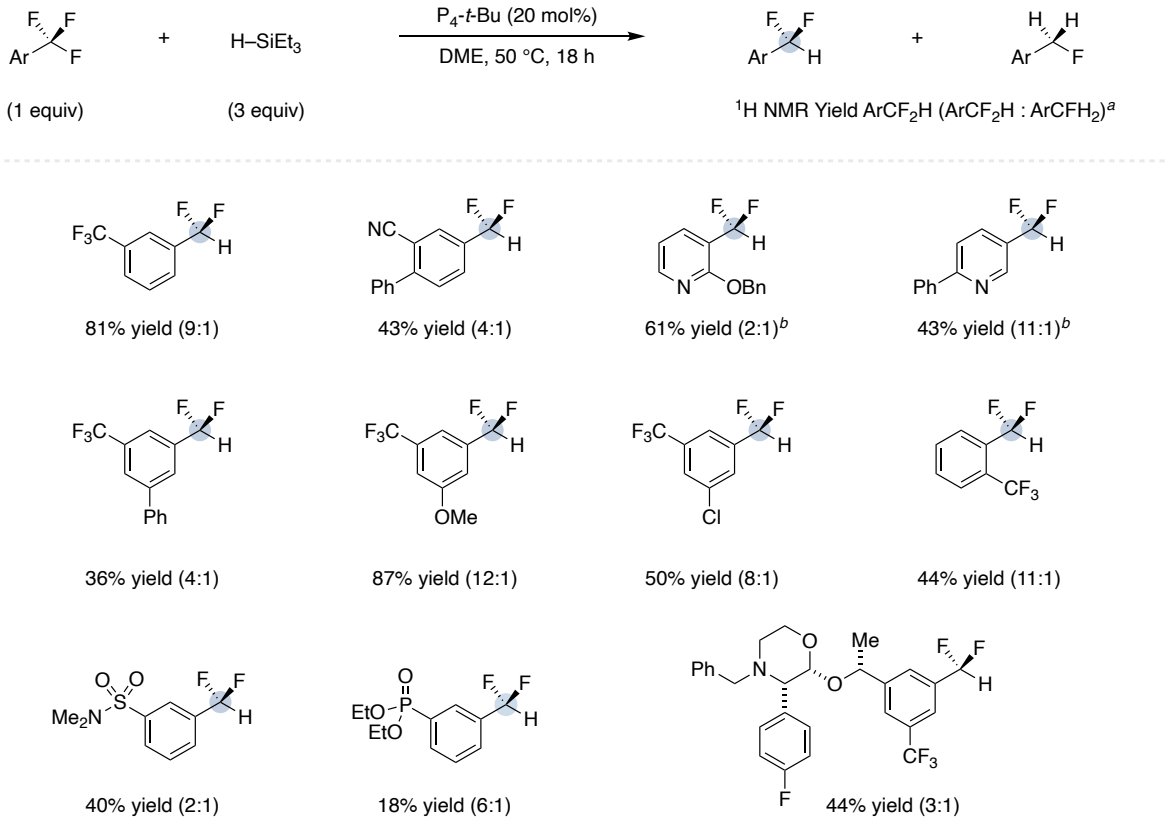

[a] Yields are ^{1}H NMR yields referened to an internal standard. [b] Reaction run at room temperature.

Figure 4-3. Preliminary scope of the P$_4$-*t*-Bu catalyzed hydrodefluorination of trifluoromethylarenes with triethylsilane.

Consideration of the mechanistic work done on the reductive coupling reaction described in Chapter 3 can allow for another mechanistic approach towards the direct hydrodefluorination reaction (Figure 4-4, top). Conducting the reductive coupling reaction to generate the difluorobenzylic silane that undergoes desilylation *in situ* by a Lewis base will produce the difluoromethylarene directly if the reaction solvent is capable of being deprotonated by the benzylic anion. This deprotonation pathway is supported by conducting the reaction in deuterated acetonitrile (MeCN-d_3), generating the difluoromethylarene **3-30** with >95% deuterium incorporation (Figure 4-4, bottom).

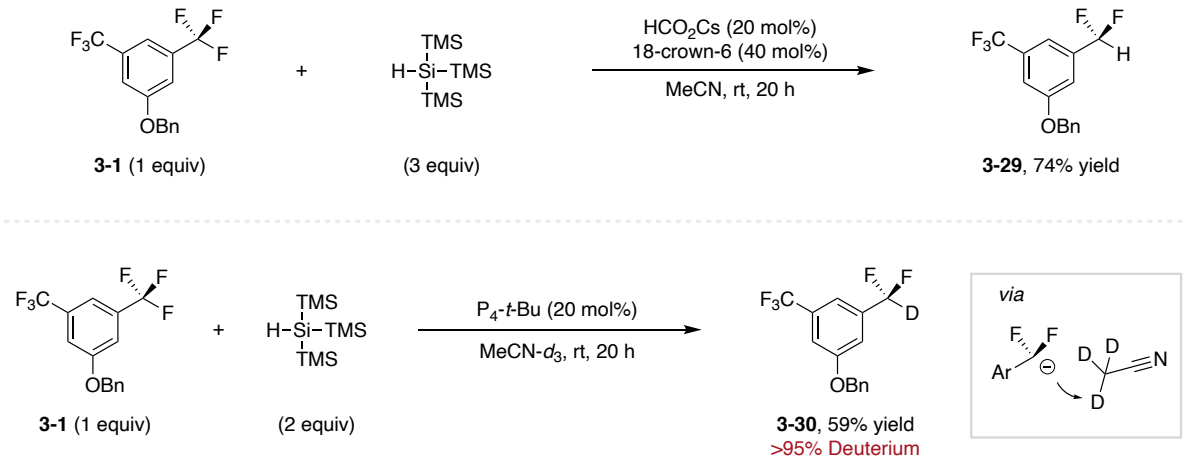

Figure 4-4. Direct generation of difluoromethylarene via reductive coupling in acidic solvent (top) and mechanistic experiment supporting the deprotonation pathway (bottom).

Since this reductive coupling hydrodefluorination pathway operates *via* a different mechanism, the scope should have differences as well. Examination of other solvents demonstrates that dimethylsulfoxide (DMSO) is a more general reaction solvent to provide higher yields. A few examples of substrates amenable to this reaction include heterocyclic substrates such as 2-trifluoroemethylpyridine and 7-trifluoromethylquinoline, and electron-deficient trifluoromethylarenes including bis(trifluoromethyl)benzenes, sulfonamides, phosphonate esters, and fluoroarenes which demonstrates similarities to the reductive coupling scope (Figure 4-5). There is still ongoing work to examine the scope and optimal conditions for the direct hydrodefluorination of trifluoromethylarenes.

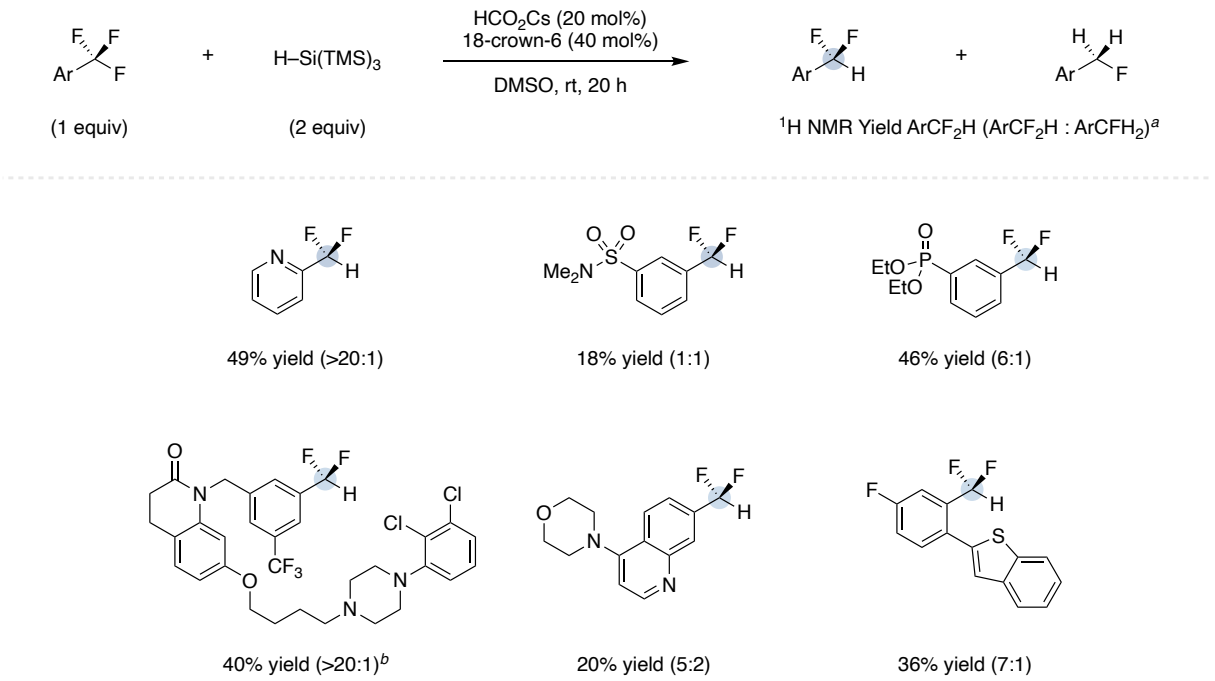

[a] Yields are ^{1}H NMR yields referened to an internal standard. [b] 1 equiv tetrabutylammonium fluoride (TBAF) added before workup

Figure 4-5. Reductive coupling reaction in acidic solvent for the hydrodefluorination of trifluoromethylarenes.

A major challenge to the development of a hydrodefluorination reaction that operates through a single electron transfer mechanism is the similarities in reduction potentials between the trifluoromethylarene and the difluoromethylarene product. The model substrate, 1,3-bis(trifluoromethyl)benzene, has a reduction potential of E_{red} = –2.67 V vs Fc^+/Fc^0 while the difluoromethylarene product **4-1** has a reduction potential of E_{red} = –2.85 V vs Fc^+/Fc^0.[22] Overcoming this challenge is part of the ongoing efforts to optimize this reaction, although the results summarized thus far provide a promising starting point.

4.7 Future work

In addition to the two reaction mechanisms described in Section 4.6 to enable the hydrodefluorination of trifluoromethylarenes, there has been additional work undertaken by a

junior graduate student, Leidy Hooker, in using the fluoride activation of hexamethyldislane to enable the hydrodefluorination of electron-neutral trifluoromethylarenes. Under these reaction conditions only the trimethylsilyl anion can be generated and the reaction is pseudo-catalytic in fluoride since mesolytic cleavage of the trifluoromethylarene radical anion after single electron reduction will generate an equivalent of fluoride anion to restart the reaction cycle. The trimethylsilyl anion is highly reducing[23] and typically causes the decomposition of electron-deficient trifluoromethylarenes but is capable of selectively reducing less activated trifluoromethylarenes. To provide an example, subjecting 1-trifluoromethylnapthalene to both of the reaction conditions I developed for the hydrodefluorination of electron-deficient trifluoromethylarenes results in no difluoromethylarene product formation (Figure 4-6, top). When 1-trifluoromethylnapthalene is subjected to the conditions developed by Leidy, using hexamethyldisilane activated by catalytic cesium fluoride, a high yield of the difluoromethylarene is obtained with near complete mono-selectivity (76%, 20:1 selectivity; Figure 4-6 bottom). This work is still ongoing and will be reported in due course.

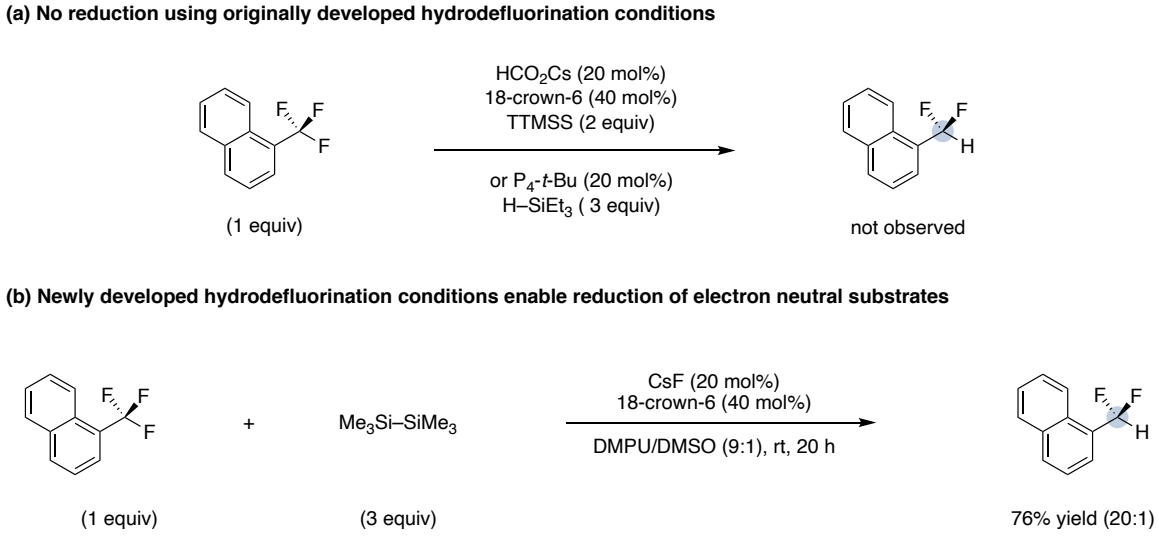

Figure 4-6. Hydrodefluorination of electron-neutral trifluoromethylarenes using hexamethyldisilane.

4.8 Conclusion and Outlook

The difluoromethylarene substructure is an important fluorinated motif due to its ability to act as a lipophilic bioisostere and therefore methods to incorporate it are in high demand. Synthetic methodologies to install a difluoromethyl motif are still underdeveloped when compared to aryl trifluoromethylation. The past few years have seen a rise in mono-selective trifluoromethylarene hydrodefluorination reactions, but the scopes of the reported methods are still limited. This chapter has detailed efforts by the Bandar group towards using the Lewis base activation of organosilanes to enable mono-selective reductions of trifluoromethylarenes.

My work described in Chapters 3 and 4 began with the discovery of the defluoroallylation reaction by the Bandar Group. After a thorough investigation of various organosilanes, I discovered a reductive coupling method to turn a trifluoromethylarene C–F bond into virtually any difluorobenzylic derivative. My discoveries inspired and guided ongoing work within the Bandar Group that will allow activation of electron-neutral trifluoromethylarenes. Thus, this work has been instrumental at advancing the aryl trifluoromethyl group into a general synthetic functional handle. The impact of this transformation stems from the perception of the ubiquitously present trifluoromethylarene as a terminal and unreactive functionality—these transformations will now allow increased access to a broad scope of difluorobenzylic derivatives that are emerging as a key substructure in modern medicines and agrochemicals.

REFERENCES

[1] Inoue, M.; Sumii, Y.; Shibata, N. Contribution of Organofluorine Compounds to Pharmaceuticals. *ACS Omega*, **2020**, *5*, 10633–10640.

[2] Erickson, J. A.; McLoughlin, J. I. Hydrogen Bond Donor Properties of the Difluoromethyl Group. *J. Org. Chem.* **1995**, *60*, 1626–1631.

[3] Sessler, C. D.; Rahm, M.; Becker, S.; Goldberg, J. M.; Wang, F.; Lippard, S. J. CF_2H, a Hydrogen Bond Donor. *J. Am. Chem. Soc.* **2017**, *139*, 9325–9332.

[4] Zafrani, Y.; Sod-Moriah, G.; Yeffet, D.; Berliner, A.; Amir, D.; Marciano, D.; Elias, S.; Katalan, S.; Ashkenazi, N.; Madmon, M.; Gershonov, E.; Saphier, S. CF_2H, a Functional Group-Dependant Hydrogen-Bond Donor: Is It a More or Less Lipophilic Bioisostere of OH, SH, and CH_3? *J. Med. Chem.* **2019**, *62*, 5628–5637.

[5] Geri, J. B.; Wade Wolfe, M. M.; Szymczak, N. K. The Difluoromethyl Group as a Masked Nucleophile: A Lewis Acid/Base Approach. *J. Am. Chem. Soc.* **2018**, *140*, 9404–9408.

[6] Santos, L.; Panossian, A.; Donnard, M.; Vors, J.-P.; Pazenok, S.; Bernier, D.; Leroux, F. R. Deprotonative Functionalization of the Difluoromethyl Group. *Org. Lett.* **2020**, *22*, 8741–8745.

[7] Erickson, J. A.; McLoughlin, J. I. Hydrogen Bond Donor Properties of the Difluoromethyl Group. *J. Org. Chem.* **1995**, *60*, 1626–1631.

[8] Rageot, D.; Bohnacker, T.; Melone, A.; Langlois, J.-B.; Borsari, C.; Hillmann, P.; Sele, A. M.; Beaufils, F.; Zvelebil, M.; Hebeisen, P.; Löscher, W.; Burke, J.; Fabbro, D.; Wymann, M. P. Discovery and Preclinical Characterization of 5-[4,6-Bis({3-oxa-8-azabicyclo[3.2.1]octan-8-yl})-1,3,5-triazn-2-yl]-4-(difluoromethyl)pyridine-2-amine (PQR620), a Highly Potent and Selective mTOC1/2 Inhibitor for Cancer and Neurological Disorders. *J. Med. Chem.* **2018**, *61*, 10084–10105.

[9] Singh, R. P.; Shreeve, J. M. Recent Advances in Nucleophilic Fluorination Reactions of Organic Compounds Using Deoxofluor and DAST. *Synthesis* **2002**, *17*, 2561–2578.

[10] (b) Ni, C.; Hu, M.; Hu, J. Good Partnership between Sulfur and Fluorine: Sulfur-Based Fluorination and Fluoroalkylation Reagents for Organic Synthesis. *Chem. Rev.* **2015**, *115*, 765– 825.

[11] Fujiwara, Y.; Dixon, J. A.; Rodriguez, R. A.; Baxter, R. D.; Dixon, D. D.; Collins, M. R.; Blackmond, D. G.; Baran, P. S. A New Reagent for Direct Difluoromethylation. *J. Am. Chem. Soc.* **2012**, *134*, 1494–1497.

[12] Sakamoto, R.; Kashiwagi H.; Maruoka, K. The Direct C–H Difluoromethylation of Heteroarenes Based on the Photolysis of Hypervalent Iodine(III) Reagents That Contain Difluoroacetoxy Ligands. *Org. Lett.* **2017**, *19*, 5126–5129.

[13] Xu, L.; Vivic, D. A.; Direct Difluoromethylation of Aryl Halides via Base Metal Catalysis at Room Temperature. *J. Am. Chem. Soc.*, **2016**, *138*, 2536–2539.

[14] Dang, H.; Whittaker, A. M.; Lalic, G. Catalytic activation of a single C–F bond in trifluoromethylarenes. *Chem. Sci.* **2016**, *7*, 505–509.

[15] Munoz, S. B.; Ni, C.; Zhang, Z.; Wang, F.; Shao, N.; Mathew, T.; Olah, G. A.; Prakash, G. K. S. Selective Late-Stage Hydrodefluorination of Trifluoromethylarenes: A Facile Access to Difluoromethylarenes. *Eur. J. Org. Chem.* **2017**, 2322–2326.

[16] Vogt, D. B.; Seath, C. P.; Wang, H.; Jui, N. T. Selective C–F Functionalization of Unactivated Trifluoromethylarenes. *J. Am. Chem. Soc.* **2019**, *141*, 13203–13211.

[17] Sap, J. B. I.; Straathof, N. J. W.; Knauber, T.; Meyer, C. F.; Médebielle, M.; Buglioni, L.; Genicot, C.; Trabanco, A. A.; Noël, T.; Ende, C. W. a.; Gouverneur, V. Organophotoredox Hydrodefluorination of Trifluoromethylarenes with Translational Applicability to Drug Discovery. *J. Am. Chem. Soc.* **2020**, *142*, 9181–9187.

[18] Schwesinger, R.; Schlemper, H.; Hasenfratz, C.; Willaredt, J.; Dambacher, T.; Breuer, T.; Ottaway, C.; Fletschinger, M.; Boele, J.; Fritz, H.; Putzas, D.; Rotter, H. W.; Bordwell, F. G.; Satish, A. V.; Ji, G.-Z.; Peters, E.-M.; Peters, K.; von Schnering, H. G.; Walz, L. Extremely Strong, Uncharged Auxiliary Bases; Monomeric and Polymer-Supported Polyaminophosphazenes (P_2–P_5). *Liebigs Ann.* **1996**, *1996*, 1055–1081.

[19] Araki, Y.; Kobayashi, K.; Yonemoto, M.; Kondo, Y. Functionalisation of heteroaromatic *N*-oxides using organic superbase catalyst. *Org. Biomol. Chem.* **2011**, *9*, 78–80.

[20] Ueno, M.; Yonemoto, M.; Hashimoto, M.; Wheatley, A. E. H.; Naka, H.; Kondo, Y. Nucleophilic aromatic substitution using Et_3SiH/cat. *t*-BuP4 as a system for nucleophile activation. *Chem. Commun.* **2007**, 2264–2266.

[21] Fu, Y.; Liu, L.; Li, R.-Q.; Liu, L.; Guo, Q.-X. First-Principal Predictions of Absolute pK_a's of Organic Acids in Dimethyl Sulfoxide Solution. *J. Am. Chem. Soc.* **2003**, *126*, 814–822.

[22] Experimentally calculated reduction potentials courtesy of the Shores group at CSU.

[23] Sakurai, H.; Akane, O.; Umino, H.; Kira, M. Silyl anions. IV. New convenient method of producing radical anions involving one-electron transfer from trimethylsilylsodium. *J. Am. Chem. Soc.* **1973**, *95*, 955–956.

APPENDIX ONE

BASE PROMOTED REDUCTIVE COUPLING REACTION FOR THE DIVERGENT DEFLUOROFUNCTIONALIZATION OF TRIFLUOROMETHYLARENES: EXPERIMENTAL

A1.1 General information

General reagent information. Cesium formate (Chem Impex catalog #26492), tris(trimethylsilyl)silane (Oakwood Chemical catalog #S21375), 18-crown-6 (Chem-Impex catalog #03901), cesium fluoride (Acros Organics catalog #315910250) were purchased from their respective vendors, stored in a nitrogen-filled glovebox and used as received. 2,2,6,6-Tetramethyl-1-piperidinyloxy (TEMPO) was purchased from Sigma-Aldrich (catalog #426369, purified by sublimation, 99%). 1-*tert*-Butyl-4,4,4-tris(dimethylamino)-2,2-bis[tris(dimethylamino)-phosphoranylidenamino]-2λ,4λ-catenadi(phosphazene) (P_4-*t*-Bu) was purchased from Millipore Sigma (product #79421) as a 0.8M solution in hexanes and was stored in a nitrogen-filled glovebox. Anhydrous solvents: dimethyl sulfoxide (DMSO, catalog #276855), tetrahydrofuran (THF, catalog #186562), 1,2-dimethoxyethane (DME, catalog #259527), *N*,*N*-dimethylformamide (DMF, catalog #227056), *N*-methyl-2-pyrrolidinone (NMP, catalog #328634), benzotrifluoride ($PhCF_3$, catalog #547948) and acetonitrile (MeCN, catalog #271004) were stored in a nitrogen-filled glovebox and used as received from Millipore Sigma. 4-Formylmorpholine (4FM, catalog #13380) was stored in a nitrogen-filled glovebox and used as received from Acros Organics. Tetrahydrofuran, toluene, diethyl ether, and dichloromethane solvents were deoxygenated and dried by passage over packed columns of neutral alumina and copper (II) oxide under positive pressure of nitrogen. All other commercially available reagents and solvents used in this study were purchased from Ambeed, Alfa Aesar, Combi-Blocks, Acros Organics, Oakwood Chemical,

or Millipore Sigma and used without further purification. Flash column chromatography was performed using 40-63 μm silica gel (SiliaFlash® F60 from Silicycle). Preparative thin-layer chromatography (PTLC) was performed on silica gel 60Å F_{254} plates (20 x 20 cm, 1000 μm, SiliaPlate from Silicycle, #TLG-R10011B-341) and visualized with UV light (254 nm). Unless otherwise noted, reactions were run in 1-dram vials (Fisherbrand 03-338A CG-4904-05) with a screw top PTFE-lined cap (Thermo Scientific, C4015-1A) for 0.10-0.50 mmol scale reactions, or 2-dram vials (ThermoFisher B7999-3) with a screw top cap (Thermo Scientific 15-SCST) and PTFE-lined silicone septum (Thermo Scientific B7995-15) for 1.0 mmol scale reactions.

General analytical information All new compounds were characterized by ^{1}H, ^{13}C and ^{19}F NMR spectroscopy, IR spectrometry, mass spectrometry, and melting point analysis (if solids). NMR spectra were recorded on Bruker Avance NEO or Varian Inova 400 spectrometers. Chemical shifts for ^{1}H NMR are reported as follows: chemical shift in reference to residual $CHCl_3$ at 7.26 ppm (δ ppm), multiplicity (s = singlet, br s = broad singlet, d = doublet, t = triplet, q = quartet, dd = doublet of doublets, dt = doublet of triplets, td = triplet of doublets, dq = doublet of quartets, qd = quartet of doublets, m = multiplet), coupling constant (Hz), and integration. Chemical shifts for ^{13}C NMR are reported in terms of chemical shift in reference to the $CDCl_3$ solvent signal (77.16 ppm). Chemical shifts for ^{19}F NMR are reported in terms of chemical shift in reference to an internal standard (fluorobenzene set to -112.96 ppm). IR spectra were recorded on a Thermo Scientific Nicolet iS-50 FT-IR spectrometer and are reported in terms of frequency of absorption (cm^{-1}). Melting points were measured on a Mel-Temp capillary melting point apparatus. High resolution mass spectra (HRMS) were recorded on an Agilent 6210 TOF interfaced to a DART 100 source, an Agilent 6230 LC-MS B-TOF equipped with a dual ESI source, or a GC-MS (Agilent 7890B with Agilent 5977A MSD) provided by Colorado State University Materials and Molecular

Analysis Center. Specific rotation analysis was measured on a Rudolph Research Analytical Autopol III polarimeter. Thin-layer chromatography (TLC) was performed on silica gel 60Å F_{254} plates (250 μm, SiliaPlate from Silicycle, #TLG- R10014B-323) and visualized with UV light (254 nm) or potassium permanganate stain.

Nomenclature: The names provided for the structures below were obtained from ChemDraw Professional 19.0.

Abbreviations: List of abbreviations used in this document.

TTMSS = tris(trimethylsilyl)silane

HCO_2Cs = cesium formate

TMS = trimethylsilane

Bn = benzyl

Ph = phenyl

Me = methyl

Et = ethyl

Ac = acetate

Piv = pivalate

PMP = paramethoxyphenyl

4FM = 4-formylmorpholine

A1.2 Reaction discovery and optimization with DMF as solvent

(a) Optimized reaction conditions for model substrate 3-1

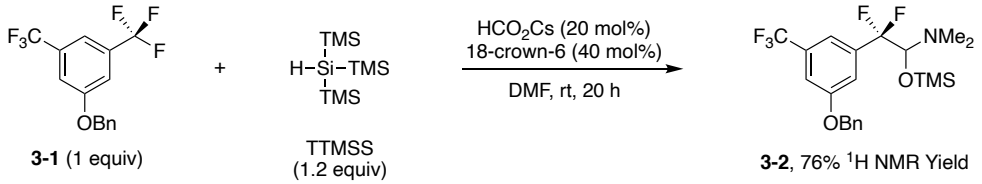

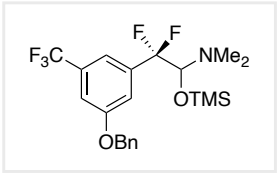

2-(3-(benzyloxy)-5-(trifluoromethyl)phenyl)-2,2-difluoro-*N*,*N*-dimethyl-1-((trimethylsilyl)oxy)ethan-1-amine (3-2). In a nitrogen-filled glovebox, to an oven-dried 1-dram glass vial charged with a Teflon-coated stir bar, was added 1-(benzyloxy)-3,5-bis(trifluoromethyl)benzene (32.0 mg, 0.1 mmol, 1.0 equiv), 18-crown-6 (10.6 mg, 0.04 mmol, 0.4 equiv), and anhydrous *N*,*N*-dimethylformamide (0.4 mL). To the solution was sequentially added tris(trimethylsilyl)silane (29.8 mg, 0.12 mmol, 1.2 equiv) and cesium formate (3.5 mg, 0.02 mmol, 0.2 equiv). The vial was capped, removed from glovebox, and the reaction solution was stirred at room temperature (rt). After 20 h, the reaction mixture was quenched with 0.1 mL $CDCl_3$, stirred for 1 min, then dibromomethane (as freshly prepared 2.0 M solution in $CDCl_3$, 50.0 µL, 0.1 mmol, 1 equiv) was added as an internal standard and an aliquot was analyzed by ^{1}H NMR spectroscopy (diagnostic peak shown in crude ^{1}H spectrum below). The ^{1}H NMR yield referenced to the dibromomethane internal standard was 76%. The compound decomposes on silica and neutral or basic alumina. Material for characterization was obtained after diluting the reaction mixture with ethyl acetate (4 mL) and washing with distilled water (3 x 3 mL) then brine (3 mL), drying over anhydrous sodium sulfate, and concentrating to provide a pale-yellow oil. **^{1}H NMR** (400 MHz, $CDCl_3$) δ 7.45–7.35 (m, 6H), 7.30–7.27 (m, 2H), 5.12 (s, 2H), 4.43 (dd, *J* = 10.6, 7.8 Hz, 1H), 2.26 (s, 6H), 0.09 (s, 9H). **^{19}F NMR** (376 MHz, $CDCl_3$) δ -62.80 (s, 3F), -104.63 (dd, *J* = 249.0, 7.7 Hz, 1F), -107.35 (dd, *J* = 249.3, 10.7 Hz, 1F). **^{13}C NMR** (101 MHz, $CDCl_3$) δ 158.8, 138.3 (t, *J* = 26.7 Hz), 136.0, 131.9 (q, *J* = 32.7 Hz), 128.8, 128.4, 127.7, 123.8 (q, *J* = 272.6 Hz), 119.9 (t, *J* = 250.2 Hz), 116.4 (t, *J* =

6.0 Hz), 116.0 (m), 113.2, 89.4 (t, J = 31.1 Hz), 70.6, 40.4, -0.1. **IR (neat):** 2956, 1737, 1672, 1357, 1250, 1043, 840, 695 (cm^{-1}). **HRMS** (DART) $[M+H]^+$ calcd. for $[C_{21}H_{27}F_5NO_2Si]^+$ 448.1726, 448.1760 found. **Note:** This is the procedure used for optimization of the reaction on a 0.1 mmol scale; for 1 mmol and 10 mmol scale reactions using this trifluoromethylarene with 4-formylmorpholine, see **Sections A1.4** and **A1.6**, respectively.

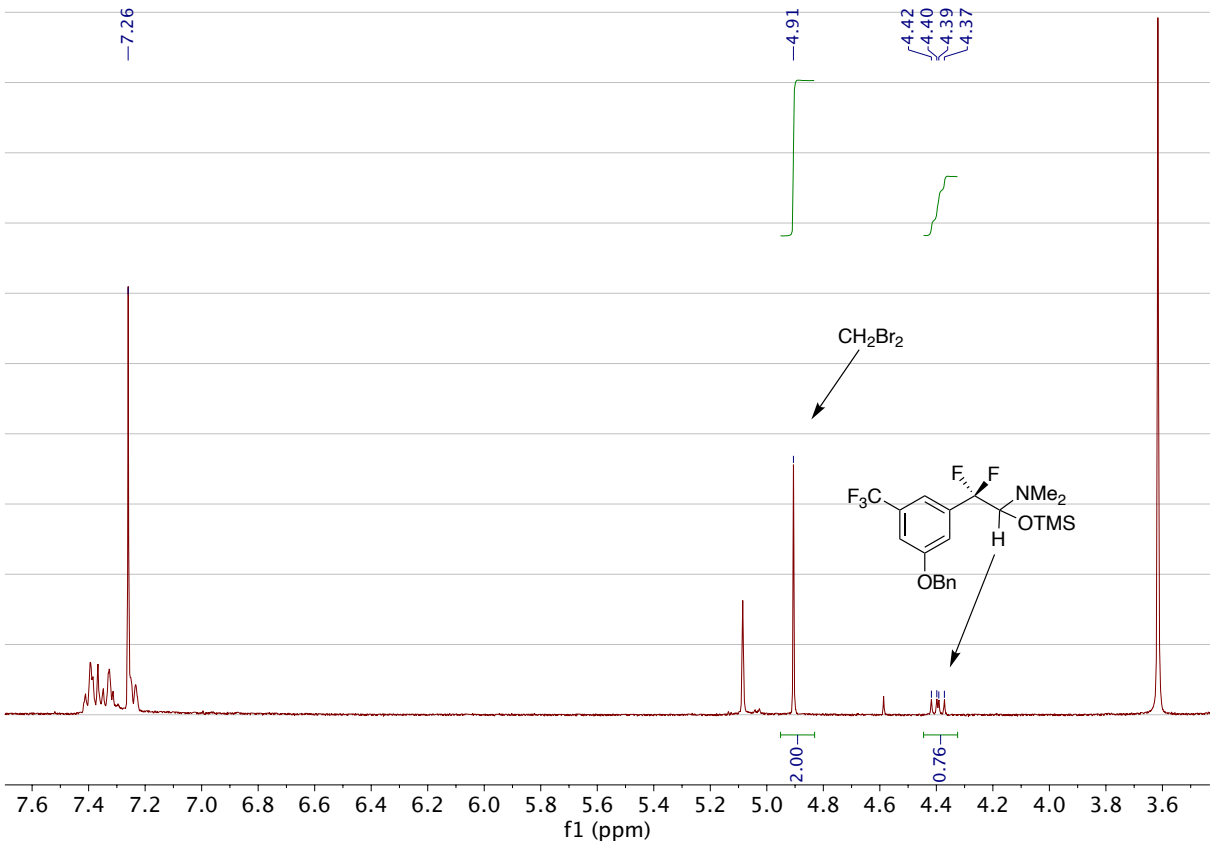

Above: Crude ^{1}H NMR spectrum showing diagnostic peak of Compound **3-2** (doublet of doublets at 4.39 ppm, 76% NMR yield) referenced to the internal standard (dibromomethane, 4.91 ppm, 0.1 mmol).

(b) Deviations from optimized reaction conditions

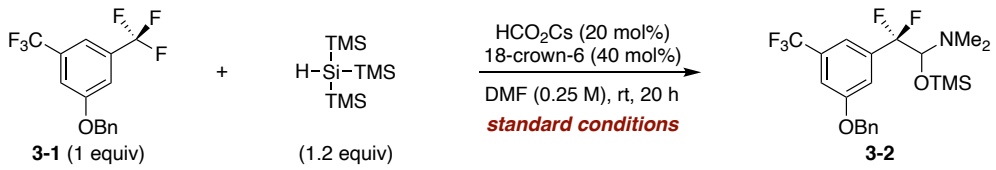

Procedure: In a nitrogen-filled glovebox, to an oven-dried 1-dram glass vial charged with a Teflon-coated stir bar, was added 1-(benzyloxy)-3,5-bis(trifluoromethyl)benzene (32.0 mg, 0.1 mmol, 1.0 equiv), 18-crown-6 (10.6 mg, 0.04 mmol, 0.4 equiv), and anhydrous *N*,*N*-dimethylformamide (0.4 mL). To the solution was sequentially added tris(trimethylsilyl)silane (29.8 mg, 0.12 mmol, 1.2 equiv), and cesium formate (3.5 mg, 0.02 mmol, 0.2 equiv). The vial was capped, removed from glovebox, and the reaction solution was stirred at rt. After 20 h, the reaction mixture was quenched with 0.1 mL $CDCl_3$, stirred for 1 min, then dibromomethane (as freshly prepared 2.0 M solution in $CDCl_3$, 50.0 µL, 0.1 mmol, 1 equiv) was added as an internal standard and an aliquot was analyzed by ^{1}H NMR spectroscopy. The ^{1}H NMR yield was referenced to dibromomethane internal standard according to the procedure described above in **Section IIa**.

Entry	Variation to above conditions	^{1}H NMR Yield (3-2)
1	None (Base = HCO_2Cs)	76%
2	Base = CsF	5%
3	Base = KOMe	30%
4	Base = HCO_2K	42%
5	Base = CsOAc	57%
6	Base = CsOPiv	19%
7	Base = Bu_4NOAc, no 18-crown-6	69%
8	No 18-crown-6	63%

9	50 mol% HCO_2Cs, no 18-crown-6	70%
10	Base = P_4-*t*-Bu, no 18-crown-6	46%
11	Base = P_4-*t*-Bu, no 18-crown-6, with 20 mol% formic acid	52%
12	Base = P_4-*t*-Bu, no 18-crown-6, with 20 mol% benzoic acid	69%
13	Base = P_4-*t*-Bu, no 18-crown-6, with 20 mol% cyclopropanecarboxylic acid	61%
14	Base = CsF, 20 mol% AcOTMS	69%
15	Base = CsF, 20 mol% $PhCO_2TMS$	73%

A1.3 Identification and optimization of a chromatographically stable hemiaminal product

a. Discussion of hemiaminal stability

The silylated hemiaminal products derived from *N*,*N*-dimethylformamide (DMF) are stable to aqueous workup but decompose when subjected to chromatography (silica or alumina). Investigation of other formamide solvents identified that the use 4-formylmorpholine (4FM) produced an adduct that was more stable to chromatography. While examining the substrate scope it became apparent that some of the 4FM hemiaminal products formed may still be sensitive to silica gel: initial purification by silica gel column chromatography for certain substrates resulted in approximately 3-10% decomposition into the difluoromethylarene and/or the aldehyde, which coelute with the desired hemiaminal product. Drying of the silica gel in a vacuum oven (120 °C for 72 h) in combination with triethylamine co-eluent and minimal time on the column typically allows isolation of product with >95% purity (as determined by ^{1}H NMR spectroscopy). The silylated hemiaminal products decompose slowly if not stored under an inert atmosphere. Storage

of **3** in a nitrogen-filled glovebox at rt showed no decomposition after three months. Conditions used for isolation is provided for each product characterized below.

b. Optimization of 4-formylmorpholine adduct 3-3

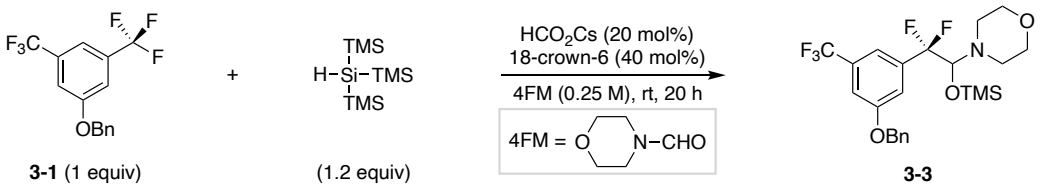

Procedure: In a nitrogen-filled glovebox, to an oven-dried 1-dram glass vial charged with a Teflon-coated stir bar, was added 1-(benzyloxy)-3,5-bis(trifluoromethyl)benzene (32.0 mg, 0.1 mmol, 1.0 equiv), 18-crown-6 (10.6 mg, 0.04 mmol, 0.4 equiv), and 4-formylmorpholine (0.4 mL). To the solution was sequentially added tris(trimethylsilyl)silane (29.8 mg, 0.12 mmol, 1.2 equiv) and cesium formate (3.5 mg, 0.02 mmol, 0.2 equiv). The vial was capped, removed from glovebox, and the reaction solution was stirred rt. After 20 h, the reaction mixture was quenched with 0.1 mL $CDCl_3$, stirred for 1 min, then dibromomethane (as freshly prepared 2.0 M solution in $CDCl_3$, 50.0 µL, 0.1 mmol, 1 equiv) was added as an internal standard and an aliquot was analyzed by ^{1}H NMR. The ^{1}H NMR yield was referenced to the dibromomethane internal standard as described above in Section IIa. Full characterization of Compound **3** is provided in **Section A1.5**.

Entry	Variation to above conditions	^{1}H NMR Yield 3
1	none	38%
2	4FM/NMP (1:1 ratio) as solvent	69% (66%)[a]
3	4FM/NMP (1:1 ratio) as solvent, 2.4 equiv TTMSS	69%
4	4FM/$PhCF_3$ (1:1 ratio) as solvent	68%

[a]Isolated yield in parenthesis, purified *via* silica gel column chromatography; see **Section A1.5** for characterization details.

A1.4 General procedure for C–F reductive hemiaminalization

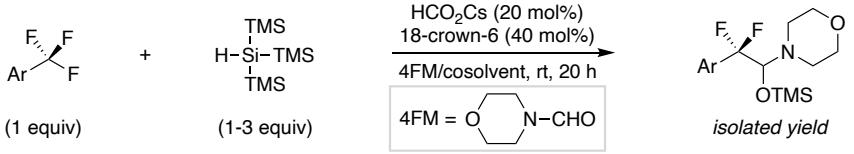

General Procedure (GP1): In a nitrogen-filled glovebox, to an oven-dried 2-dram glass vial charged with a Teflon-coated stir bar, was added trifluoromethylarene (1.0 mmol, 1 equiv), 18-crown-6 (105.7 mg, 0.4 mmol, 0.4 equiv), cesium formate (35.6 mg, 0.2 mmol, 0.2 equiv), and anhydrous solvent (either 4-formylmorpholine/*N*-methyl-2-pyrrolidinone or 4-formylmorpholine/benzotrifluoride mixture, 4.0 mL, ratio indicated for each substrate below). Tris(trimethylsilyl)silane (1-3 equiv) was then added, and the vial was capped, removed from glovebox, and the reaction mixture was stirred at rt. After 20 h, the reaction mixture was diluted with ethyl acetate (12 mL) and washed with distilled water (3 x 6 mL) [**caution:** water was added slowly due to vigorous gas evolution], then brine (8 mL), dried over anhydrous sodium sulfate, filtered, and concentrated *in vacuo*. Immediate purification by silica gel chromatography was performed using the given eluent conditions (**note:** use of silica gel that has been dried in a vacuum oven at 120 °C for 72 h was necessary for some substrates to reduce decomposition on the column and is indicated when used).

A1.5. Characterization of products from Figure 3-4

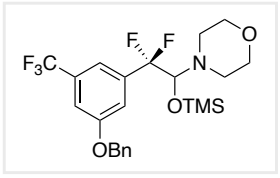

4-(2-(3-(benzyloxy)-5-(trifluoromethyl)phenyl)-2,2-difluoro-1-((trimethylsilyl)oxy)ethyl)morpholine (3-3). The General Procedure (GP1) was followed using 1-(benzyloxy)-3,5-bis(trifluoromethyl)benzene (320.2 mg, 1.0 mmol, 1 equiv), 18-crown-6 (105.7 mg, 0.4 mmol, 0.4 equiv), cesium formate (35.6

mg, 0.2 mmol, 0.2 equiv), 4-formylmorpholine/*N*-methyl-2-pyrrolidinone (1:1 ratio, 4.0 mL), and tris(trimethylsilyl)silane (298.4 mg, 1.2 mmol, 1.2 equiv). The product was isolated *via* silica gel column chromatography (5-10% ethyl acetate gradient in hexanes) as a pale-yellow oil (323.0 mg, 0.66 mmol, 66% yield). **^{1}H NMR** (400 MHz, $CDCl_3$) δ 7.47–7.35 (m, 6H), 7.30 (br s, 2H), 5.13 (s, 2H), 4.34 (dd, *J* = 10.0, 7.4 Hz, 1H), 3.62–3.54 (m, 4H), 2.61 (t, *J* = 4.6 Hz, 4H), 0.14 (s, 9H). **^{19}F NMR** (376 MHz, $CDCl_3$) δ -62.78 (s, 3F), -105.32 (dd, *J* = 248.2, 7.2 Hz, 1F), -107.31 (dd, *J* = 248.2, 10.1 Hz, 1F). **^{13}C NMR** (101 MHz, $CDCl_3$) δ 158.7, 137.8 (t, *J* = 26.5 Hz), 136.0, 131.8 (q, *J* = 32.8 Hz), 128.9, 128.5, 127.7, 123.8 (q, *J* = 272.6 Hz), 119.8 (t, *J* = 250.3 Hz), 116.5 (t, *J* = 6.5 Hz), 116.2 (m), 113.2 (m), 89.4 (t, *J* = 31.6 Hz), 70.6, 67.3, 49.0, 0.0. **IR (neat):** 2958, 2893, 2854, 1607, 1453, 1355, 1278, 1115, 840, 694 cm^{-1}. **HRMS** (DART) $[M+H]^+$ calcd. for $[C_{23}H_{29}F_5NO_3Si]^+$ 490.1831, Found: 490.1855 found.

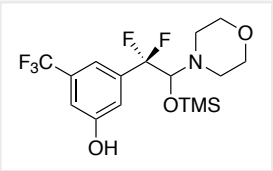

3-(1,1-difluoro-2-morpholino-2-((trimethylsilyl)oxy)ethyl)-5-(trifluoromethyl)phenol (3-4). The General Procedure (GP1) was followed using 3,5-bis(trifluoromethyl)phenol (290.1 mg, 1.0 mmol, 1 equiv), 18-crown-6 (105.7 mg, 0.4 mmol, 0.4 equiv), cesium formate (35.6 mg, 0.2 mmol, 0.2 equiv), 4-formylmorpholine/*N*-methyl-2-pyrrolidinone (1:1 ratio, 4.0 mL), and tris(trimethylsilyl)silane (522.2 mg, 2.1 mmol, 2.1 equiv). The product was isolated *via* silica gel column chromatography (15% ethyl acetate and 1% triethylamine in hexanes) as a yellow oil (230.8 mg, 0.52 mmol, 52% yield*). (**Note:** We found that this product is more stable after isolation when coeluted with triethylamine. Pure compound decomposes rapidly after purification without use of triethylamine coeluent. Product isolated and characterized as an adduct with triethylamine, 1:0.44 product/triethylamine ratio as determined by ^{1}H NMR.) *Isolated yield

determined from combined mass of mole fractions of product and triethylamine, calculation as follows: (230.8 mg isolated) / [(1 x 399.43 mg/mmol) + (0.44 x 101.19 mg/mmol)] = 0.52 mmol isolated. **^{1}H NMR** (400 MHz, $CDCl_3$) δ 10.24 (br s, 1H), 7.18 (s, 1H), 7.07–7.05 (m, 2H), 4.31 (dd, *J* = 10.5, 7.3 Hz, 1H), 3.59 (t, *J* = 4.7 Hz, 4H), 2.84 (q, *J* = 7.3 Hz, 2.6H), 2.67–2.57 (m, 4H), 1.17 (t, *J* = 7.3 Hz, 3.8H), 0.08 (s, 9H). **^{19}F NMR** (376 MHz, $CDCl_3$) δ -62.89 (s, 3F), -105.40 (dd, *J* = 247.3, 7.2 Hz, 1F), -107.47 (dd, *J* = 247.2, 10.7 Hz, 1F). **^{13}C NMR** (101 MHz, $CDCl_3$) δ 158.8, 137.7 (t, *J* = 26.3 Hz), 131.7 (q, *J* = 32.3 Hz), 124.0 (q, *J* = 272.5 Hz), 120.0 (t, *J* = 250.3 Hz), 117.9 (t, *J* = 6.3 Hz), 114.5 (m), 113.8 (m), 89.4 (t, *J* = 31.5 Hz), 67.4, 49.0, 45.5, 9.3, -0.1. **IR (neat):** 3241, 2959, 2855, 1610, 1455, 1356, 1254, 1106, 928, 842, 703 cm^{-1}. **HRMS** (DART) $[M+H]^+$ calcd. for $[C_{16}H_{23}F_5NO_3Si]^+$ 400.1362, 400.1375 found.

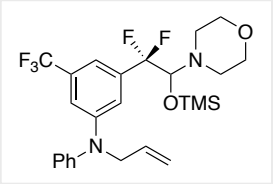

***N*-allyl-3-(1,1-difluoro-2-morpholino-2-((trimethylsilyl)oxy)ethyl)-*N*-phenyl-5-(trifluoromethyl)aniline (3-5).** The General Procedure (GP1) was followed using *N*-allyl-*N*-phenyl-3,5-bis(trifluoromethyl)aniline (345.3 mg, 1.0 mmol, 1 equiv), 18-crown-6 (105.7 mg, 0.4 mmol, 0.4 equiv), cesium formate (35.6 mg, 0.2 mmol, 0.2 equiv), 4-formylmorpholine/*N*-methyl-2-pyrrolidinone (1:1 ratio, 4 mL), and tris(trimethylsilyl)silane (497.3 mg, 2 equiv, 2 mmol). The product was isolated *via* silica gel column chromatography (1% triethylamine and 10% ethyl acetate in hexanes) as a yellow oil (282.6 mg, 0.55 mmol, 55% yield). **^{1}H NMR** (400 MHz, $CDCl_3$) δ 7.38 (t, *J* = 7.8 Hz, 2H), 7.20–7.12 (m, 6H), 5.98–5.88 (m, 1H), 5.30–5.21 (m, 2H), 4.41–4.30 (m, 3H), 3.62–3.53 (m, 4H), 2.59 (t, *J* = 4.7 Hz, 4H), 0.10 (s, 9H). **^{19}F NMR** (376 MHz, $CDCl_3$) δ -62.90 (s, 3F), -104.18 (dd, J = 247.6, 7.0 Hz, 1F), -107.66 (dd, J = 247.3, 10.1 Hz, 1F). **^{13}C NMR** (101 MHz, $CDCl_3$) δ 148.2, 146.7, 137.0 (t, *J* = 26.1 Hz), 133.2, 131.3 (q, *J* = 32.1 Hz), 130.0, 124.9, 124.8, 124.1 (q, *J* = 272.7

Hz), 119.9 (t, J = 249.9 Hz), 117.7 (t, J = 6.6 Hz), 117.2, 114.1 (m), 113.7 (m), 89.5 (t, J = 32.0 Hz), 67.3, 55.1, 49.1, 0.0. **IR (neat):** 3064, 2958, 2915, 2895, 2853, 1592, 1495, 1388, 1251, 1116, 843, 698 cm^{-1}. **HRMS** (DART) $[M+H]^+$ calcd. for $[C_{25}H_{32}F_5N_2O_2Si]^+$ 515.2148, 515.2183 found.

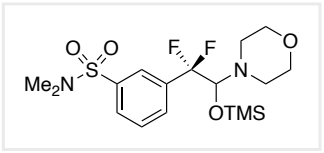

3-(1,1-difluoro-2-morpholino-2-((trimethylsilyl)oxy)ethyl)-*N*,*N*-dimethylbenzenesulfonamide (3-6). The General Procedure (GP1) was followed using *N*,*N*-dimethyl-3-(trifluoromethyl)benzenesulfonamide (253.2 mg, 1.0 mmol, 1 equiv), 18-crown-6 (105.7 mg, 0.4 mmol, 0.4 equiv), cesium formate (35.6 mg, 0.2 mmol, 0.2 equiv), 4-formylmorpholine/benzotrifluoride (1:1 ratio, 4.0 mL), and tris(trimethylsilyl)silane (298.4 mg, 1.2 mmol, 1.2 equiv). The product was isolated *via* silica gel column chromatography (vacuum oven dried silica gel, 1% triethylamine and 8% ethyl acetate in hexanes) as a pale-yellow oil (296.0 mg, 0.64 mmol, 64% yield). The purified material solidified after 3 weeks in a -20 °C freezer and a suitable crystal was extracted for analysis by x-ray crystallography. **^{1}H NMR** (400 MHz, $CDCl_3$) δ 7.90 (s, 1H), 7.81 (d, J = 7.9 Hz, 1H), 7.72 (d, J = 8.0 Hz, 1H), 7.57 (t, J = 7.8 Hz, 1H), 4.35 (dd, J = 9.6, 7.5 Hz, 1H), 3.53 (t, J = 4.7 Hz, 4H), 2.69 (s, 6H), 2.60–2.51 (m, 4H), 0.10 (s, 9H). **^{19}F NMR** (376 MHz, $CDCl_3$) δ -104.99 (dd, J = 249.7, 7.1 Hz, 1F), -107.15 (dd, J = 249.7, 9.7 Hz, 1F). **^{13}C NMR** (101 MHz, $CDCl_3$) δ 136.5 (t, J = 26.5 Hz), 135.7, 130.6 (t, J = 6.1 Hz), 129.0, 128.8, 126.0 (t, J = 6.4 Hz), 119.8 (t, J = 250.2 Hz), 89.3 (t, J = 31.7 Hz), 67.2, 48.9, 37.9, 0.0. **IR (neat):** 2965, 2848, 1456, 1338, 1249, 1160, 1018, 937, 843, 756, 700 cm^{-1}. **HRMS** (DART) $[M+H]^+$ calcd. for $[C_{17}H_{29}F_2N_2O_4SSi]^+$ 423.1580, 423.1614 found. **Melting Point:** 70-74 °C.

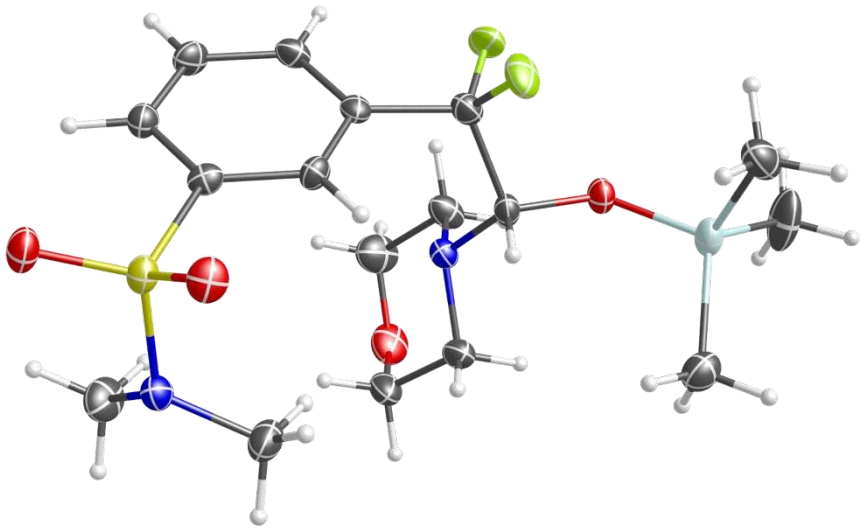

Above: X-ray crystal structure of Compound **3-6**. Thermal ellipsoids are at 50% probability. Colors of atoms are as follows: carbon (black), oxygen (red), nitrogen (blue), fluorine (green), sulfur (yellow), silicon (light blue), hydrogen (white).

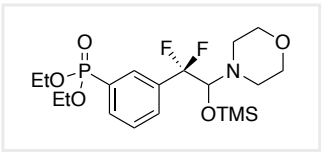

Diethyl (3-(1,1-difluoro-2-morpholino-2-((trimethylsilyl)oxy)ethyl)phenyl)phosphonate (3-7). The General Procedure (GP1) was followed using diethyl (3-(trifluoromethyl)phenyl)phosphonate (282.2 mg, 1.0 mmol, 1 equiv), 18-crown-6 (105.7 mg, 0.4 mmol, 0.4 equiv), cesium formate (35.6 mg, 0.2 mmol, 0.2 equiv), 4-formylmorpholine/*N*-methyl-2-pyrrolidinone (1:3 ratio, 4.0 mL), and tris(trimethylsilyl)silane (298.4 mg, 1.2 mmol, 1.2 equiv). The product was isolated *via* silica gel column chromatography (30-40% ethyl acetate gradient in hexanes) as a pale-yellow oil (204.8 mg, 0.45 mmol, 45% yield). **^{1}H NMR** (400 MHz, $CDCl_3$) δ 7.96–7.86 (m, 2H), 7.68 (d, J = 7.9 Hz, 1H), 7.51 (td, J = 7.7, 4.1 Hz, 1H), 4.36 (dd, J = 10.0, 7.5 Hz, 1H), 4.21–4.04 (m, 4H), 3.57 (t, J = 4.6 Hz, 4H), 2.59 (t, J = 4.6 Hz, 4H), 1.33 (t, J = 7.1 Hz, 6H), 0.11 (s, 9H). **^{19}F NMR** (376 MHz, $CDCl_3$) δ -105.30, (dd, J = 248.8, 7.6 Hz, 1F), -107.44 (dd, J = 248.9, 10.3 Hz). **^{13}C NMR** (101 MHz, $CDCl_3$) δ 135.7 (td, J = 26.2, 15.1 Hz), 133.1 (d, J = 10.0 Hz), 130.2 (td, J = 6.2, 2.9 Hz), 129.8 (dt, J = 11.7, 6.3 Hz), 128.6 (d, J = 189.4 Hz), 128.1

(d, J = 15.1 Hz), 120.1 (td, J = 250.0, 2.0 Hz), 89.3 (t, J = 31.7 Hz), 67.2, 62.2 (d, J = 5.5 Hz), 48.9, 16.4, 16.3, -0.1. **IR (neat):** 2980, 2908, 2852, 1737, 1240, 1116, 1018, 966, 869, 755 cm^{-1}. **HRMS** (DART) $[M+H]^+$ calcd. for $[C_{19}H_{33}F_2N_2O_5PSi]^+$ 452.1828, 452.1788 found.

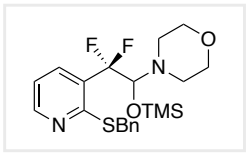

4-(2-(2-(benzylthio)pyridin-3-yl)-2,2-difluoro-1-((trimethylsilyl)oxy)ethyl)morpholine (3-8). The General Procedure (GP1) was followed using 2-(benzylthio)-3-(trifluoromethyl)pyridine (269.3 mg, 1.0 mmol, 1 equiv), 18-crown-6 (105.7 mg, 0.4 mmol, 0.4 equiv), cesium formate (35.6 mg, 0.2 mmol, 0.2 equiv), 4-formylmorpholine/benzotrifluoride (1:1 ratio, 4.0 mL), and tris(trimethylsilyl)silane (298.4 mg, 1.2 mmol, 1.2 equiv). The product was isolated *via* silica gel column chromatography (vacuum oven dried silica gel, 1% triethylamine and 3% ethyl acetate in hexanes) as a pale-yellow oil (204 mg, 0.47 mmol, 47% yield). **^{1}H NMR** (400 MHz, $CDCl_3$) δ 8.52 (d, J = 4.80 Hz, 1H), 7.67 (dd, J = 7.8, 1.8 Hz, 1H), 7.37–7.34 (m, 2H), 7.26-7.16 (m, 3H), 7.08 (dd, J = 7.8, 4.8 Hz, 1H), 4.94 (t, J = 1.0 Hz, 1H), 4.49 (dd, J = 108.1, 13.6 Hz, 2H), 3.45 (t, J = 4.8 Hz, 4H), 2.57 (ddt, J = 108.7, 11.6, 4.7, 4H), 0.03 (s, 9H). **^{19}F NMR** (376 MHz, $CDCl_3$) δ -103.04 (d, J = 256.5 Hz, 1F), -108.98 (d, J = 256.3 Hz, 1F). **^{13}C NMR** (101 MHz, $CDCl_3$) δ 155.4 (t, J = 2.1 Hz), 149.7, 138.6, 135.3 (t, J = 8.6 Hz), 129.7 (t, J = 25.8 Hz), 129.1, 128.4, 127.0, 121.0 (t, J = 253.4 Hz), 119.0, 85.6 (t, J = 27.1 Hz), 67.3, 48.4, 34.6 (t, J = 2.0 Hz), 0.1. **IR (neat):** 2958, 2849, 1580, 1559, 1401, 1261, 1117, 1059, 1029, 937, 877, 842, 752, 699 cm^{-1}. **HRMS** (DART) $[M+H]^+$ calcd. for $[C_{21}H_{29}F_2N_2O_2SSi]^+$ 439.1682, 439.1715 found.

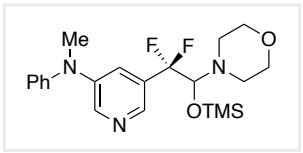

5-(1,1-difluoro-2-morpholino-2-((trimethylsilyl)oxy)ethyl)-*N*-methyl-*N*-phenylpyridin-3-amine (3-9). The General Procedure (GP1)

was followed using *N*-methyl-*N*-phenyl-5-(trifluoromethyl)pyridin-3-amine (252.2 mg, 1 mmol, 1 equiv), 18-crown-6 (105.7 mg, 0.4 mmol, 0.4 equiv), cesium formate (35.6 mg, 0.2 mmol, 0.2 equiv), 4-formylmorpholine/benzotrifluoride (1:1 ratio, 4.0 mL), and tris(trimethylsilyl)silane (298.4 mg, 1.2 mmol, 1.2 equiv). The product was isolated *via* silica gel column chromatography (vacuum oven dried silica gel, 1% triethylamine and 5% ethyl acetate in hexanes) as a dark-yellow oil (280 mg, 0.66 mmol, 66% yield). **^{1}H NMR** (400 MHz, $CDCl_3$) δ 8.29 (d, *J* = 2.8 Hz, 1H), 8.22 (d, *J* = 1.8 Hz, 1H), 7.39–7.35 (m, 2H), 7.27–7.26 (m, 1H), 7.17–7.11 (m, 3H), 4.33 (dd, *J* = 9.2, 7.8 Hz, 1H), 3.61–3.52 (m, 4H), 3.35 (s, 3H), 2.63–2.55 (m, 4H), 0.12 (s, 9H). **^{19}F NMR** (376 MHz, $CDCl_3$) δ -104.38 (dd, *J* = 252.5, 7.7 Hz, 1F), -107.30 (dd, *J* = 252.5, 9.1 Hz, 1F). **^{13}C NMR** (101 MHz, $CDCl_3$) δ 147.5, 144.5, 140.5, 138.2 (t, *J* = 6.8 Hz), 131.0 (t, *J* = 25.8 Hz), 130.0, 124.5, 123.7, 121.6 (t, *J* = 6.4 Hz), 119.7 (t, *J* = 249.8 Hz), 89.5 (t, *J* = 31.91 Hz), 67.3, 49.0, 40.2, 0.1. **IR (neat):** 2956, 2850, 1588, 1495, 1353, 1251, 1114, 1068, 1010, 869, 754, 698 cm^{-1}. **HRMS** (DART) $[M+H]^+$ calcd. for $[C_{21}H_{30}F_2N_3O_2Si]^+$ 422.2070, 422.2097 found.

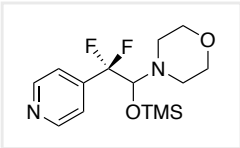

4-(2,2-difluoro-2-(pyridin-4-yl)-1-((trimethylsilyl)oxy)ethyl)morpholine (3-10). The General Procedure (GP1) was followed using 4-(trifluoromethyl)pyridine (147.1 mg, 1.0 mmol, 1 equiv), 18-crown-6 (105.7 mg, 0.4 mmol, 0.4 equiv), cesium formate (35.6 mg, 0.2 mmol, 0.2 equiv), 4-formylmorpholine/*N*-methyl-2-pyrrolidinone (1:3 ratio, 4 mL), and tris(trimethylsilyl)silane (497.3 mg, 2 equiv, 2 mmol). The reaction vial was placed into a preheated reaction block at 80 °C with stirring. The product was isolated *via* silica gel column chromatography (1% triethylamine and 10% ethyl acetate in hexanes) as a pale-yellow oil (175.6 mg, 0.55 mmol, 55% yield). **^{1}H NMR** (400 MHz, $CDCl_3$) δ 8.67 (d, *J* = 6.1 Hz, 2H), 7.39 (d, *J* = 6.1 Hz, 2H), 4.33 (t, *J* = 9.0 Hz, 1H), 3.59–3.51 (m,

4H), 2.64–2.56 (m, 4H), 0.11 (s, 9H). **^{19}F NMR** (376 MHz, $CDCl_3$) δ -107.95 (dd, *J* = 250.9, 8.0 Hz, 1F), -109.05 (dd, *J* = 250.9, 9.9 Hz, 1F). **^{13}C NMR** (101 MHz, $CDCl_3$) δ 149.8, 143.6 (t, *J* = 27.0 Hz), 121.0 (t, *J* = 6.0 Hz), 119.4 (t, *J* = 249.8 Hz), 89.2 (t, *J* = 30.8 Hz), 67.3, 48.9, 0.0. **IR (neat):** 2958, 2852, 1603, 1411, 1251, 1113, 1059, 967, 841, 675 cm^{-1}. **HRMS** (ESI) $[M+H]^+$ calcd. for $[C_{14}H_{23}F_2N_2O_2Si]^+$ 317.1491, 317.1452 found.

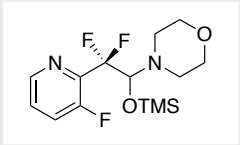

4-(2,2-difluoro-2-(3-fluoropyridin-2-yl)-1-((trimethylsilyl)oxy)ethyl)morpholine (3-11). The General Procedure (GP1) was followed using 3-fluoro-2-(trifluoromethyl)pyridine (165.1 mg, 1.0 mmol), 18-crown-6 (105.7 mg, 0.4 mmol, 0.4 equiv), cesium formate (35.6 mg, 0.2 mmol, 0.2 equiv), 4-formylmorpholine/benzotrifluoride (1:1 ratio, 4.0 mL), and tris(trimethylsilyl)silane (497.3 mg, 2 equiv, 2 mmol). The product was isolated *via* silica gel column chromatography (vacuum oven dried silica gel, 1% triethylamine and 10% ethyl acetate in hexanes) as a pale-yellow oil (136.2 mg, 0.41 mmol, 41% yield). **^{1}H NMR** (400 MHz, $CDCl_3$) δ 8.44 (d, *J* = 4.5, Hz, 1H), 7.46 (t, *J* = 9.4 Hz, 1H), 7.40–7.36 (m, 1 H), 4.75 (t, *J* = 11.2 Hz, 1H), 3.53–3.44 (m, 4H), 2.73 (ddt, *J* = 103.7, 11.6, 4.7 Hz, 2H), 0.12 (s, 9H). **^{19}F NMR** (376 MHz, $CDCl_3$) δ -104.77 (ddd, *J* = 260.8, 20.7, 10.5 Hz, 1F), -114.20 (ddd, *J* = 260.7, 20.5, 12.2 Hz, 1F), -121.89 (tdd, *J* = 20.6, 10.4, 4.0 Hz, 1F). **^{13}C NMR** (101 MHz, $CDCl_3$) δ 157.5 (d, *J* = 264.1 Hz), 144.6 (d, *J* = 5.2 Hz), 142.0 (td, *J* = 27.0, 11.0 Hz), 126.3 (d, *J* = 4.3 Hz), 124.6 (d, *J* = 20.0 Hz), 119.2 (td, *J* = 250.0, 5.5 Hz), 87.9 (ddd, *J* = 30.1, 24.9, 2.4 Hz), 67.3, 48.5, 0.1. **IR (neat):** 2958, 2853, 1452, 1252, 1116, 1071, 1017, 939, 842 cm^{-1}. **HRMS** (ESI) $[M\text{-}OSiMe_3]^+$ calcd. for $[C_{11}H_{12}F_3N_2O]^+$ 245.0896, 245.0889 found.

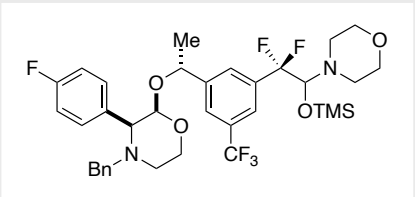

(2*R*,3*S*)-4-benzyl-2-((1*R*)-1-(3-(1,1-difluoro-2-morpholino-2-((trimethylsilyl)oxy)ethyl)-5-(trifluoromethyl)phenyl)ethoxy)-3-(4-fluorophenyl)morpholine (3-12). The General Procedure (GP1) was followed at a 0.25 mmol scale with (2*R*,3*S*)-4-benzyl-2-((*R*)-1-(3,5-bis(trifluoromethyl)phenyl)ethoxy)-3-(4-fluorophenyl)morpholine (131.0 mg, 0.25 mmol, 1 equiv), 18-crown-6 (26.4 mg, 0.1 mmol, 0.4 equiv), cesium formate (8.9 mg, 0.05 mmol, 0.2 equiv), and 4-formylmorpholine/*N*-methyl-2-pyrrolidinone (1:1 ratio, 1.0 mL), and tris(trimethylsilyl)silane (93.2 mg, 1.5 equiv, 0.375 mmol). After 15 h, the vial was brought into the glovebox and charged with another portion of tris(trimethylsilyl)silane (74.6 mg, 1.2 equiv, 0.3 mmol) and cesium formate (8.9 mg, 0.05 mmol, 0.2 equiv), then capped and stirred for another 5 h at rt. The product was isolated *via* silica gel chromatography (1% triethylamine and 10% ethyl acetate in hexanes) as a yellow oil (76.6 mg, 0.11 mmol, 44% yield). **^{1}H NMR** (400 MHz, $CDCl_3$) δ 7.53–7.43 (m, 3H), 7.30–7.19 (m, 5H), 7.16 (d, *J* = 6.2 Hz, 1H), 7.00 (q, *J* = 8.2 Hz, 2H), 6.89 (d, *J* = 5.4 Hz, 1H), 4.80 (qd, *J* = 6.5, 4.0 Hz, 1H), 4.31 (t, *J* = 3.2 Hz, 1H), 4.23–4.17 (m, 2H), 3.76 (d, *J* = 13.4 Hz, 1H), 3.56–3.53 (m, 5H), 3.39 (t, *J* = 2.9 Hz, 1H), 2.81 (d, *J* = 13.5 Hz, 2H), 2.60–2.51 (m, 4H), 2.31 (td, *J* = 11.9, 3.4 Hz, 1H), 1.42 (d, *J* = 6.5 Hz, 3H), 0.04 (d, *J* = 3.6 Hz, 9H). **^{19}F NMR** (376 MHz, $CDCl_3$) δ -62.70 (s, 3F), -104.98 (ddd, *J* = 248.8, 35.7, 6.7 Hz, 1F), -108.79 (ddd, *J* = 318.6, 248.8, 11.0 Hz), -114.73–114.77 (m, 1F). **^{13}C NMR** (101 MHz, $CDCl_3$) δ 162.6 (dd, *J* = 246.1, 4.7 Hz), 144.3 (d, *J* = 13.4 Hz), 138.0 (d, *J* = 2.1 Hz), 136.2 (t, *J* = 26.2 Hz), 133.8 (d, *J* = 3.2 Hz), 131.0–130.9 (m), 130.8 (qd, *J* = 32.6, 6.6 Hz), 129.1, 128.4, 127.8 (q, *J* = 6.3 Hz), 127.2, 124.0 (m), 123.7 (q, *J* = 272.7 Hz), 122.9 (m), 120.0 (td, *J* = 250.4, 5.3 Hz), 115.1 (dd, *J* = 21.3, 4.4 Hz), 95.6 (d, *J* = 8.0 Hz), 89.2 (t, *J* = 31.5 Hz), 72.5, 69.5, 69.4, 67.4, 59.8, 59.7, 51.9, 49.0, 24.8, 24.6, 0.0. **IR (neat):** 2957,

2918, 2853, 2801, 1509, 1263, 1115, 1058, 836, 697 cm^{-1}. **HRMS** (DART) $[M+H]^+$ calcd. for $[C_{35}H_{43}F_6N_2O_4Si]^+$ 697.2891, 697.2908 found.

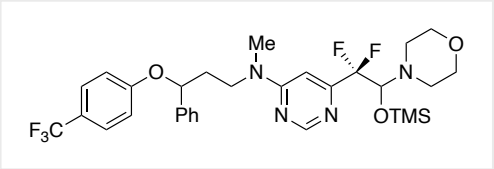

6-(1,1-difluoro-2-morpholino-2-((trimethylsilyl)oxy)ethyl)-*N*-methyl-*N*-(3-phenyl-3-(4-(trifluoromethyl)phenoxy)propyl)pyrimidin-4-amine (3-13). The General Procedure (GP1) was followed on a 0.25 mmol scale with *N*-methyl-*N*-(3-phenyl-3-(4-(trifluoromethyl)phenoxy)propyl)-6-(trifluoromethyl)pyrimidin-4-amine (113.9 mg, 0.25 mmol, 1 equiv), 18-crown-6 (26.4 mg, 0.1 mmol, 0.4 equiv), cesium formate (8.9 mg, 0.05 mmol, 0.2 equiv), 4-formylmorpholine/benzotrifluoride (1:1 ratio, 1.0 mL), and tris(trimethylsilyl)silane (74.6 mg, 1.2 equiv, 0.3 mmol). The reaction vial was placed into a preheated reaction block at 80 °C with stirring. The product was isolated *via* silica gel chromatography (1% triethylamine and 20% ethyl acetate in hexanes) as a dark-yellow oil (67.0 mg, 0.11 mmol, 43% yield).**^{1}H NMR** (400 MHz, $CDCl_3$) δ 8.55–8.51 (m, 1H), 7.43 (d, J = 8.5 Hz, 2H), 7.36–7.25 (m, 5H), 6.89 (d, J = 8.4 Hz, 2H), 6.67–6.66 (m, 1H), 5.21–5.17 (m, 1H), 4.82 (t, J = 11.3 Hz, 1H), 3.80–3.58 (m, 6H), 3.09 (br s, 3H), 2.89–2.69 (m, 4H), 2.30–2.14 (m, 2H), 0.07 (d, J = 4.62 Hz, 9H). **^{19}F NMR** (376 MHz, $CDCl_3$) δ -61.60 (s, 3F), -113f.54–115.26 (m, 2F). **^{13}C NMR** (101 MHz, $CDCl_3$) δ 162.0, 160.3, 158.2, 140.5, 129.1, 128.3, 127.0 (m), 125.7, 124.4 (q, J = 271.0 Hz), 123.4, 121.6, 119.1 (m), 115.8, 98.9 (t, J = 5.1 Hz), 87.0 (td, J = 26.5, 3.9 Hz), 78.0, 67.5, 48.6, 46.7, 46.6, 36.3, 36.2, 0.1. (**Note:** broad ^{13}C signals at 140.5 and 78.0 ppm likely due to C–N rotamers at the N-pyrimidine bond). **IR (neat):** 2958, 2854, 1603, 1516, 1326, 1111, 1067, 837, 701 cm^{-1}. **HRMS** (DART) $[M+H]^+$ calcd. for $[C_{30}H_{38}F_5N_4O_3Si]^+$ 625.2628, 625.2616 found.

A1.6 Preparative scale (10 mmol) synthesis of product 3-3

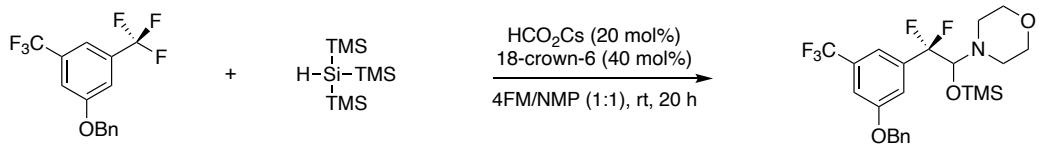

3-1, 10 mmol (1 equiv) (1.2 equiv) **3-3**, 2.6 g, 52% yield

Procedure: The following procedure was conducted without an inert atmosphere glovebox. To an oven-dried 100 mL round-bottom flask charged with a Teflon-coated stir bar was added 1-(benzyloxy)-3,5-bis(trifluoromethyl)benzene (3.20 g, 10.0 mmol, 1 equiv), 18-crown-6 (1.06 g, 4.0 mmol, 0.4 equiv), and cesium formate (356 mg, 2.0 mmol, 0.2 equiv). The flask was capped with a rubber septum and placed under vacuum and then filled with nitrogen (this operation was repeated three times) on a Schlenk manifold. 4-Formylmorpholine/*N*-methyl-2-pyrrolidinone (anhydrous, 1:1 ratio, 40 mL) was then added *via* syringe, and the reaction mixture was stirred at rt for 15 min. Tris(trimethylsilyl)silane (3.7 mL, 12.0 mmol, 1.2 equiv) was next added slowly *via* syringe. A nitrogen balloon was inserted into the septum and the Schlenk manifold nitrogen line was removed. The reaction mixture was then stirred at rt. After 20 h, the reaction mixture was slowly quenched with a few drops of water while stirring, transferred to a separatory funnel and diluted with ethyl acetate (180 mL). The mixture was then washed with distilled water (3 x 40 mL), then brine (2 x 50 mL), dried over anhydrous sodium sulfate, filtered, and concentrated *in vacuo*. The product was isolated *via* silica gel column chromatography (10% ethyl acetate in hexanes) as a yellow oil (2.6 g, 5.2 mmol, 52% yield). The characterization data matched the information provided in **Section A1.5** for Compound **3**.

A1.7 Derivatization and characterization of products from Figures 3-6 and 3-7

a. Derivatizations of Compound 3-3 (Figure 3-6)

Discussion: There can be competing reactivity from the silylated hemiaminal between the iminium and oxocarbenium modes of reactivity. Transformation to the hemiacetal (see figure below) allows selective access to the reactivity of an aldehyde.

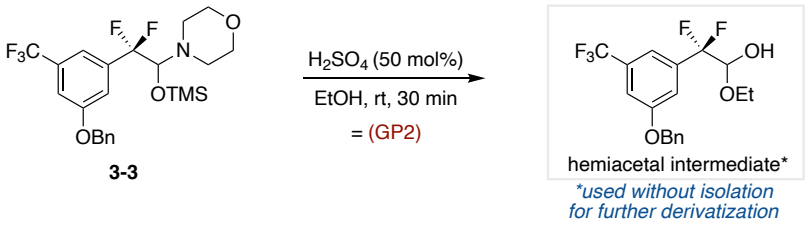

General procedure 2 for accessing hemiacetal intermediate (GP2). This general procedure was used for the formation of a hemiacetal intermediate as an entry for several derivatizations shown below. Open to air, to an oven-dried 1-dram vial charged with a Teflon-coated stir bar was added **3-3** (122.4 mg, 0.25 mmol, 1 equiv), ethanol (1 mL), and sulfuric acid (6.7 µL, 0.125 mmol, 0.5 equiv). The vial was capped and the mixture was stirred at rt for 30 min. At that time, the solution was used directly for the subsequent derivatization step as described below.

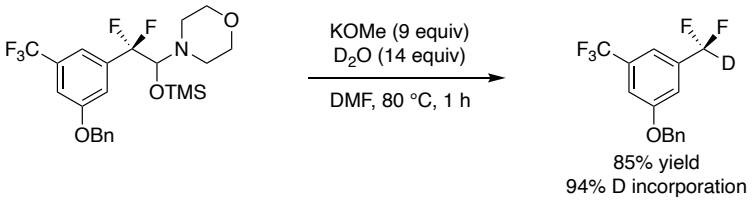

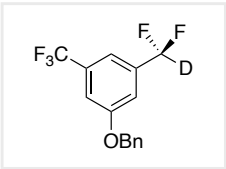

1-(benzyloxy)-3-(difluoromethyl-*d*)-5-(trifluoromethyl)benzene (3-30). Open to air, to an oven-dried 1-dram vial charged with a Teflon-coated stir bar was added **3-3** (122.4 mg, 0.25 mmol, 1 equiv) and anhydrous *N,N*-dimethylformamide (1 mL), followed by potassium methoxide (157.8 mg, 2.25 mmol, 9 equiv) then deuterium oxide (62.5 µL, 3.5 mmol, 14 equiv). The vial was capped and placed into a preheated reaction block at 80 °C with stirring. After 1 h, the reaction mixture was transferred to

a separatory funnel with ethyl acetate (10 mL), washed with water (5 x 4 mL), and brine (5 mL), then dried over anhydrous sodium sulfate, filtered, and concentrated *in vacuo*. Purification *via* silica gel column chromatography (100% hexanes) afforded the product with 94% deuterium incorporation (determined by ^{19}F NMR, see spectrum labelled below) as a clear oil (64.8 mg, 85% yield). **^{1}H NMR** (400 MHz, $CDCl_3$) δ 7.47–7.37 (m, 6H), 7.34 (br s, 1H), 7.31 (br s, 1H), 5.13 (s, 2H); **^{19}F NMR** (376 MHz, $CDCl_3$) δ -62.94 (s, 3F), -112.56 (t, J = 8.6 Hz, 2F); **^{13}C NMR** (101 MHz, $CDCl_3$) δ 159.4, 136.8 (t, J = 23.1 Hz), 135.8, 132.8 (q, J = 33.0 Hz), 128.9, 128.6, 127.8, 123.6 (q, J = 272.5 Hz), 115.4 (t, J = 5.9 Hz), 115.1 (dt, J = 10.2, 4.9 Hz), 114.3 (m), 113.4 (t, J = 28.7 Hz), 70.8; (**Note:** $–CF_2D$ carbon is not easily observable in ^{13}C NMR; a small 1:1:1 triplet is observed at 113.4 ppm). **IR (neat):** 3036, 2927, 1607, 1455, 1359, 1253, 1120, 1026, 862, 737, 695 cm^{-1}. **GC-MS (EI)** M^+ calcd. for $[C_{15}H_{10}DF_5O]^+$ 303.08, 303.10 found. **^{2}H NMR** (62 MHz, CH_3CN) δ 6.60 (t, J = 8.6 Hz, 0.94D).

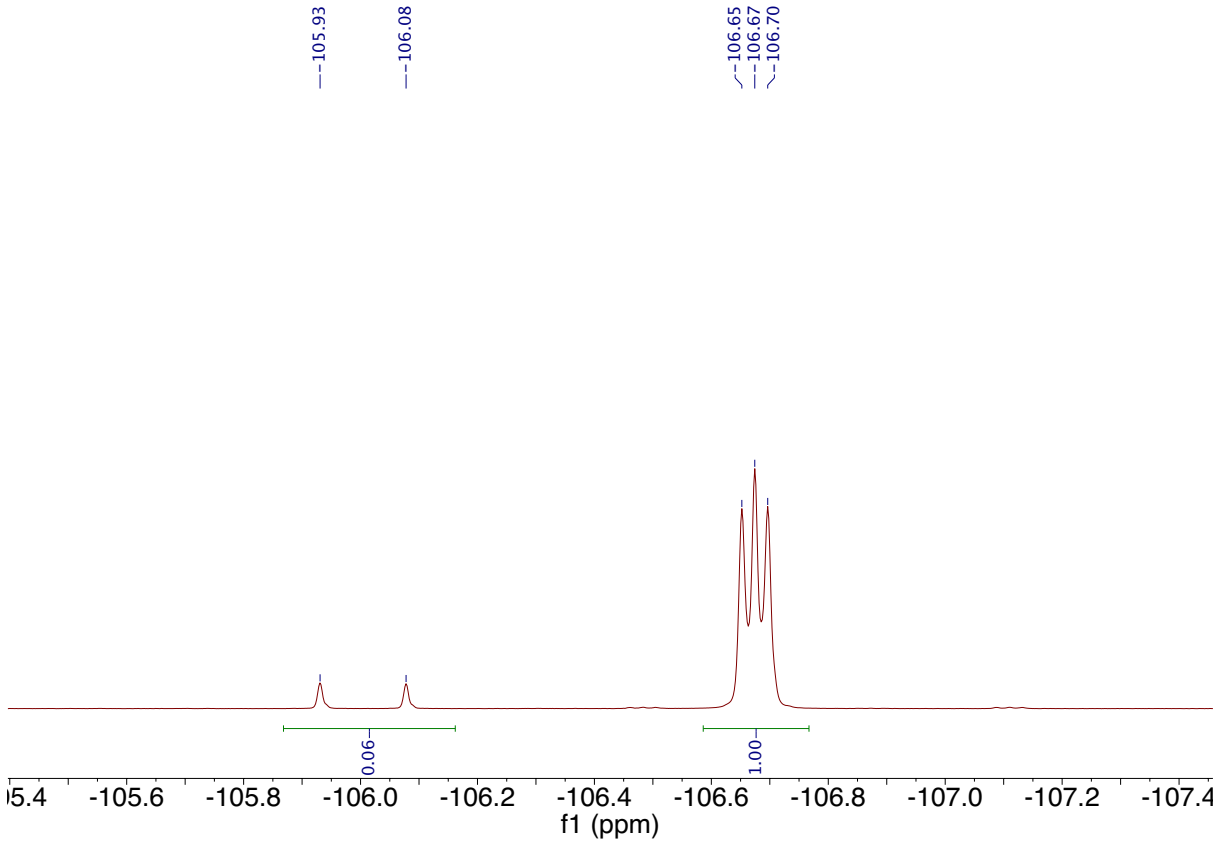

Above: ^{19}F NMR spectrum of Compound **3-30** (in DMSO-d_6) showing the deuterated compound ($ArCF_2D$) triplet at -106.67 ppm and the protonated compound ($ArCF_2H$) doublet at -106.00 ppm showing 94% deuterium incorporation (1.00/1.06 = 94%).

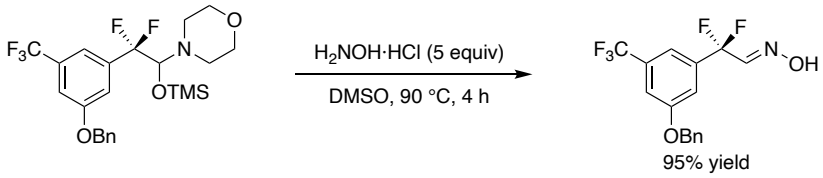

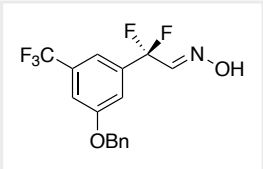

(*E*)-2-(3-(benzyloxy)-5-(trifluoromethyl)phenyl)-2,2-difluoroacetaldehyde oxime (3-14). Open to air, to an oven-dried 1-dram vial charged with a Teflon-coated stir bar was added **3-3** (122.4 mg, 0.25 mmol, 1 equiv), dry dimethyl sulfoxide (1 mL), and hydroxylamine hydrochloride (86.7 mg, 5 equiv, 1.25 mmol). The vial was capped and placed into a preheated reaction block at 90 °C for 4 h with stirring. The reaction mixture was then cooled to rt, transferred to a separatory funnel with

ethyl acetate (12 mL), washed with water (5 mL x 5), and brine (6 mL), then concentrated *in vacuo*. The resulting residue was dissolved in acetonitrile (6 mL), washed with hexanes (5 mL), then dried over anhydrous sodium sulfate, filtered, and concentrated *in vacuo* to provide the product as an off-white solid (82.4 mg, 95% yield). **^{1}H NMR** (400 MHz, $CDCl_3$) δ 8.10 (br s, 1H), 7.70 (td, J = 4.7, 1.4 Hz, 1H), 7.45–7.35 (m, 6H), 7.33 (s, 1H), 7.30 (s, 1H), 5.12 (s, 2H). **^{19}F NMR** (376 MHz, $CDCl_3$) δ -62.88 (s, 3F), -94.67 (d, J = 4.7 Hz, 2F). **^{13}C NMR** (101 MHz, $CDCl_3$) δ 159.1, 146.1 (t, J = 36.6 Hz), 136.6 (t, J = 26.6 Hz), 135.7, 132.6 (q, J = 33.1 Hz), 128.9, 128.6, 127.8, 123.5 (q, J = 272.5 Hz), 116.5 (t, J = 239.5 Hz), 116.1 (t, J = 5.8 Hz), 115.3 (m), 114.1 (m), 70.8. **IR (neat):** 3299, 3094, 3068, 2932, 1605, 1451, 1366, 1269, 1125, 1062, 979, 736, 693 cm^{-1}. **HRMS** (DART) $[M+H]^+$ calcd. for $[C_{16}H_{13}F_5NO_2]^+$ 346.0861, 346.0889 found. **Melting Point:** 67-70 °C.

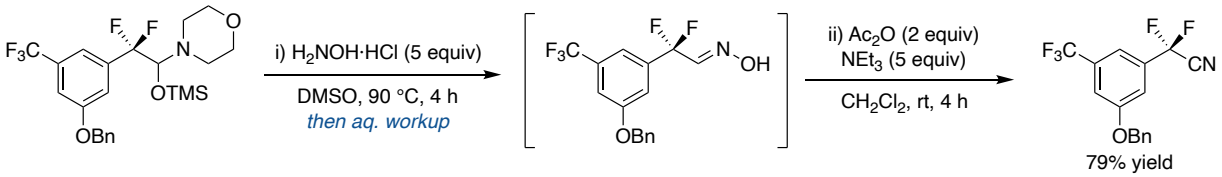

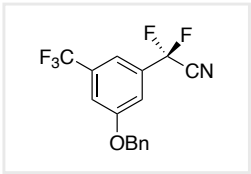

2-(3-(benzyloxy)-5-(trifluoromethyl)phenyl)-2,2-difluoroacetonitrile (3-15). Open to air, to an oven-dried 1-dram vial charged with a Teflon-coated stir bar was added **3-3** (122.4 mg, 0.25 mmol, 1 equiv), dimethyl sulfoxide (1 mL), and hydroxylamine hydrochloride (86.7 mg, 5 equiv, 1.25 mmol). The vial was capped and placed into a preheated reaction block at 90 °C for 4 h with stirring. The reaction mixture was then cooled to rt, transferred to a separatory funnel with ethyl acetate (12 mL), washed with water (5 mL x 5), and brine (6 mL), then concentrated *in vacuo*. The resulting residue was dissolved in dichloromethane (2.0 mL) and transferred to a 1-dram vial with a Teflon-coated stir bar. Triethylamine (177.2 µL, 5 equiv, 1.25 mmol) and acetic anhydride (47.3 µL, 2 equiv, 0.5 mmol) were added to the reaction mixture and then the vial was capped and stirred at rt. After 4 h,

the reaction mixture was then transferred to a separatory funnel and diluted with ethyl acetate (15 mL), washed with H_2O (5 mL) and brine (5 mL), then dried over anhydrous sodium sulfate, filtered, and concentrated *in vacuo*. The resulting residue was dissolved in acetonitrile (10 mL), washed with hexanes (5 mL), then dried over anhydrous sodium sulfate, filtered, and concentrated *in vacuo* to provide the product as dark red-brown oil (64.6 mg, 79% yield, 0.20 mmol). **^{1}H NMR** (400 MHz, $CDCl_3$) δ 7.52 (s, 1H), 7.46–7.37 (m, 7H), 5.16 (s, 2H). **^{19}F NMR** (376 MHz, $CDCl_3$) δ -63.06 (s, 3F), -84.14 (s, 2F). **^{13}C NMR** (101 MHz, $CDCl_3$) δ 159.8, 135.2, 133.7 (t, *J* = 25.8 Hz), 133.6 (q, *J* = 33.6 Hz), 129.0, 128.8, 127.8, 123.1 (q, *J* = 273.0 Hz), 116.1 (tq, *J* = 3.6, 1.9 Hz), 115.3 (t, *J* = 5.1 Hz), 114.4 (dp, 7.6, 4.1 Hz), 112.1 (t, *J* = 47.8 Hz), 107.9 (t, *J* = 244.6 Hz), 71.1. **IR (neat):** 3067, 3036, 2932, 2259, 1607, 1454, 1357, 1249, 1129, 1008, 868, 736, 695 cm^{-1}. **GC-MS** (ESI) M^+ calcd. for $[C_{16}H_{11}F_5NO]^+$ 327.07, 327.05 found.

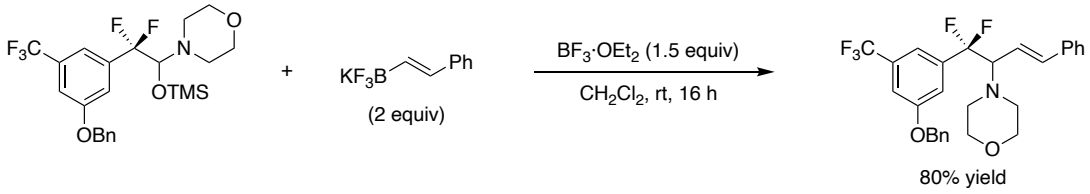

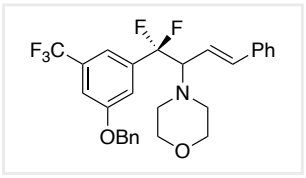

(*E*)-4-(1-(3-(benzyloxy)-5-(trifluoromethyl)phenyl)-1,1-difluoro-4-phenylbut-3-en-2-yl)morpholine (3-18) This procedure was adapted from a previous report.[1] Open to air, to an oven-dried 1-dram vial charged with a Teflon-coated stir bar was added **3-3** (122.4 mg, 0.25 mmol, 1 equiv), potassium *trans*-styryltrifluoroborate (105.0 mg, 0.5 mmol, 2 equiv), and dry dichloromethane (1.5 mL). Boron trifluoride diethyl etherate (46.3 µL, 0.375 mmol, 1.5 equiv) was then added, the vial was capped, and the reaction mixture stirred overnight at rt. The reaction mixture was then transferred to a separatory funnel with dichloromethane (12 mL), washed with water (6 mL), then brine (6

mL), dried over anhydrous sodium sulfate, filtered, and concentrated *in vacuo*. Purification *via* silica gel column chromatography (10% ethyl acetate in hexanes) afforded the product as a pale-yellow oil (101.6 mg, 80% yield). **^{1}H NMR** (400 MHz, $CDCl_3$) δ 7.40–7.18 (m, 13H), 6.55 (d, *J* = 15.9 Hz, 1H), 6.25 (dd, *J* = 15.9, 9.3 Hz, 1H), 5.07 (s, 2H), 3.57–3.49 (m, 4H), 3.40 (dt, *J* = 18.1, 9.5 Hz, 1H), 2.71 (dt, *J* = 10.1, 4.5 Hz, 2H), 2.43 (dt, *J* = 10.5, 4.6 Hz, 2H). **^{19}F NMR** (376 MHz, $CDCl_3$) δ -62.67 (s, 3F), -96.05 (dd, *J* = 250.7, 9.2 Hz, 1F), -105.65 (dd, *J* = 250.6, 17.9 Hz, 1F). **^{13}C NMR** (101 MHz, $CDCl_3$) δ 158.8, 139.1 (t *J* = 26.9 Hz), 137.8, 136.2, 135.9, 131.8 (q, *J* = 32.8 Hz), 128.9, 128.8, 128.5, 128.4, 127.7, 126.8, 123.8 (q, *J* = 272.7 Hz), 121.8 (dd, *J* = 247.9, 251.4 Hz), 119.7, 116.1 (t, *J* = 6.4 Hz), 115.8 (m), 113.0 (m), 72.9 (dd, *J* = 30.5, 24.8 Hz), 70.7, 67.3, 51.0. **IR (neat):** 3031, 2962, 2855, 1607, 1452, 1358, 1266, 1169, 1120, 1007, 861, 694 cm^{-1}. **HRMS** (DART) $[M+H]^+$ calcd. for $[C_{28}H_{27}F_5NO_2]^+$ 504.1956, 504.1989 found.

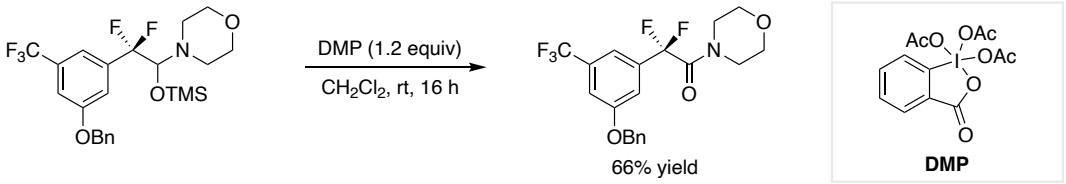

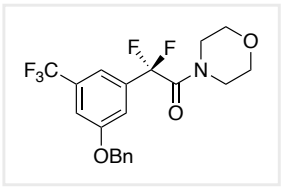

2-(3-(benzyloxy)-5-(trifluoromethyl)phenyl)-2,2-difluoro-1-morpholinoethan-1-one (3-17). Open to air, to an oven-dried 1-dram vial charged with a Teflon-coated stir bar was added **3-3** (122.4 mg, 0.25 mmol, 1 equiv) and dry dichloromethane (2 mL), followed by 1,1,1-tris(acetyloxy)-1,1-dihydro-1,2-benziodoxol-3-(1*H*)-one (DMP, 127.2 mg, 0.3 mmol, 1.2 equiv). The vial was capped and the reaction mixture was stirred at rt overnight. The reaction mixture was then transferred to a separatory funnel with dichloromethane (10 mL) and washed with 1 M aq. sodium hydroxide (8 mL), then brine (6 mL), dried over anhydrous sodium sulfate, filtered, and concentrated *in vacuo*.

Purification *via* silica gel column chromatography (10% ethyl acetate in hexanes) afforded the product as a clear oil (68.2 mg, 66% yield). **^{1}H NMR** (400 MHz, $CDCl_3$) δ 7.44–7.35 (m, 7H), 7.30 (s, 1H), 5.13 (s, 2H), 3.71–3.67 (m, 4H), 3.55 (br s, 4H). **^{19}F NMR** (376 MHz, $CDCl_3$) δ -62.87 (s, 3F), -95.29 (s, 2F). **^{13}C NMR** (101 MHz, $CDCl_3$) δ 161.5 (t, J = 30.2 Hz), 159.3, 136.2 (t, J = 25.4 Hz) 135.7, 132.8 (q, J = 33.2 Hz), 128.9, 128.6, 127.8, 123.4 (q, J = 272.7 Hz), 115.5 (t, J = 5.9 Hz), 115.3 (t, J = 253.8 Hz), 114.7 (m), 114.5 (m), 70.8, 66.8, 66.6, 46.7 (t, J = 4.2 Hz), 43.8. **IR (neat):** 2967, 2925, 2858, 1671, 1452, 1355, 1274, 1114, 998, 867, 696 cm^{-1}. **HRMS** (ESI) $[M+H]^+$ calcd. for $[C_{20}H_{19}F_5NO_3]^+$ 416.1280, 416.1283 found.

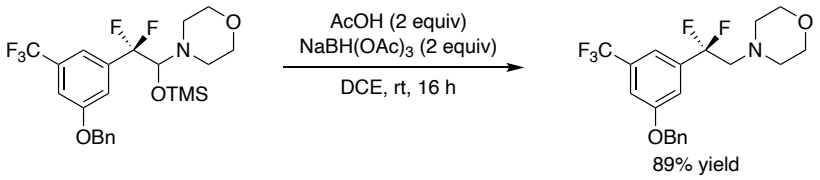

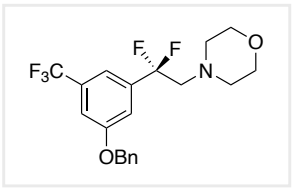

4-(2-(3-(benzyloxy)-5-(trifluoromethyl)phenyl)-2,2-difluoroethyl)morpholine (3-16). Open to air, to an oven-dried 1-dram vial charged with a Teflon-coated stir bar was added **3-3** (122.4 mg, 0.25 mmol, 1 equiv), 1,2-dichloroethane (1 mL), acetic acid (28.6 µL, 0.5 mmol, 2 equiv), and sodium triacetoxyborohydride (106.0 mg, 0.5 mmol, 2 equiv). The vial was capped and stirred at rt for 16 h. The reaction mixture was transferred to a separatory funnel with ethyl acetate (10 mL) and washed with saturated aq. sodium bicarbonate (5 mL), water (5 mL), and brine (5 mL), then dried over anhydrous sodium sulfate, filtered, and concentrated *in vacuo*. The product was isolated *via* silica gel column chromatography (20% ethyl acetate in hexanes) as a yellow oil (81.2 mg, 0.22 mmol, 89% yield). **^{1}H NMR** (400 MHz, $CDCl_3$) δ 7.46–7.34 (m, 6H), 7.30–7.29 (m, 2H), 5.13 (s, 2H), 3.62–3.59 (m, 4H), 2.92 (t, J = 13.7 Hz, 2H), 2.53–2.51 (m, 4H). **^{19}F NMR** (376 MHz, $CDCl_3$) δ -62.78 (s, 3F), -99.32 (t, J = 13.6 Hz, 2F). **^{13}C NMR** (101 MHz, $CDCl_3$) δ 158.9, 138.9 (t, J =

26.8 Hz), 135.9, 132.1 (q, J = 33.0 Hz), 128.9, 128.6, 127.7, 123.7 (q, 272.8 Hz), 121.0 (t, J = 245.1 Hz), 115.8 (t, J = 6.3 Hz), 115.3 (m), 113.2 (m), 70.7, 67.1, 64.0 (t, J = 29.5 Hz), 54.6. **IR (neat):** 2959, 2854, 2815, 1607, 1454, 1354, 1169, 1116, 1013, 865, 697 cm^{-1}. **HRMS** (ESI) $[M+H]^+$ calcd. for $[C_{20}H_{21}F_5NO_2]^+$ 402.1487, 402.1479 found.

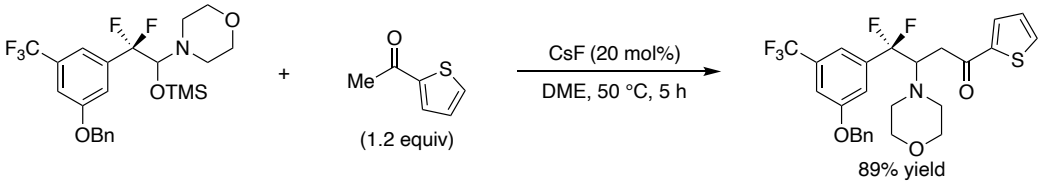

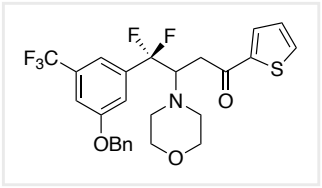

4-(3-(benzyloxy)-5-(trifluoromethyl)phenyl)-4,4-difluoro-3-morpholino-1-(thiophen-2-yl)butan-1-one (3-19). This procedure was adapted from a previous report.[2] To an oven-dried 1-dram vial charged with a Teflon-coated stir bar in a nitrogen-filled glovebox was added **3-3** (122.4 mg, 0.25 mmol, 1 equiv), 2-acetylthiophene (37.9 mg, 0.3 mmol, 1.2 equiv), 1,2-dimethoxyethane (0.5 mL) and cesium fluoride (7.6 mg, 0.05 mmol, 0.2 equiv). The vial was capped, removed from the glovebox, then placed into a preheated reaction block at 80 °C and the solution was stirred for 5 h. The reaction mixture was allowed to cool to rt and then transferred to a separatory funnel with ethyl acetate (10 mL), washed with water (2 x 5 mL), then brine (5 mL), dried over anhydrous sodium sulfate, filtered, and concentrated *in vacuo*. The product was isolated *via* silica gel column chromatography (10-15% ethyl acetate gradient in hexanes) as a yellow oil (116.7 mg, 0.22 mmol, 89% yield). **^{1}H NMR** (400 MHz, $CDCl_3$) δ 7.78 (d, J = 3.8 Hz, 1H), 7.69 (d, J = 5.0 Hz, 1H), 7.47–7.34 (m, 6H), 7.29 (s, 2H), 7.17 (t, J = 4.4 Hz, 1H), 5.14 (s, 2H), 3.91–3.81 (m, 1H), 3.48–3.18 (m, 6H), 2.74–2.69 (m, 2H), 2.49–2.44 (m, 2H). **^{19}F NMR** (376 MHz, $CDCl_3$) δ -62.73, (s, 3F), -95.87 (dd, J = 249.8, J = 8.2 Hz 1F), -108.31 (dd, J = 250.1, 21.1 Hz, 1F). **^{13}C NMR** (101

MHz, $CDCl_3$) δ 190.3, 158.8, 144.0, 138.8 (t, J = 26.7 Hz), 135.9, 134.5, 132.3, 131.9 (q, J = 32.8 Hz), 128.9, 128.5, 128.4, 127.7, 123.7 (q, J = 272.7 Hz), 122.8 (t, J = 251.4 Hz), 115.9 (t, J = 6.4 Hz), 115.6 (m), 113.2 (m), 70.7, 67.4, 65.5 (dd, J = 30.1, 24.0 Hz), 50.6, 33.7. **IR (neat):** 2958, 2853, 1730, 1662, 1607, 1355, 1248, 1168, 1116, 1014, 860, 698 cm^{-1}. **HRMS** (ESI) $[M+H]^+$ calcd. for $[C_{26}H_{25}F_5NO_3S]^+$ 526.1470, 526.1460 found.

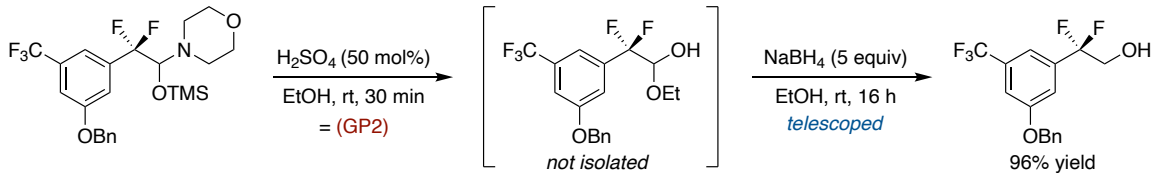

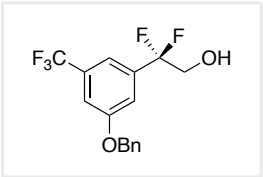

2-(3-(benzyloxy)-5-(trifluoromethyl)phenyl)-2,2-difluoroethan-1-ol (3-20). The General Procedure 2 (GP2) was followed first. To the reaction mixture was directly added sodium borohydride (47.3 mg, 1.25 mmol, 5 equiv) and the mixture was then stirred at rt for 16 h. The reaction mixture was quenched with 1 M aq. hydrochloric acid (0.5 mL), diluted with ethyl acetate (8 mL) and transferred to a separatory funnel. The organic layer was separated and washed with water (2 x 4 mL), then brine (4 mL), dried over anhydrous sodium sulfate, filtered, and concentrated *in vacuo*. The product was isolated *via* silica gel column chromatography (20% ethyl acetate in hexanes) as a pale-yellow oil (79.4 mg, 0.24 mmol, 96% yield). **^{1}H NMR** (400 MHz, $CDCl_3$) δ 7.46–7.37 (m, 6H), 7.32 (s, 2H), 5.12 (s, 2H), 3.97 (td, J = 13.1, 6.9 Hz, 2H), 2.24 (t, J = 7.1 Hz, 1H). **^{19}F NMR** (376 MHz, $CDCl_3$) δ -62.83 (s, 3F), -106.92 (t, J = 13.0 Hz, 2F). **^{13}C NMR** (101 MHz, $CDCl_3$) δ 159.2, 137.2 (t, J = 26.3 Hz), 135.8, 132.6 (q, J = 33.0 Hz), 128.9, 128.6, 127.8, 123.6 (q, J = 272.6 Hz), 119.9 (t, J = 244.7 Hz), 115.9 (t, J = 6.2 Hz), 115.0 (td, J = 6.4, 3.5 Hz), 113.7 (m), 70.8, 65.8 (t, J = 32.6 Hz). **IR (neat):** 3351, 2935, 1607, 1454, 1356, 1168, 1124, 1016, 866, 696 cm^{-1}. **HRMS** (DART) $[M+COOH]^-$ calcd. for $[C_{17}H_{14}F_5O_4]^-$ 377.0818, 377.0846 found.

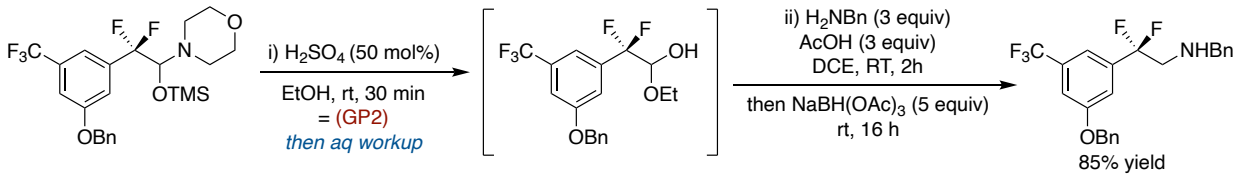

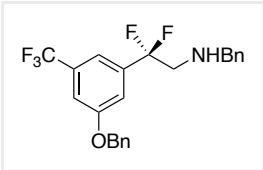

***N*-benzyl-2-(3-(benzyloxy)-5-(trifluoromethyl)phenyl)-2,2-difluoroethan-1-amine (3-21).** The General Procedure 2 (GP2) was followed first. The resulting reaction mixture from GP2 was then transfered into a seperatory funnel with ethyl acetate (8 mL), washed with water (4 mL), then brine (4 mL), dried over anhydrous sodium sulfate, filtered, and concentrated *via* a rotary evaporator into a 10 mL round bottom flask then charged with a Teflon-coated stir bar. To the resulting residue was added dry 1,2-dichloroethane (2 mL), acetic acid (42.9 µL, 3 equiv, 0.75 mmol), and benzylamine (81.9 µL, 3 equiv, 0.75 mmol). The reaction mixture was stirred for 2 h at rt, then sodium triacetoxyborohydride (264.9 mg, 5 equiv, 1.25 mmol) was added and the reaction flask was capped with a septum, a nitrogen balloon was inserted, and the mixture was stirred overnight at rt. The reaction mixture was then transfered into a seperatory funnel with dichloromethane (12 mL), washed with 1 M aq. sodium hydroxide (6 mL), water (6 mL), then brine (6 mL), dried over anhydrous sodium sulfate, filtered, and concentrated *in vacuo*. Purification *via* silica gel column chromatography (5% to 10% ethyl acetate gradient in hexanes) provided the product as a pale-yellow oil (89.4 mg, 85% yield). **^{1}H NMR** (400 MHz, $CDCl_3$) δ 7.47–7.24 (m, 13H), 5.12 (s, 2H), 3.85 (s, 2H), 3.21 (t, *J* = 14.0 Hz, 2H), 1.64 (br s, 1H). **^{19}F NMR** (376 MHz, $CDCl_3$) δ -62.75 (s, 3F), -100.83 (t, *J* = 14.0 Hz, 2F). **^{13}C NMR** (101 MHz, $CDCl_3$) δ 159.1, 139.6, 138.7 (t, *J* = 26.7 Hz), 135.9, 132.3 (q, *J* = 32.9 Hz), 128.9, 128.6, 128.56, 128.2, 127.8, 127.4, 123.7 (q, *J* = 272.6 Hz), 121.2 (t, *J* = 244.4 Hz), 115.8 (t, *J* = 6.3 Hz), 115.0 (m), 113.4 (m), 70.7, 54.5 (t, *J* = 29.5

Hz), 53.6. **IR (neat):** 3356, 3032, 2926, 2695, 2442, 1606, 1453, 1357, 1168, 1124, 1017, 866, 736, 695 cm^{-1}. **HRMS** (DART) $[M+H]^+$ calcd. for $[C_{23}H_{21}F_5NO]^+$ 422.1538, 422.1556 found.

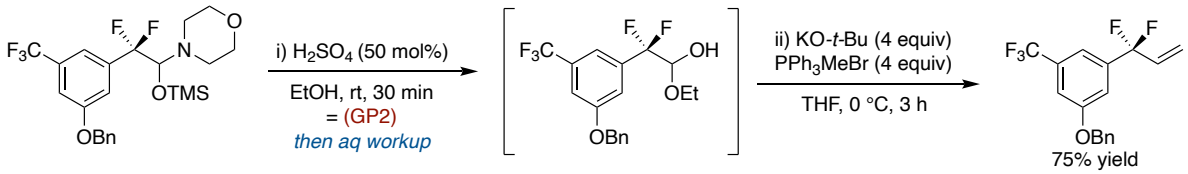

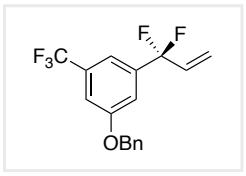

1-(benzyloxy)-3-(1,1-difluoroallyl)-5-(trifluoromethyl)benzene (3-24). This procedure was adapted from a previous report. The General Procedure 2 (GP2) was followed first. The reaction mixture from GP2 was then placed into a seperatory funnel, diluted with ethyl acetate (8 mL), then washed with water (4 mL) and brine (4 mL), dried over sodium sulfate, filtered, then concentrated *in vacuo* into a 10 mL round bottom flask and charged with a Teflon-coated stir bar. To the resulting residue was added methyltriphenylphosphonium bromide (357.2 mg, 1.0 mmol, 4 equiv), then the flask was capped with a septum and evacuated and refilled with nitrogen three times on a Schlenk line. Dry tetrahydrofuran (2.5 mL) was added *via* syringe and the flask was placed in an ice bath and cooled to 0 °C. The septum was removed, potassium *tert*-butoxide (112.2 mg, 1.0 mmol, 4 equiv) was added quickly, and the septum was replaced. The reaction mixture was stirred at 0 °C for 3 h, then quenched with water (5 mL) and transferred to a separatory funnel with ethyl acetate (10 mL). The organic layer was separated and washed with brine (5 mL), dried over anhydrous sodium sulfate, filtered, and concentrated *in vacuo*. The product was isolated *via* silica gel column chromatography (2% ethyl acetate in hexanes) as a pale-yellow oil (61.8 mg, 0.19 mmol, 75% yield). **^{1}H NMR** (400 MHz, $CDCl_3$) δ 7.47–7.35 (m, 6H), 7.31 (br s, 2H), 6.14 (dq, J = 17.2, 10.1 Hz, 1H), 5.62 (dt, J = 17.3, 2.8 Hz, 1H), 5.54 (d, J = 10.9 Hz, 1H), 5.13 (s, 2H). **^{19}F NMR** (376 MHz, $CDCl_3$) δ -62.84 (s, 3F), -93.96 (dd, J = 10.3, 2.7 Hz, 2F). **^{13}C NMR** (101 MHz, $CDCl_3$) δ 159.2, 139.0 (t, J

= 28.4 Hz), 135.8, 133.1 (t, J = 29.6 Hz), 132.5 (q, J = 32.9 Hz), 128.9, 128.6, 127.8, 123.7 (q, J = 272.6 Hz), 120.7 (t, J = 9.2 Hz), 118.6 (t, J = 239.6 Hz), 115.8 (t, J = 5.8 Hz), 115.1 (m), 113.4 (m), 70.8. **IR (neat):** 3067, 3034, 2922, 2876, 1607, 1453, 1383, 1126, 1006, 866, 695 cm^{-1}. **GC-MS (EI)** M^+ calcd. for $[C_{17}H_{13}F_5O]^+$ 328.09, 328.10 found.

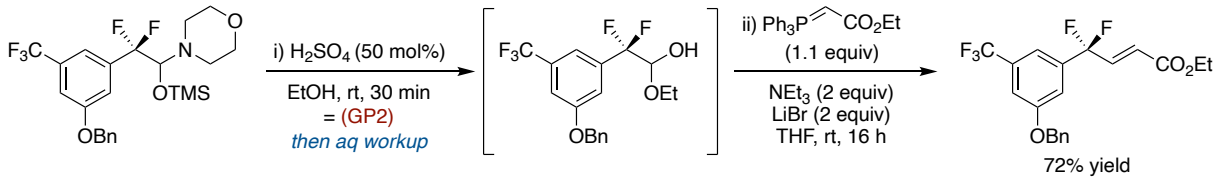

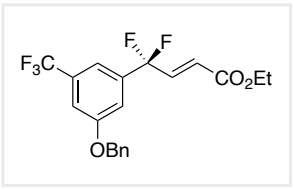

Ethyl (E)-4-(3-(benzyloxy)-5-(trifluoromethyl)phenyl)-4,4-difluorobut-2-enoate (3-25). The General Procedure 2 (GP2) was followed first. The reaction mixture from GP2 was then placed into a seperatory funnel, diluted with ethyl acetate (8 mL), washed with water (4 mL) then brine (4 mL), dried over anhydrous sodium sulfate, filtered, and concentrated *via* a rotary evaporator into a 10 mL round bottom flask then charged with a Teflon-coated stir bar. To the resulting residue was added (carbethoxymethylene)triphenylphosphorane (95.8 mg, 1.1 equiv, 0.275 mmol), lithium bromide (43.4 mg, 2 equiv, 0.5 mmol), tetrahydrofuran (5 mL), and triethylamine (69.3 µL, 2 equiv, 0.5 mmol). The reaction flask was then capped with a septum, a nitrogen balloon was inserted, and the mixture was then stirred at rt for 16 h. The reaction mixture was transferred to a seperatory funnel, diluted with ethyl acetate (10 mL), washed with water (5 mL) then brine (5 mL), dried over anhydrous sodium sulfate, filtered, and concentrated *in vacuo*. The product was isolated *via* silica gel column chromatography (5% ethyl acetate in hexanes) as a clear oil (74.0 mg, 0.18 mmol, 72% yield). **^{1}H NMR** (400 MHz, $CDCl_3$) δ 7.46–7.36 (m, 6H), 7.32 (br s, 1H), 7.28 (br s, 1H), 6.97 (dt, J = 15.7, 10.5 Hz, 1H), 6.29 (dt, J = 15.7, 2.3 Hz, 1H), 5.12 (s, 2H), 4.26 (q, J = 7.2 Hz, 2H), 1.32 (t, J = 7.1 Hz, 3H). **^{19}F NMR** (376 MHz, $CDCl_3$) δ -62.88 (s, 3F), -95.58 (dd, J =

10.5, 2.4 Hz, 2F). **^{13}C NMR** (101 MHz, $CDCl_3$) δ 164.9, 159.4, 139.0 (t, *J* = 30.1 Hz), 137.9 (t, *J* = 28.1 Hz), 135.7, 132.8 (q, *J* = 32.9 Hz), 128.9, 128.6, 127.8, 125.7 (t, *J* = 8.2 Hz), 123.5 (q, *J* = 272.8 Hz), 117.7 (t, *J* = 241.6 Hz), 115.6 (t, *J* = 5.8 Hz), 114.7 (m), 113.9 (m), 70.8, 61.5, 14.2. **IR (neat):** 3036, 2984, 2939, 1725, 1606, 1454, 1355, 1169, 1128, 1015, 865, 696 cm^{-1}. **HRMS** (DART) $[M+NH_4]^+$ calcd. for $[C_{20}H_{21}F_5NO_3]^+$ 418.1436, 418.1448 found.

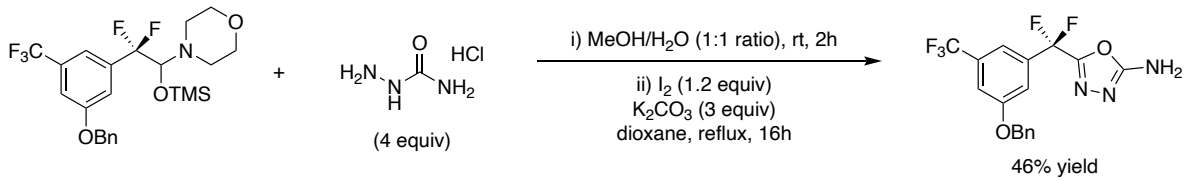

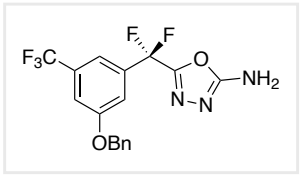

5-((3-(benzyloxy)-5-(trifluoromethyl)phenyl)difluoromethyl)-1,3,4-oxadiazol-2-amine (3-22). Open to air, to an oven-dried 1-dram vial charged with a Teflon-coated stir bar was added **3-3** (122.4 mg, 0.25 mmol, 1 equiv), semicarbazide (111.5 mg, 4 equiv, 1.0 mmol), and methanol/water (1:1 ratio, 2.0 mL). The vial was capped and the reaction mixture was stirred at rt for 2 h. The reaction mixture was then transferred to a separatory funnel with ethyl acetate (10 mL), washed with water (3 x 4 mL), and brine (5 mL). The organic layer was dried over anhydrous sodium sulfate, filtered, and concentrated into a 10 mL round bottom flask then charged with a Teflon-coated stir bar. To the concentrated residue was added 1,4-dioxane (5 mL), potassium carbonate (104 mg, 3 equiv, 0.75 mmol), and iodine (76.1 mg, 1.2 equiv, 0.3 mmol). The reaction flask was fitted with a reflux condenser, septum, and nitrogen balloon. The reaction flask was then placed in a preheated oil bath at 120 °C and the reaction solution was refluxed for 16 h with stirring. The reaction mixture was allowed to cool to rt, transferred to a separatory funnel with ethyl acetate (10 mL), washed with water (5 mL) and brine (5 mL), dried over anhydrous sodium sulfate, filtered, and concentrated *in vacuo*. Purification *via* silica gel column chromatography (1% triethylamine and

20% ethyl acetate in hexanes) provided the product as an off-white solid (44.3 mg, 46% yield). **^{1}H NMR** (400 MHz, $CDCl_3$) δ 7.49 (bs, 1H), 7.44–7.34 (m, 7H), 5.86 (bs, 2H), 5.12 (s, 2H). **^{19}F NMR** (376 MHz, $CDCl_3$) δ -62.90 (s, 3F), -94.60 (s, 2F). **^{13}C NMR** (101 MHz, $CDCl_3$) δ 164.1, 159.3, 154.5, 135.6, 135.0 (t, J = 25.9 Hz), 132.8 (q, J = 33.2 Hz), 128.9, 128.7, 127.8, 123.4 (q, J = 272.8 Hz), 116.0 (t, J = 5.7 Hz), 115.2 (m), 114.9 (m), 112.6 (t, J = 243.1 Hz), 70.9. (**Note:** Oxadiazole carbon peaks at 164.1 and 154.5 ppm are short and broad. These chemical shifts are similar to other reported oxadiazole carbon peaks.)[3] **IR (neat):** 3299, 3138, 1656, 1352, 1272, 1084, 801, 693 cm^{-1}. **HRMS** (DART) $[M+H]^+$ calcd. for $[C_{17}H_{13}F_5N_3O_2]^+$ 386.0922, 386.0957 found. **Melting Point:** 127-130 °C.

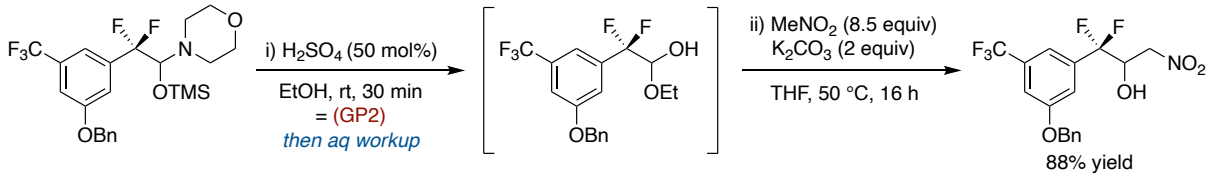

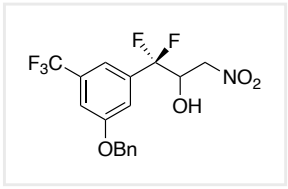

1-(3-(benzyloxy)-5-(trifluoromethyl)phenyl)-1,1-difluoro-3-nitropropan-2-ol (3-28). The General Procedure 2 (GP2) was followed first. The reaction mixture from GP2 was then placed into a seperatory funnel and diluted with ethyl acetate (8 mL) and washed with water (4 mL), then brine (4 mL), dried over anhydrous sodium sulfate, filtered, then concentrated *in vacuo* into a 10 mL round bottom flask and charged with a Teflon-coated stir bar. Dry tetrahydrofuran (4 mL) was added, followed by nitromethane (114 µL, 2.1 mmol, 8.5 equiv) and potassium carbonate (69.1 mg, 0.5 mmol, 2 equiv). The flask was sealed with a septum and placed in a preheated oil bath at 50 °C and stirred for 16 h. The reaction mixture was allowed to cool to rt and was then transferred to a seperatory funnel, diluted with ethyl acetate (10 mL), washed with water (2 x 5 mL), then brine (5 mL), dried over anhydrous sodium sulfate, filtered, and concentrated *in vacuo*. The product was

isolated *via* silica gel column chromatography (5-10% ethyl acetate gradient in hexanes) as a yellow oil (98.8 mg, 0.22 mmol, 88% yield). **^{1}H NMR** (400 MHz, $CDCl_3$) δ 7.46–7.36 (m, 7H), 7.31 (br s, 1H), 5.14 (s, 2H), 4.82–4.74 (m, 1H), 4.68 (dd, *J* = 13.9, 2.4 Hz, 1H), 4.52 (dd, *J* = 13.9, 9.6 Hz, 1H), 2.96 (br s, 1H). **^{19}F NMR** (376 MHz, $CDCl_3$) δ -62.83 (s, 3F), -102.99 (dd, *J* = 255.9, 5.5 Hz, 1F), -112.35 (dd, *J* = 255.9, 15.3 Hz, 1F). **^{13}C NMR** (101 MHz, $CDCl_3$) δ 159.3, 135.6, 135.4 (t, *J* = 26.1 Hz), 132.8 (q, *J* = 33.2 Hz), 128.9, 128.7, 127.8, 123.5 (q, *J* = 272.7 Hz), 119.2 (dd, *J* = 251.2, 248.1 Hz), 116.2 (t, *J* = 6.5 Hz), 115.1 (m), 114.4 (m), 75.1 (t, *J* = 2.7 Hz), 71.3 (dd, *J* = 34.5, 29.2 Hz), 70.9. **IR (neat):** 3271, 2978, 2930, 1560, 1455, 1353, 1127, 868, 697 cm^{-1}. **HRMS** (DART) $[M+NH_4]^+$ calcd. for $[C_{17}H_{18}F_5N_2O_4]^+$ 409.1181, 409.1192 found.

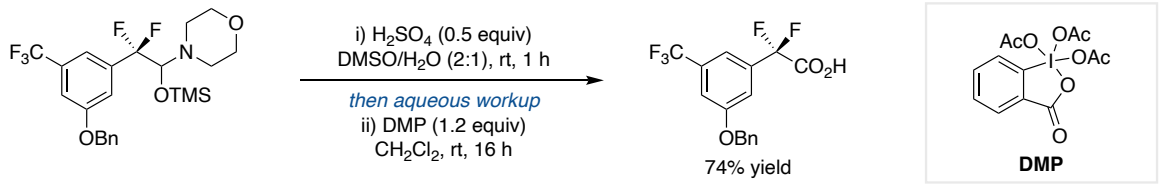

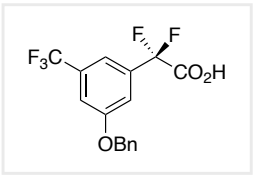

2-(3-(benzyloxy)-5-(trifluoromethyl)phenyl)-2,2-difluoroacetic acid (3-27). Open to air, to an oven-dried 1-dram vial charged with a Teflon-coated stir bar was added **3-3** (122.4 mg, 0.25 mmol, 1 equiv), dimethyl sulfoxide/water (2:1 ratio, 2 mL), and sulfuric acid (6.7 µL, 0.125 mmol, 0.5 equiv). The vial was capped and the mixture was stirred at rt for 30 min. Then the reaction mixture was then transferred to a separatory funnel with ethyl acetate (10 mL), washed with water (3 x 3 mL), and concentrated. To the resulting residue was added dichloromethane (2 mL) and 1,1,1-tris(acetyloxy)-1,1-dihydro-1,2-benziodoxol-3-(1*H*)-one (DMP, 127.2 mg, 0.3 mmol, 1.2 equiv). The vial was capped and the reaction mixture was stirred at rt overnight. The reaction mixture was then transferred to a separatory funnel with dichloromethane (10 mL), washed with 1 M aq. sodium hydroxide (8 mL),

and brine (6 mL), then dried over anhydrous sodium sulfate, filtered, and concentrated *in vacuo*. Purification *via* silica gel column chromatography (1% AcOH and 30% ethyl acetate in hexanes) afforded the product as a white solid (63.8 mg, 74% yield). **^{1}H NMR** (400 MHz, $CDCl_3$) δ 9.93 (br s, 1H), 7.41–7.32 (m, 7H), 7.29 (br s, 1H), 5.05 (s, 2H). **^{19}F NMR** (376 MHz, $CDCl_3$) δ -63.00 (s, 3F), -104.63 (s, 2F). **^{13}C NMR** (101 MHz, $CDCl_3$) δ 178.5, 168.3, 159.4, 135.6, 134.8 (t, J = 26.0 Hz), 132.9 (q, J = 33.2 Hz), 128.9, 128.7, 127.8, 123.4 (q, J = 272.8 Hz), 115.7 (t, J = 6.3 Hz), 115.0 (m), 70.9. **IR (neat):** 3032, 2931, 2875, 2695, 2539, 1759, 1607, 1358, 1271, 1116, 1002, 699 cm^{-1}. **HRMS** (DART) $[M]^-$ calcd. for $[C_{16}H_{11}F_5O_3]^-$ 346.0634, 346.0645 found. **Melting Point:** 75-78 °C.

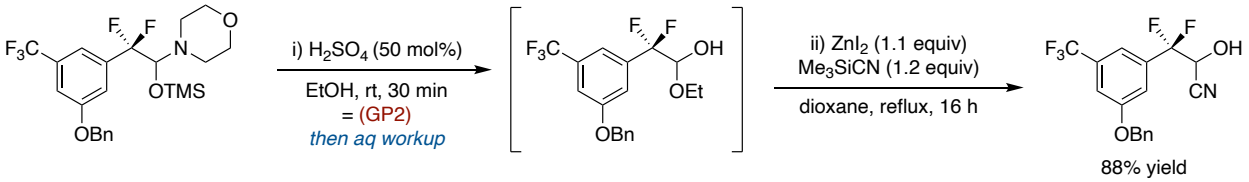

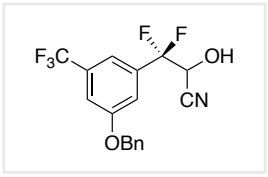

3-(3-(benzyloxy)-5-(trifluoromethyl)phenyl)-3,3-difluoro-2-hydroxypropanenitrile (3-26). This procedure was adapted from a previous report.[4] The General Procedure 2 (GP2) was followed first. The reaction mixture from GP2 was then placed into a seperatory funnel and diluted with ethyl acetate (8 mL), washed with water (4 mL), then brine (4 mL), dried over sodium sulfate, filtered, and concentrated *via* a rotary evaporator into a 10 mL round bottom flask then charged with a Teflon-coated stir bar. To the resulting residue was added anhydrous 1,4-dioxane (6 mL), zinc iodide (87.8 mg, 1.1 equiv, 0.275 mmol), and trimethylsilyl cyanide (37.5 µL, 1.2 equiv, 0.3 mmol). The flask was then fitted with a reflux condenser with a rubber septum and a nitrogen balloon, placed into a preheated oil bath at 120 °C, and the reaction solution was refluxed for 16 h with stirring. The reaction mixture was then transferred to a separatory funnel with ethyl acetate (10 mL), washed

with saturated aq. sodium bicarbonate (5 mL), then brine (5 mL), dried over anhydrous sodium sulfate, filtered, and concentrated *in vacuo*. Purification *via* silica gel column chromatography (15% ethyl acetate in hexanes) provided the product as a yellow oil (78.6 mg, 88% yield). **^{1}H NMR** (400 MHz, $CDCl_3$) δ 7.46–7.35 (m, 8H), 5.13 (s, 2H), 4.82 (dd, *J* = 9.3, 7.5 Hz, 1H), 3.41 (bs, 1H). **^{19}F NMR** (376 MHz, $CDCl_3$) δ -62.91 (s, 3F), -104.92 (dd, *J* = 254.5, 7.4 Hz, 1F), -107.08 (dd, *J* = 254.5, 9.2 Hz, 1F). **^{13}C NMR** (101 MHz, $CDCl_3$) δ 159.4, 135.5, 133.7 (t, *J* = 25.6 HZ), 132.9 (q, *J* = 33.2 Hz), 129.0, 128.7, 127.9, 123.4 (q, *J* = 272.9 Hz), 117.3 (t, *J* = 252.1 Hz), 116.4 (t, *J* = 6.2 Hz), 115.5 (m), 114.9 (m), 114.6 (m), 71.0, 65.6 (dd, *J* = 37.6, 35.8 Hz). **IR (neat):** 3377, 2933, 1607, 1454, 1360, 1127, 1015, 866, 695 cm^{-1}. **HRMS** (DART) $[M-H]^-$ calcd. for $[C_{17}H_{11}F_5NO_2]^-$ 356.0715, 356.0761 found.

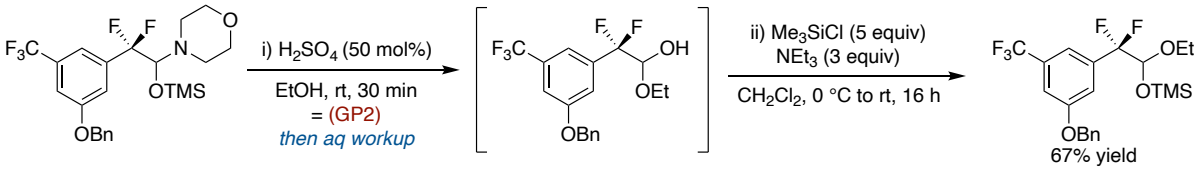

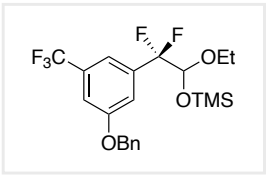

(2-(3-(benzyloxy)-5-(trifluoromethyl)phenyl)-1-ethoxy-2,2-difluoroethoxy)trimethylsilane (3-23). The General Procedure 2 (GP2) was followed first. The reaction mixture from GP2 was then placed into a seperatory funnel, diluted with ethyl acetate (8 mL), washed with water (4 mL), then brine (4 mL), dried over sodium sulfate, filtered, and concentrated *via* a rotary evaporator into a 10 mL round bottom flask then charged with a Teflon-coated stir bar. To the resulting residue was added dry dichloromethane (5 mL) and triethylamine (104 µL, 3 equiv, 0.75 mmol). The flask was placed into a 0 °C ice-bath and trimethylsilyl chloride (159 µL, 5 equiv, 1.25 mmol) was added slowly *via* syringe. The flask was capped with a septum, a positive pressure nitrogen line was inserted, and the reaction solution was stirred at rt for 16 h. The reaction mixture was then transferred to a

separatory funnel with dichloromethane (10 mL), washed with water (5 mL), then brine (5 mL), dried over anhydrous sodium sulfate, filtered, and concentrated *in vacuo*. Purification *via* silica gel column chromatography (5% ethyl acetate in hexanes) provided the product as pale-yellow oil (75.6 mg, 67% yield). **^{1}H NMR** (400 MHz, $CDCl_3$) δ 7.46–7.36 (m, 6H), 7.33 (br s, 1H), 7.29 (br s, 1H), 5.11 (s, 2H), 4.96 (t, *J* = 4.0 Hz, 1H), 3.65 (ddq, *J* = 89.9, 8.9, 7.0 Hz, 2H), 1.21 (t, *J* = 7.0 Hz, 3H), 0.20 (s, 9H). **^{19}F NMR** (376 MHz, $CDCl_3$) δ -62.84 (s, 3F), -108.00 (dd, *J* = 253.2, 4.3 Hz, 1F), -108.86 (dd, *J* = 252.7, 3.9 Hz, 1F). **^{13}C NMR** (101 MHz, $CDCl_3$) δ 158.6, 136.1, 135.7 (t, *J* = 26.1 Hz), 131.6 (q, *J* = 32.8 Hz), 128.9, 128.5, 127.8, 123.83 (q, *J* = 272.6 Hz), 118.4 (t, *J* = 247.9 Hz), 117.2 (t, *J* = 6.5 Hz), 116.9 (m), 113.5 (m), 96.4 (t, *J* = 37.1 Hz), 70.6, 64.8, 15.1, 0.3. **IR (neat):** 3035, 2933, 1607, 1455, 1358, 1254, 1121, 1019, 844, 694 cm^{-1}. **HRMS** (DART) $[M+NH_4]^+$ calcd. for $[C_{21}H_{29}F_5NO_3Si]^+$ 466.1831, 466.1855 found.

b. Complex trifluoromethylarene C–F functionalization (Figure 3-7)

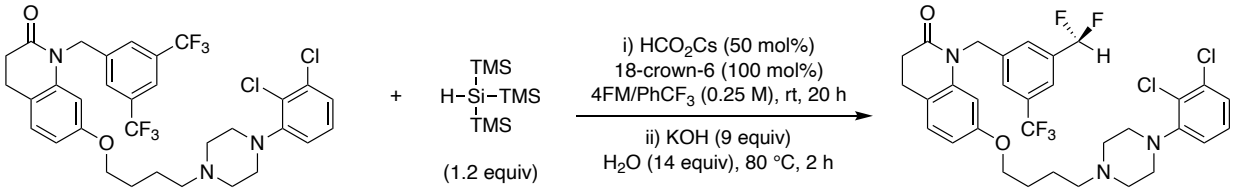

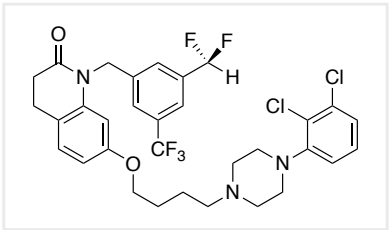

7-(4-(4-(2,3-dichlorophenyl)piperazin-1-yl)butoxy)-1-(3-(difluoromethyl)-5-(trifluoromethyl)benzyl)-3,4-dihydroquinolin-2(1*H*)-one (3-31). In a nitrogen-filled glovebox, to an oven-dried 1-dram glass vial charged with a Teflon-coated stir bar, was added 1-(3,5-bis(trifluoromethyl)benzyl)-7-(4-(4-(2,3-dichlorophenyl)piperazin-1-yl)butoxy)-3,4-dihydroquinolin-2(1*H*)-one (67.5 mg, 0.1 mmol, 1

equiv), cesium formate (8.9 mg, 0.05 mmol, 0.5 equiv), 18-crown-6 (26.4 mg, 0.1 mmol, 1 equiv), and 4-formylmorpholine/benzotrifluoride (1:1 ratio, 0.4 mL). Tris(trimethylsilyl)silane (29.8 mg, 0.12 mmol, 1.2 equiv) was then added and the vial was capped with a screw top cap and PTFE-lined silicone septum, removed from glovebox, and the reaction mixture was stirred at rt. After 20 h, the vial was opened and potassium hydroxide (50 mg, 8.9 equiv, 0.89 mmol) and water (25 µL, 13.8 equiv, 1.38 mmol) were added. The vial was capped, placed into a preheated reaction block at 80 °C, and the reaction mixture was stirred for 2 h. The reaction mixture was then diluted with ethyl acetate (6 mL) and washed with distilled water (3 x 3 mL) then brine (4 mL), dried over anhydrous sodium sulfate, filtered, and concentrated. Purification *via* preparative thin-layer chromatography (40% ethyl acetate in hexanes) provided the product as an off-white solid (38.7 mg, 59% yield). **^{1}H NMR** (400 MHz, $CDCl_3$) δ 7.66 (s, 1H), 7.61 (s, 1H), 7.56 (s, 1H), 7.19–7.13 (m, 2H), 7.09 (d, *J* = 8.2 Hz, 1H), 6.97 (dd, *J* = 7.4, 2.3 Hz), 6.81–6.51 (m, 2H), 6.35 (d, *J* = 2.3 Hz, 1H), 5.22 (s, 2H), 3.88–3.86 (m, 2H), 3.16 (br fs, 4H), 2.94–2.91 (m, 2H), 2.80–2.76 (m, 6H), 2.60 (br s, 2H), 1.76 (br s, 4H). **^{19}F NMR** (376 MHz, $CDCl_3$) δ -62.73 (s, 3F), -111.94 (d, *J* = 56.2 Hz, 2F). **^{13}C NMR** (101 MHz, $CDCl_3$) δ 170.9, 158.7, 151.3, 140.5, 139.8, 136.0 (t, *J* = 23.1 Hz), 134.2, 132.0 (q, *J* = 33.0 Hz), 128.9, 127.61, 127.58, 127.2 (t, *J* = 5.9 Hz), 125.8 (m), 124.7, 123.6 (q, *J* = 272.8 Hz), 121.7 (m), 118.7, 118.5, 113.6 (t, *J* = 240.4 Hz), 108.2, 103.2, 68.0, 58.2, 53.3, 51.3, 46.0, 32.2, 27.2, 24.8, 23.4. **IR (neat):** 2936, 2819, 1673, 1614, 1476, 1112, 1044.08, 1018, 776 cm^{-1}. **HRMS** (DART) $[M+H]^+$ calcd. for $[C_{32}H_{33}Cl_2F_5N_3O_2]^+$ 656.1865, 656.1853 found. **Melting Point:** 108-112 °C.

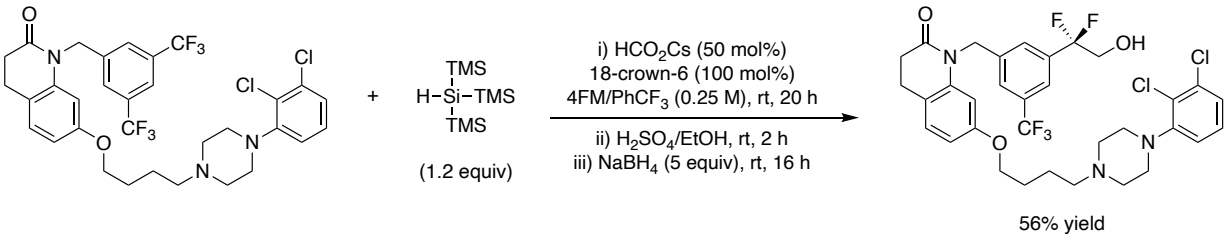

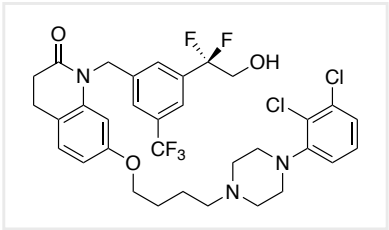

7-(4-(4-(2,3-dichlorophenyl)piperazin-1-yl)butoxy)-1-(3-(1,1-difluoro-2-hydroxyethyl)-5-(trifluoromethyl)benzyl)-3,4-dihydroquinolin-2(1*H*)-one (3-32). In a nitrogen-filled glovebox, to an oven-dried 1-dram glass vial charged with a Teflon-coated stir bar, was added 1-(3,5-bis(trifluoromethyl)benzyl)-7-(4-(4-(2,3-dichlorophenyl)piperazin-1-yl)butoxy)-3,4-dihydroquinolin-2(1*H*)-one (67.5 mg, 0.1 mmol, 1 equiv), cesium formate (8.9 mg, 0.05 mmol, 0.5 equiv), 18-crown-6 (26.4 mg, 0.1 mmol, 1 equiv), and 4-formylmorpholine/benzotrifluoride (1:1 ratio, 0.4 mL). Then tris(trimethylsilyl)silane (49.7 mg, 0.2 mmol, 2 equiv) was added and the vial was capped with a screw top cap and PTFE-lined silicone septum, removed from glovebox, and the reaction mixture was stirred at rt. After 20 h, the vial was opened and ethanol (0.2 mL) and sulfuric acid (2.7 µL, 0.05 mmol, 0.5 equiv) were added. The vial was capped and the reaction mixture was stirred at rt. After 2 h, sodium borohydride (18.9 mg, 0.5 mmol, 5 equiv) was added, the vial was recapped and the reaction mixture was stirred at rt for an additional 16 h. The reaction mixture was then diluted with ethyl acetate (6 mL) and washed with distilled water (3 x 3 mL), then brine (4 mL), dried over anhydrous sodium sulfate, filtered, and concentrated. Purification *via* preparative thin-layer chromatography (50% ethyl acetate in hexanes) provided the product as an off-white solid (38.5 mg, 56% yield). **^{1}H NMR** (400 MHz, $CDCl_3$) δ 7.68 (s, 2H), 7.59 (s, 1H), 7.18–7.13 (m, 2H), 7.06 (d, *J* = 8.2 Hz, 1H), 6.98 (dd, *J* = 6.6, 2.9 Hz, 1H), 6.50 (dd, *J* = 8.3, 2.3 Hz, 1H), 6.41 (d, *J* = 2.3 Hz, 1H), 5.21 (s, 2H), 3.97 (t, *J* = 13.1 Hz, 2H), 3.87 (t, *J* = 5.7 Hz, 2H), 3.11 (br s, 4H), 2.90 (dd, *J* = 8.8, 5.7 Hz, 2H),

2.78–2.70 (m, 6H), 2.48 (t, J = 7.6 Hz, 2H), 1.76–1.62 (m, 4H). **^{19}F NMR** (376 MHz, $CDCl_3$) δ -62.63 (s, 3F), -105.94 (t, J = 13.0 Hz, 2F). **^{13}C NMR** (101 MHz, $CDCl_3$) δ 171.0, 158.5, 151.0, 140.5, 139.4, 136.6 (t, J = 26.4 Hz), 134.2, 131.9 (q, J = 32.9 Hz), 128.8, 128.2 (t, J = 5.8 Hz), 127.7, 127.6, 125.7 (m), 125.0, 122.3, 121.9 (m), 120.2 (t, J = 244.5 Hz), 118.8, 118.6, 108.1, 103.6, 67.6, 65.2 (t, J = 32.5 Hz), 58.2, 53.3, 50.9, 46.0, 32.2, 27.0, 24.7, 23.1. **IR (neat):** 3339, 2944, 2823, 1674, 1612, 1447, 1361, 1280, 1173, 1124, 736 cm^{-1}. **HRMS** (ESI) $[M+H]^+$ calcd. for $[C_{33}H_{34}Cl_2F_5N_3O_3]^+$ 686.1970, 686.1960 found. **Melting Point:** 57-60 °C.

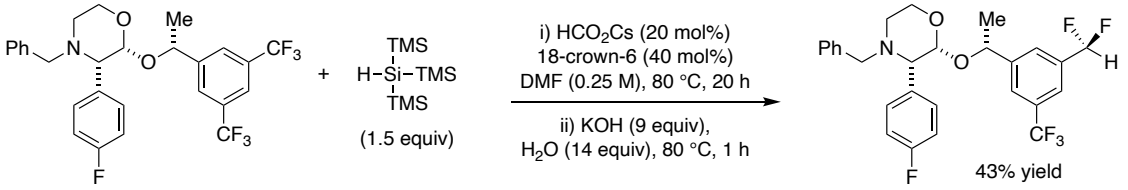

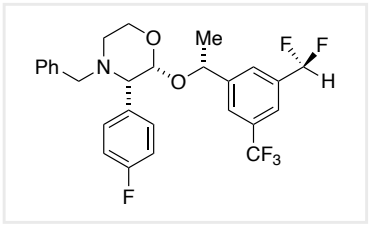

(2*R*,3*S*)-4-benzyl-2-((*R*)-1-(3-(difluoromethyl)-5-(trifluoromethyl)phenyl)ethoxy)-3-(4-fluorophenyl)morpholine (3-33). In a nitrogen-filled glovebox, to an oven-dried 1-dram vial charged with a Teflon-coated stir bar, was added (2*R*,3*S*)-4-benzyl-2-((*R*)-1-(3,5-bis(trifluoromethyl)phenyl)ethoxy)-3-(4-fluorophenyl)morpholine (131.9 mg, 0.25 mmol, 1 equiv), cesium formate (8.9 mg, 0.5 mmol, 0.2 equiv), 18-crown-6 (26.4 mg, 0.1 mmol, 0.4 equiv), and anhydrous *N*,*N*-dimethylformamide (1.0 mL). Tris(trimethylsilyl)silane (93.2 mg, 0.375 mmol, 1.5 equiv) was then added and the vial was capped with a screw top cap and PTFE-lined silicone septum, removed from glovebox, and the reaction mixture was stirred at rt. After 20 h, the vial was opened and potassium hydroxide (125 mg, 2.23 mmol, 8.9 equiv) and water (62.5 µL, 3.45 mmol, 13.8 equiv) were added. The vial was capped, placed into a preheated reaction block at 80 °C, and the reaction solution was stirred for 1

h. The reaction mixture was then transferred to a separatory funnel, diluted with ethyl acetate (6 mL), washed with water (3 x 3 mL), then brine (4 mL), dried over anhydrous sodium sulfate, filtered, and concentrated. Purification *via* silica gel chromatography (5-10% ethyl acetate gradient in hexanes) provided the product as a clear oil (54.6 mg, 43% yield). **^{1}H NMR** (400 MHz, $CDCl_3$) δ 7.56 (s, 1H), 7.49 (br s, 2H), 7.34–7.24 (m, 5H), 7.11 (s, 1H), 7.07 (t, *J* = 8.5 Hz, 2H), 6.88 (s, 1H), 6.41 (t, *J* = 56.0 Hz, 1H), 4.85 (q, *J* = 6.6 Hz, 1H), 4.33 (d, *J* = 3.0 Hz, 1H), 4.25 (td, *J* = 11.6, 2.5 Hz, 1H), 3.83 (d, *J* = 13.5 Hz, 1H), 3.58 (ddd, *J* = 11.2, 3.7, 1.6 Hz, 1H), 3.44 (d, *J* = 3.0 Hz, 1H), 2.87–2.83 (m, 2H), 2.35 (td, *J* = 11.9, 3.5 Hz, 1H), 1.45 (d, *J* = 6.6 Hz, 3H). **^{19}F NMR** (376 MHz, $CDCl_3$) δ -62.82 (s, 3F), -110.93 (dd, *J* = 377.5, 56.2 Hz, 1F),-111.73 (dd, *J* = 377.9, 55.8 Hz, 1F), -114.83 (td, *J* = 8.9, 4.5 Hz, 1F). **^{13}C NMR** (101 MHz, $CDCl_3$) δ 162.5 (d, *J* = 246.3 Hz), 145.5, 137.9, 135.4 (t, *J* = 23.0 Hz), 134.1 (d, *J* = 3.1 Hz), 131.5 (q, *J* = 32.9 Hz), 131.1 (d, *J* = 8.0 Hz), 129.1, 128.4, 127.2, 126.8 (t, *J* = 6.3 Hz), 125.4 (m), 123.5 (q, *J* = 272.6 Hz), 121.6 (m), 115.2 (d, *J* = 21.2 Hz), 113.7 (t, *J* = 240.1 Hz), 95.7, 72.5, 69.4, 59.8, 59.7, 51.9, 24.7. **IR (neat):** 3061, 2923, 2852, 1405, 1339, 1264, 1168, 1109, 1036, 889, 837, 773 cm^{-1}. **HRMS** (DART) $[M+H]^+$ calcd. for $[C_{27}H_{26}F_6NO_2]^+$ 510.1862, 510.1921 found.

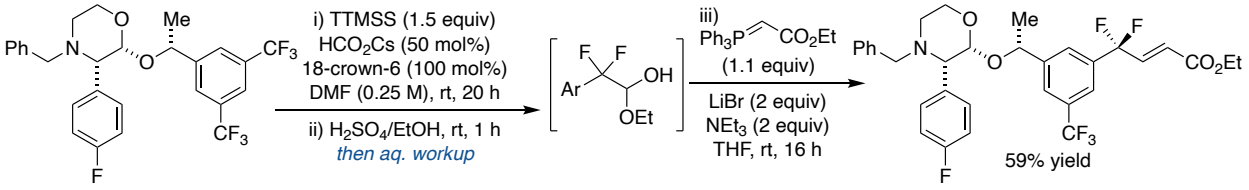

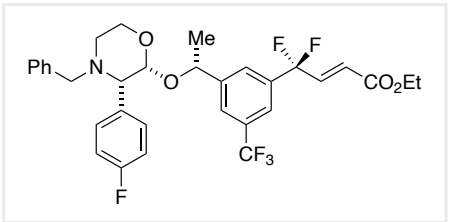

Ethyl (*E*)-4-(3-((R)-1-(((2R,3S)-4-benzyl-3-(4-fluorophenyl)morpholin-2-yl)oxy)ethyl)-5-(trifluoromethyl)phenyl)-4,4-difluorobut-2-enoate (3-34). In a nitrogen-filled glovebox, to an oven-dried 1-dram

glass vial charged with a Teflon-coated stir bar, was added (2*R*,3*S*)-4-benzyl-2-((*R*)-1-(3,5-bis(trifluoromethyl)phenyl)ethoxy)-3-(4-fluorophenyl)morpholine (131.9 mg, 0.25 mmol, 1 equiv), cesium formate (22.3 mg, 1.25 mmol, 0.5 equiv), 18-crown-6 (66.1 mg, 0.25 mmol, 1 equiv), and anhydrous *N*,*N*-dimethylformamide (1.0 mL). Tris(trimethylsilyl)silane (93.2 mg, 0.375 mmol, 1.5 equiv) was then added and the vial was capped with a screw top cap and PTFE-lined silicone septum, removed from glovebox, and the reaction mixture was stirred at rt. After 20 h, the vial was opened and ethanol (1 mL) and sulfuric acid (6.7 µL, 0.125 mmol, 0.5 equiv) were added and the vial was recapped and the reaction mixture was stirred at rt. After 1 h, the reaction mixture was diluted with ethyl acetate (6 mL) and washed with distilled water (3 x 3 mL) then brine (4 mL), dried with sodium sulfate, filtered, and concentrated into a 10 mL round bottom flask. To the resultant residue was added (carbethoxymethylene)triphenylphosphorane (95.8 mg, 1.1 equiv, 0.275 mmol), lithium bromide (43.4 mg, 2 equiv, 0.5 mmol), tetrahydrofuran (5 mL), and triethylamine (69.3 µL, 2 equiv, 0.5 mmol). The reaction flask was then capped with a septum and a nitrogen balloon was inserted, then the reaction mixture was stirred at rt for an additional 16 h. The reaction mixture was then transferred to a seperatory funnel and diluted with ethyl acetate (10 mL) and washed with water (5 mL), then brine (5 mL), dried over anhydrous sodium sulfate, filtered, and concentrated. Purification *via* silica gel chromatography (10% ethyl acetate in hexanes) provided the product as a yellow oil (88.9 mg, 59% yield). **^{1}H NMR** (400 MHz, $CDCl_3$) δ 7.50 (br s, 3H), 7.33–7.23 (m, 5H), 7.12 (s, 1H), 7.08–7.03 (m, 3H), 6.86 (dt, *J* = 15.7, 10.6 Hz, 1H), 6.22 (d, *J* = 15.7, 1H), 4.85 (q, *J* = 6.6 Hz, 1H), 4.36 (d, *J* = 2.9 Hz, 1H), 4.29–4.21 (m, 3H), 3.80 (d, *J* = 13.4 Hz, 1H), 3.58 (d, *J* = 11.2, 1H), 3.44 (s, 1H), 2.84 (d, *J* = 12.8 Hz, 2H), 2.34 (td, *J* = 11.9, 3.5 Hz, 1H), 1.46 (d, *J* = 6.6 Hz, 3H), 1.33 (t, *J* = 7.2 Hz, 3H). **^{19}F NMR** (376 MHz, $CDCl_3$) δ -62.75 (s, 3F), -94.99 (dd, *J* = 259.2, 10.9 Hz, 1F), -96.10 (dd, *J* = 259.2, 10.2 Hz, 1F),

-114.56 (t, J = 7.7 Hz, 1F). **^{13}C NMR** (101 MHz, $CDCl_3$) δ 165.0, 162.6 (d, J = 246.4 Hz), 145.7, 139.0 (t, J = 30.1 Hz), 138.0, 136.4 (t, J = 27.9 Hz), 133.8, 131.6 (q, J = 33.0 Hz), 131.0 (d, J = 7.8 Hz), 129.1, 128.4, 127.2, 126.5, (t, J = 4.9 Hz), 125.4 (t, J = 8.1 Hz), 125.0 (m), 123.4 (q, J = 272.7 Hz), 121.5 (m), 117.6 (t, J = 241.6 Hz), 115.2 (d, J = 21.3 Hz), 95.7, 72.4, 69.4, 61.5, 59.8, 59.7, 51.9, 24.7, 14.3. **IR (neat):** 2979, 2930, 2904, 2805, 1726, 1602, 1508, 1238, 1128, 1057, 1024, 835 cm^{-1}. **HRMS** (DART) $[M+H]^+$ calcd. for $[C_{32}H_{32}F_6NO_4]^+$ 608.2230, 608.2262 found.

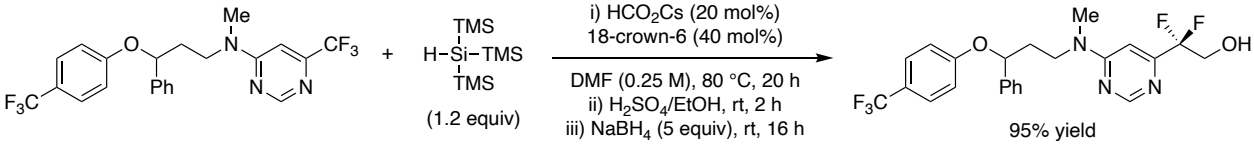

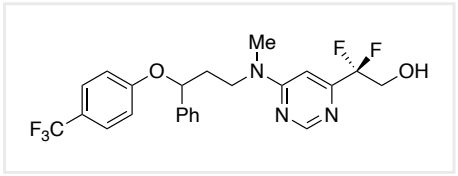

2,2-difluoro-2-(6-(methyl(3-phenyl-3-(4-(trifluoromethyl)phenoxy)propyl)amino)pyrimidin-4-yl)ethan-1-ol (3-35). In a nitrogen-filled glovebox, to an oven-dried 1-dram glass vial charged with a Teflon-coated stir bar, was added *N*-methyl-*N*-(3-phenyl-3-(4-(trifluoromethyl)phenoxy)propyl)-6-(trifluoromethyl)pyrimidin-4-amine (113.9 mg, 0.25 mmol, 1 equiv), cesium formate (8.9 mg, 0.5 mmol, 0.2 equiv), 18-crown-6 (26.4 mg, 0.1 mmol, 0.4 equiv), anhydrous *N*,*N*-dimethylformamide (1.0 mL), then tris(trimethylsilyl)silane (74.6 mg, 0.3 mmol, 1.2 equiv). The vial was capped with a screw top cap and PTFE-lined silicone septum, removed from glovebox, and placed into a preheated reaction block at 80 °C with stirring. After 20 h, the vial was opened and ethanol (2 mL) and sulfuric acid (6.7 µL, 0.125 mmol, 0.5 equiv) were added. The vial was capped and the reaction mixture was stirred for an additional 2 h at rt. Sodium borohydride (47.3 mg, 5 equiv, 1.25 mmol) was then added to the reaction mixture as a solid, the vial was capped, and the reaction solution was stirred overnight at rt. The reaction mixture was transferred to a separatory funnel, diluted with 1 M aq. sodium hydroxide (8 mL), and

extracted with ethyl acetate (3 x 10 mL). The combined organic layers were washed with brine (15 mL), dried over anhydrous sodium sulfate, filtered, and concentrated *in vacuo*. Purification *via* silica gel column chromatography (50% ethyl acetate in hexanes) provided the product as an off-white solid (111.4 mg, 95% yield). **^{1}H NMR** (400 MHz, $CDCl_3$) δ 8.50 (br s, 1H), 7.45 (d, *J* = 8.6 Hz, 2H), 7.38–7.28 (m, 5H), 6.91 (d, *J* = 8.6 Hz, 2H), 6.76 (s, 1H), 5.25 (dd, *J* = 8.7, 4.0 Hz, 1H), 4.16–3.88 (m, 5H), 3.11 (br s, 3H), 2.33–2.18 (m, 2H). **^{19}F NMR** (376 MHz, $CDCl_3$) δ -61.54 (s, 3F), -110.07 (s, 2F). **^{13}C NMR** (101 MHz, $CDCl_3$) δ 162.2, 160.3, 159.4 (t, *J* = 28.5 Hz), 157.9, 140.4, 129.0, 128.2, 126.9 (q, J = 3.8 Hz), 125.7, 124.4 (q, *J* = 271.2 Hz), 123.1 (q, *J* = 32.8 Hz), 117.5 (t, *J* = 244.5 Hz), 115.7, 99.0 (t, *J* = 4.4 Hz), 77.9, 64.0 (t, *J* = 30.7 Hz), 46.7, 36.1 **IR (neat):** 3229, 3032, 2930, 1603, 1515, 1322, 1245, 1107, 1066, 834, 700 cm^{-1}. **HRMS** (MMI) $[M+H]^+$ calcd. for $[C_{23}H_{23}F_5N_3O_2]^+$ 468.1705, 468.1726 found. **Melting Point:** 42-45 °C.

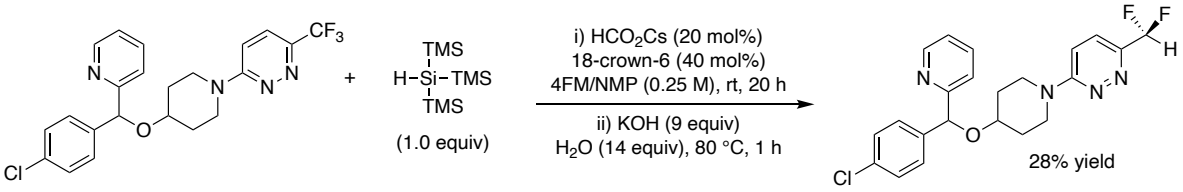

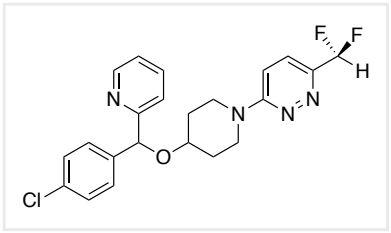

3-(4-((4-chlorophenyl)(pyridin-2-yl)methoxy)piperidin-1-yl)-6-(difluoromethyl)pyridazine (3-36). In a nitrogen-filled glovebox, to an oven-dried 1-dram vial charged with a Teflon coated stir bar, was added 3-(4-((4-chlorophenyl)(pyridin-2-yl)methoxy)piperidin-1-yl)-6-(trifluoromethyl)pyridazine (44.9 mg, 0.1 mmol, 1 equiv), cesium formate (3.5 mg, 0.02 mmol, 0.2 equiv), 18-crown-6 (10.6 mg, 0.04 mmol, 0.4 equiv), and anhydrous 4-formylmorpholine/*N*-methyl-2-pyrrolidinone (1:1 ratio, 0.4 mL). Tris(trimethylsilyl)silane (24.9 mg, 0.1 mmol, 1 equiv) was then added and the vial was capped

with a screw top cap and PTFE-lined silicone septum, removed from glovebox, and the reaction mixture was stirred at rt. After 20 h, the vial was opened and potassium hydroxide (50 mg, 8.9 equiv, 0.89 mmol) and water (25 μL, 13.8 equiv, 1.38 mmol) were added. The vial was capped and placed into a preheated reaction block at 80 °C with stirring. After 1 h, the reaction mixture was transferred to a separatory funnel, diluted with ethyl acetate (6 mL), washed with water (3 x 3 mL), then brine (4 mL), dried over anhydrous sodium sulfate, filtered, and concentrated *in vacuo*. Purification *via* preparative thin-layer chromatography (50% ethyl acetate in hexanes) provided the product as a clear oil (12.0 mg, 28% yield). **^{1}H NMR** (400 MHz, $CDCl_3$) δ 8.52 (dd, *J* = 5.1, 1.6 Hz, 1H), 7.71 (td, *J* = 7.7, 1.7 Hz, 1H), 7.54 (d, *J* = 7.9 Hz, 1H), 7.47 (d, *J* = 9.6 Hz, 1H), 7.39 (d, *J* = 8.4 Hz, 2H), 7.29 (d, *J* = 8.5 Hz, 2H), 7.19 (dd, *J* = 7.4, 4.9 Hz, 1H), 6.97 (d, *J* = 9.6 Hz, 1H), 6.76 (t, *J* = 55.0 Hz, 1H), 5.68 (s, 1H), 4.06–4.00 (m, 2H), 3.78 (tt, *J* = 7.4, 3.6 Hz, 1H), 3.52 (ddd, *J* = 12.8, 8.1, 3.6 Hz, 2H), 2.01–1.91 (m, 2H), 1.85–1.74 (m, 2H). **^{19}F NMR** (376 MHz, $CDCl_3$) δ -113.10 (d, *J* = 55.2 Hz, 2F). **^{13}C NMR** (101 MHz, $CDCl_3$) δ 161.8, 160.3, 148.9, 146.8 (t, *J* = 28.0 Hz), 140.1, 137.4, 133.7, 128.8, 128.3, 124.6, 122.8, 120.8, 114.8 (t, *J* = 237.2 Hz), 112.6, 81.2, 72.6, 42.4, 42.3, 30.81, 30.79. **IR (neat):** 3052, 2926, 2859, 1589, 1488, 1403, 1328, 1227, 1074, 1014, 820, 767 cm^{-1}. **HRMS** (DART) $[M+H]^+$ calcd. for $[C_{22}H_{22}ClF_2N_4O]^+$ 431.1445, 431.1458 found.

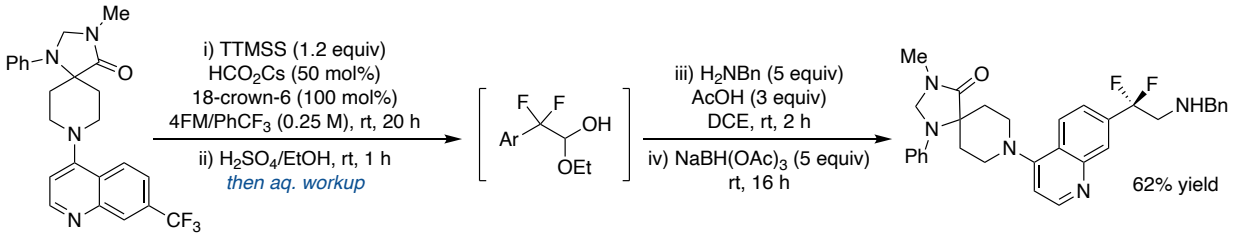

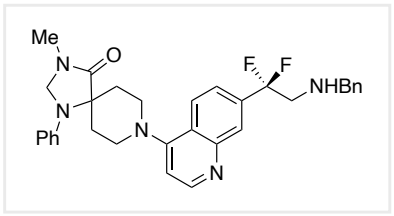

8-(7-(2-(benzylamino)-1,1-difluoroethyl)quinolin-4-yl)-3-methyl-1-phenyl-1,3,8-triazaspiro[4.5]decan-4-one (3-37). In a nitrogen-filled glovebox, to an oven-dried 1-dram glass vial charged with a Teflon-coated stir bar, was added 3-methyl-1-phenyl-8-(7-(trifluoromethyl)quinolin-4-yl)-1,3,8-triazaspiro[4.5]decan-4-one (44.0 mg, 0.1 mmol, 1 equiv), cesium formate (8.9 mg, 0.05 mmol, 0.5 equiv), 18-crown-6 (26.4 mg, 0.1 mmol, 1 equiv), and anhydrous *N*,*N*-dimethylformamide (0.4 mL). Then tris(trimethylsilyl)silane (29.8 mg, 0.12 mmol, 1.2 equiv) was added and the vial was capped with a screw top cap and PTFE-lined silicone septum, removed from glovebox, and the reaction mixture was stirred at rt. After 20 h, the vial was opened and ethanol (0.2 mL) and sulfuric acid (2.7 µL, 0.05 mmol, 0.5 equiv) were added, the vial was recapped and the reaction mixture was stirred at rt. After 1 h, the reaction mixture was diluted with ethyl acetate (6 mL) and washed with distilled water (3 x 3 mL), then brine (4 mL), dried with sodium sulfate, and concentrated into a 10 mL round bottom flask. To the resulting residue was added 1,2-dichloroethane (3 mL), acetic acid (17.2 µL, 3 equiv, 0.3 mmol), and benzylamine (54.6 µL, 5 equiv, 0.5 mmol). The reaction flask was capped with a septum and the reaction mixture was stirred for 2 h. Sodium triacetoxyborohydride (106.0 mg, 5 equiv, 0.5 mmol) was then added and the vial was capped with a septum, a nitrogen balloon was inserted, and the reaction mixture was stirred overnight at rt. The reaction mixture was then transfered into a seperatory funnel with dichloromethane (4 mL) and washed with 1 M aq. sodium hydroxide (3 mL), then water (3 mL) and brine (4 mL), dried over anhydrous sodium sulfate, filtered, and concentrated. Purification *via* preparative thin-layer chromatography (1% triethylamine and 1% methanol in dichloromethane) provided the product as a pale-yellow oil (33.7 mg, 62% yield). **^{1}H NMR** (400 MHz, $CDCl_3$) δ 8.75 (d, *J* = 5.2 Hz, 1H), 8.28 (s, 1H), 8.07 (d, *J* = 8.7 Hz, 1H), 7.62

(dd, J = 8.9, 1.8 Hz, 1H), 7.36–7.20 (m, 7H), 6.97–6.89 (m, 4H), 4.75 (s, 2H), 3.88–3.81 (m, 4H), 3.65–3.61 (m, 2H), 3.31 (t, J = 14.2 Hz, 2H), 3.04 (s, 3H), 2.98 (td, J = 13.0, 5.0 Hz, 2H), 1.88 (d, J = 14.2 Hz, 2H). **^{19}F NMR** (376 MHz, $CDCl_3$) δ -100.76 (t, J = 14.3 Hz, 2F). **^{13}C NMR** (101 MHz, $CDCl_3$) δ 174.3, 157.7, 151.2, 148.4, 142.8, 139.7, 137.1 (t, J = 26.4 Hz), 129.7, 128.6, 128.2, 127.2 127.0 (t, J = 6.8 Hz), 124.4, 124.1, 122.1 (t, J = 5.6 Hz), 121.8 (t, J = 244.3 Hz), 119.3, 115.0, 109.8, 65.4, 60.1, 54.7 (t, J = 29.1 Hz), 53.6, 49.1, 29.6, 27.8. **IR (neat):** 3330, 2967, 2927, 2854, 1672, 1614, 1511, 1450, 1180, 1127, 1086, 713 cm^{-1}. **HRMS** (DART) $[M+H]^+$ calcd. for $[C_{32}H_{34}F_2N_5O]^+$ 542.2726, 542.2725 found.

A1.8 Mechanistic experiments

a. Solvent Dependent Product Formation

Discussion: The experiments below demonstrate that the major product of the reaction is dependent upon the solvent used. When the reaction solvent is NMP, the major product is the difluorobenzylsilane **3-38**. When the reaction solvent is MeCN, the major product is the difluoromethylarene **3-29**. The implication of these results is expanded upon in the next section.

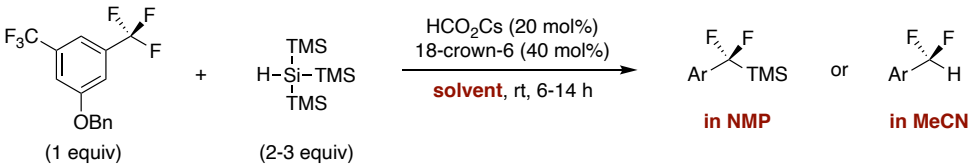

General Procedure 3 (GP3): In a nitrogen-filled glovebox, to an oven-dried 1-dram glass vial charged with a Teflon-coated stir bar, was added 1-(benzyloxy)-3,5-bis(trifluoromethyl)benzene (32.0 mg, 0.1 mmol, 1.0 equiv), 18-crown-6 (10.6 mg, 0.04 mmol, 0.4 equiv), cesium formate (3.5 mg, 0.02 mmol, 0.2 equiv), and anhydrous solvent (0.4 mL). Tris(trimethylsilyl)silane (1.2 to 3

equiv) was then added, and the vial was capped with a screw top PTFE-lined cap, removed from glovebox, and the reaction mixture was stirred at rt. After 16 h, the reaction mixture was quenched with 0.1 mL $CDCl_3$, stirred for 1 min, then dibromomethane (as freshly prepared 2.0 M solution in $CDCl_3$, 50.0 µL, 0.1 mmol, 1 equiv) was added as an internal standard and an aliquot was analyzed by ^{1}H NMR spectroscopy by integration of characteristic aryl C–H protons of the benzyl silane (singlets at 7.08 or 7.17 ppm) or the difluoromethylarene's characteristic $ArCF_2$–H shift (triplet at 6.65 ppm). Yields and characterization data are provided below for each reaction.

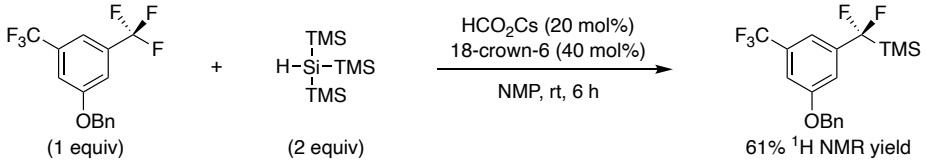

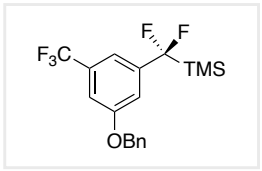

((3-(benzyloxy)-5-(trifluoromethyl)phenyl)difluoromethyl)trimethylsilane (3-38). The General Procedure 3 (GP3) was followed using anhydrous *N*-methyl-2-pyrrolidinone as solvent (0.4 mL) and tris(trimethylsilyl)silane (49.7 mg, 0.2 mmol, 2 equiv). Analysis of the chemical shifts for the aryl C–H protons of the benzyl silane (singlets at 7.08 and 7.17 ppm) provided the ^{1}H NMR yield referenced to a dibromomethane internal standard as 61%. Pure product was isolated for characterization by preparative thin layer chromatography (100% hexanes) as a white solid. **^{1}H NMR** (400 MHz, $CDCl_3$) δ 7.45–7.33 (m, 5H), 7.23 (s, 1H), 7.17 (s, 1H), 7.08 (s, 1H), 5.12 (s, 2H), 0.11 (s, 9H). **^{19}F NMR** (376 MHz, $CDCl_3$) δ -62.85 (s, 3F), -112.55 (s, 2F). **^{13}C NMR** (101 MHz, $CDCl_3$) δ 159.1, 141.0 (t, J = 20.9 Hz), 136.1, 132.3 (q, J = 32.7 Hz), 128.9, 128.5, 127.7, 127.6 (t, J = 266.2 Hz), 123.8 (q, J = 272.6 Hz), 114.7 (t, J = 7.8 Hz), 114.2 (tq, J = 8.0, 3.9 Hz), 112.5 (qt, J = 3.9, 2.0 Hz), 70.6, -4.9 (t, J = 1.7 Hz). **IR (neat):** 2961,

2903, 1331, 1253, 1218, 1128, 1047, 1002, 840, 705 cm^{-1}. **GC-MS (EI)** M^+ calcd. for $[C_{18}H_{19}F_5OSi]^+$ 374.11, 374.15 found. **Melting Point:** 70-73 ºC.

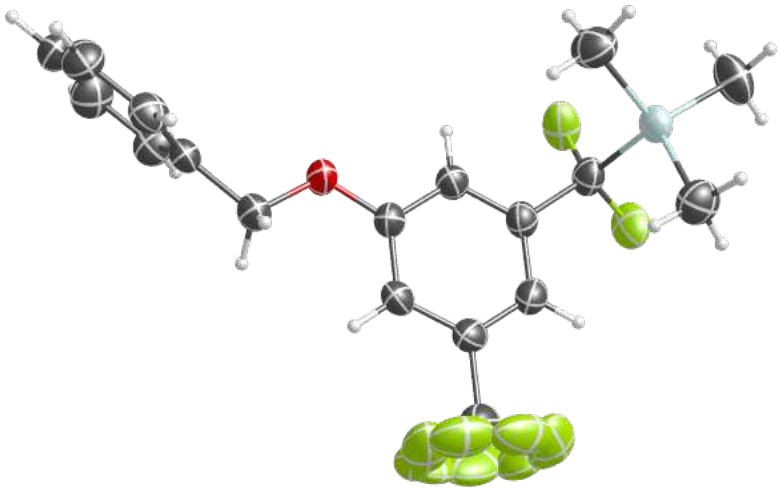

Above: X-ray crystal structure of Compound **3-38**. Thermal ellipsoids are at 50% probability. Colors of atoms are as follows: carbon (black), oxygen (red), fluorine (green), silicon (light blue), hydrogen (white).

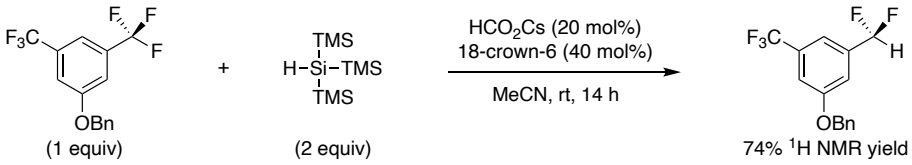

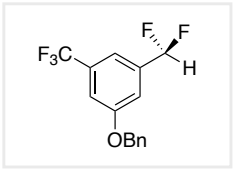

1-(benzyloxy)-3-(difluoromethyl)-5-(trifluoromethyl)benzene (3-29). The General Procedure 3 (GP3) was followed using anhydrous acetonitrile as solvent (0.4 mL) and tris(trimethylsilyl)silane (74.6 mg, 0.3 mmol, 3 equiv). Analysis of the chemical shifts for the difluoromethylarene's characteristic $ArCF_2$–H peak (triplet at 6.65 ppm) provided the ^{1}H NMR yield referenced to a dibromomethane internal standard as 74%. Pure product was isolated for characterization by preparative thin layer chromatography (100% hexanes) as a clear oil. **^{1}H NMR** (400 MHz, $CDCl_3$) δ 7.45–7.37 (m, 6H), 7.34 (s, 1H), 7.30 (s, 1H), 6.65 (t, J = 56.1 Hz), 5.13 (s, 2H). **^{19}F NMR** (376 MHz, $CDCl_3$) δ -62.92 (s, 3F), -111.84 (d, J = 56.2 Hz, 2F). **^{13}C NMR** (101 MHz, $CDCl_3$) δ 159.4, 136.9 (t, J = 23.0 Hz), 135.8,

132.8 (q, J = 33.1 Hz), 128.9, 128.6, 127.8, 123.6 (q, J = 272.8 Hz), 115.4 (t, J = 5.9 Hz), 115.1 (td, J = 6.4, 3.5 Hz), 114.3 (dt, J = 3.6, 1.8 Hz), 113.7 (t, J = 240.4 Hz), 70.8. **IR (neat):** 3035, 2919, 1608, 1455, 1340, 1240, 1169, 1126, 1026, 864, 738, 694 cm^{-1}. **GC-MS (EI)** M^+ calcd. for $[C_{15}H_{12}F_5O]^+$ 302.07, 302.10 found.

b. Defluorosilylation is a likely intermediate to other defluorofunctionalization products

Discussion: To test the identity of benzylsilane **3-38** as an intermediate towards hemiaminal **3-2**, isolated benzylsilane **3-38** was subjected to catalytic base (cesium formate or cesium fluoride) in DMF solvent with either 0 or 1 equiv TTMSS. Under all conditions benzylsilane **3-38** was transformed into hemiaminal **3-2** without any starting material (**3-38**) remaining.

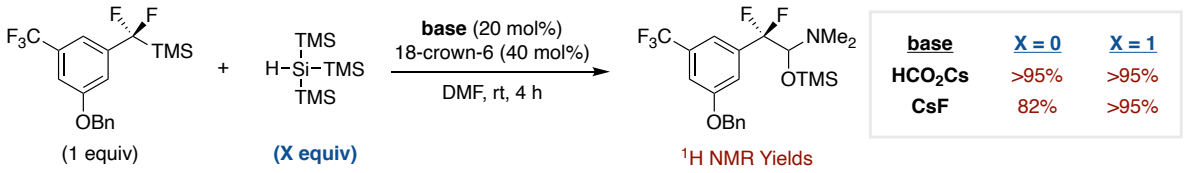

Procedure: In a nitrogen-filled glovebox, to an oven-dried 1-dram glass vial charged with a Teflon-coated stir bar was added ((3-(benzyloxy)-5-(trifluoromethyl)phenyl)difluoromethyl)trimethylsilane (37.4 mg, 0.1 mmol, 1.0 equiv), 18-crown-6 (10.6 mg, 0.04 mmol, 0.4 equiv), and anhydrous *N*,*N*-dimethylformamide (0.4 mL). To the solution was sequentially added tris(trimethylsilyl)silane (if used: 24.9 mg, 0.1 mmol, 1 equiv) and cesium formate (3.5 mg, 0.02 mmol, 0.2 equiv). The vial was capped with a screw top PTFE-lined cap, removed from glovebox, and the reaction solution was stirred at rt. After 4 h, the reaction mixture was quenched with 0.1 mL $CDCl_3$, stirred for 1 min, then dibromomethane (as freshly prepared 2.0 M solution in $CDCl_3$, 50.0 µL, 0.1 mmol, 1 equiv) was added as an internal standard and an aliquot was analyzed by ^1H NMR spectroscopy using the diagnostic chemical shift of

product **2** (doublet of doublets at 4.39 ppm) referenced to the dibromomethane internal standard (singlet at 4.91 ppm). The obtained ^{1}H NMR yields are shown in the scheme above.

Discussion: To test the identity of benzylsilane **3-38** as an intermediate towards difluoromethylarene **3-39**, isolated benzylsilane **3-38** was subjected to basic conditions in acetonitrile. The following two reactions show the protodesilylation using cesium formate and cesium fluoride. At rt, catalytic cesium formate did not turn over and only provided 14% ^{1}H NMR yield of **3-39**, but heating to 80 °C provided full conversion and 86% ^{1}H NMR yield of **3-39**. Conversely, catalytic cesium fluoride provided full conversion of **3-38** and 80% ^{1}H NMR yield of the **3-39** at rt.

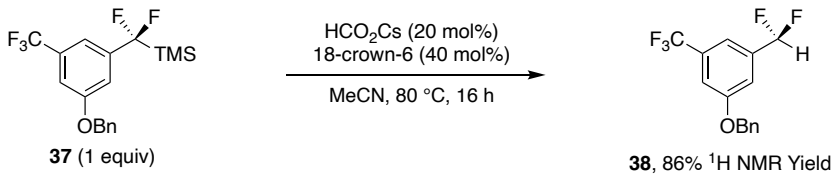

37 (1 equiv)

38, 86% ^{1}H NMR Yield

Procedure: In a nitrogen-filled glovebox, to an oven-dried 1-dram glass vial charged with a Teflon-coated stir bar was added ((3-(benzyloxy)-5-(trifluoromethyl)phenyl)difluoromethyl)trimethylsilane (37.4 mg, 0.1 mmol, 1.0 equiv), 18-crown-6 (10.6 mg, 0.04 mmol, 0.4 equiv), anhydrous acetonitrile (0.4 mL) and cesium formate (3.5 mg, 0.02 mmol, 0.2 equiv). The vial was capped with a screw top PTFE-lined cap, removed from glovebox, and the reaction solution was stirred at 80 °C. After 16 h, the reaction mixture was quenched with 0.1 mL $CDCl_3$, stirred for 1 min, then dibromomethane (as freshly prepared 2.0 M solution in $CDCl_3$, 50.0 μL, 0.1 mmol, 1 equiv) was added as an internal standard and an aliquot was analyzed by ^{1}H NMR spectroscopy using the diagnostic $ArCF_2$–H chemical shift (triplet at

6.65 ppm) referenced to the dibromomethane internal standard (singlet at 4.91 ppm). The ^{1}H NMR yield was determined to be 86%.

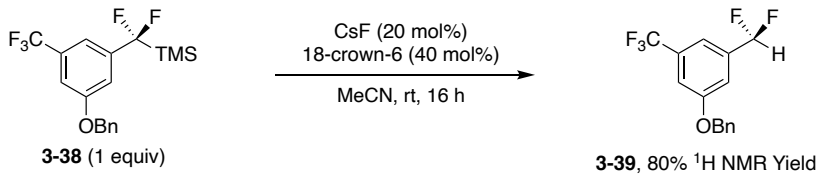

3-38 (1 equiv)

3-39, 80% ^{1}H NMR Yield

Procedure: In a nitrogen-filled glovebox, to an oven-dried 1-dram glass vial charged with a Teflon-coated stir bar was added ((3-(benzyloxy)-5-(trifluoromethyl)phenyl)difluoromethyl)trimethylsilane (37.4 mg, 0.1 mmol, 1.0 equiv), 18-crown-6 (10.6 mg, 0.04 mmol, 0.4 equiv), anhydrous acetonitrile (0.4 mL) and cesium fluoride (3.0 mg, 0.02 mmol, 0.2 equiv). The vial was capped with a screw top PTFE-lined cap, removed from glovebox, and the reaction solution was stirred at rt. After 16 h, the reaction mixture was quenched with 0.1 mL $CDCl_3$, stirred for 1 min, then dibromomethane (as freshly prepared 2.0 M solution in $CDCl_3$, 50.0 μL, 0.1 mmol, 1 equiv) was added as an internal standard and an aliquot was analyzed by ^{1}H NMR spectroscopy using the diagnostic $ArCF_2$–H chemical shift (triplet at 6.65 ppm) referenced to the dibromomethane internal standard (singlet at 4.91 ppm). The ^{1}H NMR yield was determined to be 80%.

c. Reaction profile analysis

Discussion: A reaction profile was conducted to verify the intermediacy of benzylsilane **3-38** towards the production of silylated hemiaminal **3-2**. Concurrent formation of **3-2** and **3-38** can be observed. The starting material (**3-1**) is completely consumed at the 75 minute timepoint and the remaining **3-38** is converted to **3-2** at the 90 minute timepoint.

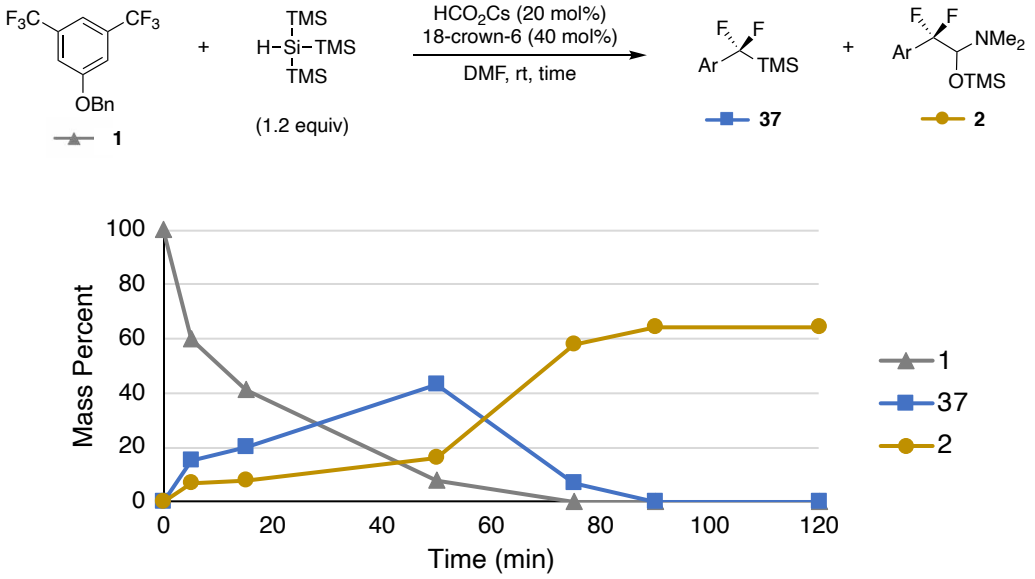

Procedure: In a nitrogen-filled glovebox, a stock solution was created with 1-(benzyloxy)-3,5-bis(trifluoromethyl)benzene (320.2 mg, 1.0 mmol, 1.0 equiv), cesium formate (35.6 mg, 0.2 mmol, 0.2 equiv), 18-crown-6 (105.6 mg, 0.4 mmol, 0.4 equiv), 4-fluorobiphenyl (81.2 mg, 0.47 mmol, 0.47 equiv), and anhydrous *N*,*N*-dimethylformamide (4.0 mL). The solution was stirred until completely homogenized. In the nitrogen-filled glovebox, 400 µL of the stock solution was added to eight different oven-dried 1-dram vials charged with Teflon-coated stir bars. Tris(trimethylsilyl)silane (37.0 µL, 0.12 mmol, 1.2 equiv) was then added to each vial, the vials were capped with a screw top PTFE-lined cap, removed from glovebox, and reaction solutions were stirred at rt. After the time indicated, a reaction vial was quenched with 0.1 mL $CDCl_3$ and an aliquot was analyzed by ^{19}F NMR spectroscopy using 4-fluorobiphenyl as the internal standard (multiplet centered at -116.31 ppm) to provide ^{19}F NMR yields of the starting material ($ArCF_3$ **3-1**, singlet at -63.26 ppm), deflurosilylation intermediate (**3-38**, singlet at -112.82 ppm), and hemiaminal product (**3-2**, doublet of doublets at -105.28 and -107.51 ppm). The data points are tabulated below. Vial 0 is an analysis of the stock solution before addition of

tris(trimethylsilyl)silane. **Note:** A 15 second relaxation delay was necessary to achieve accurate integration using the 4-fluorobiphenyl internal standard in ^{19}F NMR.

Vial	Time (min)	$ArCF_3$ (3-1)	$ArCF_2TMS$ (3-38)	3-2
0	0	100%	0%	0%
1	5	60%	15%	7%
2	15	41%	20%	8%
3	50	8%	43%	16%
4	75	0%	7%	58%
5	90	0%	0%	64%
6	120	0%	0%	64%
7	180	0%	0%	64%

d. Evidence of silyl anion formation under reaction conditions

Section Discussion: The experiments in this section were conducted to probe the identity of the active silyl species generated from the activation of TTMSS with 18-crown-6 ligated cesium formate in DMF. Replacement of the trifluoromethylarene electrophile with other electrophiles (1,2,3,4-tetrafluorobenzene, 3-chloropropylbenzene, and styrene oxide) resulted in substitution or elimination products that support the formation of two different silyl anions (the trimethylsilyl anion and the 1,1,1,3,3,3-hexamethyltrisilyl anion) under the reaction conditions. The 1,2,3,4-tetrafluorobenzene electrophile undergoes substitution from a trimethylsilyl anion. The 3-chloropropylbenzene electrophile undergoes substitution from the 1,1,1,3,3,3-hexamethyltrisilyl anion. The styrene oxide electrophile undergoes ring opening from a trimethylsilyl anion, followed

by a Peterson-type elimination to generate styrene and a trimethylsilyloxy anion that is silylated *in situ* to generate hexamethyldisiloxane.

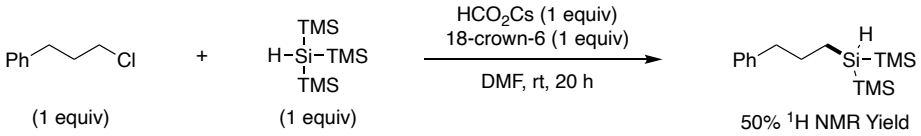

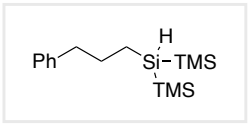

1,1,1,3,3,3-hexamethyl-2-(3-phenylpropyl)trisilane (3-40). In a nitrogen-filled glovebox, to an oven-dried 2-dram glass vial charged with a Teflon-coated stir bar was added (3-chloropropyl)benzene (77.3 mg, 0.5 mmol, 1.0 equiv), 18-crown-6 (132.2 mg, 0.5 mmol, 1 equiv), anhydrous *N*,*N*-dimethylformamide (4.0 mL) and cesium formate (89.0 mg, 0.5 mmol, 1 equiv). Tris(trimethylsilyl)silane (124.3 mg, 0.5 mmol, 1 equiv) was then added and the vial was capped with a screw top PTFE-lined cap, removed from glovebox, and the reaction solution was stirred at rt. After 20 h, the reaction mixture was quenched with 1.0 mL $CDCl_3$, stirred for 1 min, then dibromomethane (69.5 µL, 1.0 mmol, 2 equiv) was added as an internal standard and an aliquot was analyzed by ^{1}H NMR spectroscopy using the multiplet centered at 0.79 ppm referenced to the dibromomethane internal standard (singlet at 4.91 ppm). The ^{1}H NMR yield was determined to be 50%. Pure product was isolated for characterization by an aqueous workup followed by preparative thin layer chromatography (100% hexanes), providing the product as a clear oil. **^{1}H NMR** (400 MHz, C_6D_6) δ 7.20–7.05 (m, 5H), 3.38 (t, J = 4.6 H, 1H), 2.59 (t, J = 7.5 Hz, 2H), 1.83–1.75 (m, 2H), 0.86–0.81 (m, 2H), 0.19 (s, 18H). **^{13}C NMR** (101 MHz, C_6D_6) δ 142.5, 128.8, 128.7, 126.1, 39.9, 31.0, 7.1, 0.4. **IR (neat):** 3927, 2951, 2893, 2060, 1399, 1244, 1040, 831, 745, 695, 614 cm^{-1}. **GC-MS (EI)** M^+ calcd. for $[C_{15}H_{30}Si_3]^+$ 294.17, 294.20 found.

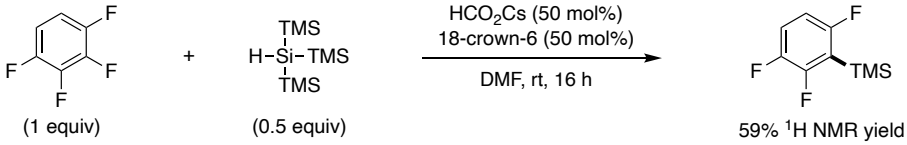

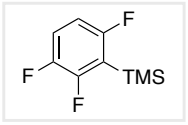

Trimethyl(2,3,6-trifluorophenyl)silane (3-39). In a nitrogen-filled glovebox, to an oven-dried 1-dram glass vial charged with a Teflon-coated stir bar, was added 1,2,3,4-tetrafluorobenzene (150.1 mg, 1.0 mmol, 1.0 equiv), 18-crown-6 (132.2 mg, 0.5 mmol, 0.5 equiv), anhydrous *N*,*N*-dimethylformamide (4.0 mL) and cesium formate (89.0 mg, 0.5 mmol, 0.5 equiv). Tris(trimethylsilyl)silane (124.4 mg, 0.5 mmol, 0.5 equiv) was then added and the vial was capped with a screw top PTFE-lined cap, removed from glovebox, and the reaction solution was stirred at rt. After 16 h, the reaction mixture was transferred to a separatory funnel and was diluted with ethyl acetate (12 mL), washed with H_2O (3 x 4 mL), then brine (6 mL), dried over anhydrous sodium sulfate and concentrated *in vacuo*. To the residue was added dibromomethane (69.5 µL, 1.0 mmol, 1.0 equiv) as an internal standard and an aliquot was analyzed by ^{1}H NMR spectroscopy using an aromatic peak (qd at 7.05 or dddd at 6.66 ppm) referenced to the internal standard (singlet at 4.90 ppm). The ^{1}H NMR yield was determined to be 59%. **^{1}H NMR** (400 MHz, $CDCl_3$) δ 7.05 (qd, *J* = 9.2, 5.1 Hz, 1H), 6.66 (dddd, *J* = 9.3, 7.9, 3.1, 2.0 Hz), 0.33 (s, 9H). **^{19}F NMR** (376 MHz, $CDCl_3$) δ -103.35 (dt, *J* = 15.3, 6.3 Hz, 1F), -122.49 (dd, *J* = 23.0, 9.1 Hz, 1F), -143.75 (dddd, *J* = 23.1, 16.8, 9.5, 3.3 Hz, 1F); spectral data matches reported values.[5] Crude ^{1}H and ^{19}F NMR spectrum provided below.

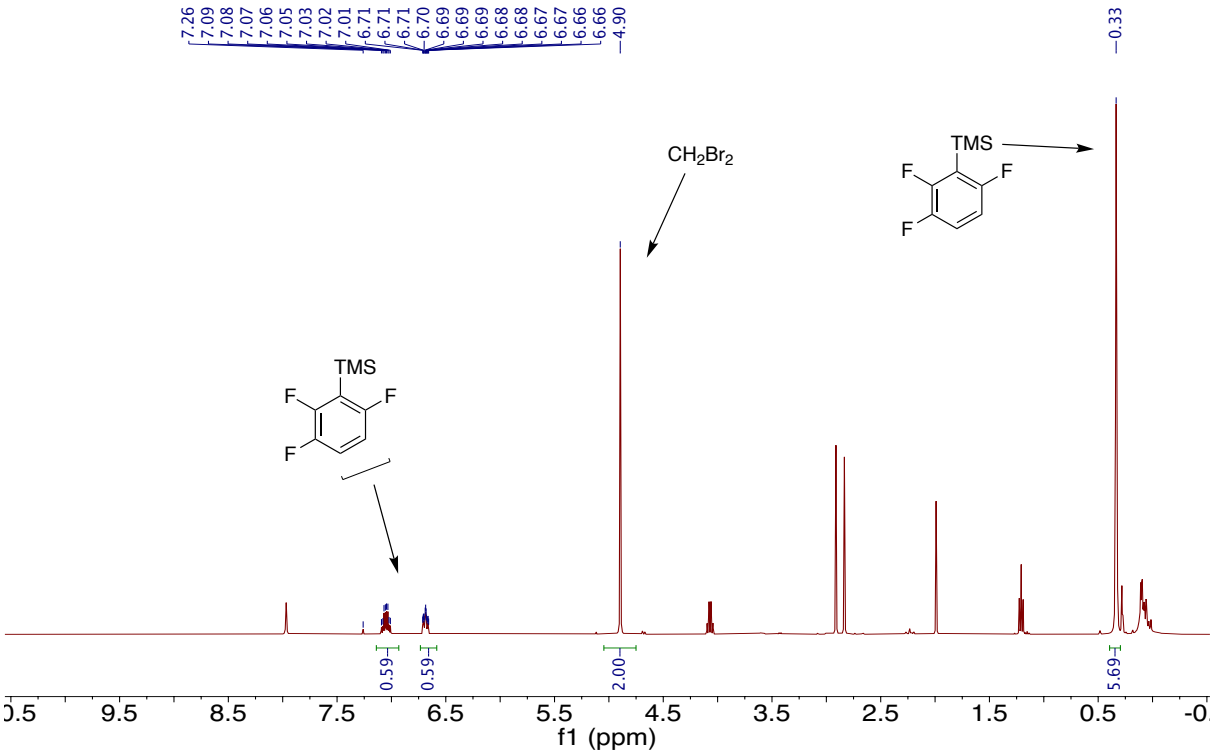

Above: ^{1}H NMR spectrum of crude reaction (after aqueous workup) of the defluorosilylation of 1,2,3,4-tetrafluorobenzene with TTMSS activated by 18-crown-6 ligated cesium formate in DMF. Reference to the dibromomethane internal standard shows an ^{1}H NMR yield of 59% of trimethyl(2,3,6-trifluorophenyl)silane (3-39). Residual DMF and EtOAc peaks are visible in the spectrum.

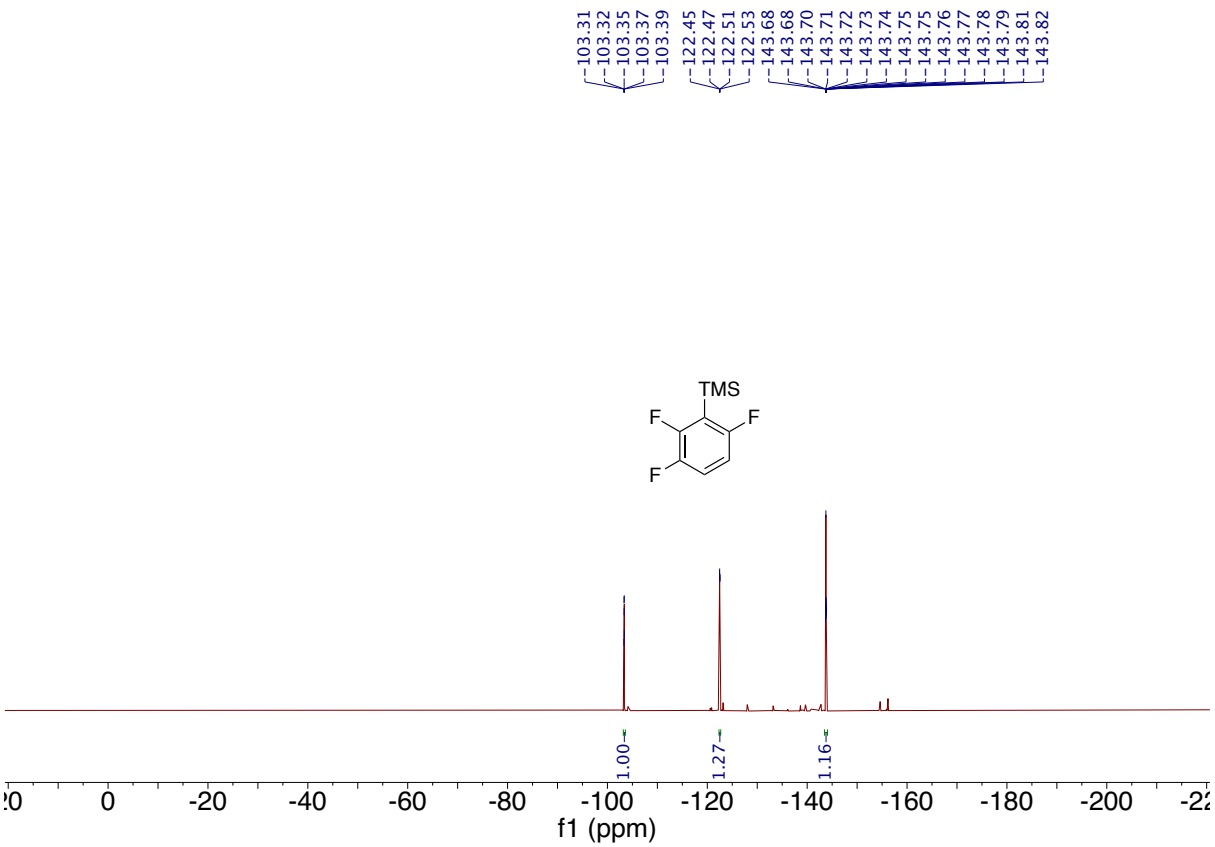

Above: ^{19}F NMR spectrum of the crude trimethyl(2,3,6-trifluorophenyl)silane (3-39)

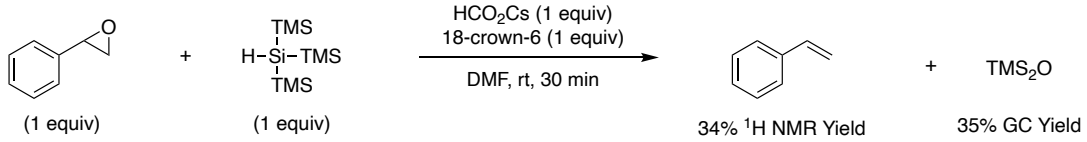

Procedure: In a nitrogen-filled glovebox, to an oven-dried 2-dram glass vial charged with a Teflon-coated stir bar, was added styrene oxide (60.1 mg, 0.5 mmol, 1.0 equiv), 18-crown-6 (132.2 mg, 0.5 mmol, 1.0 equiv), anhydrous *N*,*N*-dimethylformamide (2.0 mL) and cesium formate (89.0 mg, 0.5 mmol, 1.0 equiv). Tris(trimethylsilyl)silane (124.3 mg, 0.5 mmol, 0.5 equiv) was then added and the vial was capped with a screw top PTFE-lined cap, removed from glovebox, and the reaction solution was stirred at rt. After 30 min, the reaction mixture was quenched with 1.0 mL $CDCl_3$, stirred for 1 min, then biphenyl (157.3 mg, 1.02 mmol, 2.04 equiv) and dibromomethane (34.8 μL, 0.5 mmol, 1.0 equiv) were added as internal standards. An aliquot was analyzed by ^1H

NMR spectroscopy using the vinyl peaks from styrene (doublet at 5.66 ppm) referenced to the dibromomethane internal standard (singlet at 4.87 ppm). The ^{1}H NMR yield was determined to be 34%. An aliquot was also analyzed by gas chromatography using biphenyl as the internal standard to quantify the amount of hexamethyldisiloxane (TMS_2O) produced in the reaction. A calibration curve of TMS_2O and biphenyl provides a GC yield of 35% TMS_2O. **^{1}H NMR** (400 MHz, $CDCl_3$) δ 7.34–7.15 (m, 5H), 6.64 (dd, *J* = 17.6, 10.9 Hz, 1H), 5.67 (d, *J* = 17.6 Hz, 1H), 5.16 (d, *J* = 10.9 Hz, 1H). Spectral data matches an authentic sample (Acros Catalog #220532500) and spiking authentic styrene into the crude reaction mixture verifies the formation of styrene as the product. The ^{1}H NMR spectrum of the crude reaction mixture is shown below.

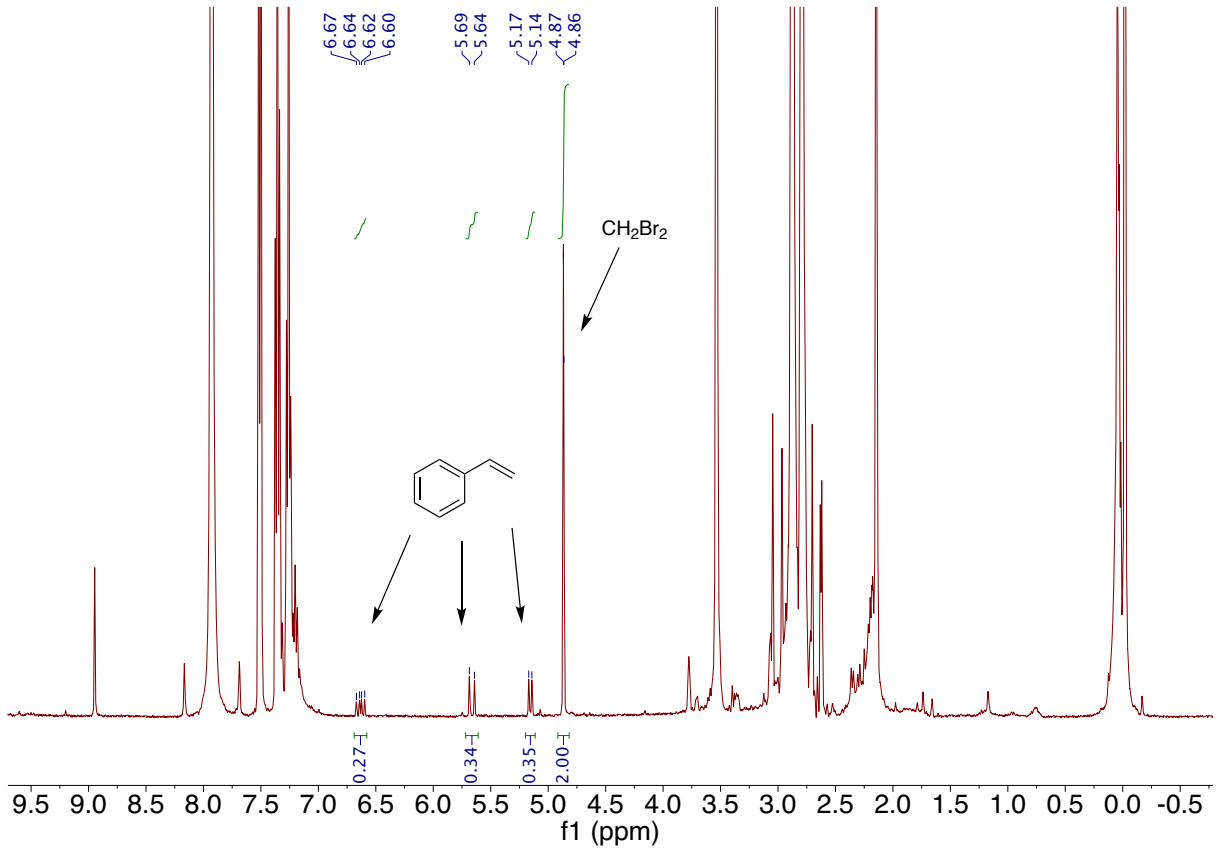

Above: ^{1}H NMR spectrum of the crude reaction mixture showing the formation of styrene from styrene oxide using TTMSS activated by 18-crown-6 ligated cesium formate in DMF. The ^{1}H NMR yield of styrene is 34% referenced to the dibromomethane internal standard.

e. Effect of additives on reaction yield

Discussion: To probe the reaction mechanism, the model reaction was carried out with various additives to gauge their effect on the reaction yield. Chlorobenzene had a negligible effect on the yield, whereas bromo- and iodobenzene completely shut down any reactivity. Arylbromides and aryliodides have been reported to undergo halophilic attack by silyl anions.[6] Phenyl triflate also results no reactivity, which can be attributed to preferential reduction over the trifluoromethylarene. The presence of radical traps (TEMPO and BHT) have a negligible effect on the yield as well.

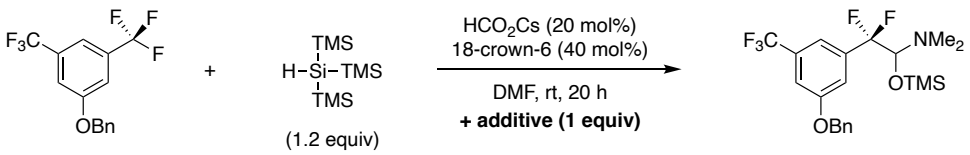

Additive:	none	PhCl	PhBr	PhI	$PhSO_2CF_3$	TEMPO	BHT
^{1}H NMR Yield:	76%	69%	0%	0%	0%	65%	75%

Procedure: In a nitrogen-filled glovebox, to an oven-dried 1-dram glass vial charged with a Teflon-coated stir bar, was added 1-(benzyloxy)-3,5-bis(trifluoromethyl)benzene (32.0 mg, 0.1 mmol, 1.0 equiv), 18-crown-6 (10.6 mg, 0.04 mmol, 0.4 equiv), the additive (0.1 mmol, 1.0 equiv), and anhydrous *N*,*N*-dimethylformamide (0.4 mL). To the solution was sequentially added tris(trimethylsilyl)silane (29.8 mg, 0.12 mmol, 1.2 equiv), and cesium formate (3.5 mg, 0.02 mmol, 0.2 equiv). The vial was capped, removed from glovebox, and the reaction solution was stirred at rt. After 20 h, the reaction mixture was quenched with 0.1 mL $CDCl_3$, stirred for 1 min, then dibromomethane (as freshly prepared 2.0 M solution in $CDCl_3$, 50.0 μL, 0.1 mmol, 1 equiv) was added as an internal standard and an aliquot was analyzed by ^{1}H NMR spectroscopy. The ^{1}H NMR yield was referenced to the dibromomethane internal standard according to the procedure described above in Section IIa.

f. Use of other disilane reagents instead of TTMSS

Discussion: A variety of R–Si(TMS)$_3$ reagents were evaluated to see if they can promote the reductive coupling reaction. TTMSS, where R = H, provided the highest yield of the product in the model reaction. When R = TMS, Me, Ph, pyrrolidine, the yield was substantially lower at around 10% yield. When R = allyl, the hemiaminal was formed in 6% yield when the reaction was heated to 80 °C. These results suggest that TTMSS possesses the right balance of steric and electronic properties to successfully promote the reductive coupling reaction.

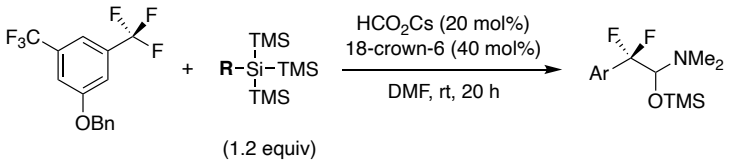

R	^{1}H NMR Yield
H	69 %
TMS	7%
Me	12 %
Ph	trace
pyrrolidine	12 %
allyl (@ 80 °C)	6 %

Procedure: In a nitrogen-filled glovebox, to an oven-dried 1-dram glass vial charged with a Teflon-coated stir bar, was added 1-(benzyloxy)-3,5-bis(trifluoromethyl)benzene (32.0 mg, 0.1 mmol, 1.0 equiv), 18-crown-6 (10.6 mg, 0.04 mmol, 0.4 equiv), and anhydrous *N*,*N*-dimethylformamide (0.4 mL). To the solution was sequentially added silane reagent (0.12 mmol, 1.2 equiv), and cesium formate (3.5 mg, 0.02 mmol, 0.2 equiv). The vial was capped, removed from glovebox, and the reaction solution was stirred at rt. After 20 h, the reaction mixture was quenched with 0.1 mL $CDCl_3$, stirred for 1 min, then dibromomethane (as freshly prepared 2.0 M solution in $CDCl_3$, 50.0 μL, 0.1 mmol, 1 equiv) was added as an internal standard and an aliquot was analyzed by ^{1}H NMR spectroscopy. The ^{1}H NMR yield was referenced to the dibromomethane internal standard according to the procedure described above in Section IIa.

Discussion: The use of the common disilane reagent, hexamethyldisilane, does not promote the reductive coupling reaction. Use of cesium formate at rt provides no reactivity, with all of the trifluoromethylarene remaining at the end of the reaction. Use of cesium fluoride does not provide appreciable amounts of product, and a low mass balance remains of the trifluoromethylarene. These conditions can only possibly generate the trimethylsilyl anion, suggesting that the trimethylsilyl anion alone cannot promote the reductive coupling reaction.

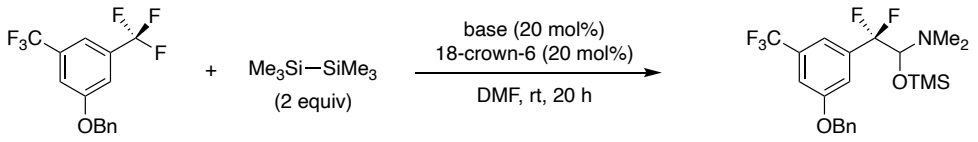

Base	^{1}H NMR Yield
HCO_2Cs	0% (100% SM)
CsF	0% (29% SM)

Procedure: In a nitrogen-filled glovebox, to an oven-dried 1-dram glass vial charged with a Teflon-coated stir bar, was added 1-(benzyloxy)-3,5-bis(trifluoromethyl)benzene (32.0 mg, 0.1 mmol, 1.0 equiv), 18-crown-6 (10.6 mg, 0.04 mmol, 0.4 equiv), and anhydrous *N*,*N*-dimethylformamide (0.4 mL). To the solution was sequentially added hexamethyldisilane (20.5 µL, 0.2 mmol, 2.0 equiv), and cesium formate (3.5 mg, 0.02 mmol, 0.2 equiv) or cesium fluoride (3.0 mg, 0.02 mmol. 0.2 equiv). The vial was capped, removed from glovebox, and the reaction solution was stirred at rt. After 20 h, the reaction mixture was quenched with 0.1 mL $CDCl_3$, stirred for 1 min, then dibromomethane (as freshly prepared 2.0 M solution in $CDCl_3$, 50.0 µL, 0.1 mmol, 1 equiv) was added as an internal standard and an aliquot was analyzed by ^{1}H NMR spectroscopy. The ^{1}H NMR yield was referenced to the dibromomethane internal standard according to the procedure described above in Section **A1.2a**.

g. Deuterium incorporation through use of deuterated reaction solvent

Discussion: Deuterium is incorporated into the derivatized product using DMF-d_7 as the reaction solvent for the reductive coupling reaction. Full deuterium incorporation from the reductive coupling suggests that the TTMSS hydrogen [H–Si(TMS)$_3$] is not incorporated into the product.

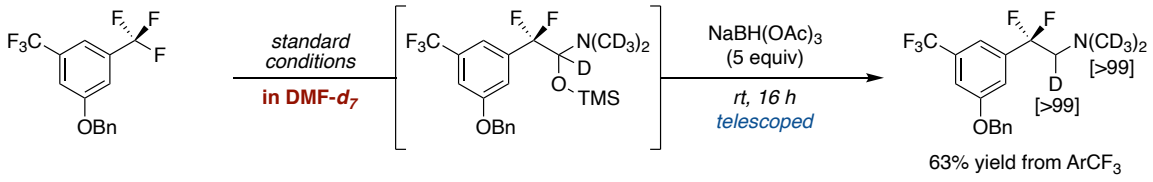

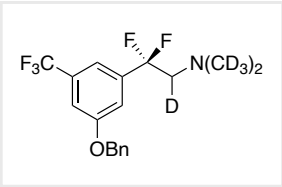

2-(3-(benzyloxy)-5-(trifluoromethyl)phenyl)-2,2-difluoro-*N*,*N*-bis(methyl-*d*3)ethan-1-amine-1-*d* (A1-3). In a nitrogen-filled glovebox, to an oven-dried 1-dram glass vial charged with a Teflon-coated stir bar, was added 1-(benzyloxy)-3,5-bis(trifluoromethyl)benzene (64.0 mg, 0.2 mmol, 1.0 equiv), cesium formate (7.0 mg, 0.04 mmol, 0.2 equiv), 18-crown-6 (21.2 mg, 0.08 mmol, 0.4 equiv), and *N*,*N*-dimethylformamide-D7 (>99.5% D, 0.75 mL ampoule purchased from Oakwood Chemical: #099937-2x0.75ml). To the solution was added tris(trimethylsilyl)silane (59.7 mg, 0.24 mmol, 1.2 equiv). The vial was then capped, removed from glovebox, and the reaction solution was stirred at rt. After 16 h, to the reaction mixture was directly added sodium triacetoxyborohydride (211.9 mg, 1.0 mmol, 5 equiv) and the mixture was then stirred at rt for 16 h. The reaction mixture was transferred to a separatory funnel and diluted with ethyl acetate (16 mL). The organic layer was washed with 1M aq. sodium hydroxide (2 x 5 mL), water (5 mL), then brine (5 mL), dried over anhydrous sodium sulfate, filtered, and concentrated *in vacuo*. The product was isolated *via* silica gel column chromatography (1% triethylamine and 10% ethyl acetate in hexanes) as a pale-yellow oil (45.8 mg, 0.13 mmol, 63% yield). **^{1}H NMR** (400 MHz, $CDCl_3$) δ 7.46–7.34 (m, 6H), 7.31 (s, 1H), 7.29 (s, 1H), 5.12 (s, 2H), 2.89 (t, *J* = 14.1 Hz, 1H). **^{19}F NMR** (376 MHz, $CDCl_3$) δ -62.74 (s, 3F), -99.20 (t, *J* = 14.3 Hz, 2F). **^{13}C NMR** (101 MHz, $CDCl_3$) δ 159.0, 139.1 (t, *J* = 26.6 Hz), 136.0, 132.3 (q, *J* = 32.9 Hz), 128.9, 128.5, 127.8, 123.7 (q, *J* = 272.7 Hz), 121.3 (t, *J* = 244.9 Hz), 115.8 (t, *J* = 6.4 Hz), 114.9 (m), 113.2 (m), 70.7, 64.6–63.7 (m), 45.9 (t, *J* = 20.9 Hz), 29.9, 26.0 (t, *J* = 29.5 Hz). **IR (neat):** 3067, 3036, 2932, 2259, 1607, 1454, 1357, 1249, 1129, 1008, 868, 695 (cm^{-1}). **GC-MS** (ESI) M^+ calcd. for $[C_{18}H_{12}D_7F_5NO]^+$ 366.17, 366.15 found. **^{2}H NMR** (62 MHz, $CHCl_3$) δ 2.94 (br s, 1D), 2.30 (br s, 6D).

A1.9 Isolation and derivatization of products in Figure 3-12

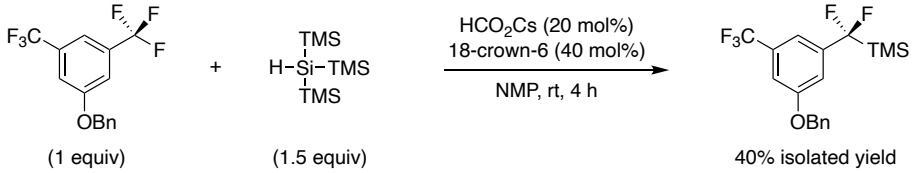

Procedure: In a nitrogen-filled glovebox, to an oven-dried 100 mL round bottom flask charged with a Teflon-coated stir bar, was added 1-(benzyloxy)-3,5-bis(trifluoromethyl)benzene (1.60 g, 5.0 mmol, 1 equiv), 18-crown-6 (528.6 mg, 2.0 mmol, 0.4 equiv), cesium formate (177.9 mg, 1.0 mmol, 0.2 equiv), and anhydrous *N*-methyl-2-pyrrolidinone (25 mL). Tris(trimethylsilyl)silane (2.3 mL, 7.5 mmol, 1.5 equiv) was then added and the flask was capped with a rubber septum, removed from glovebox, and a nitrogen filled balloon was inserted, and the reaction mixture was stirred at rt. After 4 h, the reaction mixture was extracted with hexanes (10 x 10 mL) [**Note:** directly washing the reaction solution with water results in extensive protodesilylation]. The combined hexanes layer was washed with brine (25 mL), dried over anhydrous sodium sulfate, filtered, and concentrated *in vacuo*. Purification *via* silica gel chromatography (100% hexanes) provided the product as a white solid (0.749 g, 2.0 mmol, 40% yield). The characterization data matched that provided in **Section A1.8a** for compound **3-38**.

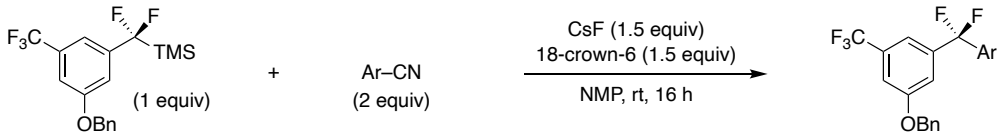

General Procedure 4 for Arylation (GP4): This procedure was adapted from a previous report.[7] In a nitrogen-filled glovebox, to an oven-dried 1-dram glass vial charged with a Teflon-coated stir bar was added ((3-(benzyloxy)-5-(trifluoromethyl)phenyl)difluoromethyl)trimethylsilane (74.9

mg, 0.2 mmol, 1.0 equiv), cyanoarene (2.0 equiv), 18-crown-6 (63.4 mg, 0.24 mmol, 1.2 equiv), and anhydrous *N*,*N*-dimethylformamide (0.8-1.2 mL). The reaction solution was stirred for 1 min, then cesium fluoride (36.5 mg, 0.24 mmol, 1.2 equiv) was added. The vial was capped with a screw top PTFE-lined cap, removed from glovebox, and the reaction solution was stirred at rt. After 16 h, the reaction mixture was transferred to a separatory funnel and diluted with ethyl acetate (8 mL), then washed with water (2 mL x3) and brine (3 mL). The organic layer was dried over anhydrous sodium sulfate, filtered, and concentrated *in vacuo*. The product was isolated *via* silica gel column chromatography using the given eluent conditions.

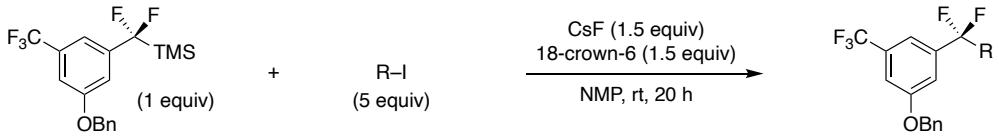

General Procedure 5 for Alkylation (GP5): In a nitrogen-filled glovebox, to an oven-dried 1-dram glass vial charged with a Teflon-coated stir bar was added ((3-(benzyloxy)-5-(trifluoromethyl)phenyl)difluoromethyl)trimethylsilane (74.9 mg, 0.2 mmol, 1.0 equiv), alkyl iodide (5.0 equiv), 18-crown-6 (79.3 mg, 0.3 mmol, 1.5 equiv), and anhydrous *N*-methyl-2-pyrrolidinone (0.8 mL). The reaction solution was stirred for 1 min, then cesium fluoride (45.6 mg, 0.3 mmol, 1.5 equiv) was added. The vial was capped with a screw top PTFE-lined cap, removed from glovebox, and the reaction mixture was stirred at rt. After 20 h, the reaction mixture was transferred to a separatory funnel and diluted with ethyl acetate (8 mL), then washed with water (2 mL) and brine (4 mL). The organic layer was dried over anhydrous sodium sulfate, filtered, and concentrated *in vacuo*. The product was isolated *via* silica gel column chromatography using the given eluent conditions.

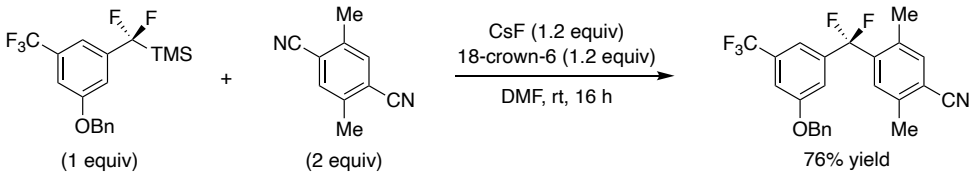

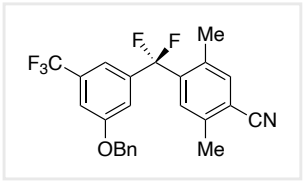

4-((3-(benzyloxy)-5-(trifluoromethyl)phenyl)difluoromethyl)-2,5-dimethylbenzonitrile (3-41). The General Procedure 4 (GP4) was followed with ((3-(benzyloxy)-5-(trifluoromethyl)phenyl)difluoromethyl)trimethylsilane (74.9 mg, 0.2 mmol, 1.0 equiv), 2,5-dimethylterephthalonitrile (62.5 mg, 0.4 mmol, 2.0 equiv), 18-crown-6 (63.4 mg, 0.24 mmol, 1.2 equiv), anhydrous *N*,*N*-dimethylformamide (0.8 mL), and cesium fluoride (36.5 mg, 0.24 mmol, 1.2 equiv). Purification *via* silica gel column chromatography (0-10% diethyl ether gradient in hexanes) provided the product as an off-white solid (65.6 mg, 0.15 mmol, 76% yield). **^{1}H NMR** (400 MHz, $CDCl_3$) δ 7.56 (s, 1H), 7.43 (s, 1H), 7.39–7.36 (m, 5H), 7.32–7.30 (m, 2H), 7.10 (s, 1H), 5.09 (s, 2H), 2.58 (s, 3H), 2.12 (s, 3H). **^{19}F NMR** (376 MHz, $CDCl_3$) δ -62.78 (s, 3F), -88.20 (s, 2F). **^{13}C NMR** (101 MHz, $CDCl_3$) δ 159.2, 139.8, 138.8 (t, J = 28.3 Hz), 138.4 (t, J = 25.5 Hz), 135.8, 135.6, 134.9 (t, J = 2.8 Hz), 132.8 (q, J = 32.9 Hz), 128.9, 127.7, 128.1 (t, J = 8.5 Hz), 127.7, 123.5 (q, J = 272.8 Hz), 119.6 (t, J = 243.6 Hz), 117.4, 116.4 (t, J = 5.5 Hz), 115.2 (m), 114.9, 113.7 (m), 70.8, 20.3, 19.6 (t, J = 2.5 Hz). **IR (neat):** 3092, 2921, 2229, 1608, 1451, 1362, 1245, 1162, 1064, 1040, 894, 718, 706 cm^{-1}. **HRMS** (DART) $[M+H]^+$ calcd. for $[C_{24}H_{19}F_5NO]^+$ 432.1381, 432.1345 found. **Melting Point:** 77-79 °C.

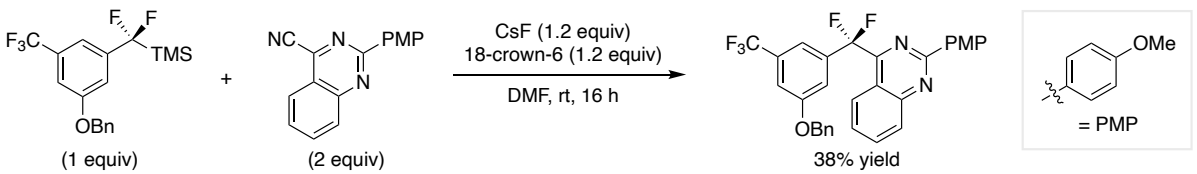

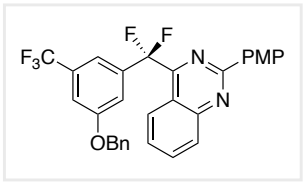

4-((3-(benzyloxy)-5-(trifluoromethyl)phenyl)difluoromethyl)-2-(4-methoxyphenyl)quinazoline (3-42). The General Procedure 4 (GP4) was followed with ((3-(benzyloxy)-5-(trifluoromethyl)phenyl)difluoromethyl)trimethylsilane (74.9 mg, 0.2 mmol, 1.0 equiv), 2-(4-methoxyphenyl)quinazoline-4-carbonitrile[7] (104.5 mg, 0.4 mmol, 2.0 equiv), 18-crown-6 (63.4 mg, 0.24 mmol, 1.2 equiv), anhydrous *N*,*N*-dimethylformamide (1.2 mL), and cesium fluoride (36.5 mg, 0.24 mmol, 1.2 equiv). Purification *via* silica gel column chromatography (10% diethyl ether in hexanes) provided the product as a yellow solid (41.1 mg, 0.076 mmol, 38% yield). **^{1}H NMR** (400 MHz, $CDCl_3$) δ 8.41–8.37 (m, 3H), 8.12 (d, *J* = 8.7 Hz, 1H), 7.90 (ddd, *J* = 8.4, 6.9, 1.4 Hz, 1H), 7.62–7.58 (m, 2H), 7.46–7.29 (m, 7H), 6.98 (d, *J* = 8.9 Hz, 2H), 5.12 (s, 2H), 3.88 (s, 3H). **^{19}F NMR** (376 MHz, $CDCl_3$) δ -62.76 (s, 3F), -90.09 (s, 2F). **^{13}C NMR** (101 MHz, $CDCl_3$) δ 162.3, 160.9 (t, *J* = 31.6 Hz), 159.1, 159.0, 153.0, 138.1 (t, *J* = 26.4 Hz), 135.8, 134.3, 132.2 (q, *J* = 32.9 Hz), 130.4, 129.9, 129.6, 128.9, 128.5, 127.7, 127.6, 125.5 (t, *J* = 5.1 Hz), 123.7 (q, *J* = 272.6 Hz), 120.01 (t, *J* = 246.2 Hz), 119.5, 116.6 (t, *J* = 6.1 Hz), 116.2 (m), 114.2, 113.8 (m), 70.8, 55.5. **IR (neat):** 3073, 2937, 2842, 1603, 1573, 1548, 1453, 1360, 1249, 1165, 1127, 1030, 845, 765, 723 cm^{-1}. **HRMS** (DART) $[M+H]^+$ calcd. for $[C_{30}H_{22}F_5N_2O_2]^+$ 537.1596, 537.1603 found. **Melting Point:** 103-106 °C.

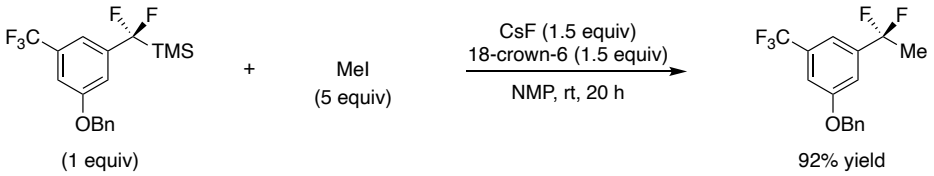

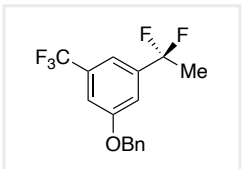

1-(benzyloxy)-3-(1,1-difluoroethyl)-5-(trifluoromethyl)benzene (3-43). The General Procedure 5 (GP5) was followed with ((3-(benzyloxy)-5-(trifluoromethyl)phenyl)difluoromethyl)trimethylsilane (74.9 mg, 0.2 mmol,

1.0 equiv), iodomethane (62.3 µL, 1.0 mmol, 5.0 equiv), 18-crown-6 (79.3 mg, 0.3 mmol, 1.5 equiv), anhydrous *N*-methyl-2-pyrrolidinone (0.8 mL). and cesium fluoride (45.6 mg, 0.3 mmol, 1.5 equiv). Purification *via* silica gel column chromatography (100% hexanes) provided the product as a clear oil (58.4 mg, 0.18 mmol, 92% yield). **^{1}H NMR** (400 MHz, $CDCl_3$) δ 7.48–7.38 (m, 6H), 7.32–7.29 (m, 2H), 5.13 (s, 2H), 1.94 (t, *J* = 18.2 Hz, 3H). **^{19}F NMR** (376 MHz, $CDCl_3$) δ -62.83 (s, 3F), -88.20 (q, *J* = 18.2 Hz, 2F). **^{13}C NMR** (101 MHz, $CDCl_3$) δ 159.3, 140.8 (t, *J* = 27.4 Hz), 135.9, 132.5 (q, *J* = 32.8 Hz), 128.9, 128.6, 127.8, 123.7 (q, *J* = 272.7 Hz), 121.1 (t, *J* = 240.2 Hz), 115.0 (t, *J* = 6.1 Hz), 114.2 (td, *J* = 6.3, 3.0 Hz), 113.1 (m), 70.7, 26.0 (t, *J* = 29.5 Hz). **IR (neat):** 3068, 3035, 3006, 2876, 1607, 1458, 1358, 1263, 1123, 1025, 695 cm^{-1}. **GC-MS (EI)** M^+ calcd. for $[C_{16}H_{13}F_5NO]^+$ 316.09, 316.10 found.

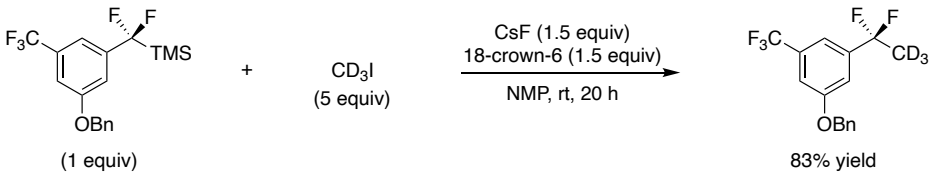

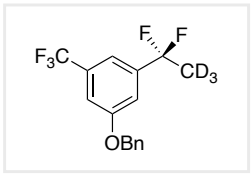

1-(benzyloxy)-3-(1,1-difluoroethyl-2,2,2-*d*$_3$)-5-(trifluoromethyl)benzene (3-44). The General Procedure 5 (GP5) was followed with ((3-(benzyloxy)-5-(trifluoromethyl)phenyl)difluoromethyl)trimethylsilane (74.9 mg, 0.2 mmol, 1.0 equiv), iodomethane-d_3 (62.2 µL, 1.0 mmol, 5.0 equiv), 18-crown-6 (79.3 mg, 0.3 mmol, 1.5 equiv), anhydrous *N*-methyl-2-pyrrolidinone (0.8 mL), and cesium fluoride (45.6 mg, 0.3 mmol, 1.5 equiv). Purification *via* silica gel column chromatography (100% hexanes) provided the product as a clear oil (53.0 mg, 0.17 mmol, 83% yield). **^{1}H NMR** (400 MHz, $CDCl_3$) δ 7.47–7.38 (m, 6H), 7.31–7.29 (m, 2H), 5.13 (s, 2H). **^{19}F NMR** (376 MHz, $CDCl_3$) δ -62.83 (s, 3F), -88.60 (s, 2F). **^{13}C NMR** (101 MHz, $CDCl_3$) δ 159.3, 140.8 (t, *J* = 27.4 Hz), 135.9, 132.5 (q, *J* = 32.8 Hz), 128.9, 128.6, 127.8, 123.7 (q, *J* = 272.6 Hz), 121.1 (t, *J* = 240.2 Hz), 115.0 (t, *J* = 6.2

Hz), 114.2 (m), 113.1 (m), 70.7. (**Note:** The CD_3 carbon is not clearly visible in ^{13}C NMR, a small blip can be seen on the baseline at 25.0 ppm—we hypothesize that this is due to effects arising from the neighboring ^{2}H and ^{19}F atoms). **IR (neat):** 3067, 3036, 2877, 1607, 1454, 1359, 1259, 1169, 1119, 1012, 868, 736 cm^{-1}. **GC-MS (EI)** M^+ calcd. for $[C_{16}H_{10}D_3F_5O]^+$ 319.11, 319.10 found. **^{2}H NMR** (62 MHz, $CHCl_3$)**:** δ 1.96 (br s, >2.95D).

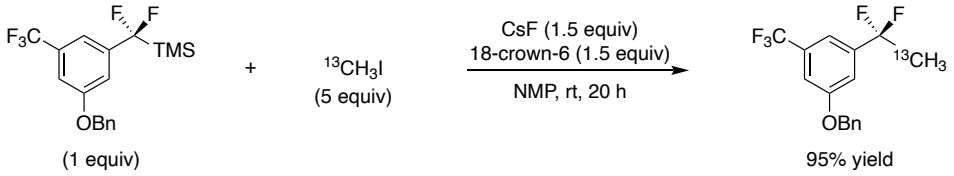

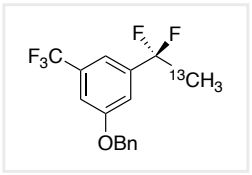

1-(benzyloxy)-3-(1,1-difluoroethyl-2-^{13}C)-5-(trifluoromethyl)benzene (3-45). The General Procedure 5 (GP5) was followed with ((3-(benzyloxy)-5-(trifluoromethyl)phenyl)difluoromethyl)trimethylsilane (74.9 mg, 0.2 mmol, 1.0 equiv), iodomethane-^{13}C (62.4 μL, 1.0 mmol, 5.0 equiv), 18-crown-6 (79.3 mg, 0.3 mmol, 1.5 equiv), anhydrous *N*-methyl-2-pyrrolidinone (0.8 mL), and cesium fluoride (45.6 mg, 0.3 mmol, 1.5 equiv). Purification *via* silica gel column chromatography (100% hexanes) provided the product as a clear oil (60.4 mg, 0.19 mmol, 95% yield). **^{1}H NMR** (400 MHz, $CDCl_3$) δ 7.48–7.37 (m, 6H), 7.32–7.30 (m, 2H), 5.13 (s, 2H), 1.94 (dt, *J* = 129.2, 18.2 Hz, 3H). **^{19}F NMR** (376 MHz, $CDCl_3$) δ -62.80 (s, 3F), -88.19 (dq, *J* = 29.4, 18.3 Hz, 2F). **^{13}C NMR** (101 MHz, $CDCl_3$) δ 159.3, 140.8 (td, *J* = 27.4, 4.1 Hz), 135.9, 132.5 (q, *J* = 32.8 Hz), 128.9, 128.6, 127.8, 123.7 (q, *J* = 272.6 Hz), 121.11 (td, *J* = 240.2, 48.2 Hz), 115.0 (t, *J* = 6.1 Hz), 114.2 (td, *J* = 6.2, 3.5 Hz), 113.1 (m), 70.7, 26.0 (t, *J* = 29.4 Hz), 23.9, 15.3. **IR (neat):** 3068, 2995, 2936, 1607, 1457, 1357, 1261, 1123, 1024, 880, 708 cm^{-1}. **GC-MS (EI)** M^+ calcd. for $[C_{15}{}^{13}CH_{13}F_5NO]^+$ 317.09, 317.10 found.

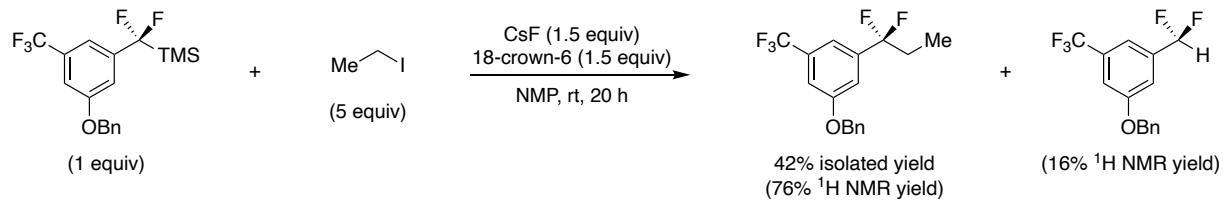

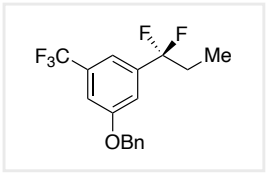

1-(benzyloxy)-3-(1,1-difluoropropyl)-5-(trifluoromethyl)benzene (3-46). The General Procedure 5 (GP5) was followed with ((3-(benzyloxy)-5-(trifluoromethyl)phenyl)difluoromethyl)trimethylsilane (74.9 mg, 0.2 mmol, 1.0 equiv), iodoethane (80.4 µL, 1.0 mmol, 5.0 equiv), 18-crown-6 (79.3 mg, 0.3 mmol, 1.5 equiv), anhydrous *N*-methyl-2-pyrrolidinone (0.8 mL), and cesium fluoride (45.6 mg, 0.3 mmol, 1.5 equiv). Analysis of the crude reaction mixture was carried out by quenching the reaction with $CDCl_3$ (0.5 mL), addition of dibromomethane internal standard (100.0 µL of 2.0 M stock solution in $CDCl_3$), and analysis of an aliquot of the reaction mixture *via* ^{1}H NMR. Referenced to the dibromomethane internal standard (singlet at 4.93 ppm), the product signal (quartet at 3.47 ppm) provided an ^{1}H NMR yield of 72%. Purification *via* silica gel column chromatography (100% hexanes) provided the product as a clear oil (27.6 mg, 0.084 mmol, 42% isolated yield). [**Note:** A lower isolated yield compared to the ^{1}H NMR yield is due to coelution of protodesilylation side product (16% ^{1}H NMR yield, triplet at 6.64 ppm) in some fractions, which were discarded.] **^{1}H NMR** (400 MHz, $CDCl_3$) δ 7.40–7.26 (m, 6H), 7.22–7.18 (m, 2H), 5.06 (s, 2H), 2.08 (tq, J = 15.6, 7.5 Hz, 2H), 0.93 (t, J = 7.5 Hz, 3H). **^{19}F NMR** (376 MHz, $CDCl_3$) δ -62.82 (s, 3F), -97.89 (t, J = 16.2 Hz, 2F). **^{13}C NMR** (101 MHz, $CDCl_3$) δ 159.2, 140.0 (t, J = 27.6 Hz), 135.9, 132.4 (q, J = 32.8 Hz), 128.9, 128.6, 127.8, 123.9 (q, J = 243.3) 122.4 (t, J = 272.5 Hz), 115.4 (t, J = 6.3 Hz), 114.6 (td, J = 6.3, 3.6 Hz), 113.0 (m), 70.7, 32.3 (t, J = 27.9 Hz), 6.9 (t, J = 5.0 Hz). **IR (neat):** 3035, 2984, 2939, 1606, 1454, 1346, 1246, 1168, 1125, 987, 866, 696 cm^{-1}. **GC-MS (EI)** M^+ calcd. for $[C_{17}H_{15}F_5O]^+$ 330.10, 330.10 found.

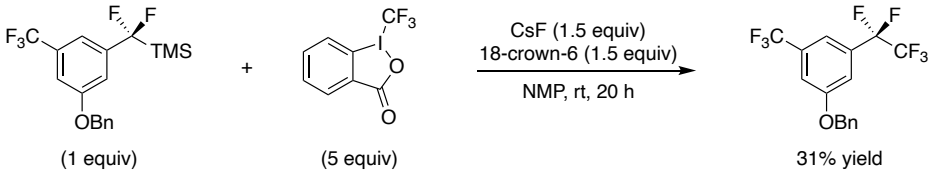

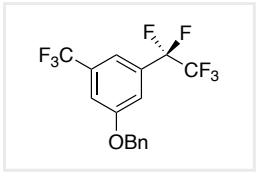

1-(benzyloxy)-3-(perfluoroethyl)-5-(trifluoromethyl)benzene (3-47). The General Procedure 5 (GP5) was followed with ((3-(benzyloxy)-5-(trifluoromethyl)phenyl)difluoromethyl)trimethylsilane (74.9 mg, 0.2 mmol, 1.0 equiv), 1-trifluoromethyl-1,2-benziodoxol-3-(1*H*)-one (Togni II, 316.0 mg, 1.0 mmol, 5.0 equiv), 18-crown-6 (79.3 mg, 0.3 mmol, 1.5 equiv), anhydrous *N*-methyl-2-pyrrolidinone (0.8 mL), and cesium fluoride (45.6 mg, 0.3 mmol, 1.5 equiv). Purification *via* silica gel column chromatography (100% hexanes) provided the product as a clear oil (16.4 mg, 0.068 mmol, 31% yield). **^{1}H NMR** (400 MHz, $CDCl_3$) δ 7.47–7.38 (m, 8H), 5.15 (s, 2H). **^{19}F NMR** (376 MHz, $CDCl_3$) δ -63.05 (s, 3F), -84.63 (s, 3F), -114.98 (s, 2F) **^{13}C NMR** (101 MHz, $CDCl_3$) δ 159.4, 135.4, 133.1 (q, J = 33.4 Hz), 131.3 (t, J = 24.7 Hz), 129.0, 128.8, 127.9, 123.3 (q, J = 272.7 Hz), 119.0 (qt, J = 286.0, 38.8 Hz), 116.8 (t, J = 6.6 Hz), 115.8 (m), 115.4 (m), 112.8 (tq, J = 254.7, 38.5 Hz), 71.0. **IR (neat):** 2918, 2850, 1609, 1456, 1362, 1259, 1174, 1112, 1607, 998, 867, 739, 693 cm^{-1}. **GC-MS (EI)** M^+ calcd. for $[C_{16}H_{10}F_8O]^+$ 370.06, 370.10 found.

A1.10 C–H Functionalization of a Difluoromethylarene

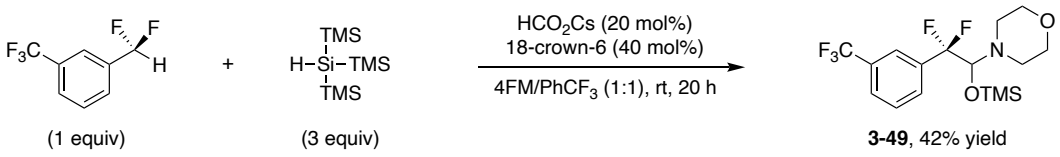

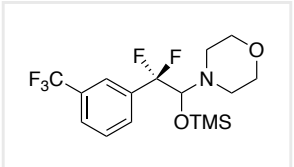

4-(2,2-difluoro-2-(3-(trifluoromethyl)phenyl)-1-((trimethylsilyl)oxy)ethyl)morpholine (3-49). In a nitrogen-filled glovebox, to an oven-dried 2-dram glass vial charged with a Teflon-

coated stir bar, was added 1-(difluoromethyl)-3-(trifluoromethyl)benzene (196.1 mg, 1.0 mmol, 1 equiv), 18-crown-6 (105.7 mg, 0.4 mmol, 0.4 equiv), cesium formate (35.6 mg, 0.2 mmol, 0.2 equiv), 4-formylmorpholine/benzotrifluoride (1:1 ratio, 4.0 mL), and tris(trimethylsilyl)silane (746.0 mg, 3.0 mmol, 3 equiv). The vial was then capped, removed from glovebox, and placed on a stir plate and stirred at rt. After 20 h, the reaction mixture was diluted with ethyl acetate (12 mL) and washed with distilled water (3 x 6 mL) [**Caution**: add water slowly due to vigorous gas evolution] then brine (8 mL), dried over anhydrous sodium sulfate, filtered, and concentrated *in vacuo*. Purification *via* silica gel column chromatography (1% triethylamine and 5% ethyl acetate in hexanes) provided the product as a pale-yellow oil (156.4 mg, 0.43 mmol, 42% yield). **^{1}H NMR** (400 MHz, $CDCl_3$) δ 7.79 (s, 1H), 7.68 (d, *J* = 7.9 Hz, 2 H), 7.52 (t, *J* = 7.8 Hz, 2H), 4.35 (dd, *J* = 10.1, 7.0 Hz, 1H), 3.58–3.55 (m, 4H), 2.60–2.57 (m, 4H), 0.10 (s, 9H). **^{19}F NMR** (376 MHz, $CDCl_3$) δ -62.85 (s, 3F), -105.38 (d, *J* = 249.0 Hz, 1F), -108.00 (d, *J* = 249.1 Hz, 1F). **^{13}C NMR** (101 MHz, $CDCl_3$) δ 136.3 (t, *J* = 26.5 Hz), 130.6 (q, *J* = 32.8 Hz), 129.8 (t, *J* = 6.3 Hz), 128.6, 126.7–126.6 (m), 124.0 (q, *J* = 272.2 Hz), 123.9 (td, *J* = 6.6, 3.4 Hz), 120.0 (t, *J* = 249.9 Hz), 89.4 (t, *J* = 31.8 Hz), 67.3, 49.1, 1.8, -0.1. **IR (neat):** 3036.18, 2958.48, 2854.29, 1607.36, 1453.55, 1354.75, 1249.73, 1128.88, 1306.75, 841.83, 754.40, 695.80 cm^{-1}. **GC-MS** (EI) M^+ calcd. for $[C_{16}H_{22}F_5NO_2Si]^+$ 383.13, 383.10 found.

A1.11 Preparation and characterization of starting materials

Discussion: All substrates that are not described below were purchased and used as received. All non-commercial substrates and reagents used are described below.

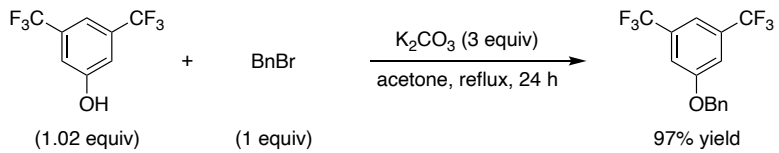

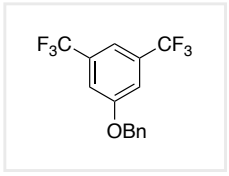

1-(benzyloxy)-3,5-bis(trifluoromethyl)benzene (A1-2). To an oven-dried round bottom flask charged with a Teflon-coated stir bar was added 3,5-bis(trifluoromethyl)phenol (5.8 mL, 32.6 mmol, 1.02 equiv), benzyl bromide (6.0 mL, 32 mmol, 1 equiv), acetone (150 mL), and potassium carbonate (13.3g, 96 mmol, 3 equiv). A reflux condensor fitted with a rubber septum and a nitrogen-filled balloon were then placed onto the flask, and the reaction mixture was placed into a preheated oil bath at 70 °C and stirred under reflux. After 24 h, the flask was removed from the oil bath and the solution was allowed to cool to rt. The reaction mixture was filtered and concentrated *in vacuo*. Silica gel column chromatography (5-10% ethyl acetate in hexanes) provided the product as a white solid (9.99 g, 31 mmol, 97% yield). **^{1}H NMR** (400 MHz, $CDCl_3$) δ 7.48 (br s, 1H), 7.46–7.33 (m, 7H), 5.09 (s, 2H). **Melting Point:** 31-32 ºC. The spectroscopic data matches a previous report.[9]

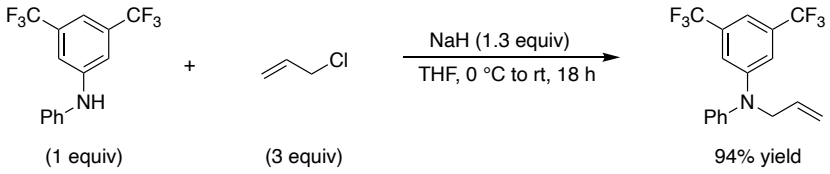

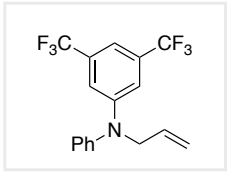

***N*-allyl-*N*-phenyl-3,5-bis(trifluoromethyl)aniline (A1-3).** To an oven-dried round bottom flask charged with a Teflon-coated stir bar was added *N*-phenyl-3,5-bis(trifluoromethyl)aniline (3.1 mL, 10 mmol, 1.0 equiv), allyl chloride (2.4 mL, 30 mmol, 3 equiv), and tetrahydrofuran (40 mL). The flask was capped with a septum and a nitrogen-filled balloon was inserted, then the flask was placed into a 0 °C ice-bath and stirred for 15 min. The septum was then removed and sodium hydride (60% in mineral oil, 0.52g, 13

mmol, 1.3 equiv) was added portion-wise and the septum was placed onto the flask again. The reaction mixture was stirred and allowed to warm to rt overnight. After 18 h, the reaction mixture was diluted with ethyl acetate (100 mL), washed with water (60 mL) and brine (40 mL), then dried over anhydrous sodium sulfate, filtered, and concentrated *in vacuo*. Silica gel column chromatography (5% ethyl acetate in hexanes) provided the product as a yellow oil (3.24 g, 9.4 mmol, 94% yield). **^{1}H NMR** (400 MHz, $CDCl_3$) δ 7.43 (t, *J* = 7.8 Hz, 2H), 7.27–7.23 (m, 4H), 7.18 (s, 2H), 5.93 (ddt, *J* = 17.3, 10.0, 4.8 Hz, 1H), 5.32 (dd, *J* = 17.2, 1.9 Hz, 1H), 5.27 (dd, *J* = 10.4, 1.7 Hz, 1H), 4.40 (dd, *J* = 4.7, 2.2 Hz, 2H). The spectroscopic data matches a previous report.[10]

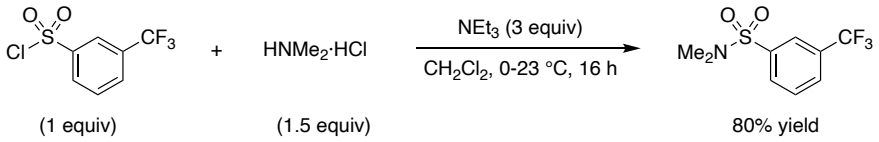

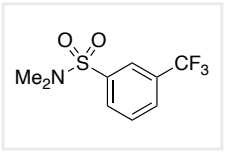

***N*,*N*-dimethyl-3-(trifluoromethyl)benzenesulfonamide (A1-4).** To an oven-dried round bottom flask charged with a Teflon-coated stir bar was added 3-(trifluoromethyl)benzenesulfonyl chloride (3.2 mL, 20 mmol, 1 equiv), dimethylamine hydrochloride (2.4 g, 30 mmol, 1.5 equiv), and dichloromethane (40 mL). A rubber septum with a nitrogen-filled balloon was placed onto the flask and the flask was placed into a 0 °C ice-bath and stirred for 15 min. Triethylamine (8.3 mL, 60 mmol, 3 equiv) was then added slowly through the septum *via* syringe. The reaction solution was stirred and allowed to warm to rt overnight. After 16 h, the reaction mixture was diluted with water (50 mL) and the organic layer was seperated. The aqueous layer was extracted with dichloromethane (3 x 15 mL). The combined organic layers were washed with saturated aq. ammonium chloride (40 mL), then brine (40 mL), dried over anhydrous sodium sulfate, filtered, and concentrated *in vacuo*. Silica gel column

chromatography (10% ethyl acetate in hexanes) provided the product as clear oil (4.05 g, 16 mmol, 80% yield). **^{1}H NMR** (400 MHz, $CDCl_3$) δ 8.02 (s, 1H), 7.96 (d, *J* = 7.9 Hz, 1H), 7.86 (d, *J* = 7.9 Hz, 1H), 7.71 (t, *J* = 7.9 Hz, 1H), 2.73 (s, 6H). The spectroscopic data matches a previous report.[11]

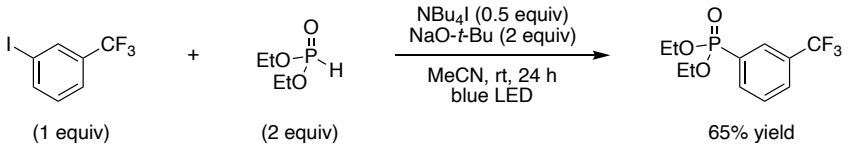

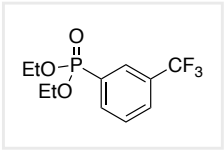

diethyl (3-(trifluoromethyl)phenyl)phosphonate (A1-5). This procedure was adapted from a previous report.[12] To an oven-dried round bottom flask charged with a Teflon-coated stir bar was added diethyl (3-iodophenyl)phosphonate (0.72 g, 5 mmol, 1 equiv), diethyl phosphonate (1.29 mL, 10 mmol, 2 equiv), tetrabutylammonium iodide (0.92 g, 2.5 mmol, 0.5 equiv), and sodium *tert*-butoxide (0.96 g, 10 mmon, 2 equiv). A rubber septum was placed onto the flask, the flask was attached to a Schlenk manifold, and placed under vacuum and filled with nitrogen (this operation was repeated three times). Acetonitrile (50 mL) was then added through the septum *via* syringe and the reaction solution was sparged with nitrogen for 15 min. The reaction mixture was then irradiated with blue LEDs (Product Code: CL-FRS5050WPDD-5M-12V-BL from www.creativelightings.com) placed around the flask at a distance of about 4 cm with a small fan to provide air circulation while stirring. After 24 h, the reaction mixture was diluted with ethyl acetate (50 mL), pushed through a plug of celite, and concentrated *in vacuo*. Silica gel column chromatography (30-50% ethyl acetate in hexanes) provided the product as a pale-yellow oil (0.92 g, 3.3 mmol, 65% yield). **^{1}H NMR** (400 MHz, $CDCl_3$) δ 8.03 (d, *J* = 13.7 1H), 7.96 (dd, *J* = 13.1, 7.6 Hz, 1H), 7.76 (d, *J* = 7.9 Hz, 1H), 7.61 (td, *J* = 7.8, 3.8, Hz, 1H), 4.19–4.02 (m, 4H), 1.30 (t, *J* = 7.1, 6H). The spectroscopic data matches a previous report.[12]

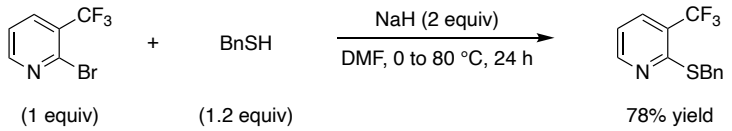

(1 equiv) (1.2 equiv) 78% yield

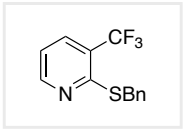

2-(benzylthio)-3-(trifluoromethyl)pyridine (A1-6). To an oven-dried round bottom flask charged with a Teflon-coated stir bar was added 2-bromo-3-(trifluoromethyl)pyridine (3.39 g, 15 mmol, 1 equiv), phenylmethanethiol (2.1 mL, 18 mmol, 1.2 equiv), and dry *N*,*N*-dimethylformamide (50 mL). The reaction mixture was cooled to 0 °C in an ice bath then sodium hydride (60% in mineral oil, 1.20 g, 30 mmol, 2 equiv) was added portionwise. A rubber septum and nitrogen-filled balloon were then placed onto the flask, and the reaction mixture was stirred at 0 °C for 10 min, then the flask was placed into a preheated oil bath at 80 °C with stirring. After 24 h, the flask was removed from the oil bath and allowed to cool to rt. The reaction mixture was diluted with ethyl acetate (150 mL) and washed with 1 M aq. sodium hydroxide (40 mL), water (3 x 40 mL), and brine (80 mL), then dried over anhydrous sodium sulfate, filtered, and concentrated *in vacuo*. Silica gel column chromatography (5-10% ethyl acetate in hexanes) provided the product as a yellow oil (3.16 g, 12 mmol, 78% yield). **^{1}H NMR** (400 MHz, $CDCl_3$) δ 8.42 (dd, *J* = 5.0, 1.6 Hz, 1H), 7.63 (dd, *J* = 7.8, 1.7 Hz), 7.30 (d, *J* = 7.2 Hz, 2H), 7.17 (t, *J* = 7.4 Hz, 2H), 7.12–7.07 (m, 1H), 6.90 (dd, *J* = 7.9, 4.9 Hz, 1H), 4.40 (s, 2H). **^{19}F NMR** (376 MHz, $CDCl_3$) δ -63.22 (s, 3F). **^{13}C NMR** (101 MHz, $CDCl_3$) δ 158.1, 151.5 (d, *J* = 1.6 Hz), 137.2, 134.3 (q, *J* = 5.2 Hz), 129.3, 128.6, 127.6, 123.5 (q, *J* = 273.2 Hz), 123.4 (q, *J* = 32.7 Hz), 118.5, 34.6 (d, *J* = 1.5 Hz). **IR (neat):** 3062, 3029, 1583, 1559, 1403, 1314, 1236, 1165, 1126, 1110, 1026, 803, 715 cm^{-1}. **GC-MS (EI)** M^+ calcd. for $[C_{13}H_{10}F_3NS]^+$ 269.05, 269.10 found.

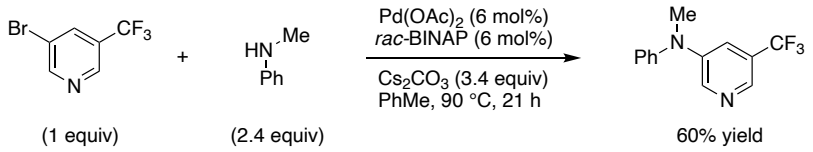

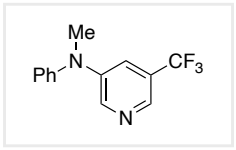

***N*-methyl-*N*-phenyl-5-(trifluoromethyl)pyridin-3-amine (A1-7).** In a nitrogen-filled glovebox, to an oven-dried round bottom flask charged with a Teflon-coated stir bar was added 3-bromo-5-(trifluoromethyl)pyridine (3.11 g, 13.7 mmol, 1 equiv), *N*-methylaniline (3.58 mL, 33.0 mmol, 2.4 equiv), palladium(II) acetate (185 mg, 0.83 mmol, 0.06 equiv), (±)-2,2′-bis(diphenylphosphino)-1,1′-binaphthalene (547 mg, 0.83 mmol, 0.06 equiv), cesium carbonate (15.3 g, 46.6 mmol, 3.4 equiv), and toluene (50 mL). The flask was capped with a rubber septum, removed from the glovebox, placed into a preheated oil bath at 90 °C, and a nitrogen-filled balloon was inserted. After 21 h, the flask was removed from the oil bath and allowed to cool to rt. The reaction mixture was diluted with water (50 mL) and the organic layer was separated. The aqeuous layer was then extracted with ethyl acetate (3 x 30 mL). The combined organic layers were washed with brine (80 mL), dried over anhydrous sodium sulfate, filtered, and concentrated *in vacuo*. Silica gel column chromatography (3-8% ethyl acetate in hexanes) provided the product as a yellow oil (2.07 g, 8.2 mmol, 60% yield). **^{1}H NMR** (400 MHz, $CDCl_3$) δ 8.26 (d, J = 2.8 Hz, 1H), 8.20 (d, J = 1.8 Hz, 1H), 7.32 (t, J = 8.8 Hz, 2H), 7.17–7.08 (m, 4 H), 3.27 (s, 3H). **^{19}F NMR** (376 MHz, $CDCl_3$) δ -62.57 (s, 3F). **^{13}C NMR** (101 MHz, $CDCl_3$) δ 146.8, 144.9, 141.1 (d, J = 3.8 Hz), 135.8 (q, J = 4.2 Hz), 130.2, 126.6 (q, J = 32.1 Hz), 125.7, 125.0, 123.8 (q, J = 272.8 Hz),117.7 (q, J = 3.8 Hz), 40.1. **IR (neat):** 3059, 2886, 2822, 1692, 1602, 1495, 1358, 1122, 1076, 918, 867, 698 cm^{-1}. **GC-MS (EI)** M^+ calcd. for $[C_{13}H_{11}F_3N_2]^+$ 252.09, 252.05 found.

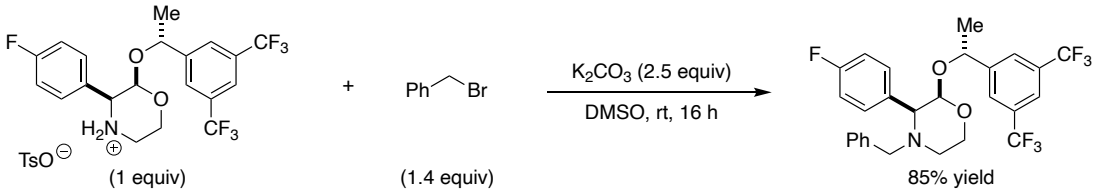

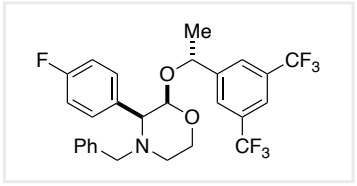

(2*R*,3*S*)-4-benzyl-2-((*R*)-1-(3,5-bis(trifluoromethyl)phenyl)ethoxy)-3-(4-fluorophenyl)morpholine (A1-8). To an oven-dried round bottom flask charged with a Teflon-coated stir bar was added (2*R*,3*S*)-2-((*R*)-1-(3,5-bis(trifluoromethyl)phenyl)ethoxy)-3-(4-fluorophenyl)morpho-line 4-methylbenzenesulfonate (2.95 g, 4.8 mmol, 1.0 equiv), benzyl bromide (0.80 mL, 6.7 mmol, 1.4 equiv), dimethylsulfoxide (20 mL), and potassium carbonate (1.66 g, 12 mmol, 2.5 equiv). The flask was capped with a rubber septum, a nitrogen-filled balloon was inserted, and the reaction mixture was stirred at rt. After 21 h, the reaction mixture was diluted with water (30 mL), and washed with ethyl acetate (3 x 50 mL). The combined organic layers were then washed with brine (60 mL), dried over anhydrous sodium sulfate, filtered, and concentrated *in vacuo*. Silica gel column chromatography (1% triethylamine and 10% diethyl ether in hexanes) provided the product as a clear, viscous resin-like substance (2.14 g, 4.1 mmol, 85% yield). **^{1}H NMR** (400 MHz, $CDCl_3$) δ 7.63 (s, 1H), 7.46 (br s, 2H), 7.32–7.21 (m, 5H), 7.14 (s, 2H), 7.04 (t, *J* = 8.6 Hz, 2H), 4.85 (q, *J* = 6.6 Hz, 1H), 4.33 (d, *J* = 2.9 Hz, 1H), 4.22 (td, *J* = 11.6, 2.4 Hz, 1H), 3.80 (d, *J* = 13.5 Hz, 1H), 3.57 (dd, *J* = 11.1, 3.6, 1.6 Hz, 1H), 3.42 (d, *J* = 3.0 Hz, 1H), 2.83 (d, *J* = 13.5 Hz, 2H), 2.33 (td, *J* = 11.9, 3.5 Hz, 1H), 1.44 (d, *J* = 6.6 Hz, 3H). The spectroscopic data matches a previous report.[11]

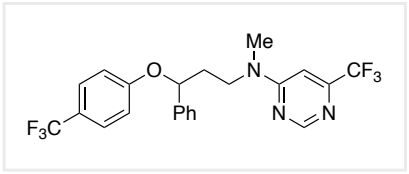

_N_-methyl-_N_-(3-phenyl-3-(4-(trifluoromethyl)phenoxy)propyl)-6-(trifluoromethyl)pyrimidin-4-amine (A1-9). To an oven-dried round bottom flask charged with a Teflon-coated stir bar was added 4-chloro-6-(trifluoromethyl)pyrimidine (0.92 g, 5.05 mmol, 1.05 equiv), fluoxetine hydrochloride (1.73 g, 5 mmol, 1 equiv), triethylamine (2.1 mL, 15 mmol, 3 equiv), and *N*,*N*-dimethylformamide (20 mL). A rubber septum and a nitrogen-filled balloon were placed onto the flask, then the flask was placed into a preheated oil bath at 80 °C with stirring. After 22 h, the reaction mixture was cooled to rt, diluted with ethyl acetate (100 mL), washed with water (5 x 20 mL), then brine (40 mL), dried over anhydrous sodium sulfate, filtered, and concentrated *in vacuo*. Silica gel column chromatography (10% ethyl acetate in hexanes) provided the product as slightly pink, viscous oil (2.1 g, 4.6 mmol, 92% yield). **^{1}H NMR** (400 MHz, $CDCl_3$) δ 8.55 (br s, 1H), 7.39 (d, *J* = 8.6 Hz, 2H), 7.32–7.22 (m, 5H), 6.84 (d, *J* = 8.6 Hz, 2H), 6.64 (br s, 1H), 5.18 (dd, *J* = 8.5, 4.1 Hz, 1H), 3.87 (br s, 2H), 3.06 (br s, 3H), 2.28–2.13 (m, 2H). **^{19}F NMR** (376 MHz, $CDCl_3$) δ -61.58 (s, 3F), -70.64 (s, 3F). **^{13}C NMR** (101 MHz, $CDCl_3$) δ 162.1, 160.2, 158.8, 154.2 (q, *J* = 34.5 Hz), 140.3, 129.1, 128.3, 126.9 (q, *J* = 3.8 Hz), 125.7, 125.4, 124.4 (q, *J* = 271.2 Hz), 123.3, 121.1 (q, *J* = 274.7 Hz), 115.7, 98.7 (q, *J* = 3.4 Hz), 77.9, 46.7, 36.1. **IR (neat):** 3030, 2927, 1604, 1513, 1319, 1248, 1105, 1064, 833, 701 cm^{-1}. **HRMS** (DART) $[M+H]^+$ calcd. for $[C_{22}H_{20}F_6N_3O]^+$ 456.1505, 456.1533 found.

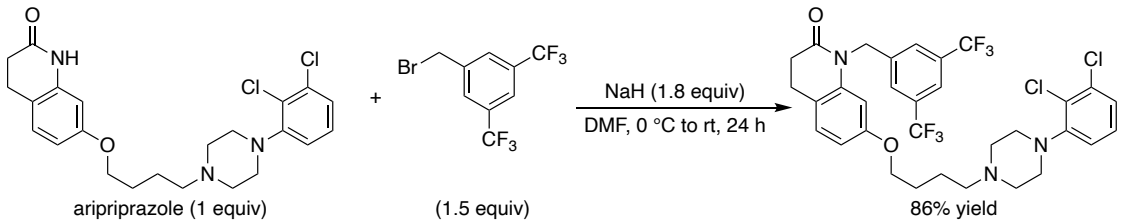

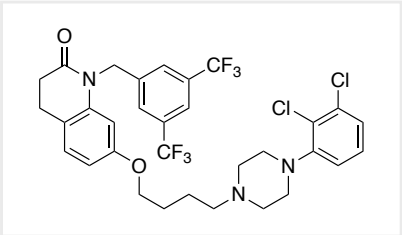

1-(3,5-bis(trifluoromethyl)benzyl)-7-(4-(4-(2,3-dichlorophenyl)piperazin-1-yl)butoxy)-3,4-dihydroquinolin-2(1H)-one (A1-10). To an oven-dried round bottom flask charged with a Teflon-coated stir bar was added aripriprazole (2.24 g, 5.0 mmol, 1 equiv), 1-(bromomethyl)-3,5-bis(trifluoromethyl)benzene (1.37 mL, 7.5 mmol, 1.5 equiv), and dry *N*,*N*-dimethylformamide (50 mL). The reaction mixture was cooled to 0 °C in an ice bath and then sodium hydride (60% in mineral oil, 0.36 g, 9.0 mmol, 1.8 equiv) was added portionwise. A rubber septum and nitrogen-filled balloon were then placed onto the flask, and the reaction mixture was stirred at 0 °C for 30 min, then the flask was allowed to warm slowly to rt with stirring. After 24 h, the reaction mixture was diluted with ethyl acetate (150 mL) and washed with water (5 x 50 mL) and brine (80 mL), then dried over anhydrous sodium sulfate, filtered, and concentrated *in vacuo*. Silica gel column chromatography (5-10% ethyl acetate in hexanes) provided the product as a pale-yellow solid (3.16 g, 3.9 mmol 78% yield). **^{1}H NMR** (400 MHz, $CDCl_3$) δ 7.77 (s, 1H), 7.67 (s, 2H), 7.15–7.08 (m, 3H), 6.96–6.92 (m, 1H), 6.54 (dd, *J* = 8.3, 2.3 Hz, 1H), 6.34 (d, *J* = 2.3 Hz, 1H), 5.23 (s, 2H), 3.87 (t, *J* = 6.3 Hz, 2H), 3.05 (br s, 4H), 2.92 (dd, *J* = 8.7, 5.7 Hz, 2H), 2.78 (dd, *J* = 8.8, 5.7 Hz, 2H), 2.62 (br s, 4H), 2.46–2.42 (m, 2H), 1.79–1.60 (m, 4H). **^{19}F NMR** (376 MHz, $CDCl_3$) δ -62.81 (s, 6F). **^{13}C NMR** (101 MHz, $CDCl_3$) δ 170.8, 158.7, 151.3, 140.3, 140.2, 134.1, 132.1 (q, *J* = 33.4 Hz), 128.9, 127.54, 127.52, 126.9 (m), 124.6, 123.3 (q, *J* = 272.9 Hz), 121.5 (p, *J* = 3.9 Hz), 118.7, 118.5, 108.1, 103.1, 68.0, 58.1, 53.3, 51.3, 45.8, 32.2, 27.2, 24.7, 23.4. **IR (neat):** 3060, 2942, 2815, 1678, 1616, 1512, 1446, 1348, 1281, 1164, 1118, 968, 777 cm^{-1}. **HRMS** (DART) $[M+H]^+$ calcd. for $[C_{32}H_{32}Cl_2F_6N_3O_2]^+$ 674.1770, 674.1770 found. **Melting Point:** 119-123 ºC.

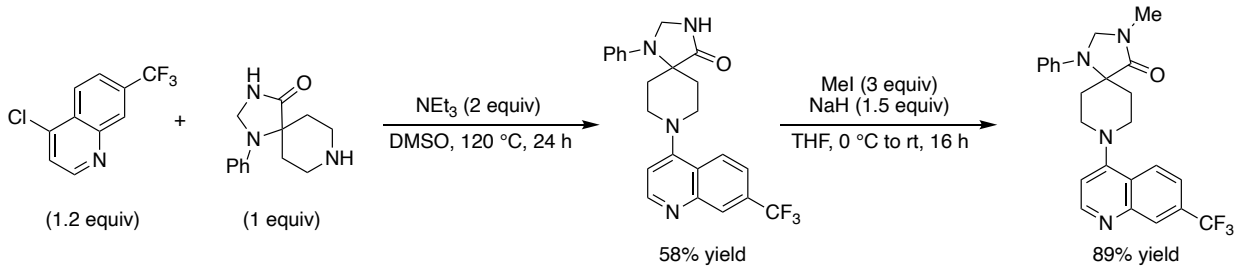

3-methyl-1-phenyl-8-(7-(trifluoromethyl)quinolin-4-yl)-1,3,8-triazaspiro[4.5]decan-4-one (A1-11).

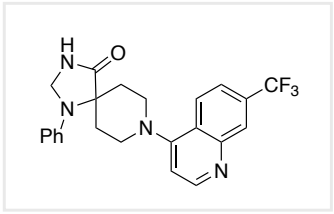

Step 1: To an oven-dried round bottom flask charged with a Teflon-coated stir bar was added 4-chloro-7-(trifluoromethyl)quinoline (1.39 g, 6.0 mmol, 1.2 equiv), 1-phenyl-1,3,8-triazaspiro[4.5]decan-4-one (1.16 g, 5.0 mmol, 1 equiv), triethylamine (1.4 mL, 10 mmol, 2 equiv), and dimethylsulfoxide (10 mL). The flask was capped with a rubber septum and nitrogen-filled balloon, and placed into a preheated oil bath at 120 °C with stirring. After 24 h, the reaction mixture was cooled to rt, transferred to a separatory funnel, diluted with ethyl acetate (30 mL), and washed with water (5 x 10 mL) and brine (20 mL), then dried over anhydrous sodium sulfate, filtered, and concentrated *in vacuo*. Purification *via* silica gel column chromatography (100% ethyl acetate) provided 1-phenyl-8-(7-(trifluoromethyl)quinolin-4-yl)-1,3,8-triazaspiro[4.5]decan-4-one as an off-white solid (1.23 g, 2.9 mmol, 58% yield). **^{1}H NMR** (400 MHz, $CDCl_3$) δ 8.81 (d, *J* = 5.1 Hz, 1H), 8.40 (s, 1H), 8.15 (d, *J* = 8.8 Hz, 1H), 7.69 (dd, *J* = 8.8, 1.9 Hz, 1H), 7.35 (dd, *J* = 8.7, 7.3 Hz, 2H), 7.03–6.93 (m, 4H), 6.48 (bs, 1H), 4.84 (s, 2H), 3.79 (t, *J* = 12.2 Hz, 2H), 3.61 (d, *J* = 12.2 Hz, 2H), 2.99 (td, *J* = 13.2, 5.2 Hz, 2H), 1.97 (d, *J* = 13.8 Hz).

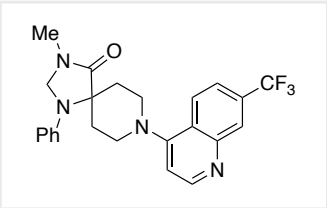

Step 2: To an oven-dried round bottom flask charged with a Teflon-coated stir bar was added 1-phenyl-8-(7-(trifluoromethyl)quinolin-4-yl)-1,3,8-triazaspiro[4.5]decan-4-one (600 mg, 1.4 mmol, 1 equiv), iodomethane (0.27 mL, 4.3 mmol, 3 equiv), and tetrahydrofuran (10 mL). The reaction flask was capped with a rubber septum and a nitrogen-filled balloon, and placed into a 0 °C ice-bath with stirring. The septum was removed and sodium hydride (60% in mineral oil, 88.0 mg, 2.2 mmol, 1.5 equiv) was added in one portion and the septum was placed back onto the flask. The reaction mixture was stirred at 0 °C for 30 min, then the ice-bath was removed and the reaction mixture was allowed to warm to rt overnight with stirring. After 16 h, the reaction mixture was diluted with ethyl acetate (20 mL), washed with water (10 mL) and brine (20 mL), dried over anhydrous sodium sulfate, filtered, and concentrated *in vacuo*. Purification *via* silica gel column chromatography (80-100% ethyl acetate gradient in hexanes) provided the title compound as a pale-yellow solid (550 mg, 1.2 mmol, 89% yield). **^{1}H NMR** (400 MHz, $CDCl_3$) δ 8.81 (d, *J* = 4.9 Hz, 1H), 8.36 (s, 1H), 8.15 (d, *J* = 8.7 Hz, 1H), 7.67 (dd, *J* = 8.8, 2.1 Hz, 1H), 7.34 (t, *J* = 7.4 Hz, 1H), 7.01 (d, *J* = 5.0 Hz, 1H), 6.97 (d, *J* = 8.1 Hz, 1H), 6.91 (t, *J* = 7.3 Hz, 1H), 4.76 (s, 2H), 3.80 (td, *J* = 12.5, 3.0 Hz, 2H), 3.57 (dd, *J* = 12.5, 4.9 Hz, 2H), 3.05 (s, 3H), 2.99 (td, *J* = 13.1, 6.8 Hz, 2H), 1.88 (d, *J* = 13.8 Hz, 2H). **^{19}F NMR** (376 MHz, $CDCl_3$) δ -62.70 (s, 3F). **^{13}C NMR** (101 MHz, $CDCl_3$) δ 174.3, 157.4, 152.3, 148.8, 142.8, 130.9 (q, *J* = 32.6 Hz), 129.7, 128.0 (q, *J* = 4.4 Hz), 125.5, 125.1, 124.1 (q, *J* = 272.4 Hz), 121.0 (q, *J* = 3.2 Hz), 119.3, 115.0, 110.7, 65.4, 60.1. 49.2, 29.6, 27.7. **IR (neat):** 3051, 2967, 2933, 2868, 1690, 1577, 1510, 1325, 1292, 1161, 1111, 747, 702 cm^{-1}. **HRMS** (DART) $[M+H]^+$ calcd. for $[C_{24}H_{24}F_3N_4O]^+$ 441.1897, 441.1912 found. **Melting Point:** 185-190 ºC.

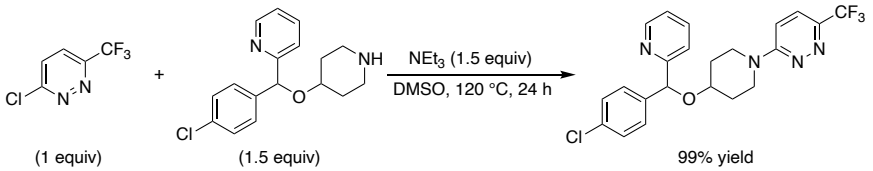

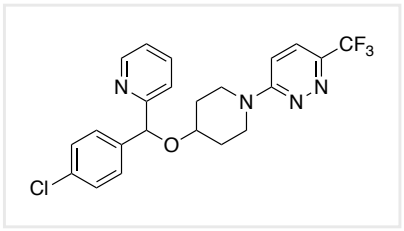

3-(4-((4-chlorophenyl)(pyridin-2-yl)methoxy)piperidin-1-yl)-6-(trifluoromethyl)pyridazine (A1-12). To an oven-dried round bottom flask charged with a Teflon-coated stir bar was added 3-chloro-6-(trifluoromethyl)pyridazine (1.00 g, 5.48 mmol, 1 equiv), dry dimethylsulfoxide (20 mL), and 2-((4-chlorophenyl)(piperidin-4-yloxy)methyl)pyridine (2.49 g, 8.22 mmol, 1.5 equiv). The flask was fitted with a rubber septum and then evacuated and refilled with nitrogen three times on a Schlenk line, and a nitrogen-filled balloon was then inserted. Triethylamine (1.2 mL, 8.22 mL, 1.5 equiv) was added through the septum and the flask was placed into a preheated oil bath at 120 °C with stirring. After 24 h, the reaction mixture was quenched with saturated aq. sodium bicarbonate (5 mL) and diluted with ethyl acetate (40 mL) and water (40 mL). The aqeous layer was seperated and washed with ethyl acetate (3 x 30 mL). The combined organic layers were washed with brine (50 mL), dried over anhydrous sodium sulfate, filtered, and concentrated *in vacuo*. Purification *via* silica gel column chromatography (50-60% ethyl acetate gradient in hexanes) provided the title compound as an off-white solid (2.44 g, 5.4 mmol, 99% yield). **^{1}H NMR** (400 MHz, $CDCl_3$) δ 8.46 (dd, *J* = 5.0, 1.7 Hz, 1H), 7.64 (td, *J* = 7.7, 1.8 Hz, 1H), 7.48 (d, *J* = 7.9 Hz, 1H), 7.37 (d, *J* = 9.6 Hz, 1H), 7.34 (d, *J* = 8.3 Hz, 2H), 7.23 (d, *J* = 8.4 Hz, 2H), 7.12 (dd, *J* = 7.7, 4.8 Hz, 1H), 6.87 (d, *J* = 9.6 Hz, 1H), 5.61 (s, 1H), 4.05–3.96 (m, 2H), 3.74 (tt, *J* = 7.3, 3.6 Hz, 1H), 3.52 (ddd, *J* = 13.4, 8.0, 3.7 Hz, 2H), 1.95–1.85 (m, 2H), 1.81–1.70 (m, 2H). **^{19}F NMR** (376 MHz, $CDCl_3$) δ -66.12 (s, 3F). **^{13}C NMR** (101 MHz, $CDCl_3$) δ 161.7, 160.1, 149.1, 142.4 (q, *J* = 34.9 Hz), 140.1, 137.1, 133.5, 128.7, 128.2, 124.6 (q, *J* = 2.1 Hz), 122.7, 122.3 (q, *J* = 272.5 Hz), 120.7, 111.3, 81.2, 72.3, 42.2, 42.1,

30.7. **IR (neat):** 3069, 2935, 2898, 1589, 1489, 1405, 1337, 1179, 1093, 1072, 1022, 839, 789 cm^{-1}. **HRMS** (DART) $[M+H]^+$ calcd. for $[C_{22}H_{21}ClF_3N_4O]^+$ 449.1351, 449.1350 found. **Melting Point:** 128-130 ºC.

A1.12 References

[1] Billard, T.; Langlois, B. R. *J. Org. Chem.* **2002**, *67*, 997–1000.
[2] Blond, G.; Billard, T.; Langlois, B. R. *J. Org. Chem.* **2001**, *66*, 4826–4830.
[3] Matheau-Raven, D.; Dixon, D. J. Angew. Chem. Int. Ed. **2021**, *60*, 19725–19729.
[4] Kubota, T.; Iijima, M.; Tanaka, T. *Tet. Lett.* **1992**, *33*, 1351–1354.
[5] Elsby, M. R.; Johnson, S. A.; *J. Am. Chem. Soc.*, **2017**, *139*, 9401–9407.
[6] Shippey, M. A.; Dervan, P. B. *J. Org. Chem.* **1977**, *42*, 2654–2655.
[7] Reidl, T. R.; Bandar, J. S. *J. Am. Chem. Soc.* **2021**, *143*, 11939–11945.
[8] Zhao, X.; Zhou, Y.; Yang, Q.; Xie, Y.; Ding, Q.; Deng, Z.; Zhang, M.; Xu, J.; Peng, Y. *Synthesis*, **2013**, *45*, 3245–3250.
[9] Marquard, S. L.; Hartwig, J. F. *Angew. Chem. Int. Ed.* **2011**, *50*, 7119–7123.
[10] Schwarz, J. L.; Schäfers, F.; Tlahuext-Aca, A.; Lückemeier, L.; Glorius, F. *J. Am. Chem. Soc*. **2018**, *140*, 12705–12709.
[11] Luo, C.; Bandar, J. S. *J. Am. Chem. Soc.* **2019**, *141*, 14120–14125.
[12] Zeng, H.; Dou, Q.; Li, C.-L. *Org. Lett.* **2019**, *21*, 1301–1305.

A1.13 X-ray crystallography experimental procedure and data

Structures were determined for the Compounds **3-6** and **3-38**. Single crystals were coated with Paratone-N oil and mounted under a cold stream of dinitrogen gas. Single crystal X-ray diffraction data were acquired on a Bruker D8 QUEST diffractometer equipped with a Photon50 CMOS detector and curved graphite monochromator using Mo Kα radiation (λ = 0.71073 Å). Initial lattice parameters were obtained from a least-squares analysis of more than 100 reflections; these parameters were later refined against all data. None of the crystals showed significant decay during data collection. Data were integrated and corrected for Lorentz and polarization effects using Bruker APEX4 software, and semiempirical absorption corrections were applied using SCALE.[13] Space group assignments were based on systematic absences, E statistics, and successful refinement of the structures. Structures were solved using Direct Methods and were refined with the aid of successive Fourier difference maps against all data using the SHELXTL 6.14 software package.[14] Thermal parameters for all non-hydrogen atoms were refined anisotropically. All hydrogen atoms were assigned to ideal positions and refined using a riding model with an isotropic thermal parameter 1.2 times that of the attached carbon atom (1.5 times for methyl hydrogens). Selected bond distances and angles for crystals of Compound **3-6** are collected in Table S1-10 below. Selected bond distances and angles for crystals of Compound **3-38** are collected in Table S11-19 below. All other metric parameters can be found in the cif files included with the Supporting Information.

[13] Sheldrick, G. M. *SADABS – a program for area detector absorption corrections*.
[14] Sheldrick, G, M. *SHELXTL*, v. 6.14; Bruker AXS: Madison, WI, 1999.

Definitions of R_1 and $wR2$.
$R_1 = \Sigma \, ||F_o| - |F_c|| \, / \, \Sigma \, |F_o|$; $wR2 = \{\Sigma[w(F_o^2 - F_c^2)^2] \, / \, \Sigma[w(F_o^2)^2]\}^{1/2}$

a. Crystal Structure Report for Compound 3-6

A clear colourless, rod-like specimen of $C_{17}H_{28}F_2N_2O_4SSi$, approximate dimensions 0.054 mm x 0.078 mm x 0.124 mm, was used for the X-ray crystallographic analysis. The X-ray intensity data were measured on a Fixed χ Bruker D8 QUEST system equipped with a Siemens KFF Mo2K-90 sealed tube (Mo Kα, λ = 0.71073 Å) and a curved graphite monochromator.

Table S1: Data collection details for Compound 3-6.

Axis	dx/mm	2θ/°	ω/°	φ/°	χ/°	Width/°	Frames	Time/s	Wavelength/Å	Voltage/kV	Current/mA	Temperature/K
Phi	34.993	20.00	-7.44	0.00	54.71	0.50	360	10.00	0.71076	50	30.0	116
Omega	35.693	41.86	-130.39	-40.00	54.71	0.50	319	15.00	0.71076	50	30.0	116
Omega	35.693	41.86	-131.08	120.00	54.71	0.50	319	15.00	0.71076	50	30.0	116
Omega	35.693	41.86	-130.39	-120.00	54.71	0.50	319	15.00	0.71076	50	30.0	116
Omega	35.693	41.86	-131.08	40.00	54.71	0.50	319	15.00	0.71076	50	30.0	116
Omega	35.693	11.86	-161.08	180.00	54.71	0.50	319	15.00	0.71076	50	30.0	116
Omega	35.693	41.86	-131.08	-160.00	54.71	0.50	319	15.00	0.71076	50	30.0	116
Omega	35.693	26.86	-146.08	0.00	54.71	0.50	319	15.00	0.71076	50	30.0	116
Omega	35.693	62.79	50.04	0.00	54.71	0.50	319	15.00	0.71076	50	30.0	116
Omega	35.693	11.86	-161.08	0.00	54.71	0.50	319	15.00	0.71076	50	30.0	116
Omega	35.693	26.86	-146.08	180.00	54.71	0.50	319	15.00	0.71076	50	30.0	116
Omega	35.693	41.86	-131.08	80.00	54.71	0.50	319	15.00	0.71076	50	30.0	116
Omega	35.693	41.86	29.11	160.00	54.71	0.50	319	15.00	0.71076	50	30.0	116
Omega	35.693	31.71	-141.23	120.00	54.71	0.50	319	15.00	0.71076	50	30.0	116
Omega	35.693	41.86	-131.08	-80.00	54.71	0.50	319	15.00	0.71076	50	30.0	116

A total of 4826 frames were collected. The total exposure time was 19.61 hours. The frames were integrated with the Bruker SAINT software package using a narrow-frame algorithm. The integration of the data using a monoclinic unit cell yielded a total of 83054 reflections to a maximum θ angle of 26.37° (0.80 Å resolution), of which 4276 were independent (average redundancy 19.423, completeness = 99.9%, R_{int} = 14.84%, R_{sig} = 4.33%) and 3101 (72.52%) were

greater than $2\sigma(F^2)$. The final cell constants of a = 9.5216(6) Å, b = 9.3831(6) Å, c = 23.5240(15) Å, β = 95.734(3)°, volume = 2091.2(2) $Å^3$, are based upon the refinement of the XYZ-centroids of 9989 reflections above 20 σ(I) with 4.677° < 2θ < 52.08°. Data were corrected for absorption effects using the Multi-Scan method (SADABS). The ratio of minimum to maximum apparent transmission was 0.837. The calculated minimum and maximum transmission coefficients (based on crystal size) are 0.9690 and 0.9860.

The structure was solved and refined using the Bruker SHELXTL Software Package, using the space group P 1 21/n 1, with Z = 4 for the formula unit, $C_{17}H_{28}F_2N_2O_4SSi$. The final anisotropic full-matrix least-squares refinement on F^2 with 249 variables converged at R1 = 4.71%, for the observed data and wR2 = 13.69% for all data. The goodness-of-fit was 1.047. The largest peak in the final difference electron density synthesis was 0.600 $e^-/Å^3$ and the largest hole was -0.378 $e^-/Å^3$ with an RMS deviation of 0.075 $e^-/Å^3$. On the basis of the final model, the calculated density was 1.342 g/cm^3 and F(000), 896 e^-.

Table S2. Sample and crystal data for Compound 3-6.

Identification code	jb002r
Chemical formula	$C_{17}H_{28}F_2N_2O_4SSi$
Formula weight	422.56 g/mol
Temperature	116(2) K
Wavelength	0.71073 Å
Crystal size	0.054 x 0.078 x 0.124 mm
Crystal habit	clear colourless rod

Crystal system	monoclinic	
Space group	P 1 21/n 1	
Unit cell dimensions	a = 9.5216(6) Å	α = 90°
	b = 9.3831(6) Å	β = 95.734(3)°
	c = 23.5240(15) Å	γ = 90°
Volume	2091.2(2) $Å^3$	
Z	4	
Density (calculated)	1.342 g/cm^3	
Absorption coefficient	0.254 mm^{-1}	
F(000)	896	

Table S3. Data collection and structure refinement for Compound 3-6.

Diffractometer	Fixed χ Bruker D8 QUEST
Radiation source	Siemens KFF Mo2K-90 sealed tube (Mo Kα, λ = 0.71073 Å)
Theta range for data collection	2.78 to 26.37°
Index ranges	-11<=h<=11, -11<=k<=11, -29<=l<=29
Reflections collected	83054
Independent reflections	4276 [R(int) = 0.1484]
Coverage of independent reflections	99.9%
Absorption correction	Multi-Scan

Max. and min. transmission	0.9860 and 0.9690
Structure solution technique	direct methods
Structure solution program	XT, VERSION 2018/2
Refinement method	Full-matrix least-squares on F^2
Refinement program	SHELXL-2019/1 (Sheldrick, 2019)
Function minimized	$\Sigma\ w(F_o^2 - F_c^2)^2$
Data / restraints / parameters	4276 / 0 / 249
Goodness-of-fit on F^2	1.047
Final R indices	3101 data; $I>2\sigma(I)$ R1 = 0.0471, wR2 = 0.1203
	all data R1 = 0.0776, wR2 = 0.1369
Weighting scheme	$w=1/[\sigma^2(F_o^2)+(0.0680P)^2+2.0964P]$ where $P=(F_o^2+2F_c^2)/3$
Largest diff. peak and hole	0.600 and -0.378 eÅ^{-3}
R.M.S. deviation from mean	0.075 eÅ^{-3}

Table S4. Atomic coordinates and equivalent isotropic atomic displacement parameters (Å^2) for Compound 3-6.

U(eq) is defined as one third of the trace of the orthogonalized U_{ij} tensor.

	x/a	y/b	z/c	U(eq)
S1	0.68750(7)	0.33613(7)	0.44766(3)	0.01839(17)
Si1	0.17367(8)	0.98143(9)	0.40317(3)	0.0232(2)

	x/a	y/b	z/c	U(eq)
F1	0.21320(18)	0.66055(18)	0.28846(7)	0.0300(4)
F2	0.19192(17)	0.60405(19)	0.37683(8)	0.0318(4)
O1	0.7645(2)	0.2105(2)	0.43597(8)	0.0252(5)
O2	0.6007(2)	0.3366(2)	0.49410(8)	0.0234(4)
O3	0.2495(2)	0.8928(2)	0.35350(8)	0.0218(4)
O4	0.6902(2)	0.9757(3)	0.28511(11)	0.0396(6)
N1	0.8033(2)	0.4643(3)	0.46047(10)	0.0209(5)
N2	0.4808(2)	0.8172(3)	0.33605(10)	0.0211(5)
C1	0.5801(3)	0.3813(3)	0.38456(11)	0.0179(6)
C2	0.4763(3)	0.4839(3)	0.38731(11)	0.0180(5)
C3	0.3956(3)	0.5246(3)	0.33733(11)	0.0180(5)
C4	0.4167(3)	0.4591(3)	0.28587(12)	0.0216(6)
C5	0.5201(3)	0.3557(3)	0.28414(12)	0.0239(6)
C6	0.6038(3)	0.3169(3)	0.33340(11)	0.0210(6)
C7	0.2893(3)	0.6429(3)	0.34037(12)	0.0214(6)
C8	0.3543(3)	0.7851(3)	0.36202(11)	0.0188(6)
C9	0.0413(3)	0.8679(4)	0.43369(14)	0.0328(7)
C10	0.3070(3)	0.0426(3)	0.46078(13)	0.0306(7)
C11	0.0864(5)	0.1338(4)	0.36408(16)	0.0496(11)
C12	0.4590(3)	0.8647(4)	0.27639(12)	0.0286(7)

	x/a	y/b	z/c	U(eq)
C13	0.5713(3)	0.9203(3)	0.36849(12)	0.0248(6)
C14	0.6008(4)	0.8777(4)	0.25291(15)	0.0422(9)
C15	0.7100(3)	0.9309(4)	0.34272(15)	0.0332(7)
C16	0.9039(3)	0.4834(4)	0.41770(14)	0.0325(7)
C17	0.7522(3)	0.6011(3)	0.48101(13)	0.0280(7)

Table S5. Bond lengths (Å) for Compound 3-6.

S1-O1	1.429(2)	S1-O2	1.4342(19)
S1-N1	1.639(2)	S1-C1	1.768(3)
Si1-O3	1.657(2)	Si1-C9	1.850(3)
Si1-C11	1.851(3)	Si1-C10	1.853(3)
F1-C7	1.366(3)	F2-C7	1.374(3)
O3-C8	1.420(3)	O4-C15	1.414(4)
O4-C14	1.419(4)	N1-C16	1.468(4)
N1-C17	1.472(4)	N2-C8	1.436(3)
N2-C13	1.459(4)	N2-C12	1.467(4)
C1-C6	1.385(4)	C1-C2	1.386(4)
C2-C3	1.392(4)	C2-H2	0.950000
C3-C4	1.390(4)	C3-C7	1.508(4)
C4-C5	1.386(4)	C4-H4	0.950000

C5-C6	1.388(4)	C5-H5	0.950000
C6-H6	0.950000	C7-C8	1.536(4)
C8-H8	1.000000	C9-H9A	0.980000
C9-H9B	0.980000	C9-H9C	0.980000
C10-H10A	0.980000	C10-H10B	0.980000
C10-H10C	0.980000	C11-H11A	0.980000
C11-H11B	0.980000	C11-H11C	0.980000
C12-C14	1.514(4)	C12-H12A	0.990000
C12-H12B	0.990000	C13-C15	1.511(4)
C13-H13A	0.990000	C13-H13B	0.990000
C14-H14A	0.990000	C14-H14B	0.990000
C15-H15A	0.990000	C15-H15B	0.990000
C16-H16A	0.980000	C16-H16B	0.980000
C16-H16C	0.980000	C17-H17A	0.980000
C17-H17B	0.980000	C17-H17C	0.980000

Table S6. Bond angles (°) for Compound 3-6.

O1-S1-O2	119.65(12)	O1-S1-N1	106.99(12)
O2-S1-N1	106.60(12)	O1-S1-C1	107.52(12)
O2-S1-C1	108.05(12)	N1-S1-C1	107.49(12)

O3-Si1-C9	110.25(13)	O3-Si1-C11	104.05(13)
C9-Si1-C11	110.38(18)	O3-Si1-C10	110.87(13)
C9-Si1-C10	109.77(15)	C11-Si1-C10	111.40(18)
C8-O3-Si1	127.37(16)	C15-O4-C14	109.6(3)
C16-N1-C17	112.2(2)	C16-N1-S1	115.91(19)
C17-N1-S1	117.55(19)	C8-N2-C13	113.1(2)
C8-N2-C12	115.2(2)	C13-N2-C12	108.6(2)
C6-C1-C2	121.5(2)	C6-C1-S1	119.6(2)
C2-C1-S1	118.9(2)	C1-C2-C3	119.2(2)
C1-C2-H2	120.400000	C3-C2-H2	120.400000
C4-C3-C2	119.9(2)	C4-C3-C7	121.5(2)
C2-C3-C7	118.6(2)	C5-C4-C3	120.0(3)
C5-C4-H4	120.000000	C3-C4-H4	120.000000
C4-C5-C6	120.6(3)	C4-C5-H5	119.700000
C6-C5-H5	119.700000	C1-C6-C5	118.8(3)
C1-C6-H6	120.600000	C5-C6-H6	120.600000
F1-C7-F2	105.1(2)	F1-C7-C3	110.2(2)
F2-C7-C3	109.4(2)	F1-C7-C8	110.5(2)
F2-C7-C8	107.3(2)	C3-C7-C8	113.9(2)
O3-C8-N2	113.5(2)	O3-C8-C7	108.5(2)
N2-C8-C7	111.6(2)	O3-C8-H8	107.700000

N2-C8-H8	107.700000	C7-C8-H8	107.700000
Si1-C9-H9A	109.500000	Si1-C9-H9B	109.500000
H9A-C9-H9B	109.500000	Si1-C9-H9C	109.500000
H9A-C9-H9C	109.500000	H9B-C9-H9C	109.500000
Si1-C10-H10A	109.500000	Si1-C10-H10B	109.500000
H10A-C10-H10B	109.500000	Si1-C10-H10C	109.500000
H10A-C10-H10C	109.500000	H10B-C10-H10C	109.500000
Si1-C11-H11A	109.500000	Si1-C11-H11B	109.500000
H11A-C11-H11B	109.500000	Si1-C11-H11C	109.500000
H11A-C11-H11C	109.500000	H11B-C11-H11C	109.500000
N2-C12-C14	109.1(3)	N2-C12-H12A	109.900000
C14-C12-H12A	109.900000	N2-C12-H12B	109.900000
C14-C12-H12B	109.900000	H12A-C12-H12B	108.300000
N2-C13-C15	109.1(2)	N2-C13-H13A	109.900000
C15-C13-H13A	109.900000	N2-C13-H13B	109.900000
C15-C13-H13B	109.900000	H13A-C13-H13B	108.300000
O4-C14-C12	111.5(3)	O4-C14-H14A	109.300000
C12-C14-H14A	109.300000	O4-C14-H14B	109.300000
C12-C14-H14B	109.300000	H14A-C14-H14B	108.000000
O4-C15-C13	111.5(2)	O4-C15-H15A	109.300000
C13-C15-H15A	109.300000	O4-C15-H15B	109.300000

C13-C15-H15B	109.300000	H15A-C15-H15B	108.000000
N1-C16-H16A	109.500000	N1-C16-H16B	109.500000
H16A-C16-H16B	109.500000	N1-C16-H16C	109.500000
H16A-C16-H16C	109.500000	H16B-C16-H16C	109.500000
N1-C17-H17A	109.500000	N1-C17-H17B	109.500000
H17A-C17-H17B	109.500000	N1-C17-H17C	109.500000
H17A-C17-H17C	109.500000	H17B-C17-H17C	109.500000

Table S7. Torsion angles (°) for Compound 3-6.

C9-Si1-O3-C8	-76.2(2)	C11-Si1-O3-C8	165.5(2)
C10-Si1-O3-C8	45.6(3)	O1-S1-N1-C16	51.0(2)
O2-S1-N1-C16	-179.8(2)	C1-S1-N1-C16	-64.2(2)
O1-S1-N1-C17	-172.3(2)	O2-S1-N1-C17	-43.2(2)
C1-S1-N1-C17	72.4(2)	O1-S1-C1-C6	-13.3(3)
O2-S1-C1-C6	-143.7(2)	N1-S1-C1-C6	101.6(2)
O1-S1-C1-C2	168.5(2)	O2-S1-C1-C2	38.1(3)
N1-S1-C1-C2	-76.6(2)	C6-C1-C2-C3	-1.1(4)
S1-C1-C2-C3	177.1(2)	C1-C2-C3-C4	2.1(4)
C1-C2-C3-C7	-176.2(2)	C2-C3-C4-C5	-1.4(4)
C7-C3-C4-C5	176.8(3)	C3-C4-C5-C6	-0.3(4)

C2-C1-C6-C5	-0.6(4)	S1-C1-C6-C5	-178.8(2)
C4-C5-C6-C1	1.3(4)	C4-C3-C7-F1	6.3(4)
C2-C3-C7-F1	-175.4(2)	C4-C3-C7-F2	121.3(3)
C2-C3-C7-F2	-60.4(3)	C4-C3-C7-C8	-118.6(3)
C2-C3-C7-C8	59.7(3)	Si1-O3-C8-N2	-122.9(2)
Si1-O3-C8-C7	112.5(2)	C13-N2-C8-O3	77.3(3)
C12-N2-C8-O3	-48.4(3)	C13-N2-C8-C7	-159.7(2)
C12-N2-C8-C7	74.5(3)	F1-C7-C8-O3	45.2(3)
F2-C7-C8-O3	-68.9(3)	C3-C7-C8-O3	169.8(2)
F1-C7-C8-N2	-80.6(3)	F2-C7-C8-N2	165.4(2)
C3-C7-C8-N2	44.1(3)	C8-N2-C12-C14	-173.5(3)
C13-N2-C12-C14	58.5(3)	C8-N2-C13-C15	171.8(2)
C12-N2-C13-C15	-58.9(3)	C15-O4-C14-C12	58.5(4)
N2-C12-C14-O4	-58.9(4)	C14-O4-C15-C13	-58.9(3)
N2-C13-C15-O4	60.0(3)		

Table S8. Anisotropic atomic displacement parameters (Å^2) for Compound 3-6.

The anisotropic atomic displacement factor exponent takes the form: $-2\pi^2[h^2 a^{*2} U_{11} + ... + 2 h k a^* b^* U_{12}]$

	U_{11}	U_{22}	U_{33}	U_{23}	U_{13}	U_{12}
S1	0.0212(3)	0.0175(3)	0.0168(3)	0.0010(3)	0.0033(2)	0.0036(3)

	U_{11}	U_{22}	U_{33}	U_{23}	U_{13}	U_{12}
Si1	0.0243(4)	0.0243(4)	0.0213(4)	-0.0004(3)	0.0041(3)	0.0079(3)
F1	0.0244(9)	0.0299(9)	0.0325(9)	-0.0054(8)	-0.0121(7)	0.0041(7)
F2	0.0194(9)	0.0295(10)	0.0489(11)	0.0010(8)	0.0147(8)	-0.0009(7)
O1	0.0304(11)	0.0202(10)	0.0250(10)	0.0000(8)	0.0025(9)	0.0090(9)
O2	0.0280(11)	0.0246(10)	0.0187(9)	0.0036(8)	0.0069(8)	0.0012(9)
O3	0.0214(10)	0.0224(10)	0.0218(10)	0.0004(8)	0.0025(8)	0.0061(8)
O4	0.0282(12)	0.0409(13)	0.0524(15)	-0.0013(12)	0.0172(11)	-0.0060(11)
N1	0.0177(11)	0.0228(12)	0.0221(12)	-0.0022(10)	0.0023(9)	0.0024(10)
N2	0.0166(12)	0.0241(13)	0.0225(12)	-0.0020(10)	0.0014(9)	0.0015(10)
C1	0.0214(14)	0.0162(13)	0.0162(13)	0.0015(10)	0.0025(10)	-0.0031(11)
C2	0.0208(13)	0.0176(13)	0.0162(12)	-0.0024(10)	0.0050(10)	0.0011(11)
C3	0.0136(12)	0.0170(13)	0.0234(13)	-0.0004(11)	0.0028(10)	-0.0031(10)
C4	0.0180(14)	0.0272(15)	0.0188(13)	-0.0008(11)	-0.0018(11)	-0.0018(11)
C5	0.0254(15)	0.0269(16)	0.0202(14)	-0.0069(12)	0.0059(11)	-0.0007(12)
C6	0.0204(14)	0.0192(14)	0.0237(14)	-0.0016(11)	0.0033(11)	0.0017(11)
C7	0.0172(14)	0.0254(15)	0.0212(13)	-0.0011(11)	-0.0002(11)	0.0010(12)
C8	0.0166(13)	0.0197(14)	0.0203(13)	-0.0012(11)	0.0023(11)	0.0043(11)
C9	0.0215(15)	0.047(2)	0.0306(16)	-0.0055(14)	0.0042(13)	-0.0007(14)
C10	0.0349(17)	0.0301(17)	0.0279(16)	-0.0052(13)	0.0077(13)	-0.0025(14)
C11	0.067(3)	0.044(2)	0.039(2)	0.0056(16)	0.0133(19)	0.035(2)

	U_{11}	U_{22}	U_{33}	U_{23}	U_{13}	U_{12}
C12	0.0212(15)	0.0433(19)	0.0215(14)	0.0007(13)	0.0031(12)	-0.0010(13)
C13	0.0220(15)	0.0248(15)	0.0265(15)	-0.0024(12)	-0.0034(12)	0.0011(12)
C14	0.0346(19)	0.060(2)	0.0344(18)	-0.0079(17)	0.0139(15)	-0.0078(17)
C15	0.0194(15)	0.0301(17)	0.050(2)	-0.0077(15)	0.0000(14)	-0.0006(13)
C16	0.0247(15)	0.0360(18)	0.0389(18)	-0.0056(15)	0.0146(13)	-0.0017(14)
C17	0.0275(16)	0.0222(15)	0.0349(17)	-0.0059(13)	0.0070(13)	0.0013(13)

Table S9. Hydrogen atomic coordinates and isotropic atomic displacement parameters (Å^2) for Compound 3-6.

	x/a	y/b	z/c	U(eq)
H2	0.4604	0.5260	0.4228	0.022000
H4	0.3602	0.4853	0.2519	0.026000
H5	0.5338	0.3109	0.2489	0.029000
H6	0.6759	0.2474	0.3321	0.025000
H8	0.3803	0.7757	0.4041	0.023000
H9A	-0.0190	0.9272	0.4555	0.049000
H9B	0.0895	0.7965	0.4590	0.049000
H9C	-0.0169	0.8197	0.4027	0.049000
H10A	0.2595	1.0898	0.4907	0.046000

	x/a	y/b	z/c	U(eq)
H10B	0.3717	1.1098	0.4450	0.046000
H10C	0.3604	0.9604	0.4771	0.046000
H11A	0.0328	1.1888	0.3900	0.074000
H11B	0.0222	1.0982	0.3321	0.074000
H11C	0.1581	1.1950	0.3495	0.074000
H12A	0.4103	0.9580	0.2742	0.034000
H12B	0.3992	0.7951	0.2534	0.034000
H13A	0.5881	0.8896	0.4089	0.030000
H13B	0.5246	1.0147	0.3674	0.030000
H14A	0.6469	0.7831	0.2536	0.051000
H14B	0.5865	0.9099	0.2127	0.051000
H15A	0.7722	0.9995	0.3651	0.040000
H15B	0.7571	0.8367	0.3449	0.040000
H16A	0.9847	0.5394	0.4343	0.049000
H16B	0.8576	0.5336	0.3844	0.049000
H16C	0.9367	0.3900	0.4059	0.049000
H17A	0.8320	0.6555	0.4995	0.042000
H17B	0.6835	0.5834	0.5086	0.042000
H17C	0.7071	0.6556	0.4486	0.042000

Table S10. Hydrogen bond distances (Å) and angles (°) for Compound 3-6.

	Donor-H	Acceptor-H	Donor-Acceptor	Angle
C2-H2···O2#4	0.95	2.46	3.400(3)	171.1
C8-H8···O2#4	1.00	2.61	3.557(3)	158.9
C12-H12A···F1#3	0.99	2.61	3.496(4)	148.8
C12-H12B···F1	0.99	2.39	3.059(4)	124.5
C15-H15A···O1#1	0.99	2.59	3.426(4)	141.6
C16-H16A···F2#2	0.98	2.57	3.202(3)	122.0

Symmetry transformations used to generate equivalent atoms:

#1 x, y+1, z

#2 x+1, y, z

#3 -x+1/2, y+1/2, -z+1/2

#4 -x+1, -y+1, -z+1

b. Crystal Structure Report for Compound 3-38

A clear colourless, rod-like specimen of $C_{18}H_{19}F_5OSi$, approximate dimensions 0.043 mm x 0.107 mm x 0.234 mm, was used for the X-ray crystallographic analysis. The X-ray intensity data were measured on a Fixed χ Bruker D8 QUEST system equipped with a Siemans KFF Mo2K-90 sealed tube (Mo Kα, λ = 0.71073 Å) and a curved graphite monochromator.

Table S11: Data collection details for Compound 3-38.

Axis	dx/mm	2θ/°	ω/°	φ/°	χ/°	Width/°	Frames	Time/s	Wavelength/Å	Voltage/kV	Current/mA	Temperature/K
Phi	34.886	20.00	-7.50	0.00	54.71	0.50	360	1.00	0.71076	50	30.0	250
Omega	35.686	35.34	-137.60	160.00	54.71	0.50	319	15.00	0.71076	50	30.0	250
Omega	35.686	35.34	-137.60	-40.00	54.71	0.50	319	15.00	0.71076	50	30.0	250
Omega	35.686	35.34	22.59	80.00	54.71	0.50	319	15.00	0.71076	50	30.0	250
Omega	35.686	35.34	-137.60	-120.00	54.71	0.50	319	15.00	0.71076	50	30.0	250
Omega	35.686	54.80	42.05	36.00	54.71	0.50	319	15.00	0.71076	50	30.0	250
Omega	35.686	16.71	-156.23	270.00	54.71	0.50	319	15.00	0.71076	50	30.0	250
Omega	35.686	16.71	-156.23	90.00	54.71	0.50	319	15.00	0.71076	50	30.0	250
Omega	35.686	53.01	40.26	0.00	54.71	0.50	319	15.00	0.71076	50	30.0	250
Omega	35.686	16.71	-156.23	0.00	54.71	0.50	319	15.00	0.71076	50	30.0	250
Omega	35.686	20.34	-152.60	180.00	54.71	0.50	319	15.00	0.71076	50	30.0	250
Omega	35.686	35.34	22.59	-160.00	54.71	0.50	319	15.00	0.71076	50	30.0	250
Omega	35.686	35.34	22.59	120.00	54.71	0.50	319	15.00	0.71076	50	30.0	250

A total of 4188 frames were collected. The total exposure time was 16.05 hours. The frames were integrated with the Bruker SAINT software package using a narrow-frame algorithm. The integration of the data using a monoclinic unit cell yielded a total of 64335 reflections to a maximum θ angle of 25.68° (0.82 Å resolution), of which 3486 were independent (average redundancy 18.455, completeness = 99.9%, R_{int} = 4.83%, R_{sig} = 1.63%) and 2963 (85.00%) were greater than $2\sigma(F^2)$. The final cell constants of $\underline{a}$ = 5.7614(2) Å, $\underline{b}$ = 26.3432(7) Å, $\underline{c}$ = 12.1590(3) Å, β = 91.8200(10)°, volume = 1844.49(9) $Å^3$, are based upon the refinement of the XYZ-centroids of 9085 reflections above 20 σ(I) with 4.560° < 2θ < 55.39°. Data were corrected for absorption effects using the Multi-Scan method (SADABS). The ratio of minimum to maximum apparent transmission was 0.883. The

calculated minimum and maximum transmission coefficients (based on crystal size) are 0.9600 and 0.9920.

The structure was solved and refined using the Bruker SHELXTL Software Package, using the space group P 1 21/n 1, with Z = 4 for the formula unit, $C_{18}H_{19}F_5OSi$. The final anisotropic full-matrix least-squares refinement on F^2 with 287 variables converged at R1 = 3.93%, for the observed data and wR2 = 10.29% for all data. The goodness-of-fit was 1.047. The largest peak in the final difference electron density synthesis was 0.242 $e^-/Å^3$ and the largest hole was -0.225 $e^-/Å^3$ with an RMS deviation of 0.035 $e^-/Å^3$. On the basis of the final model, the calculated density was 1.348 g/cm^3 and F(000), 776 e^-.

Table S12. Sample and crystal data for Compound 3-38.

Identification code	jb001
Chemical formula	$C_{18}H_{19}F_5OSi$
Formula weight	374.42 g/mol
Temperature	250(2) K
Wavelength	0.71073 Å
Crystal size	0.043 x 0.107 x 0.234 mm
Crystal habit	clear colourless rod
Crystal system	monoclinic
Space group	P 1 21/n 1
Unit cell dimensions	a = 5.7614(2) Å α = 90°

	b = 26.3432(7) Å β = 91.8200(10)°
	c = 12.1590(3) Å γ = 90°
Volume	1844.49(9) $Å^3$
Z	4
Density (calculated)	1.348 g/cm^3
Absorption coefficient	0.178 mm^{-1}
F(000)	776

Table S13. Data collection and structure refinement for Compound 3-38.

Diffractometer	Fixed χ Bruker D8 QUEST
Radiation source	Siemans KFF Mo2K-90 sealed tube (Mo Kα, λ = 0.71073 Å)
Theta range for data collection	2.28 to 25.68°
Index ranges	-7<=h<=7, -32<=k<=32, -14<=l<=14
Reflections collected	64335
Independent reflections	3486 [R(int) = 0.0483]
Coverage of independent reflections	99.9%
Absorption correction	Multi-Scan
Max. and min. transmission	0.9920 and 0.9600
Structure solution technique	direct methods

Structure solution program	SHELXT 2018/2 (Sheldrick, 2018)
Refinement method	Full-matrix least-squares on F^2
Refinement program	SHELXL-2018/3 (Sheldrick, 2018)
Function minimized	$\Sigma\ w(F_o^2 - F_c^2)^2$
Data / restraints / parameters	3486 / 361 / 287
Goodness-of-fit on F^2	1.047
Δ/σ_{max}	0.011
Final R indices	2963 data; I>2σ(I) R1 = 0.0393, wR2 = 0.0972 all data R1 = 0.0476, wR2 = 0.1029
Weighting scheme	$w=1/[\sigma^2(F_o^2)+(0.0477P)^2+0.7139P]$ where $P=(F_o^2+2F_c^2)/3$
Largest diff. peak and hole	0.242 and -0.225 eÅ^{-3}
R.M.S. deviation from mean	0.035 eÅ^{-3}

Table S14. Atomic coordinates and equivalent isotropic atomic displacement parameters (Å^2) for Compound 3-38.

U(eq) is defined as one third of the trace of the orthogonalized U_{ij} tensor.

	x/a	y/b	z/c	U(eq)
Si1	0.29349(8)	0.77875(2)	0.22018(4)	0.03983(14)
F1	0.0127(2)	0.71179(5)	0.32333(10)	0.0625(3)

	x/a	y/b	z/c	U(eq)
F2	0.9921(2)	0.70650(5)	0.14358(10)	0.0614(3)
O1	0.6584(2)	0.60206(5)	0.44197(10)	0.0513(3)
C1	0.5783(3)	0.61551(6)	0.33923(13)	0.0405(4)
C2	0.4074(3)	0.65269(6)	0.33564(14)	0.0410(4)
C3	0.3126(3)	0.66898(6)	0.23585(14)	0.0396(4)
C4	0.3877(3)	0.64768(7)	0.13853(14)	0.0444(4)
C5	0.5583(3)	0.61118(6)	0.14299(14)	0.0444(4)
C6	0.6558(3)	0.59465(6)	0.24228(14)	0.0427(4)
C7	0.6434(5)	0.58866(8)	0.03839(16)	0.0630(6)
F1A	0.617(2)	0.5396(3)	0.0367(10)	0.082(3)
F2A	0.8814(12)	0.5940(5)	0.0313(8)	0.086(3)
F3A	0.553(3)	0.6093(6)	0.9511(8)	0.101(5)
F4A	0.730(3)	0.5434(4)	0.0486(7)	0.070(3)
F5A	0.782(3)	0.6179(4)	0.9861(11)	0.096(4)
F6A	0.4597(17)	0.5797(6)	0.9650(8)	0.093(3)
F7A	0.851(3)	0.5677(8)	0.0507(8)	0.108(5)
F8A	0.652(3)	0.6213(6)	0.9583(13)	0.092(5)
F9A	0.492(3)	0.5533(6)	0.0028(11)	0.122(4)
C8	0.1480(3)	0.71312(7)	0.23163(14)	0.0428(4)
C9	0.4806(4)	0.78692(9)	0.34570(17)	0.0597(5)

	x/a	y/b	z/c	U(eq)
C10	0.0614(4)	0.82710(8)	0.2112(2)	0.0636(6)
C11	0.4594(4)	0.77774(8)	0.09241(17)	0.0572(5)
C12	0.8485(3)	0.56712(7)	0.44895(15)	0.0461(4)
C13	0.8999(3)	0.55639(6)	0.56800(14)	0.0380(4)
C14	0.7471(3)	0.52829(8)	0.62865(16)	0.0503(5)
C15	0.1027(3)	0.57329(7)	0.61892(16)	0.0468(4)
C16	0.7948(4)	0.51808(9)	0.73828(17)	0.0585(5)
C17	0.1504(4)	0.56296(8)	0.72827(17)	0.0552(5)
C18	0.9965(4)	0.53556(8)	0.78803(15)	0.0550(5)

Table S15. Bond lengths (Å) for Compound 3-38.

Si1-C10	1.848(2)	Si1-C11	1.850(2)
Si1-C9	1.853(2)	Si1-C8	1.9282(19)
F1-C8	1.381(2)	F2-C8	1.387(2)
O1-C1	1.365(2)	O1-C12	1.431(2)
C1-C6	1.387(2)	C1-C2	1.389(2)
C2-C3	1.383(2)	C2-H2	0.940000

C3-C4	1.391(2)	C3-C8	1.500(2)
C4-C5	1.375(3)	C4-H4	0.940000
C5-C6	1.386(2)	C5-C7	1.500(3)
C6-H6	0.940000	C7-F3A	1.287(8)
C7-F5A	1.292(8)	C7-F4A	1.297(8)
C7-F1A	1.301(7)	C7-F8A	1.302(9)
C7-F7A	1.323(9)	C7-F9A	1.339(9)
C7-F6A	1.383(7)	C7-F2A	1.383(6)
C9-H9A	0.970000	C9-H9B	0.970000
C9-H9C	0.970000	C10-H10A	0.970000
C10-H10B	0.970000	C10-H10C	0.970000
C11-H11A	0.970000	C11-H11B	0.970000
C11-H11C	0.970000	C12-C13	1.495(2)
C12-H12A	0.980000	C12-H12B	0.980000
C13-C15	1.378(3)	C13-C14	1.381(3)
C14-C16	1.379(3)	C14-H14	0.940000
C15-C17	1.376(3)	C15-H15	0.940000
C16-C18	1.373(3)	C16-H16	0.940000
C17-C18	1.370(3)	C17-H17	0.940000
C18-H18	0.940000		

Table S16. Bond angles (°) for Compound 3-38.

C10-Si1-C11	110.66(11)	C10-Si1-C9	111.69(11)
C11-Si1-C9	113.00(10)	C10-Si1-C8	107.87(9)
C11-Si1-C8	106.57(9)	C9-Si1-C8	106.71(9)
C1-O1-C12	117.20(13)	O1-C1-C6	124.51(15)
O1-C1-C2	115.51(15)	C6-C1-C2	119.99(16)
C3-C2-C1	120.42(16)	C3-C2-H2	119.800000
C1-C2-H2	119.800000	C2-C3-C4	119.75(16)
C2-C3-C8	120.14(15)	C4-C3-C8	119.80(15)
C5-C4-C3	119.34(16)	C5-C4-H4	120.300000
C3-C4-H4	120.300000	C4-C5-C6	121.59(16)
C4-C5-C7	119.72(17)	C6-C5-C7	118.69(17)
C5-C6-C1	118.91(16)	C5-C6-H6	120.500000
C1-C6-H6	120.500000	F5A-C7-F4A	110.6(6)
F3A-C7-F1A	111.3(7)	F8A-C7-F7A	107.9(7)
F8A-C7-F9A	104.9(8)	F7A-C7-F9A	108.8(7)
F5A-C7-F6A	104.9(6)	F4A-C7-F6A	101.0(5)
F3A-C7-F2A	106.3(6)	F1A-C7-F2A	102.3(5)
F3A-C7-C5	113.4(6)	F5A-C7-C5	113.9(4)
F4A-C7-C5	114.7(4)	F1A-C7-C5	111.5(5)
F8A-C7-C5	113.1(9)	F7A-C7-C5	112.9(5)

F9A-C7-C5	108.8(5)	F6A-C7-C5	110.5(4)
F2A-C7-C5	111.3(3)	F1-C8-F2	104.58(14)
F1-C8-C3	108.97(14)	F2-C8-C3	108.80(15)
F1-C8-Si1	109.80(12)	F2-C8-Si1	109.24(11)
C3-C8-Si1	114.94(12)	Si1-C9-H9A	109.500000
Si1-C9-H9B	109.500000	H9A-C9-H9B	109.500000
Si1-C9-H9C	109.500000	H9A-C9-H9C	109.500000
H9B-C9-H9C	109.500000	Si1-C10-H10A	109.500000
Si1-C10-H10B	109.500000	H10A-C10-H10B	109.500000
Si1-C10-H10C	109.500000	H10A-C10-H10C	109.500000
H10B-C10-H10C	109.500000	Si1-C11-H11A	109.500000
Si1-C11-H11B	109.500000	H11A-C11-H11B	109.500000
Si1-C11-H11C	109.500000	H11A-C11-H11C	109.500000
H11B-C11-H11C	109.500000	O1-C12-C13	107.86(14)
O1-C12-H12A	110.100000	C13-C12-H12A	110.100000
O1-C12-H12B	110.100000	C13-C12-H12B	110.100000
H12A-C12-H12B	108.400000	C15-C13-C14	118.59(17)
C15-C13-C12	120.85(17)	C14-C13-C12	120.54(17)
C16-C14-C13	120.65(18)	C16-C14-H14	119.700000
C13-C14-H14	119.700000	C17-C15-C13	120.71(18)
C17-C15-H15	119.600000	C13-C15-H15	119.600000

C18-C16-C14	120.03(19)	C18-C16-H16	120.000000
C14-C16-H16	120.000000	C18-C17-C15	120.25(19)
C18-C17-H17	119.900000	C15-C17-H17	119.900000
C17-C18-C16	119.75(18)	C17-C18-H18	120.100000
C16-C18-H18	120.100000		

Table S17. Torsion angles (°) for Compound 3-38.

C12-O1-C1-C6	5.4(3)	C12-O1-C1-C2	-174.70(16)
O1-C1-C2-C3	-179.56(16)	C6-C1-C2-C3	0.3(3)
C1-C2-C3-C4	0.5(3)	C1-C2-C3-C8	-173.10(16)
C2-C3-C4-C5	-1.0(3)	C8-C3-C4-C5	172.62(17)
C3-C4-C5-C6	0.7(3)	C3-C4-C5-C7	-178.90(18)
C4-C5-C6-C1	0.1(3)	C7-C5-C6-C1	179.75(18)
O1-C1-C6-C5	179.22(17)	C2-C1-C6-C5	-0.7(3)
C4-C5-C7-F3A	4.4(10)	C6-C5-C7-F3A	-175.3(10)
C4-C5-C7-F5A	76.6(11)	C6-C5-C7-F5A	-103.0(11)
C4-C5-C7-F4A	-154.5(9)	C6-C5-C7-F4A	25.8(9)
C4-C5-C7-F1A	-122.2(7)	C6-C5-C7-F1A	58.2(7)
C4-C5-C7-F8A	36.2(10)	C6-C5-C7-F8A	-143.4(10)
C4-C5-C7-F7A	159.1(11)	C6-C5-C7-F7A	-20.5(11)

C4-C5-C7-F9A	-80.0(11)	C6-C5-C7-F9A	100.4(11)
C4-C5-C7-F6A	-41.2(9)	C6-C5-C7-F6A	139.2(9)
C4-C5-C7-F2A	124.2(7)	C6-C5-C7-F2A	-55.4(7)
C2-C3-C8-F1	-35.9(2)	C4-C3-C8-F1	150.44(16)
C2-C3-C8-F2	-149.40(16)	C4-C3-C8-F2	37.0(2)
C2-C3-C8-Si1	87.76(18)	C4-C3-C8-Si1	-85.86(18)
C1-O1-C12-C13	-177.75(15)	O1-C12-C13-C15	-111.37(18)
O1-C12-C13-C14	70.1(2)	C15-C13-C14-C16	1.0(3)
C12-C13-C14-C16	179.60(18)	C14-C13-C15-C17	-0.9(3)
C12-C13-C15-C17	-179.42(17)	C13-C14-C16-C18	-0.5(3)
C13-C15-C17-C18	0.1(3)	C15-C17-C18-C16	0.4(3)
C14-C16-C18-C17	-0.3(3)		

Table S18. Anisotropic atomic displacement parameters (Å^2) for Compound 3-38.

The anisotropic atomic displacement factor exponent takes the form: $-2\pi^2[h^2 a^{*2} U_{11} + ... + 2 h k a^* b^* U_{12}]$

	U_{11}	U_{22}	U_{33}	U_{23}	U_{13}	U_{12}
Si1	0.0377(3)	0.0400(3)	0.0417(3)	0.0026(2)	-0.00023(19)	0.0082(2)
F1	0.0535(7)	0.0676(7)	0.0678(8)	0.0192(6)	0.0227(6)	0.0173(6)
F2	0.0515(6)	0.0601(7)	0.0711(8)	0.0037(6)	-0.0215(6)	0.0037(5)
O1	0.0687(8)	0.0512(8)	0.0339(6)	0.0021(5)	-0.0005(6)	0.0288(7)

	U_{11}	U_{22}	U_{33}	U_{23}	U_{13}	U_{12}
C1	0.0514(10)	0.0356(9)	0.0346(9)	0.0038(7)	0.0012(7)	0.0063(7)
C2	0.0485(10)	0.0381(9)	0.0366(9)	0.0027(7)	0.0058(7)	0.0076(7)
C3	0.0431(9)	0.0353(9)	0.0404(9)	0.0055(7)	0.0011(7)	0.0015(7)
C4	0.0583(11)	0.0384(9)	0.0361(9)	0.0040(7)	-0.0054(8)	0.0010(8)
C5	0.0631(11)	0.0336(9)	0.0365(9)	-0.0008(7)	0.0030(8)	0.0018(8)
C6	0.0551(10)	0.0318(9)	0.0413(9)	0.0008(7)	0.0039(8)	0.0093(7)
C7	0.1024(18)	0.0463(11)	0.0407(11)	-0.0017(9)	0.0068(11)	0.0136(11)
F1A	0.118(8)	0.049(3)	0.081(6)	-0.031(3)	0.014(5)	-0.008(4)
F2A	0.091(3)	0.104(8)	0.064(6)	-0.024(5)	0.034(3)	-0.010(4)
F3A	0.159(12)	0.112(9)	0.031(3)	0.001(5)	0.005(6)	0.052(8)
F4A	0.111(9)	0.060(5)	0.041(3)	0.001(4)	0.013(6)	0.038(5)
F5A	0.151(10)	0.076(6)	0.063(7)	-0.011(4)	0.054(7)	-0.013(7)
F6A	0.127(6)	0.103(8)	0.046(5)	-0.026(5)	-0.031(4)	0.027(5)
F7A	0.141(8)	0.128(12)	0.057(4)	0.022(8)	0.046(6)	0.073(7)
F8A	0.135(13)	0.087(6)	0.059(8)	0.028(6)	0.045(8)	0.035(8)
F9A	0.207(12)	0.078(7)	0.080(8)	-0.035(5)	0.001(7)	-0.022(7)
C8	0.0397(9)	0.0479(10)	0.0406(9)	0.0072(7)	-0.0001(7)	0.0070(8)
C9	0.0590(12)	0.0670(13)	0.0524(12)	-0.0083(10)	-0.0080(10)	0.0052(10)
C10	0.0507(11)	0.0477(11)	0.0923(17)	0.0084(11)	0.0011(11)	0.0145(9)
C11	0.0614(12)	0.0604(12)	0.0502(11)	0.0050(9)	0.0093(9)	-0.0032(10)

	U_{11}	U_{22}	U_{33}	U_{23}	U_{13}	U_{12}
C12	0.0518(10)	0.0441(10)	0.0422(10)	0.0003(8)	-0.0003(8)	0.0160(8)
C13	0.0425(9)	0.0323(8)	0.0391(9)	-0.0006(7)	-0.0002(7)	0.0105(7)
C14	0.0408(10)	0.0591(12)	0.0509(11)	0.0000(9)	-0.0009(8)	-0.0025(8)
C15	0.0498(10)	0.0366(9)	0.0541(11)	0.0006(8)	0.0005(8)	-0.0028(8)
C16	0.0590(12)	0.0670(13)	0.0502(11)	0.0115(10)	0.0134(10)	0.0013(10)
C17	0.0563(12)	0.0532(12)	0.0551(12)	-0.0081(9)	-0.0144(9)	0.0015(9)
C18	0.0710(13)	0.0569(12)	0.0366(10)	-0.0017(8)	-0.0050(9)	0.0199(10)

Table S19. Hydrogen atomic coordinates and isotropic atomic displacement parameters ($Å^2$) for Compound 3-38.

	x/a	y/b	z/c	U(eq)
H2	0.3558	0.6669	0.4015	0.049000
H4	0.3225	0.6581	0.0704	0.053000
H6	0.7726	0.5697	0.2439	0.051000
H9A	0.6065	0.7625	0.3452	0.089000
H9B	0.3892	0.7815	0.4103	0.089000
H9C	0.5440	0.8210	0.3473	0.089000
H10A	-0.0347	0.8213	0.1454	0.095000
H10B	0.1304	0.8606	0.2080	0.095000

	x/a	y/b	z/c	U(eq)
H10C	-0.0335	0.8247	0.2755	0.095000
H11A	0.3573	0.7681	0.0310	0.086000
H11B	0.5851	0.7534	0.1000	0.086000
H11C	0.5229	0.8112	0.0792	0.086000
H12A	0.9852	0.5818	0.4151	0.055000
H12B	0.8077	0.5356	0.4101	0.055000
H14	0.6092	0.5160	0.5949	0.060000
H15	1.2095	0.5921	0.5785	0.056000
H16	0.6891	0.4991	0.7790	0.070000
H17	1.2892	0.5748	0.7621	0.066000
H18	1.0290	0.5287	0.8628	0.066000

A1.14 NMR Spectra

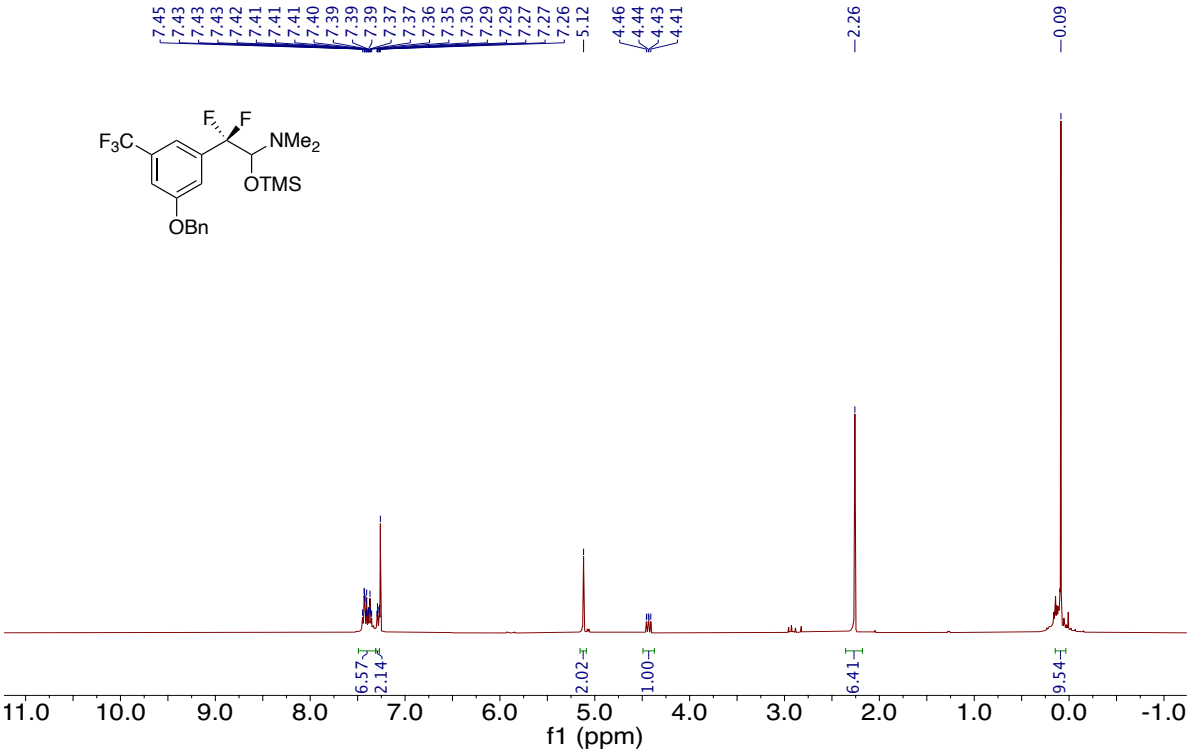

^{1}H NMR of Compound **3-2** (400 MHz, $CDCl_3$)

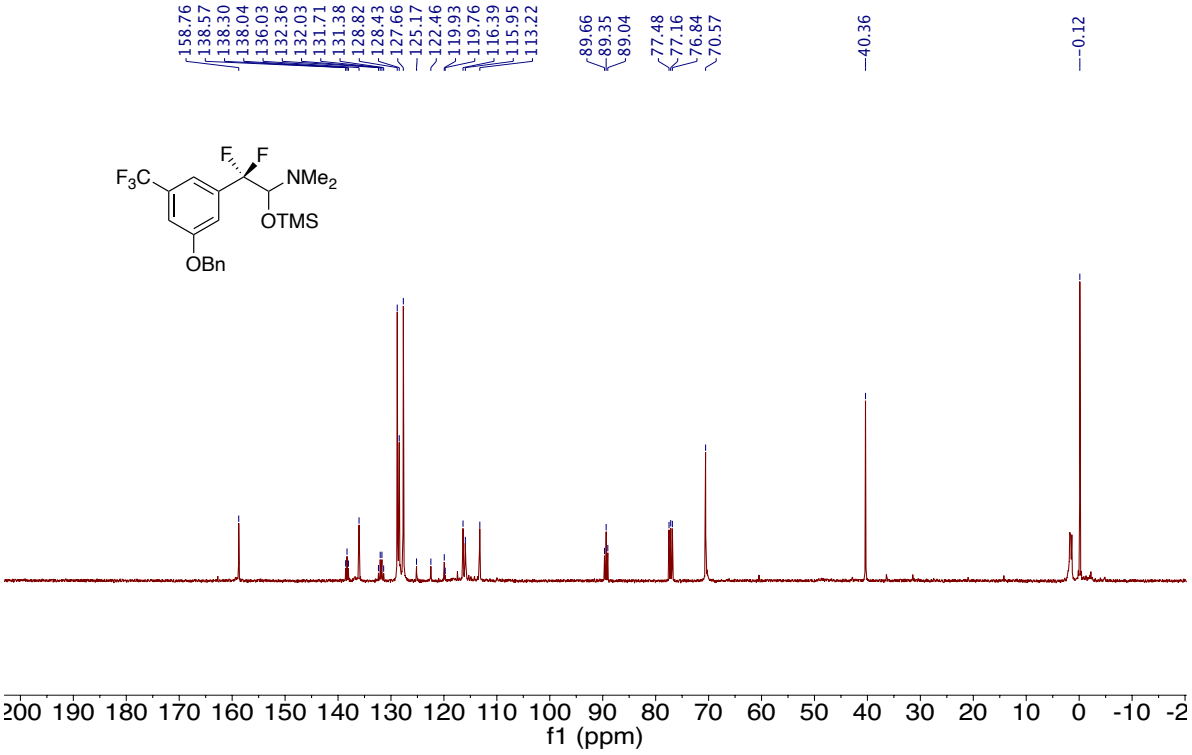

^{13}C NMR of Compound **3-2** (101 MHz, $CDCl_3$)

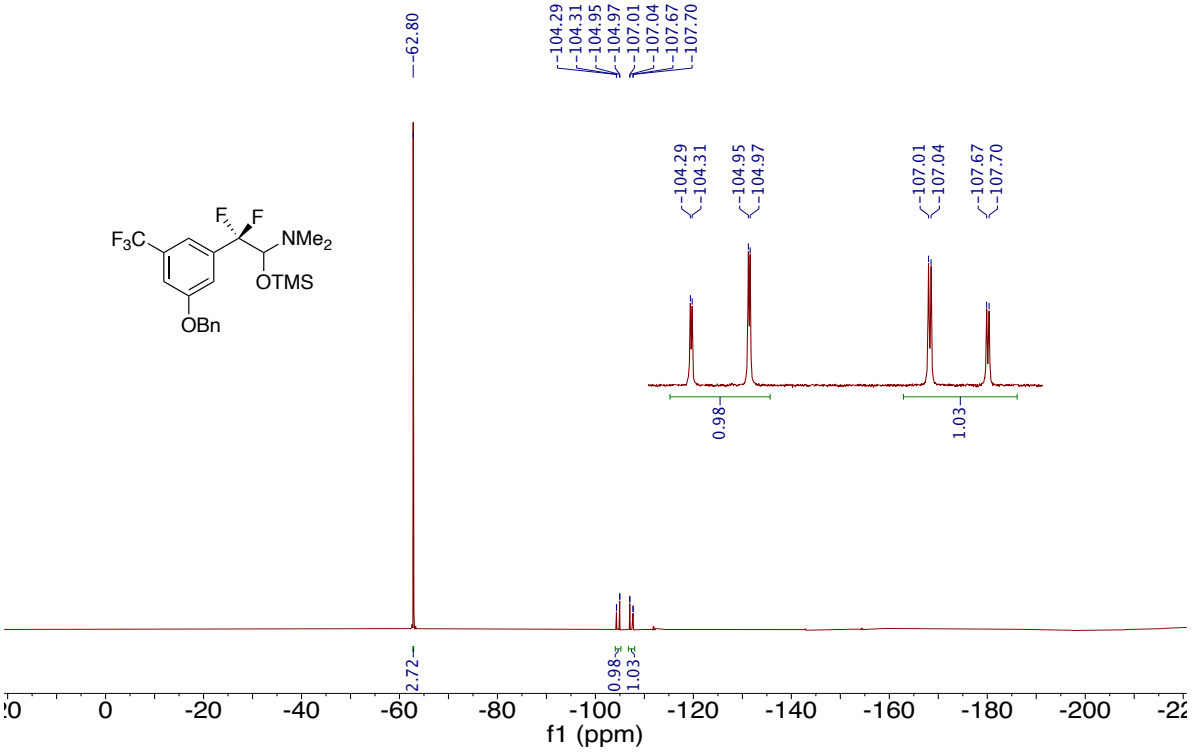

^{19}F NMR of Compound **3-2** (376 MHz, $CDCl_3$)

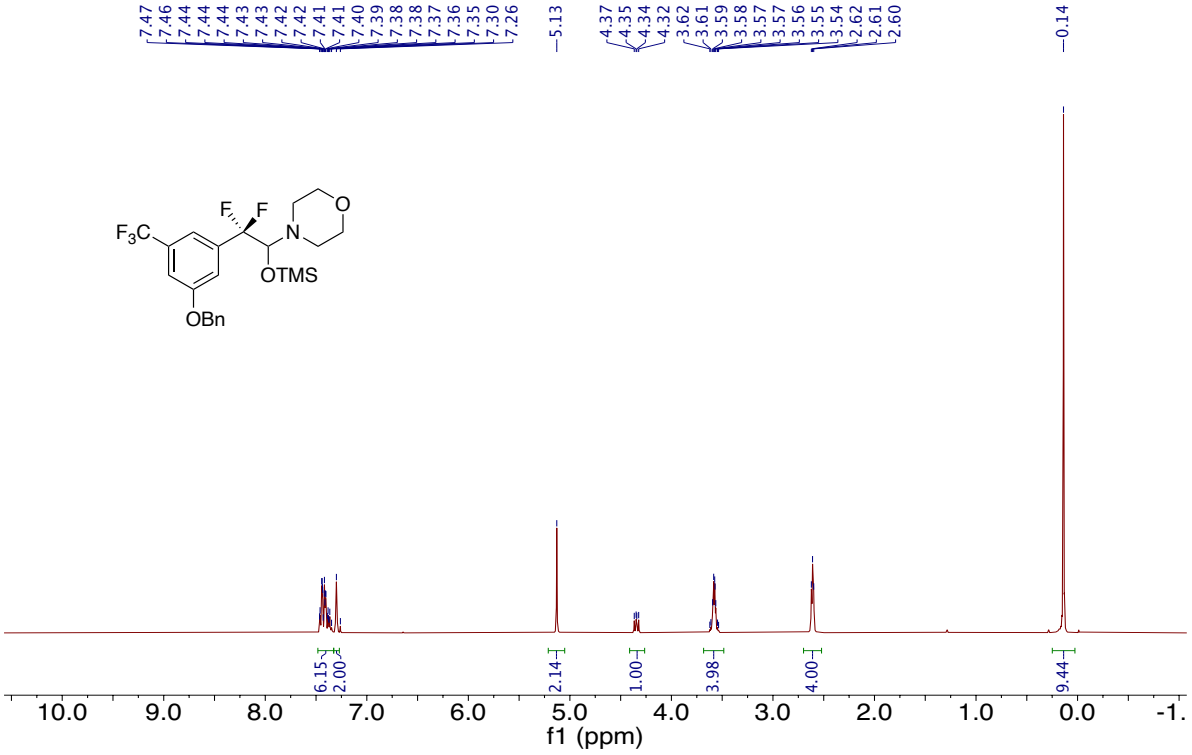

^{1}H NMR of Compound **3-3** (400 MHz, $CDCl_3$)

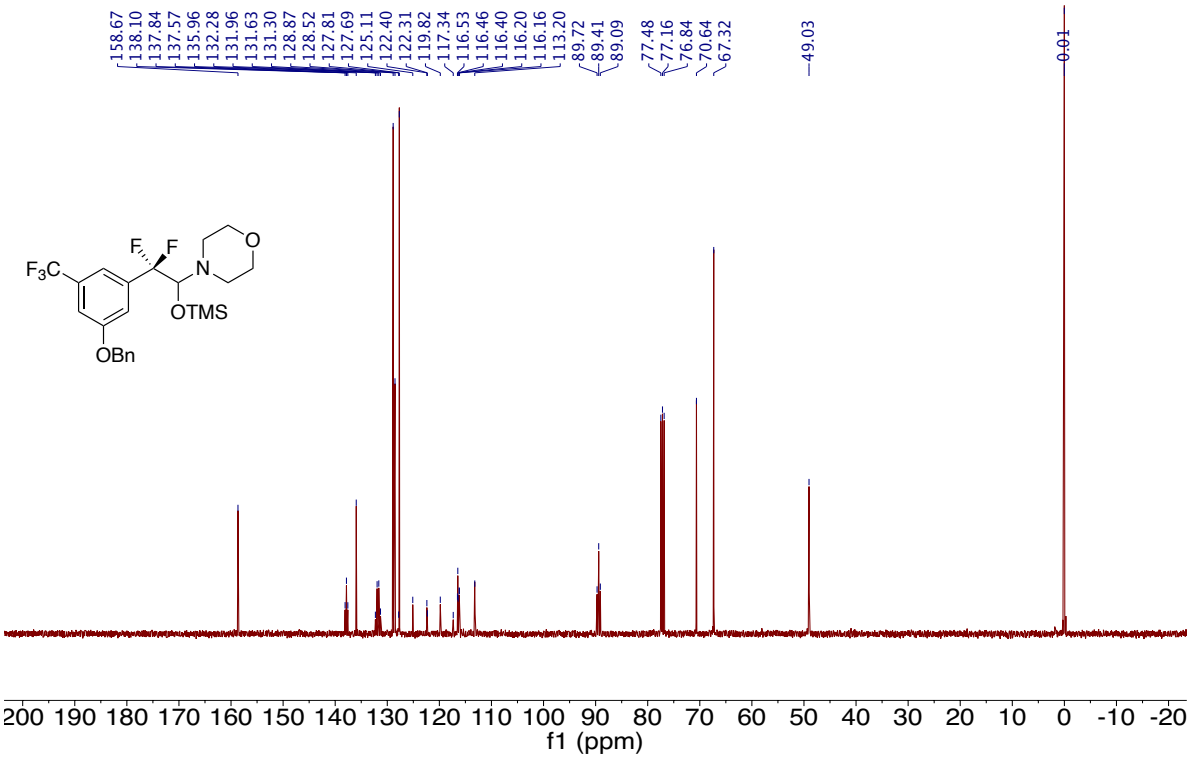

^{13}C NMR of Compound **3-3** (101 MHz, $CDCl_3$)

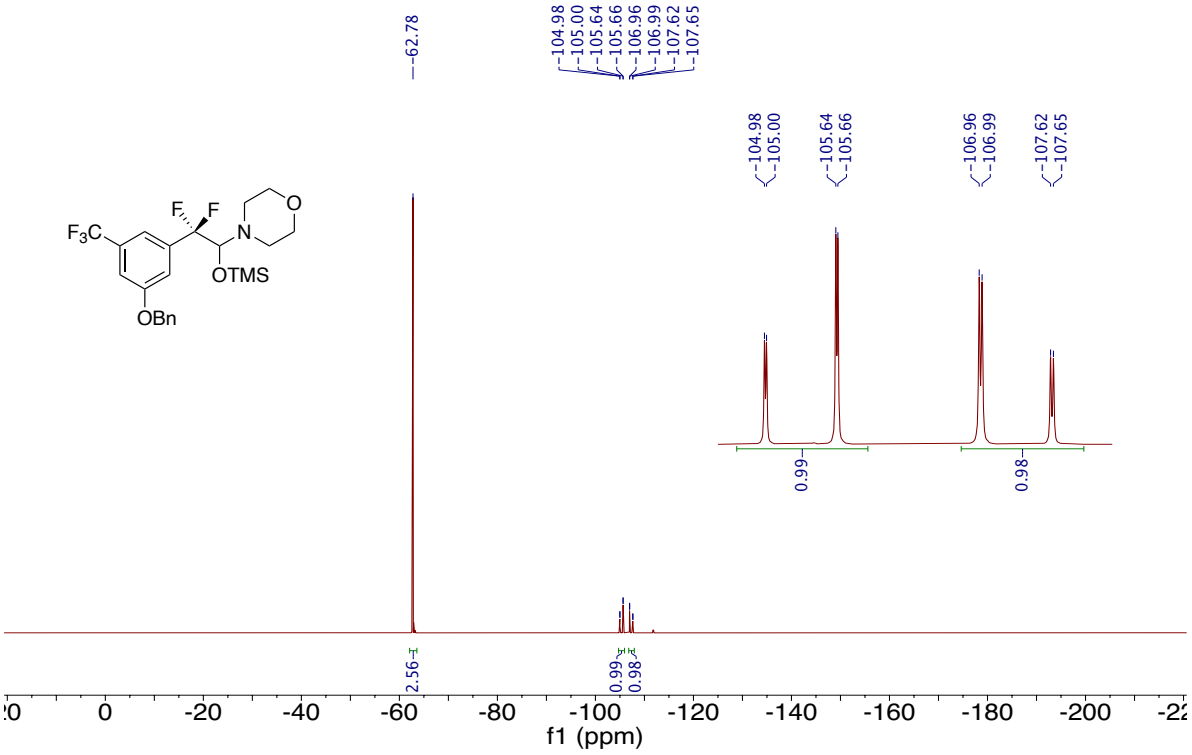

^{19}F NMR of Compound **3-3** (376 MHz, $CDCl_3$)

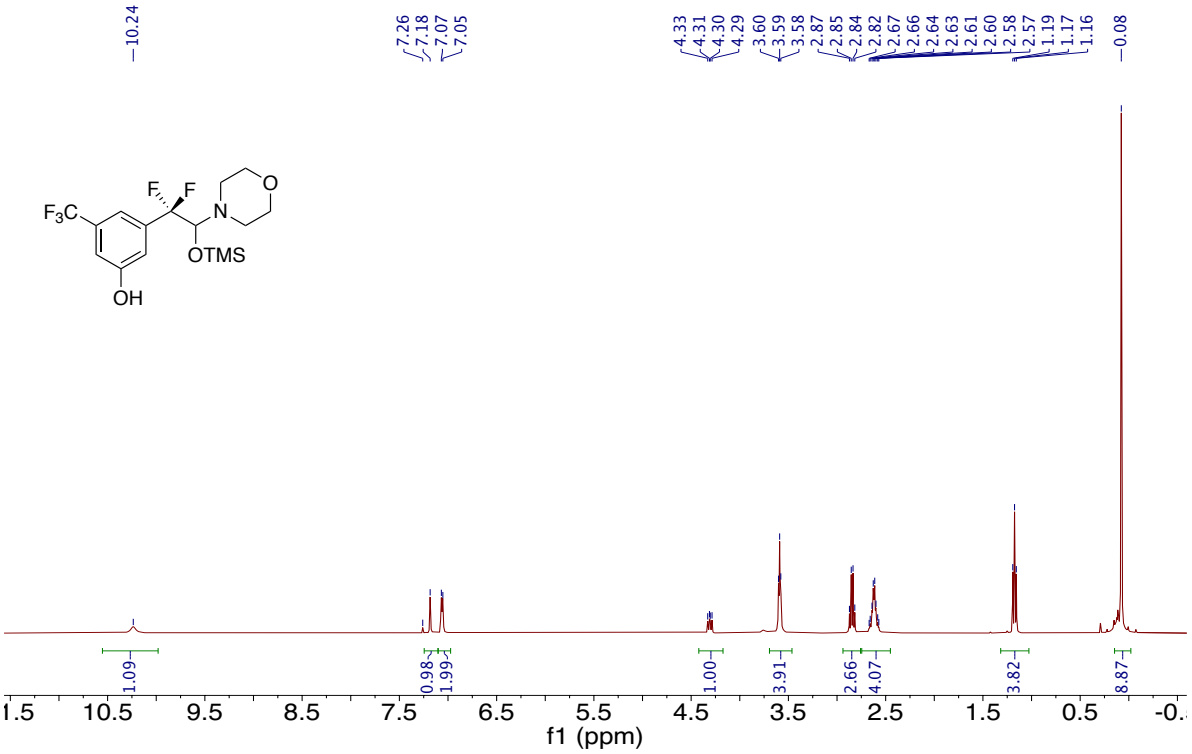

^{1}H NMR of Compound **3-4** (400 MHz, $CDCl_3$)

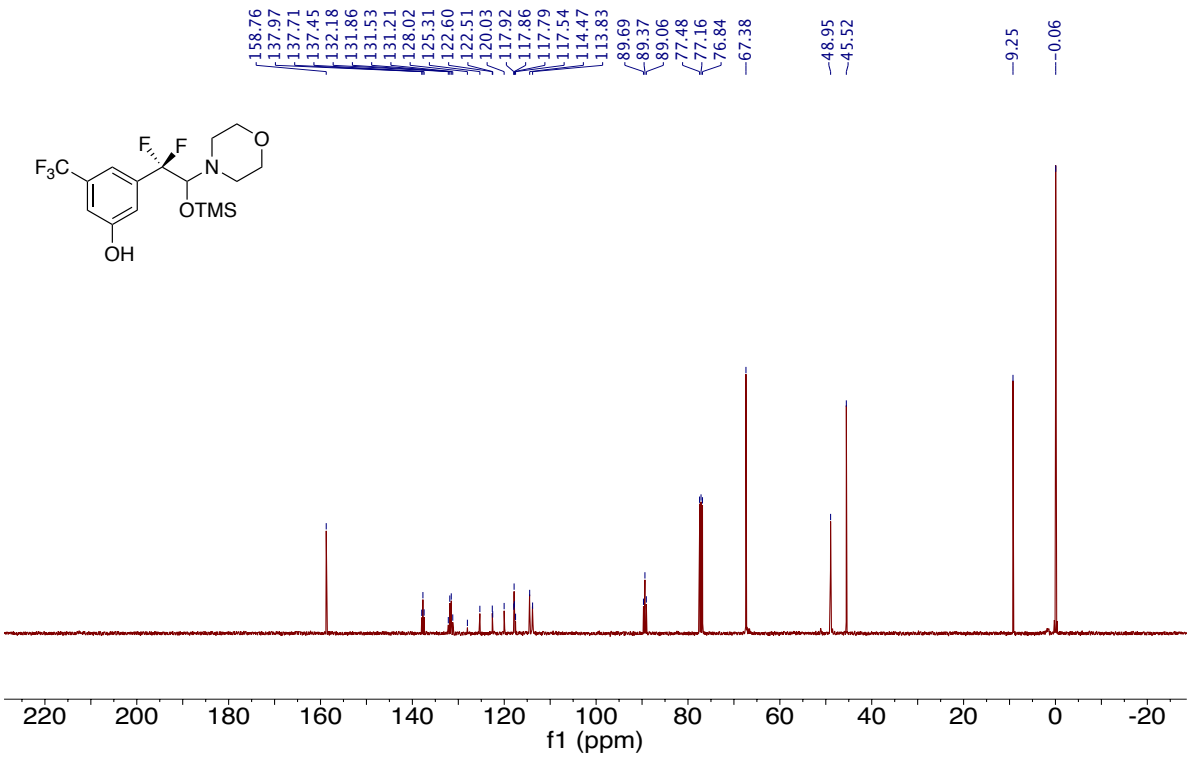

^{13}C NMR of Compound **3-4** (101 MHz, $CDCl_3$)

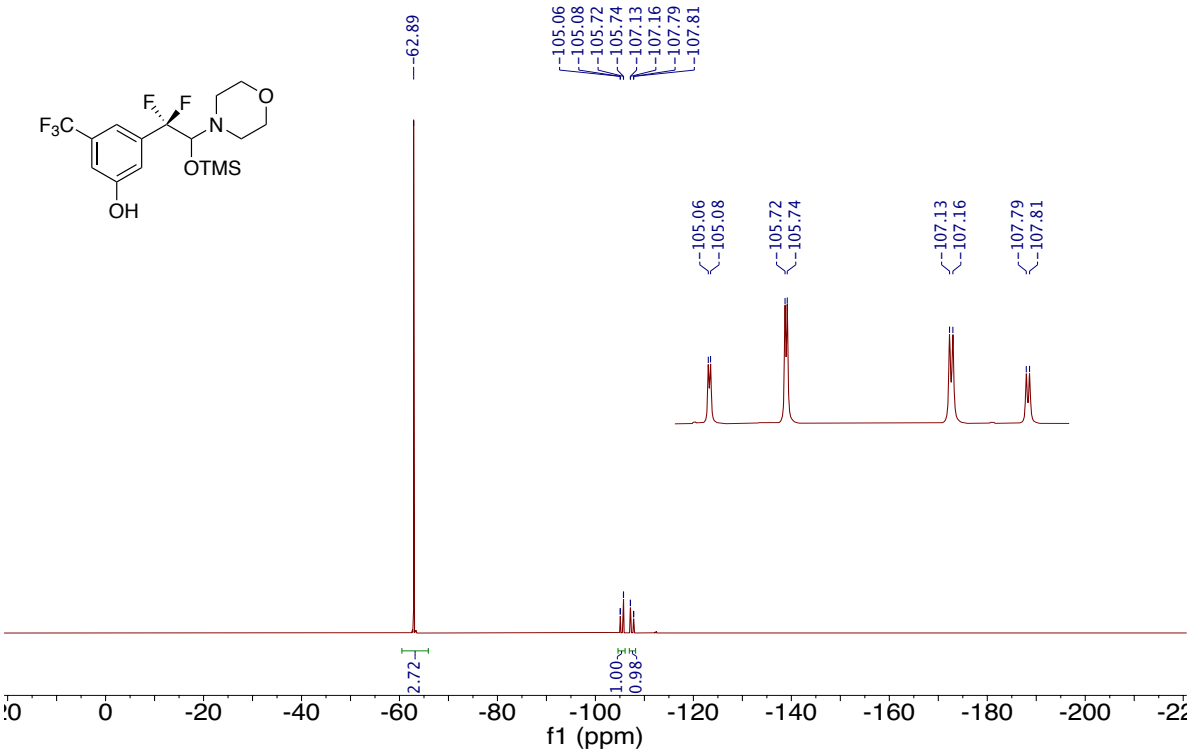

^{19}F NMR of Compound **3-4** (376 MHz, $CDCl_3$)

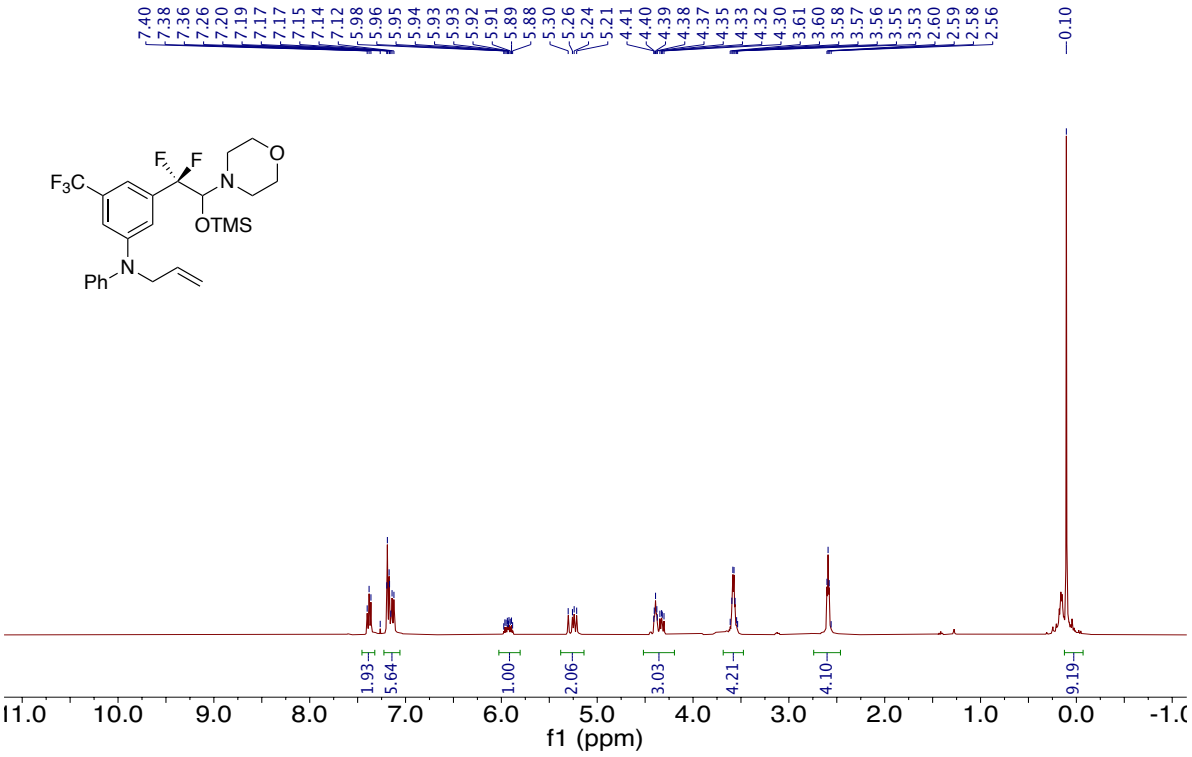

^{1}H NMR of Compound **3-5** (400 MHz, $CDCl_3$)

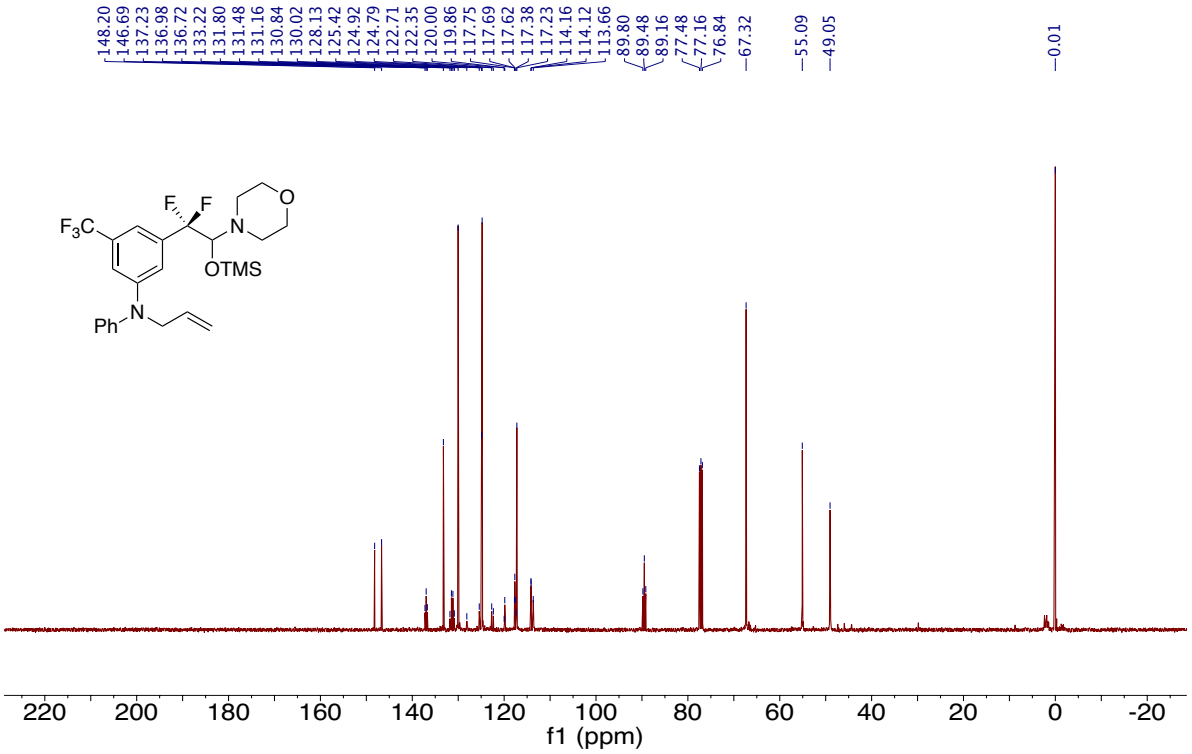

^{13}C NMR of Compound **3-5** (101 MHz, $CDCl_3$)

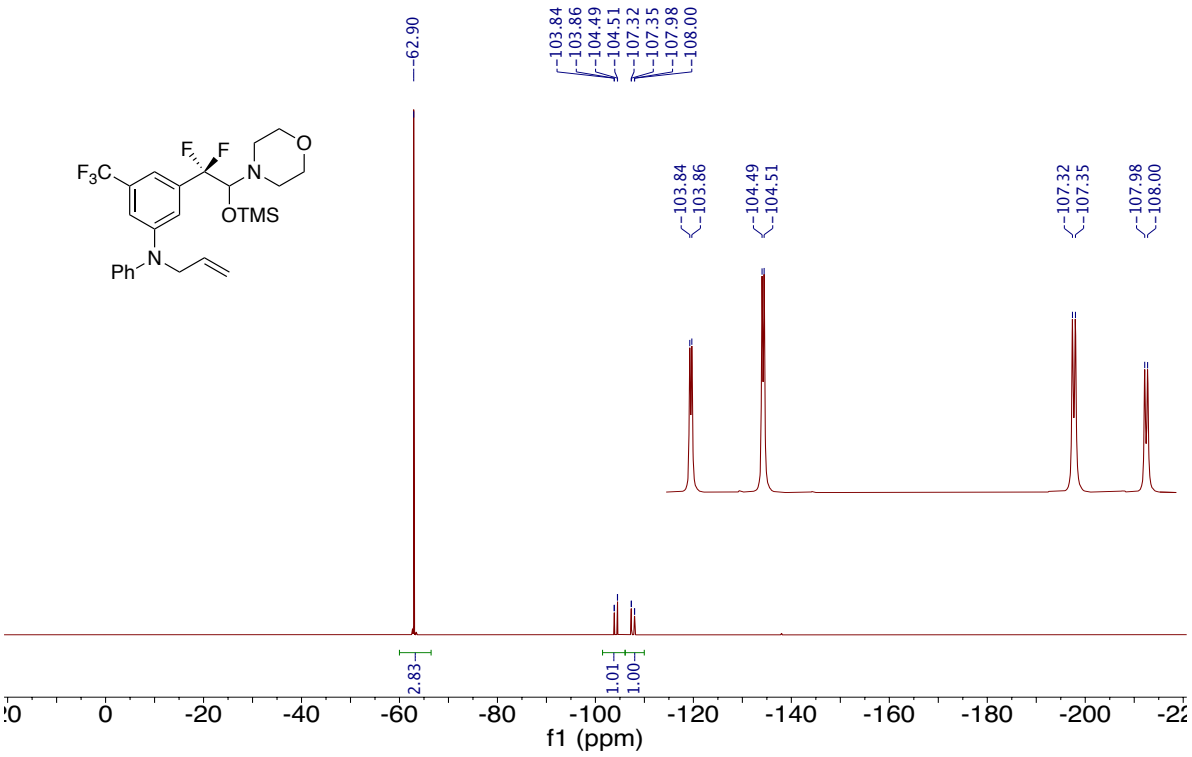

^{19}F NMR of Compound **3-5** (376 MHz, $CDCl_3$)

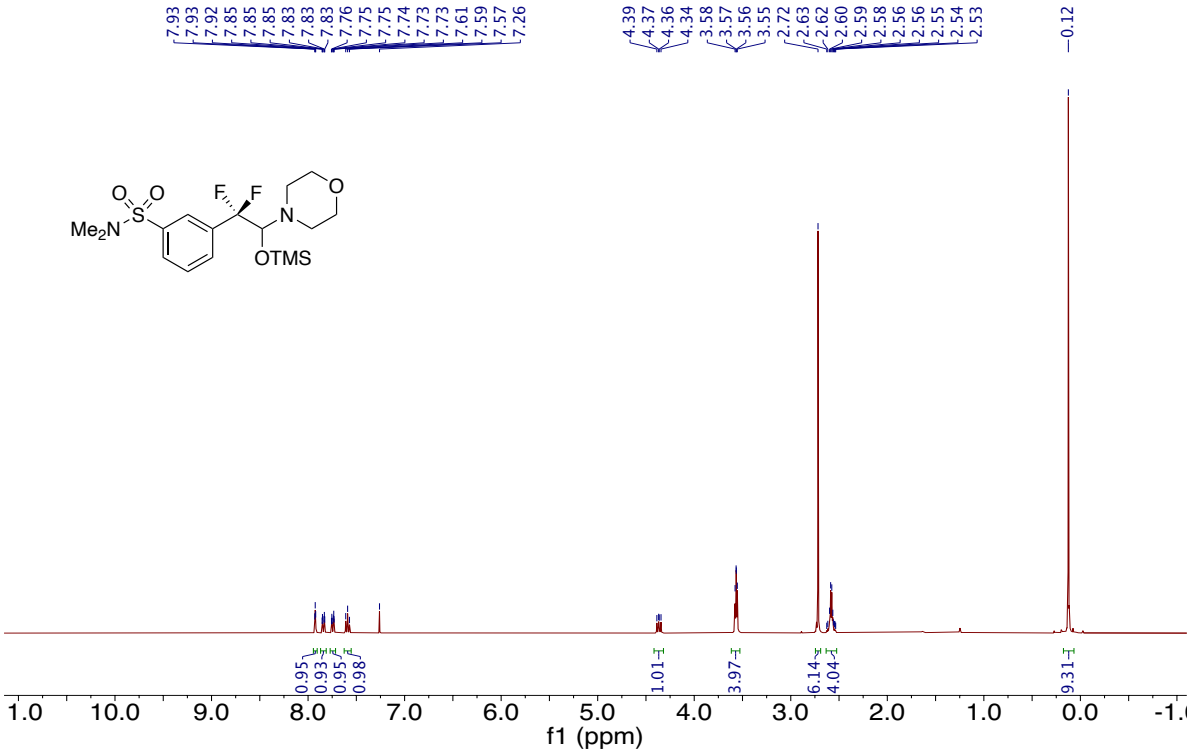

^{1}H NMR of Compound **3-6** (400 MHz, $CDCl_3$)

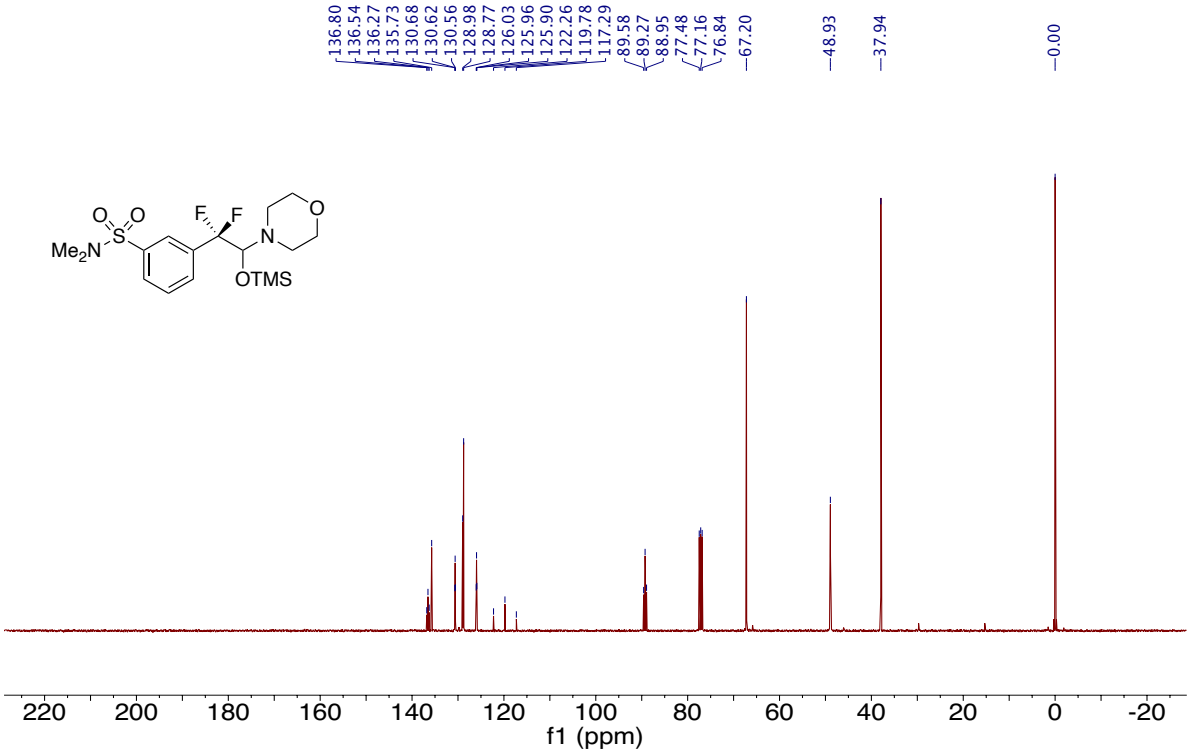

^{13}C NMR of Compound **3-6** (101 MHz, $CDCl_3$)

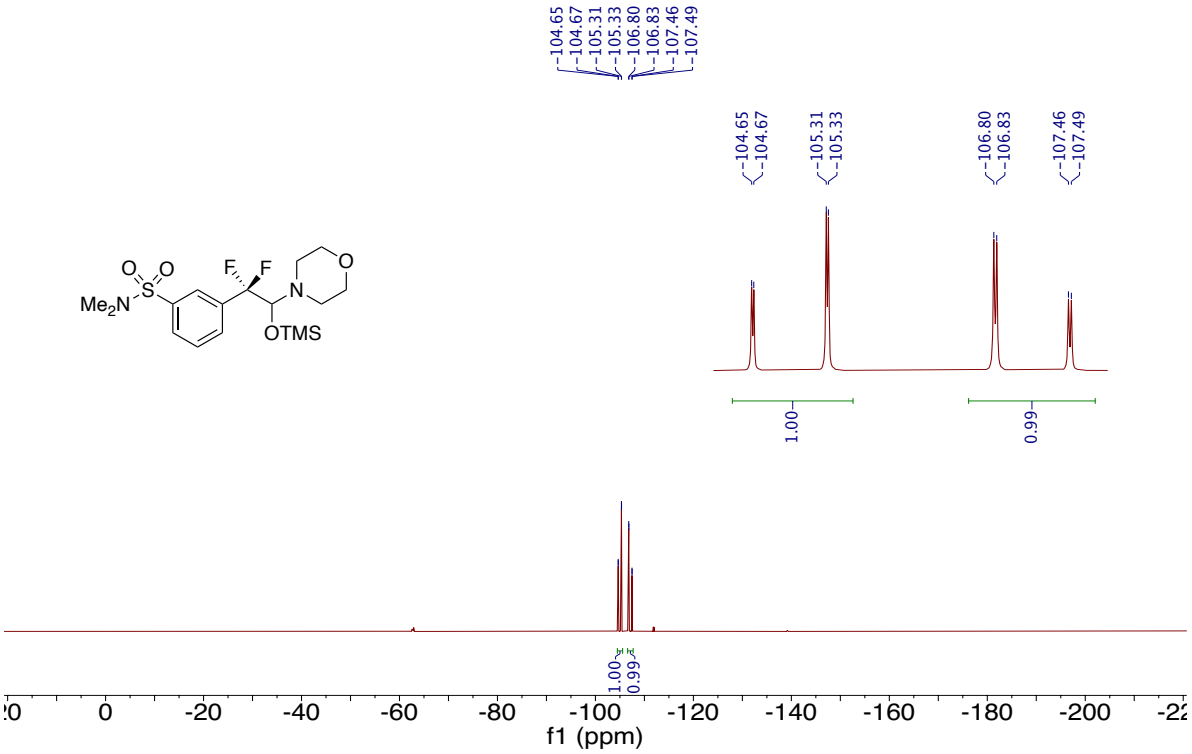

^{19}F NMR of Compound **3-6** (376 MHz, $CDCl_3$)

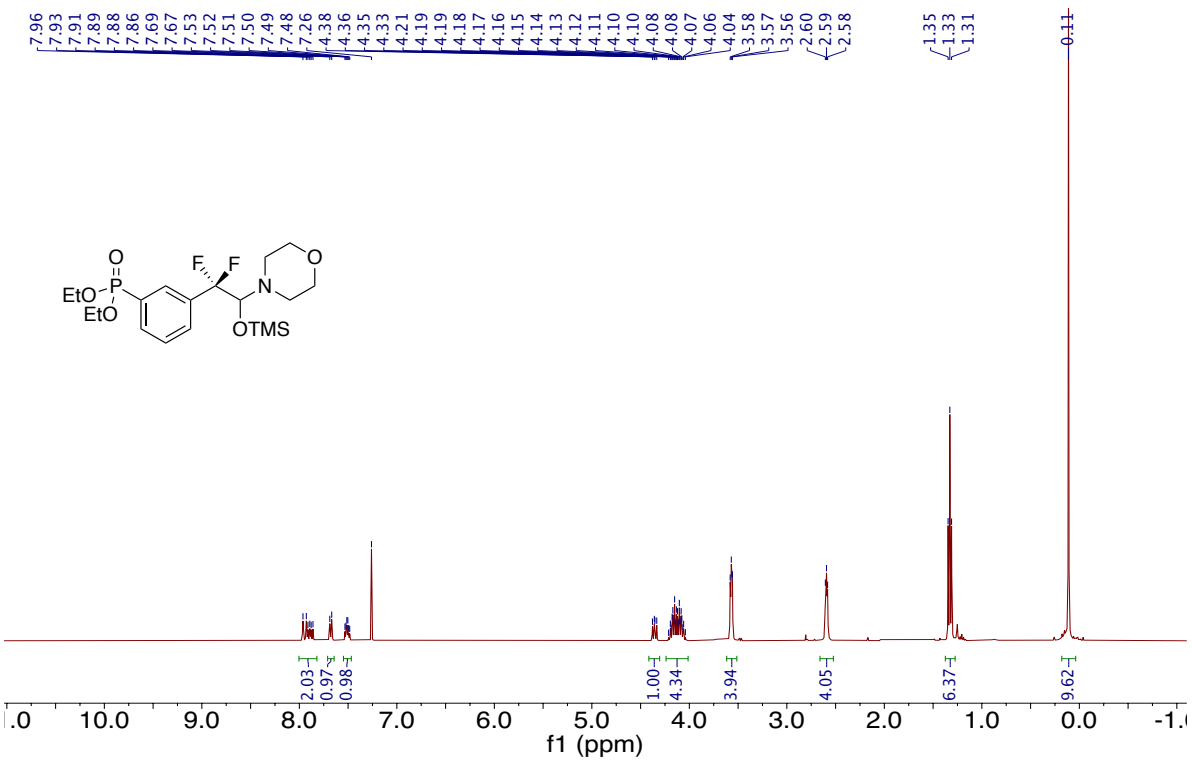

^{1}H NMR of Compound **3-7** (400 MHz, $CDCl_3$)

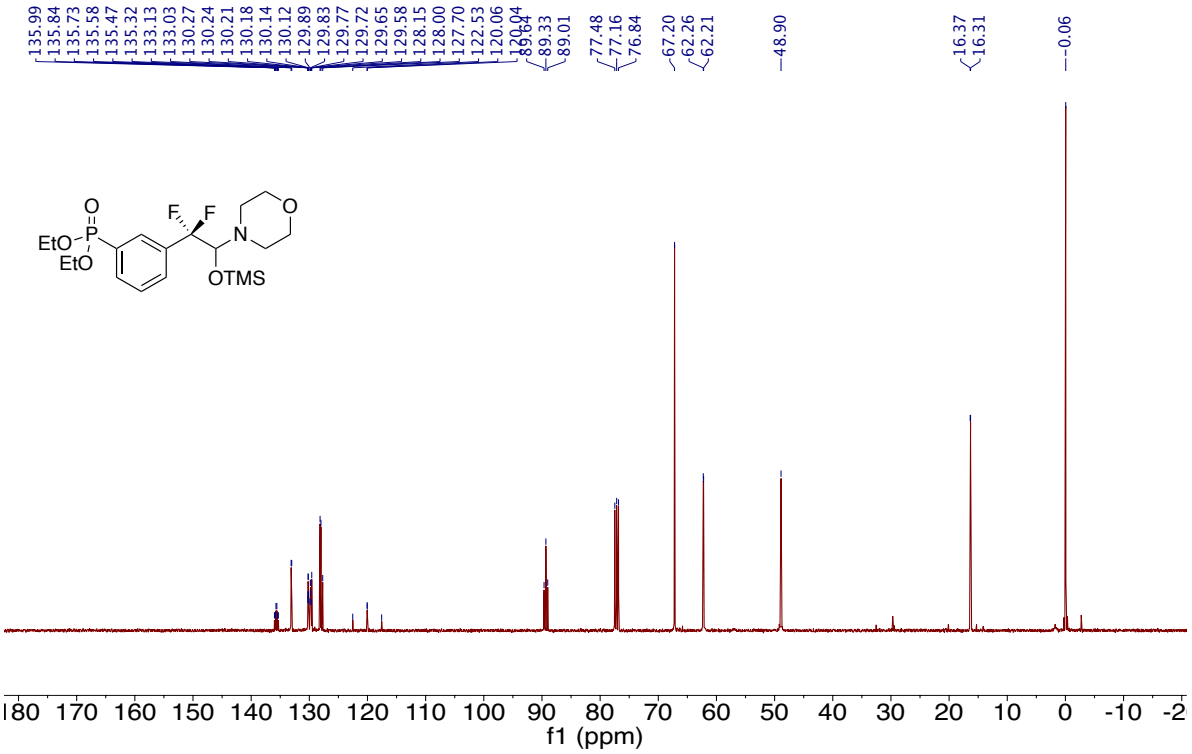

^{13}C NMR of Compound **3-7** (101 MHz, $CDCl_3$)

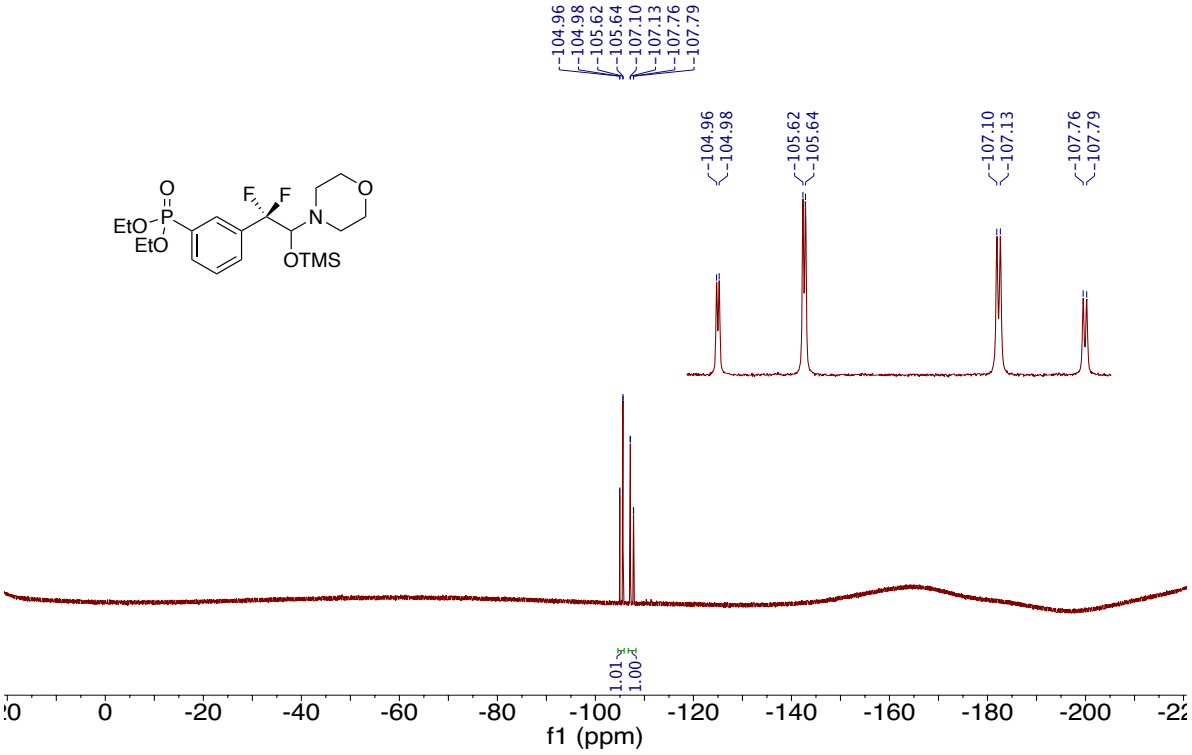

^{19}F NMR of Compound **3-7** (376 MHz, $CDCl_3$)

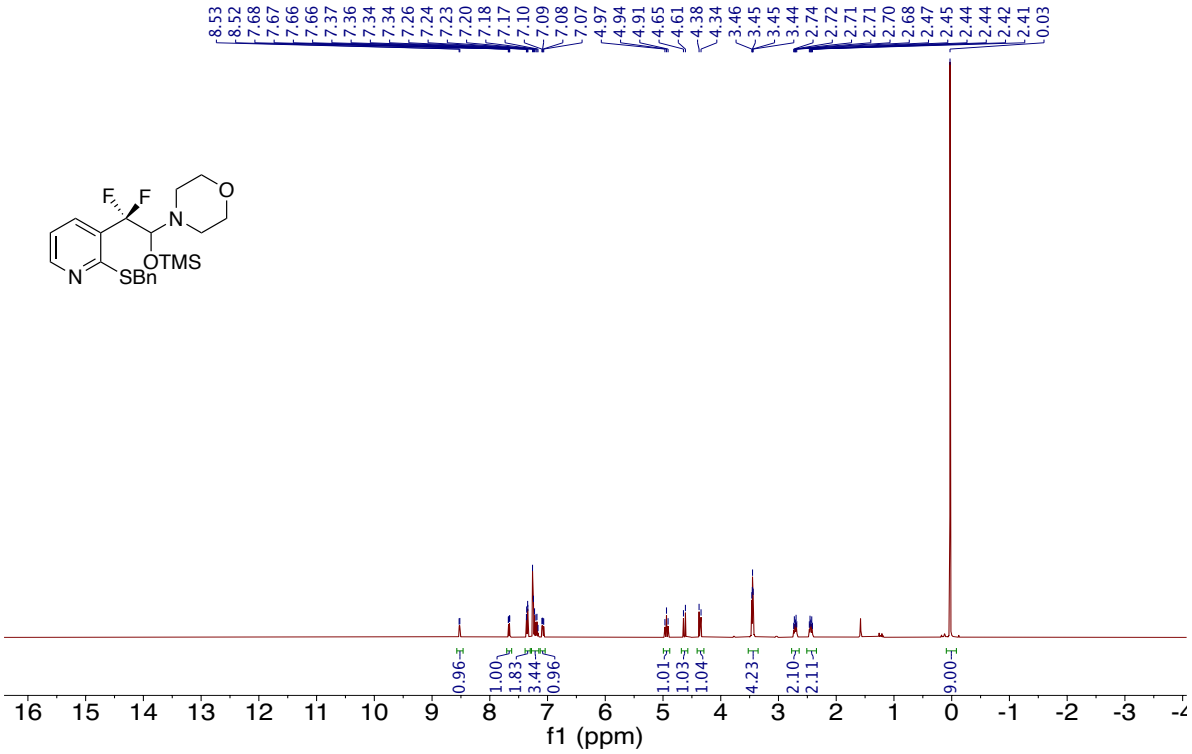

^{1}H NMR of Compound **3-8** (400 MHz, $CDCl_3$)

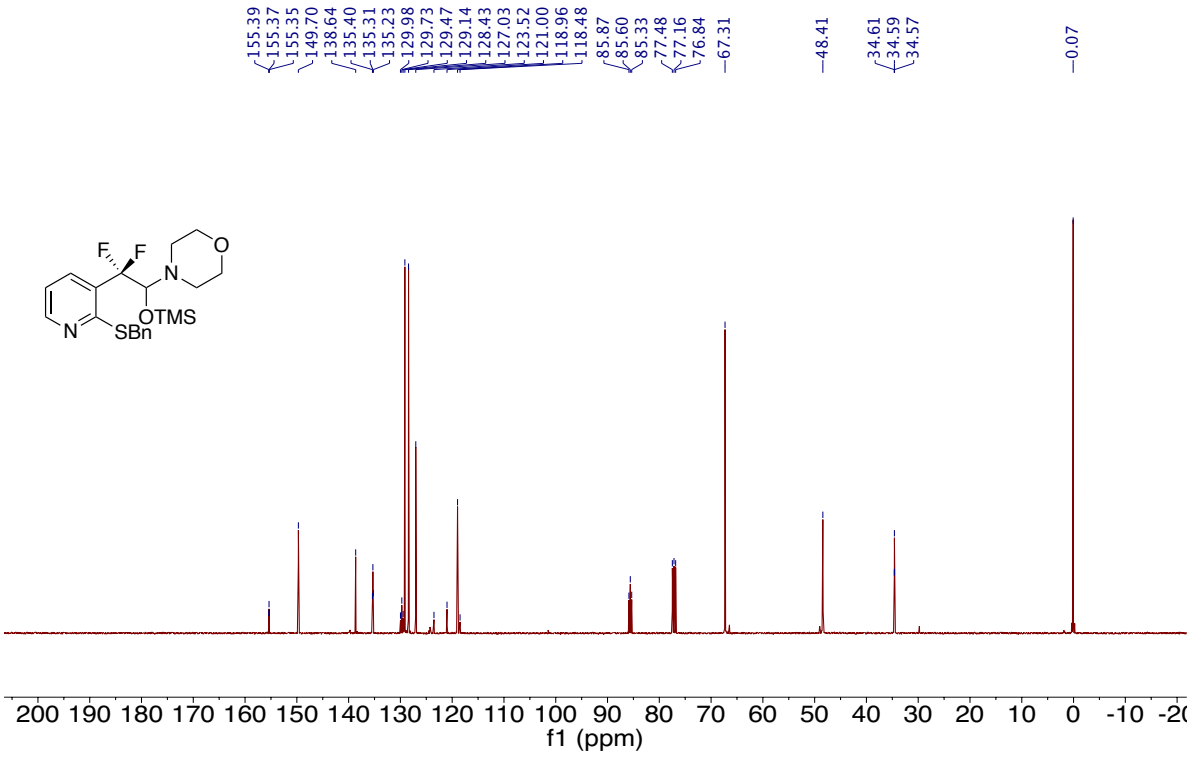

^{13}C NMR of Compound **3-8** (101 MHz, $CDCl_3$)

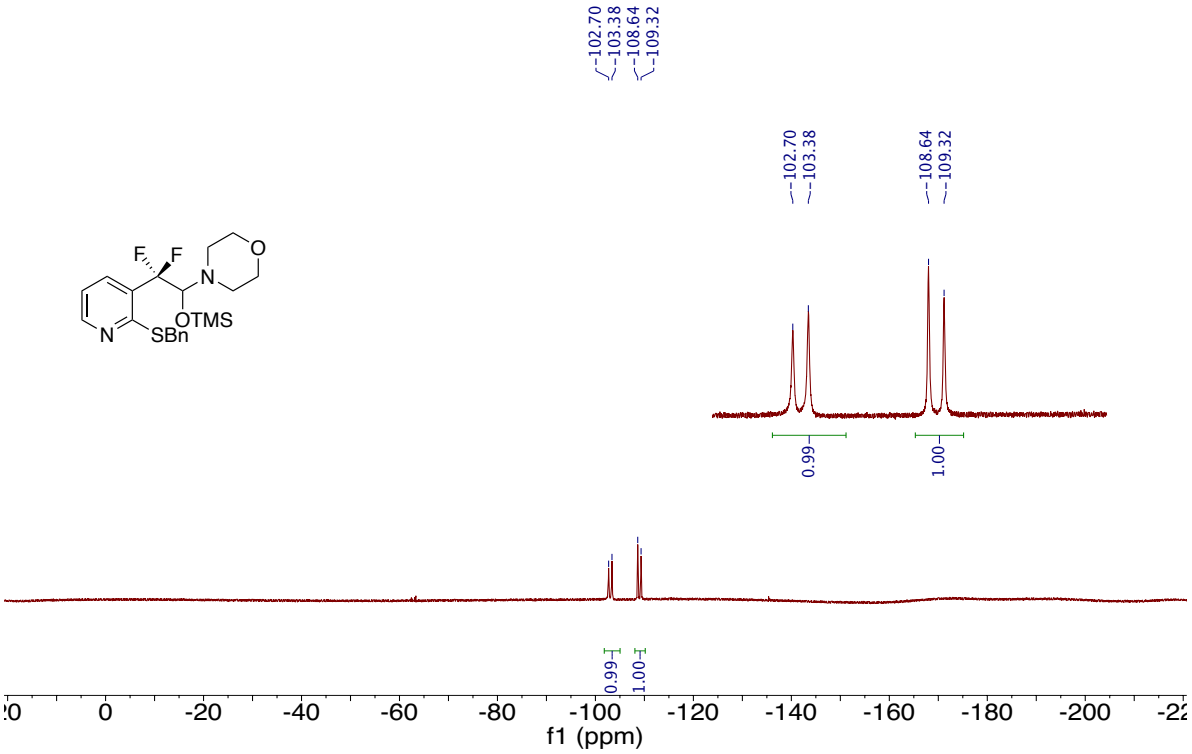

^{19}F NMR of Compound **3-8** (376 MHz, $CDCl_3$)

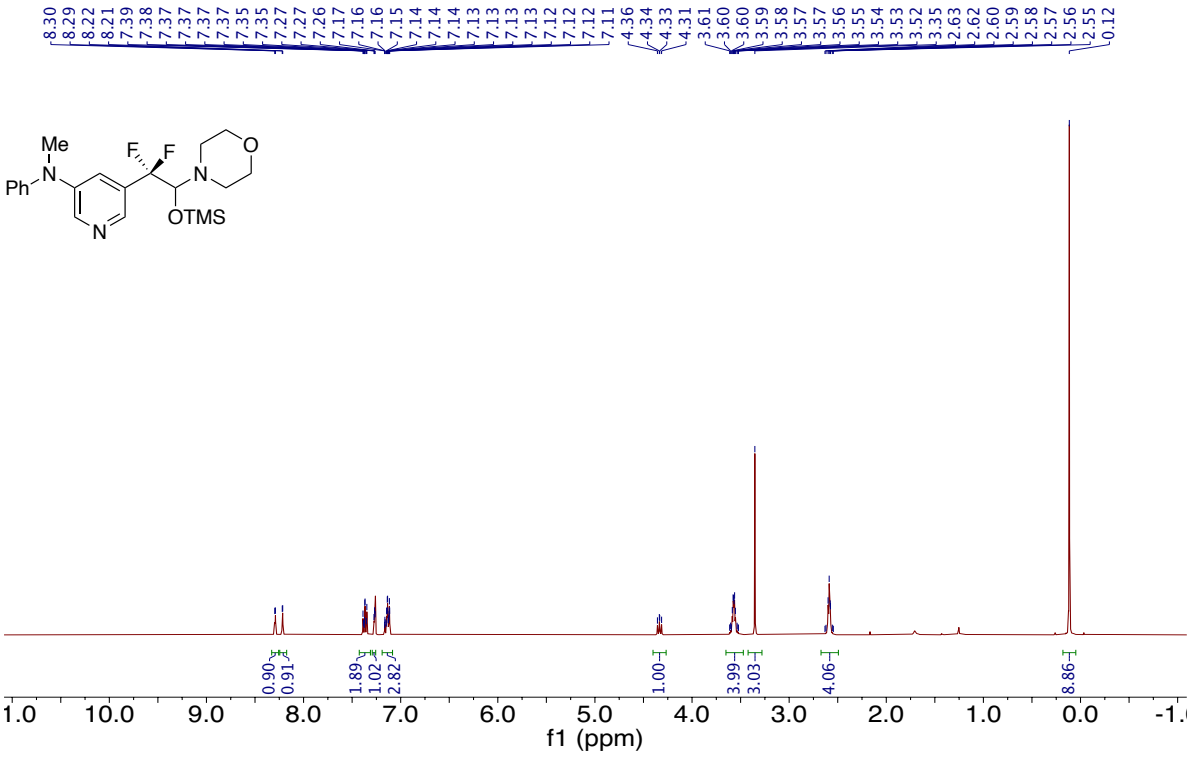

^{1}H NMR of Compound **3-9** (400 MHz, $CDCl_3$)

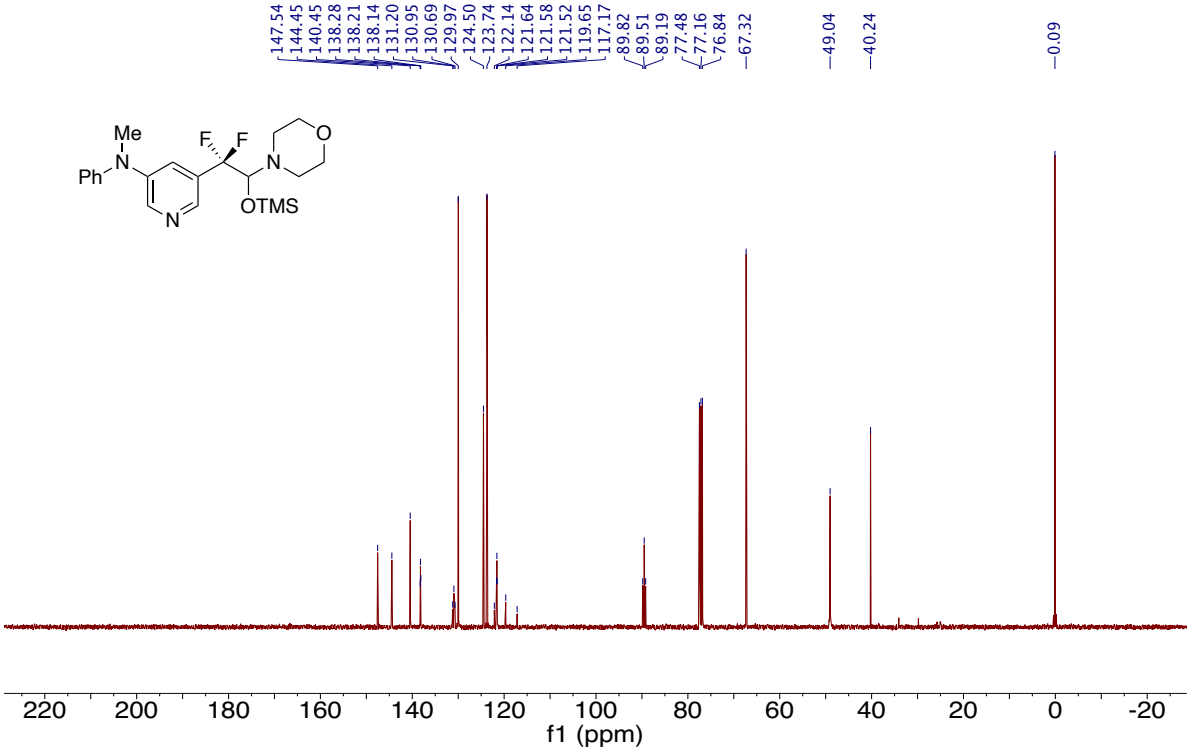

^{13}C NMR of Compound **3-9** (101 MHz, $CDCl_3$)

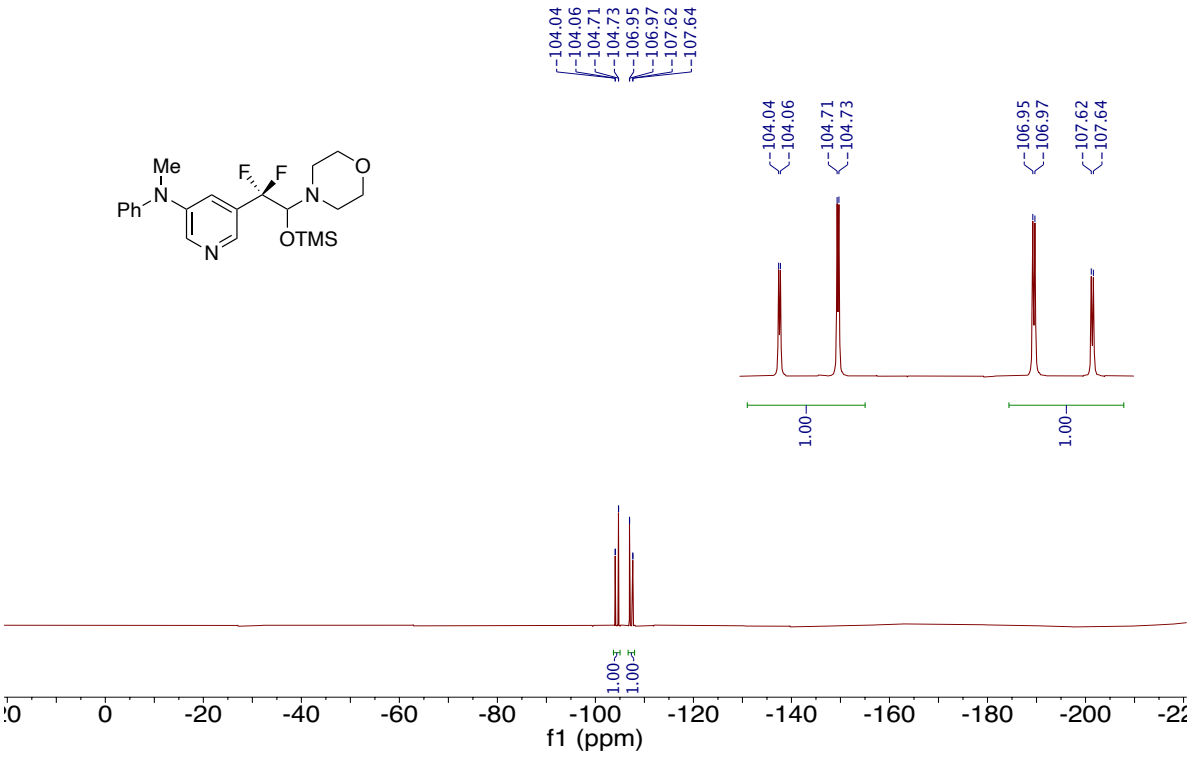

^{19}F NMR of Compound **3-9** (376 MHz, $CDCl_3$)

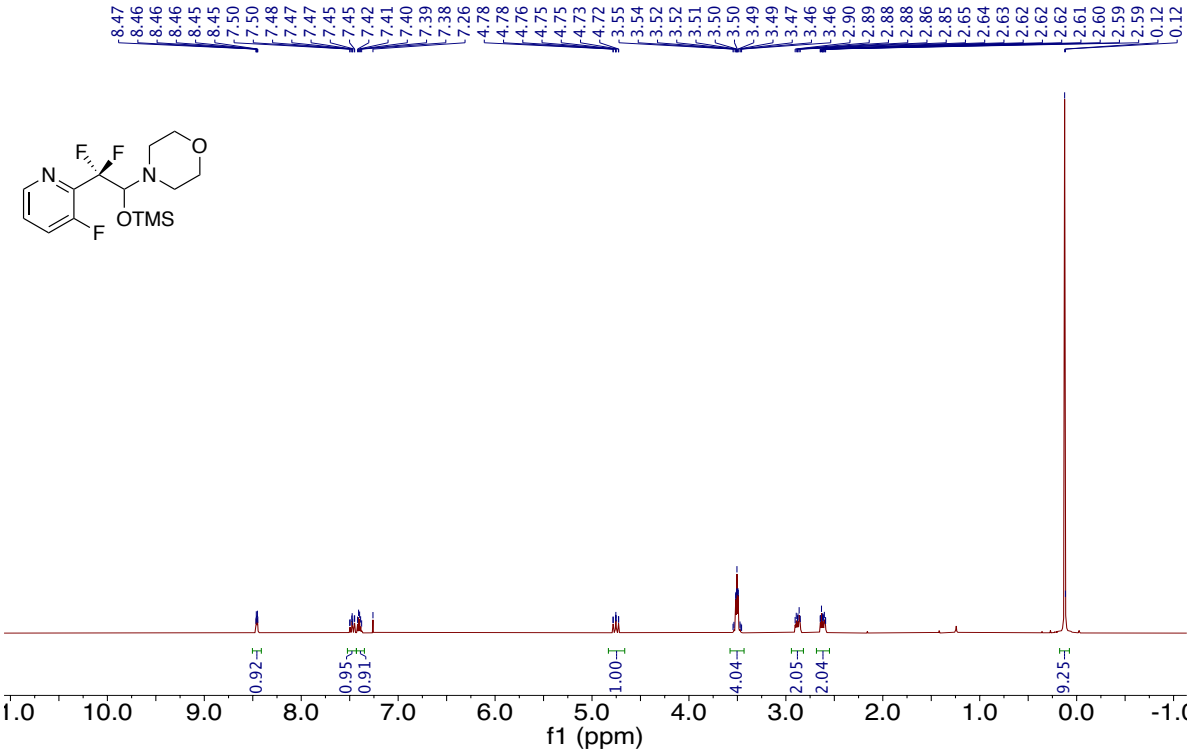

^{1}H NMR of Compound **10** (400 MHz, $CDCl_3$)

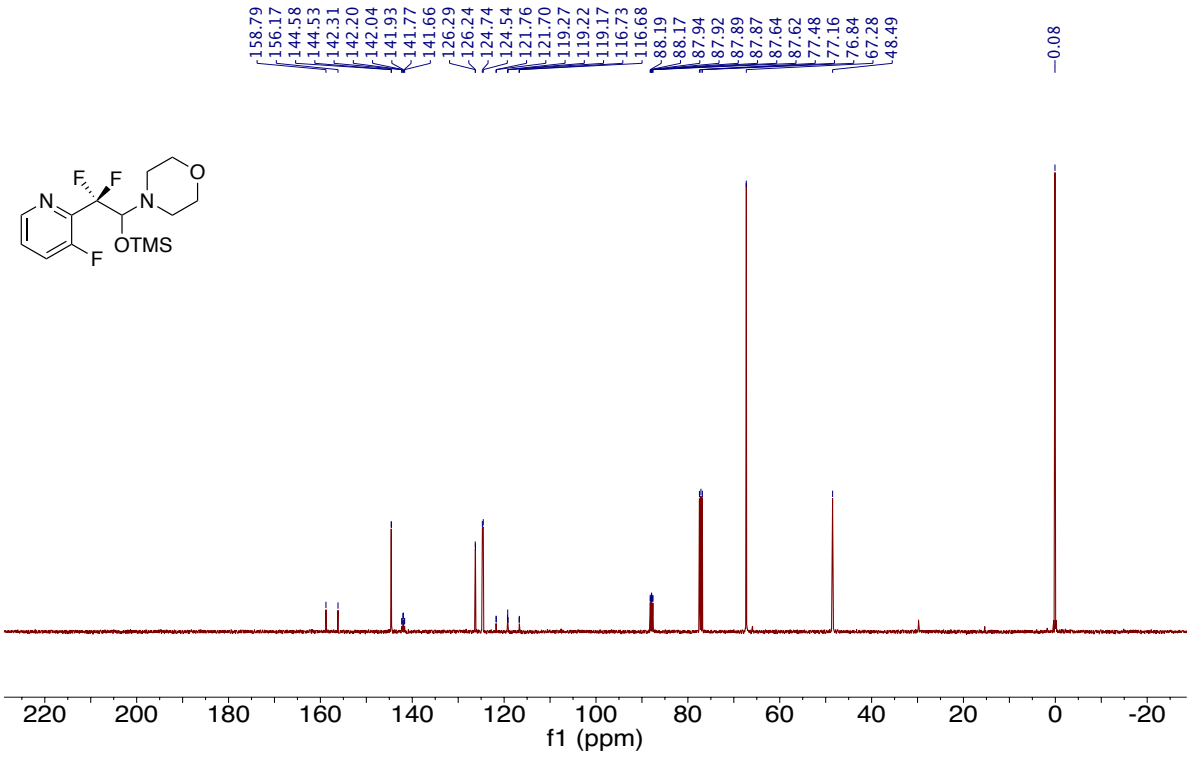

^{13}C NMR of Compound **3-10** (101 MHz, $CDCl_3$)

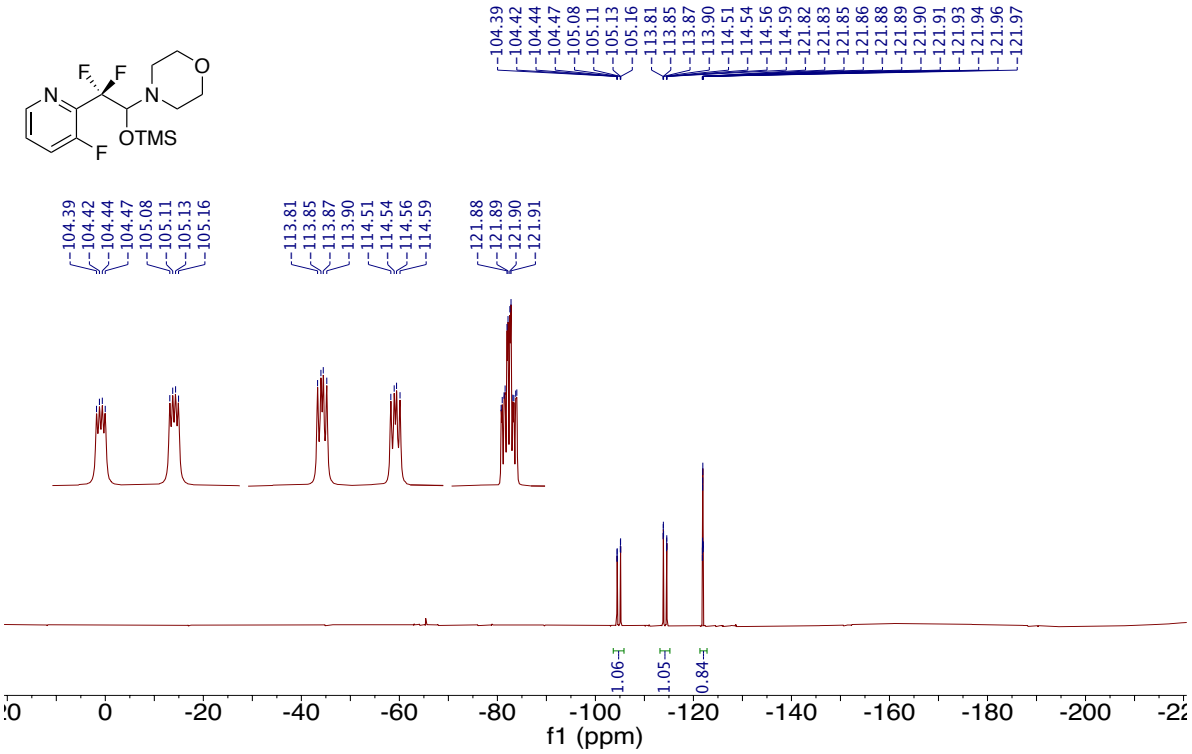

[19]F NMR of Compound **3-10** (376 MHz, $CDCl_3$)

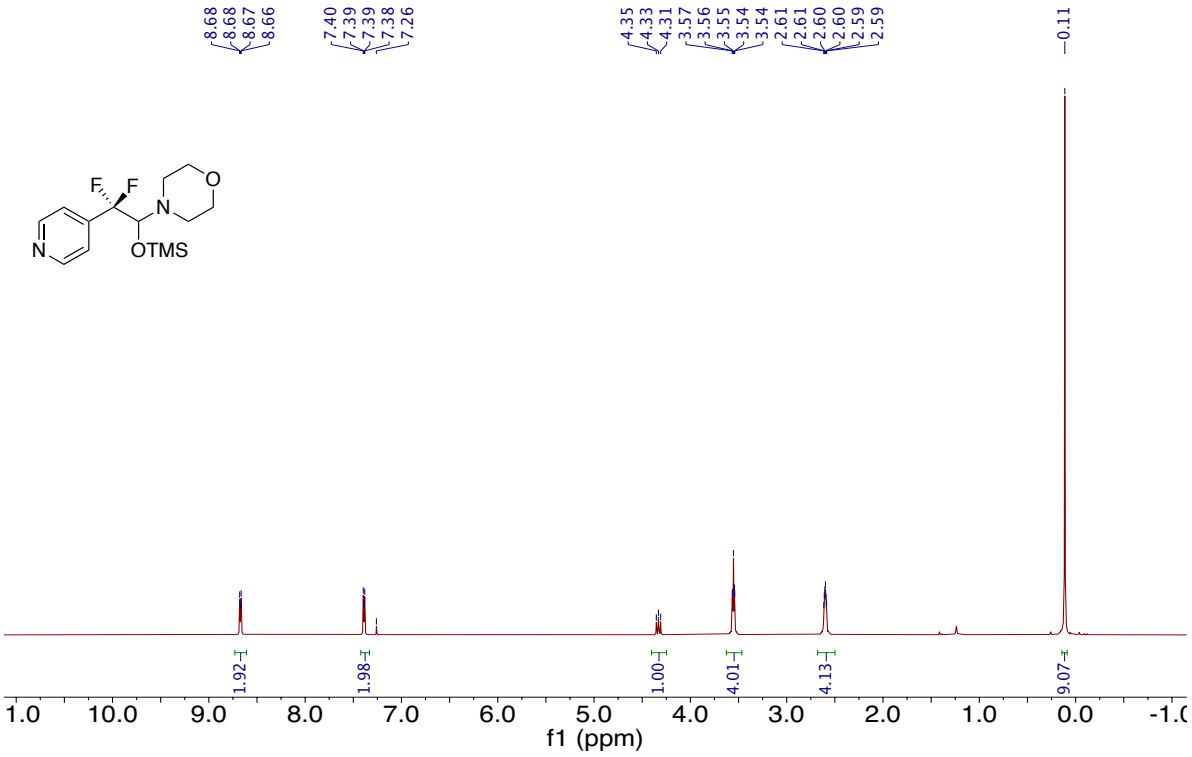

[1]H NMR of Compound **3-11** (400 MHz, $CDCl_3$)

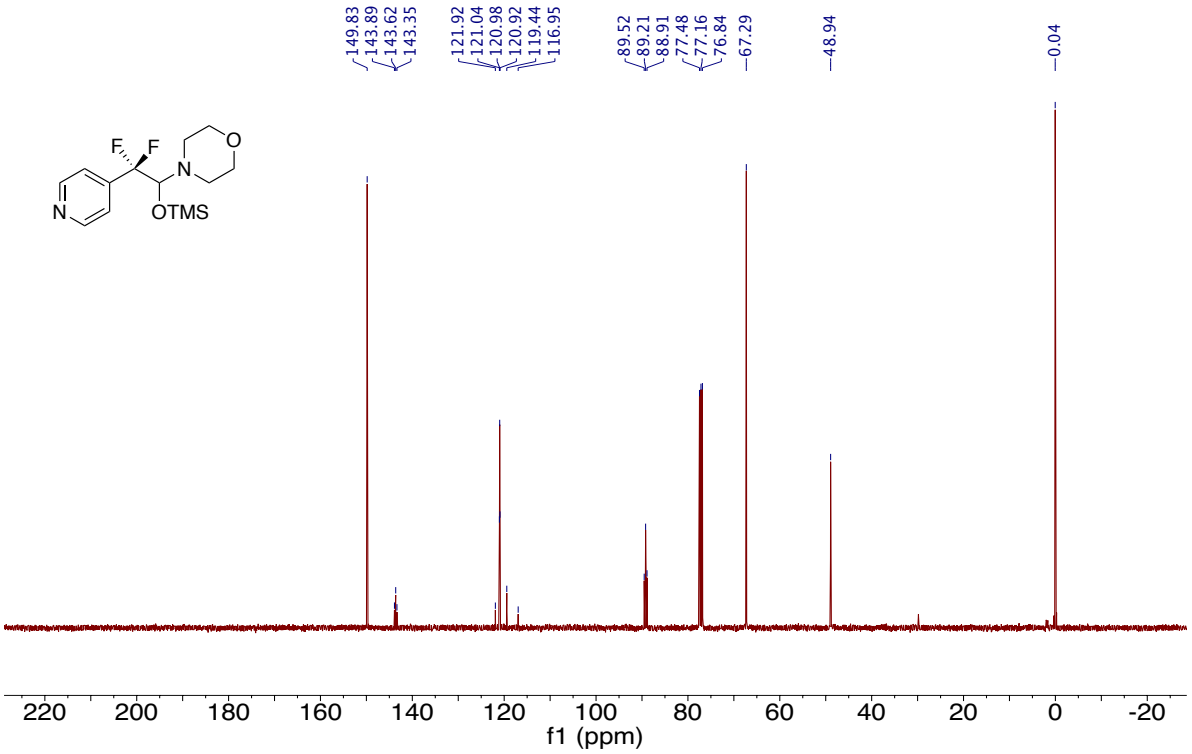

^{13}C NMR of Compound **3-11** (101 MHz, $CDCl_3$)

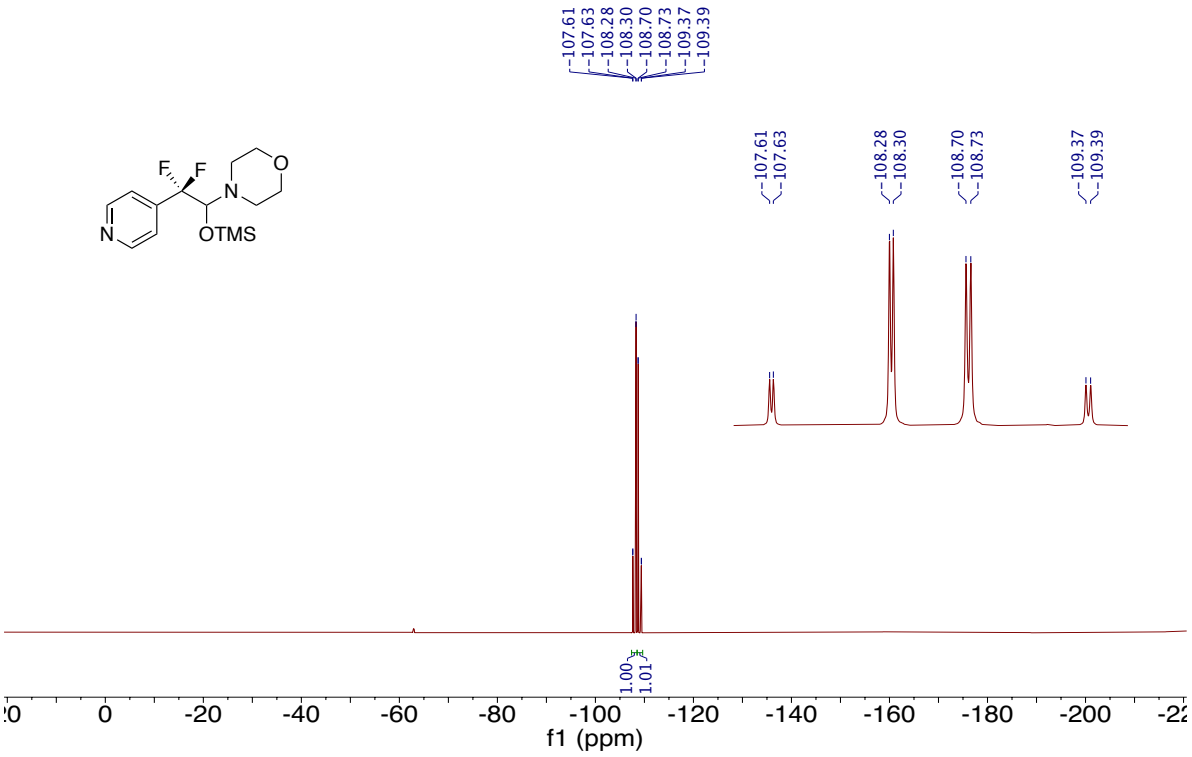

^{19}F NMR of Compound **3-11** (376 MHz, $CDCl_3$)

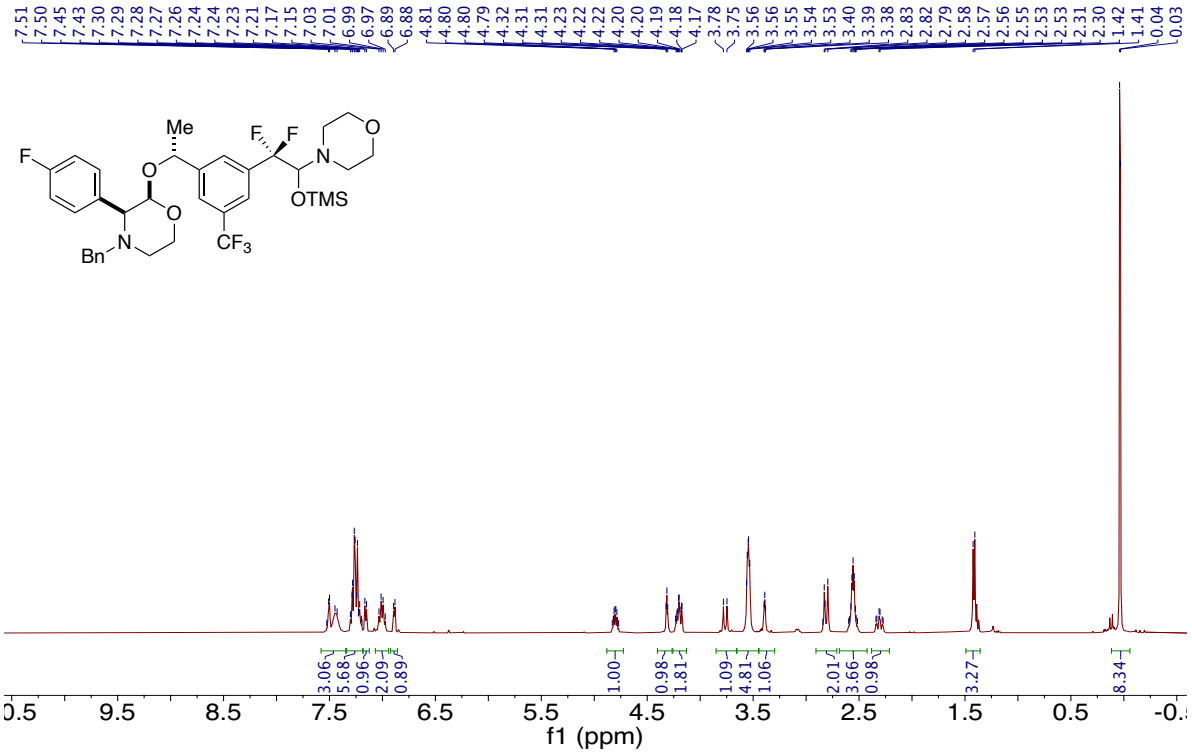

^{1}H NMR of Compound **3-12** (400 MHz, $CDCl_3$)

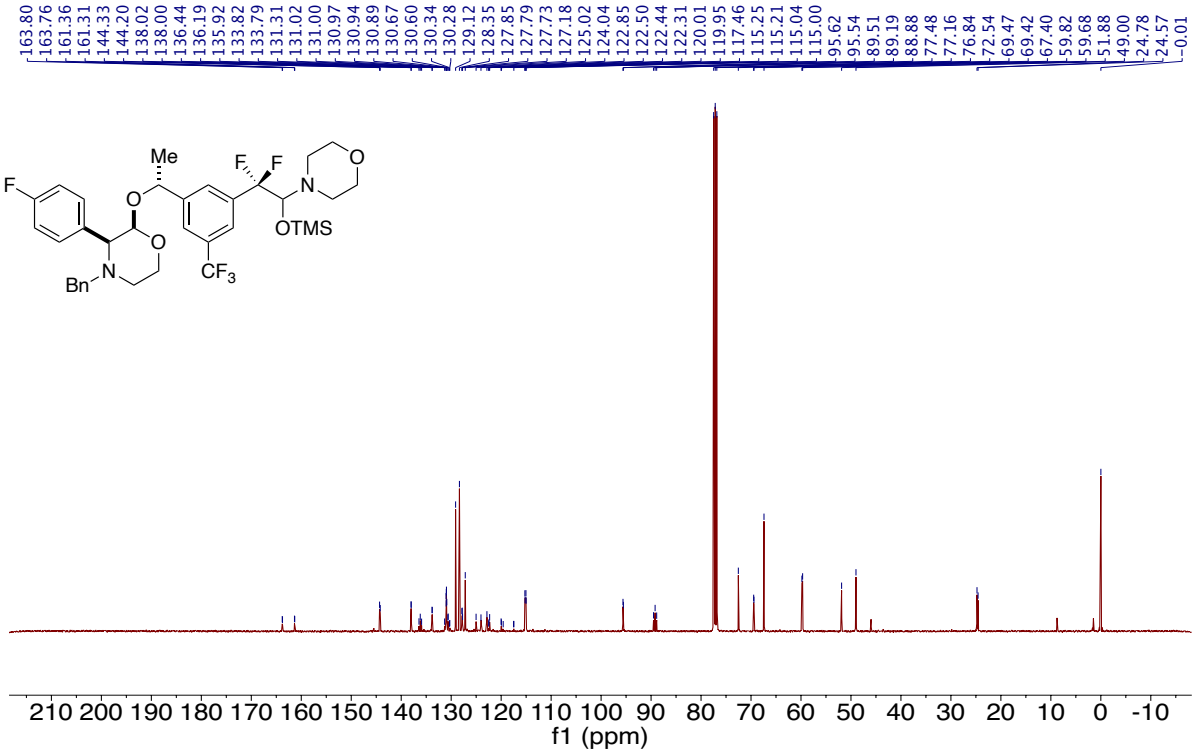

^{13}C NMR of Compound **3-12** (101 MHz, $CDCl_3$)

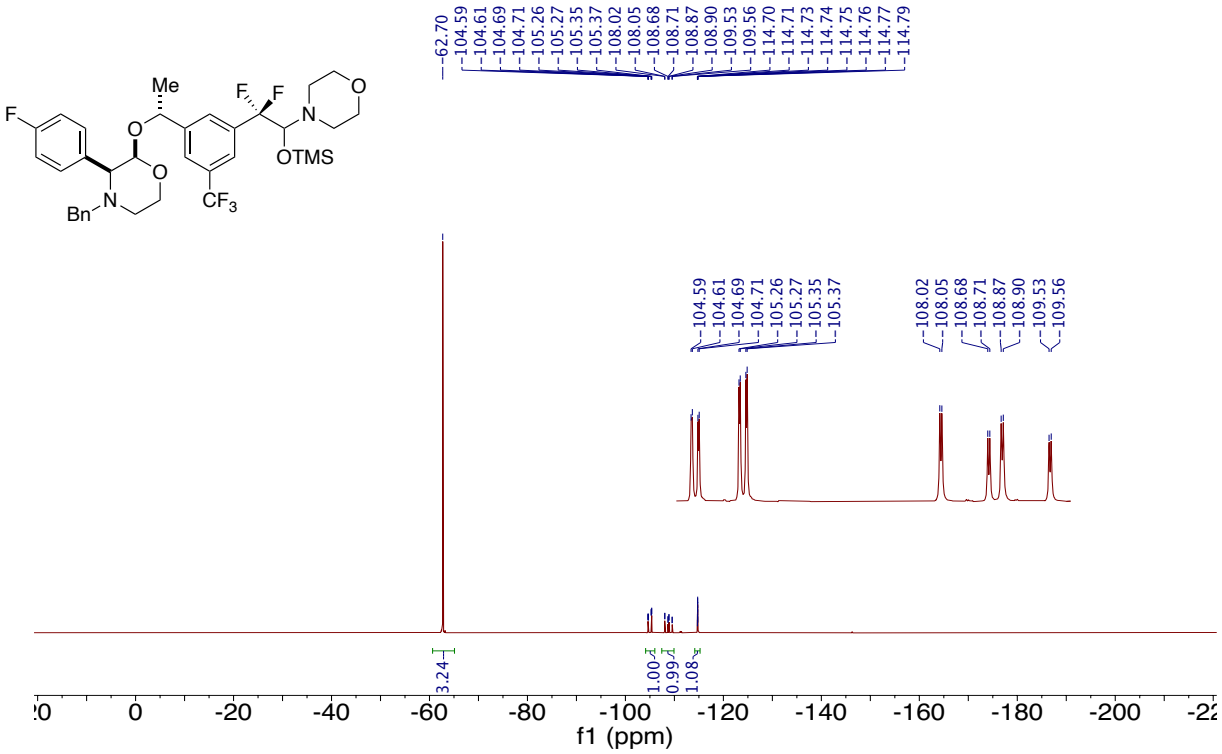

[19]F NMR of Compound **3-12** (376 MHz, $CDCl_3$)

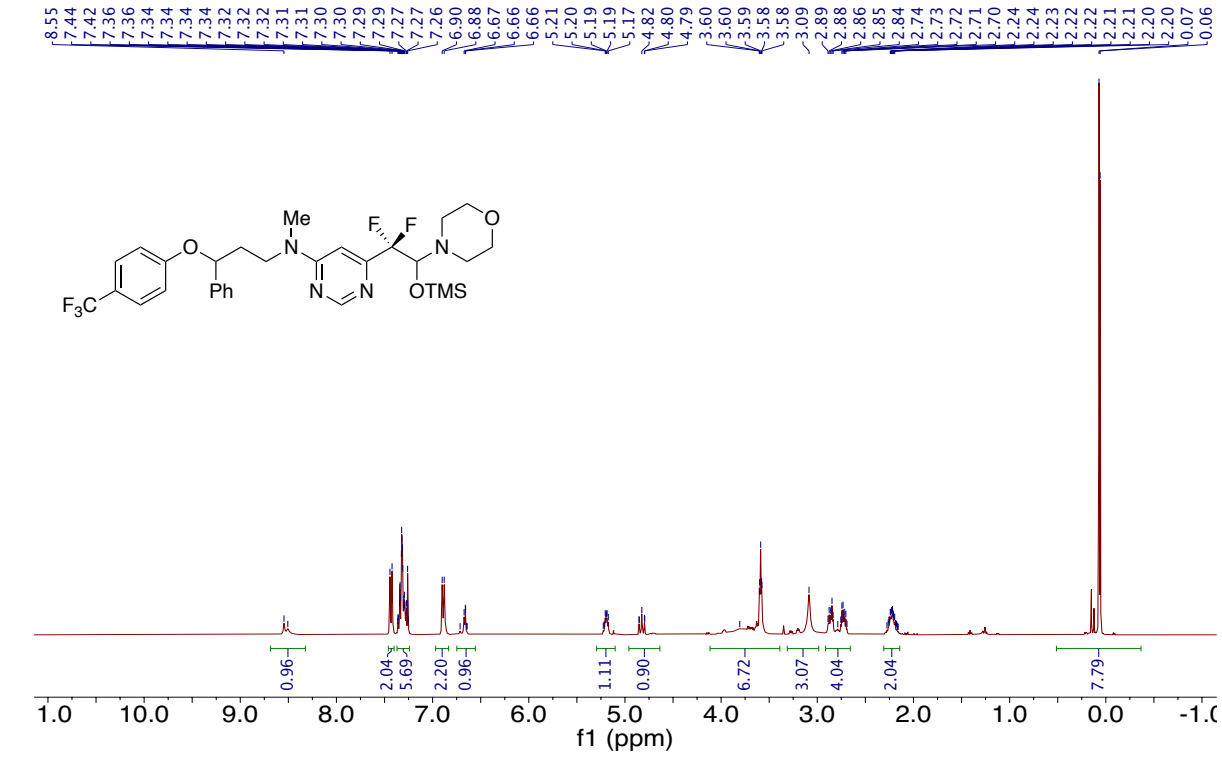

[1]H NMR of Compound **3-13** (400 MHz, $CDCl_3$)

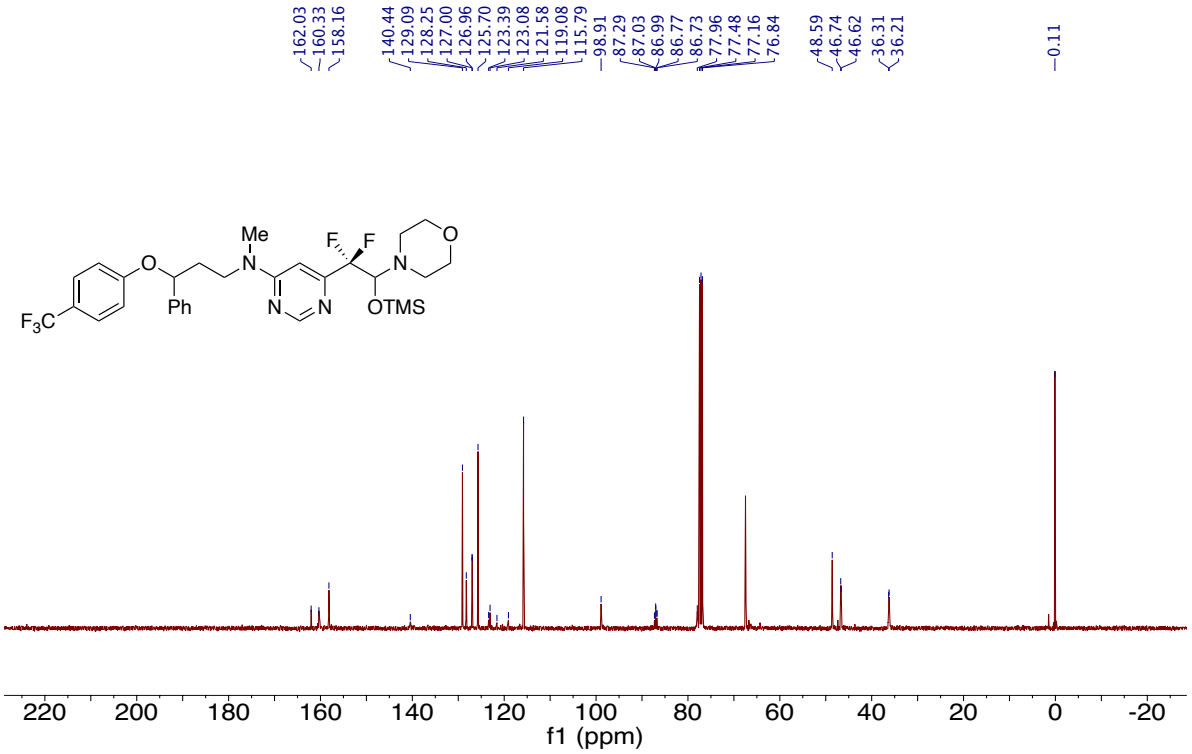

^{13}C NMR of Compound **3-13** (101 MHz, $CDCl_3$)

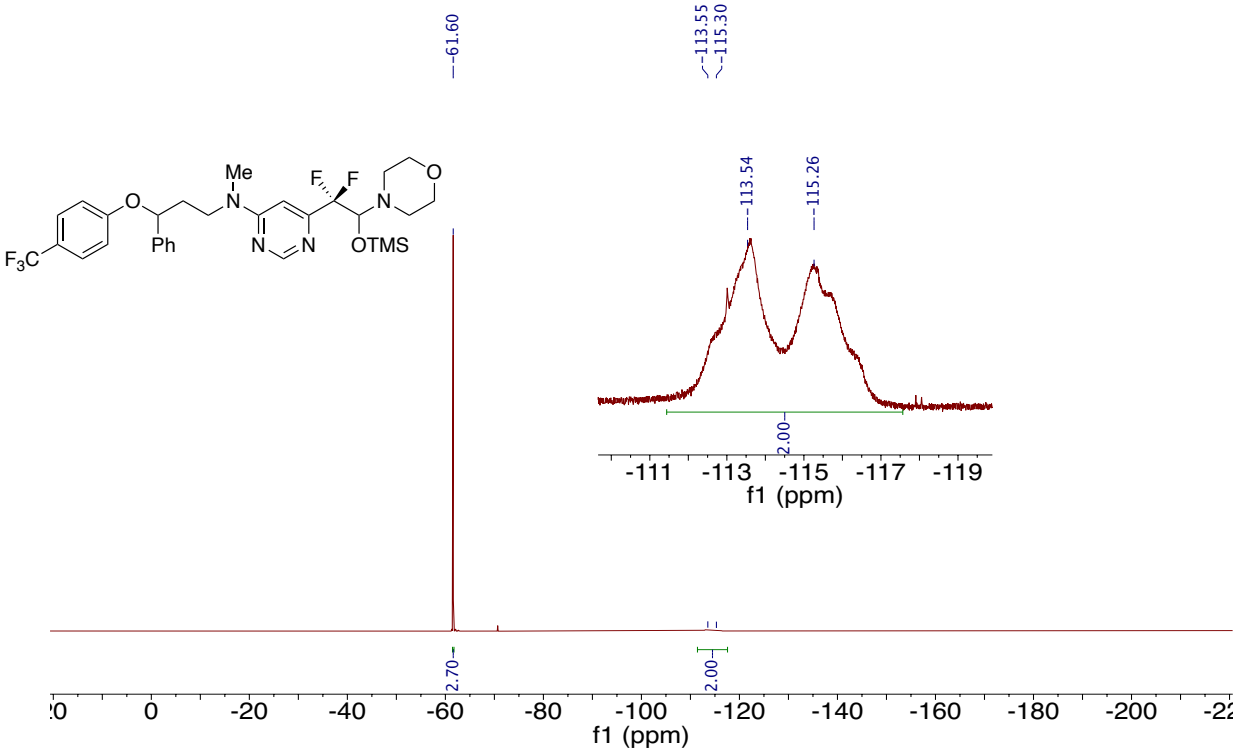

^{19}F NMR of Compound **3-13** (376 MHz, $CDCl_3$)

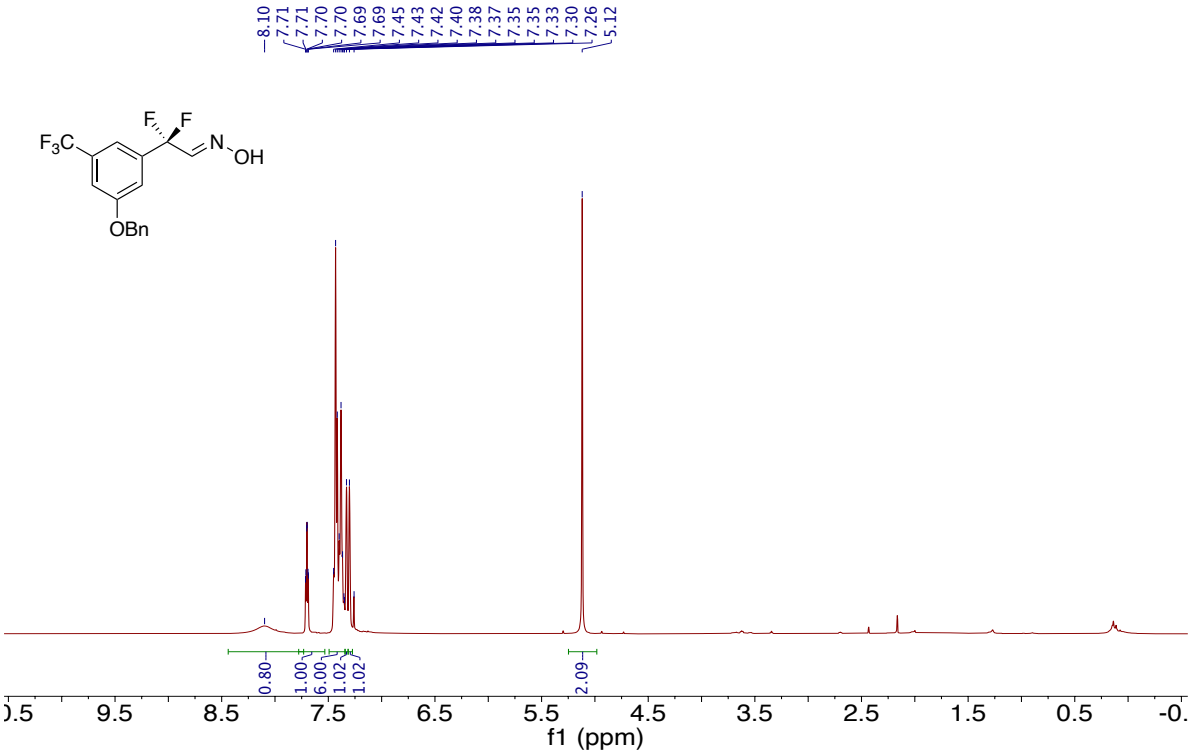

^{1}H NMR of Compound **3-14** (400 MHz, $CDCl_3$)

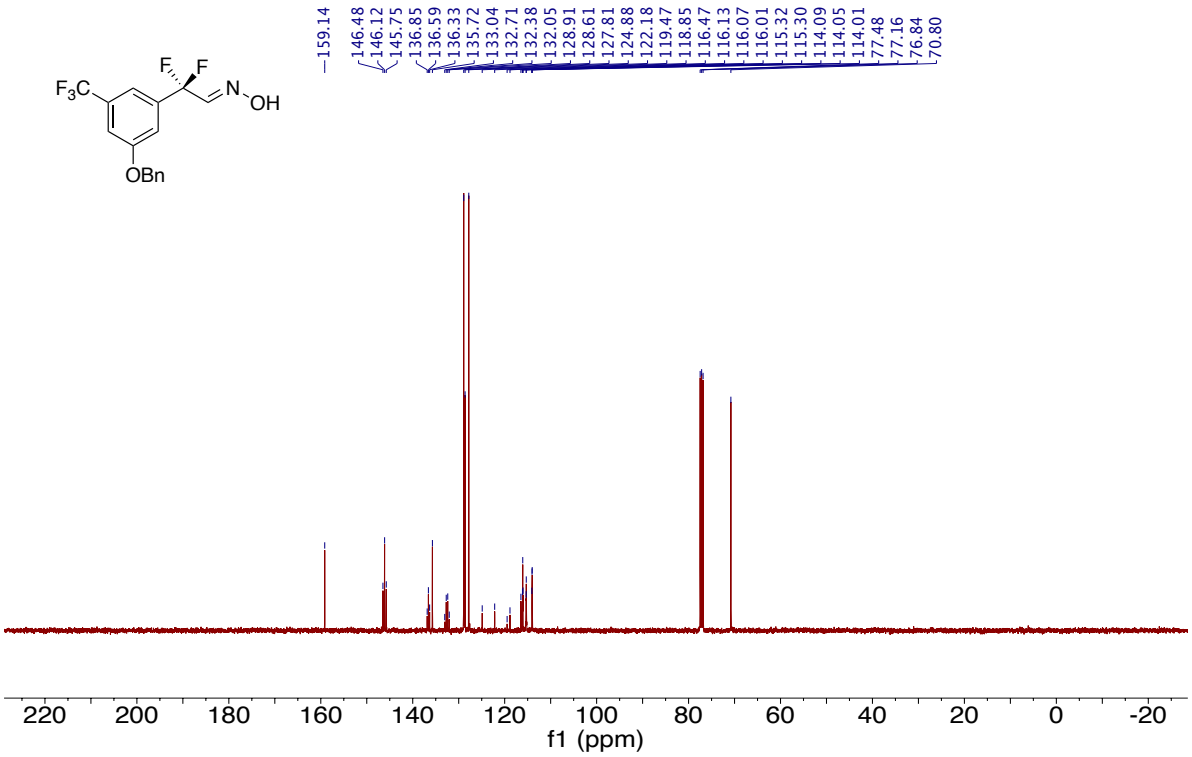

^{13}C NMR of Compound **3-14** (101 MHz, $CDCl_3$)

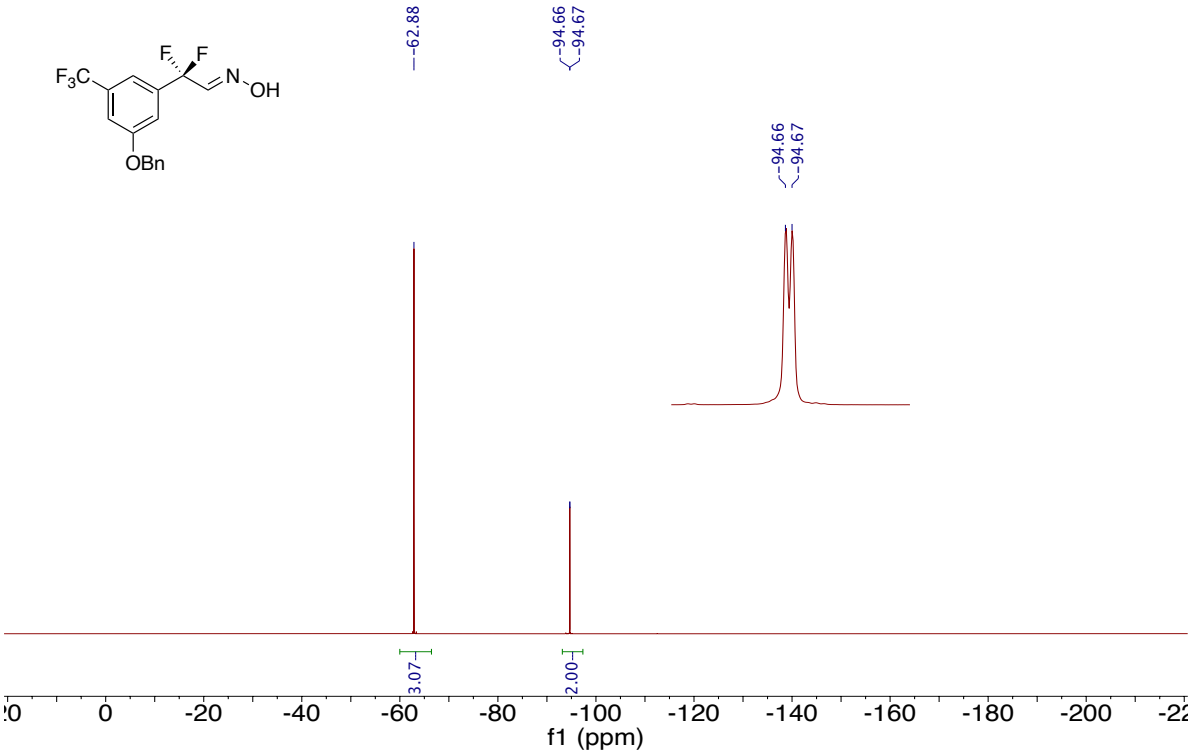

^{19}F NMR of Compound **3-14** (376 MHz, $CDCl_3$)

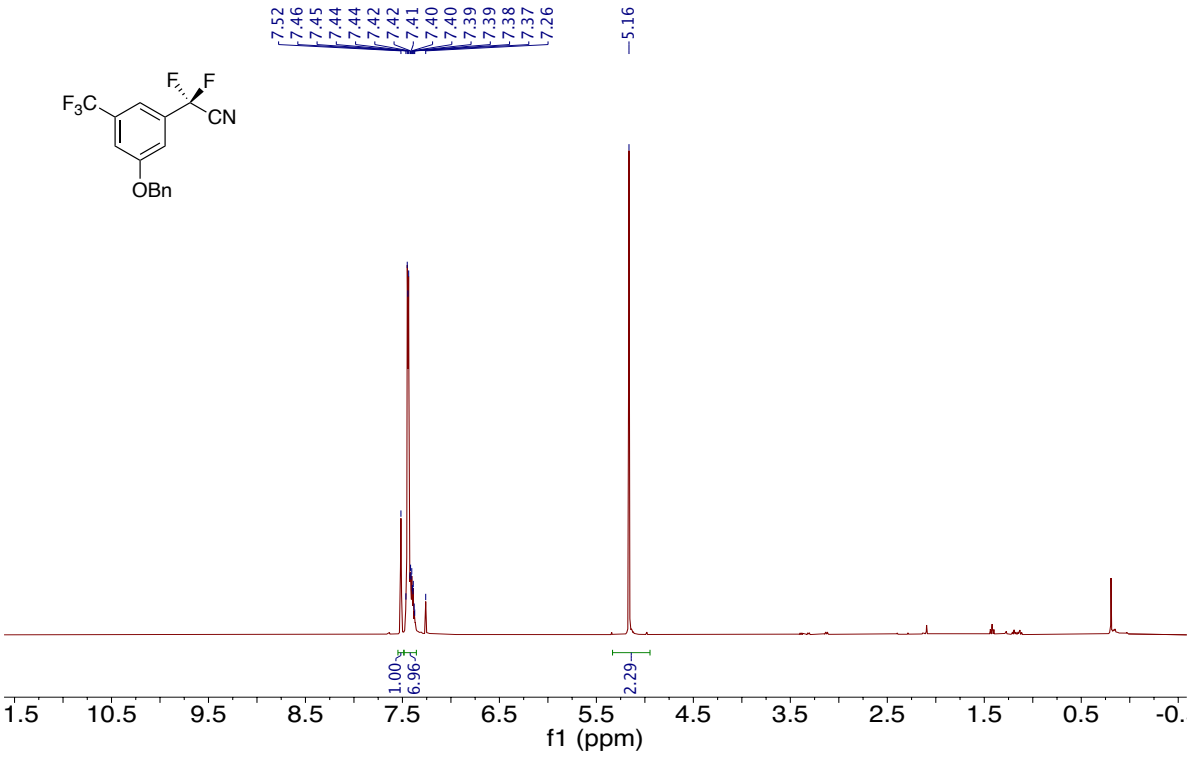

^{1}H NMR of Compound **3-15** (400 MHz, $CDCl_3$)

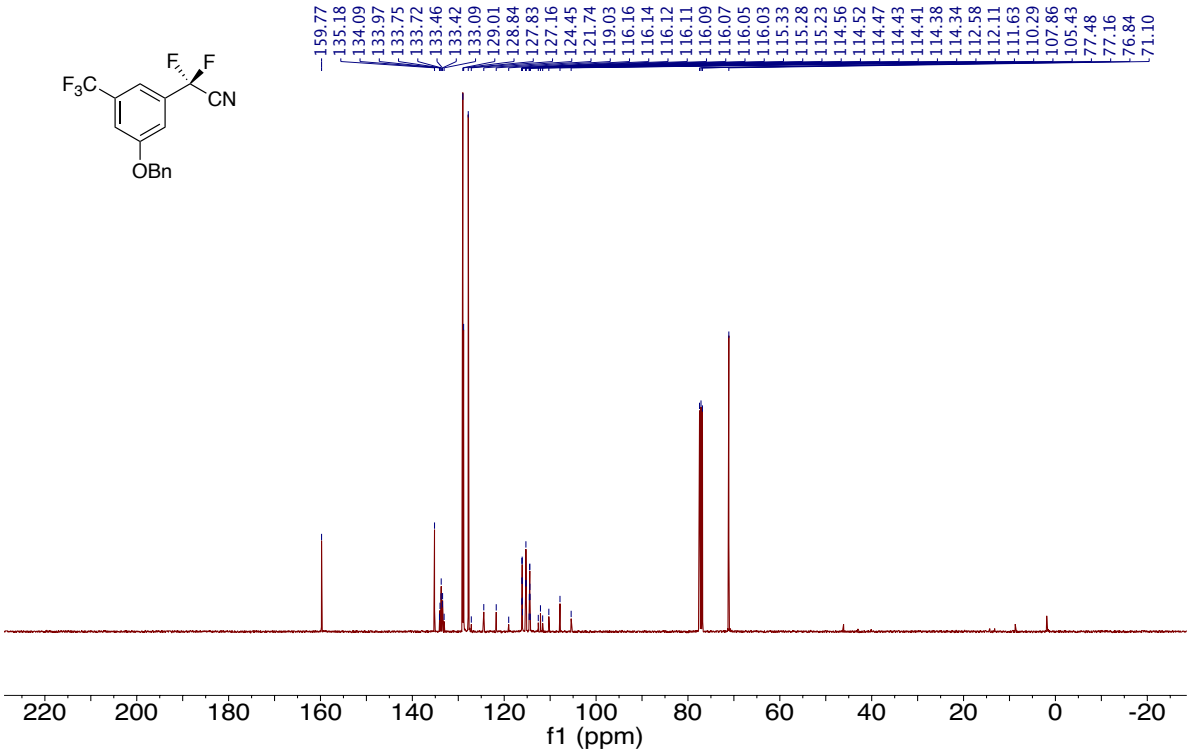

^{13}C NMR of Compound **3-15** (101 MHz, $CDCl_3$)

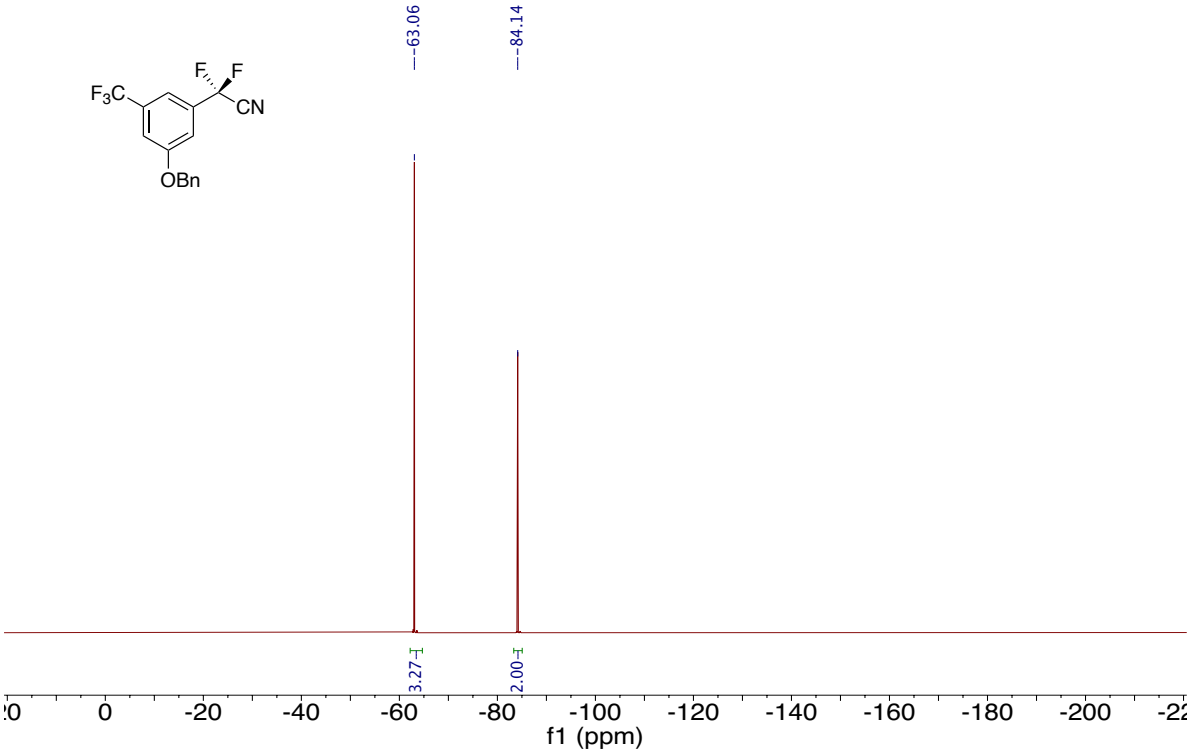

^{19}F NMR of Compound **3-15** (376 MHz, $CDCl_3$)

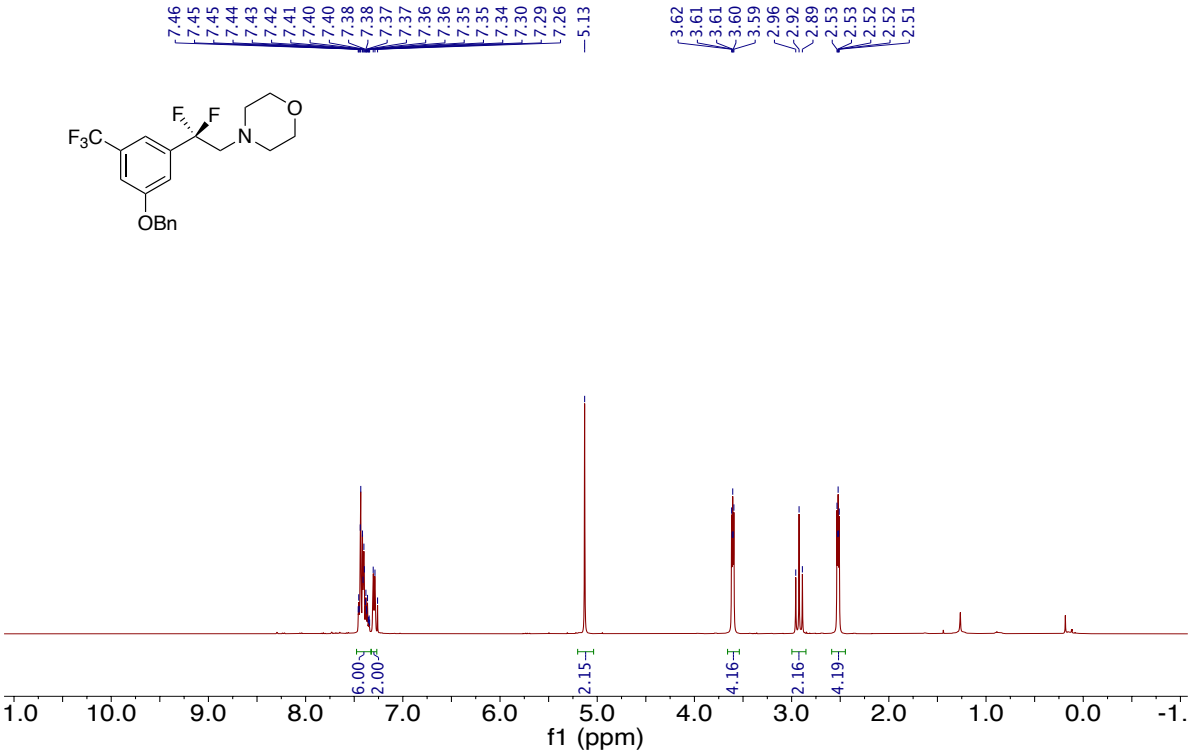

^{1}H NMR of Compound **3-16** (400 MHz, $CDCl_3$)

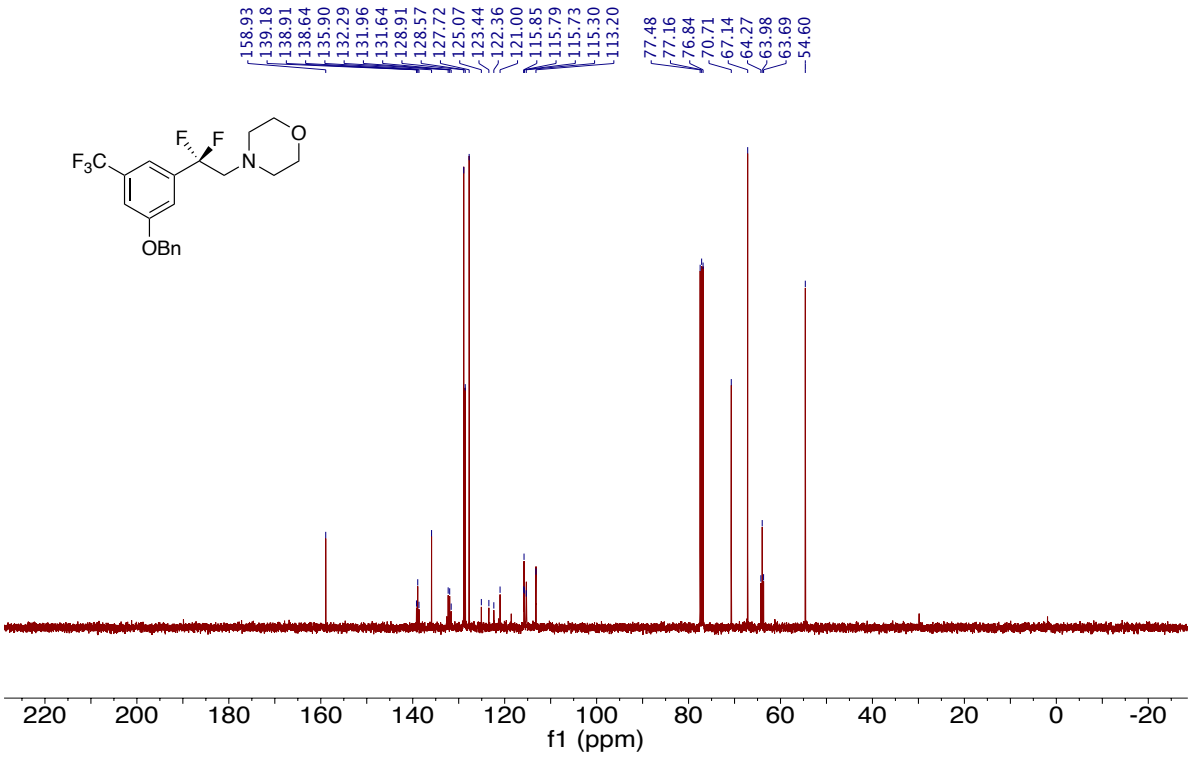

^{13}C NMR of Compound **3-16** (101 MHz, $CDCl_3$)

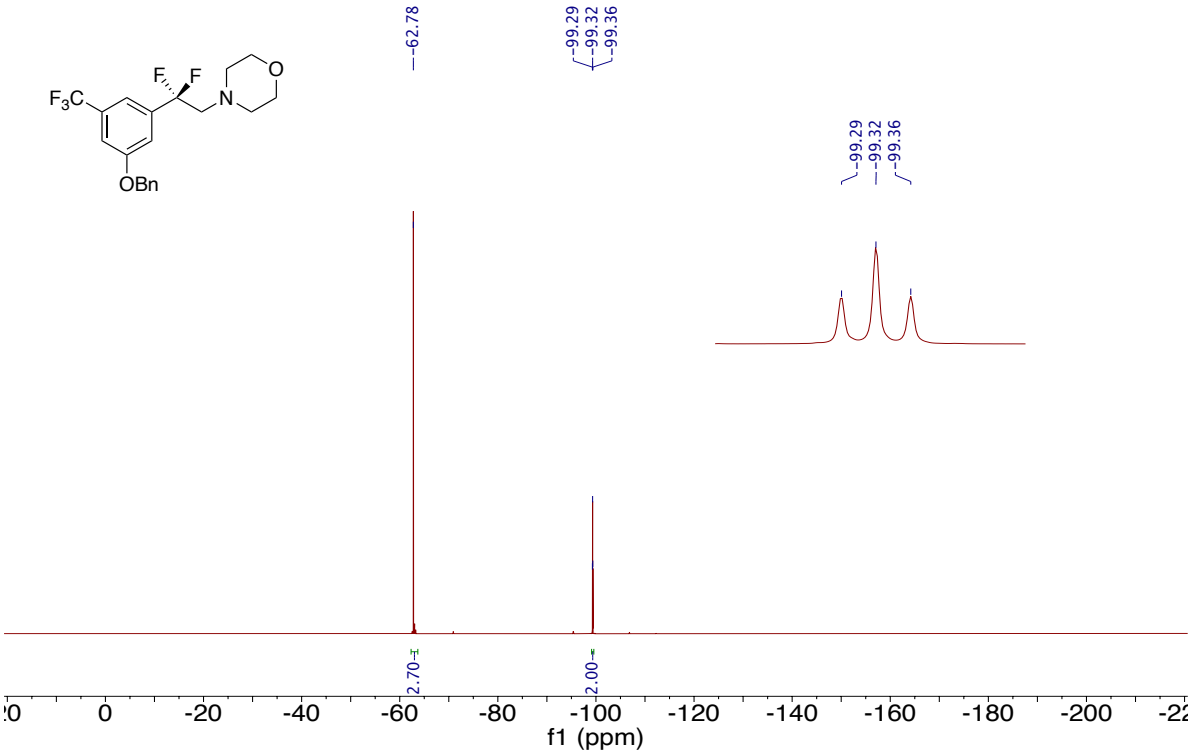

^{19}F NMR of Compound **3-16** (376 MHz, $CDCl_3$)

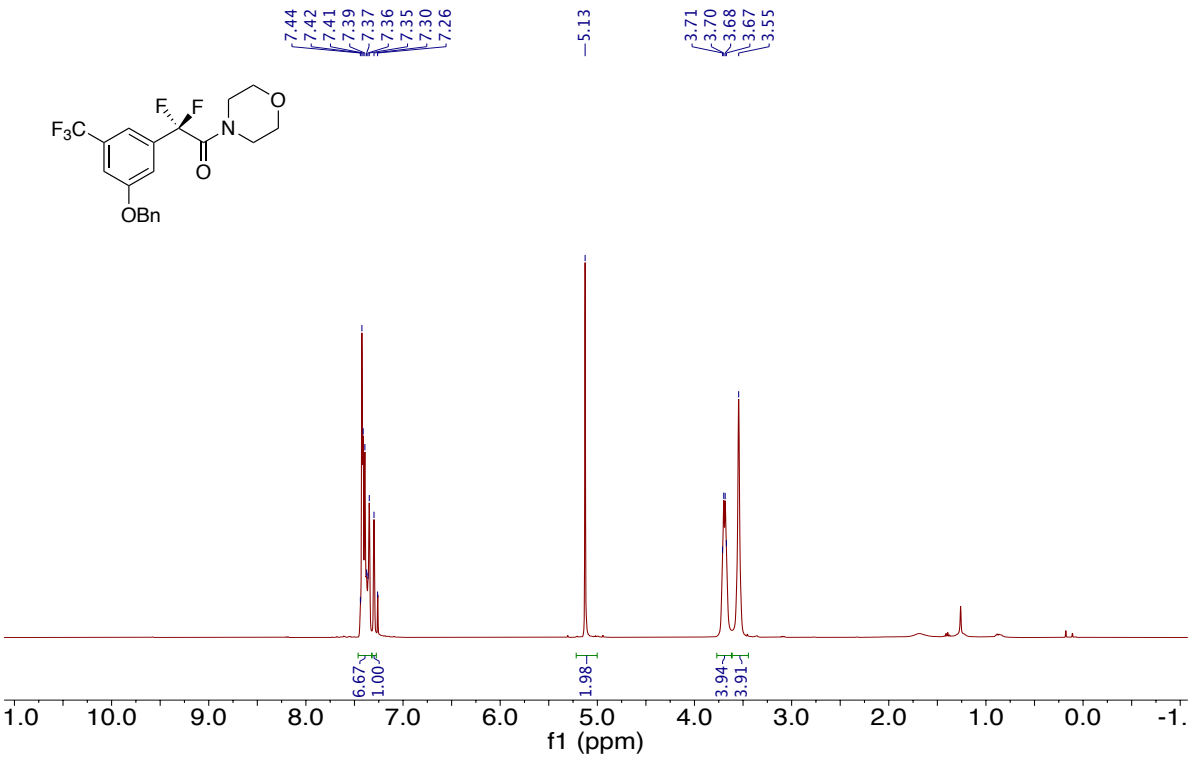

^{1}H NMR of Compound **3-17** (400 MHz, $CDCl_3$)

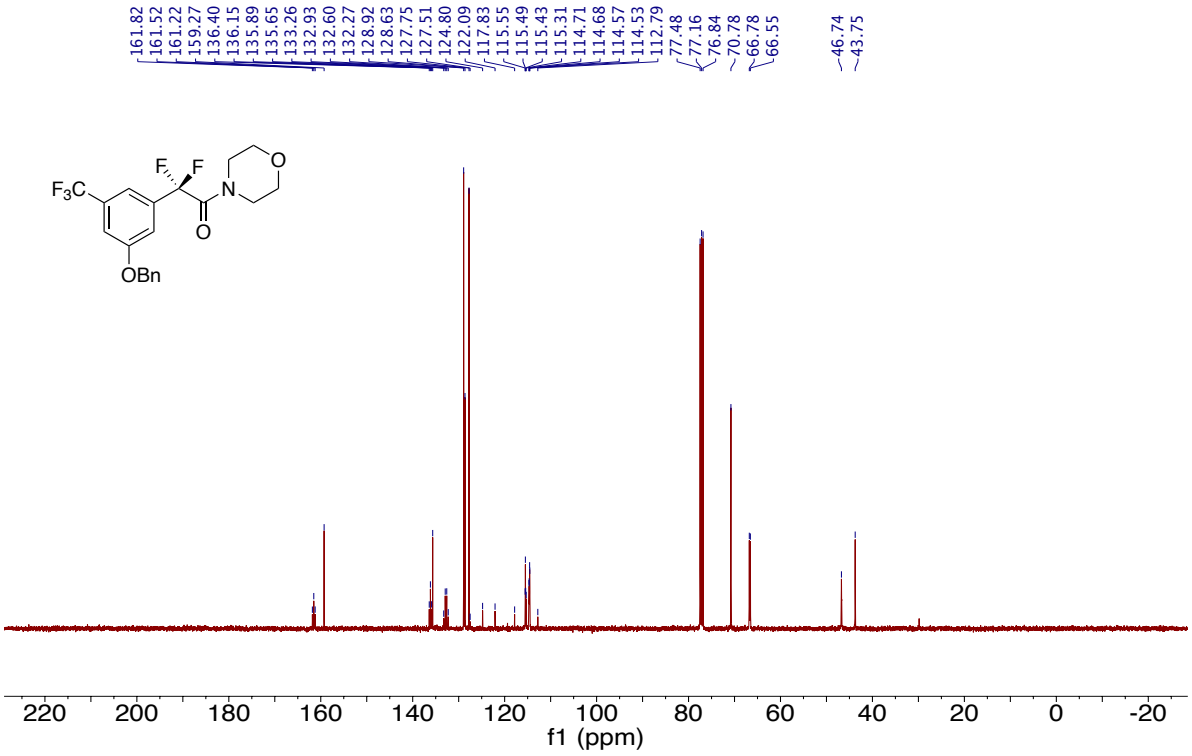

^{13}C NMR of Compound **3-17** (101 MHz, $CDCl_3$)

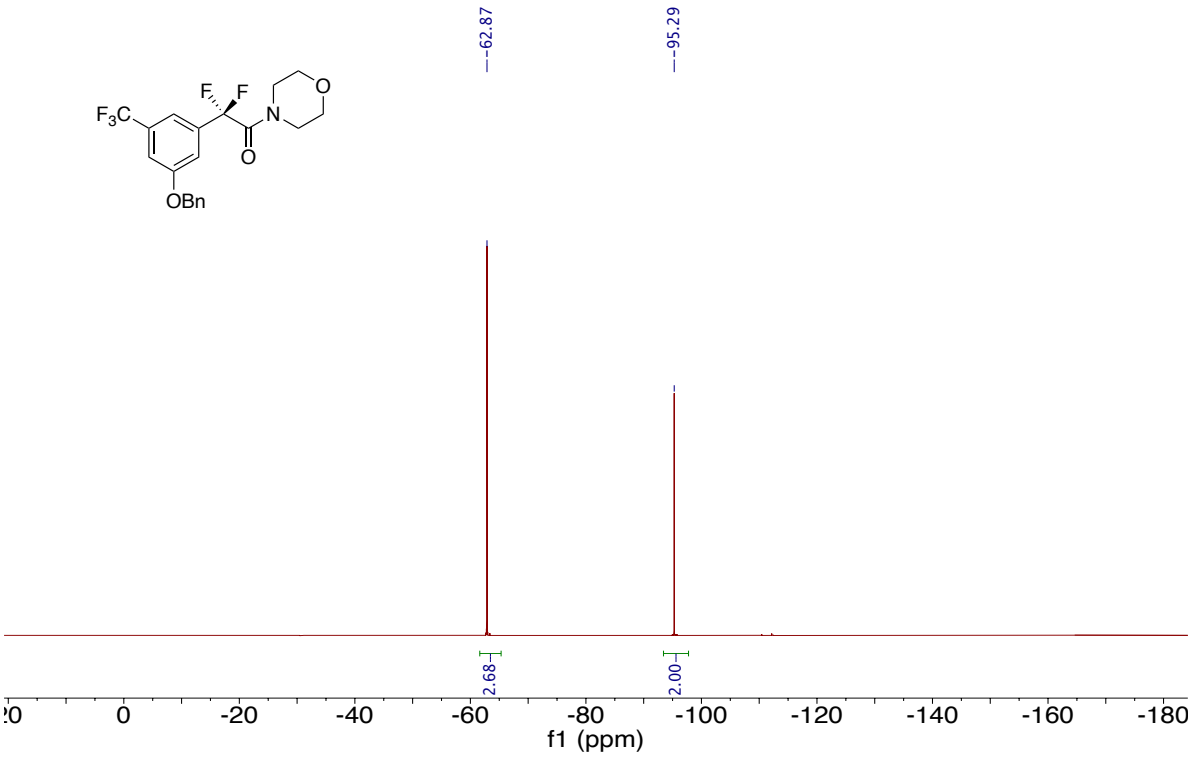

^{19}F NMR of Compound **3-17** (376 MHz, $CDCl_3$)

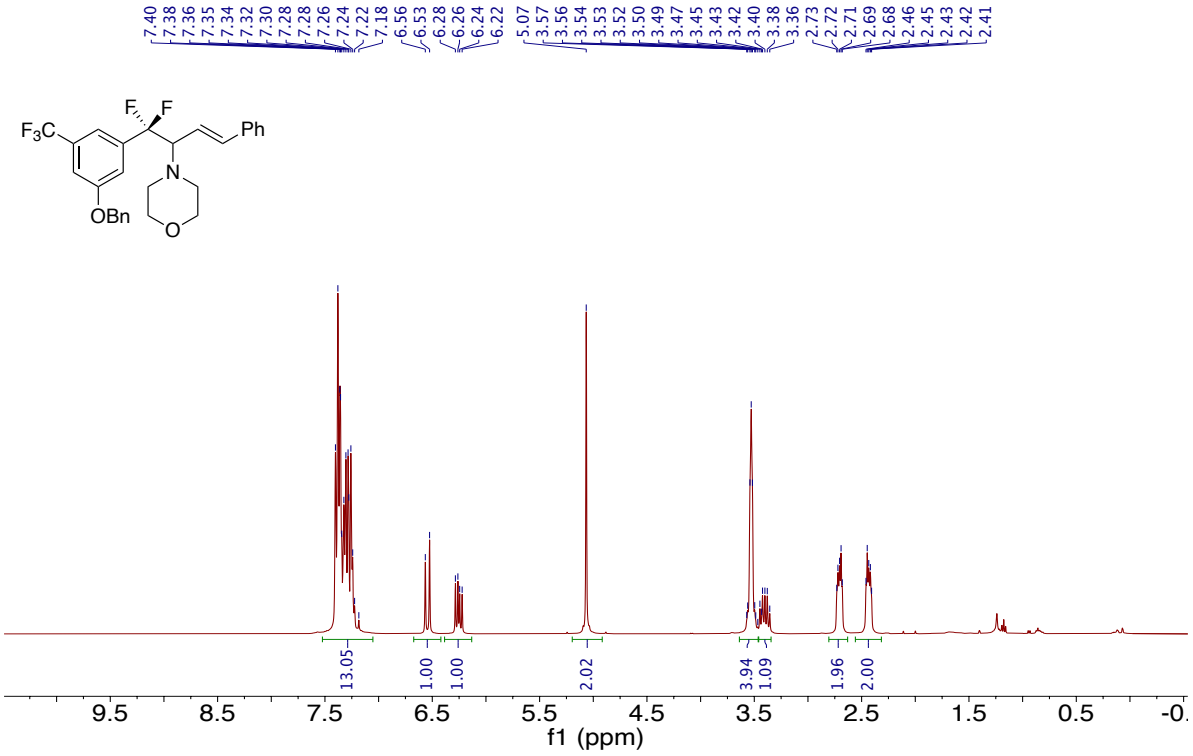

^{1}H NMR of Compound **3-18** (400 MHz, $CDCl_3$)

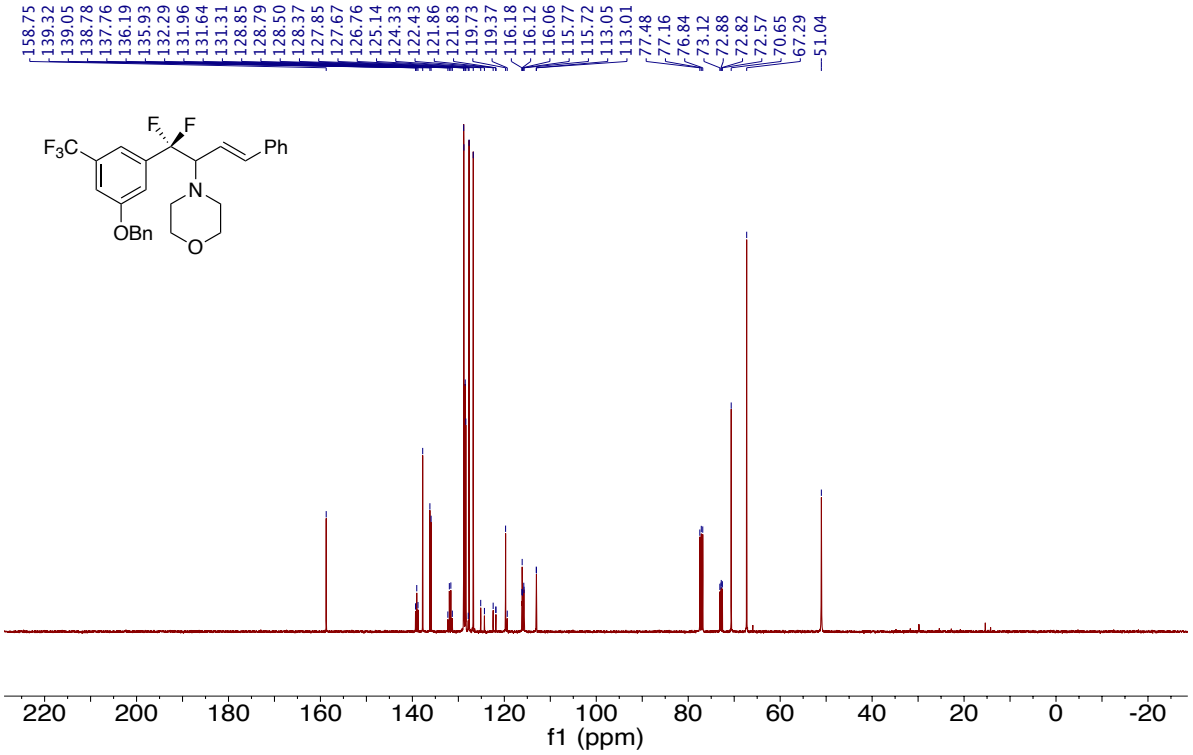

^{13}C NMR of Compound **3-18** (101 MHz, $CDCl_3$)

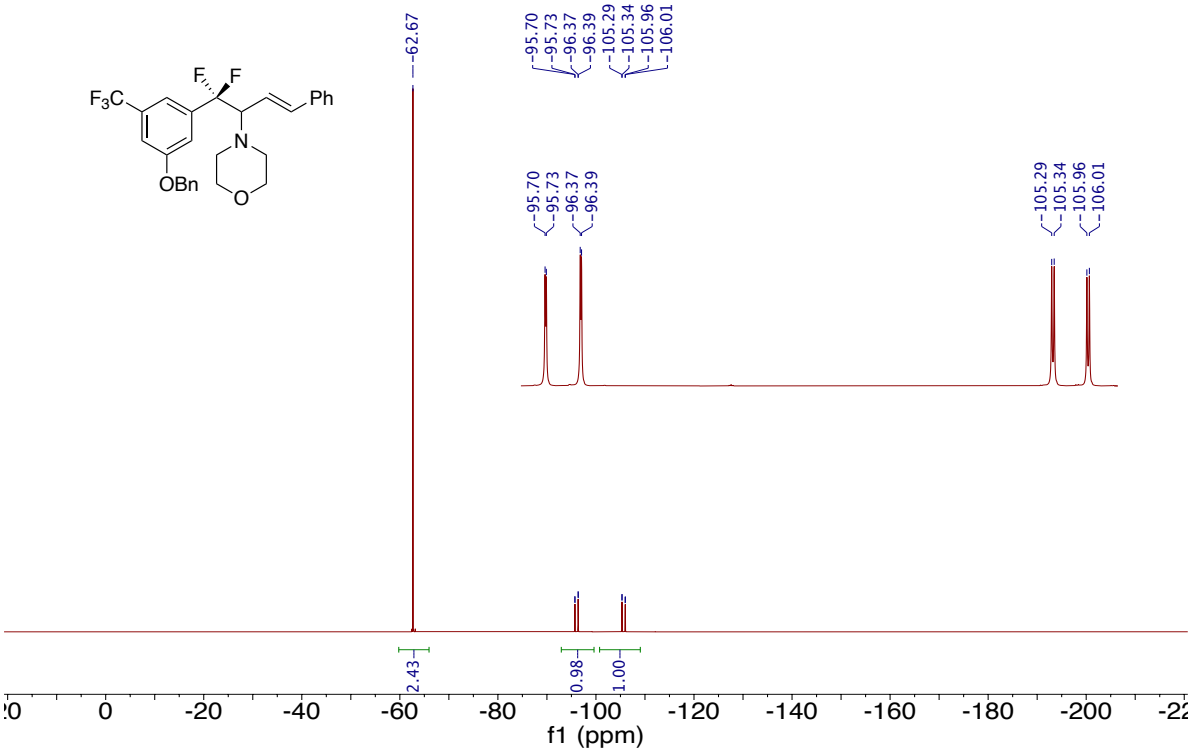

^{19}F NMR of Compound **3-18** (376 MHz, $CDCl_3$)

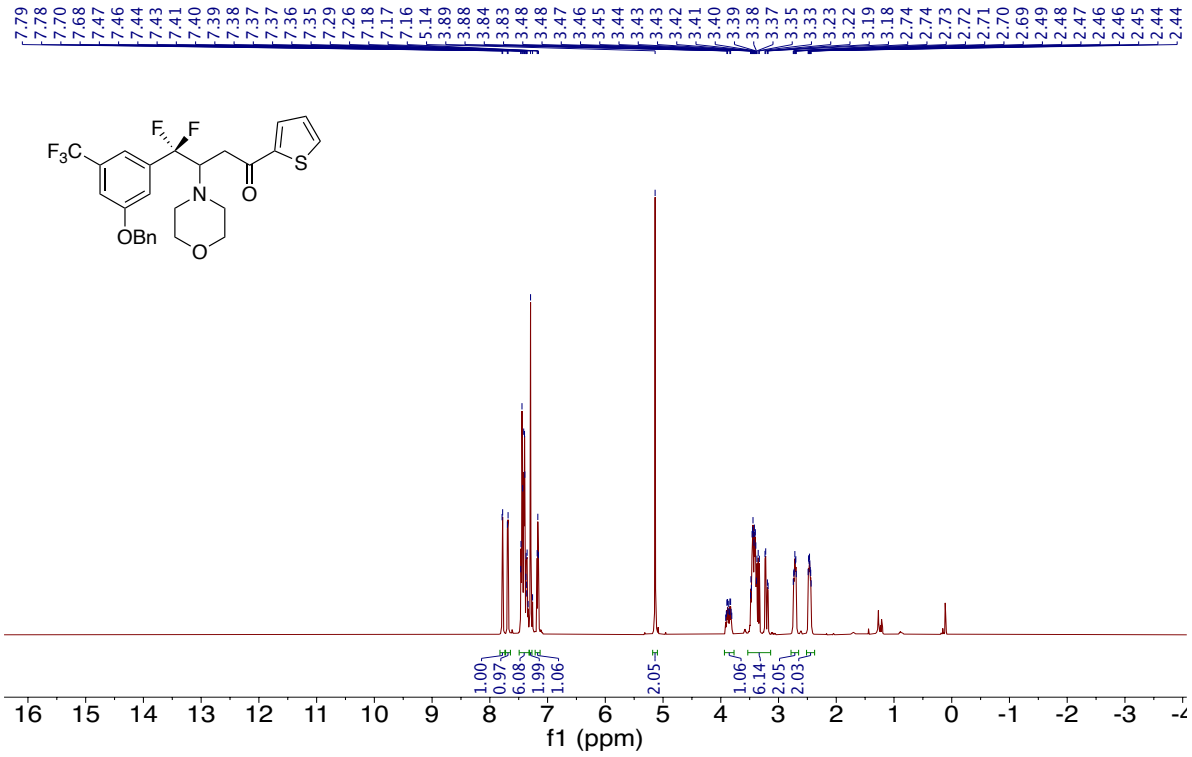

^{1}H NMR of Compound **3-19** (400 MHz, $CDCl_3$)

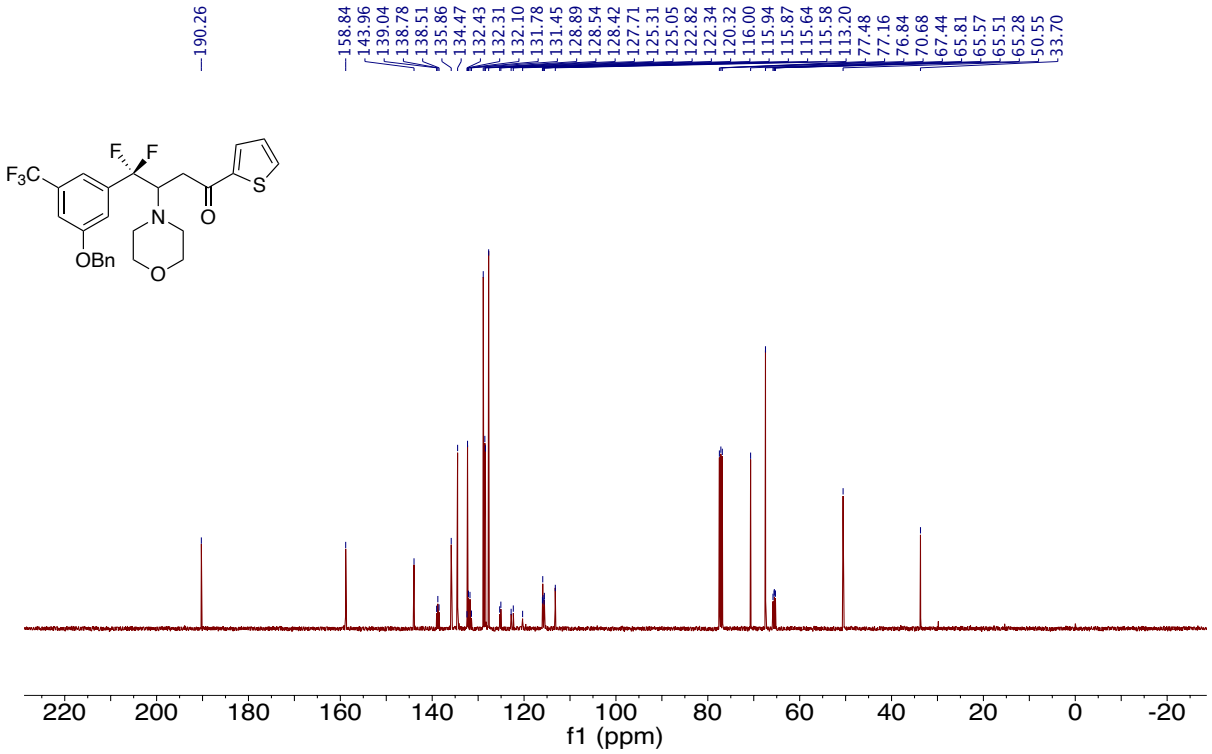

^{13}C NMR of Compound **3-19** (101 MHz, $CDCl_3$)

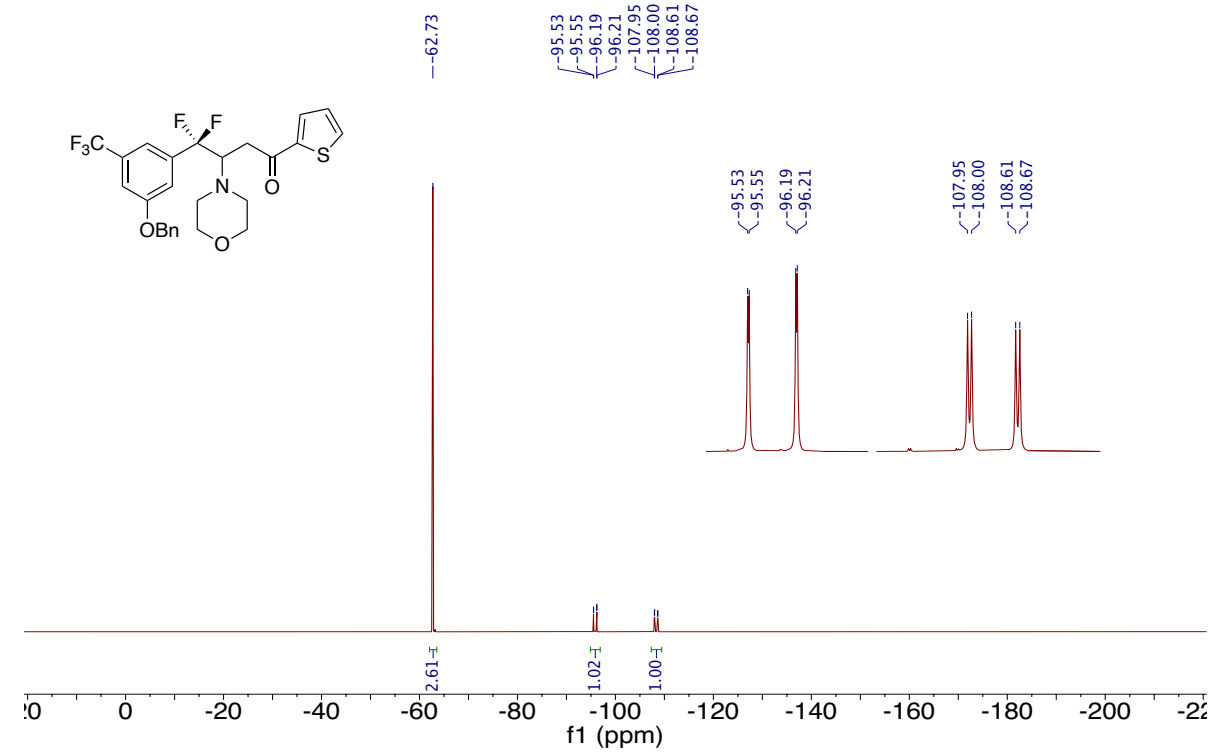

^{19}F NMR of Compound **3-19** (376 MHz, $CDCl_3$)

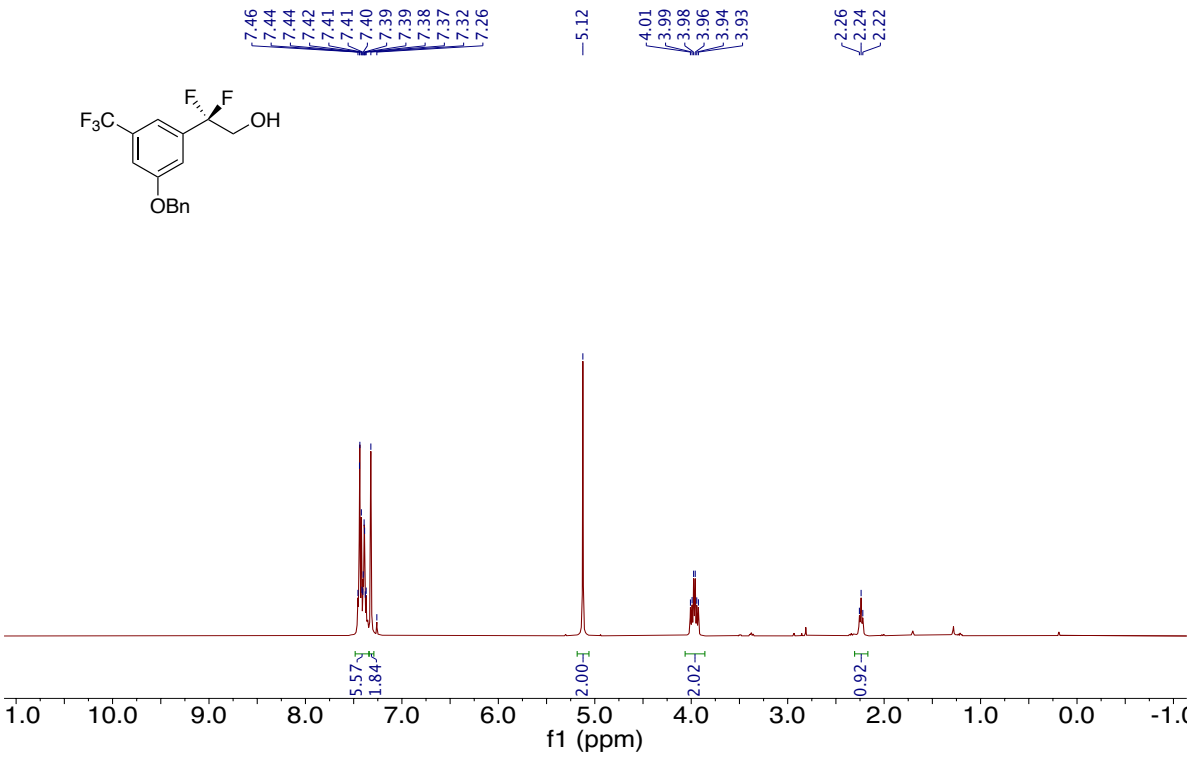

^{1}H NMR of Compound **3-20** (400 MHz, $CDCl_3$)

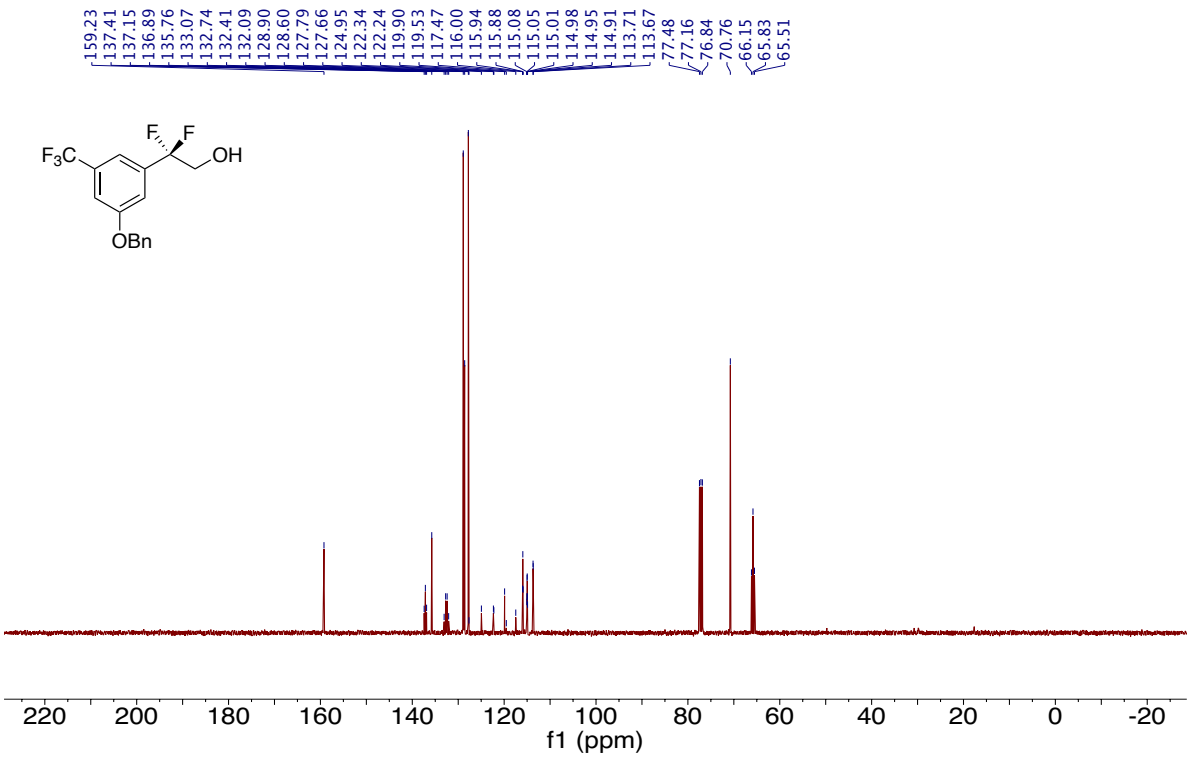

^{13}C NMR of Compound **3-20** (101 MHz, $CDCl_3$)

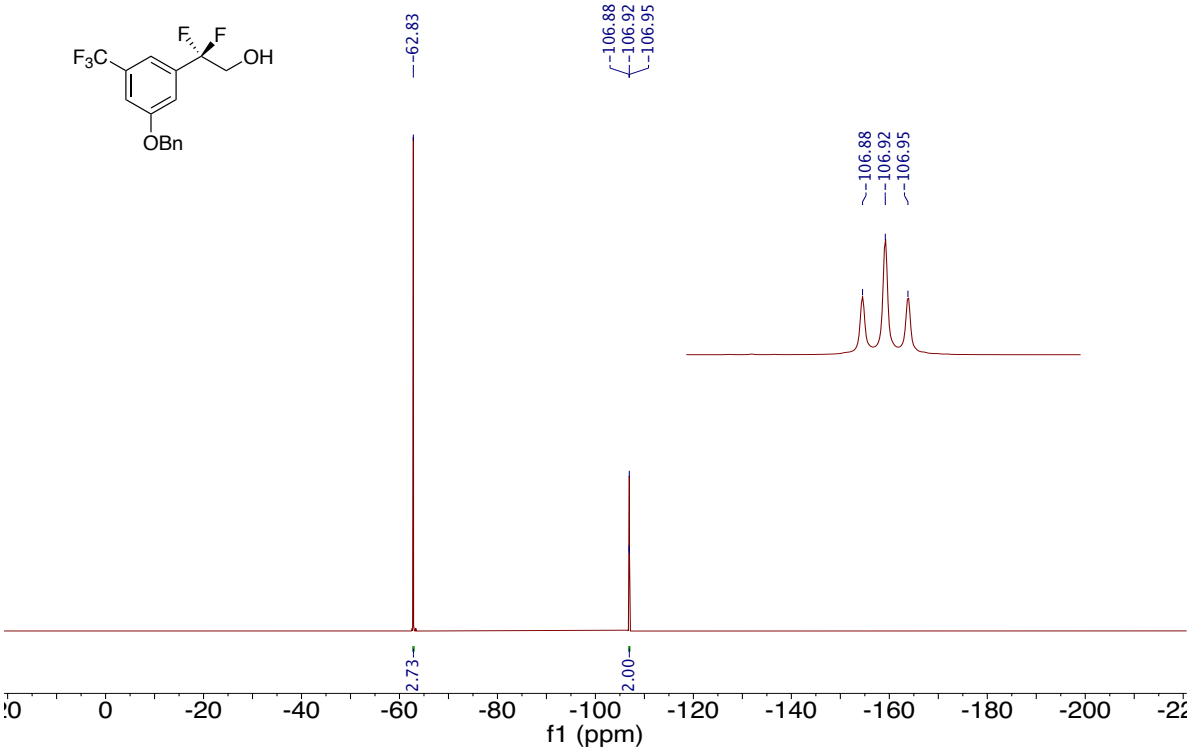

^{19}F NMR of Compound **3-20** (376 MHz, $CDCl_3$)

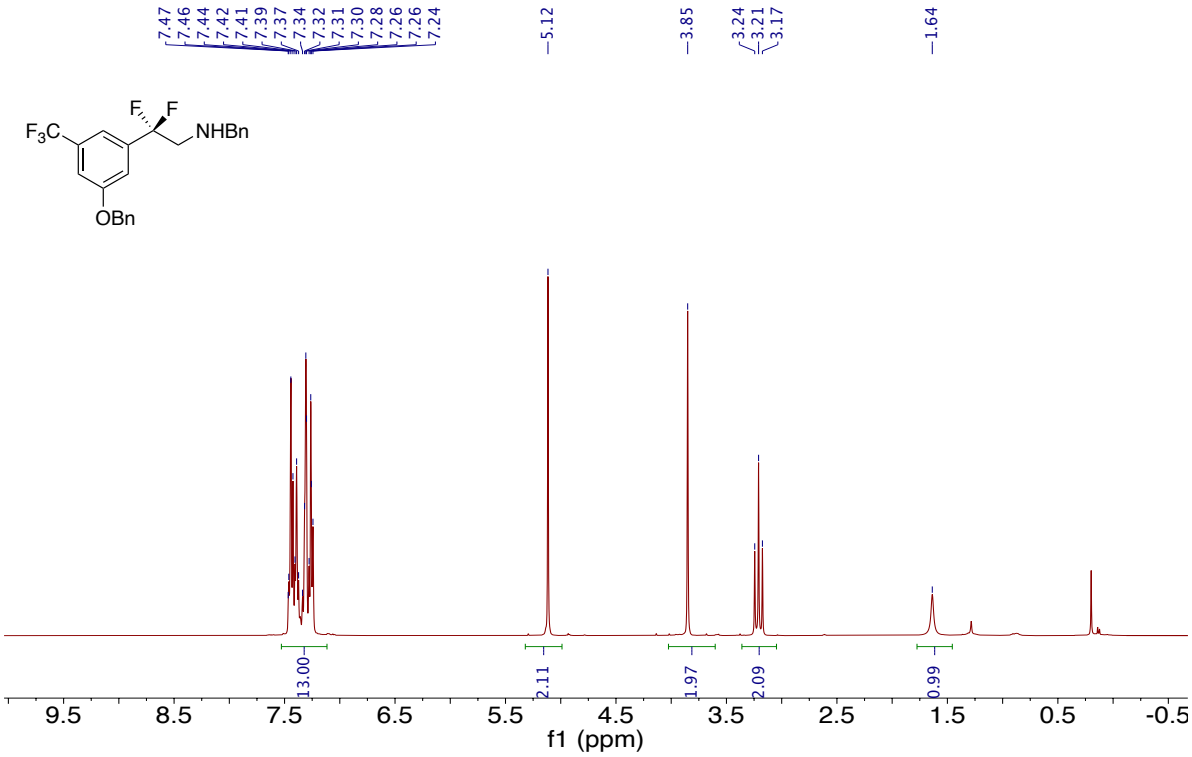

^{1}H NMR of Compound **3-21** (400 MHz, $CDCl_3$)

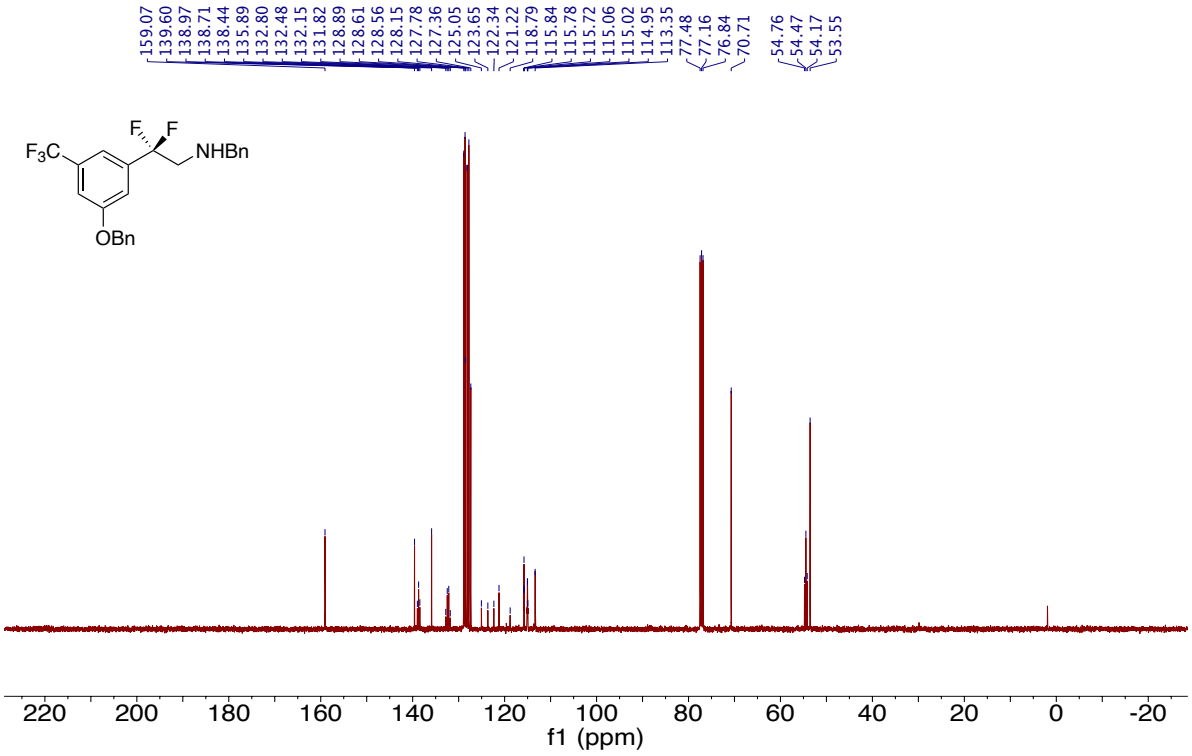

^{13}C NMR of Compound **3-21** (101 MHz, $CDCl_3$)

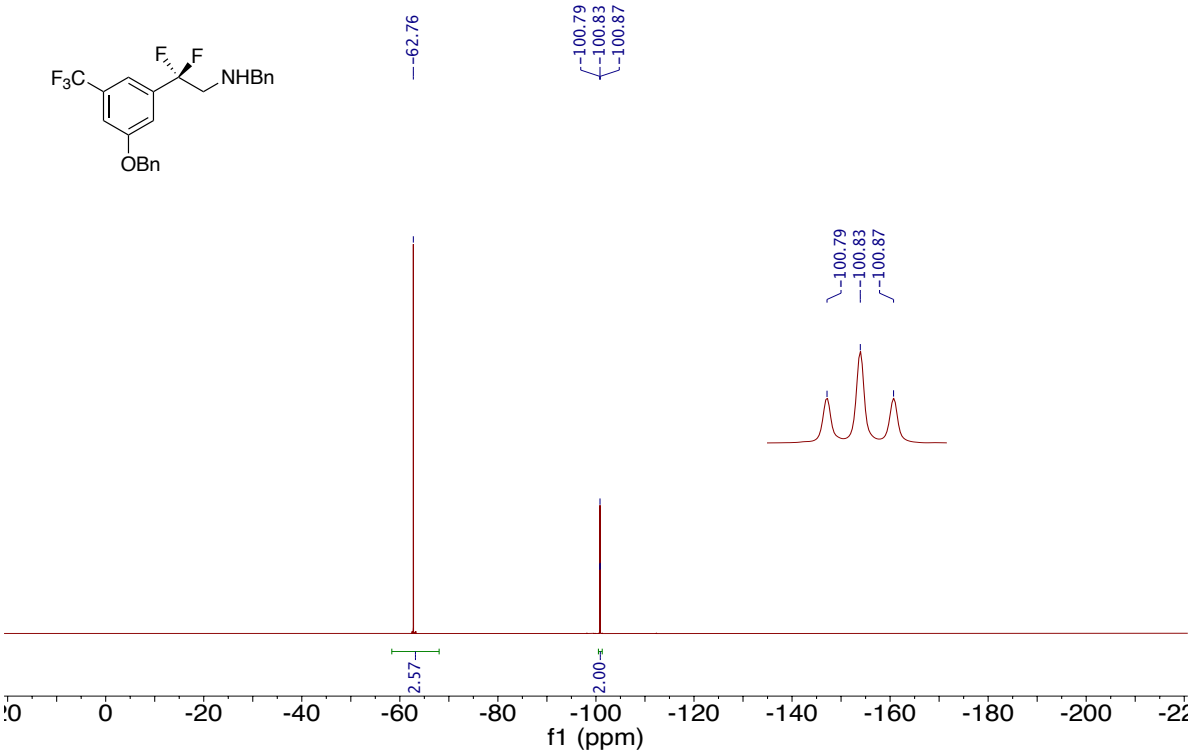

^{19}F NMR of Compound **3-21** (376 MHz, $CDCl_3$)

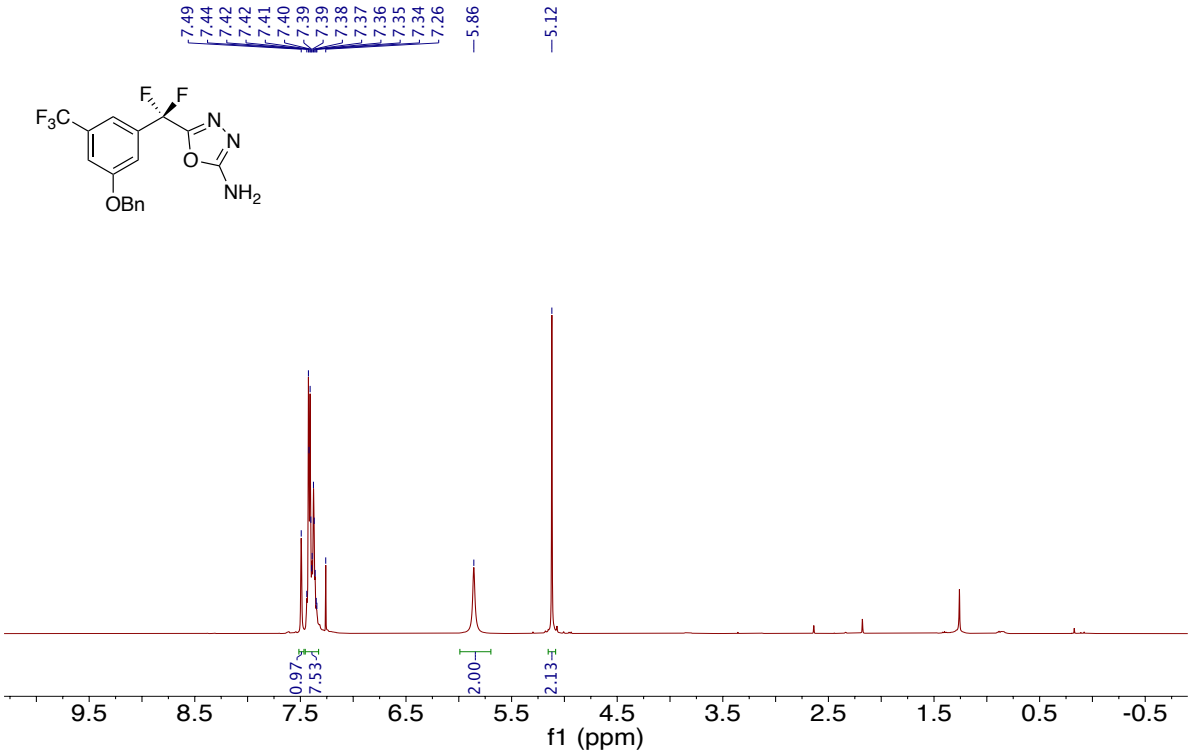

^{1}H NMR of Compound **3-22** (400 MHz, $CDCl_3$)

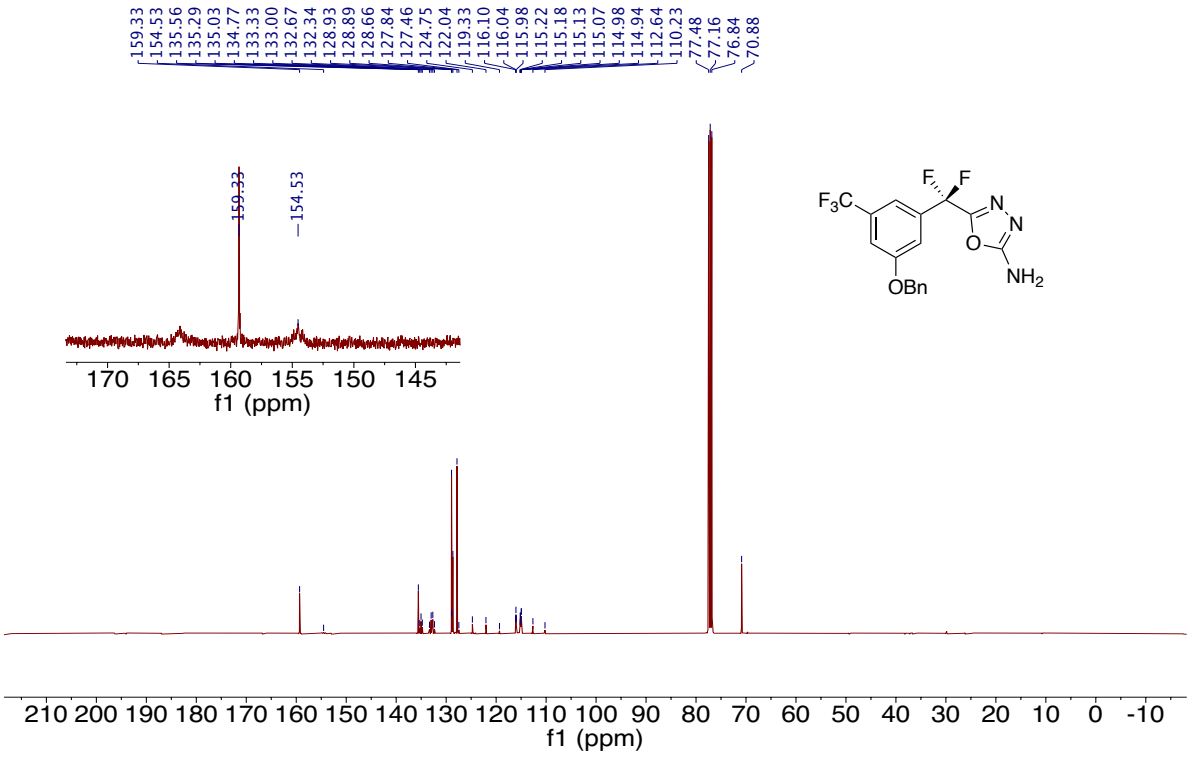

^{13}C NMR of Compound **3-22** (101 MHz, $CDCl_3$)

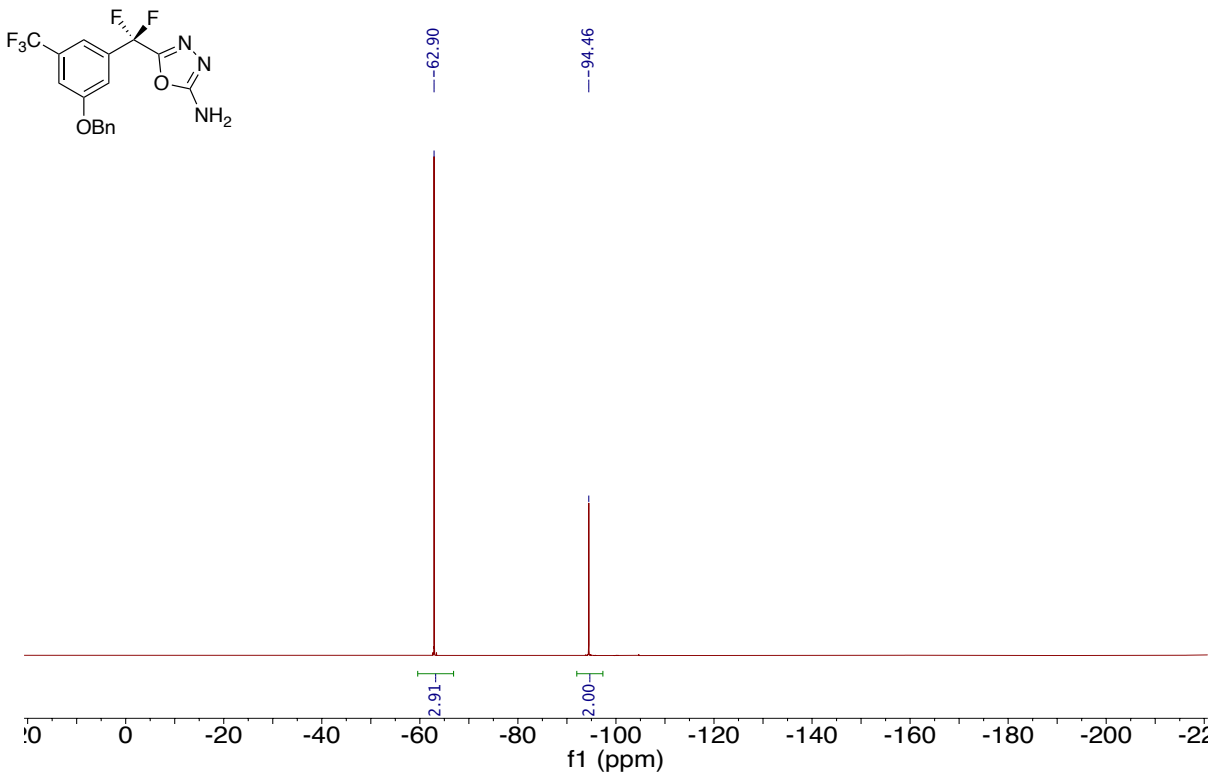

^{19}F NMR of Compound **3-22** (376 MHz, $CDCl_3$)

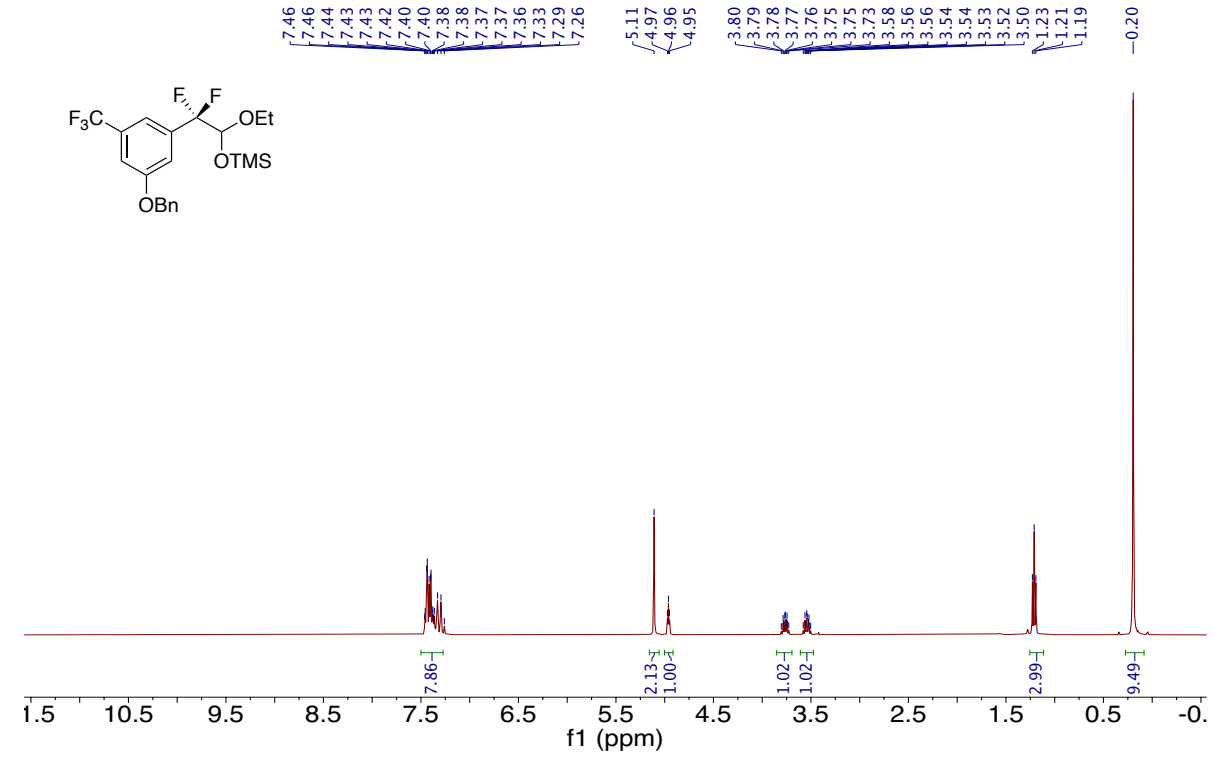

^{1}H NMR of Compound **3-23** (400 MHz, $CDCl_3$)

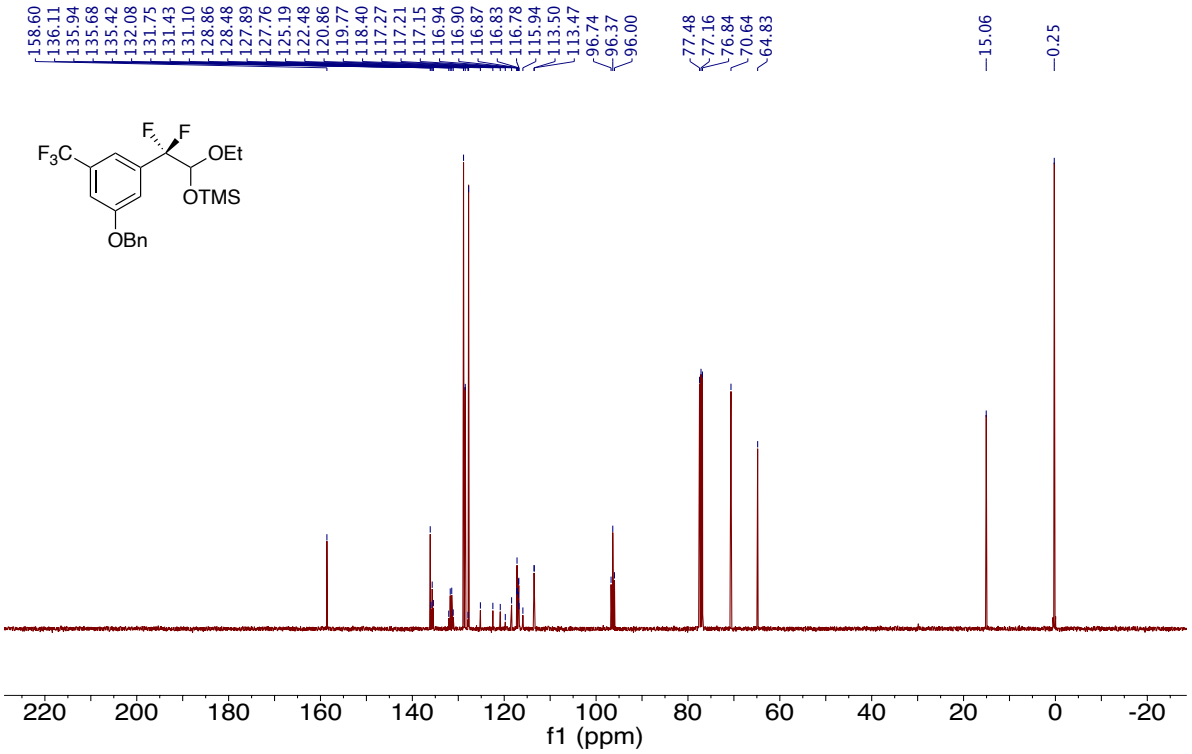

^{13}C NMR of Compound **3-23** (101 MHz, $CDCl_3$)

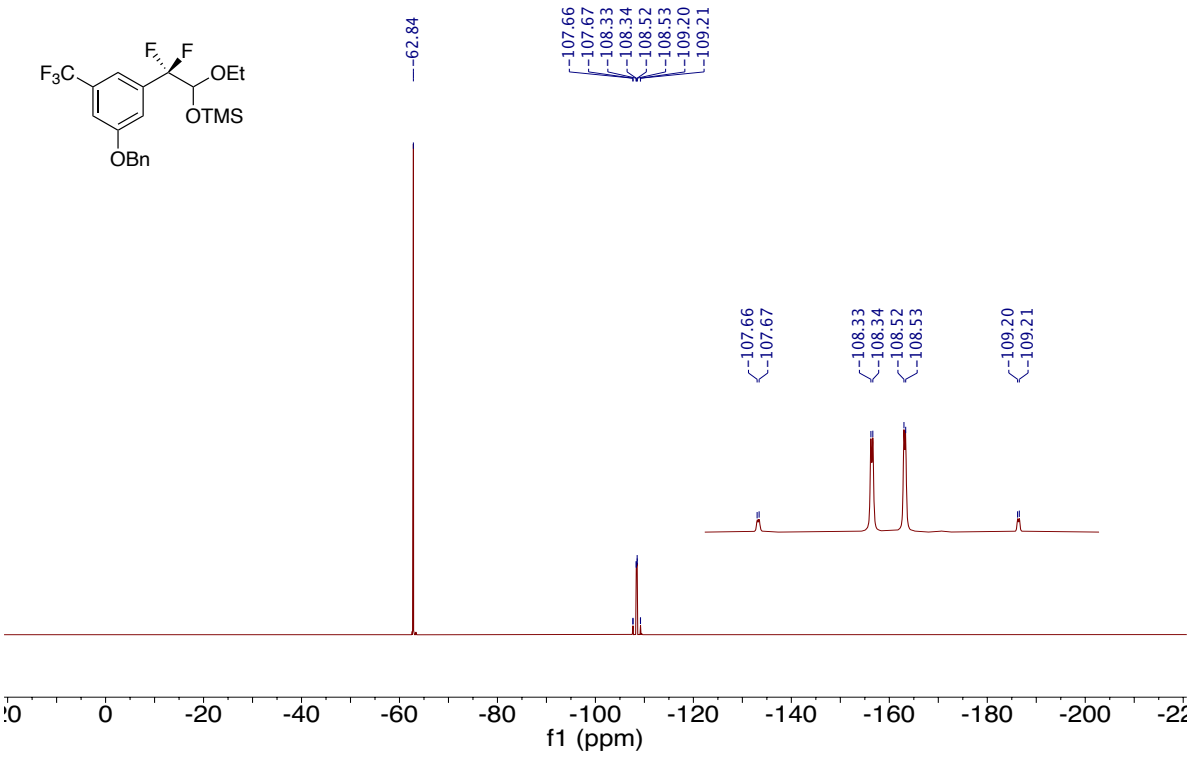

^{19}F NMR of Compound **3-23** (376 MHz, $CDCl_3$)

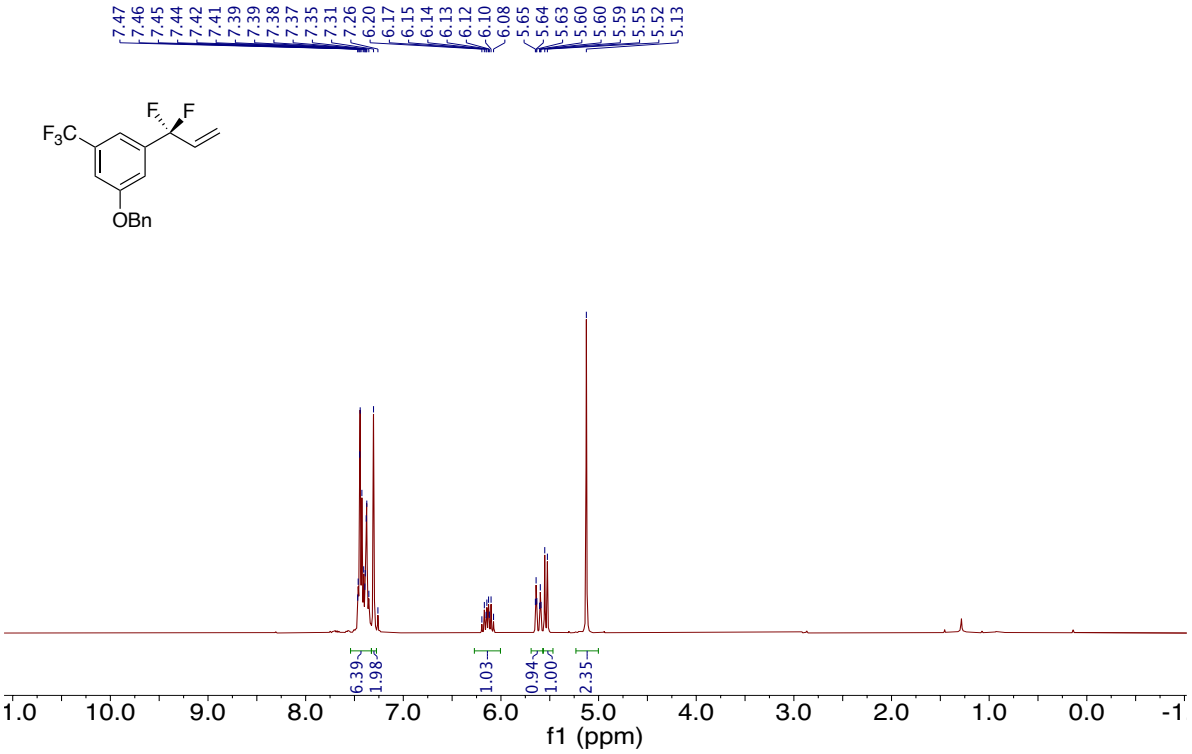

^{1}H NMR of Compound **3-24** (400 MHz, $CDCl_3$)

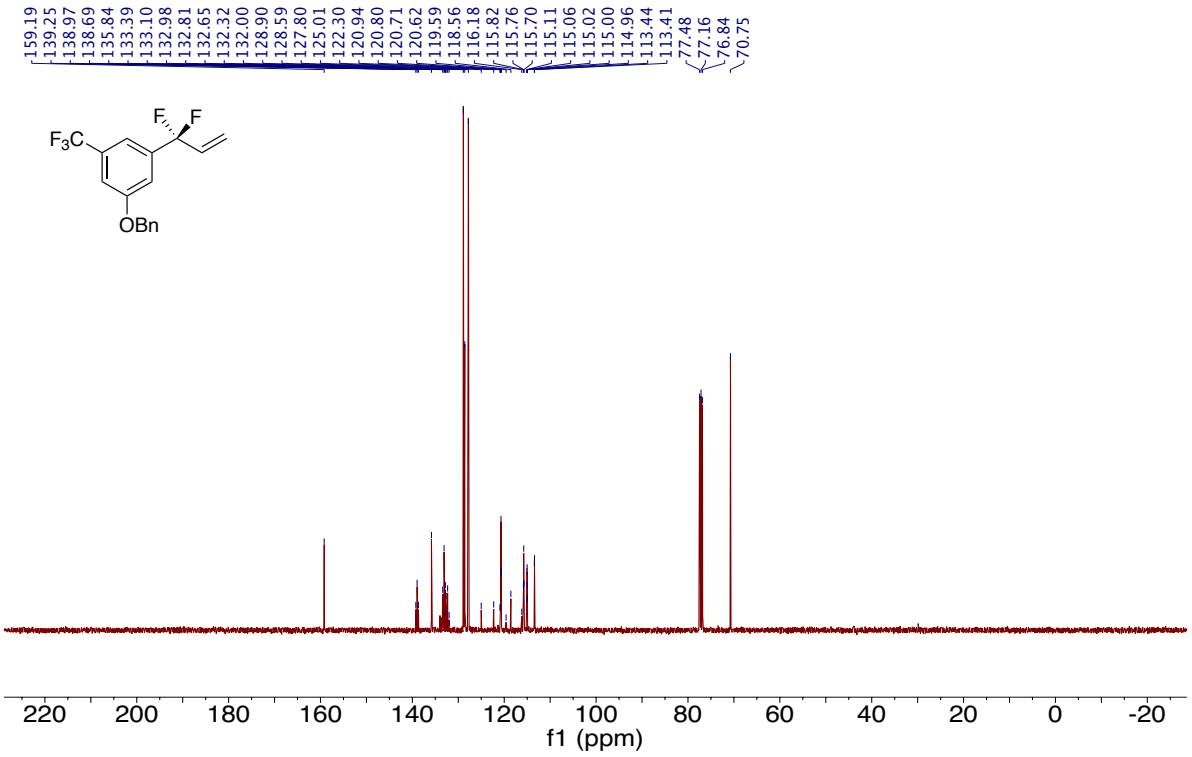

^{13}C NMR of Compound **3-24** (101 MHz, $CDCl_3$)

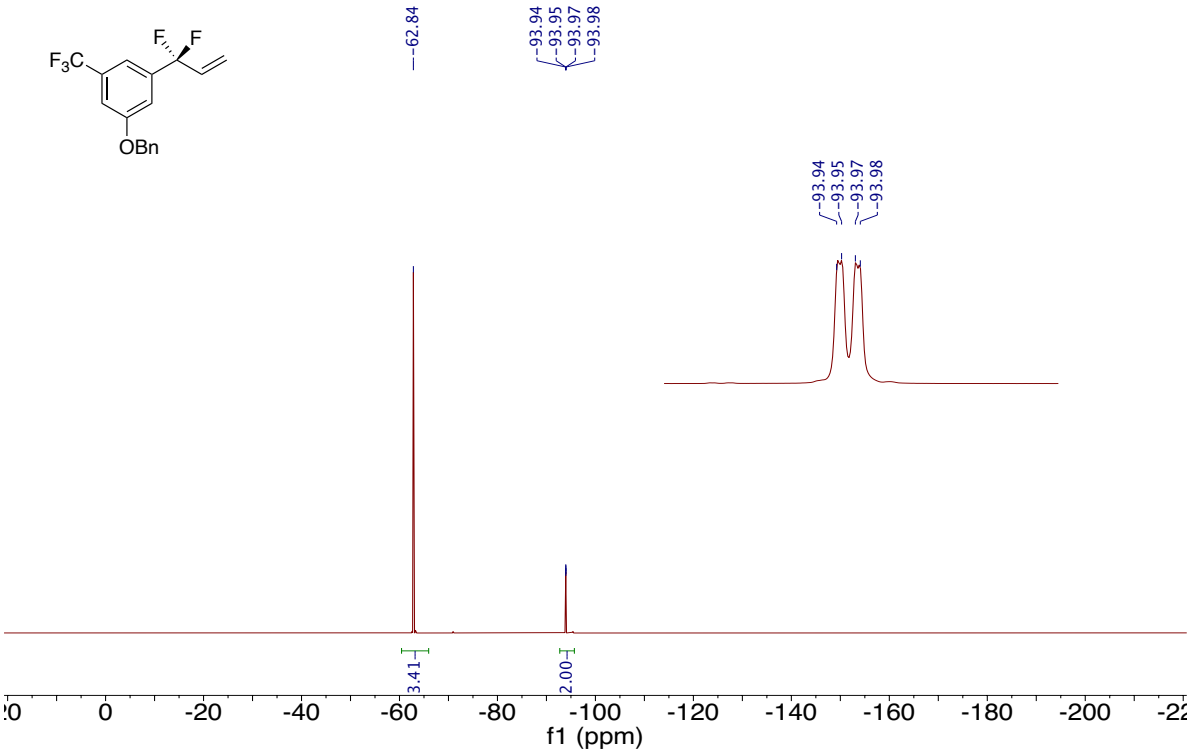

^{19}F NMR of Compound **3-24** (376 MHz, $CDCl_3$)

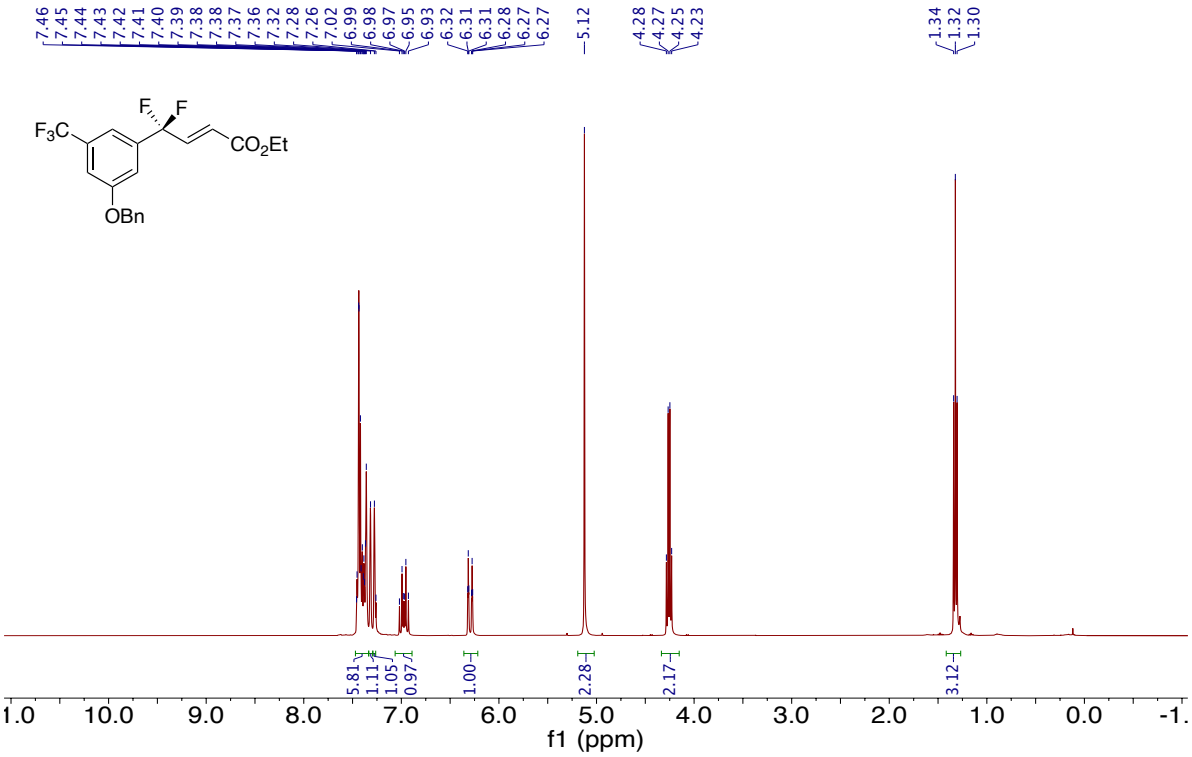

^{1}H NMR of Compound **3-25** (400 MHz, $CDCl_3$)

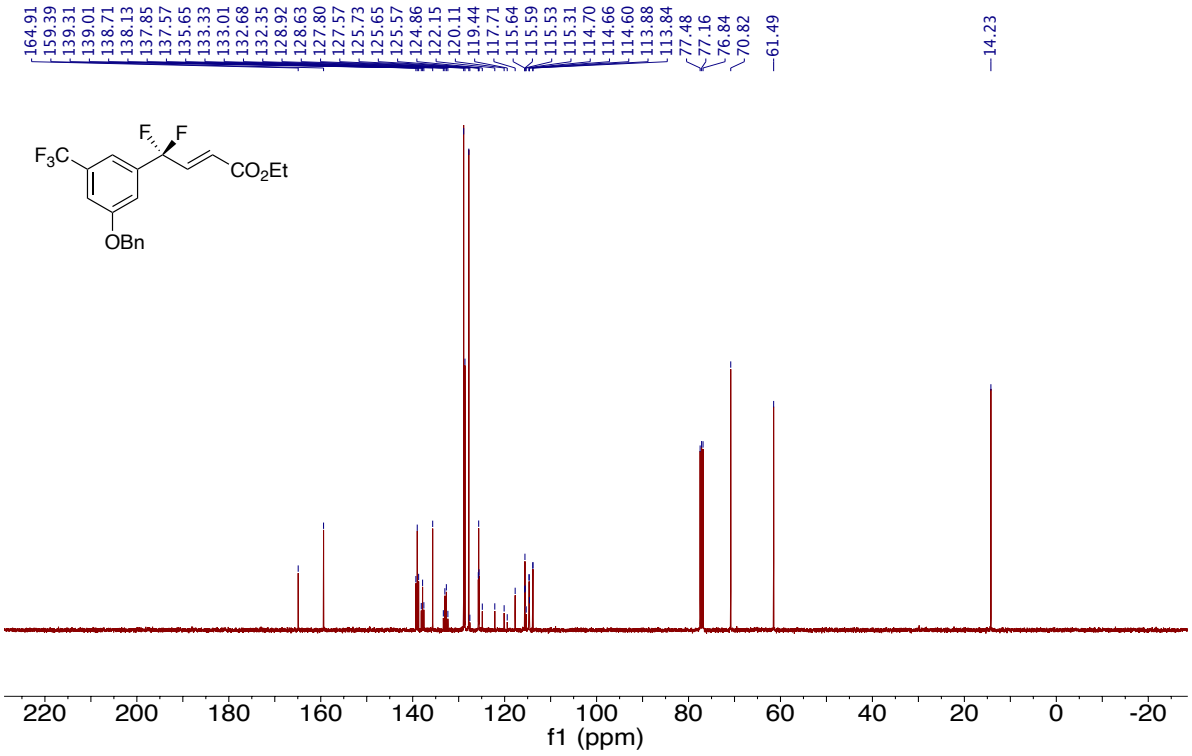

^{13}C NMR of Compound **3-25** (101 MHz, $CDCl_3$)

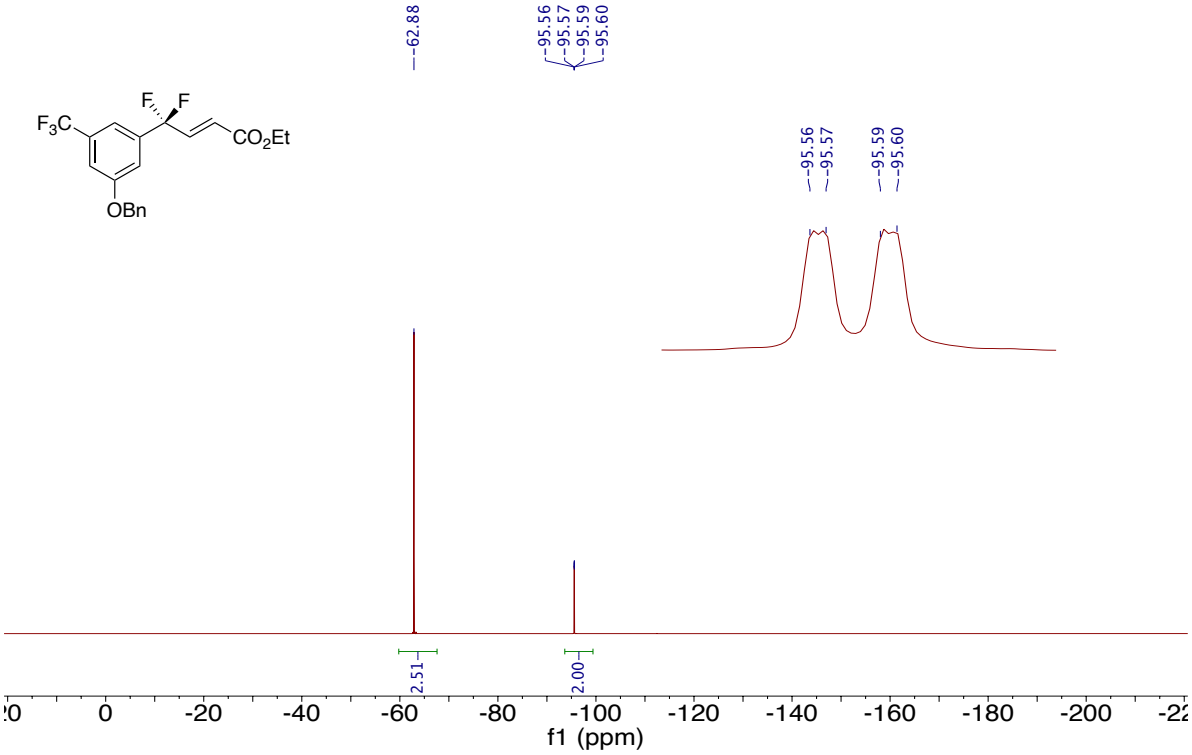

^{19}F NMR of Compound **3-25** (376 MHz, $CDCl_3$)

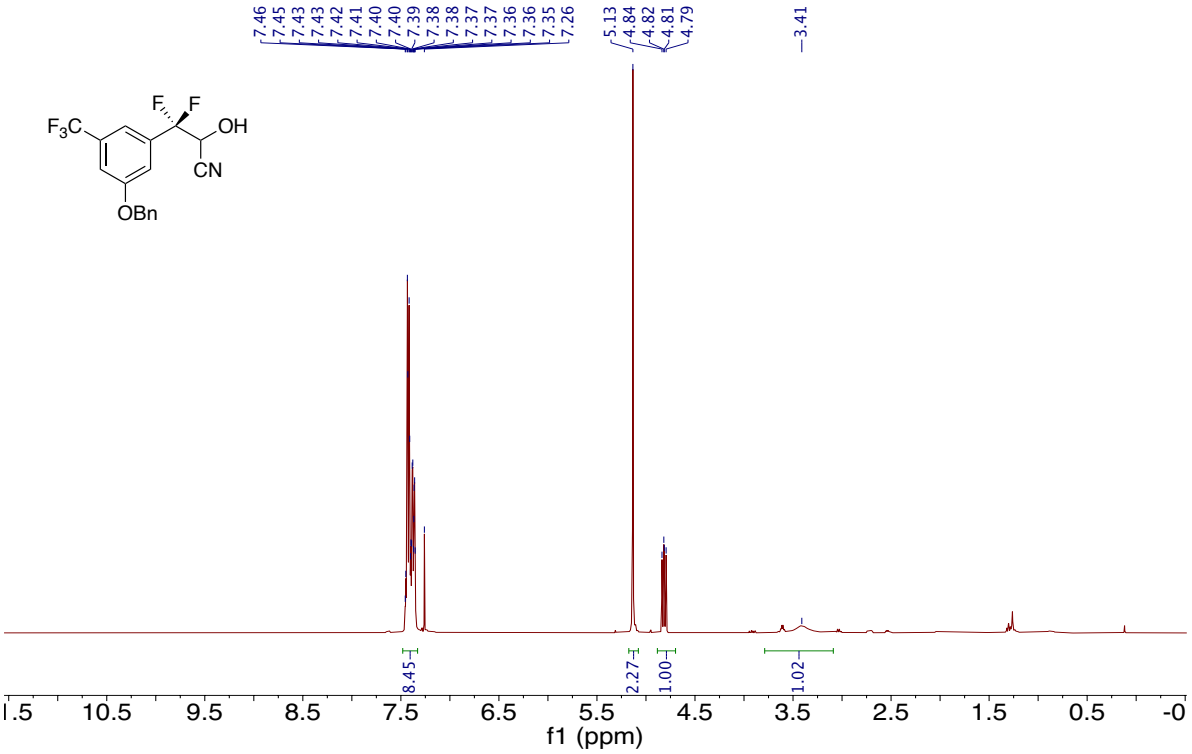

^{1}H NMR of Compound **3-26** (400 MHz, $CDCl_3$)

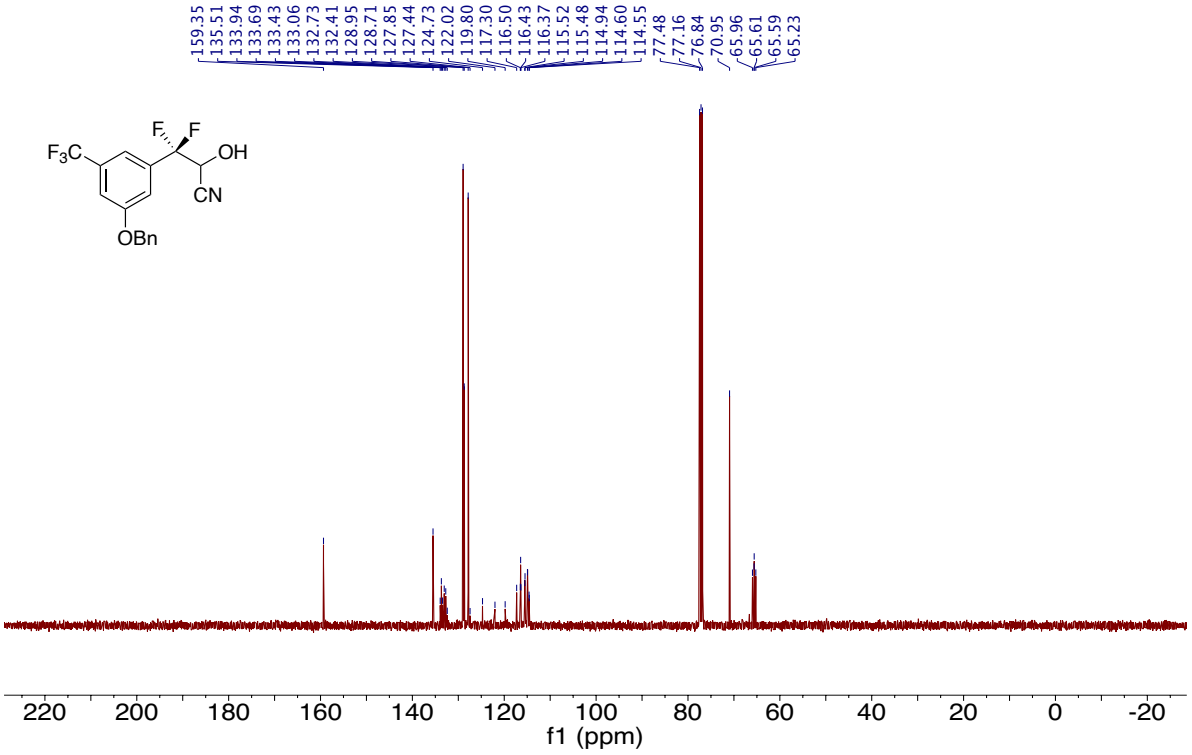

^{13}C NMR of Compound **3-26** (101 MHz, $CDCl_3$)

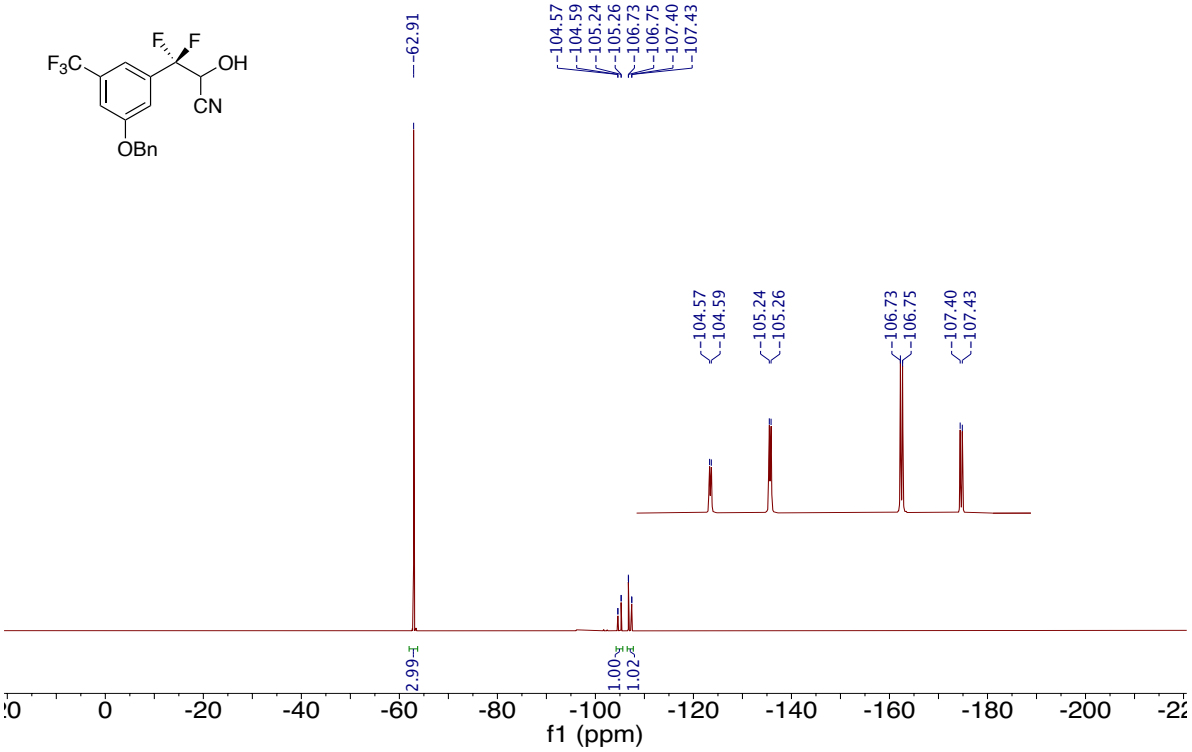

^{19}F NMR of Compound **3-26** (376 MHz, $CDCl_3$)

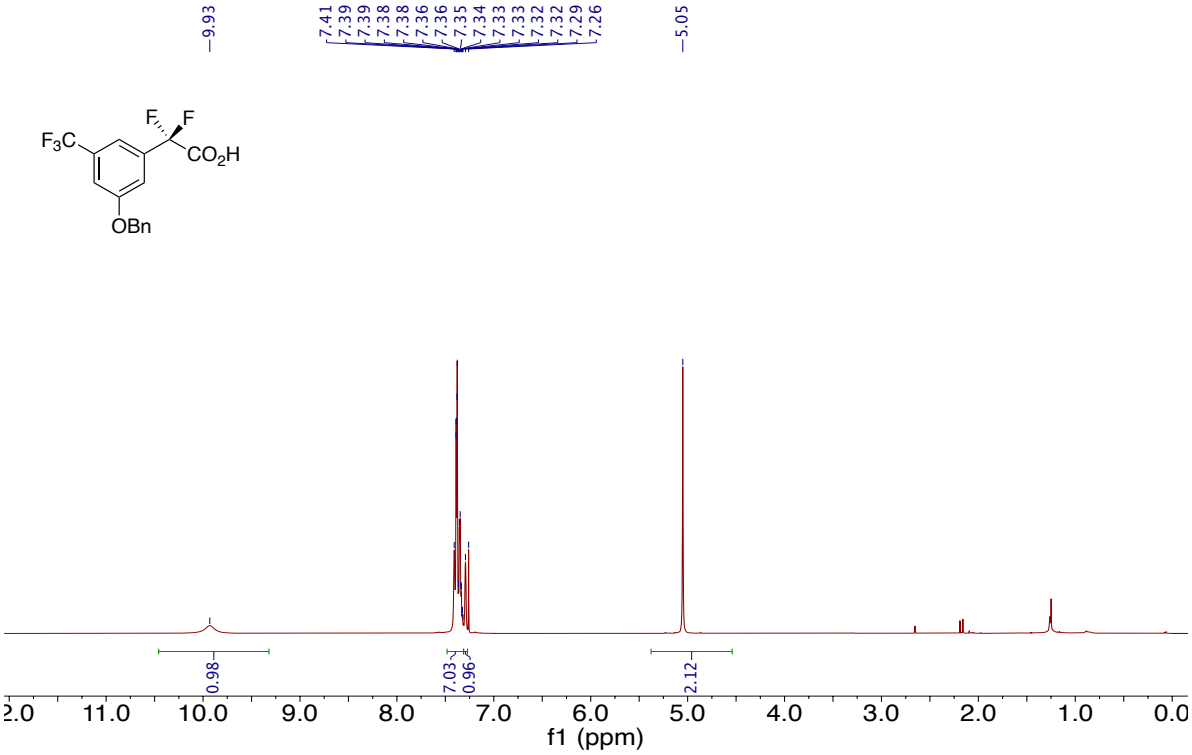

^{1}H NMR of Compound **3-27** (400 MHz, $CDCl_3$)

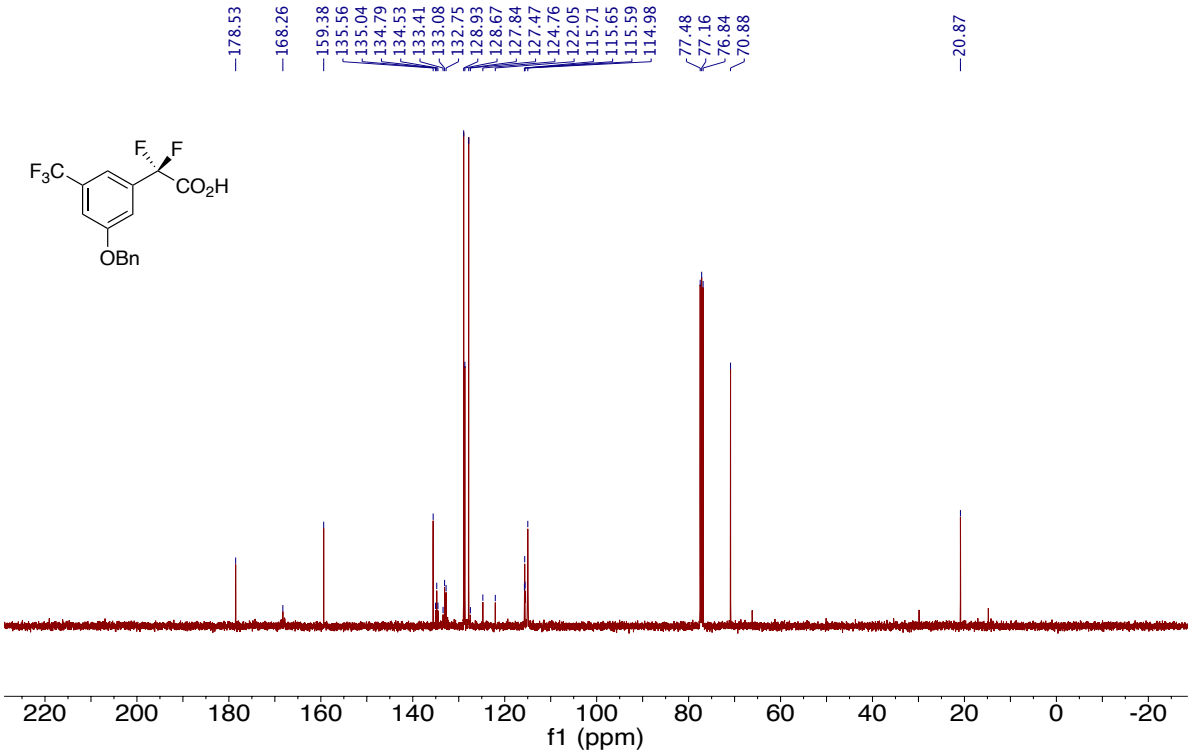

^{13}C NMR of Compound **3-27** (101 MHz, $CDCl_3$)

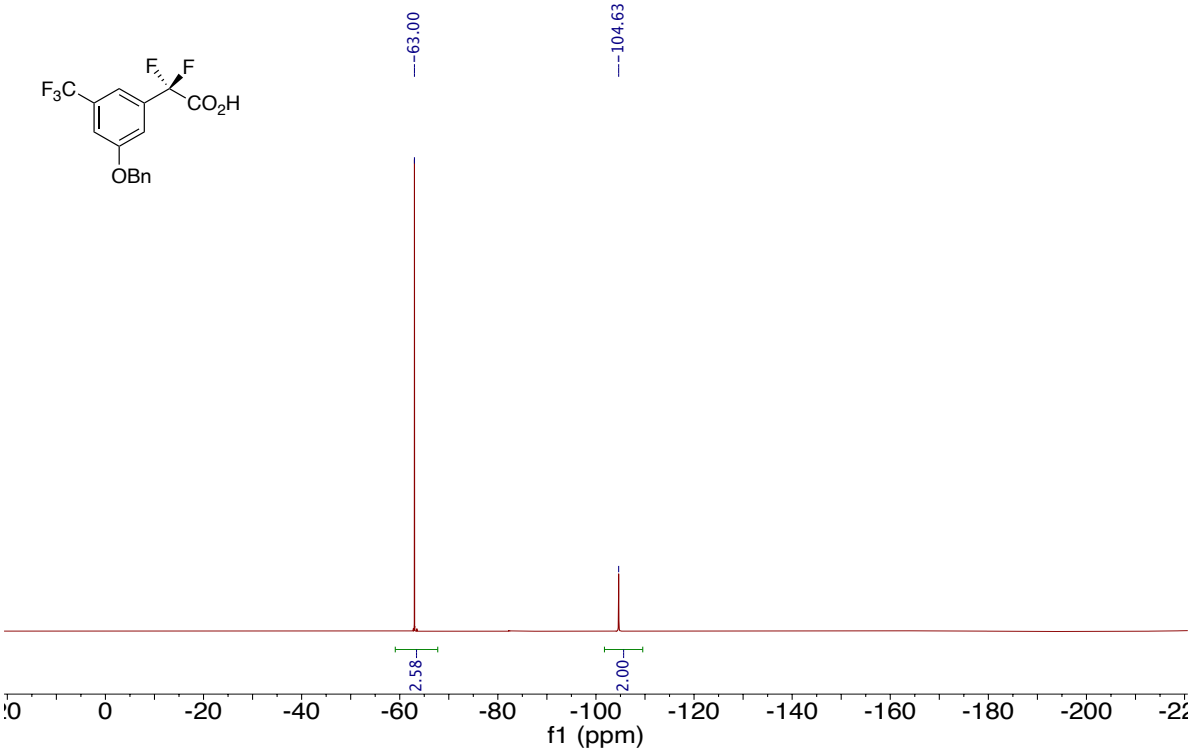

^{19}F NMR of Compound **3-27** (376 MHz, $CDCl_3$)

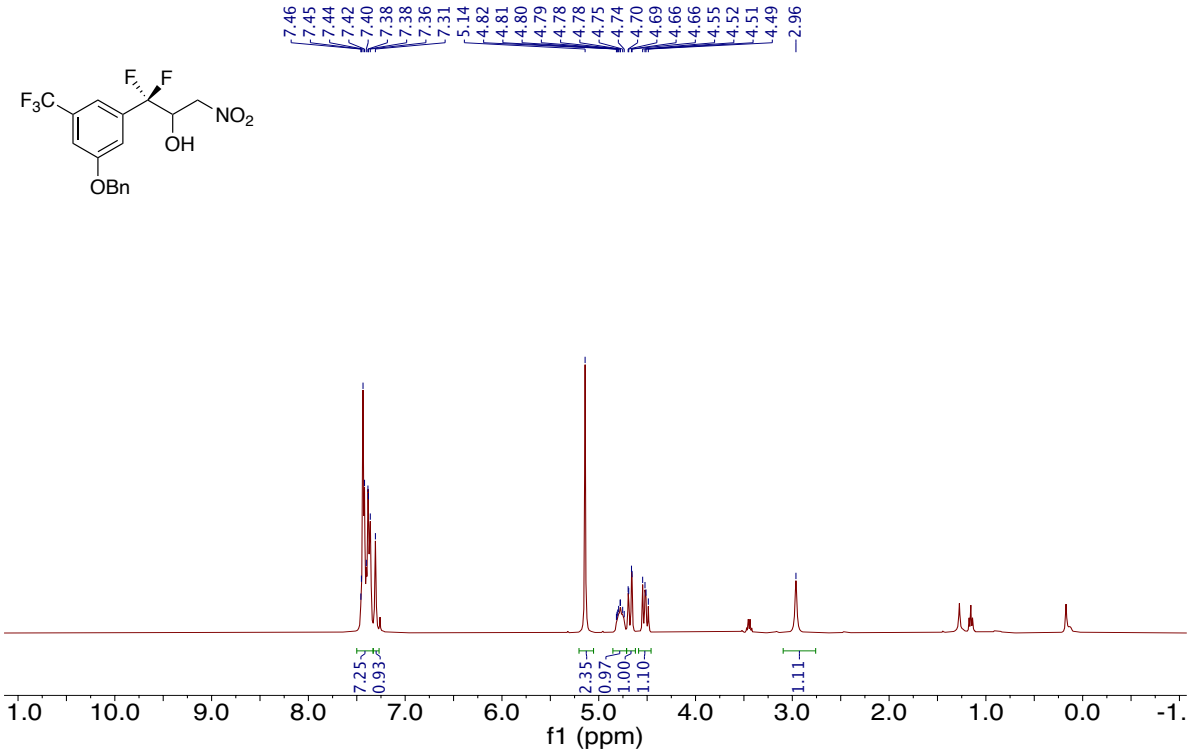

^{1}H NMR of Compound **3-28** (400 MHz, $CDCl_3$)

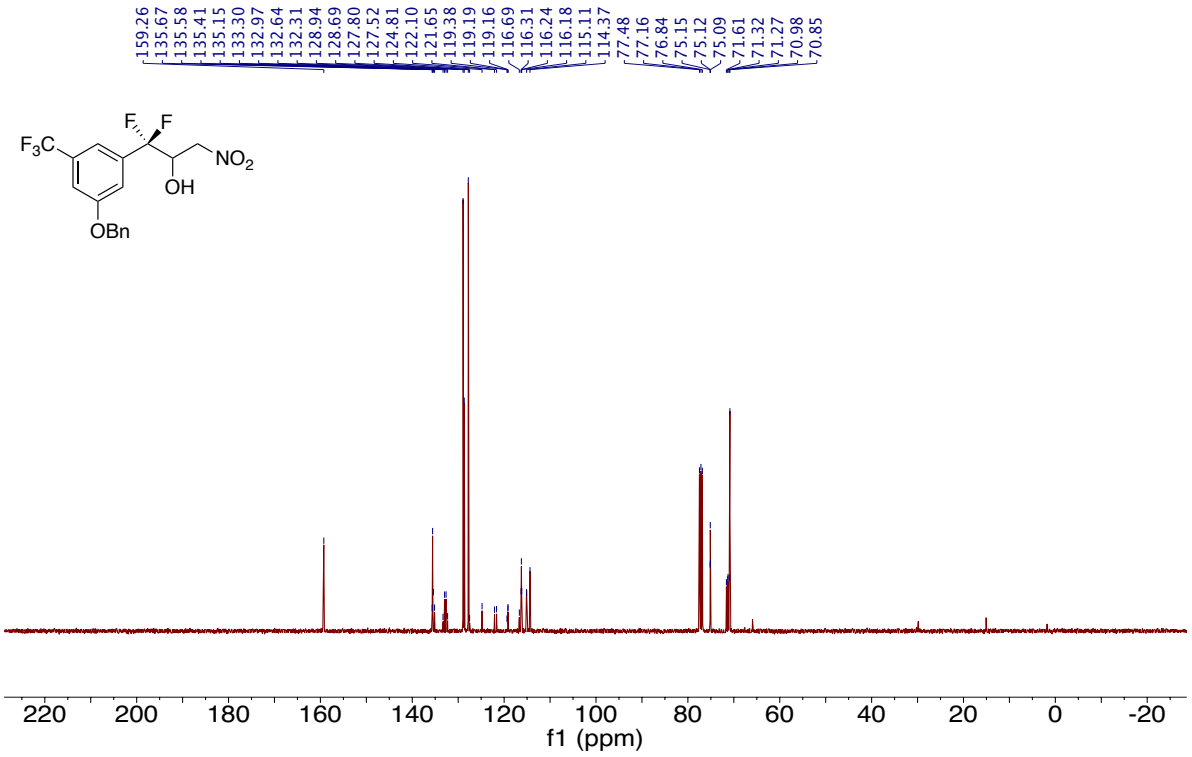

^{13}C NMR of Compound **3-28** (101 MHz, $CDCl_3$)

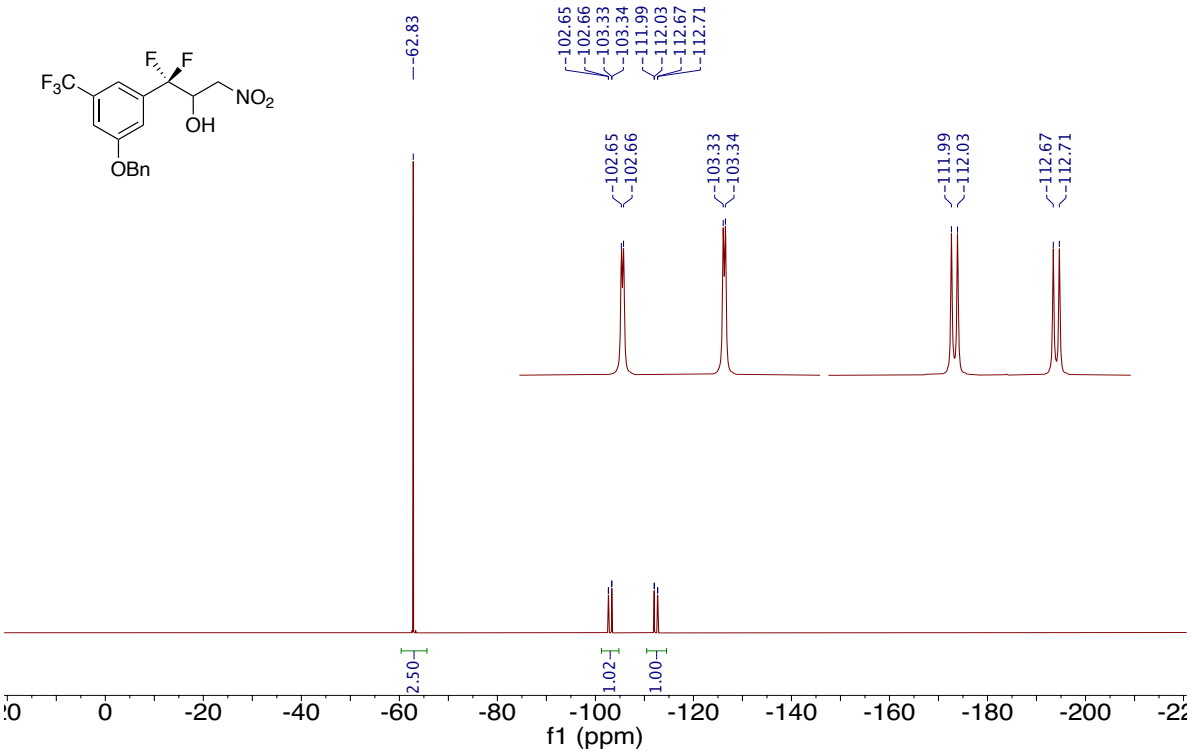

^{19}F NMR of Compound **3-28** (376 MHz, $CDCl_3$)

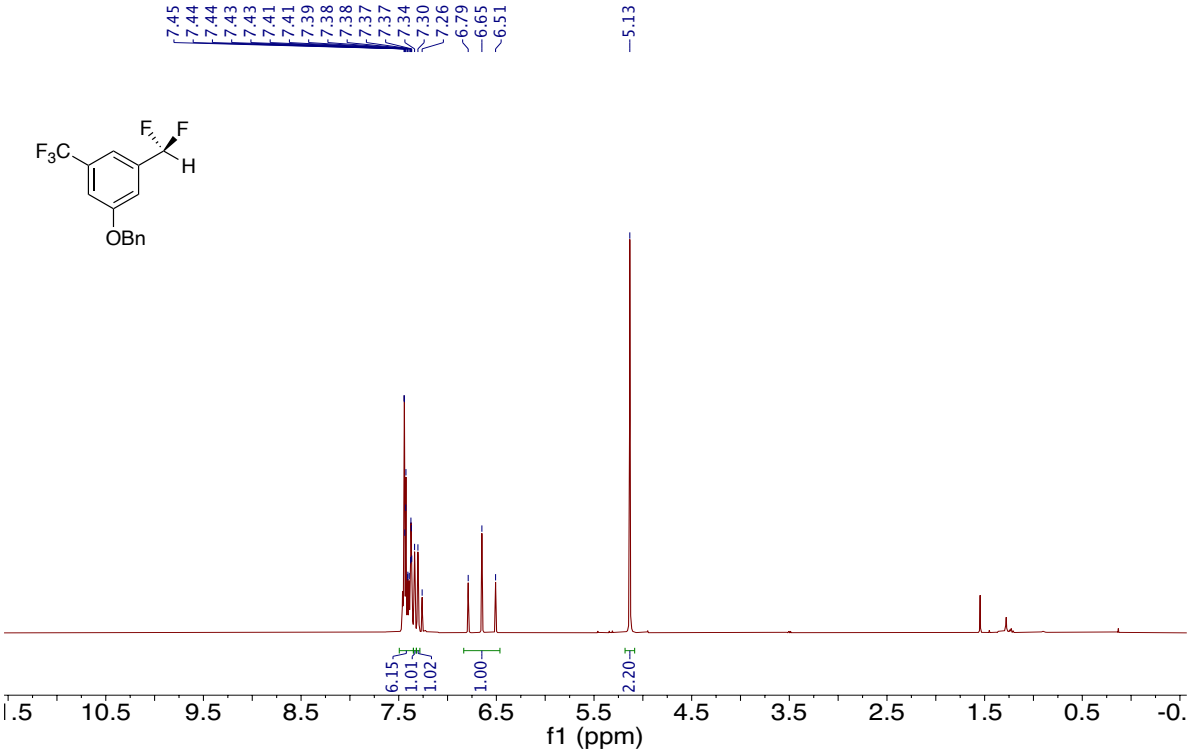

^{1}H NMR of Compound **3-29** (400 MHz, $CDCl_3$)

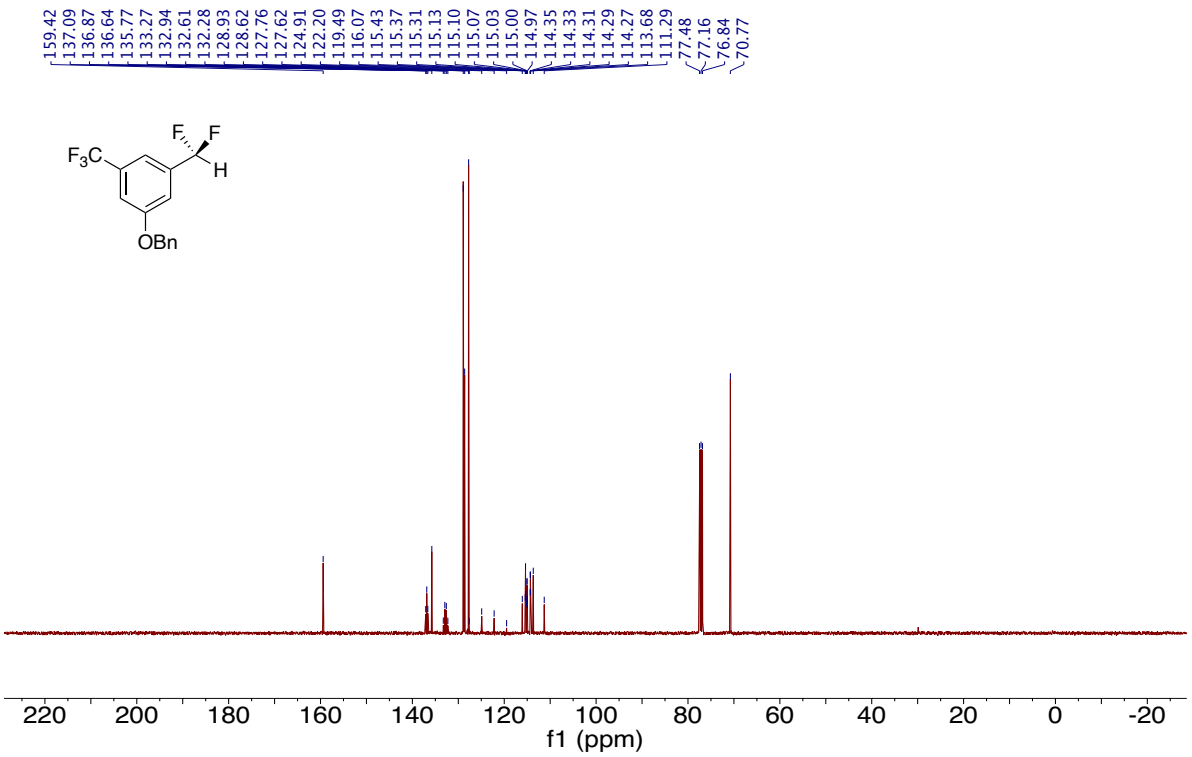

^{13}C NMR of Compound **3-29** (101 MHz, $CDCl_3$)

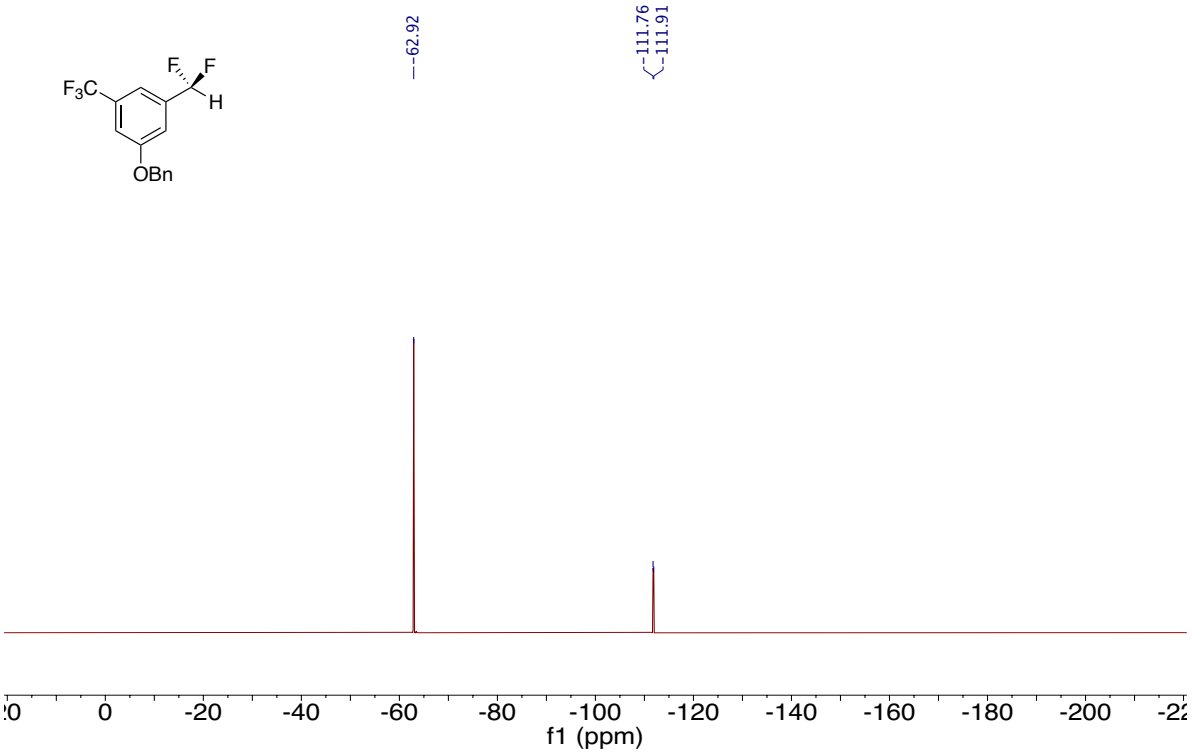

^{19}F NMR of Compound **3-29** (376 MHz, $CDCl_3$)

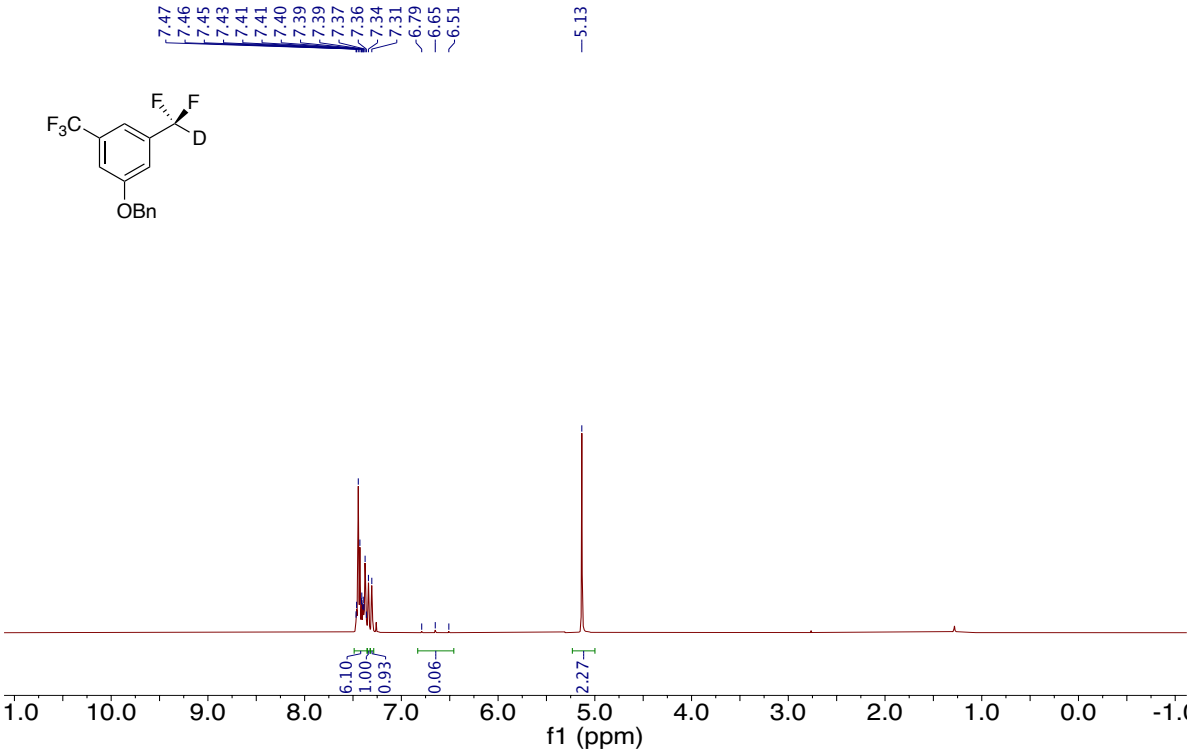

^{1}H NMR of Compound **3-30** (400 MHz, $CDCl_3$)

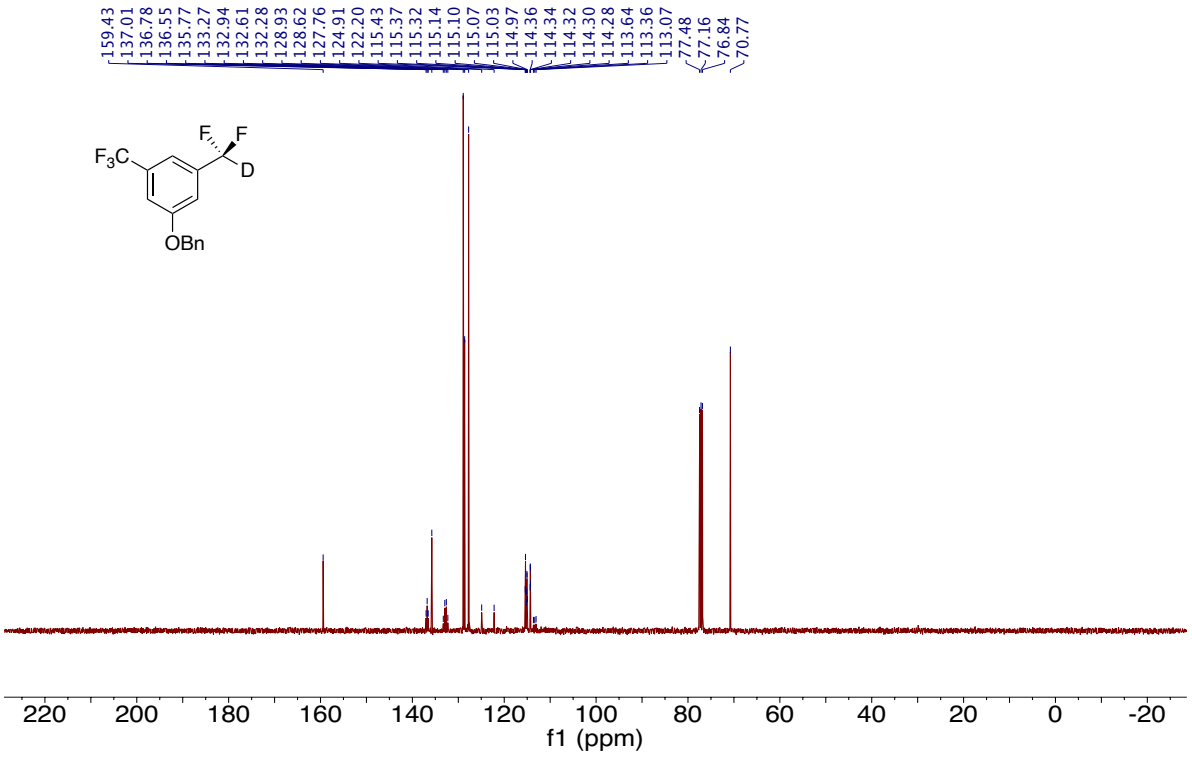

^{13}C NMR of Compound **3-30** (101 MHz, $CDCl_3$)

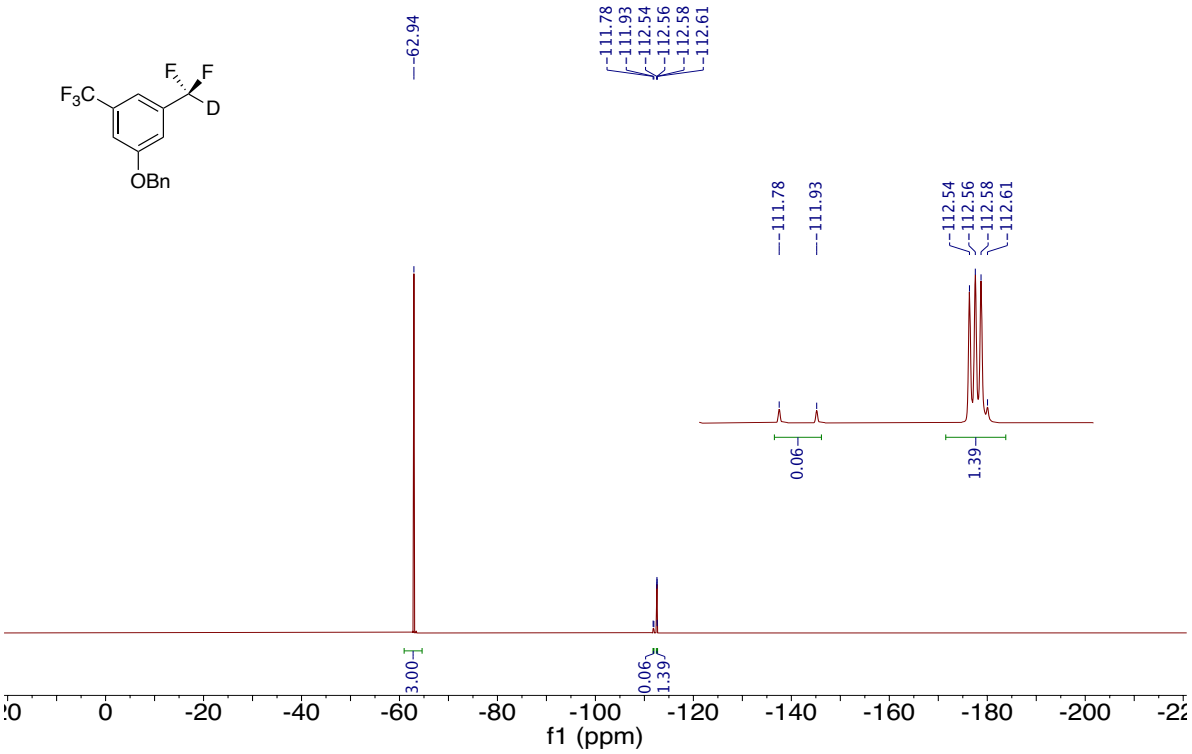

^{19}F NMR of Compound **3-30** (376 MHz, $CDCl_3$)

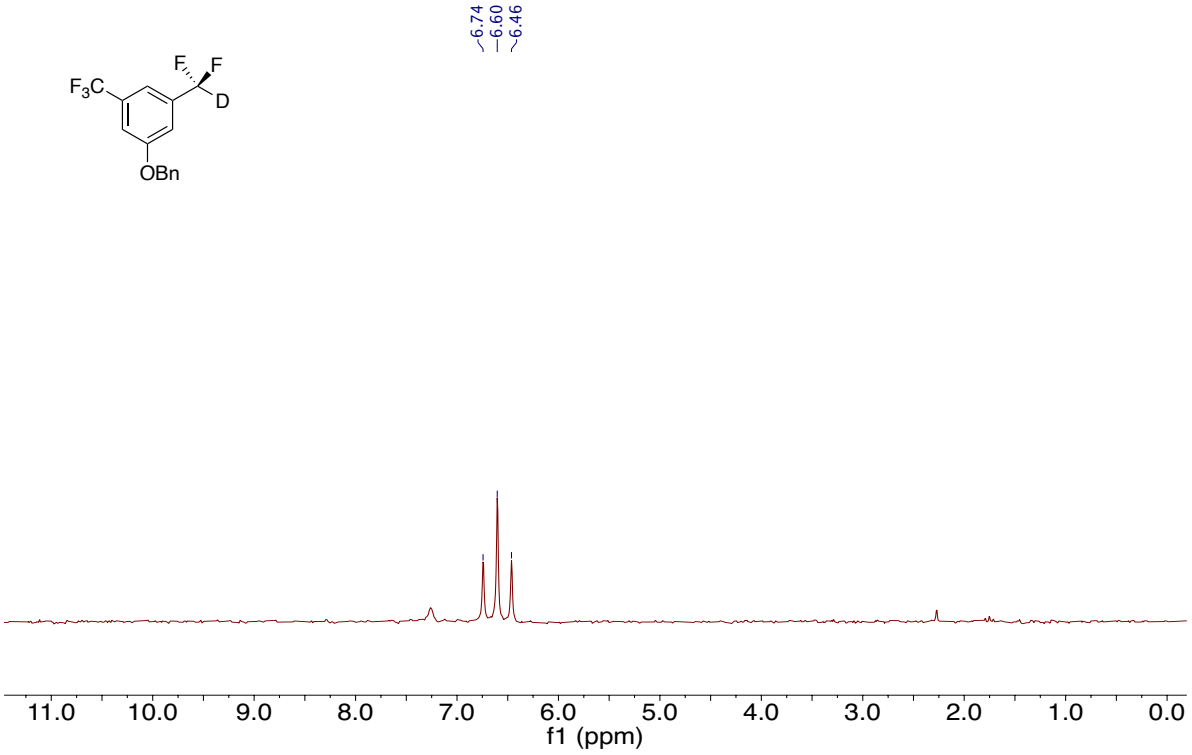

^{2}H NMR of Compound **3-30** (62 MHz, CH_3CN)

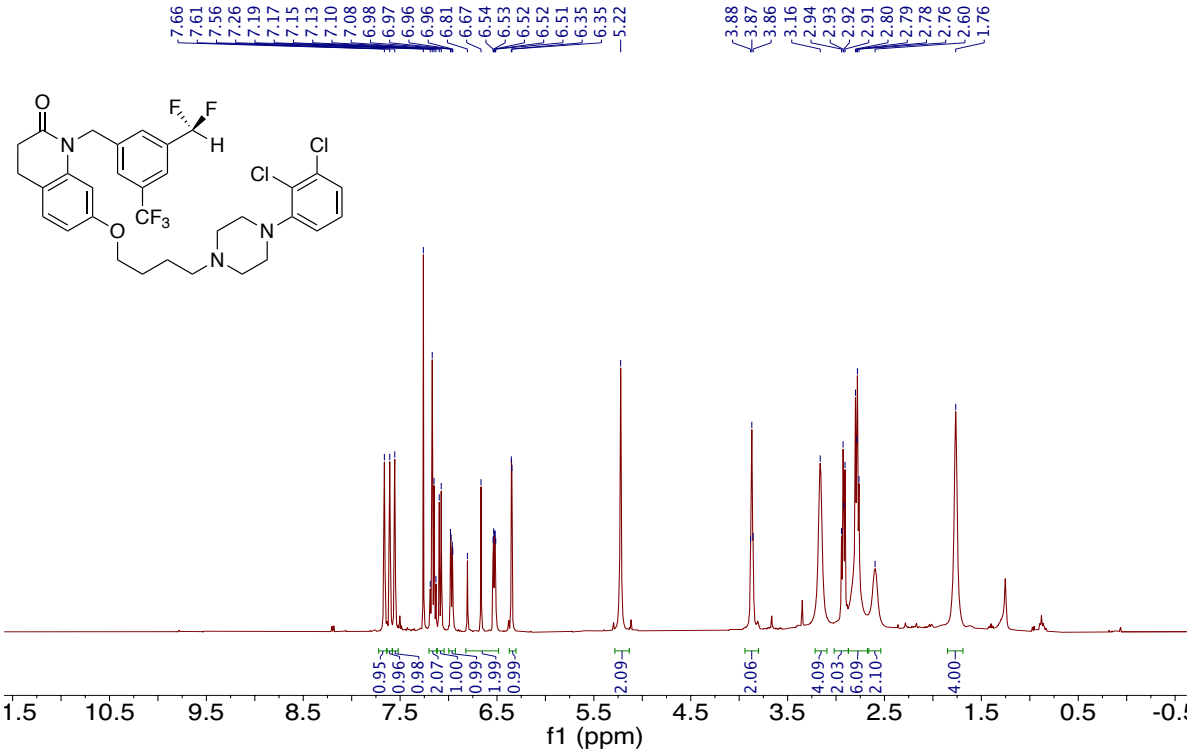

^{1}H NMR of Compound **3-31** (400 MHz, $CDCl_3$)

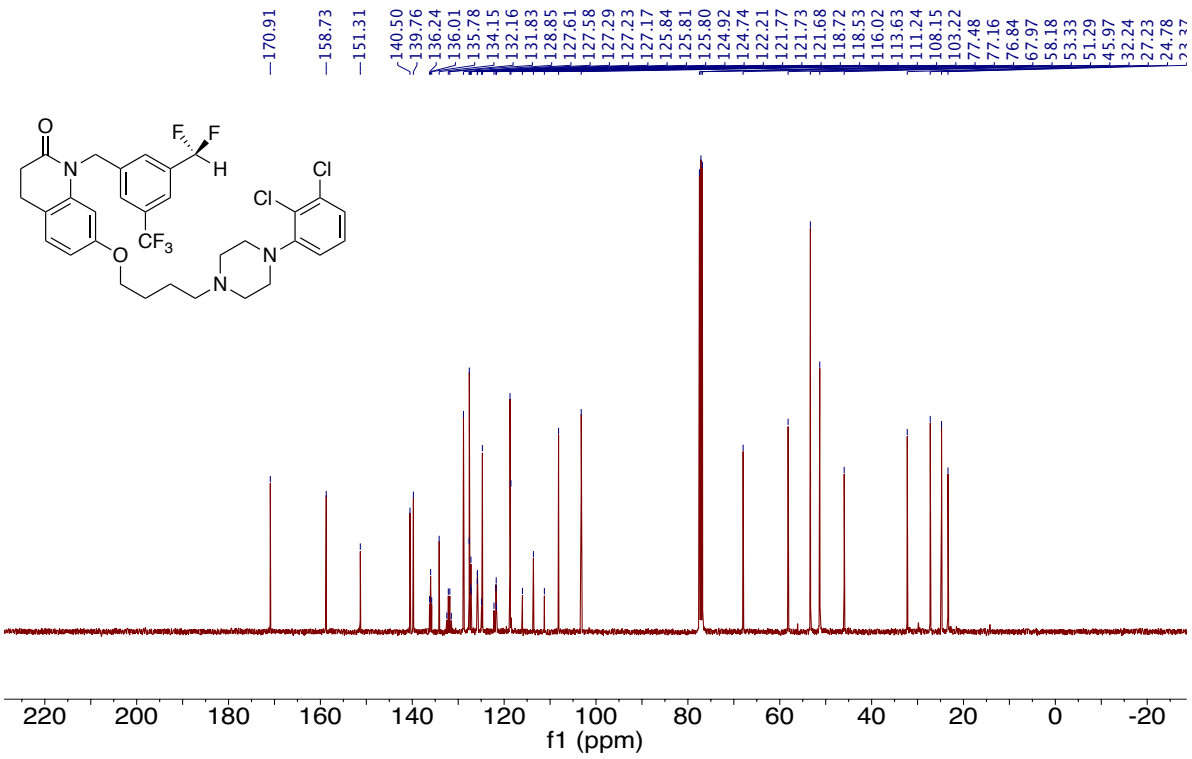

^{13}C NMR of Compound **3-31** (101 MHz, $CDCl_3$)

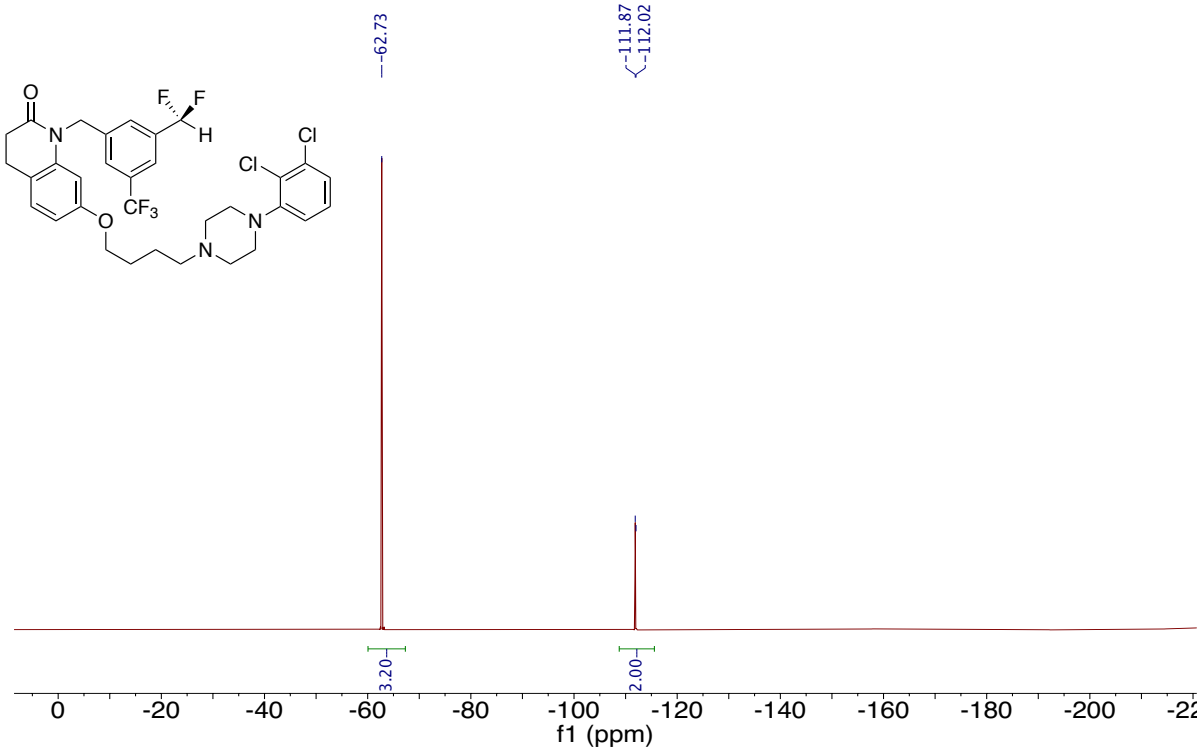

^{19}F NMR of Compound **3-31** (376 MHz, $CDCl_3$)

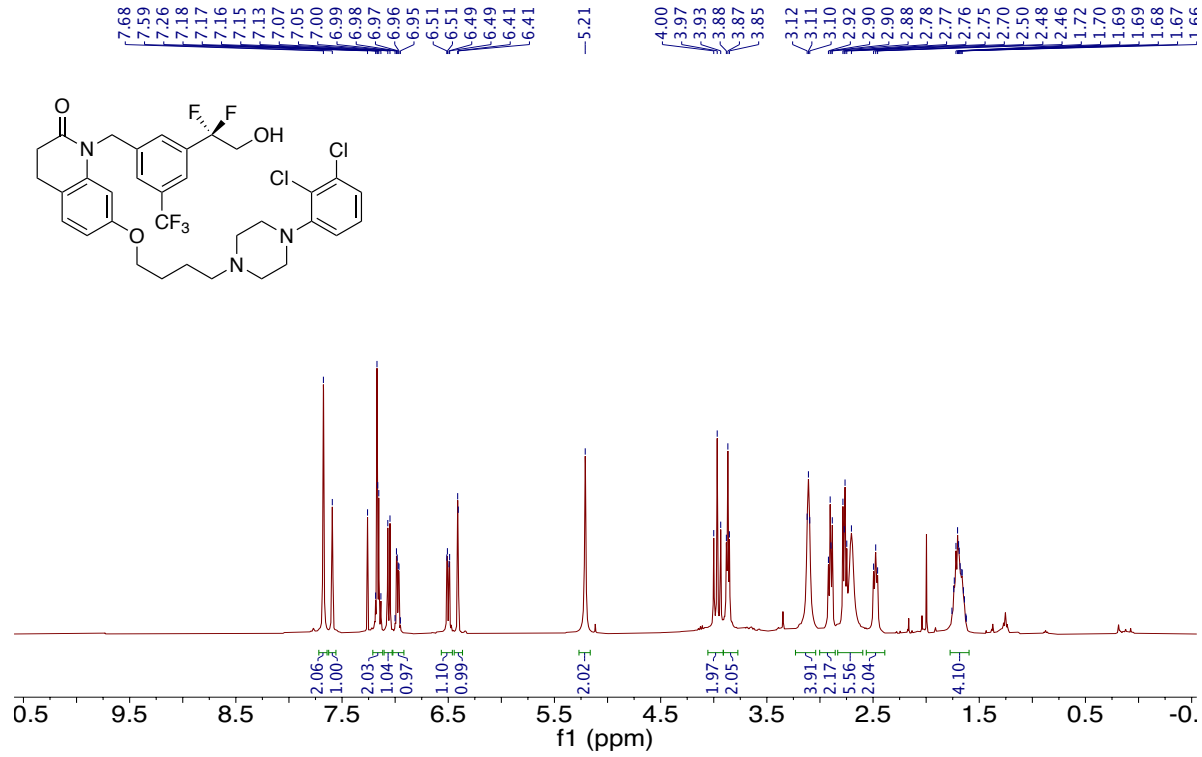

^{1}H NMR of Compound **3-32** (400 MHz, $CDCl_3$)

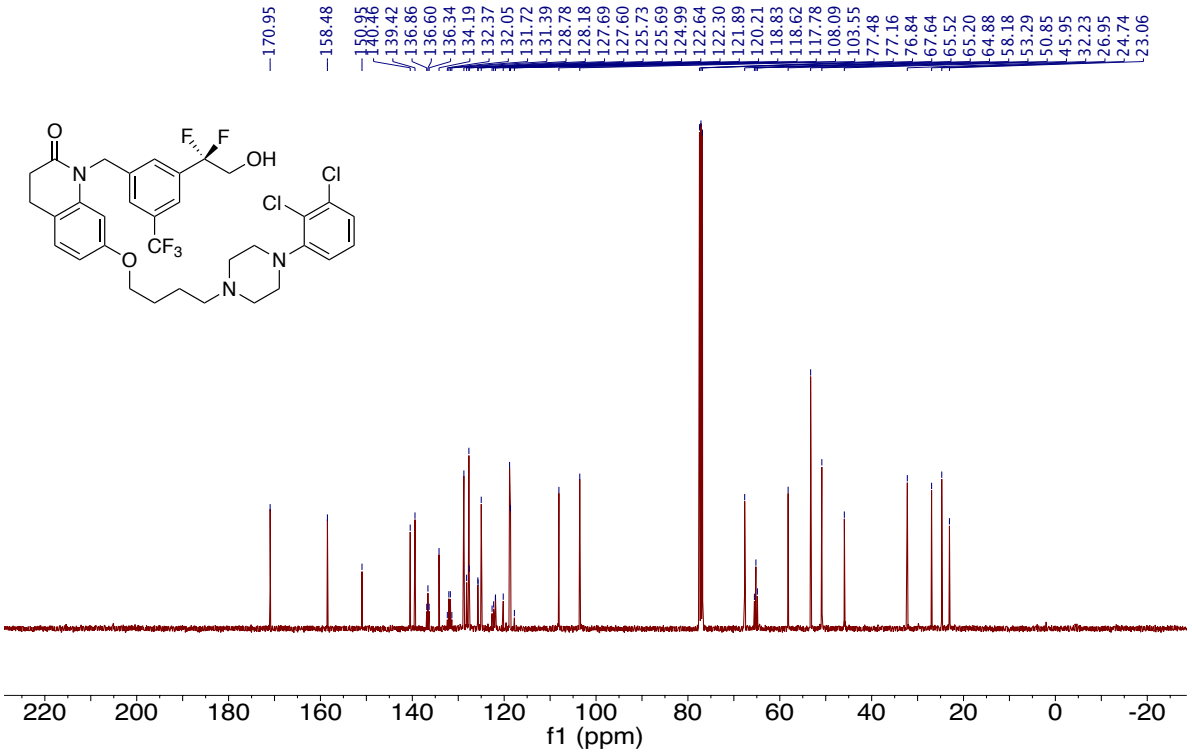

^{13}C NMR of Compound **3-32** (101 MHz, $CDCl_3$)

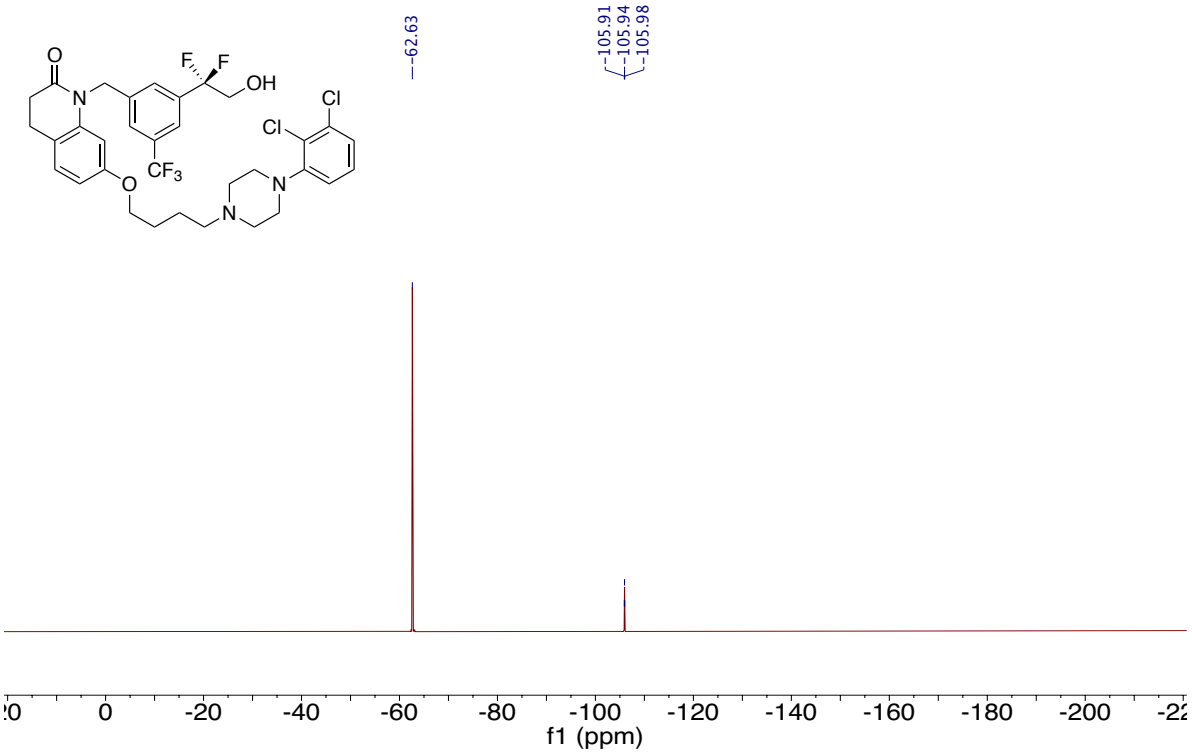

^{19}F NMR of Compound **3-32** (376 MHz, $CDCl_3$)

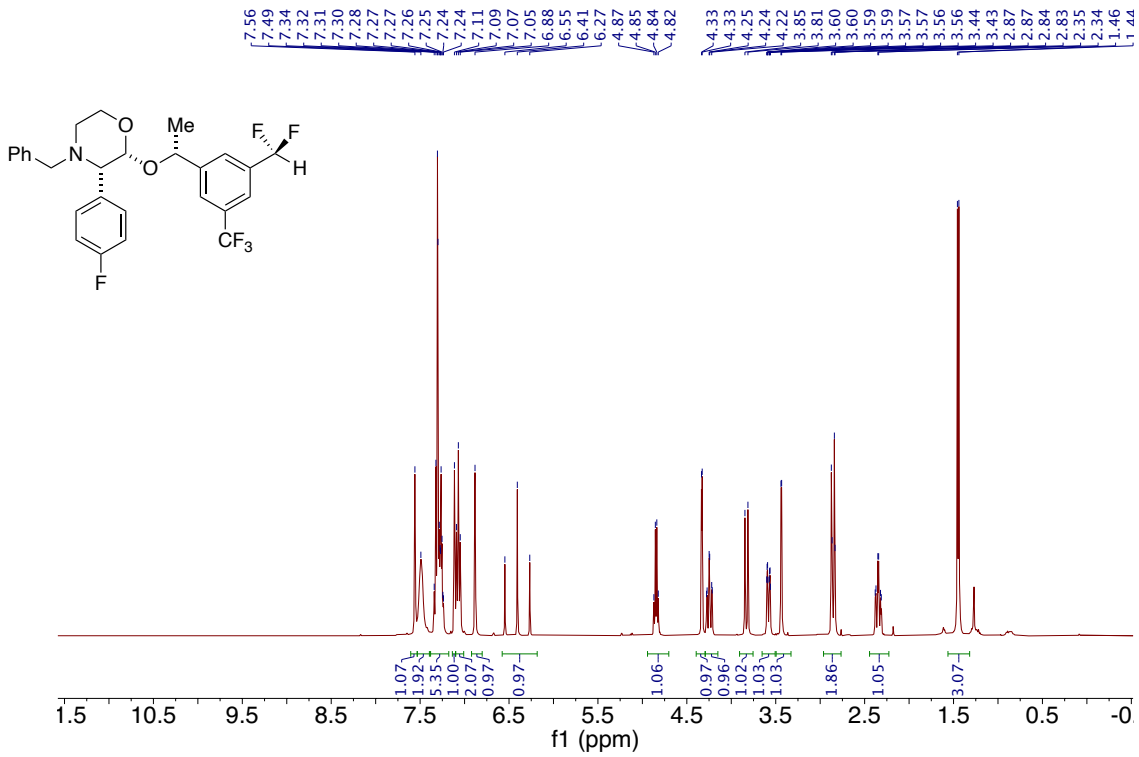

^{1}H NMR of Compound **3-33** (400 MHz, $CDCl_3$)

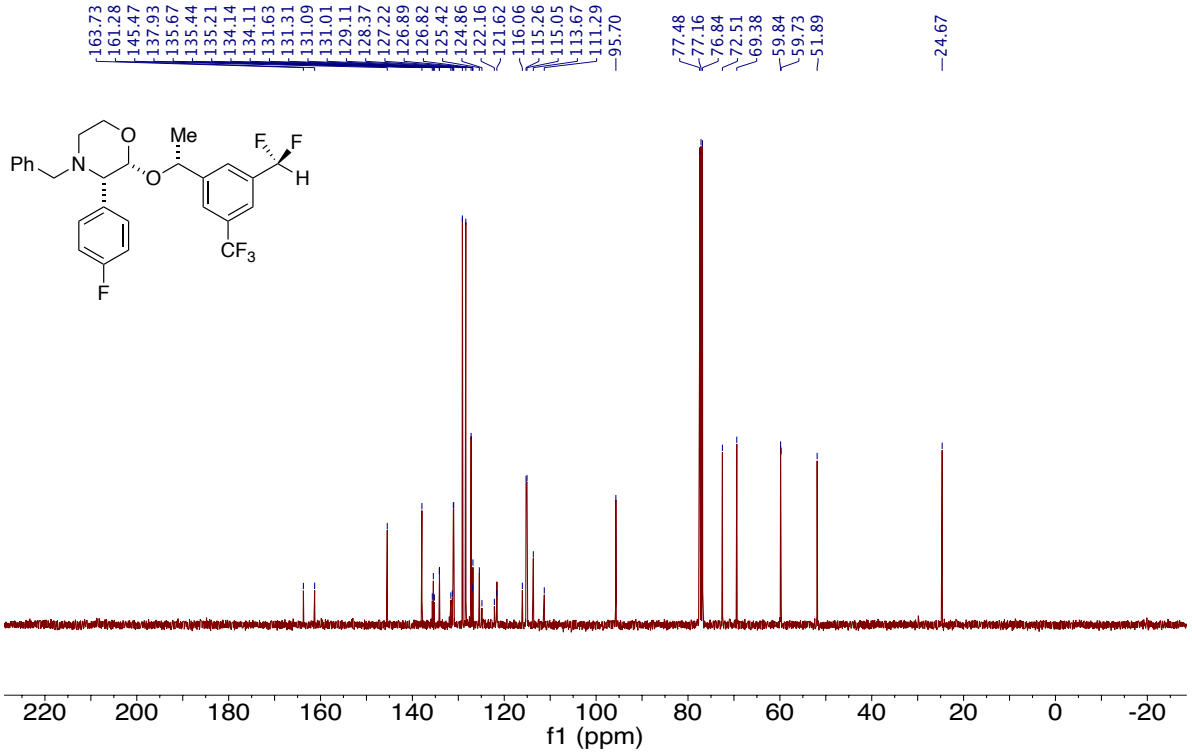

^{13}C NMR of Compound **3-33** (101 MHz, $CDCl_3$)

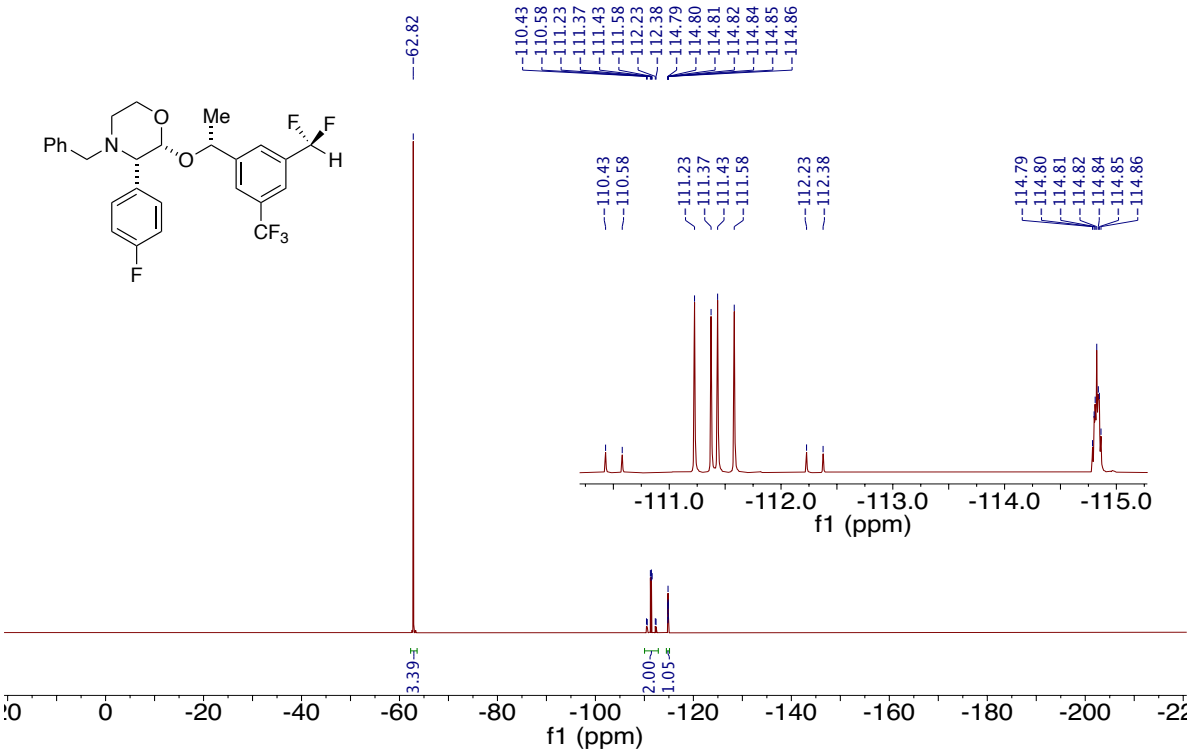

^{19}F NMR of Compound **3-33** (376 MHz, $CDCl_3$)

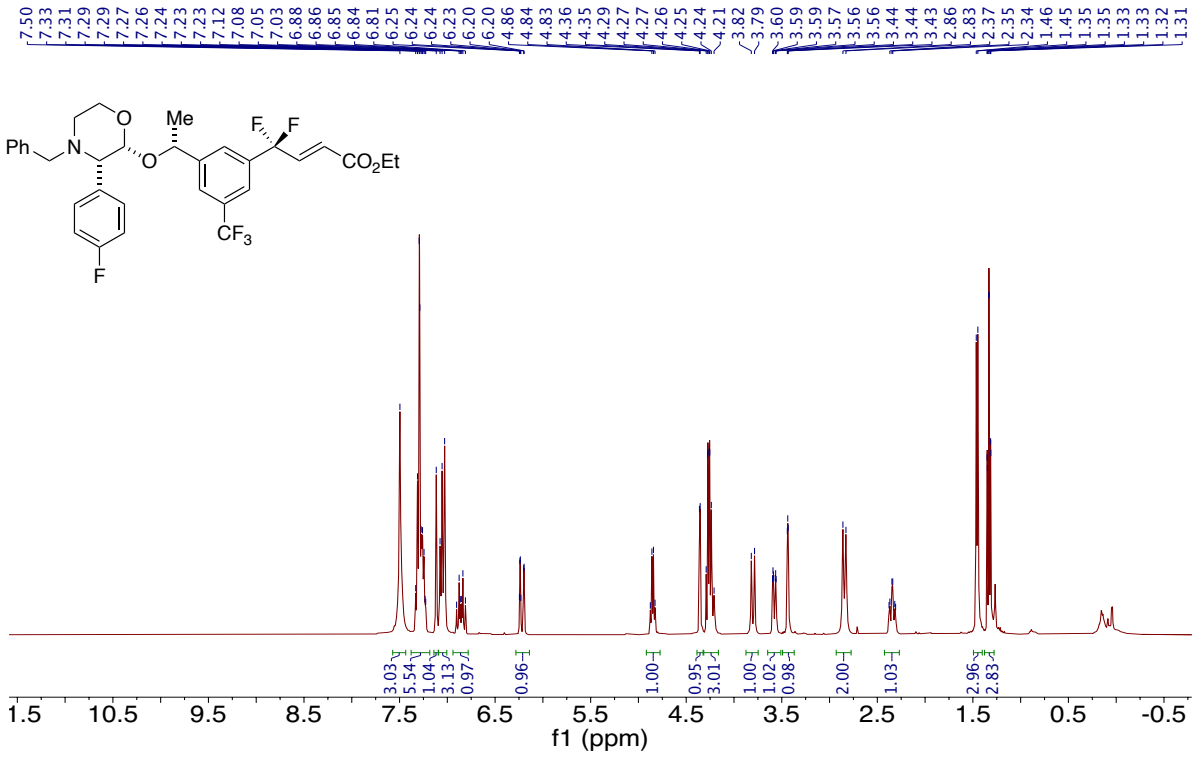

^{1}H NMR of Compound **3-34** (400 MHz, $CDCl_3$)

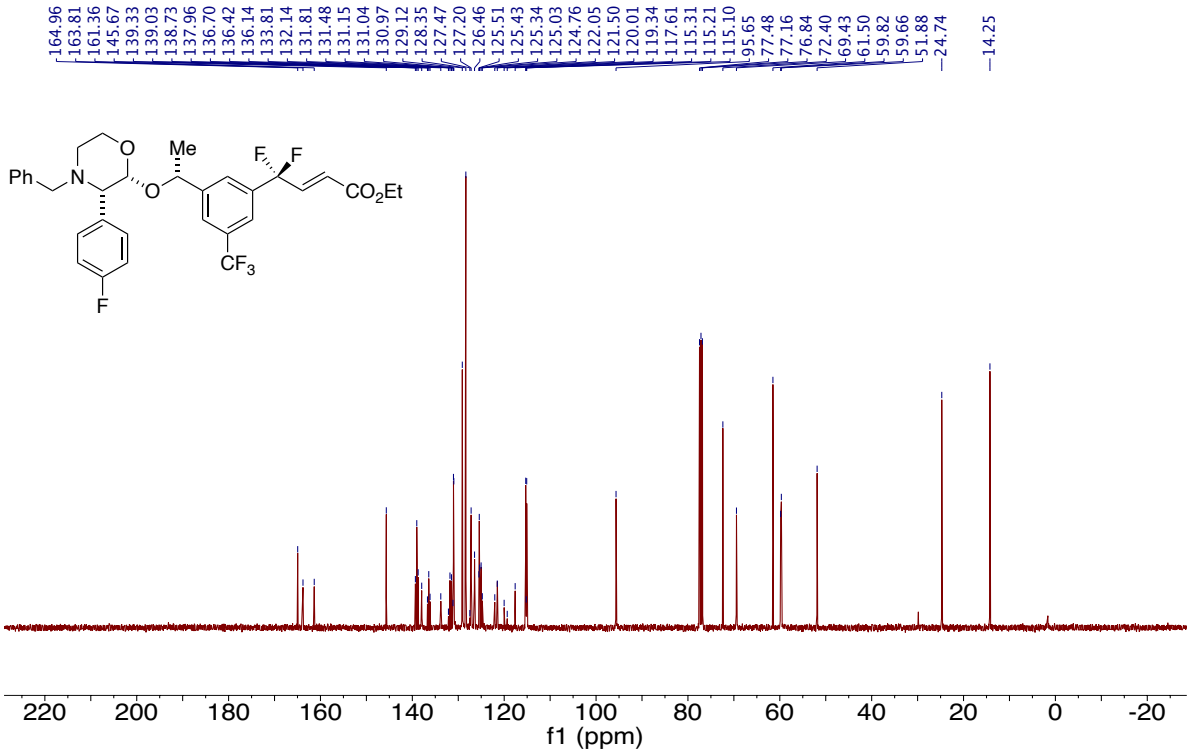

^{13}C NMR of Compound **3-34** (101 MHz, $CDCl_3$)

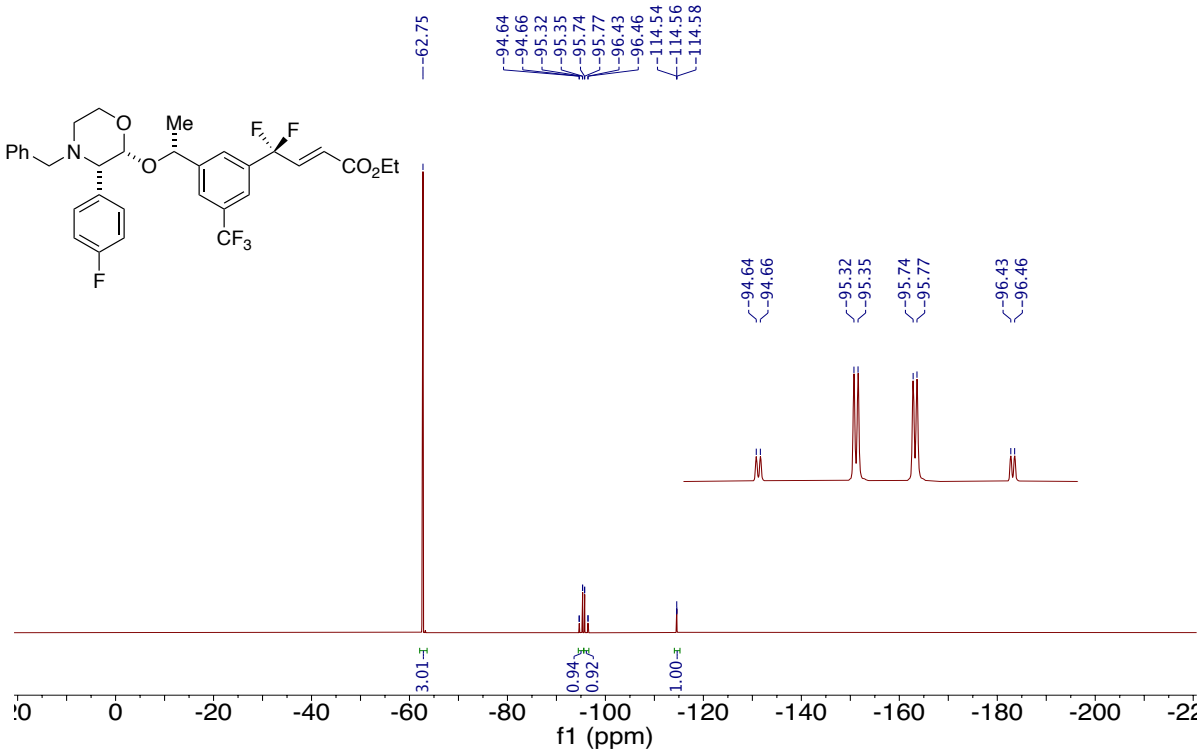

^{19}F NMR of Compound **3-34** (376 MHz, $CDCl_3$)

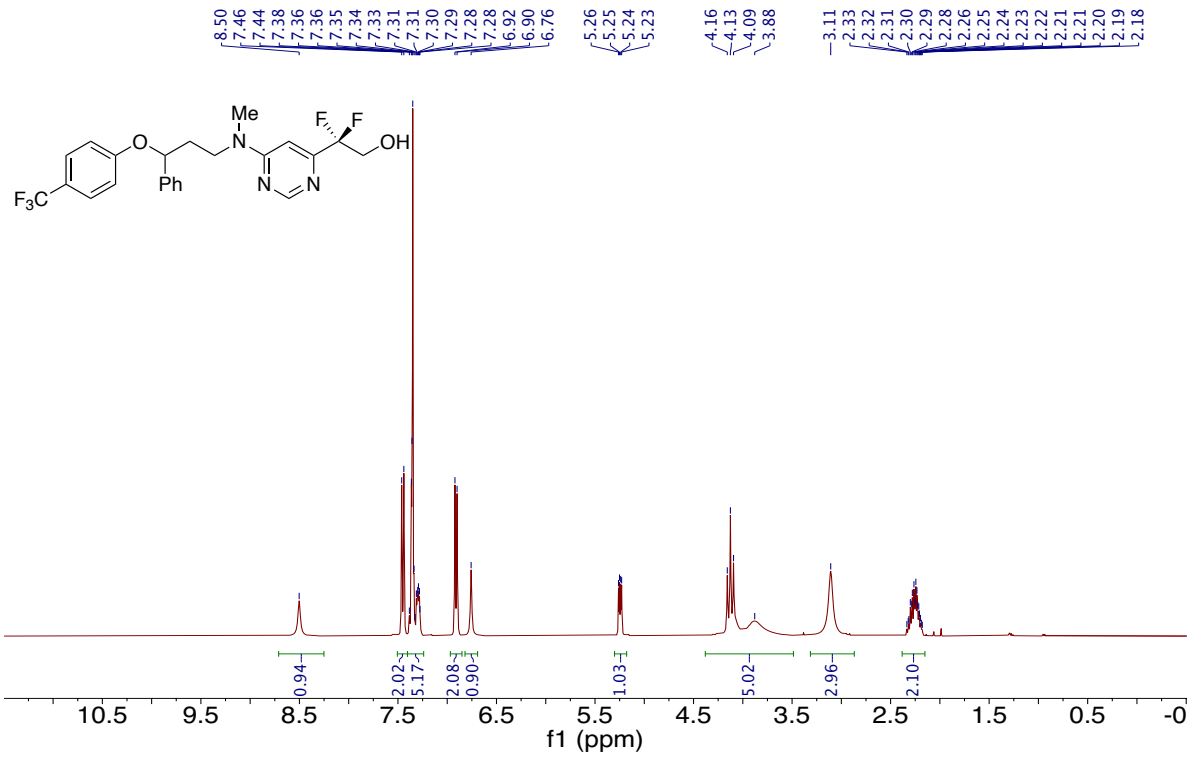

^{1}H NMR of Compound **3-35** (400 MHz, $CDCl_3$)

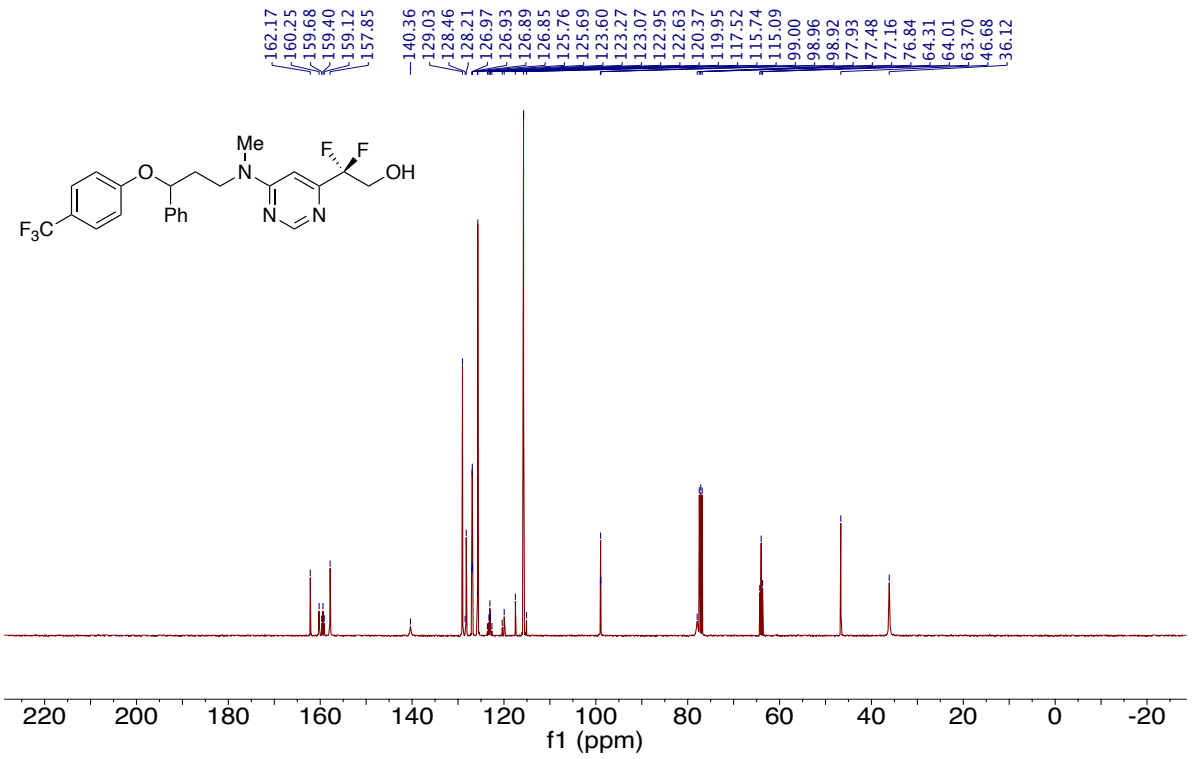

^{13}C NMR of Compound **3-35** (101 MHz, $CDCl_3$)

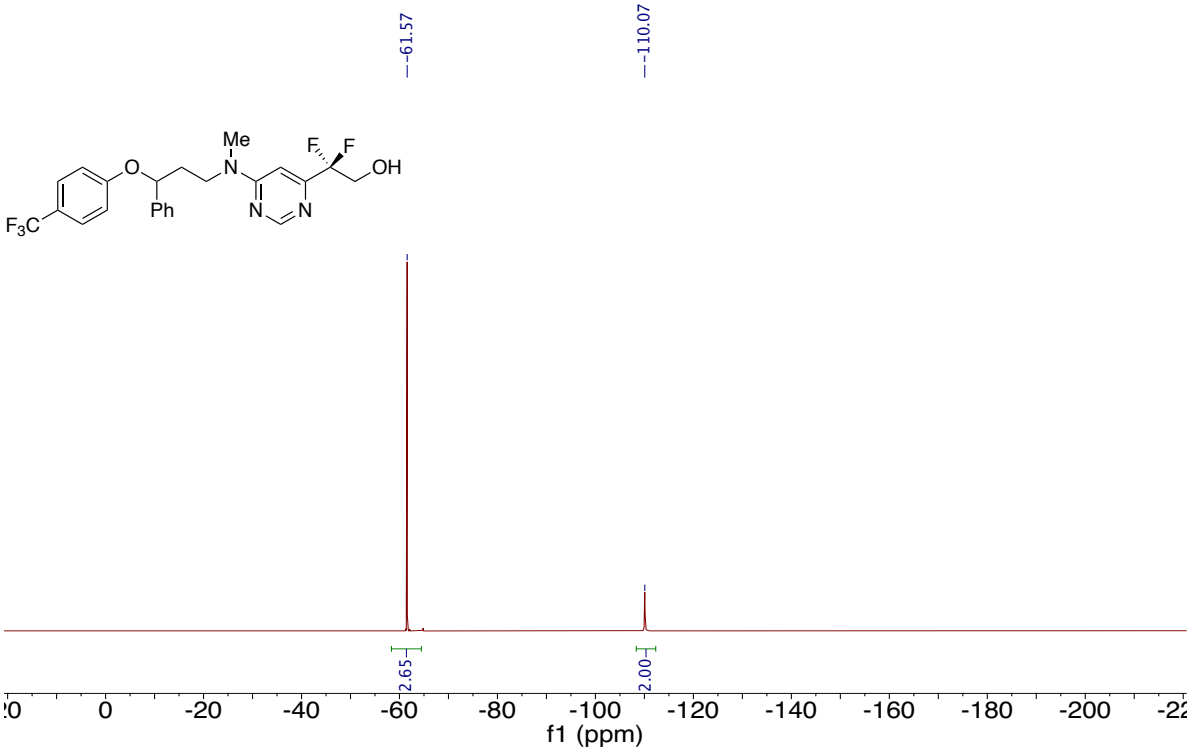

^{19}F NMR of Compound **3-35** (376 MHz, $CDCl_3$)

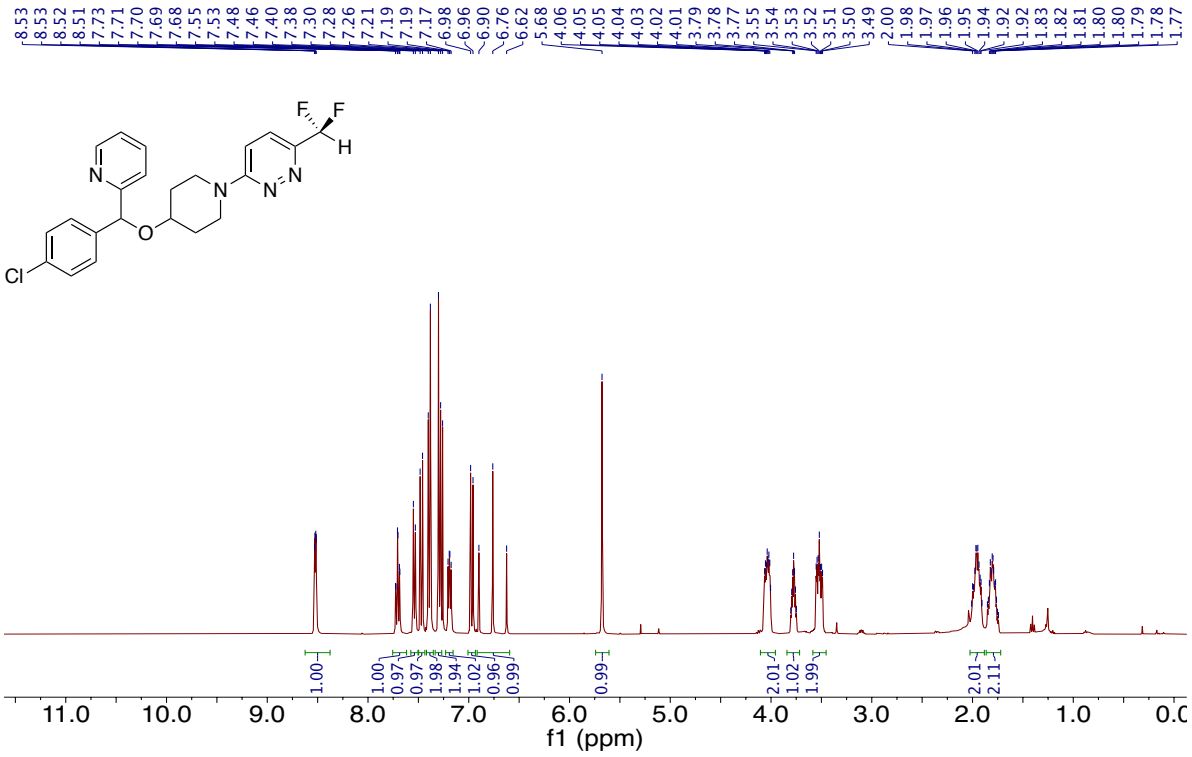

^{1}H NMR of Compound **3-36** (400 MHz, $CDCl_3$)

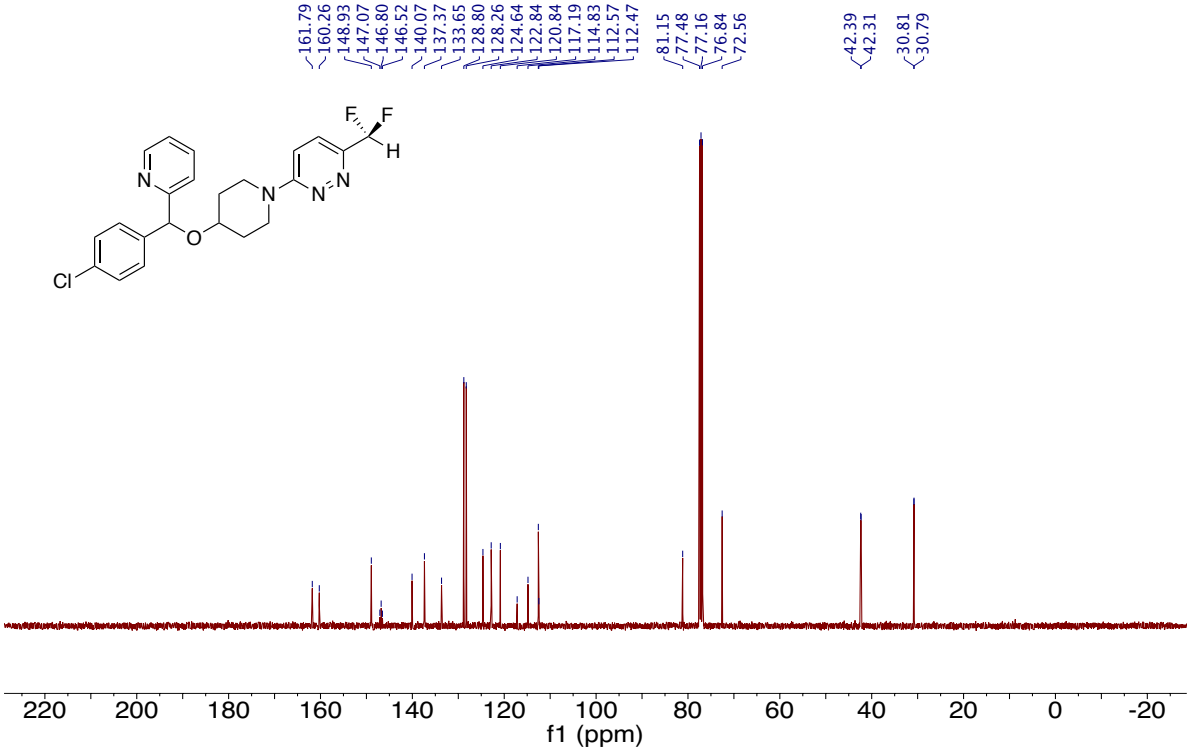

^{13}C NMR of Compound **3-36** (101 MHz, $CDCl_3$)

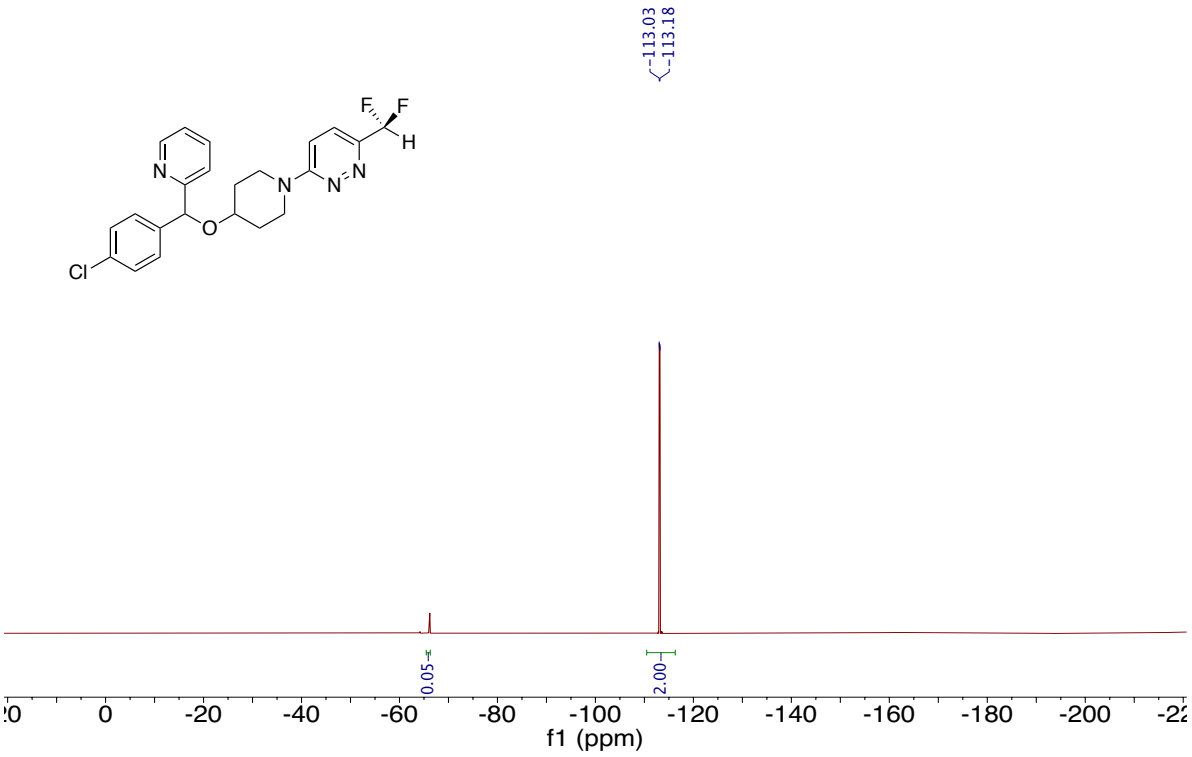

^{19}F NMR of Compound **3-36** (376 MHz, $CDCl_3$)

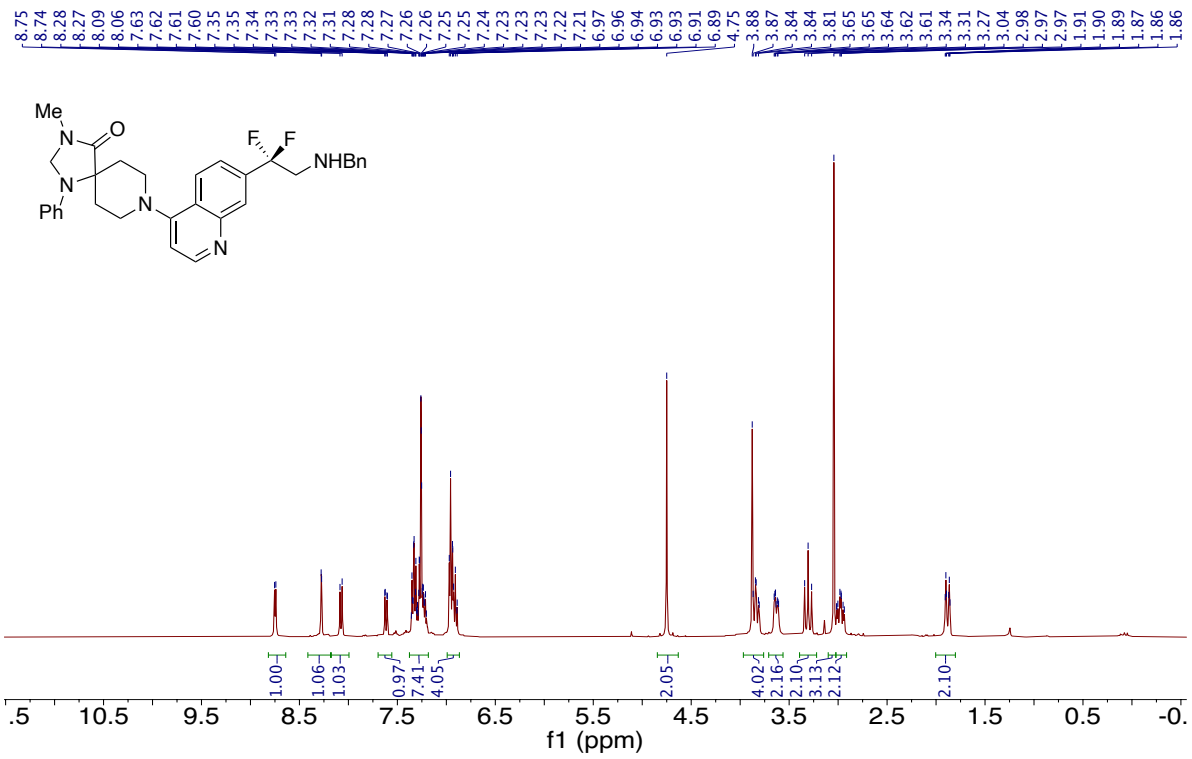

^{1}H NMR of Compound **3-37** (400 MHz, $CDCl_3$)

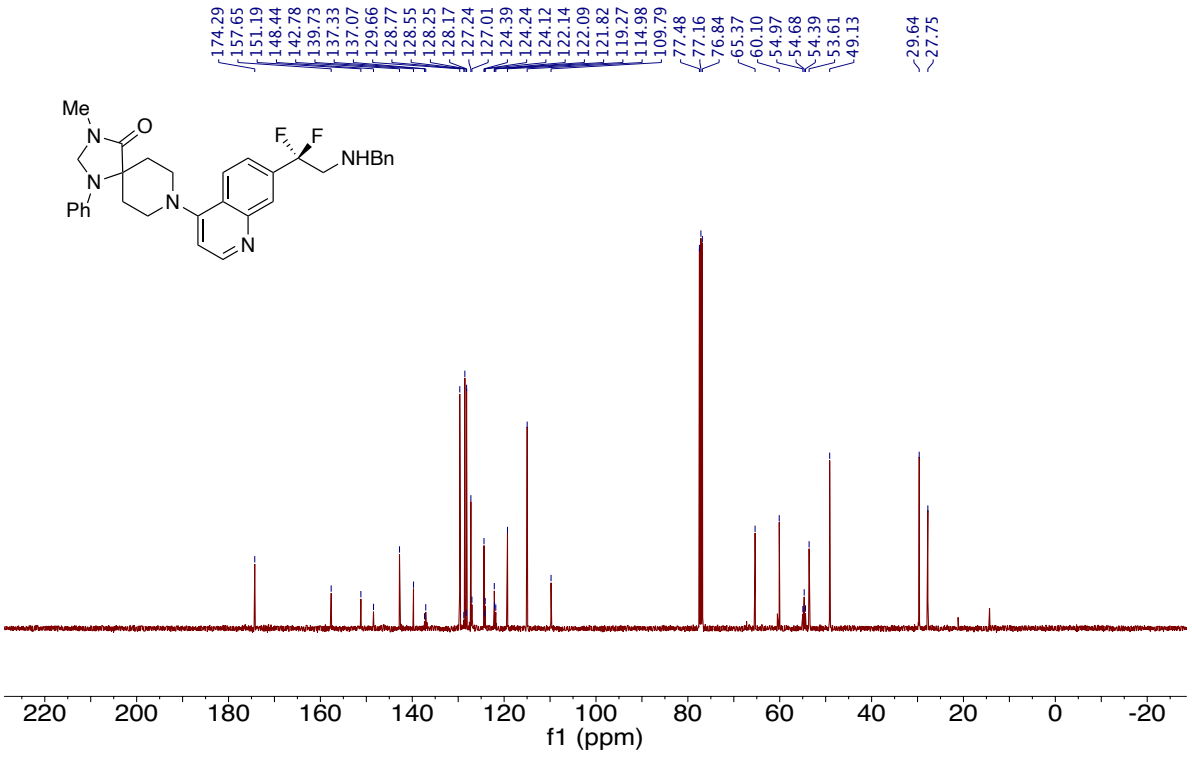

^{13}C NMR of Compound **3-37** (101 MHz, $CDCl_3$)

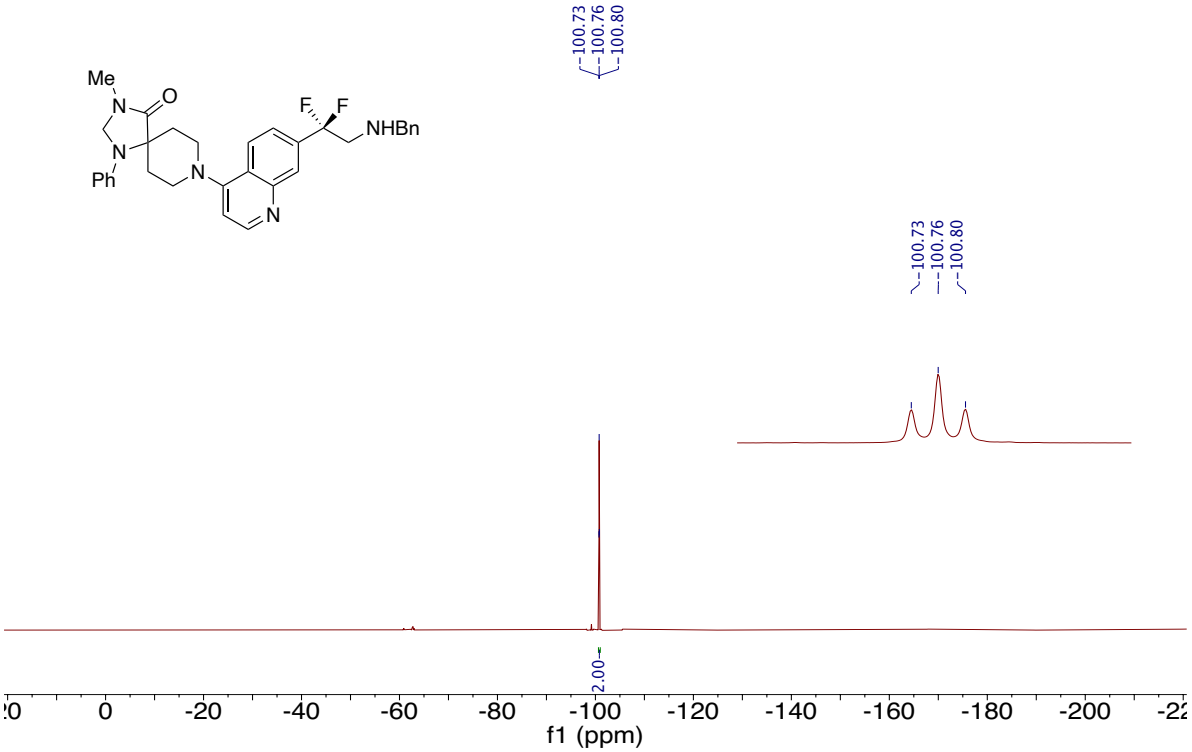

^{19}F NMR of Compound **3-37** (376 MHz, $CDCl_3$)

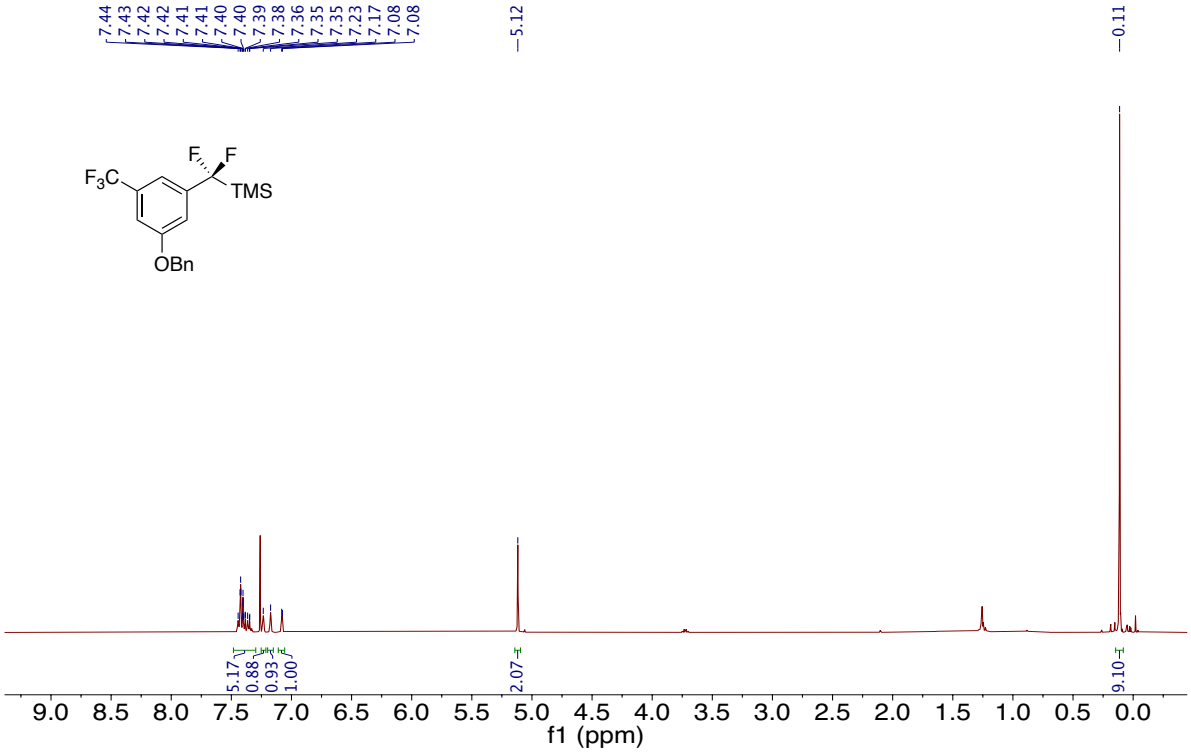

^{1}H NMR of Compound **3-38** (400 MHz, $CDCl_3$)

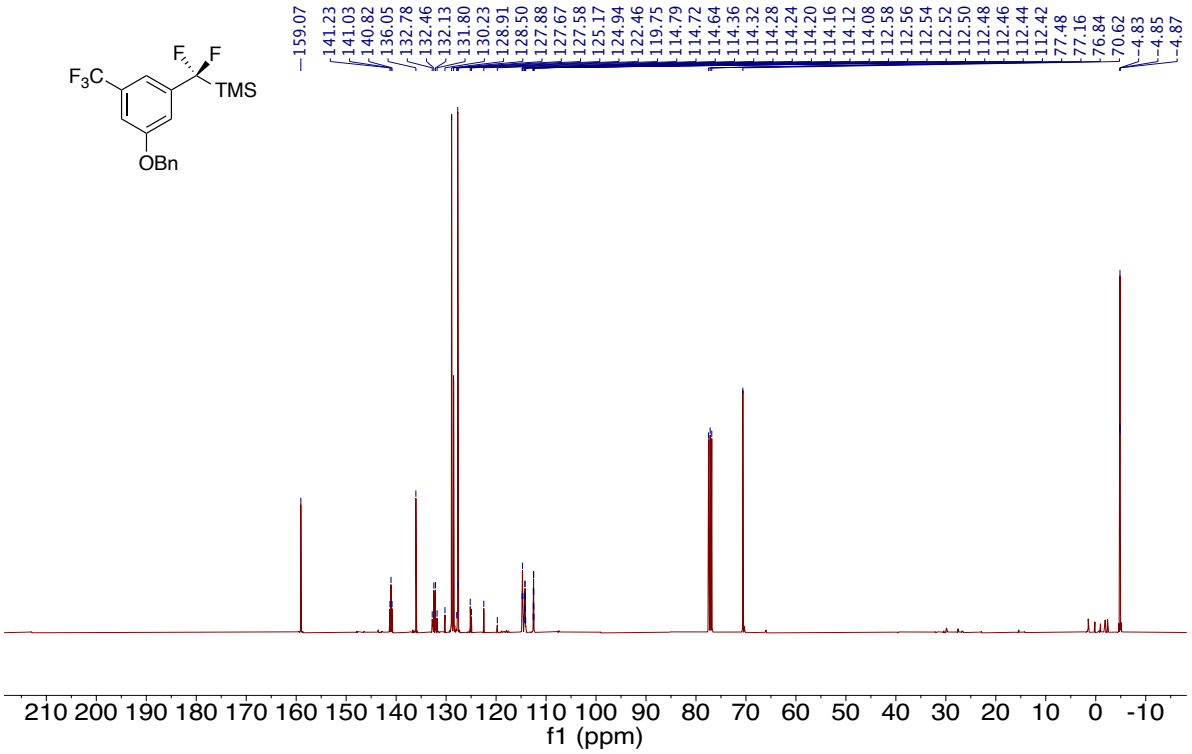

^{13}C NMR of Compound **3-38** (101 MHz, $CDCl_3$)

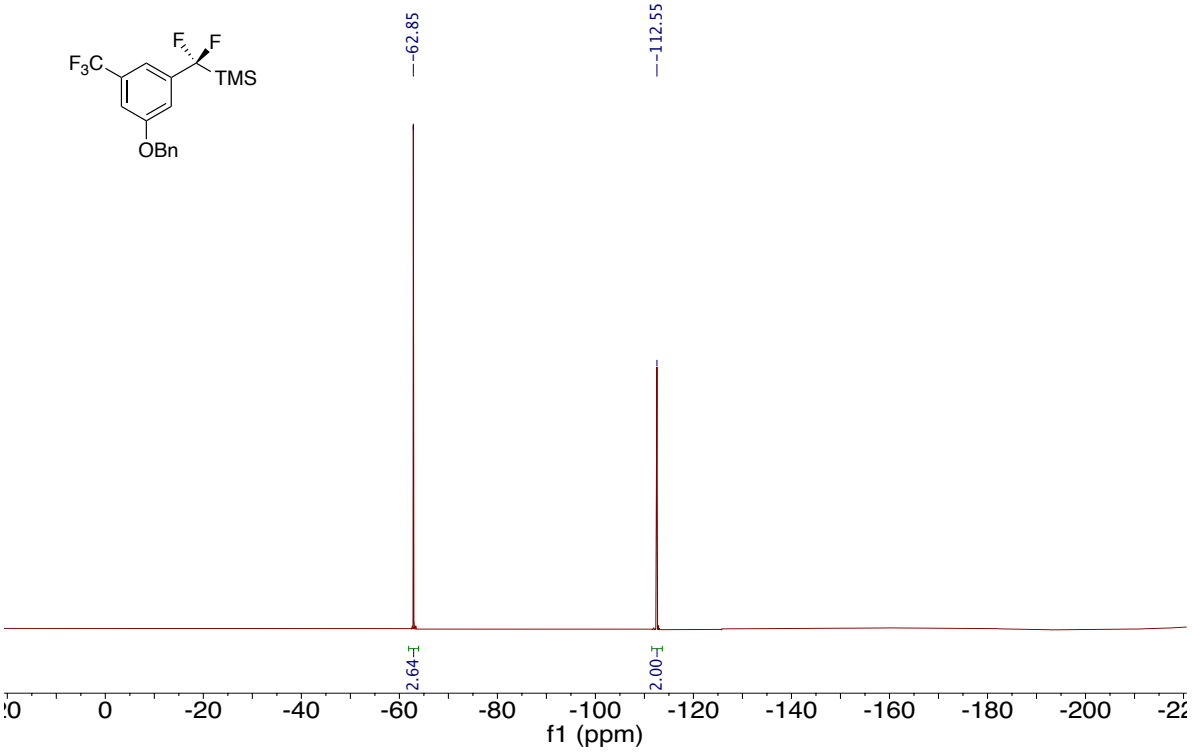

^{19}F NMR of Compound **3-38** (376 MHz, $CDCl_3$)

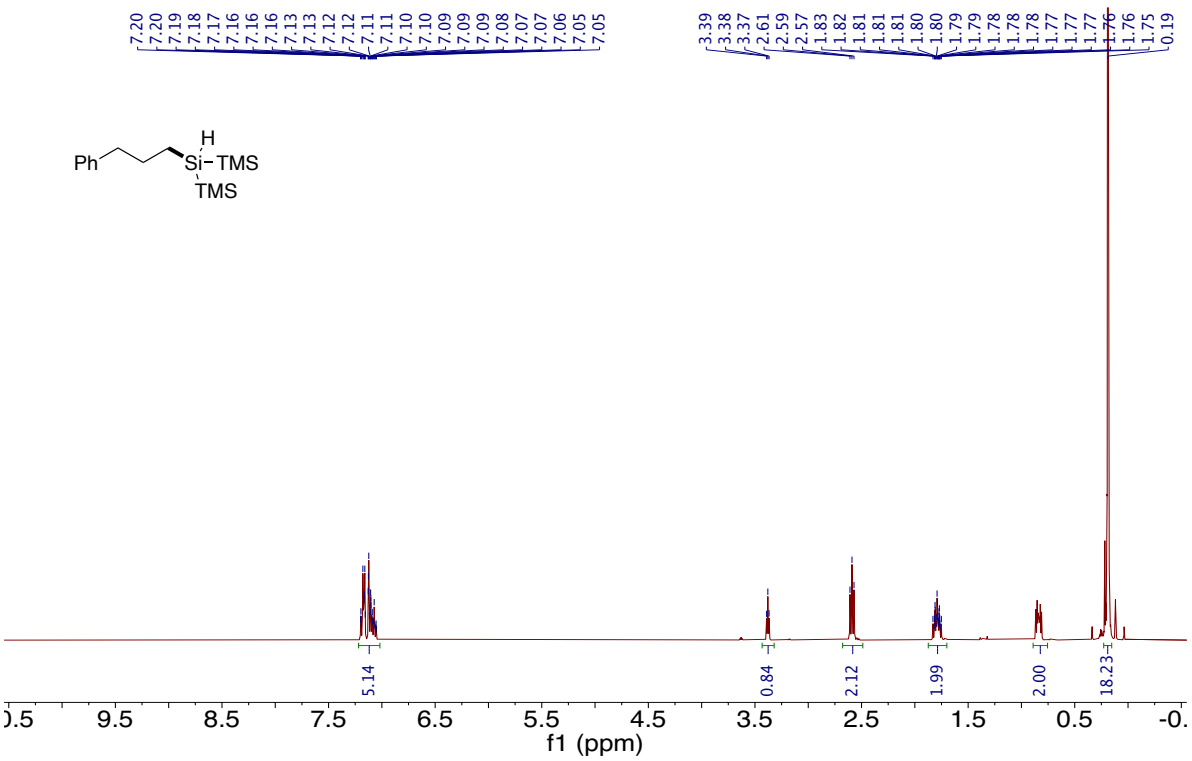

^{1}H NMR of Compound **3-40** (400 MHz, C_6D_6)

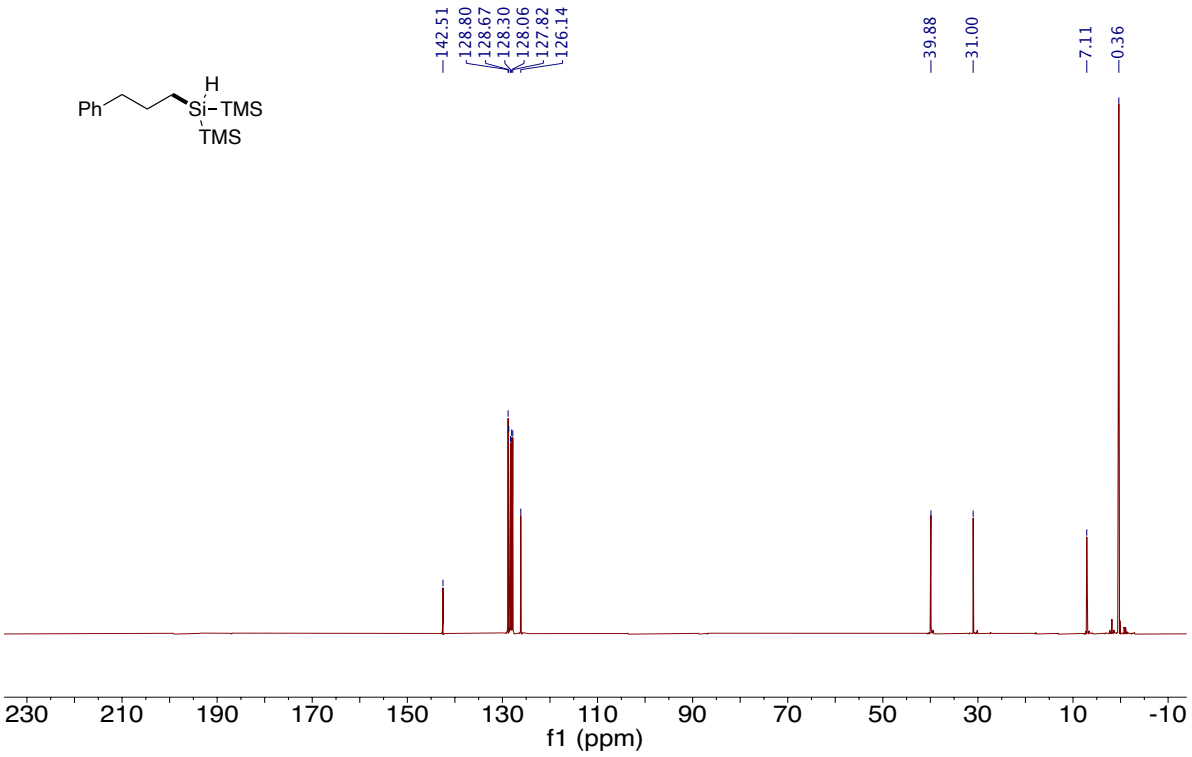

^{13}C NMR of Compound **3-40** (101 MHz, C_6D_6)

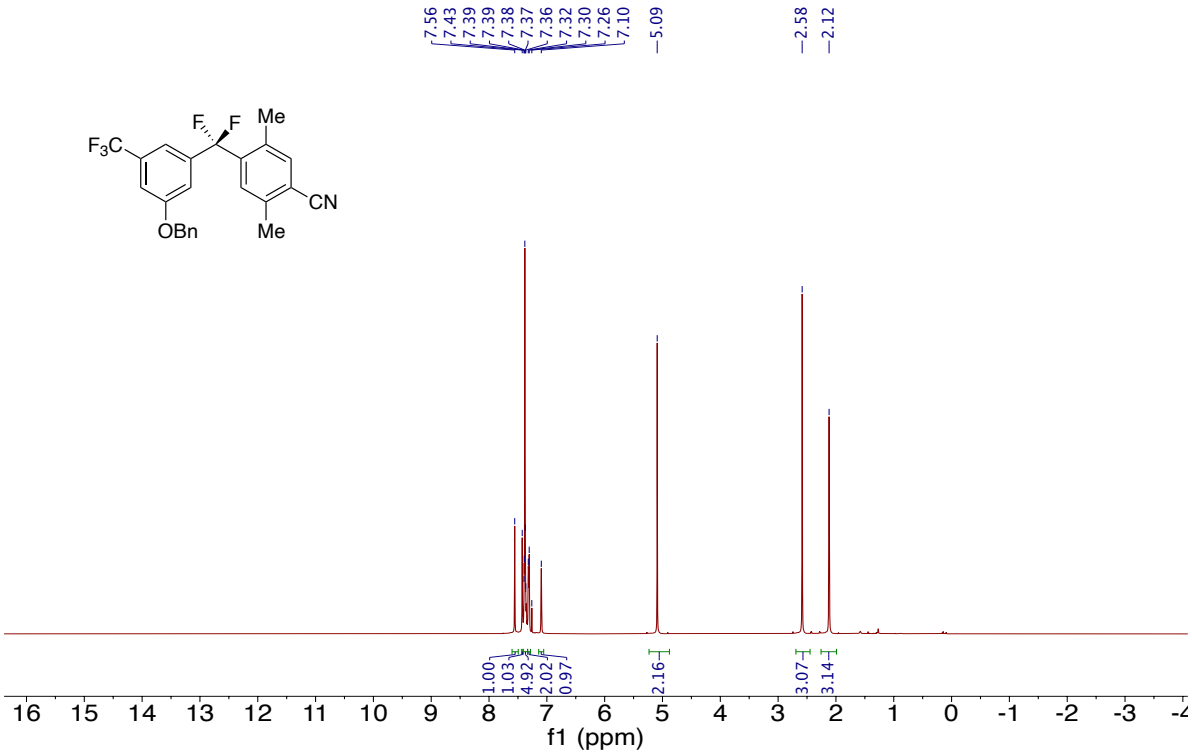

^{1}H NMR of Compound **3-41** (400 MHz, $CDCl_3$)

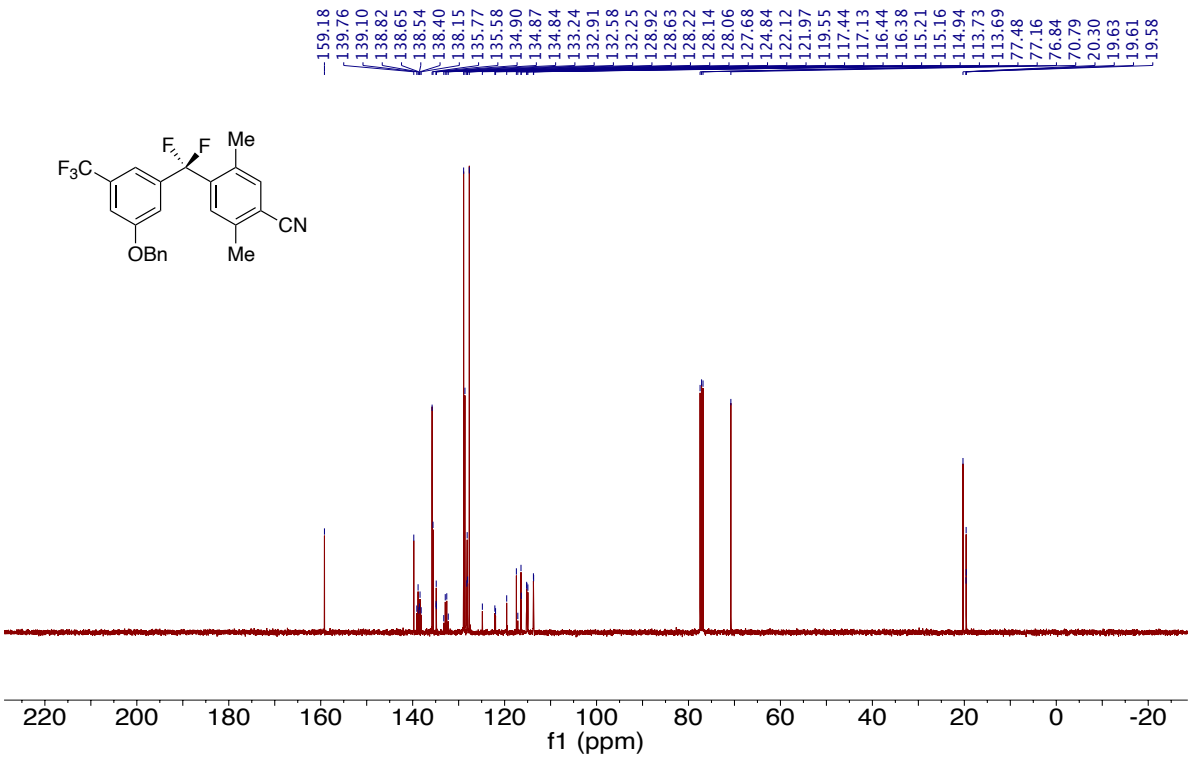

^{13}C NMR of Compound **3-41** (101 MHz, $CDCl_3$)

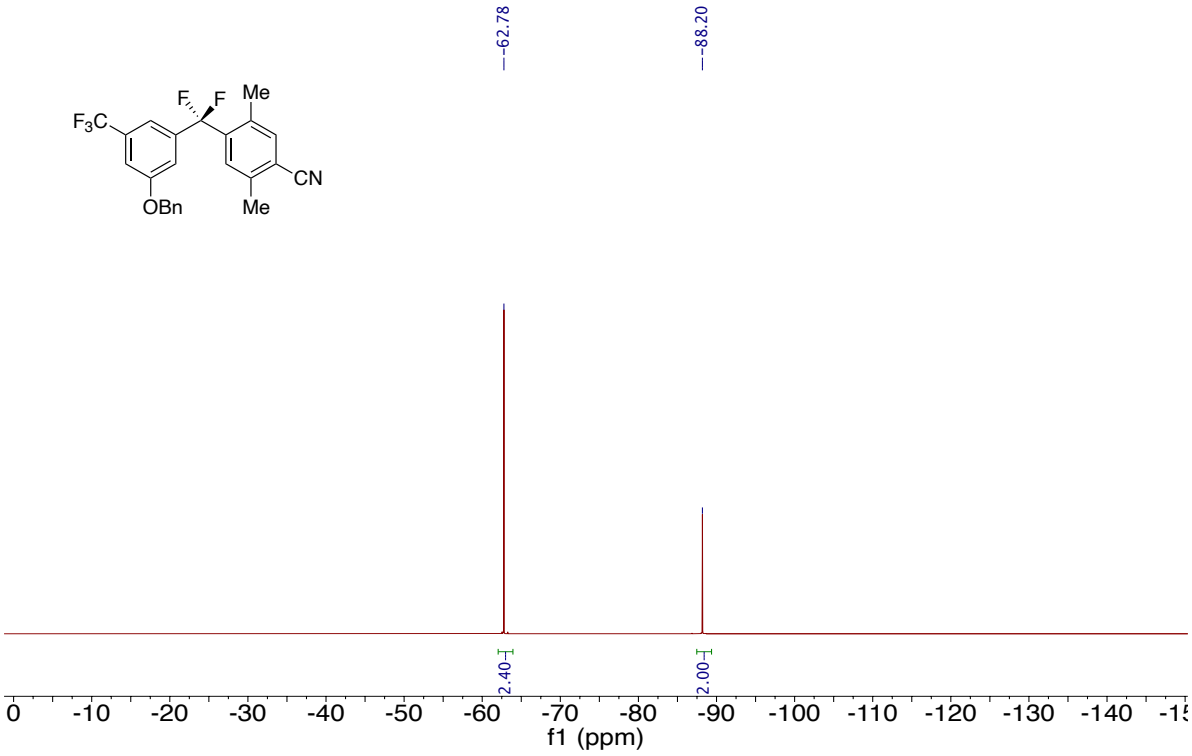

^{19}F NMR of Compound **3-41** (376 MHz, $CDCl_3$)

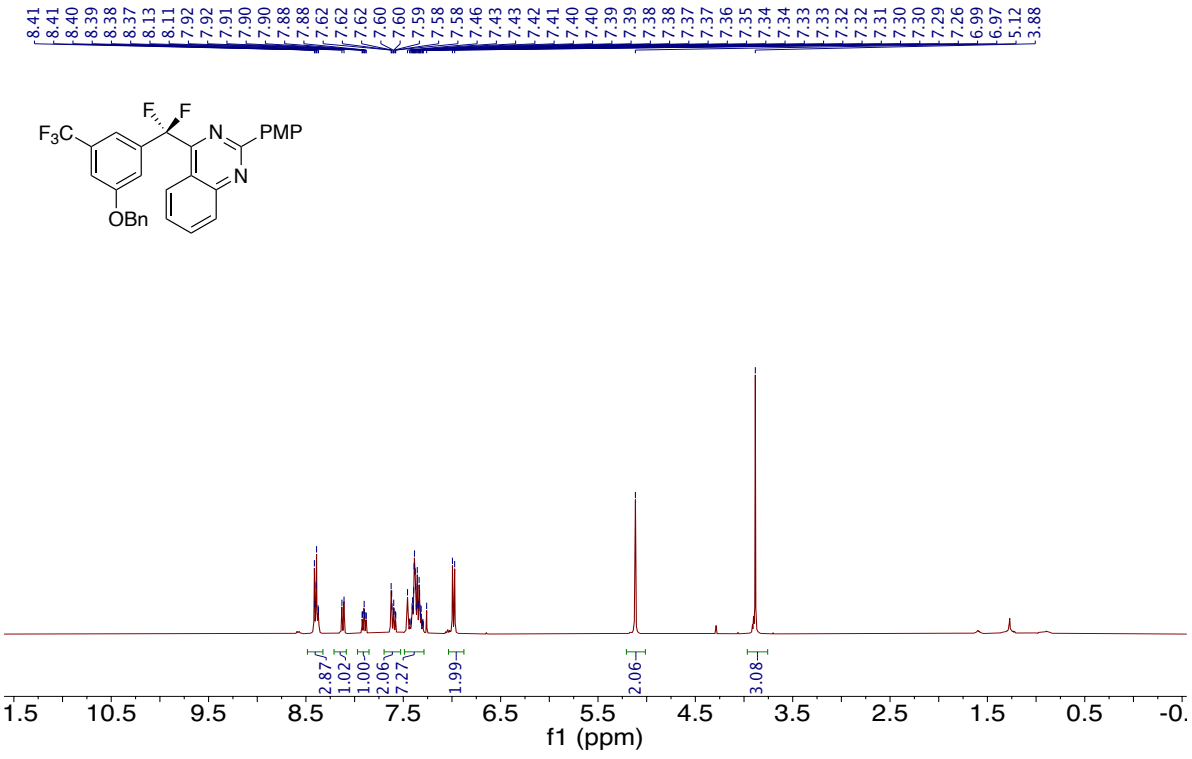

^{1}H NMR of Compound **3-42** (400 MHz, $CDCl_3$)

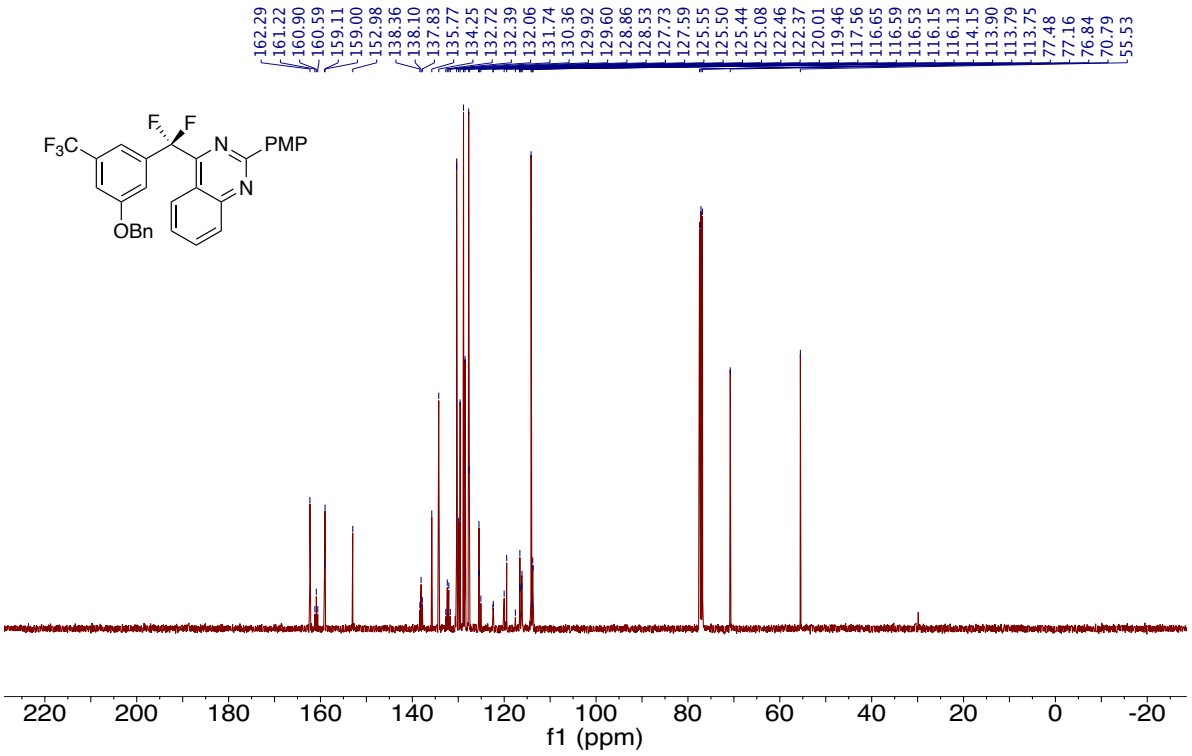

^{13}C NMR of Compound **3-42** (101 MHz, $CDCl_3$)

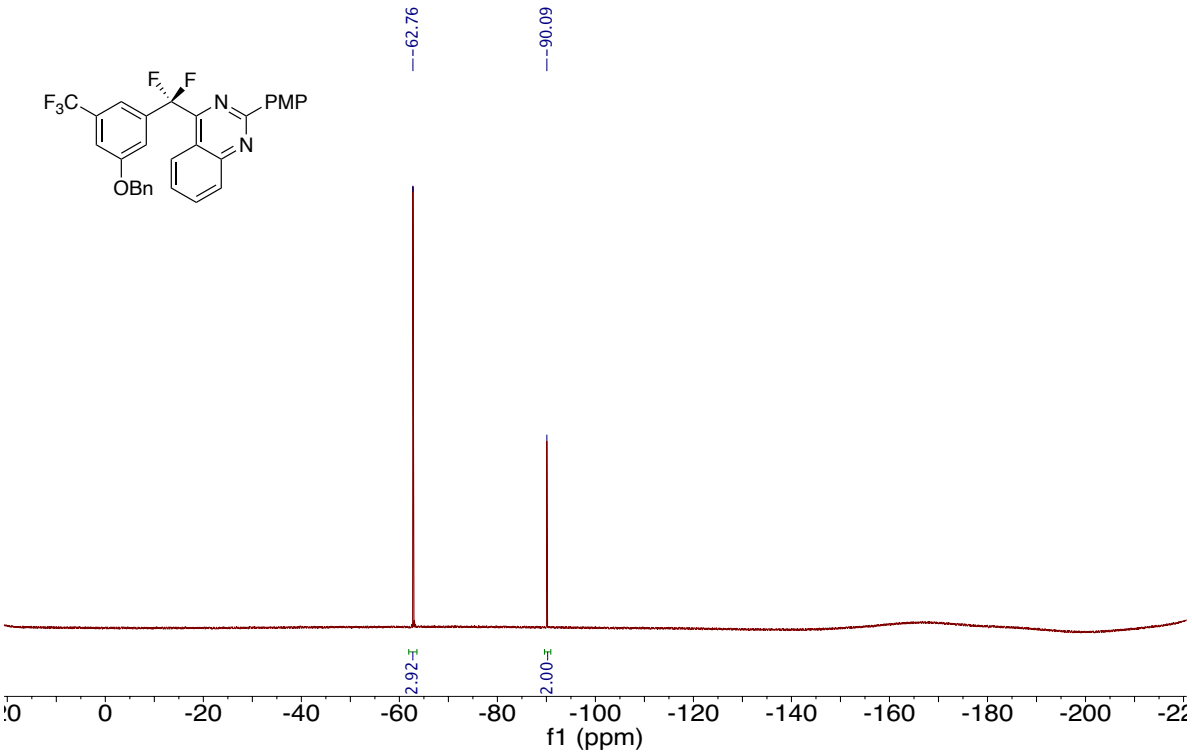

^{19}F NMR of Compound **3-42** (376 MHz, $CDCl_3$)

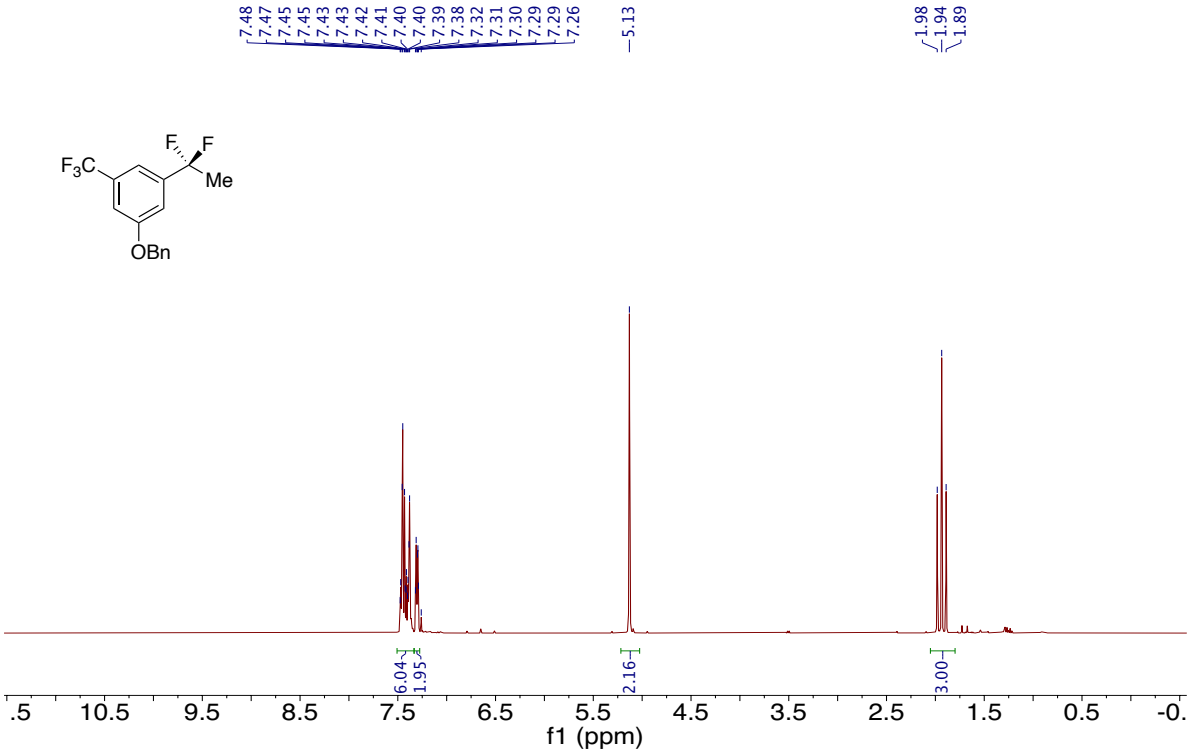

^{1}H NMR of Compound **3-43** (400 MHz, $CDCl_3$)

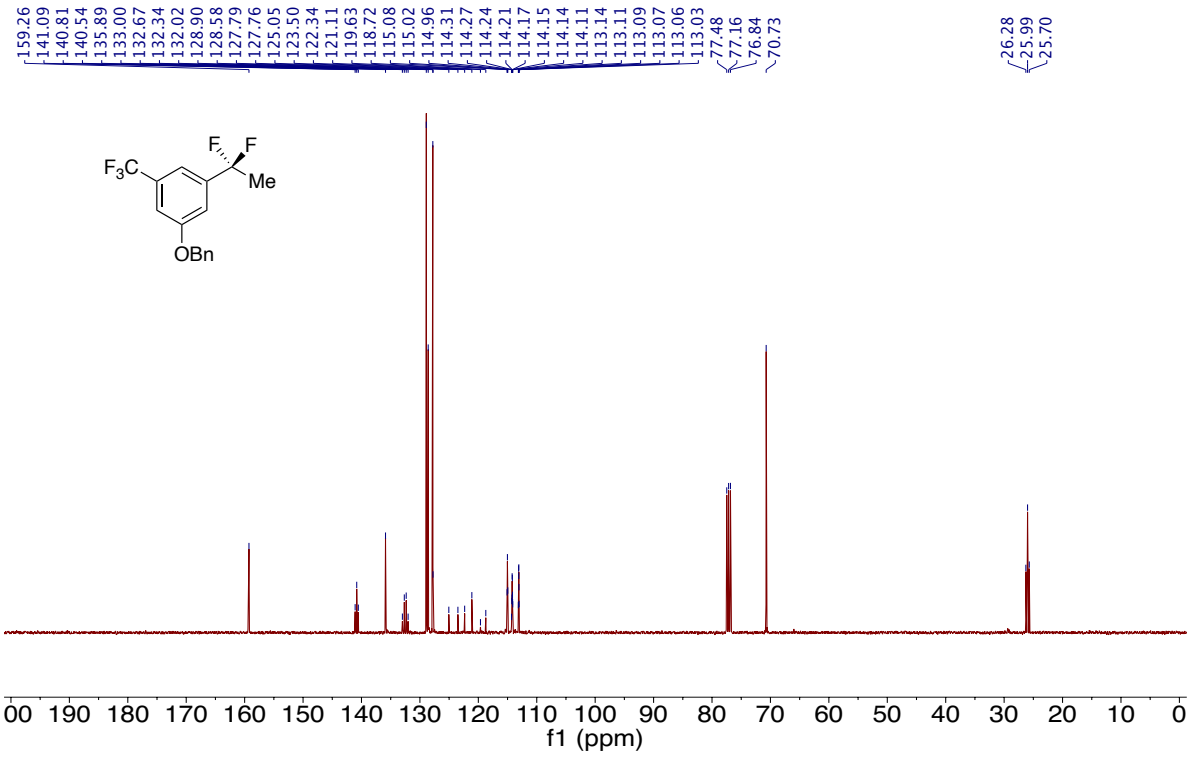

^{13}C NMR of Compound **3-43** (101 MHz, $CDCl_3$)

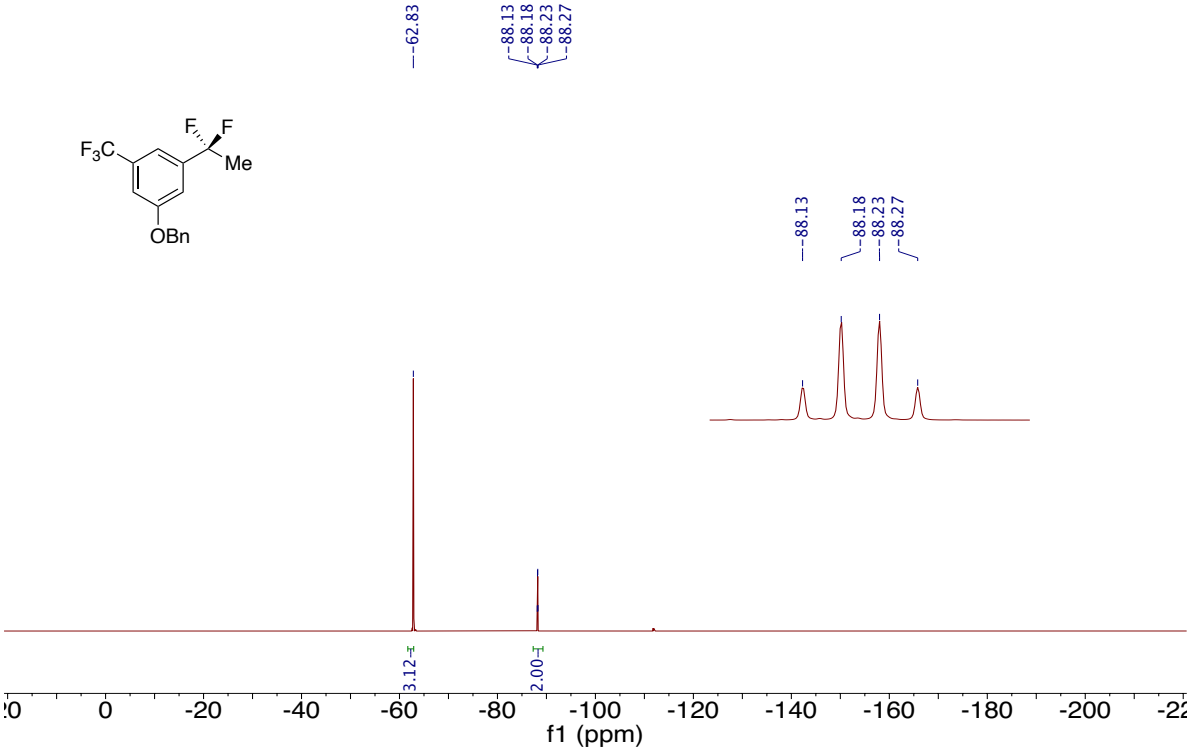

^{19}F NMR of Compound **3-43** (376 MHz, $CDCl_3$)

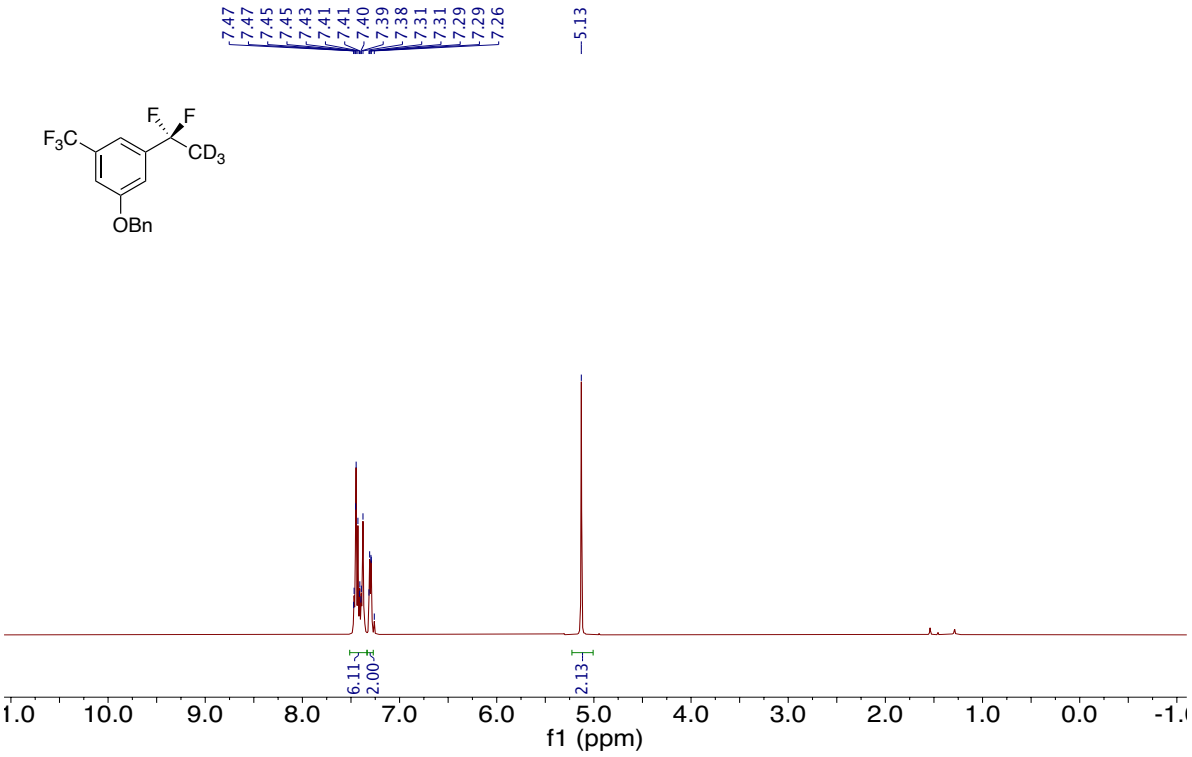

^{1}H NMR of Compound **3-44** (400 MHz, $CDCl_3$)

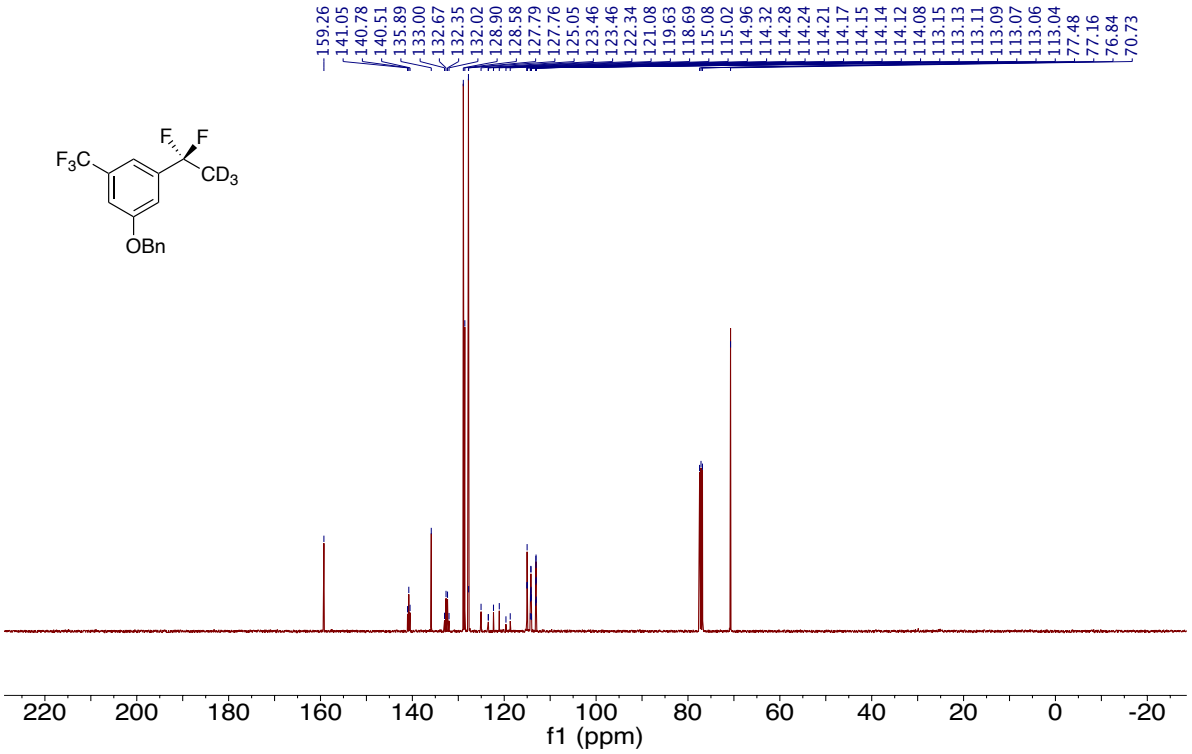

^{13}C NMR of Compound **3-44** (101 MHz, $CDCl_3$)

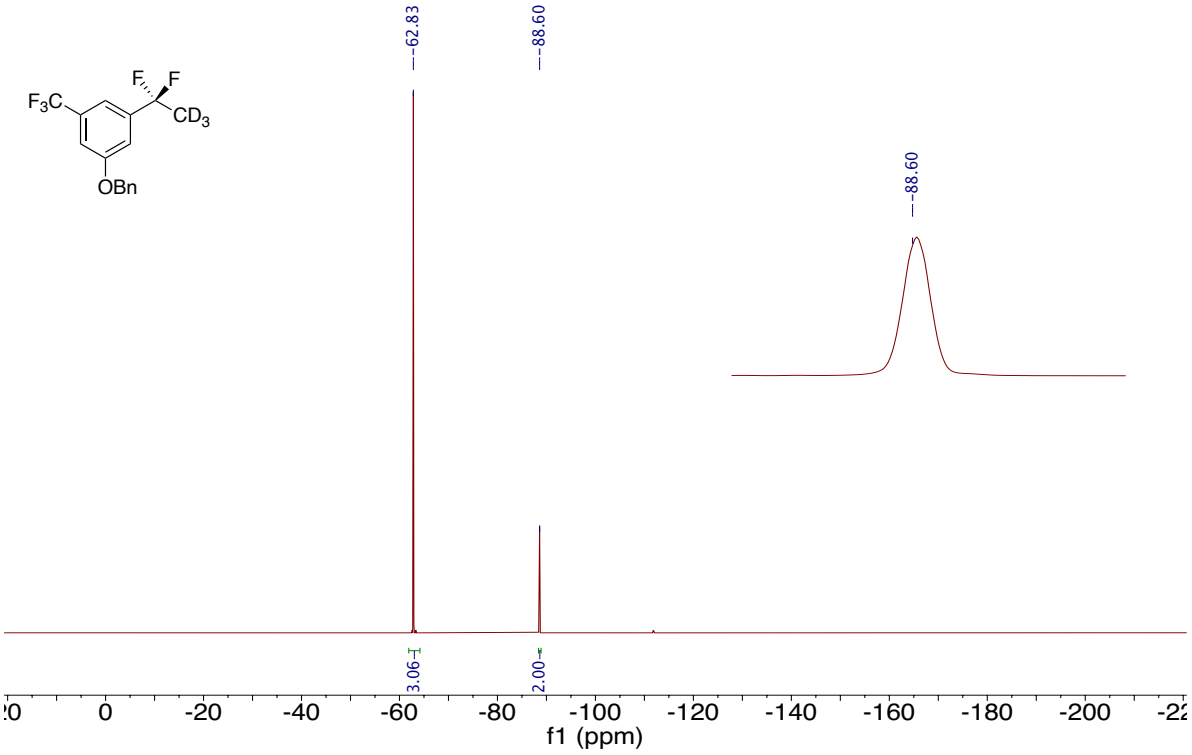

^{19}F NMR of Compound **3-44** (376 MHz, $CDCl_3$)

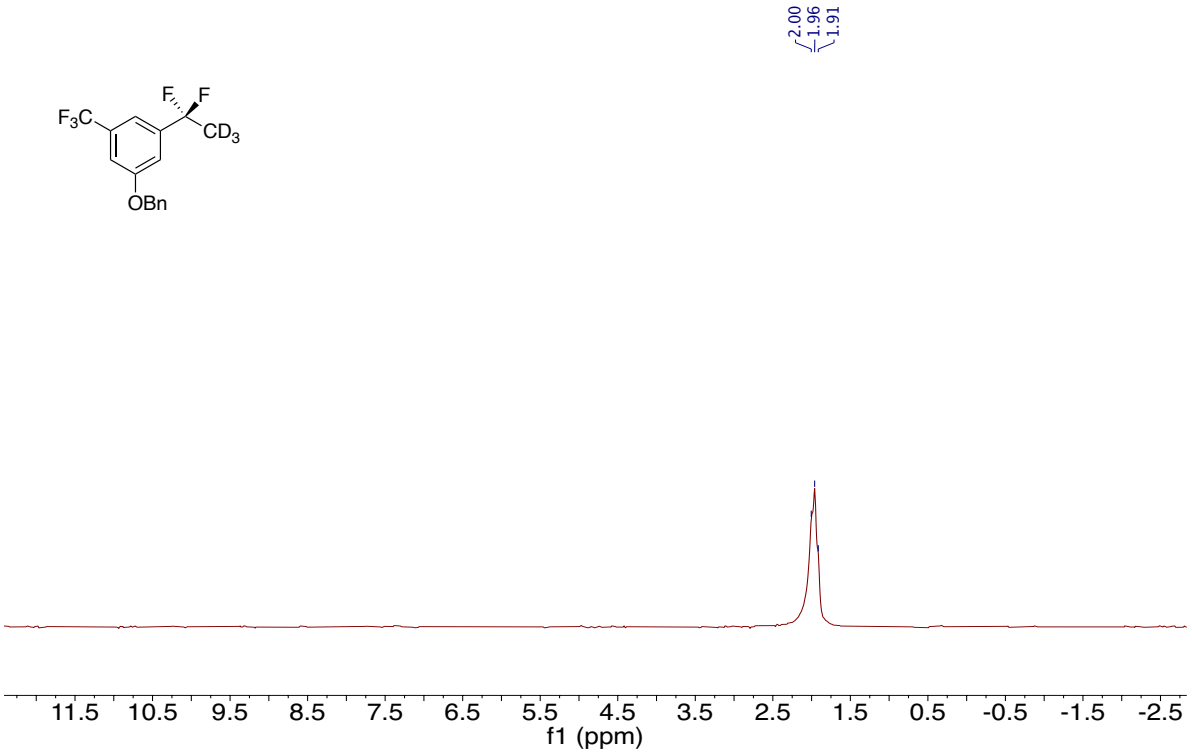

^{2}H NMR of Compound **3-44** (62 MHz, $CHCl_3$)

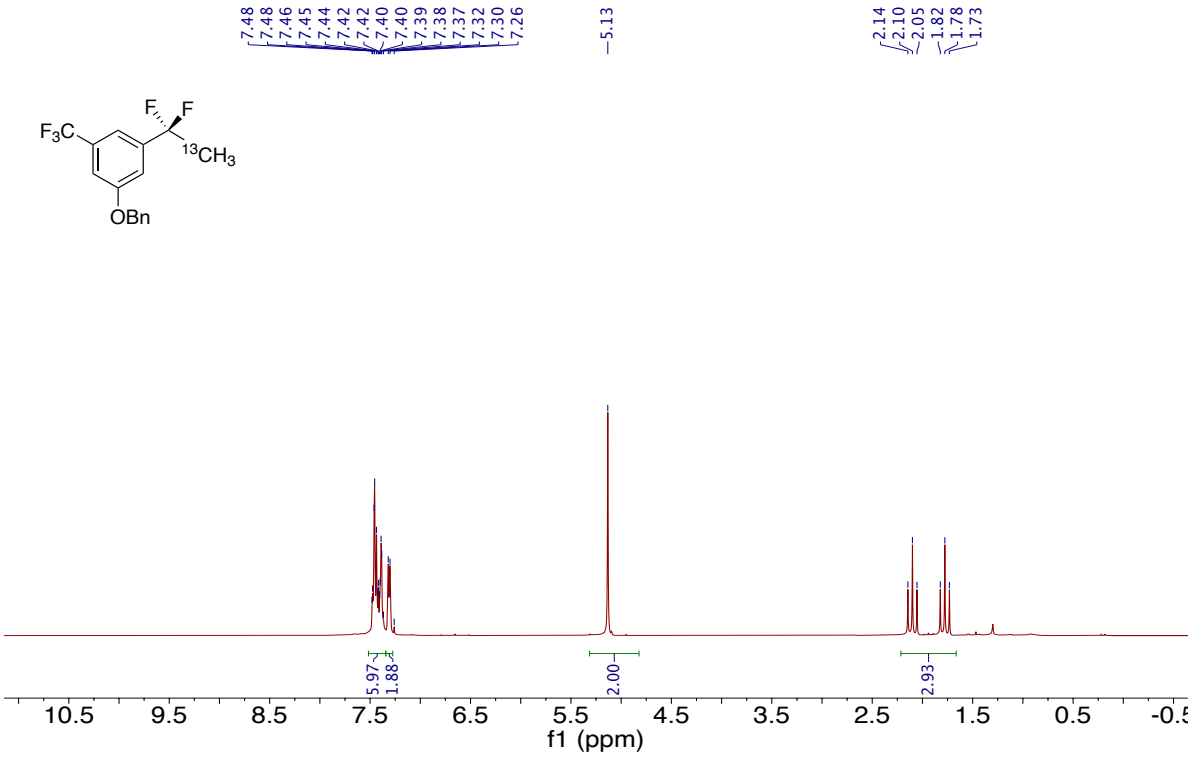

^{1}H NMR of Compound **3-45** (400 MHz, $CDCl_3$)

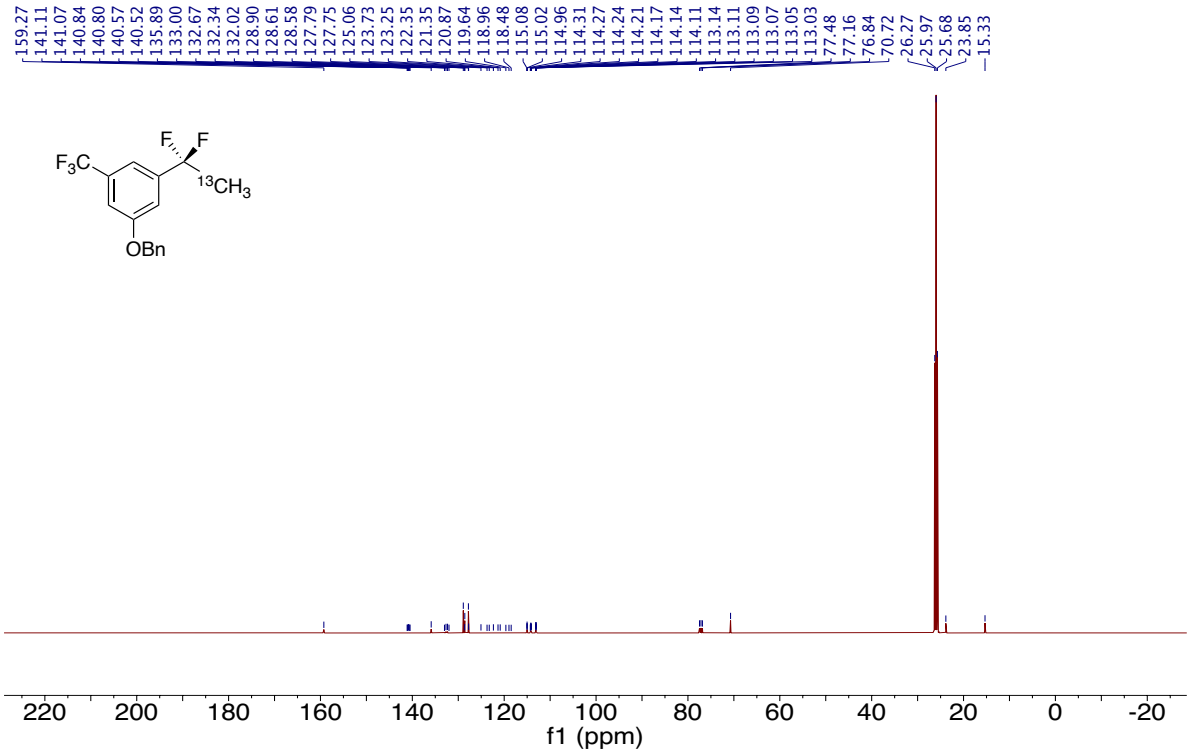

^{13}C NMR (Full Spectrum) of Compound **3-45** (101 MHz, $CDCl_3$)

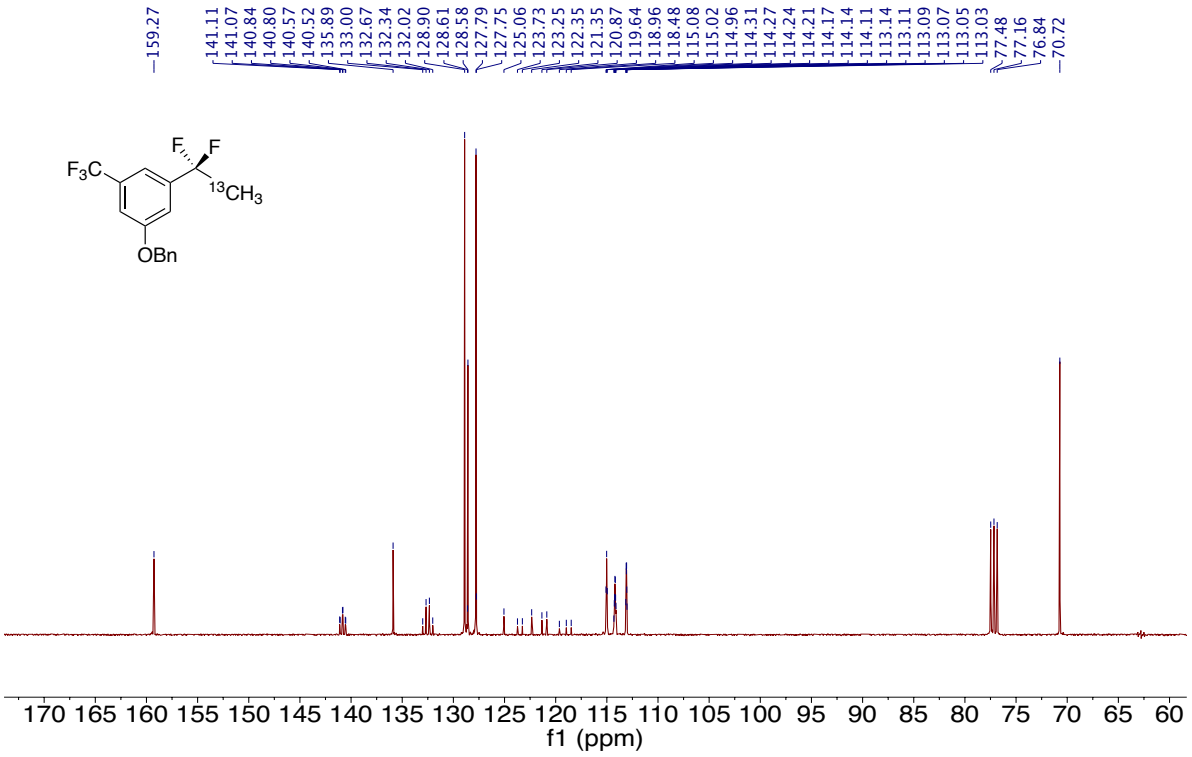

^{13}C NMR (Zoomed in 170-60ppm) of Compound **3-45** (101 MHz, $CDCl_3$)

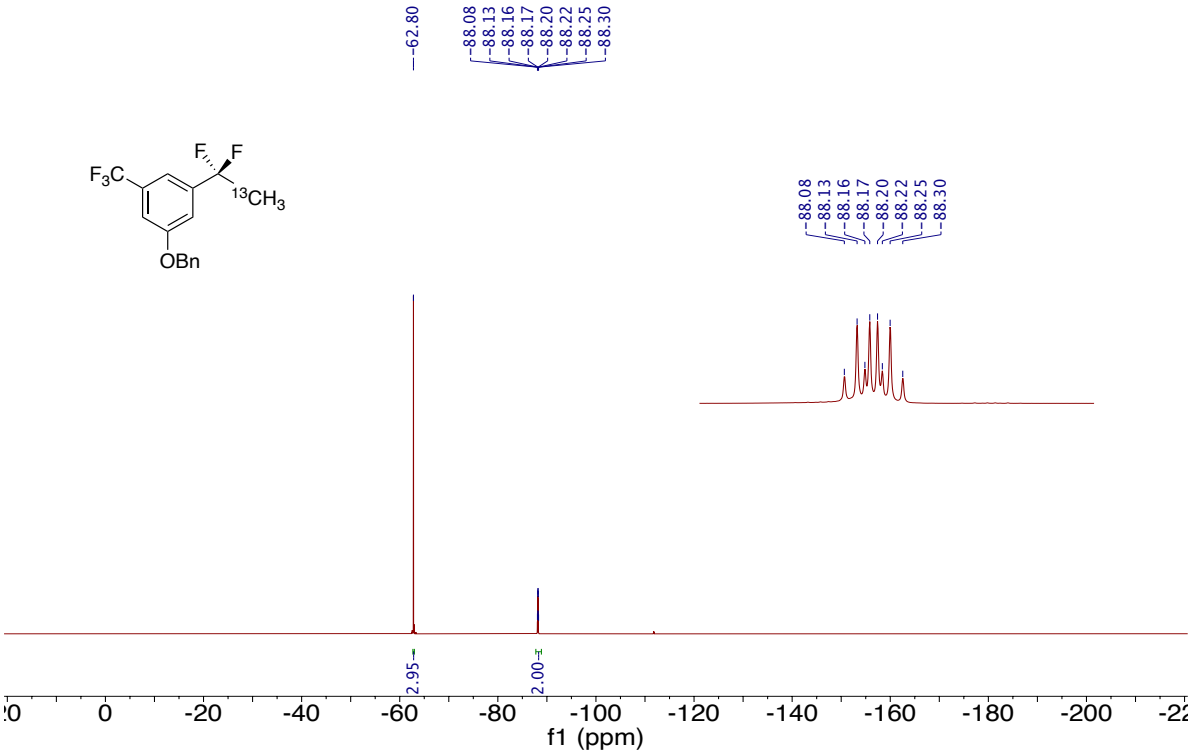

^{19}F NMR of Compound **3-45** (376 MHz, $CDCl_3$)

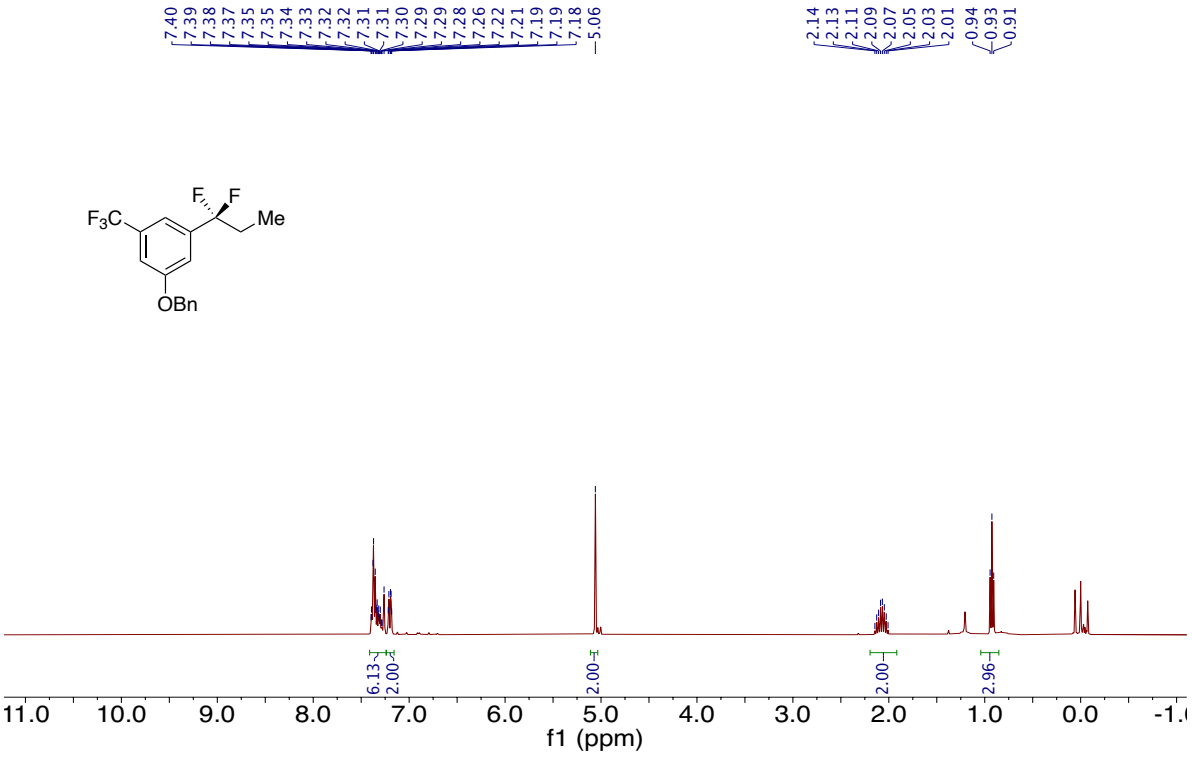

^{1}H NMR of Compound **3-46** (400 MHz, $CDCl_3$)

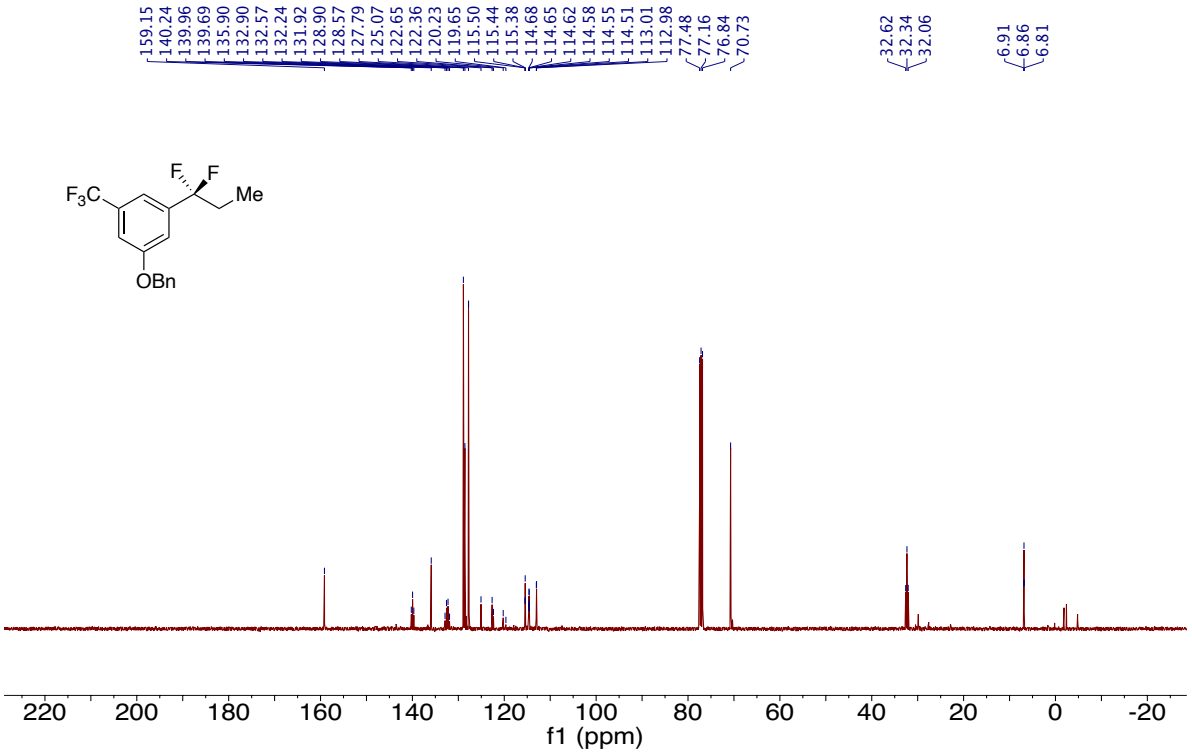

^{13}C NMR of Compound **3-46** (101 MHz, $CDCl_3$)

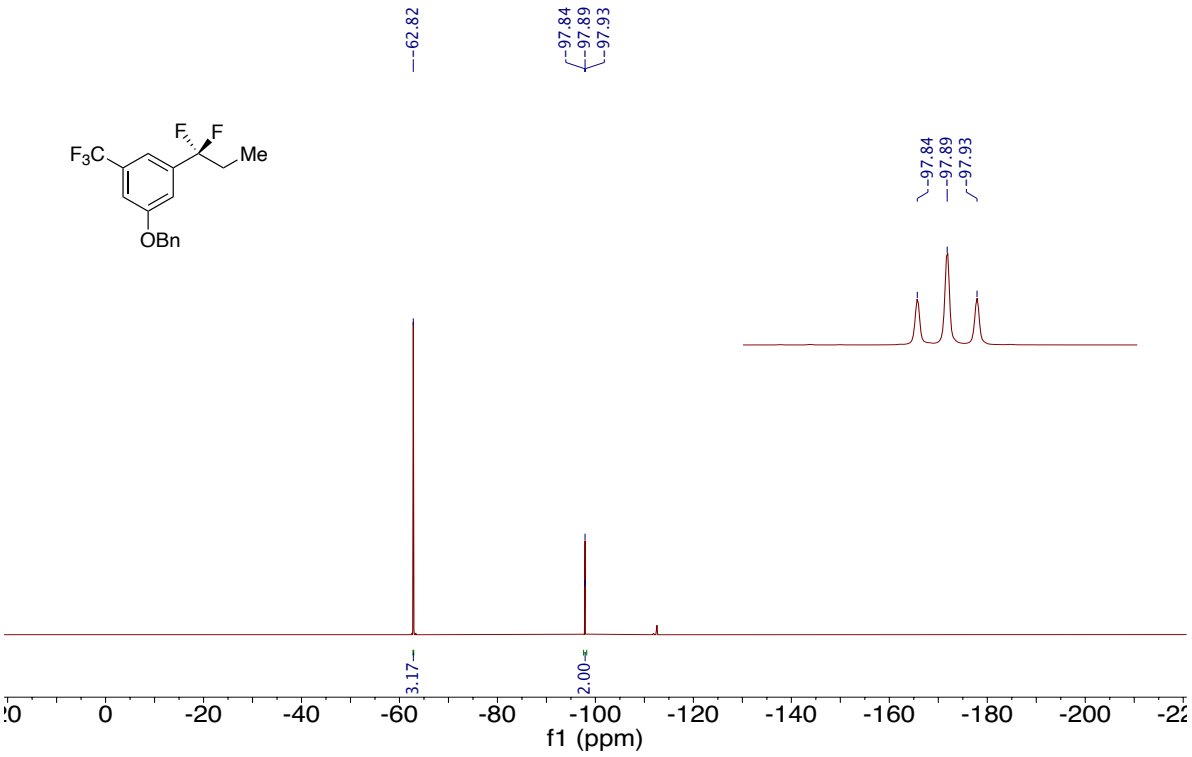

^{19}F NMR of Compound **3-46** (376 MHz, $CDCl_3$)

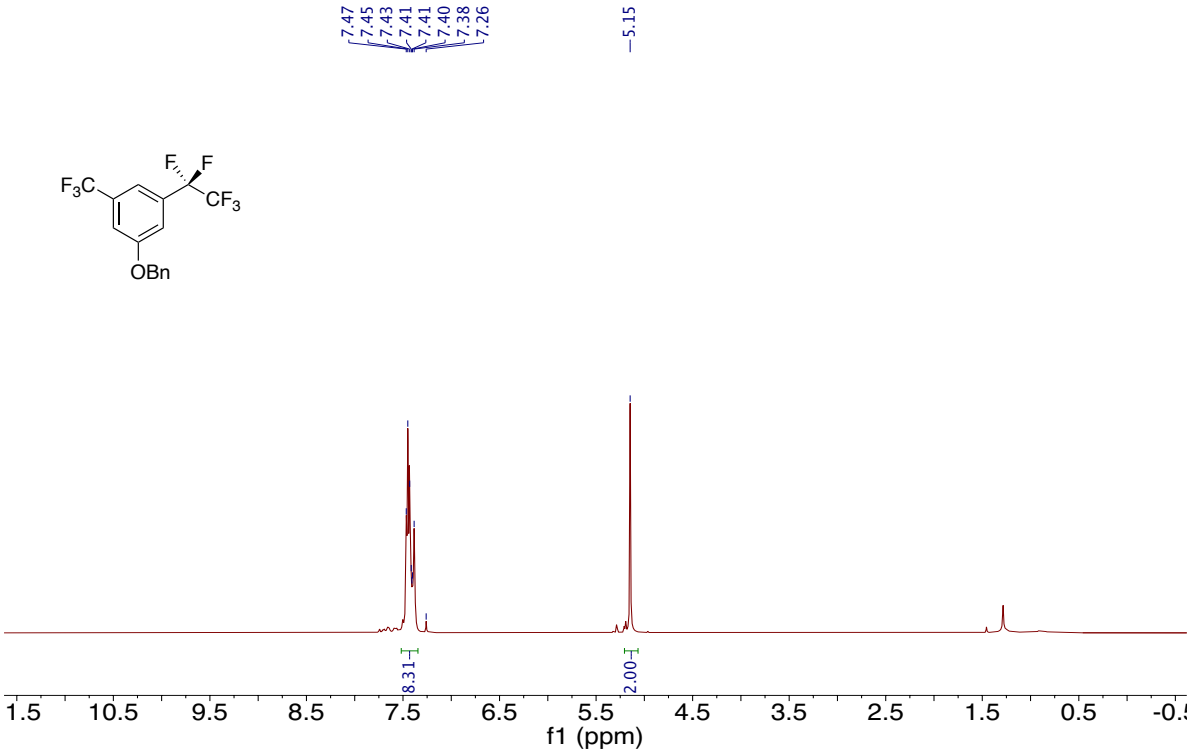

^{1}H NMR of Compound **3-47** (400 MHz, $CDCl_3$)

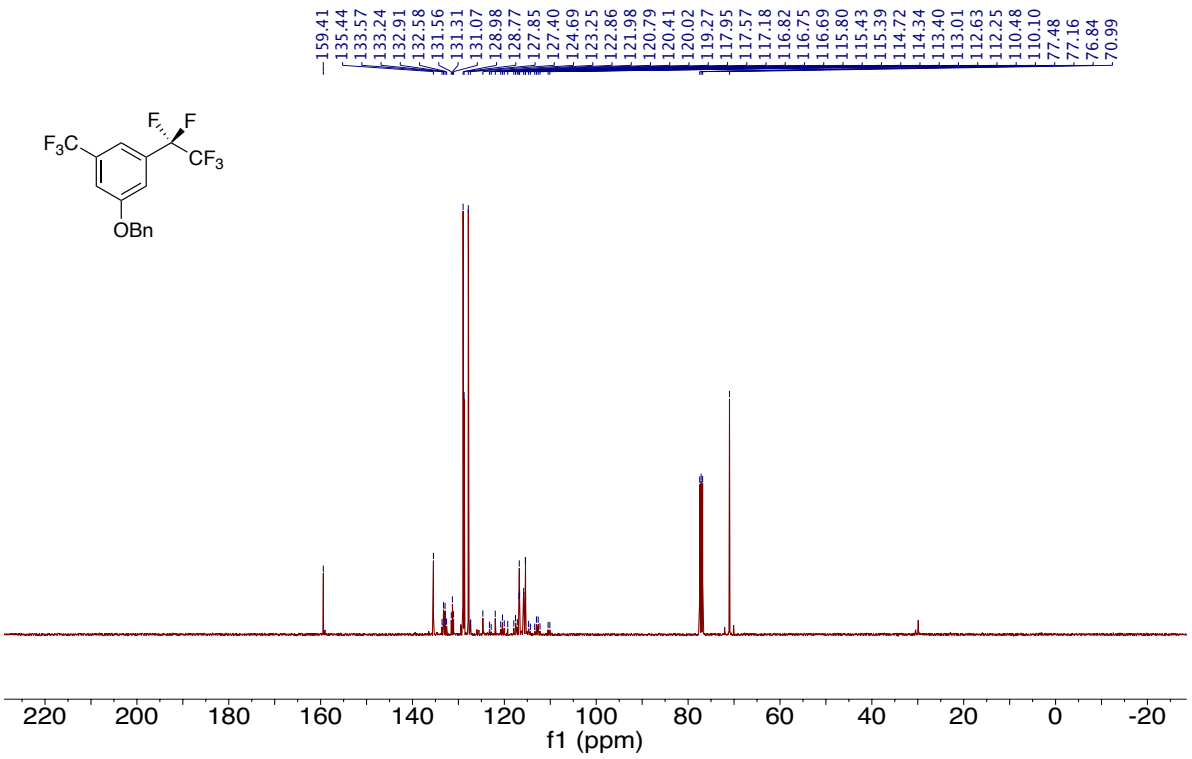

^{13}C NMR of Compound **3-47** (101 MHz, $CDCl_3$)

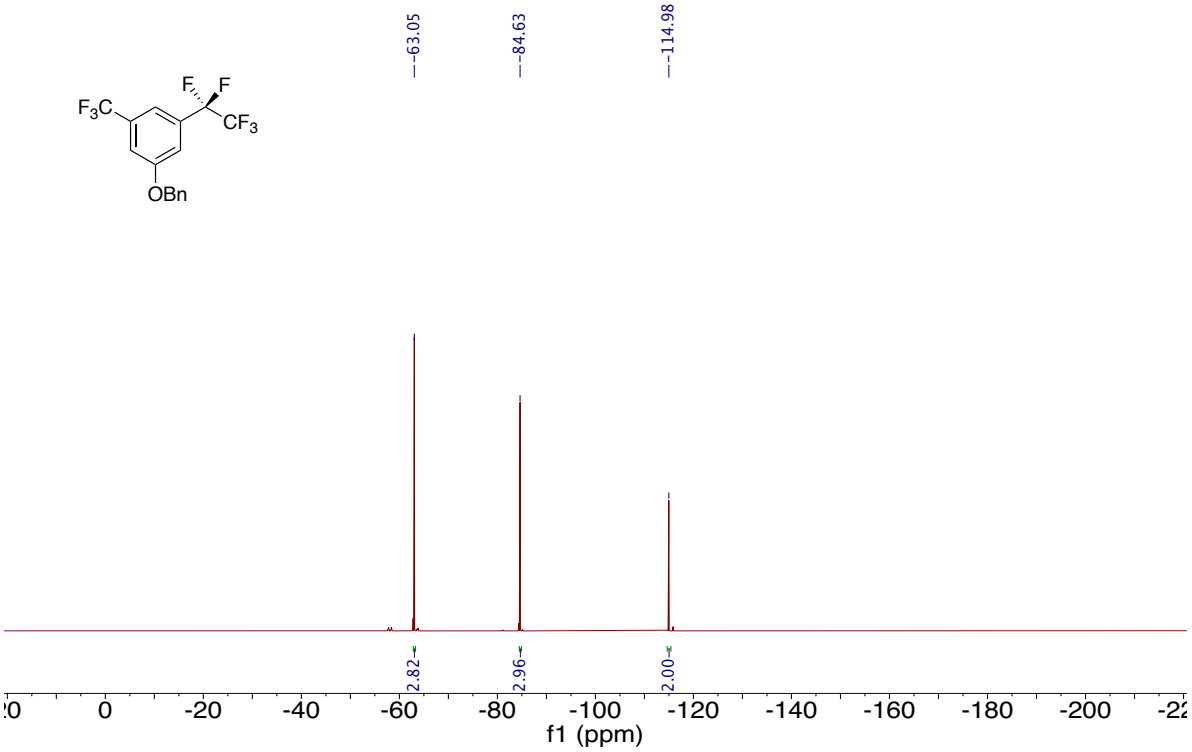

^{19}F NMR of Compound **3-47** (376 MHz, $CDCl_3$)

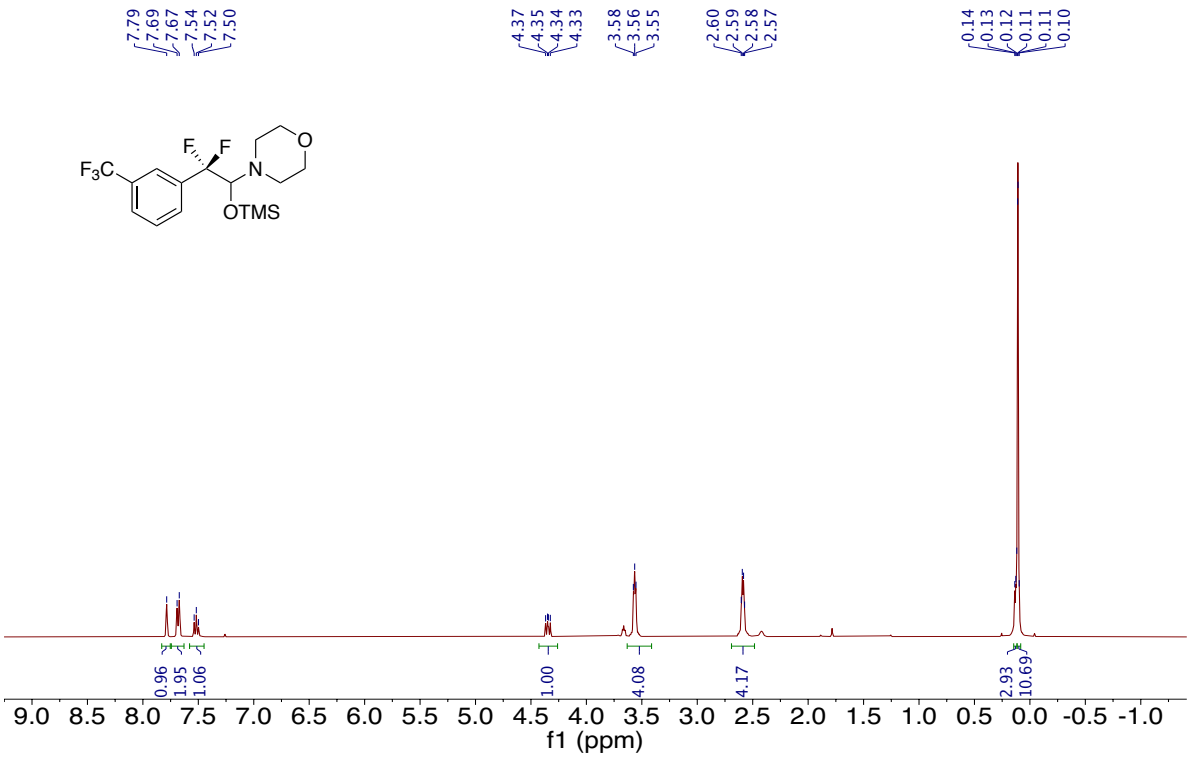

^{1}H NMR of Compound **3-49** (400 MHz, $CDCl_3$)

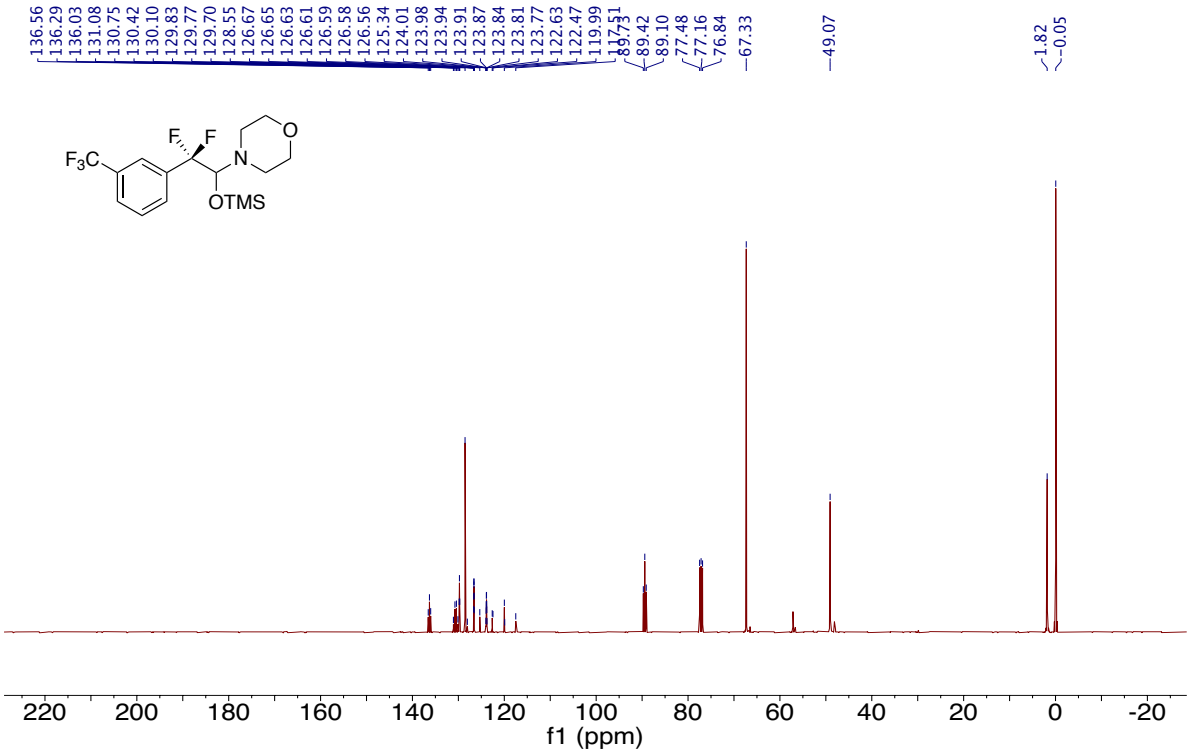

^{13}C NMR of Compound **3-49** (101 MHz, $CDCl_3$)

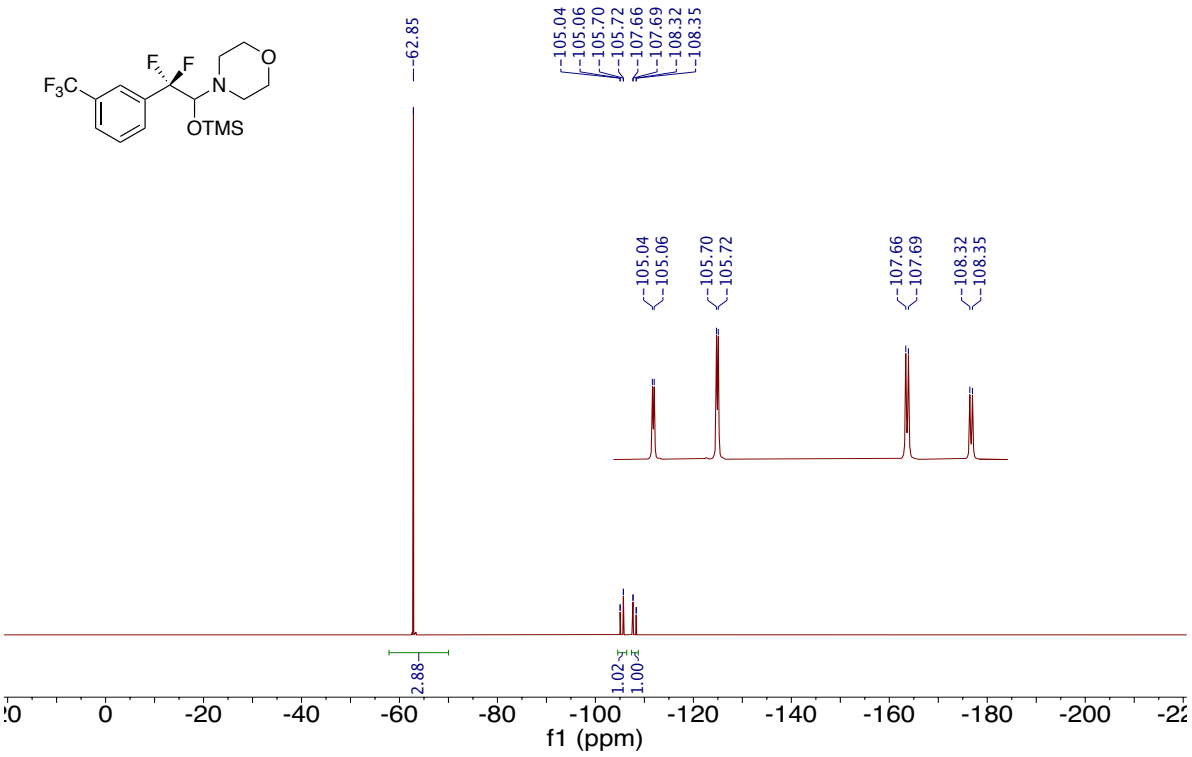

^{19}F NMR of Compound **3-49** (376 MHz, $CDCl_3$)

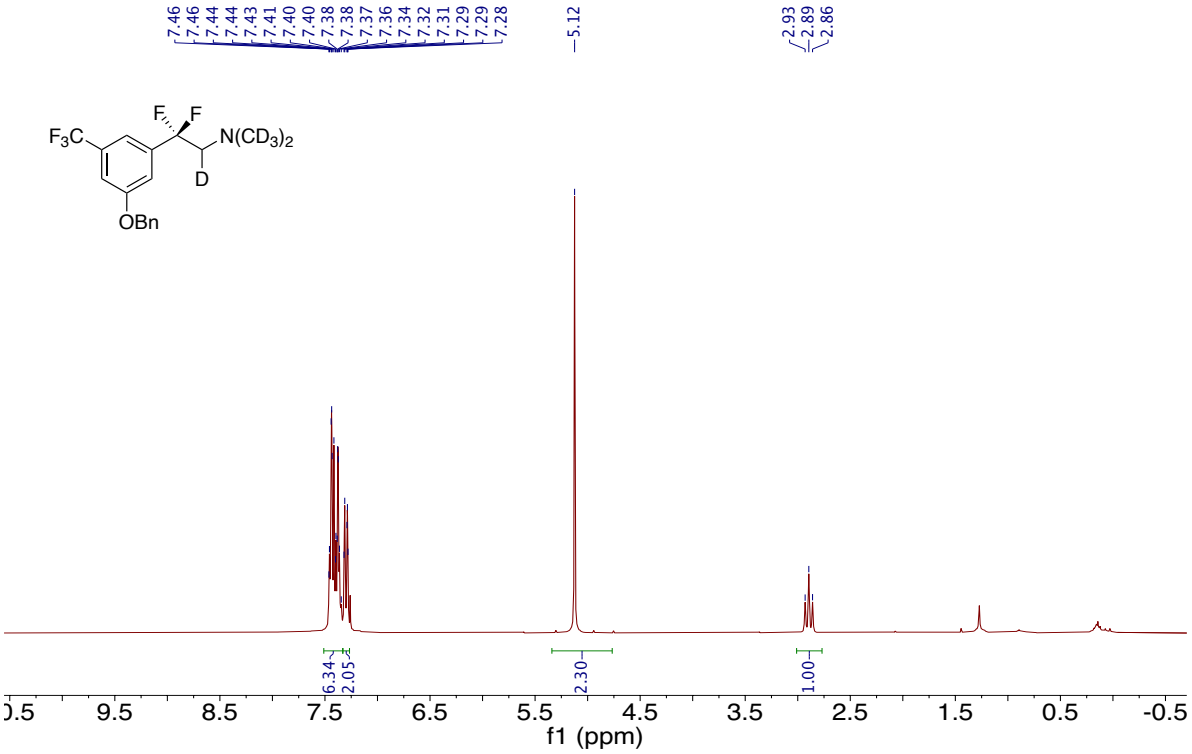

^{1}H NMR of Compound **A1-1** (400 MHz, $CDCl_3$)

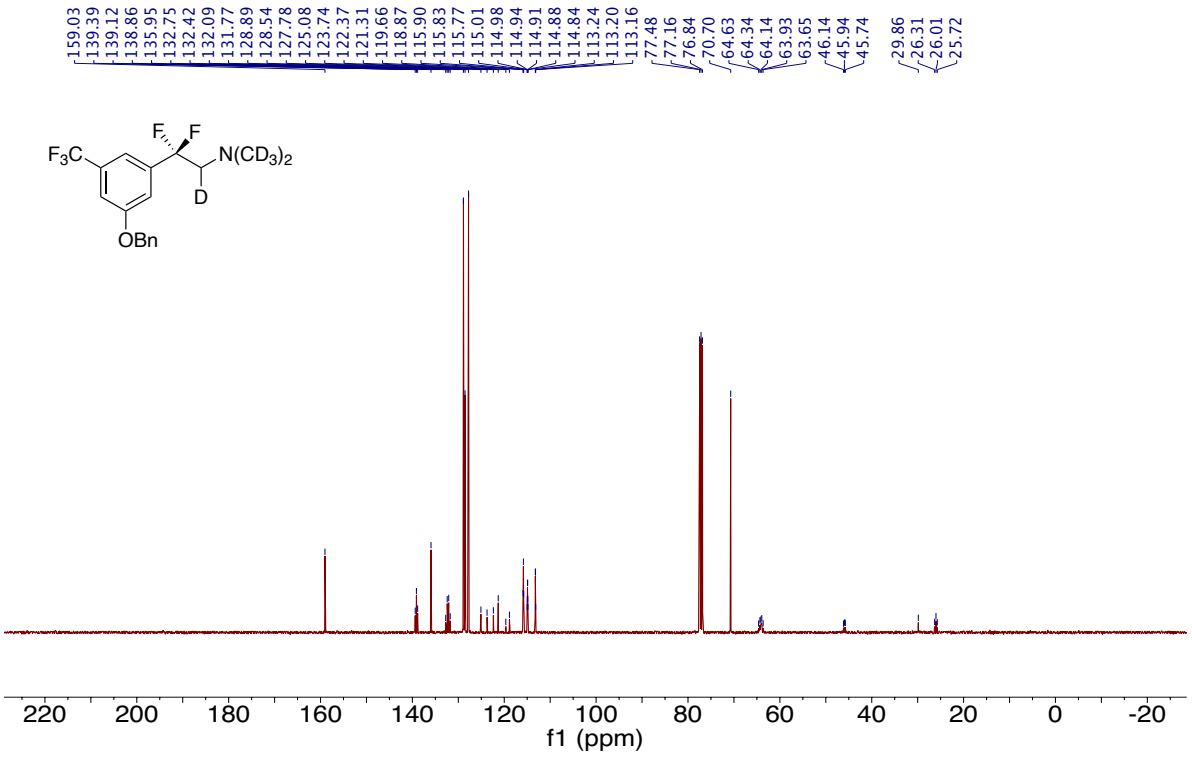

^{13}C NMR of Compound **A1-1** (101 MHz, $CDCl_3$)

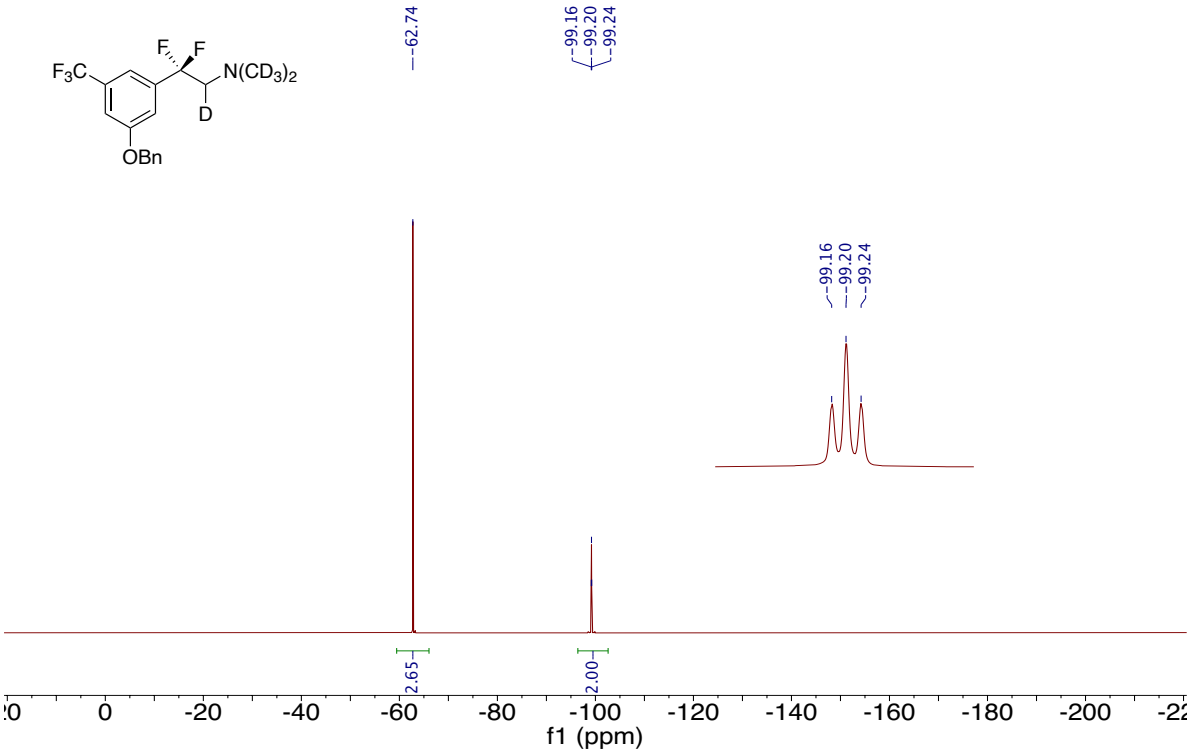

^{19}F NMR of Compound **A1-1** (376 MHz, $CDCl_3$)

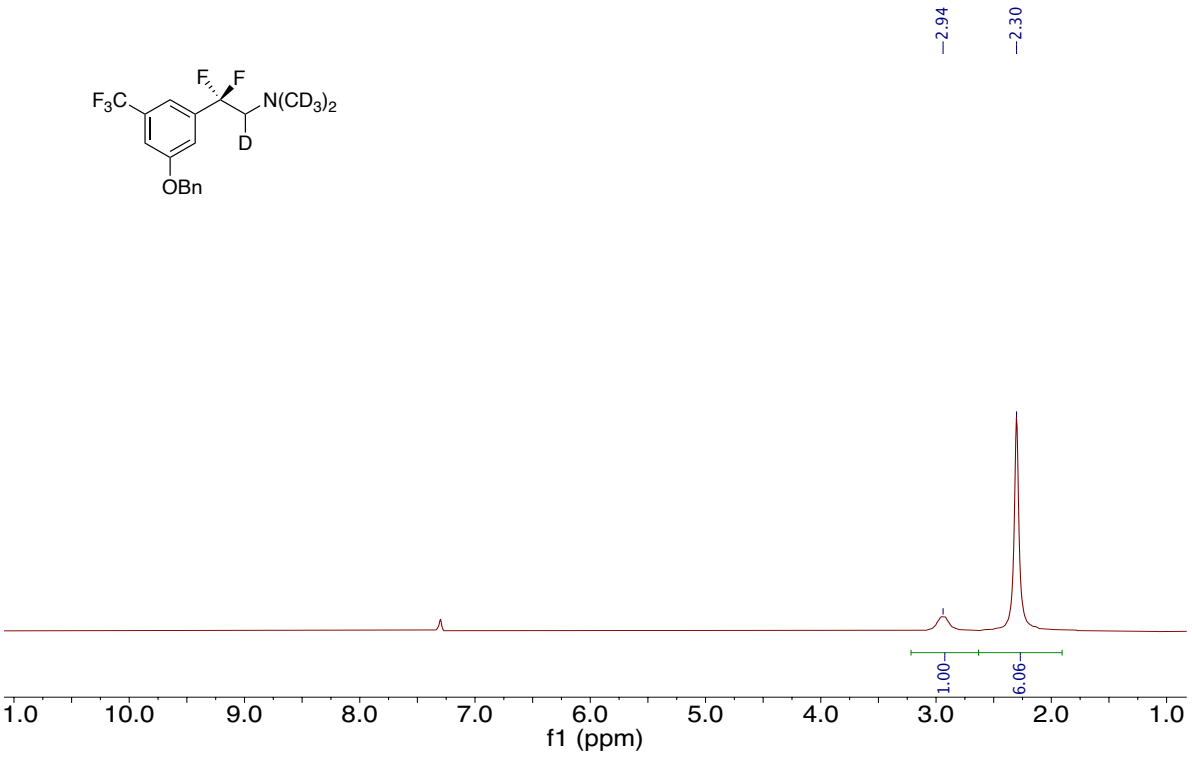

^{2}H NMR of Compound **SI-3** (62 MHz, $CHCl_3$)

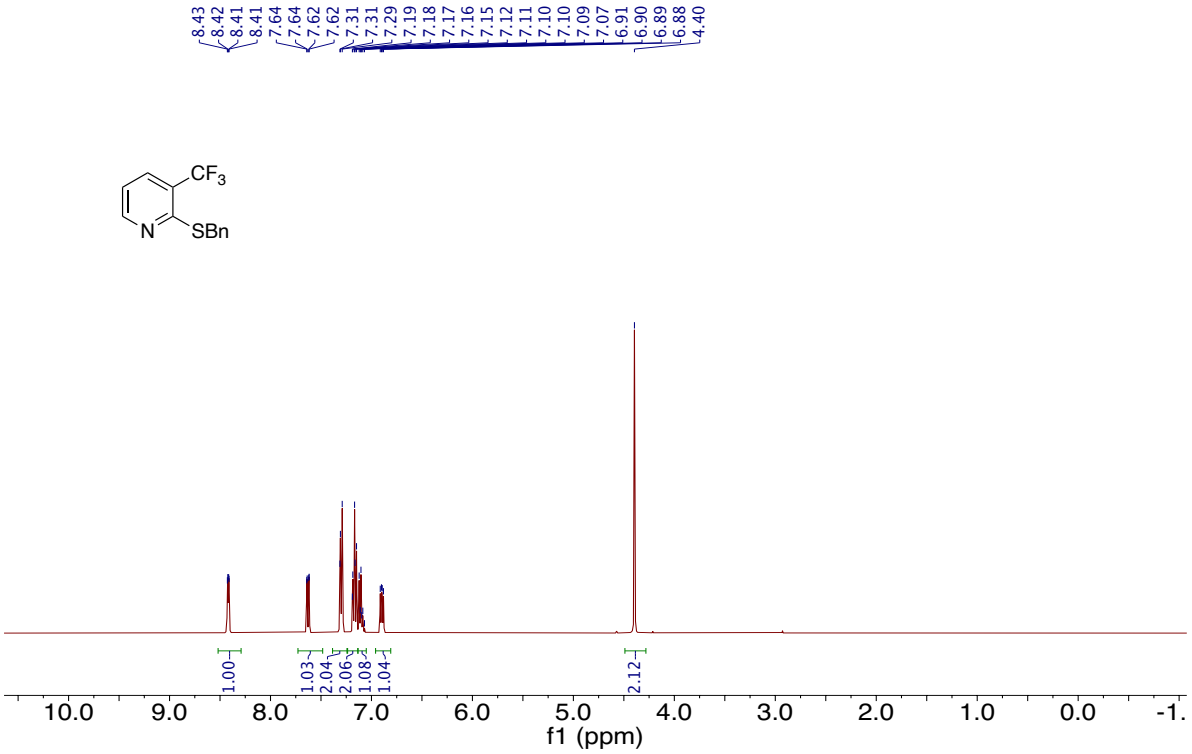

^{1}H NMR of Compound **A1-6** (400 MHz, $CDCl_3$)

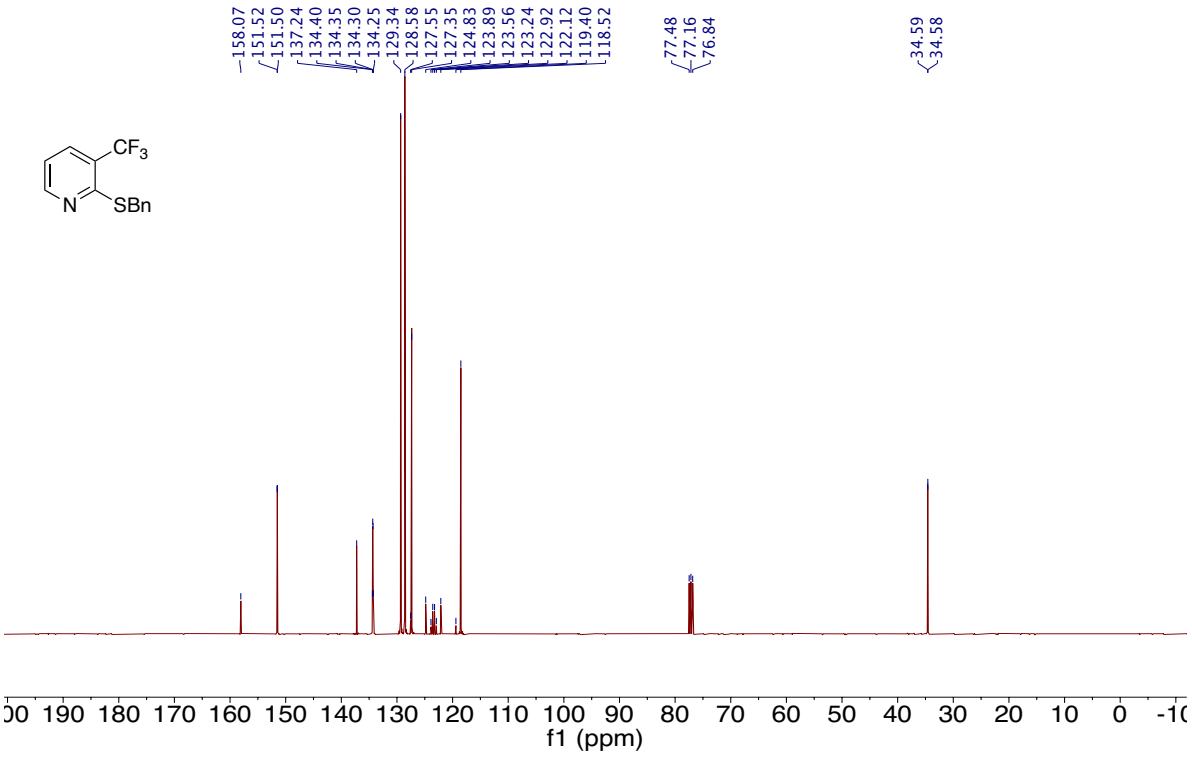

^{13}C NMR of Compound **A1-6** (101 MHz, $CDCl_3$)

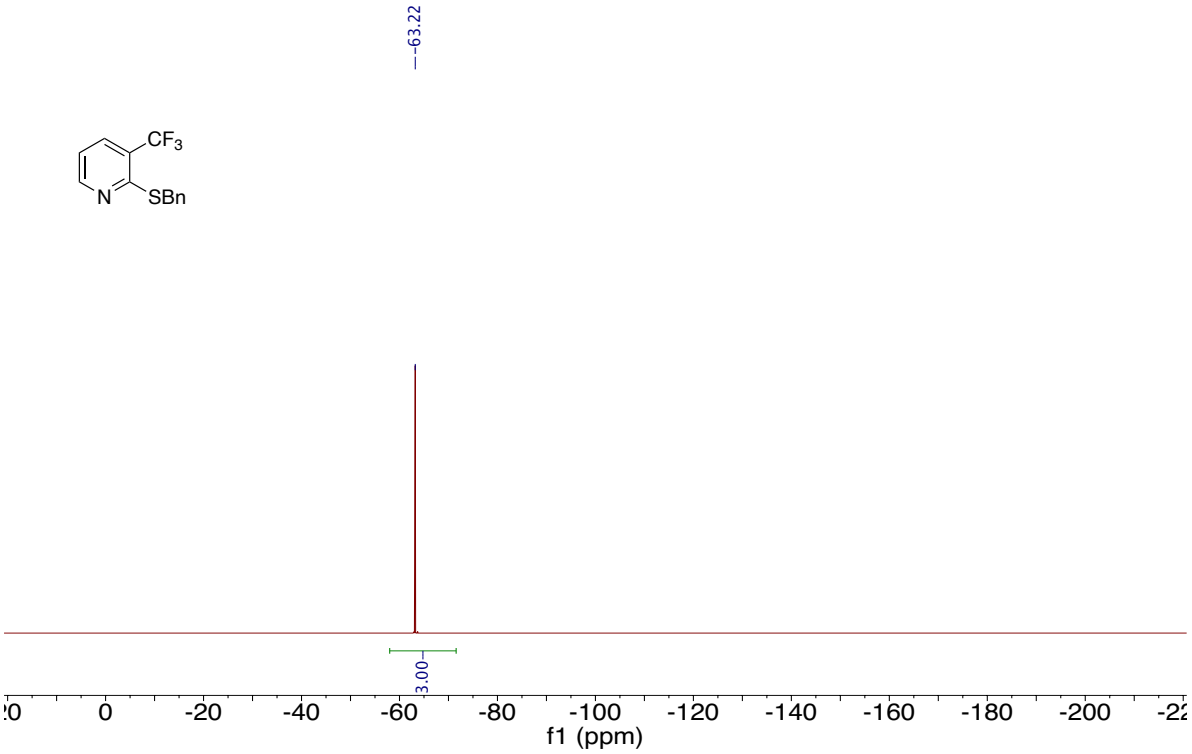

^{19}F NMR of Compound **A1-6** (376 MHz, $CDCl_3$)

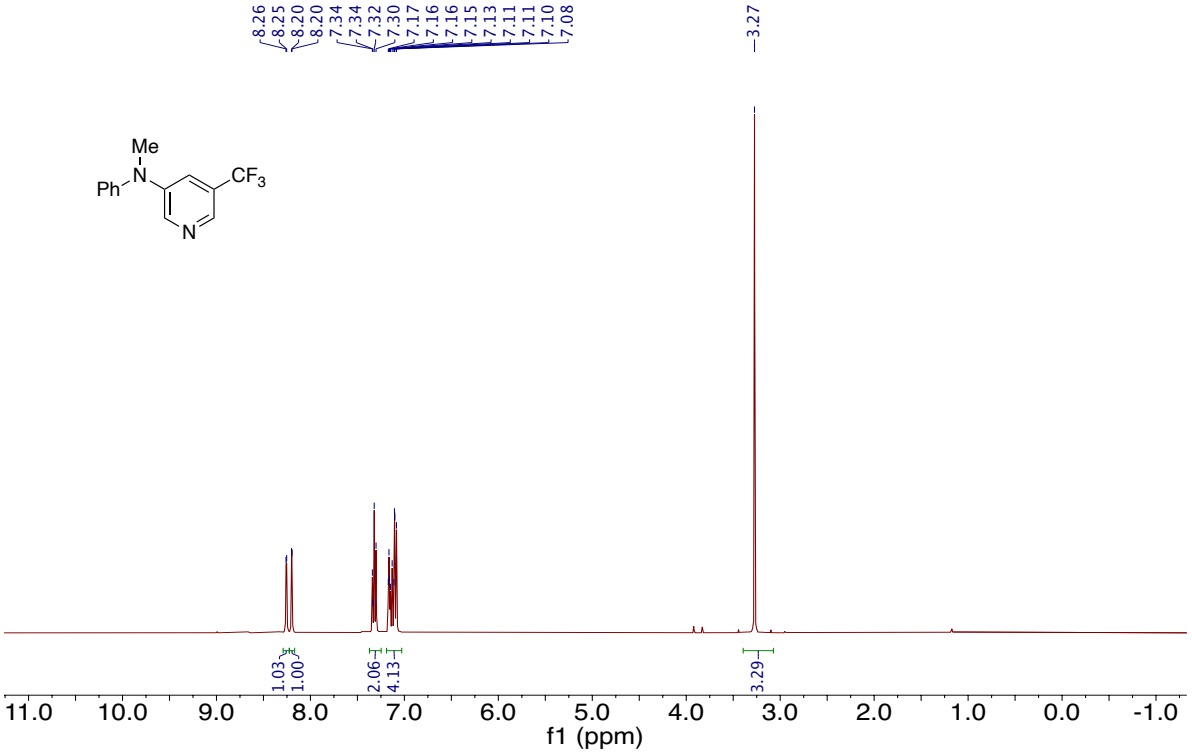

^{1}H NMR of Compound **A1-7** (400 MHz, $CDCl_3$)

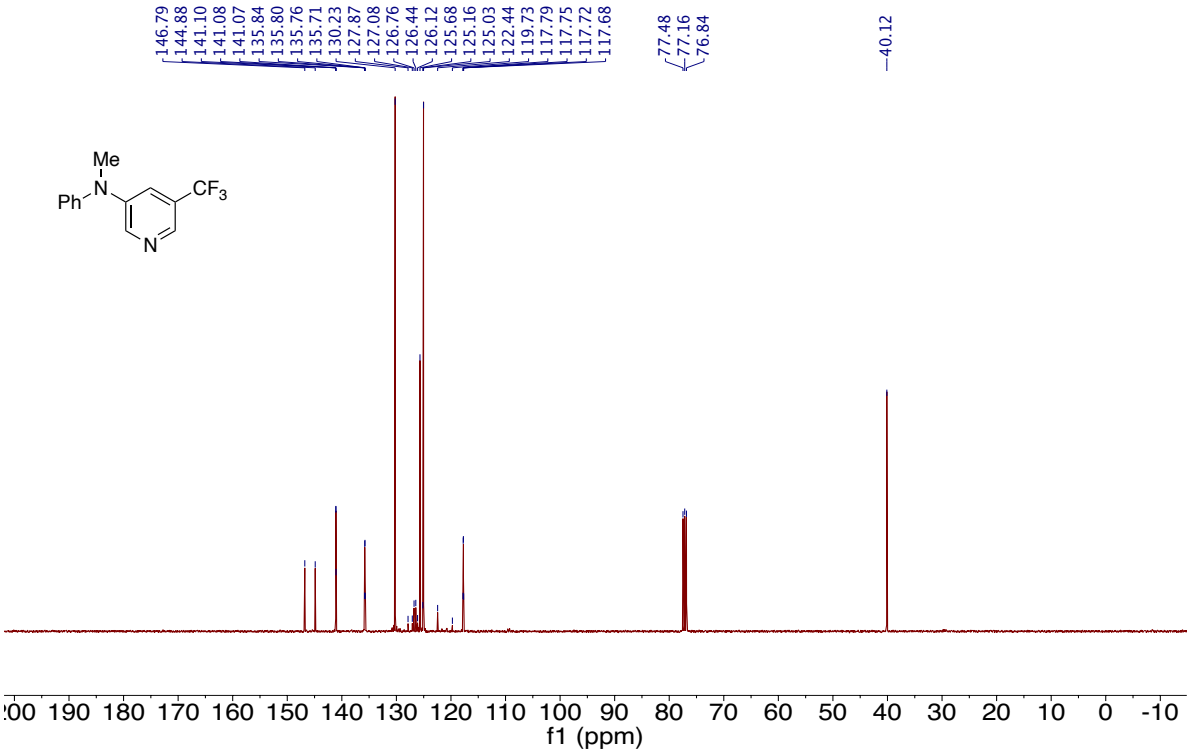

^{13}C NMR of Compound **A1-7** (101 MHz, $CDCl_3$)

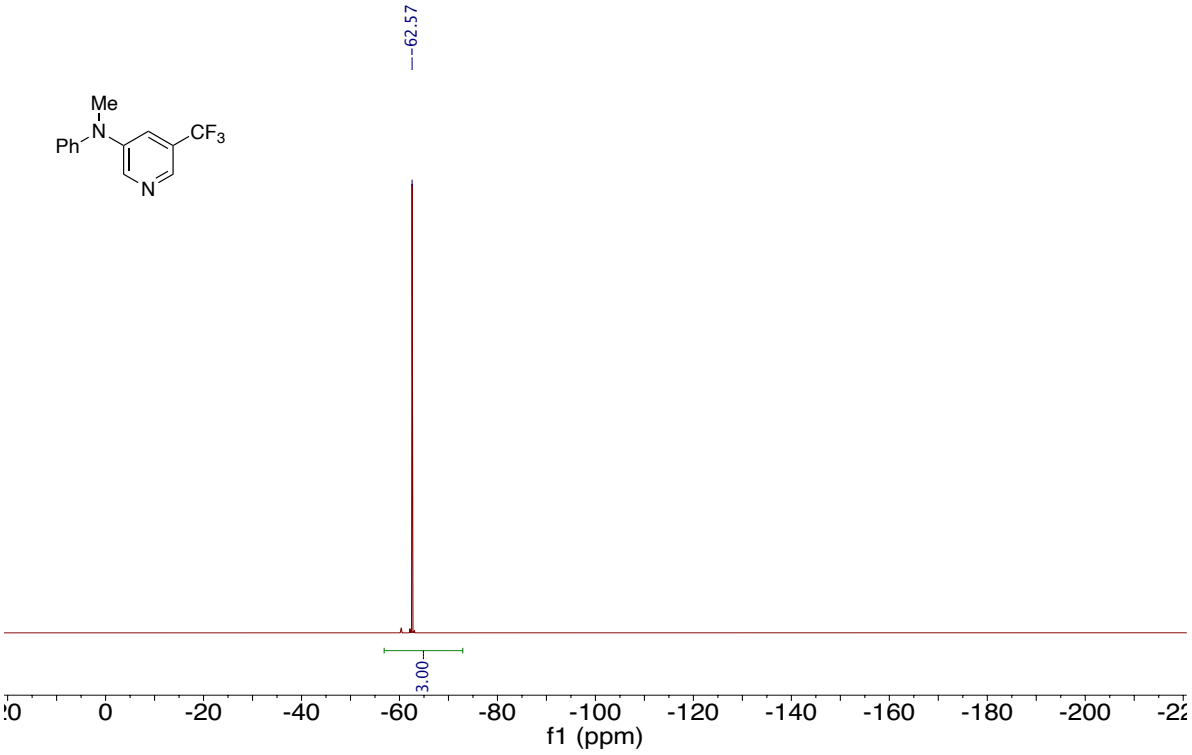

^{19}F NMR of Compound **A1-7** (376 MHz, $CDCl_3$)

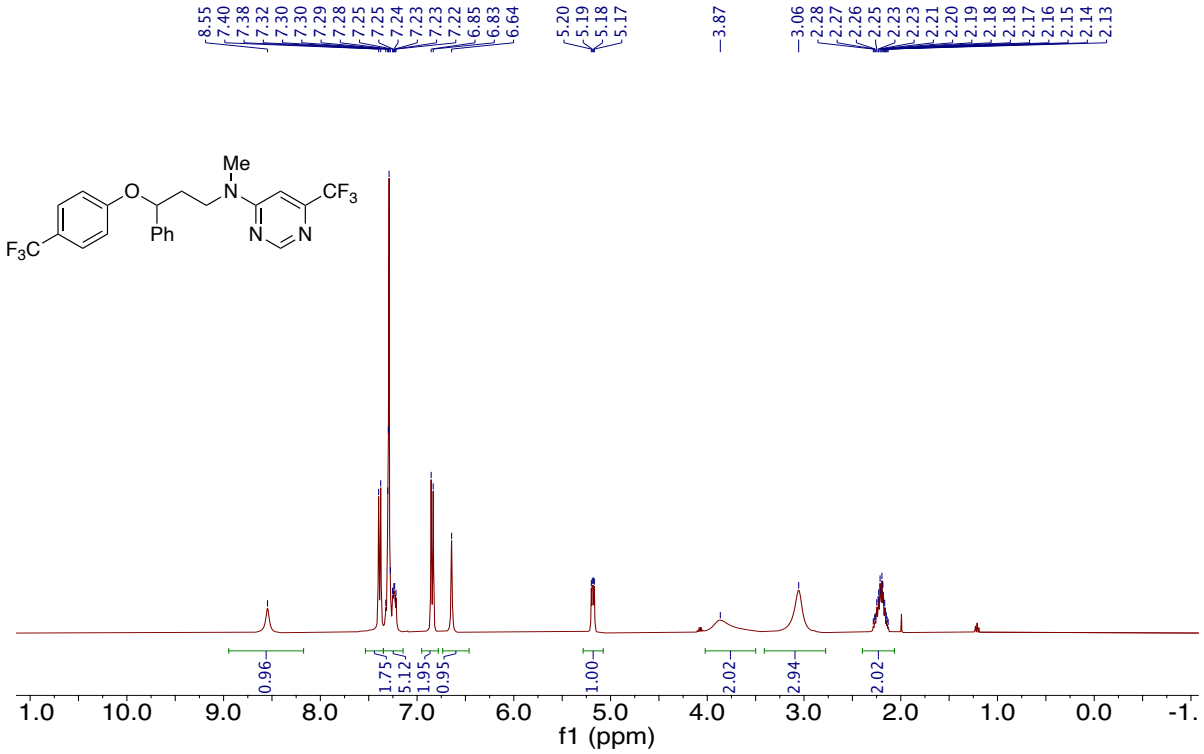

[1]H NMR of Compound **A1-9** (400 MHz, $CDCl_3$)

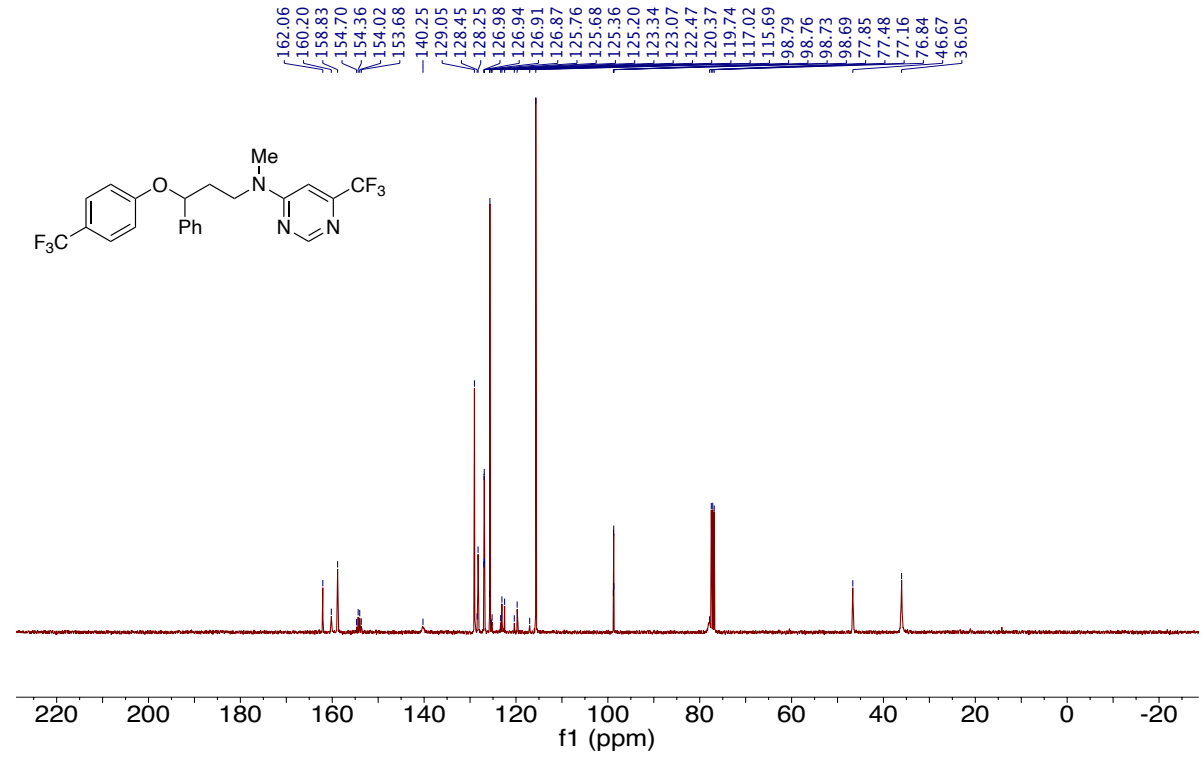

[13]C NMR of Compound **A1-9** (101 MHz, $CDCl_3$)

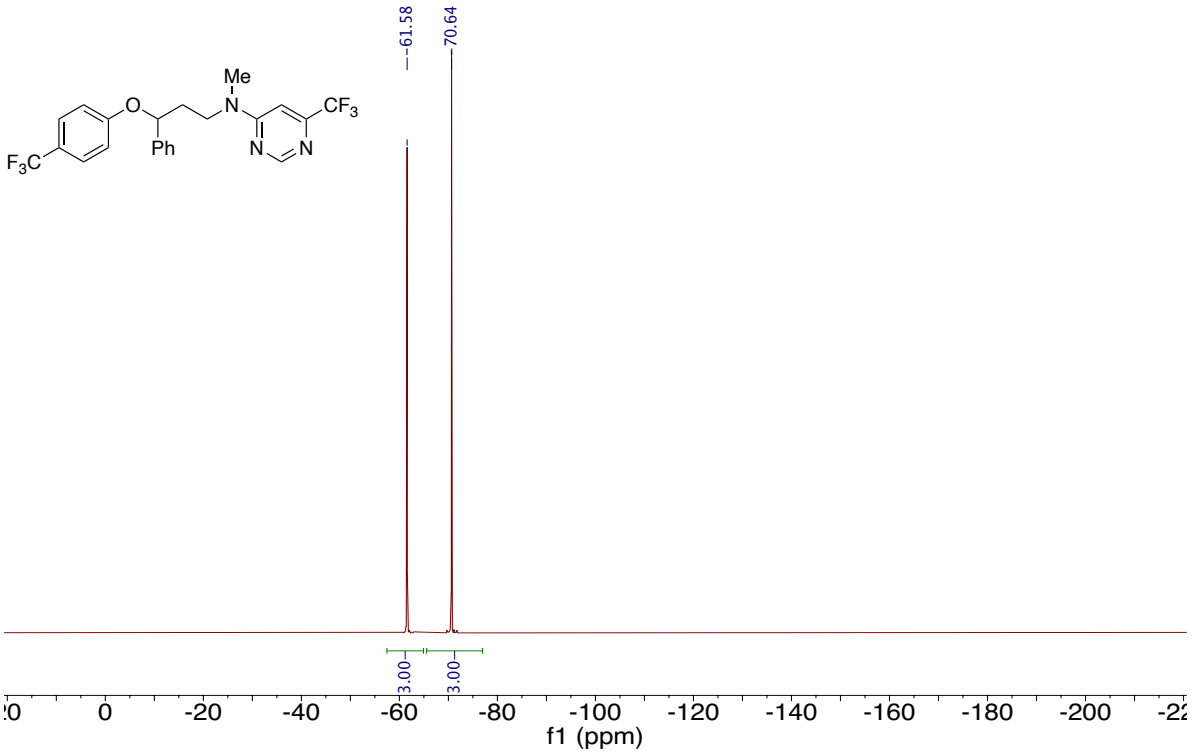

^{19}F NMR of Compound **A1-9** (376 MHz, $CDCl_3$)

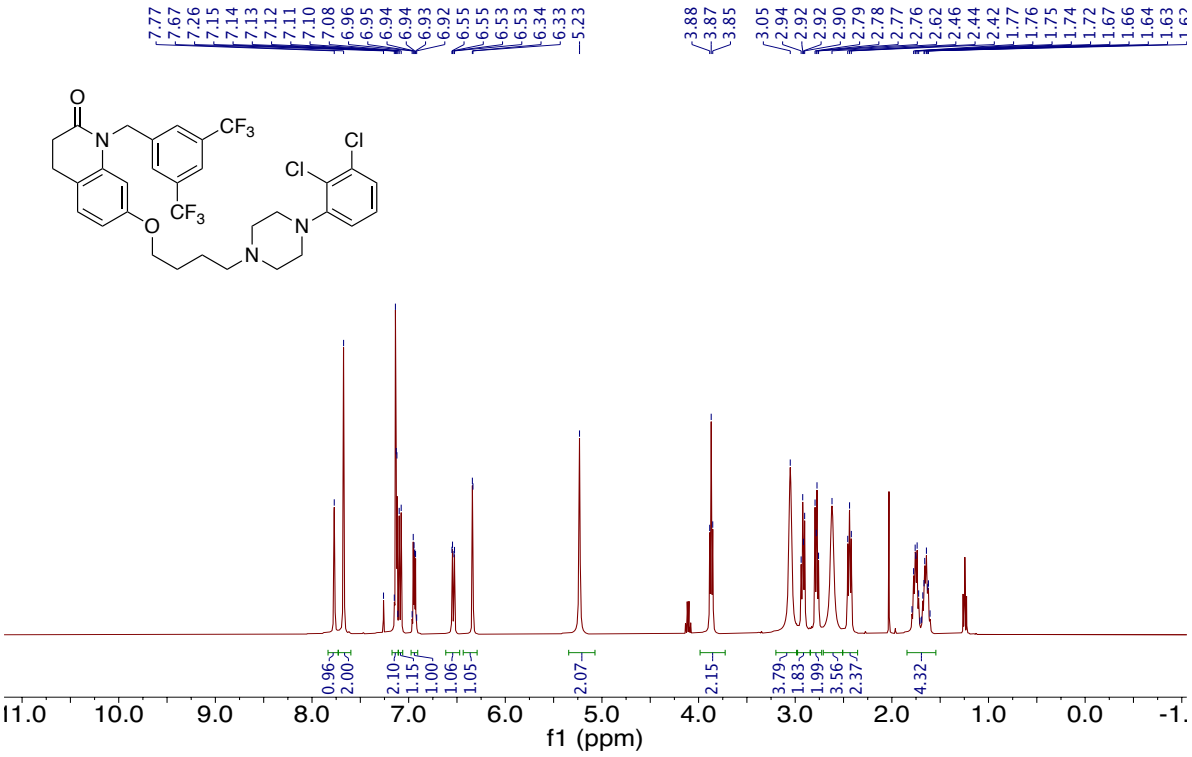

^{1}H NMR of Compound **A1-10** (400 MHz, $CDCl_3$)

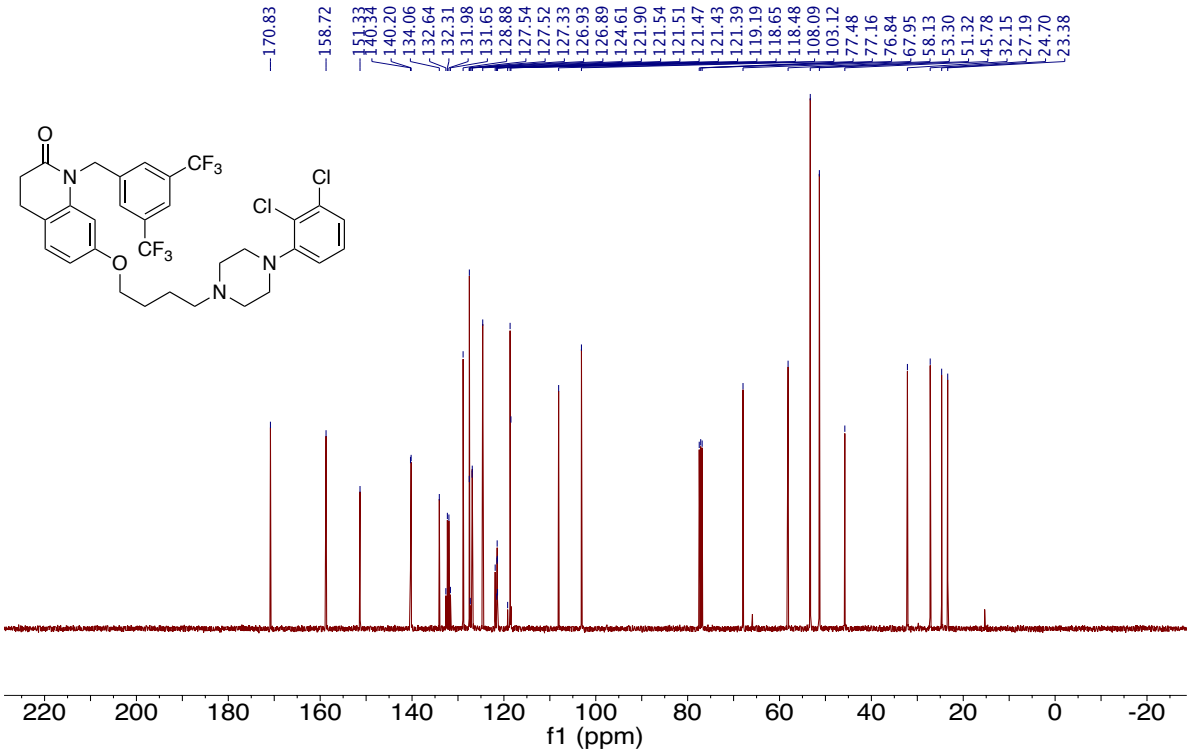

^{13}C NMR of Compound **A1-10** (101 MHz, $CDCl_3$)

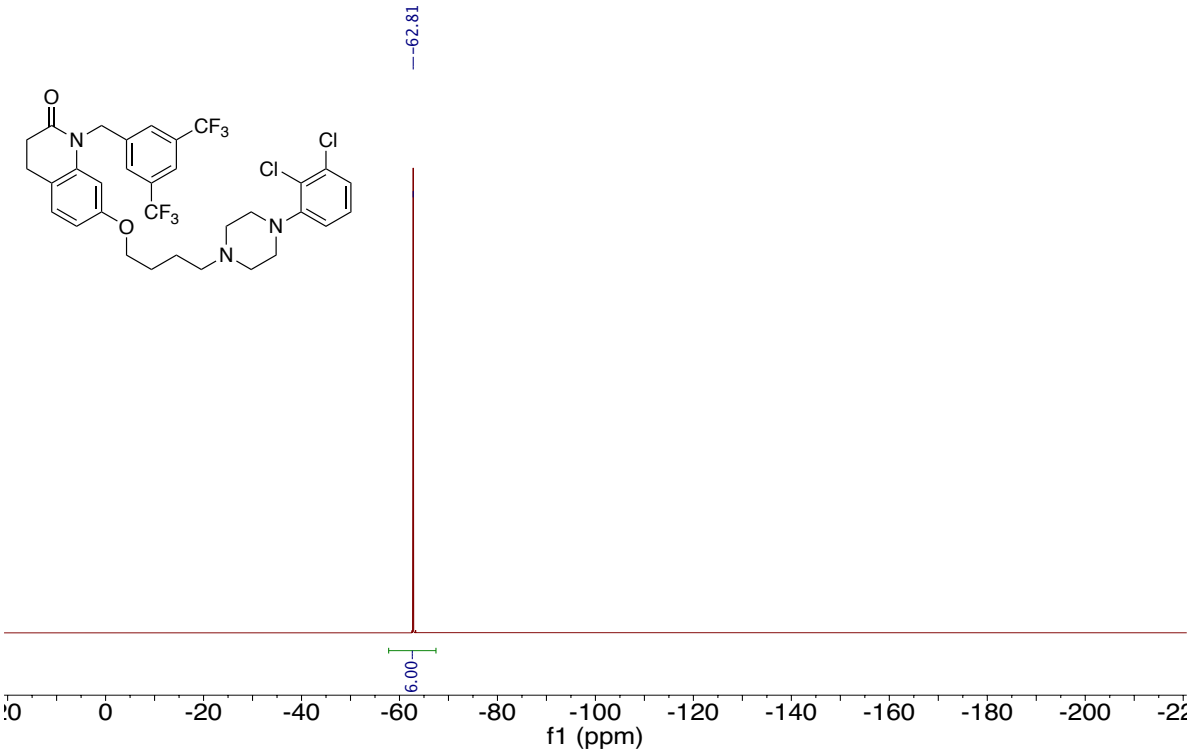

^{19}F NMR of Compound **A1-10** (376 MHz, $CDCl_3$)

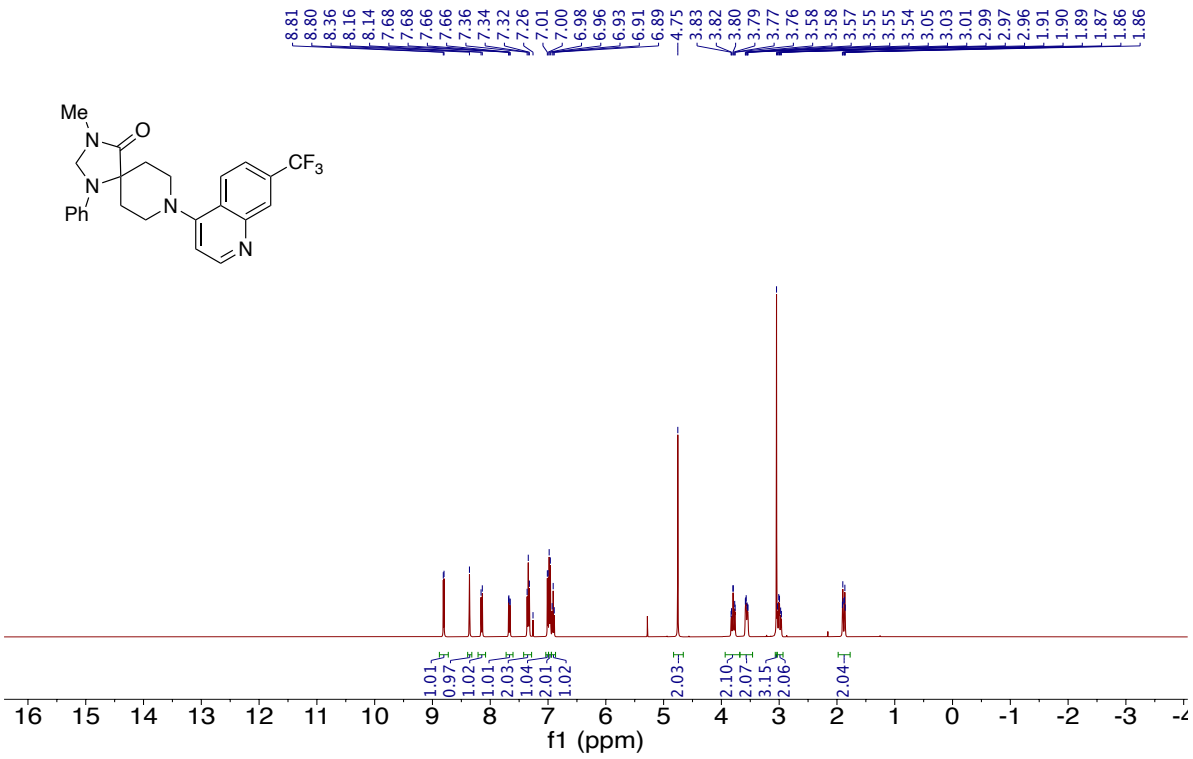

^{1}H NMR of Compound **A1-11** (400 MHz, $CDCl_3$)

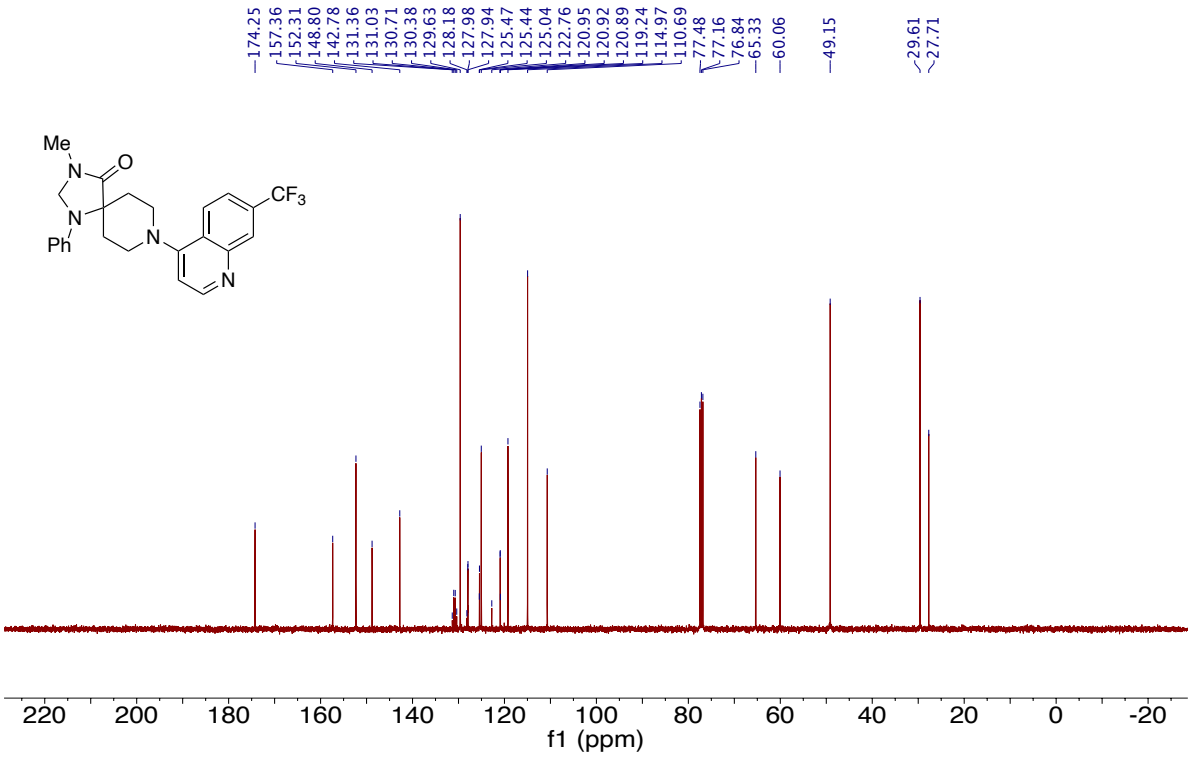

^{13}C NMR of Compound **A1-11** (101 MHz, $CDCl_3$)

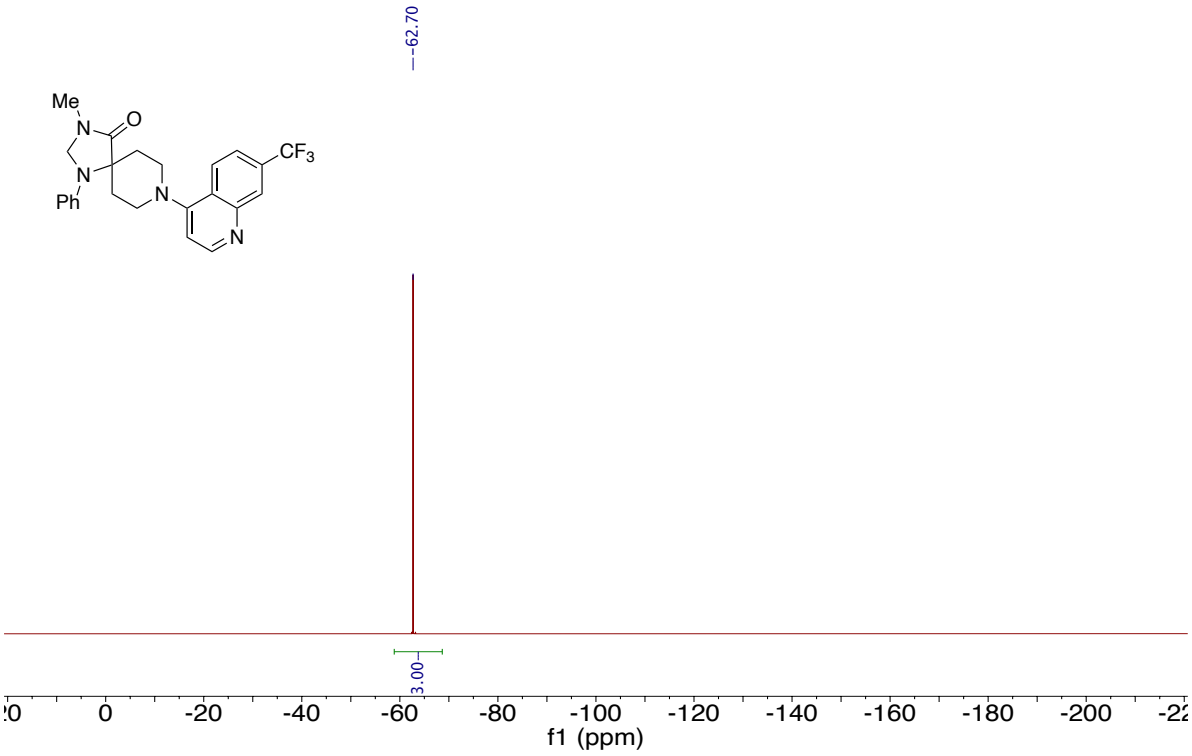

^{19}F NMR of Compound **A1-11** (376 MHz, $CDCl_3$)

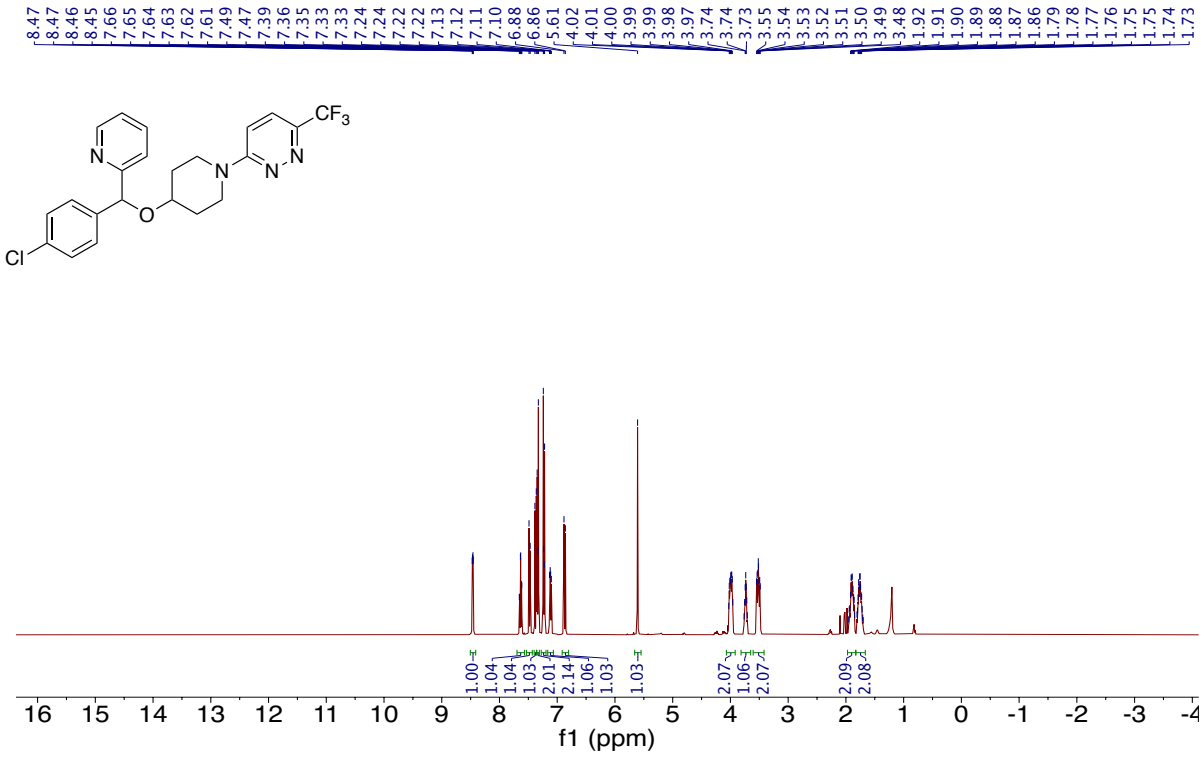

^{1}H NMR of Compound **A1-12** (400 MHz, $CDCl_3$)

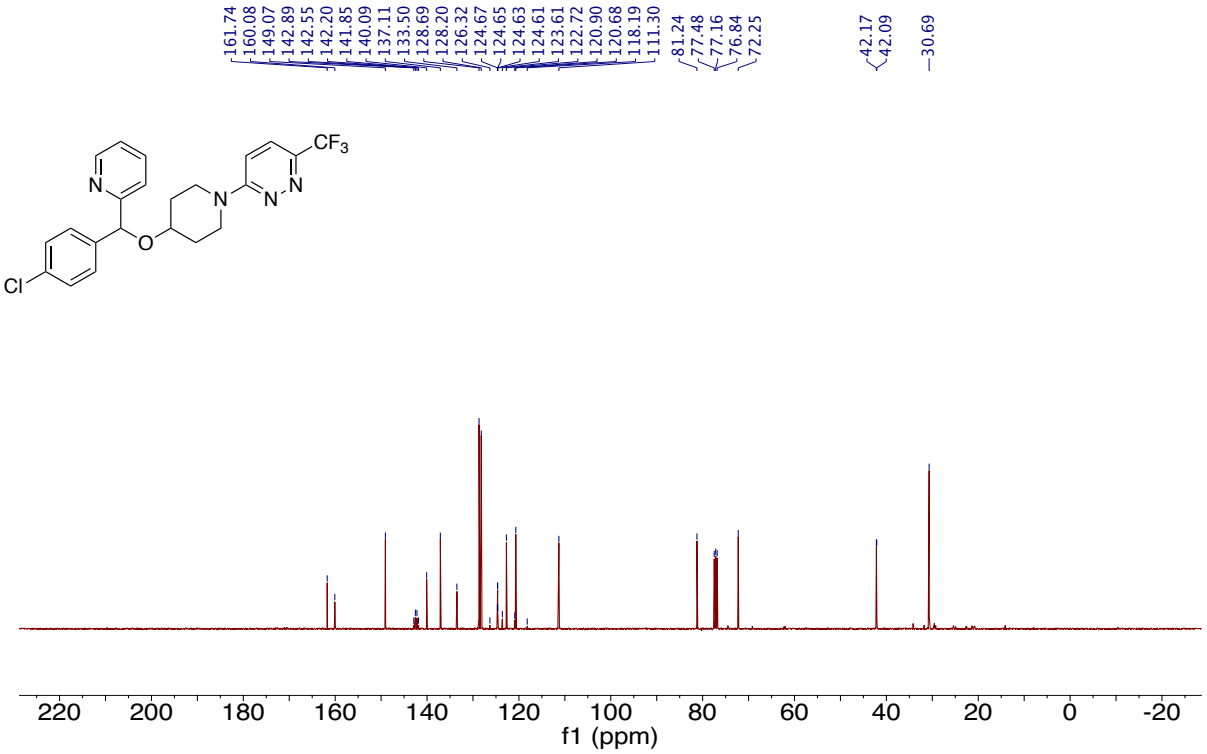

^{13}C NMR of Compound **A1-12** (101 MHz, $CDCl_3$)

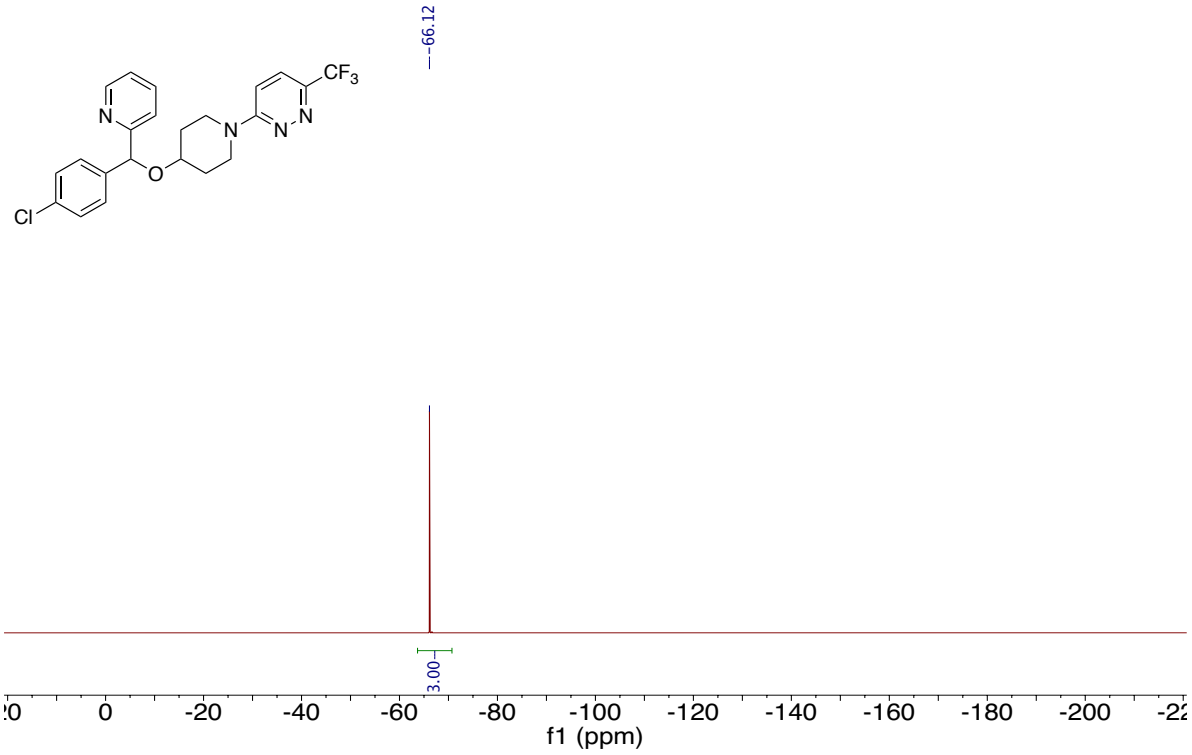

^{19}F NMR of Compound **A1-12** (376 MHz, $CDCl_3$)